

**STRUCTURAL AND ASSOCIATIONAL
ASPECTS OF SOME DIELECTROPOLAR
LIQUID MOLECULES IN NONPOLAR
SOLVENTS FROM RELAXATION
PHENOMENA**

THESIS SUBMITTED FOR THE DEGREE OF DOCTOR OF
PHILOSOPHY (SCIENCE) OF THE UNIVERSITY OF
NORTH BENGAL
2002

**North Bengal University
Library**

NILANJAN GHOSH
M.Sc., B. Ed.

Ref
539.6
6292712

149646

13 MAR 2003

STOCK TAKING - 2011 |

Dedicated to my parents
Sri Nirode Ranjan Ghosh
&
Smt. Sabita Ghosh

ACKNOWLEDGEMENT

I am highly grateful to Dr. S. Acharyya M.Sc., D. Phil (Cal), Reader in Physics of Raiganj College (University College), P.O. Raiganj, Dist. Uttar Dinajpur 733134, India for his kind guidance, active cooperation and helpful supervision for the research works presented in the thesis entitled 'Structural and associational aspects of some dielectropolar liquid molecules in nonpolar solvents from relaxation phenomena.'

I am particularly indebted to Dr. R. Ghosh, Reader of the Department of Physics of the University of North Bengal for his kind permission to perform experimental works in his Dielectric Laboratory. I convey my thanks to Dr. A. K. Nanda, Reader of the Department of Chemistry NBU for providing the author with the chemicals used in the experiment.

The author is grateful to Dr. S. K. Ghoshal, Professor of the Department of Physics and Dr. T. K. Chatterjee, Registrar of North Bengal University for their constant encouragement and inspiration towards the progress of the research work.

He is thankful to Dr. S. K. Sit of Raiganj Polytechnic, Dr. R.C. Basak of Raiganj College, Mr. K. Dutta, Mr. A. Karmakar, research workers for their helpful cooperation in the development of the thesis work.

I am particularly indebted to all of my family members, my wife Mrs. Sanchita Ghosh M.A. and my son "Purbayan" because without their cooperation the thesis works could not be possible.

Nilanjan Ghosh 06.5.02
(Nilanjan Ghosh)

Assistant Teacher in Physics
Department of Physics
Sudarsanpur D.P.U. Vidyachakra
P.O. Raiganj, Dist. Uttar Dinajpur
Pin : 733134, India.

CONTENTS

Synopsis of Thesis Work

CHAPTER 1

General Introduction and Brief Review of Previous Works..... 1-52

- 1.1. Introduction
- 1.2. Dielectric Polarisation
- 1.3. Static Relative Permittivity
- 1.4. Static Dielectric Susceptibility
- 1.5. Dipole moment, Polarisability and Clausius-Mosotti relation
- 1.6. Debye Equation
- 1.7. Dielectric Equations based on different models
- 1.8. Dielectric Dispersion
- 1.9. Representation of permittivity in the complex plane
- 1.10. Relaxation time and distribution function
- 1.11. Double relaxations due to molecular and intramolecular rotations..
- 1.12. Dielectric loss and high frequency conductivity
- 1.13. Relaxation mechanism of polar solute in nonpolar solvent under high frequency electric field
- 1.14. Relaxation mechanism of polar-nonpolar liquid mixture from Debye equation under low frequency electric field.
- 1.15. Extrapolation technique and Guggenheim equation
- 1.16. Gopalakrishna's method to estimate τ and μ
- 1.17. Eyrings rate theory
- 1.18. Relaxation time and its relationship with viscosity
- 1.19. Dielectric relaxation of polar liquid molecules in nonpolar solvent under radio frequency electric field.
- 1.20. A brief review of the previous works

CHAPTER 2

Scope and objective of the Present Work 53-74

2.1 Introduction

2.2. Theoretical formulation to estimate $hf\tau_j$ and μ_j .

2.3. Static experimental parameter X_{ij} and static μ_s

2.4. Double relaxation times τ_1, τ_2 and dipole moments μ_1, μ_2 .

2.5. Relaxation parameters under rf electric field.

2.6. Rf resistance and conductivity of a polar liquid

2.7. Washing of dielectric cell and purification of dipolar liquids.

2.8. Coefficient of viscosity of dipolar liquids.

2.9. Formulations for n, τ_j and μ_j under rf electric field.

2.10. Eyrings rate theory

2.11. Structural aspects of dipolar molecules from μ_{theo} .

CHAPTER 3

Structural and associational aspects of binary and single polar liquids in nonpolar solvent under high frequency electric field..... 75-83

CHAPTER 4

Double relaxations of some isomeric octyl alcohols by high frequency absorption in nonpolar solvent..... 84-99

CHAPTER 5

Dielectric relaxation of para polar liquids under high frequency electric field..... 100-112

CHAPTER 6

Structural and associational aspects of dielectropolar straight chain alcohols from relaxation phenomena..... 113-138

CHAPTER 7

**Structural and associational aspects of isomers of anisidine
and toluidine under a gigahertz electric field..... 139-161**

CHAPTER 8

**Double relaxation phenomena of monosubstituted
anilines in benzene under high frequency electric field..... 162-188**

CHAPTER 9

**Structural conformation and associational aspects of some
normal alcohols in benzene and their mixtures under
rf electric field at single and different temperatures..... 189-214**

CHAPTER 10

**Relaxation phenomena of aprotic polar liquid molecules
under a kilohertz electric field..... 215-239**

CHAPTER 11

Summary and Conclusion..... 240-248

List of Published and communicated papers

SYNOPSIS OF THESIS WORK

The relaxation mechanism of polar molecules in nonpolar solvents under high frequency (hf) electric field is of special interest as it throws much light on various types of molecular associations like solute-solvent (monomer) and solute solute (dimer) formations in a given solvent. One may get an idea about the stability or unstability of the systems in the relaxation phenomena through the measured thermodynamic energy parameters. It also offers valuable information of size, shape and structure of a dipolar liquid molecule from the measured permittivities like real ϵ'_{ij} , imaginary ϵ''_{ij} parts of complex permittivity ϵ^*_{ij} under hf electric field, static ϵ_{oij} and infinite frequency permittivity $\epsilon_{\infty ij}$ at different weight fractions w_j of a dipolar liquid at a given temperature.

An extensive study is, therefore, made in this thesis to get relaxation time τ_j of a large number of polar liquids assuming the existence of single broad or two Debye type dispersions in order to arrive at the structural and associational aspects of them. τ_j 's are subsequently used to calculate the hf dipole moments μ_j 's of those polar molecules in terms of slope β of hf conductivity k_{ij} or σ_{ij} against w_j curve. τ_j 's are usually estimated from the ratio of the slopes of $k''_{ij}-w_j$ or $\sigma''_{ij}-w_j$ and $k'_{ij}-w_j$ or $\sigma'_{ij}-w_j$ curves at $w_j \rightarrow 0$ where k''_{ij} or σ''_{ij} and k'_{ij} or σ'_{ij} are the imaginary and real parts of the hf complex conductivity k^*_{ij} or σ^*_{ij} in c.g.s. and SI units. The variation of hf conductivity k_{ij} or σ_{ij} against w_j alongwith other measured parameters have been well displayed to get hf μ_j . The obtained τ_j 's from the methodology so far developed are finally compared with the existing methods of Murthy et al and Gopalakrishna. In the present method polar-polar interactions are thought to be fully eliminated.

The estimated hf μ_j 's are compared with the static dipole moment μ_s obtained from linear coefficient of $X_{ij}-w_j$ variation from the measured relaxation parameters under static or low frequency electric field within the frame work of Debye and Smyth model. The theoretical dipole moments μ_{theo} 's have conveniently

been obtained from available bond angles and bond moments of the substituent polar groups attached to the polar molecules. In almost all cases μ_{theo} 's are found to differ from experimental hf μ'_j 's and static μ_s 's suggesting the very existence of inductive and mesomeric moments of the substituent polar groups attached to the parent molecule.

The recent trend is to study the orientational polarisation of molecules in terms of measured orientational susceptibilities like real χ'_{ij} , imaginary χ''_{ij} and static χ_{0ij} rather than permittivities. $\epsilon_{\infty ij}$ includes the fast polarisation and appears frequently as a subtracted term in Bergmann's equation. The existence of double relaxation times τ_1 and τ_2 due to rotation of the flexible parts and the whole molecules themselves were also expressed in terms of measured susceptibilities.

To test the dielectric relaxation theories so far developed a rigorous study is, however, made on a number of dipolar molecules like long chain normal and octyl alcohols, anilines, aprotic polar liquids, para-compounds like parahydroxy propiophenone, parachloropropiophenone, paraacetamidobenzaldehyde, parabenzoyloxy benzaldehyde in dioxane, paraanisidine, paraphenitidine, orthochloroparanitroaniline and parabromonitrobenzene in C_6H_6 at various concentrations and temperatures in $^{\circ}C$. Different thermodynamic energy parameters like enthalpy ΔH_{τ} , entropy ΔS_{τ} and free energy ΔF_{τ} of activation due to dielectric relaxation from Eyring's rate theory at different experimental temperatures in $^{\circ}C$ establish the structural and associational aspects of dielectropolar liquid molecules.

It is observed that in addition to displacement current, conduction current due to existence of free ions in the dipolar liquids is playing its role to yield rf conductivity under radio frequency (rf) electric field. But the displacement current alone gives rise to conduction under the microwave electric field. An attempt is, therefore, made to provide the feasibility of applying hf conductivity technique on some combinations of simpler dipolar molecules like alcohols in a suitable solvent or in pure states at a single or different experimental

temperatures in °C. The object of such study is to measure the dielectric relaxation parameters in order to yield the molecular dynamics of the systems under 1 MHz frequency of electric field. Some of the works of the author in c.g.s. units have been published in different journals of international repute. But nowadays the modern trend is to study the dielectric relaxation phenomena of polar molecules in nonpolar solvent in SI units because of its unified, coherent and rationalised nature. Later research works have been made in SI unit to get the interesting insight into the interactions of the dipolar molecules.

Thus the subject matter of this thesis is directed to get a concrete concept of structural and associational aspects of several dielectropolar molecules in liquid state from their measured relaxation parameters under GHz and rf electric fields. The new powerful theoretical approach enables one to test the adequacy or otherwise of the theories based on Debye-Smyth model which are usually found to deviate from the traditional dielectric theories prevailing elsewhere.

CHAPTER -1

GENERAL INTRODUCTION AND BRIEF REVIEW OF PREVIOUS WORKS

GENERAL INTRODUCTION AND BRIEF REVIEW OF PREVIOUS WORKS

1.1. Introduction

At the beginning of the present century the subject matter of dielectrics was scattered in different journals of many countries and in various languages. This field becomes the centre of interest to the scientific community and technologists all over the world when Debye [1] published a comprehensive monograph : "Polar Molecules". Since then a large number of research workers [2-6] were engaged themselves to explore the different aspects of pure polar liquid molecule and polar - nonpolar liquid mixture. Series of monographs were gradually published one after the other starting from Fröhlich [7], Smyth [8] Hill [9] to Jonscher [10] to enhance the scientific content of this particular field of research. The structural and associational aspect of the complicated and nonspherical polar molecules could, however, be reached from the study of dielectric relaxation phenomena involved with the orientational polarisation.

1.2. Dielectric Polarisation

When an isotropic nonpolar dielectric material is placed between two charged plates of a condenser, the positive nuclei of dielectric molecule are attracted by the negative plate while the negatively charged electrons by the positive plate. As a result an induced electric dipole is formed. This is known as induced polarisation due to distortion of the electric lines of force by the molecule as well as molecule itself by the electric field. The distortion polarisation is the sum of electronic and atomic polarisations. They occur both in the nonpolar and polar dielectrics, although the polar molecule has the molecular asymmetry. The asymmetric nature of molecules occur due to noncoincidence of centre of positive and negative charges. The centre of gravity of the positive and negative charges of the nonpolar molecule coincides in

absence of the applied electric field. The part of the polarisation on the other hand, for the permanent dipole of the molecule is called the orientational polarisation. In addition to distortion polarisation, the orientational polarisation takes place in case of polar molecules which are nonspherical in shape.

The induced electric dipole moment per unit volume or the polarisation charge per unit area of the nonpolar substance is commonly known as dielectric polarisation. It is a vector quantity parallel to the electric field. If we consider a unit charge in cylindrical cavity of small cross section with its axis in the direction of lines of force the actual force acting on this unit charge is called the electric field intensity \vec{E} . On the other hand, let a cavity is made in the space between two closely situated planes and perpendicular to electric lines of force, a unit charge between the planes is acted upon by the electric displacement vector \vec{D} . In Maxwell's electromagnetic theory it is assumed that

$$\vec{D} = \epsilon \vec{E} \quad (1.1)$$

where ϵ = absolute permittivity of dielectric material = $\epsilon_0 \epsilon_r$, ϵ_0 is called the permittivity of free space = $\frac{1}{4\pi c^2 \times 10^{-7}} = 8.854 \times 10^{-12}$. Farad metre⁻¹.

where c is the velocity of light in vacuum and ϵ_r is called the relative permittivity.

1.3. Static Relative Permittivity

If two charges of opposite signs are supposed to be placed on two separate conductors of a condenser having a homogeneous dielectric medium the forces on each of them is reduced by a factor ϵ_r compared to when they are placed in vacuum. ϵ_r being greater than unity is a scalar quantity called the static relative permittivity of the medium. Hence the capacitor filled with a dielectric material has a capacitance ϵ_r times greater than a capacitor with the same electrodes in vacuum. Except for exceedingly high electric field unlike normally to be reached, ϵ_r is independent of the magnitude of the applied electric field for all dielectric materials used in practice excluding ferroelectrics.

1.4. Static Dielectric Susceptibility

The introduction of a dielectric material between two charged plates reduces the electric field by a factor ϵ_r . The medium produces a flux in Coulomb metre⁻² (C.m⁻²) known as polarisation \vec{P} which opposes the electric displacement vector \vec{D} produced by the capacitor. The reduction in electric field \vec{E} can be expressed by :

$$\vec{E} = \frac{\vec{D} - \vec{P}}{\epsilon_0} \quad (1.2)$$

$$\text{or } \frac{\vec{P}}{\epsilon_0 \vec{E}} = \frac{\vec{D}}{\epsilon_0 \vec{E}} - 1$$

$$\text{or } \frac{\vec{P}}{\epsilon_0 \vec{E}} = \epsilon_r - 1 \quad (1.3)$$

The dimensionless ratio of P to $\epsilon_0 E$ is called the dielectric susceptibility χ_e of the dielectric i.e.

$$\chi_e = \epsilon_r - 1 \quad (1.4)$$

represents the component of the static relative permittivity for the electrical response of the medium itself to the applied electric field.

1.5. Dipole Moment, Polarizability and Clausius–Mosotti Relation

When two charges of equal magnitude q but of opposite signs are separated by a distance d , they constitute what is known as electric dipole of moment μ in Coulomb metre (C.m)

$$\mu = qd \quad (1.5)$$

In a dielectric material in which a polarisation \vec{P} exists, an elementary cuboid may be imagined of volume δV with two faces perpendicular to P of area δA

separated by a distance δx . Its dipole moment is $P \delta A \delta x$ or $P \delta V$. So the polarisation \vec{P} is defined as the dipole moment per unit volume of the dielectrics. This dipole moment is determined by the microscopic entity called the polarisability of the material.

When an isotropic dielectric is subjected to an external electric field \vec{E} , it causes the charge distribution within the dielectric to modify it into local field \vec{E}_1 . In nonpolar dielectrics, the dipole moments μ_a and μ_e due to atomic and electronic polarisations are proportional to \vec{E}_1 i.e.

$$\mu_a = \alpha_a E_1 \quad (1.6)$$

$$\mu_e = \alpha_e E_1 \quad (1.7)$$

where α_a and α_e are the proportionality constants called atomic and electronic polarisabilities. For a polar molecule having a permanent dipole moment μ_p arising out of molecular orientational polarisation i.e.

$$\mu_p = \alpha_p E_1 \quad (1.8)$$

Now, $\alpha_t = \alpha_a + \alpha_e + \alpha_p = \alpha_d + \alpha_p$, is the total electric polarisability. Thus the polarisation \vec{P} is, however, obtained by multiplying α with \vec{E}_1 and number density n of molecules.

$$\vec{P} = n\alpha\vec{E}_1 \quad (1.9)$$

Substituting \vec{P} from Eq (1.3) in Eq (1.9) one obtains

$$\epsilon_r - 1 = \frac{n \alpha \vec{E}_1}{\epsilon_0 \vec{E}} \quad (1.10)$$

A classical calculation made by Lorentz [11] gives the expression for E_1 where

$$\vec{E}_1 = \vec{E} + \frac{\vec{P}}{3\epsilon_0} \quad (1.11)$$

From Eqs. (1.10) and (1.11) one gets.

$$\frac{\epsilon_r - 1}{\epsilon_r + 2} = \frac{n\alpha}{3\epsilon_0} \quad (1.12)$$

Multiplying both sides by $\frac{M}{\rho}$ we have

$$\frac{\epsilon_r - 1}{\epsilon_r + 2} \cdot \frac{M}{\rho} = \frac{N\alpha}{3\epsilon_0} \quad (1.13)$$

where $nM/\rho = N =$ the Avogadro's number, $M =$ molecular weight, $\rho =$ mass density of the dielectric material.

Equation (1.13) is Clausius - Mosotti relation [12,13] which relates the macroscopic quantity ϵ_r with the microscopic quantity α for a material.

According to Maxwell's electromagnetic theory $\epsilon_r = n_D^2$, then Eq (1.13) becomes.

$$\frac{n_D^2 - 1}{n_D^2 + 2} \cdot \frac{M}{\rho} = \frac{N\alpha}{3\epsilon_0} \quad (1.14)$$

which is Lorentz-Lorentz equation [14], for molar refraction. where n_D is the refractive index.

1.6. Debye Equation

The variable $\frac{\epsilon_r - 1}{\epsilon_r + 2} \cdot \frac{M}{\rho}$ of Eq (1.13) does not vary with temperature. However, according to experimental observation ϵ_r and ρ are temperature dependent quantities. $\frac{\epsilon_r - 1}{\epsilon_r + 2} \cdot \frac{M}{\rho}$ was found to be independent of temperature for nonpolar dielectrics.

The variation of $\frac{\epsilon_r - 1}{\epsilon_r + 2} \frac{M}{\rho}$ against $\frac{1}{T}$ was, however, observed [1] for

some molecules called polar molecules. The charge distribution of such molecule is that even in absence of electric field it possesses a permanent dipole moment μ_p . The permanent μ of the molecule is randomly directed and hence the net moment is zero. The applied electric field tends to align μ_p along the field direction whereas thermal motions tries to disorganise the orderly state so produced. The resulting orientational polarisation \vec{P}_o is inversely proportional to absolute temperature T K and except for exceedingly high electric field is directly proportional to \vec{E}_1 .

$$\text{It can be shown [15] that } P_o = \frac{n\mu_p^2 \vec{E}_1}{3kT} \quad (1.15)$$

Now $\vec{P}_o/n\vec{E}_1$ is defined as the orientational polarisability α_p given by :

$$\alpha_p = \frac{\mu_p^2}{3kT}$$

Thus the total polarisability in case of polar dielectric is

$$\alpha_T = \alpha_a + \alpha_e + \frac{\mu_p^2}{3kT}$$

$$\alpha_T = \alpha_d + \frac{\mu_p^2}{3kT} \quad (1.16)$$

where α_d is the polarisability due to fast polarisation. The Clausius - Mosotti equation (Eq. 1.13) becomes :

$$\frac{\epsilon_r - 1}{\epsilon_r + 2} \frac{M}{\rho} = \frac{N}{3\epsilon_0} \left(\alpha_d + \frac{\mu_p^2}{3kT} \right) \quad (1.17)$$

This is known as Debye equation [1] for a dipolar gaseous molecule. It can be represented by a straight line between experimentally measured variables of

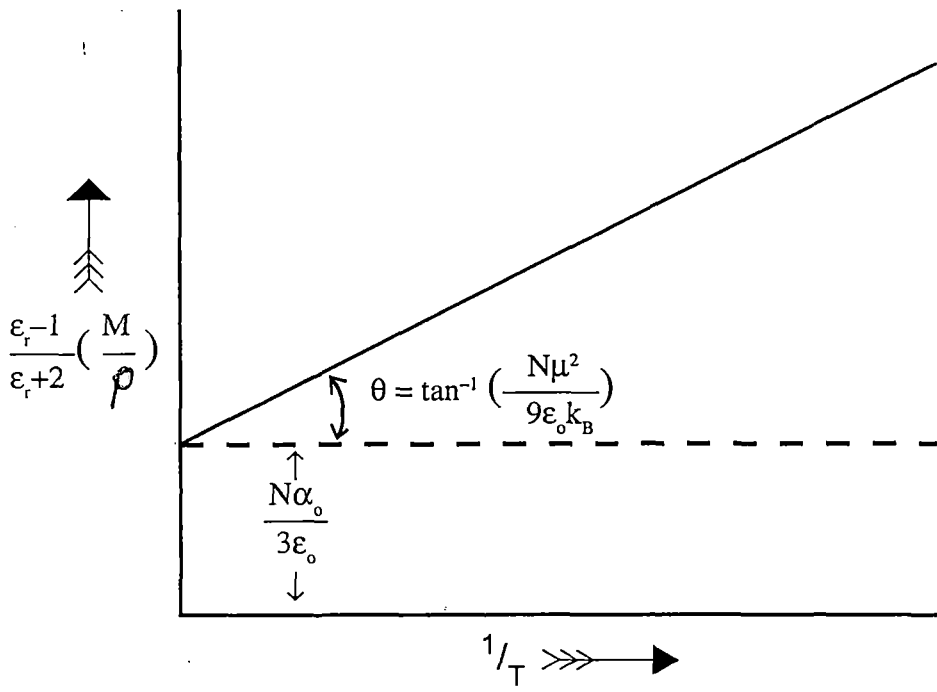


Figure 1.1

$\frac{\epsilon_r - 1}{\epsilon_r + 2} \frac{M}{\rho}$ and $\frac{1}{T}$ of Figure. 1.1., whose slope may yield μ a of a dipolar gas molecule to arrive at the valuable information of the structural aspects of a molecule.

1.7. Dielectric Equation Based on Different Models

For almost spherical polar liquid molecule Onsager equation is applicable [2]. A relation between the relative permittivity and dipole moment is, however, obtained by considering the reaction field \vec{R} for the external applied electric field and the cavity field \vec{G} , in a continuous medium of static relative permittivity ϵ .

$$\frac{(\epsilon_{oij} - n_{Dij}^2) \cdot (2 \epsilon_{oij} + n_{Dij}^2)}{\epsilon_{oij} (n_{Dij}^2 + 2)^2} = \frac{N\rho\mu^2}{9MkT\epsilon} \quad (1.18)$$

Later on, a large number of workers modified Debye and Onsager equations to obtain μ of a highly nonspherical polar liquid molecule.

Kirkwood [3] pointed out the fact of hindered rotation of the polar molecule in a dielectric medium under polarisation. The effect of short range forces was considered to generalise Onsager equation [2]. The macroscopic relative permittivities of the medium are then connected by :

$$\frac{(\epsilon_{oij} - n_{Dij}^2) \cdot (2 \epsilon_{oij} + n_{Dij}^2)}{\epsilon_{oij} (n_{Dij}^2 + 2)^2} = \frac{N\rho\mu^2}{9MkT\epsilon} g \quad (1.19)$$

The correlation parameter “g” measures the hindered molecular rotation arising out of short range intermolecular forces. It can, however, be calculated from the knowledge of the structure of the liquid molecule. For normal liquids of nearly spherical shape and size “g” is equal to unity. But for highly nonspherical and associative liquids “g” values deviates significantly from unity.

Fröhlich and Sack [16] also extended Onsager equation to solids. They

applied it to the model having two equilibrium orientations for the molecules separated by an angle of 180° . The equation may be written as :

$$\frac{(\epsilon_{oij} - \epsilon_{\infty ij}) \cdot (2\epsilon_{oij} + \epsilon_{\infty ij})}{3 \epsilon_{oij}} = \left[1 + \frac{(\epsilon_{oij} - \epsilon_{\infty ij})^2}{3\epsilon_{oij} \epsilon_{\infty ij}} \right] \frac{\mu^2}{a^3 kT} \quad (1.20)$$

Where 'a' is the molecular radius. The equation (1.20) may be applied to highly viscous liquids as well as to solids. But for liquids of low viscosity it reduces to Onsager equation. The difficulties in Fröhlich equation are associated with the evaluation of interaction of the sample with the surrounding medium. Thus there exists experimental limitation in determining the required parameters involved in various equations presented. For nonassociative dipolar liquids where short range forces are absent one can use Onsager equation to analyse the experimental data to estimate μ .

1.8 Dielectric Dispersion

When an alternating electric field is applied to a dielectric material electronic, atomic and orientational polarisations operate effectively. The inertia of sub microscopic entities increases with the frequency and thereby ceases to operate. The frequency range over which all the polarisations is dropping is known as dispersion. The springlike nature of the forces involved in electronic and atomic polarisations tend to disappear with the frequency of the applied electric field. The dropping out of the orientational polarisation is, however, accompanied by relaxation process which involves with a relaxation time over a much wider range of frequencies. When the frequency of the impressed electric field exceeds a certain critical value, the permanent dipoles of molecules can not follow the exact alternation of the applied electric field. The measurable lag is commonly known as dielectric relaxation and the relaxation time τ is defined as the lag in response of the polar molecule with the forces to which it is

subjected. Thus when the electric field is switched off all the polarisations decay exponentially with time. The time in which the polarisation is reduced to $1/e$ times its initial value is called relaxation time τ [17]. Typically the mid frequency f_0 is 10^{15} Hz for electronic polarisation and 10^{12} Hz for atomic polarisation. But the orientational polarisation has a wide range of f_0 lying between 10^4 to 10^9 Hz [18] depending on the nature of the material and temperature.

Each region of dispersion is associated with an energy loss i.e. absorption of energy per second per unit volume. It has a peak at f_0 . The existence of energy loss means that electric displacement vector \vec{D} instead of being inphase with \vec{E} lags by a phase angle δ . Thus it is evident from Eq (1.1) that ϵ_r^* is a complex quantity given by :

$$\epsilon_r^* = \epsilon_r' - j\epsilon_r'' \quad (1.21)$$

$$\epsilon_r''/\epsilon_r' = \tan \delta \quad (1.22)$$

ϵ_r'' and $\tan \delta$ are known as the dielectric loss factor and loss tangent respectively.

Also the real χ_e' and imaginary χ_e'' parts of hf complex susceptibility χ_e^* are related to complex relative permittivity ϵ_r^* by :

$$\chi_e = \chi_e' - j\chi_e'' \quad (1.23)$$

$$\chi_e' = \epsilon_r' - 1 \quad (1.24)$$

$$\chi_e'' = \epsilon_r'' \quad (1.25)$$

When the measured ϵ_r' and ϵ_r'' are plotted against frequency 'f' of the applied alternating electric field the observed variations are shown in Figure 1.2. The resulting curves exhibit sharp resonance of ϵ_r'' at a particular frequency f_0 . It indicates the regions for electronic, atomic and orientational polarisations (Figure 1.2). Almost similar behaviour of the molecular orientational polarisation process is observed in the plot of $\bar{\chi}_p'' = (\chi''/\chi_{ps})$ against $\log_{10}(\omega\tau)$ as seen in Figure 1.3[18]. χ_{ps} is the static orientational susceptibility and $\omega (=2\pi f)$

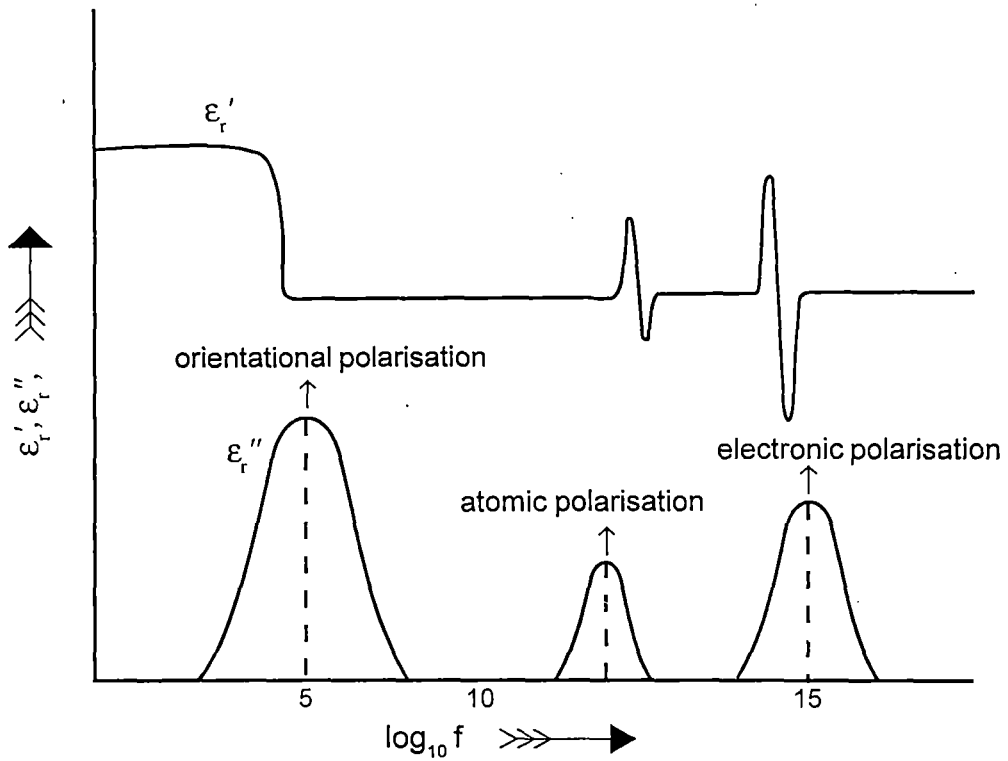


Figure 1.2

(Variation of ϵ' , and ϵ'' , with frequency f . Abscissa is $\log_{10} f$, where f is expressed in hertz)

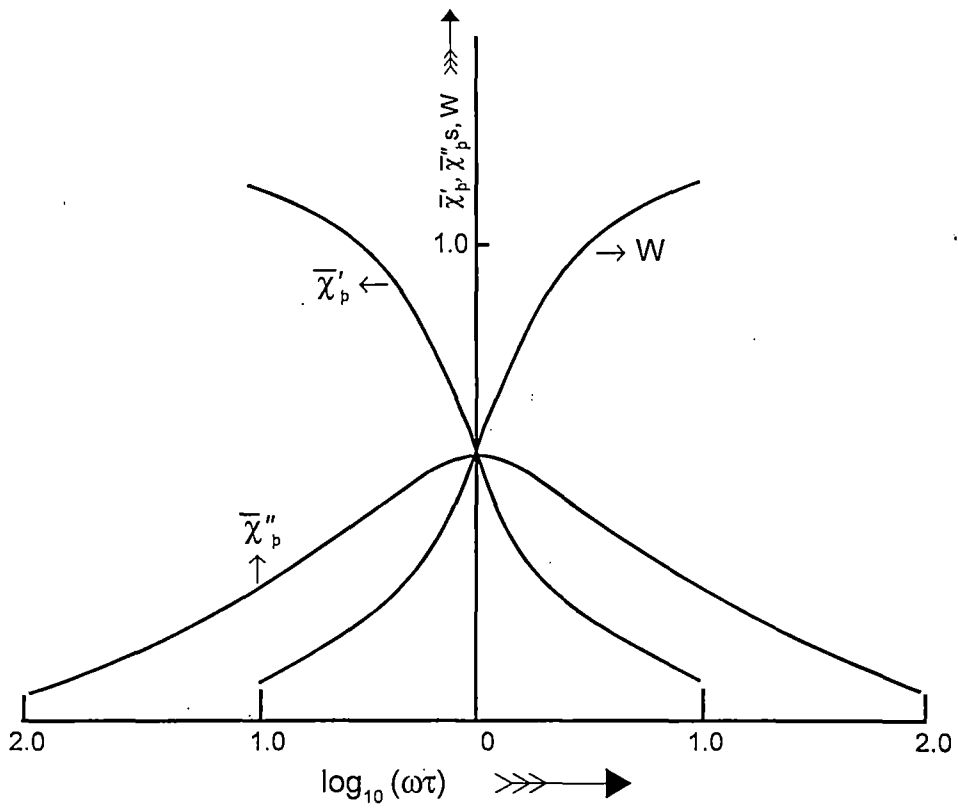


Figure 1.3

Plot of $\bar{\chi}'_p = \chi'/\chi_{ps}$, $\bar{\chi}''_p = \chi''/\chi_{ps}$, and $W = W_\tau/\epsilon_0\chi_{ps}E^2$ for Debye behaviour (χ_{ps} is the static orientational susceptibility)

is the angular frequency of the applied electric field. The frequency variation of ϵ'_r and ϵ''_r are not independent. The drop in ϵ'_r from beginning to end of a dispersion region namely $\Delta\epsilon'_r$ is called the strength of the dispersion and is governed by Kramers - Kronig [18] relation :

$$\Delta\epsilon'_r = \frac{2}{\pi} \int_{-\infty}^{+\infty} \epsilon''_r d(\ln f) \quad (1.26)$$

In practice, the integral is truncated to avoid the inclusion of area attributable to other mechanism.

At optical frequencies it is usual practice to characterize the material by its complex refractive index n^*_D given by :

$$n^*_D = n_D - jk \quad (1.27)$$

where n_D is the real part of refractive index and k is the absorption coefficient n^*_D is related to ϵ_r by $\epsilon_r = n^2_D$. So from Eq (1.21) we have :

$$n^*_D = n^2_D - k^2 \quad (1.28)$$

$$\epsilon''_r = 2n_D \cdot k \quad (1.29)$$

The use of the above relationship allows one to locate the value of ϵ_r at high frequencies. For the optical measurements k is very low and hence one gets $\epsilon_r \simeq n^2_D$.

1.9. Representation of Permittivity in the Complex Plane

A. Debye Behaviour

The variation of ϵ_r^* with angular frequency ω is [1] :

$$\frac{\epsilon_r^* - \epsilon_\infty}{\epsilon_s - \epsilon_\infty} = \frac{1}{1 + j\omega\tau} \quad (1.30)$$

where ϵ_∞ and ϵ_s are the relative permittivities at much higher and lower

frequencies respectively than ε_r^* in the dispersion regions arising out of relaxation of permanent dipoles. Equating the real and imaginary parts of Eq.(1.30) one gets.

$$\frac{\varepsilon_r' - \varepsilon_\infty}{\varepsilon_s - \varepsilon_\infty} = \frac{1}{1 + \omega^2\tau^2} \quad (1.31)$$

$$\frac{\varepsilon_r''}{\varepsilon_s - \varepsilon_\infty} = \frac{\omega\tau}{1 + \omega^2\tau^2} \quad (1.32)$$

On eliminating the parameter $\omega\tau$ and rearranging it is obtained :

$$\left(\varepsilon_r' - \frac{\varepsilon_s + \varepsilon_\infty}{2}\right)^2 + \varepsilon_r''^2 = \left(\frac{\varepsilon_s - \varepsilon_\infty}{2}\right)^2 \quad (1.33)$$

This is a parametric equation of a circle. If ε_r'' be plotted against ε_r' a semicircular arc of radius $\left(\frac{\varepsilon_s - \varepsilon_\infty}{2}\right)^2$ results in the Figure 1.4 with its centre at $\{\frac{1}{2}(\varepsilon_s + \varepsilon_\infty), 0\}$

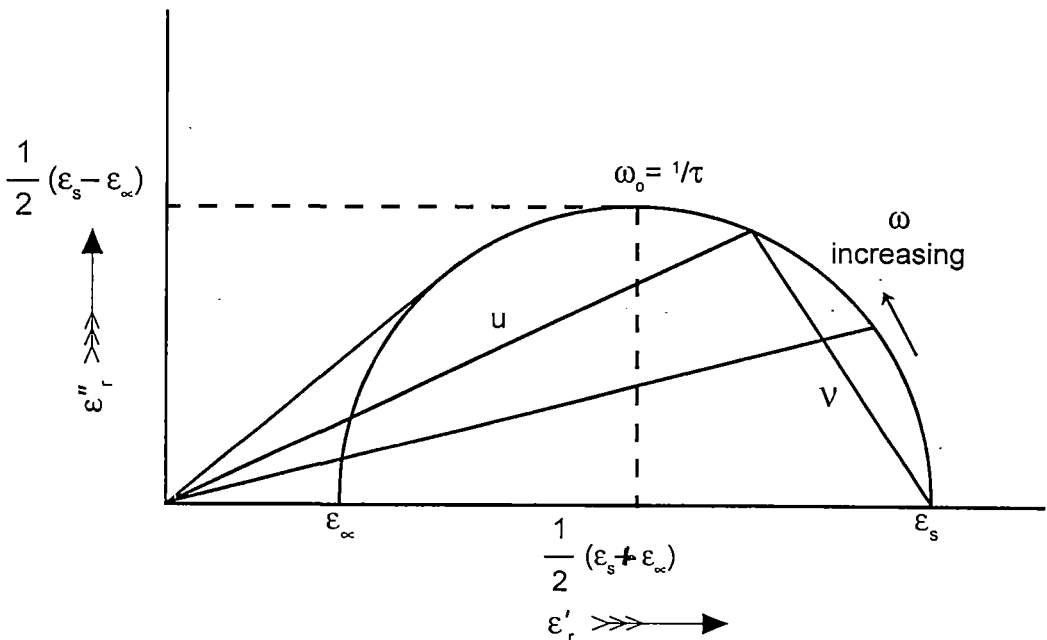


Figure 1.4

(Plot of ε_r'' versus ε_r' for Debye behaviour)

on the ϵ_r' axis, making intercept of ϵ_s and ϵ_∞ in the lower and higher ω . The loss factor has its maximum value when $\omega_0 = 1/\tau$ and on the semicircle the frequency ω is given by

$$\frac{\omega}{\omega_0} = \frac{v}{u} \quad (1.34)$$

where u and v are the distances of the point from the intercept of the semicircle with ϵ_r' axis as shown in Figure 1.4.

The value ϵ_r'' gives a semicircle when plotted against ϵ_r' . It indicates that the data conform to the Debye theory. Results of permittivity measurements when are analysed in this way for many simple liquids, the experimental points do not always lie on the expected Debye semicircle. The method has the disadvantage that the frequency, which is the independent variable, is very difficult to be known accurately.

B. The Cole - Cole arc

The universally well known contribution of Cole -Cole [19] to the study of dielectric relaxation are found to satisfy materials including long chain alcohols and polymers. The measured permittivities at different frequencies follow the empirical equation :

$$\frac{\epsilon_r^* - \epsilon_\infty}{\epsilon_s - \epsilon_\infty} = \frac{1}{1 + (j\omega\tau)^{1-\gamma}} \quad (1.35)$$

where $0 \leq \gamma < 1$. When ϵ_r'' be plotted against ϵ_r' a circular arc results in with its centre at $\{1/2 (\epsilon_s + \epsilon_\infty), -1/2 (\epsilon_s - \epsilon_\infty) \tan \pi\gamma/2\}$ and radius $1/2 (\epsilon_s - \epsilon_\infty) \text{Sec } \pi\gamma/2$. The physical significance of this plot as shown in Figure 1.5 is that τ can be obtained by using.

$$\omega\tau = \left(\frac{v}{u}\right)^{1-\gamma} \quad (1.36)$$

149646

3 MAR 2003

Uttarakhand University
Library
Dehra Dun

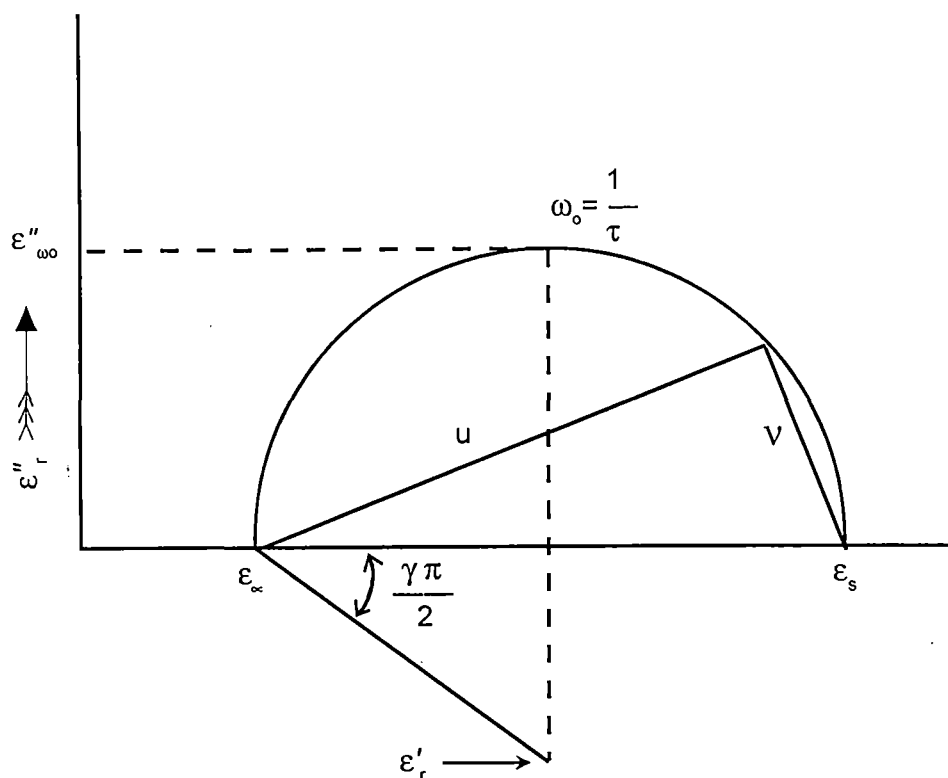


Figure 1.5

(Cole - Cole Plot)

Where u and v are distances of the point from the intercept on the ϵ'_r axis. The value of γ found experimentally, show a tendency to increase with increasing number of internal degrees of freedom in the molecules and with decreasing temperature. In the limit $\gamma = 0$ the Cole - Cole arc reduces to the Debye semi circle.

C. The Cole - Davidson arc

The Cole-Cole symmetrical arc results in for certain materials like glycerol into a skewed arc by Cole and Davidson [20,21]. They suggested that behaviour of this kind could be represented by the equation

$$\frac{\epsilon'_r - \epsilon_\infty}{\epsilon_s - \epsilon_\infty} = \frac{1}{(1 + j\omega\tau)^\delta} \quad (1.37)$$

Where δ is a constant, $0 < \delta \leq 1$

When ϵ_r'' 's are plotted against ϵ_r' in Figure 1.6 it represents the skewed arc. The ϵ_r' axis of the skewed arc cuts at an acute angle $\pi\delta/2$ to yield $\epsilon_r' = \epsilon_\infty$ at right angles and $\epsilon_r' = \epsilon_s$ at the high and low frequencies ends respectively. The maximum value of ϵ_r' occurs at angular frequency

$$\omega_m = \frac{1}{\tau} \tan \frac{\pi}{2(1+\delta)} \quad (1.38)$$

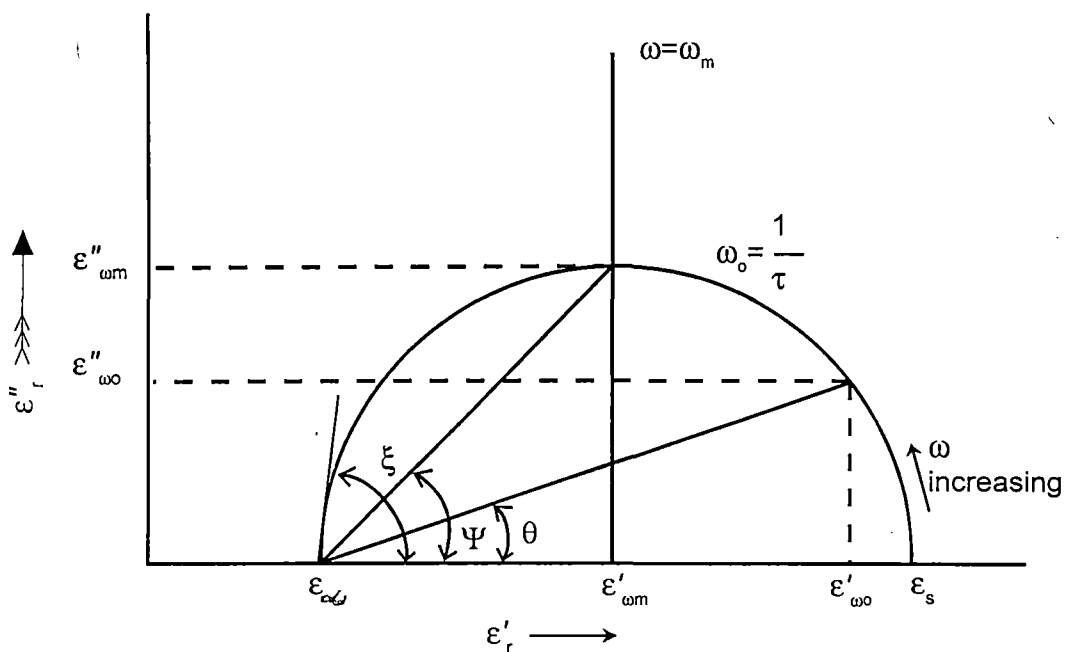


Figure 1.6

Cole-Davidson plot $\xi = \frac{\pi}{2} \delta$; $\Psi = \frac{\pi}{2} \delta/(1+\delta)$, $\theta = \frac{\pi}{4} \delta$.

The physical significance of this plot is that τ can be estimated by using Eq. (1.38) with the knowledge of ω_m and δ . Also Eq. (1.38) seems to be very successful in representing the behaviour of substances at low temperature. As the temperature increases δ tends to 1 showing Debye semicircular arc.

1.10. Relaxation Time and Distribution Function

Many experimental results of dipolar liquids were found to satisfy Cole-Cole and Cole-Davidson plots almost quantitatively. The left hand side of both Eqs. (1.35) and (1.37) are associated with two physical constraints [22] and hence it is very difficult to draw any concrete physical conclusion from them. In addition to the semicircular and skewed arc plots a number of circular arc plots could, however, be observed for multiple relaxation times. For this reason the original Debye equations (1.31) and (1.32) can be considered.

$$\frac{\epsilon_r' - \epsilon_\infty}{\epsilon_s - \epsilon_\infty} = \int_0^\infty \frac{G(\tau) d\tau}{1 + \omega^2 \tau^2} \quad (1.39)$$

$$\frac{\epsilon_r''}{\epsilon_s - \epsilon_\infty} = \int_0^\infty \frac{G(\tau) d\tau}{1 + \omega^2 \tau^2} \quad (1.40)$$

Where $G(\tau)$ is the distribution function of relaxation times which satisfies the normalisation condition

$$\int_0^\infty G(\tau) d\tau = 1 \quad (1.41)$$

$G(\tau)d\tau$ is the fraction of the group of dipoles at a given instant having individual relaxation time in a range $d\tau$.

A large number of workers suggested the distribution functions. Wagner [23] and Yager [24] applied the Gaussian error distribution function to observe some of the experimental data satisfactorily i.e.

$$G(\tau) d\tau = b\pi^{-1/2} \exp(-b^2 y^2) dy \quad (1.42)$$

Where 'b' is a constant which determines the breadth of distribution and

$$y = \ln(\tau/\tau_0)$$

where τ_0 is the most probable relaxation time.

In long chain polar molecules such as alcohols and polymers there are many possibilities of internal rotations bending and twisting each with characteristic relaxation time. In averaging to the macroscopic condition a distribution of relaxation time is observed by Kirkwood and Fous [25].

$$G(\tau) = \frac{1}{2 \cosh y + 2} \quad (1.43)$$

where $y = \ln (\tau/\tau_0)$

This Eq. (1.43) failed to explain experimental results in most cases. Fous and Kirkwood [26] further observed that the experimental data should be represented by another empirical relation :

$$\epsilon'' = \epsilon_m'' \operatorname{sech} (\beta \ln \omega/\omega_m) \quad (1.44)$$

where β is a distribution parameter. ω_m is the angular frequency corresponding to the maximum value of ϵ_m'' of ϵ'' . The distribution function is

$$G(\tau) = \frac{\beta}{\pi} \frac{\cos (\beta\pi/2) \cosh (\beta y)}{\cos^2 (\beta\pi/2) + \sinh^2 (\beta y)} \quad (1.45)$$

A useful empirical relation developed by Cole and Cole [19]. It is given by:

$$G(\tau)d\tau = \frac{1}{2\pi} \frac{\sin \alpha\pi}{\cosh (1-\alpha)\ln (\tau_0/\tau) - \cos \alpha\pi} \quad (1.46)$$

Where α is a distribution parameter which measures the width of distribution.

Fröhlich [7] derived the distribution function as :

$$G(\tau) = (\epsilon_0 - \epsilon_\infty) \frac{kT}{V_0} \frac{1}{\tau} \text{ if } \tau_0 \leq \tau \leq \tau_1 \quad (1.47)$$

$$\tau_1 = \tau_0 \exp(V_0/kT)$$

$$G(\tau) = 0 \text{ if } \tau < \tau_0 \text{ and } \tau > \tau_1$$

V_0 is the width of potential barrier.

A more general form of distribution function has recently been described by Matsumoto and Higasi [27] as

$$G(\tau) = \frac{1}{A\tau^n} \text{ where } 0 < n < \infty \text{ if } \tau_1 < \tau < \tau_2$$

but $G(\tau) = 0$ if $\tau < \tau_1$ and $\tau > \tau_2$ (1.48)

1.11. Double Relaxations Due to Molecular and Intramolecular Rotations

For a number of non interacting Debye type dispersions Budo [28] assumed that Debye equation (1.30) can be put into the form :

$$\frac{\epsilon_r^* - \epsilon_\infty}{\epsilon_s - \epsilon_\infty} = \sum \frac{c_k}{1 + j\omega\tau_k} \quad (1.49)$$

Where c_k is the relative contribution for the k th type of relaxation process, such that $\sum c_k = 1$.

For almost all dipolar molecules the relaxation process is involved with two separate broad dispersions of relaxation times τ_1 and τ_2 . The relative contributions c_1 and c_2 due to τ_1 and τ_2 towards relaxation can also be estimated. Eq. (1.49) is written as

$$\frac{\epsilon_r' - \epsilon_\infty}{\epsilon_s - \epsilon_\infty} = c_1 \frac{1}{1 + \omega^2\tau_1^2} + c_2 \frac{1}{1 + \omega^2\tau_2^2} \quad (1.50)$$

$$\frac{\epsilon_r''}{\epsilon_s - \epsilon_\infty} = c_1 \frac{\omega\tau_1}{1 + \omega^2\tau_1^2} + c_2 \frac{\omega\tau_2}{1 + \omega^2\tau_2^2} \quad (1.51)$$

such that $c_1 + c_2 = 1$

Bergmann et al [29] used a graphical method to obtain τ_1 and τ_2 from Eqs (1.50) and (1.51). The above equations are :

$$Y = c_1 Y_1 + c_2 Y_2 \quad (1.52)$$

$$Z = c_1 Z_1 + c_2 Z_2 \quad (1.53)$$

where

$$Y = \frac{\epsilon_r''}{\epsilon_s - \epsilon_\infty}, \quad Y_1 = \frac{\omega\tau_1}{1 + \omega^2\tau_1^2}, \quad Z_1 = \frac{1}{1 + \omega^2\tau_1^2}$$

$$Z = \frac{\epsilon_r' - \epsilon_\infty}{\epsilon_s - \epsilon_\infty}, \quad Y_2 = \frac{\omega\tau_2}{1 + \omega^2\tau_2^2}, \quad Z_2 = \frac{1}{1 + \omega^2\tau_2^2}$$

with reference to Figure 1.7. Z is plotted against Y for different experimental frequencies ω of the applied electric field. An experimental point (Y, Z) lies on a chord between the points (Y_1, Z_1) and (Y_2, Z_2) on the normalised Debye semicircle of Figure 1.7. The selected point divides the chord in the ratio c_1/c_2 . When this ratio is known, the analysis is made by drawing a chord through the experimental points (Y, Z) such that it is divided in that ratio. The consistent values of τ_1, τ_2 and c_1, c_2 are then estimated.

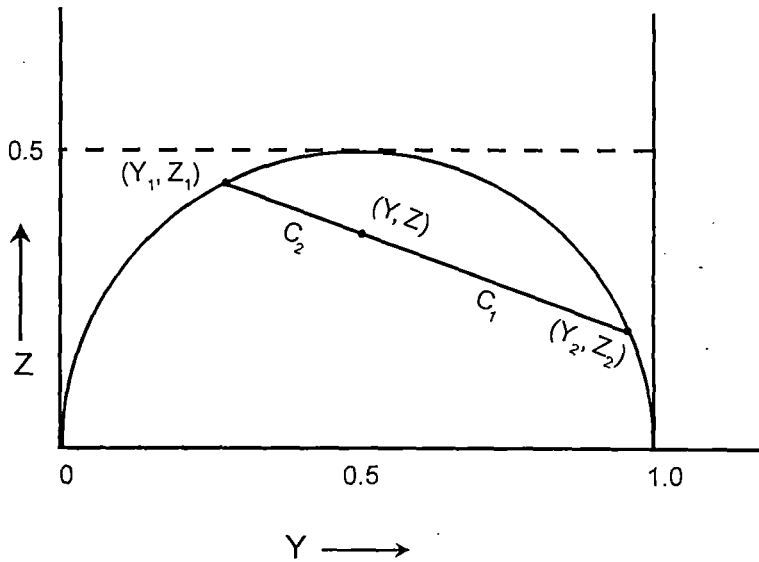


Figure 1.7

(Plot of normalised semi circle)

Bhattacharyya et al [30] subsequently simplified the above procedure to calculate τ_1 and τ_2 when the relative permittivities were measured at two different frequencies of the applied electric field. Let $X_1 = \omega\tau_1$, $X_2 = \omega\tau_2$, $\xi = 1/(1+X^2)$ and $\eta = X/(1+X^2)$. Eqs. (1.52) and (1.53) becomes :

$$a = c_1 \xi_1 + c_2 \xi_2 \quad (1.54)$$

$$b = c_1 \eta_1 + c_2 \eta_2 \quad (1.55)$$

where $a = \frac{\epsilon_r' - \epsilon_\infty}{\epsilon_s - \epsilon_\infty}$ and $b = \frac{\epsilon_r''}{\epsilon_s - \epsilon_\infty}$

From Eqs. (1.54) and (1.55) one obtains

$$c_1 = \frac{(b - aX_2)(1+X_1^2)}{X_1 - X_2} \quad (1.56)$$

$$c_2 = \frac{(aX_1 - b)(1+X_2^2)}{X_1 - X_2} \quad (1.57)$$

such that $X_1 > X_2$

Since $c_1 + c_2 = 1$ Eqs. (1.56) and (1.57) are solved to get :

$$\frac{1-a}{b} = (X_1 + X_2) - \frac{a}{b} X_1 X_2 \quad (1.58)$$

to yield τ_1 and τ_2 , provided the data are measured at two different known frequencies of the electric field. The c_1 and c_2 can be estimated from Eqs (1.56) and (1.57) respectively.

Higasi et al [31] made a analysis to estimate τ_1 and τ_2 of polar liquid molecules in nonpolar solvents graphically under single frequency electric field. Saha et al [32] and Sit et al [33] put forward an analytical method based on single frequency measurement of relative permittivities ϵ'_{ij} , ϵ''_{ij} , ϵ_{oij} and $\epsilon_{\infty ij}$ of polar-nonpolar liquid mixtures of different weight fractions w_j 's at a given temperature

to get τ_1 , τ_2 and c_1 , c_2 respectively. Earlier investigation had been made on different long chained molecules like alcohols in nonpolar solvents [34,35] to see the double relaxation phenomena at three different electric field frequencies in terms of relative permittivities. Recently Ghosh et al [36] has derived a formulation in terms of dielectric orientational susceptibilities to obtain τ_1 and τ_2 as presented in chapter 2.

1.12. Dielectric Loss and High Frequency Conductivity

The dielectric absorption measures the energy dissipation in a dielectric medium due to dielectric relaxation. This is of smaller magnitude and related to dc conductivity of the medium. The effect of Joule's heat arises from the conductivity associated with the loss factor ϵ'' .

In an ideal dielectric, there is actually no free-ion conduction still Joule heat is produced in dielectric by the drift of electrons or free ions under the applied alternating electric field. Let a potential V is established between the parallel plates of a condenser having dielectric material of complex dielectric constant ϵ^* and d is the distance of separation between the plates of surface area A . A charge q per unit area appears on each plate. An electric displacement D is then created in the dielectric material. The current density i is then given by

$$i = \frac{dq}{dt} \quad (1.59)$$

In SI unit, $q = D$ and $D = \epsilon_r^* \epsilon_0 E$

Where $E = \frac{V}{d}$ = intensity of applied electric field and ϵ_0 = permittivity of

free space = $8.854 \times 10^{-12} \text{ Fm}^{-1}$

$$\text{or } i = \frac{d}{dt} (\epsilon_r^* \epsilon_0 E) = \epsilon_r^* \epsilon_0 \frac{d}{dt} \left(\frac{V}{d} \right)$$

under the alternating electric field potential $V = V_0 e^{j\omega t}$ (1.60)

the above equation is :

$$i = \frac{\epsilon_r^* \epsilon_0}{d} \frac{d}{dt} (V_0 e^{j\omega t})$$

$$= j\omega \epsilon_r^* \epsilon_0 E \quad (1.61)$$

The current density i in terms of hf complex conductivity σ^* is :

$$i = \sigma^* E \quad (1.62)$$

From Eqs (1.61) and (1.62) one gets

$$\sigma^* = j\omega \epsilon_r^* \epsilon_0 \quad (1.63)$$

Murphy and Morgan [37], however, deduced σ^* :

$$\sigma^* = \sigma' + j\sigma'' \quad (1.64)$$

From Eqs. (1.63) and (1.64) one obtains

$$\sigma' + j\sigma'' = \omega \epsilon_0 \epsilon_r'' + j\omega \epsilon_0 \epsilon_r'$$

$$\text{since } \epsilon_r^* = \epsilon_r' - j\epsilon_r''$$

where $\sigma' = \omega \epsilon_0 \epsilon_r''$ and $\sigma'' = \omega \epsilon_0 \epsilon_r'$ are the real and imaginary parts of hf complex conductivity σ^* .

1.13. Relaxation Mechanism of Polar Solute in Nonpolar Solvent under High Frequency Electric Field

If α_i and α_j be the polarisabilities of a nonpolar and polar molecule of molecular weights M_i and M_j respectively the Eq (1.17) becomes :

$$\frac{\epsilon_\infty - 1}{\epsilon_\infty + 2} \frac{f_i M_i + f_j M_j}{\rho_{ij}} = \frac{N}{3\epsilon_0} f_i \alpha_i + \frac{N}{3\epsilon_0} f_j \alpha_j \quad (1.65)$$

$$\frac{\epsilon_s - 1}{\epsilon_s + 2} \frac{f_i M_i + f_j M_j}{\rho_{ij}} = \frac{N}{3\epsilon_0} f_i \alpha_i + \frac{N}{3\epsilon_0} f_j \alpha_j + \frac{N \mu_j^2 f_j}{9\epsilon_0 kT} \quad (1.66)$$

where ϵ_∞ and ϵ_s are the dielectric constants of the solution at infinite frequency and static electric fields respectively. The mole fractions f_i and f_j of the components are

$$f_i = \frac{n_i}{n_i + n_j} \quad \text{and} \quad f_j = \frac{n_j}{n_i + n_j}$$

n_i and n_j are the number of solvent and solute molecules per unit volume of the solution. From Eqs (1.65) and (1.66) one obtains :

$$\epsilon_s - \epsilon_\infty = \frac{N c_j \mu_j^2}{27 \epsilon_0 kT} (\epsilon_s + 2) (\epsilon_\infty + 2) \quad (1.67)$$

c_j is the concentration of the solute molecule in moles /c.c. Using $(\epsilon_s - \epsilon_\infty)$ from Eq. (1.32) one gets.

$$\epsilon_r'' = \frac{N c_j \mu_j^2}{27 \epsilon_0 kT} (\epsilon_s + 2) (\epsilon_\infty + 2) \frac{\omega \tau}{1 + \omega^2 \tau^2} \quad (1.68)$$

In dilute polar-nonpolar liquid mixture, it is assumed that $\epsilon_s \simeq \epsilon_\infty \simeq \epsilon_r'$

$$\epsilon_r'' = \frac{N c_j \mu_j^2}{27 \epsilon_0 kT} (\epsilon_r' + 2)^2 \frac{\omega \tau}{1 + \omega^2 \tau^2} \quad (1.69)$$

ϵ_r'' in Eq (1.69) depends linearly on c_j . At infinite dilution of $c_j = 0$, ϵ_r' may be replaced by ϵ_i , the relative permittivity of the solvent used.

$$\epsilon_r'' = \frac{N c_j \mu_j^2}{27 \epsilon_0 kT} (\epsilon_i + 2)^2 \frac{\omega \tau}{1 + \omega^2 \tau^2} \quad (1.70)$$

The Eq. (1.70) with $\sigma' = \omega \epsilon_0 \epsilon_r''$ becomes

$$\sigma' = \frac{Nc_j \mu_j^2 (\epsilon_i + 2)^2 \omega^2 \tau}{27kT(1 + \omega^2 \tau^2)} \quad (1.71)$$

The Eq (1.71) may be used to estimate $hf \mu_j$ in order to arrive at the structural aspects of a dielectropolar liquid molecule.

From Eq (1.31) it can be written as :

$$\epsilon_r' = \epsilon_\infty + \left(\frac{\epsilon_s - \epsilon_\infty}{1 + \omega^2 \tau^2} \right) \quad (1.72)$$

Multiplying both sides by $\omega \epsilon_0$ and introducing the term $\sigma'' = \omega \epsilon_0 \epsilon_r'$ and $\sigma' = \omega \epsilon_0 \epsilon_r''$, the Eq (1.72) with the help of Eq(1.32) becomes :

$$\sigma'' = \sigma_\infty + \left(\frac{1}{\omega \tau} \right) \cdot \sigma' \quad (1.73)$$

The Eq (1.73) is linear between the variables σ'' and σ' . The slope $1/\omega\tau$ may conveniently be used [38] to estimate τ of a polar unit.

1.14. Relaxation Mechanism of Polar - Nonpolar Liquid Mixture from Debye Equation under Low Frequency Electric Field :

The Eq. (1.17) is applied to estimate static μ_s under static or low frequency electric field. For a mixture of two liquids : one of the i th type (nonpolar) and the other of the j th type (polar) Eq. (1.17) is :

$$\frac{\epsilon_{ij} - 1}{\epsilon_{ij} + 2} \frac{M_i f_i + M_j f_j}{\rho_{ij}} = \frac{N}{3\epsilon_0} (\alpha_i f_i + \alpha_j f_j + \frac{\mu_s^2}{3kT} f_j) \quad (1.74)$$

ϵ_{ij} is the relative permittivity of solution. As $\alpha_i = \alpha_j$ Eq. (1.74) reduces to :

$$\frac{\epsilon_{ij} - 1}{\epsilon_{ij} + 2} V_{ij} = \frac{N\alpha_i}{3\epsilon_0} + \frac{N}{3\epsilon_0} \frac{\mu_s^2}{3kT} f_j$$

$$\frac{\epsilon_{ij} - 1}{\epsilon_{ij} + 2} V_{ij} = \frac{\epsilon_i - 1}{\epsilon_i + 2} V_i + \frac{N\mu_s^2}{9\epsilon_0 kT} f_j \quad (1.75)$$

where V_{ij} and V_i are the specific volumes of the solution and solvent respectively.

As $\epsilon = n_D^2$ where n_D is the refractive index, Eq (1.75) for a neutral dielectrics is :

$$\frac{n_{Dij}^2 - 1}{n_{Dij}^2 + 2} V_{ij} = \frac{n_{Di}^2 - 1}{n_{Di}^2 + 2} V_i \quad (1.76)$$

From Eqs (1.75) and (1.76) one gets :

$$\left(\frac{\epsilon_{ij} - 1}{\epsilon_{ij} + 2} - \frac{n_{Dij}^2 - 1}{n_{Dij}^2 + 2} \right) = \left(\frac{\epsilon_i - 1}{\epsilon_i + 2} - \frac{n_{Di}^2 - 1}{n_{Di}^2 + 2} \right) \frac{V_i}{V_{ij}} + \frac{N}{3\epsilon_0} \frac{\mu_s^2}{3kT} \frac{f_j}{V_{ij}}$$

$f_j/V_{ij} = c_j$ is the molar concentration per unit volume. Since $V_i/V_{ij} \rightarrow 1$ at infinite dilution, the above equation becomes :

$$\left(\frac{\epsilon_{ij} - 1}{\epsilon_{ij} + 2} - \frac{n_{Dij}^2 - 1}{n_{Dij}^2 + 2} \right) = \left(\frac{\epsilon_i - 1}{\epsilon_i + 2} - \frac{n_{Di}^2 - 1}{n_{Di}^2 + 2} \right) + \frac{N\mu_s^2}{9\epsilon_0 kT} c_j \quad (1.77)$$

which is Debye equation for polar-nonpolar liquid mixture. At extremely low concentration of $c_j = 0$ Eq. (1.77) is used to compute μ_s . The disadvantage of this method is that it could not be applied for a concentrated solution. The different parameters like ϵ_{ij} , n_{Dij} , ρ_{ij} were to be determined at infinite dilution by extrapolation technique.

1.15. Extrapolation Technique and Guggenheim Equation

The extrapolation technique was usually made to smooth out the curve through the experimentally measured relaxation parameters. The errors involved in the measurement were estimated by Hedestrand [39], Cohen Henrique [40] and others [41, 42]. They suggested various types of extrapolation to obtain the desired parameters including polarisation at infinite dilution. But all the methods are not free from inherent difficulties to locate the exact magnitudes of the quantities required to be measured. The difficulty arises to get $(\delta\rho_{ij}/\delta f_j)f_j \rightarrow 0$ and $(\delta n_{Dij}^2/\delta f_j)f_j \rightarrow 0$ from the graphical extrapolation. Böttcher [42], however, compared the results obtained from different extrapolation methods to compute μ_s . A marked difference was, however, noticed in a solution of phenol in benzene to calculate μ_s by different extrapolation techniques.

Higasi [43] put forward an empirical formula for the easy determination of μ_s :

$$\mu_s = \beta (\Delta\varepsilon/f_j)^{1/2} \quad (1.78)$$

where the constant β depends entirely on the solvents used. As for example $\beta = (0.90 \pm 0.10) D$ in C_6H_6 . Krishna and Srivastava [44] used the following relation:

$$\mu_s = \beta (d\varepsilon_{ij}/df_j)^{1/2} \quad (1.79)$$

to compute μ_s of some polar solutes in liquid state. Here $(d\varepsilon_{ij}/df_j)$ is the slope of ε_{ij} vs. f_j curve. It is observed that Eq. (1.79) is valid in the straight part of $\varepsilon_{ij}-f_j$ curve. Here, $\beta = 0.828 D$.

Again, Srivastava and Chandra [45] obtained different values of β for different solutes. A question, therefore arises for the validity of Higasi's method. Jaiprakash [46], however, showed that Eq (1.79) is a special case of Eq (1.77) when $\varepsilon_{ij} \simeq 1$. But no such polar-nonpolar liquid mixture is available for which $\varepsilon_{ij} \simeq 1$. Higasi's method is thus not a universal one to locate μ_s at all concentrations.

Guggenheim [47] however, introduced fictitious atomic polarisability γ'_{ja} of the polar molecule. It was, further, assumed that γ'_{ja} is equal to atomic polarisability γ_{ja} so that they cancel each other to make the solution free from atomic polarisation. From Eq. (1.77) a curve might be drawn with $3(\epsilon_{ij} - n_{Dij}^2) / (\epsilon_{ij} + 2)(n_{Dij}^2 + 2)$ against c_j . The slope of the curve was used to obtain μ_s . Writing $\Delta = (\epsilon_{ij} - n_{Dij}^2) - (\epsilon_i - n_{Di}^2)$ in Eq. (1.77) one obtains.

$$\mu_s^2 = \frac{9\epsilon_0 kT}{N} \cdot \frac{3}{(\epsilon_i + 2)(n_{Di}^2 + 2)} \cdot \frac{\Delta}{c_j} \quad (1.80)$$

taking $\epsilon_i = n_{Di}^2$ [48,49]. Smith [50], however, introduced the concept of weight fraction w_j in place of c_j

$$c_j = \rho_{ij} w_j / M_j \quad (1.81)$$

Guggenheim [51] also accepted Eq (1.81) to formulate the equation

$$\mu_s^2 = \frac{9\epsilon_0 kT}{N} \cdot \frac{3}{(\epsilon_i + 2)^2} \cdot \frac{M_j}{\rho_i} \left(-\frac{\Delta}{w_j} \right) \quad (1.82)$$

where

$$\frac{\Delta}{w_j} = \left[\left(\frac{\delta\epsilon_{ij}}{\delta w_j} \right) w_j \rightarrow 0 - 2n_{Di} \left(\frac{\delta n_{Di}^2}{\delta w_j} \right) w_j \rightarrow 0 \right] \quad (1.83)$$

In Eq (1.82), M_j is the molecular weight of a polar liquid and ρ_i is the density of the nonpolar solvent. The $\epsilon_{ij} - w_j$ and $n_{Di}^2 - w_j$ curves are extrapolated at $w_j \rightarrow 0$ to estimate μ_s from Eqs (1.82) and (1.83). Hence a large number of data of ϵ_{ij} and n_{Dij}^2 for different w_j 's for a given solute-solvent mixture were experimentally measured. Jaiprakash [46] later on deduced

$$\mu_s^2 = \frac{27\epsilon_0 M_j kT}{N\rho_i} \left(-\frac{\delta X_{ij}}{\delta w_j} \right) w_j \rightarrow 0 \quad (1.84)$$

where

$$\left(\frac{\delta X_{ij}}{\delta w_j}\right)_{w_j \rightarrow 0} = \left[\frac{1}{(\epsilon_i + 2)^2} \left(\frac{\delta \epsilon_{ij}}{\delta w_j}\right)_{w_j \rightarrow 0} - \frac{2n_{Di}}{(n_{Di}^2 + 2)} \left(\frac{\delta n_{Di}}{\delta w_j}\right)_{w_j \rightarrow 0} \right]$$

from Eq (1.80) to obtain μ_s . The Eq (1.84) reduces to Guggenheim equation Eq. (1.82) when $\epsilon_i = n_{Di}^2$. Guggenheim equation is thus a special case of Debye equation (1.77). The Eq (1.84) is valid for low concentrated solution of polar liquid of low μ_s in non-polar solvent. The evaluation of μ_s depends on the theory of extrapolation of ϵ_{ij} , n_{Dij} , ρ_{ij} , of polar-nonpolar liquid mixture with w_j 's of solute at any given temperature. For trimethyl amine in benzene Lefevre and Smyth [41] applied the technique of ratio of finite differences, and Guggenheim [51], on the other hand, used his personal judgement on the measured parameters against w_j 's to obtain μ_s 's of 0.91D and 0.83D respectively. Such affairs often put the experimentalists to choose as to what method of extrapolation is needed to get accurate μ_s of a dipolar liquid in a given solvent.

Recently, Ghosh et al [52], extended the theory of polar-nonpolar liquid mixture based on Debye and Smyth model as Guggenheim equation is derived from Debye's equation. This theoretical development has been described in Chapter 2.

1.16. Gopalakrishna's Method to Estimate τ and μ

Debyes' equation (Eq (1.30) for complex dielectric constant ϵ_{ij}^* of a polar non-polar liquid mixture is :

$$\frac{\epsilon_{ij}^* - 1}{\epsilon_{ij}^* + 2} = \frac{\epsilon_{\infty ij} - 1}{\epsilon_{\infty ij} + 2} + \frac{n\mu^2}{9\epsilon_0 kT} \frac{1}{1 + j\omega\tau} \quad (1.85)$$

Equating the real and imaginary parts from both sides of Eq (1.85) one gets :

$$\frac{\epsilon_{ij}''^2 + \epsilon_{ij}' + \epsilon_{ij}''^2 - 2}{(\epsilon_{ij}' + 2)^2 + \epsilon_{ij}''^2} = \frac{\epsilon_{\infty ij} - 1}{\epsilon_{\infty ij} + 2} + \frac{n\mu^2}{9\epsilon_0 kT} \frac{1}{1 + \omega^2\tau^2} \quad (1.86)$$

$$\frac{3\varepsilon_{ij}''}{(\varepsilon_{ij}' + 2)^2 + \varepsilon_{ij}''^2} = \frac{n\mu^2}{9\varepsilon_0 kT} \cdot \frac{\omega\tau}{1 + \omega^2\tau^2} \quad (1.87)$$

writing $(\varepsilon_{\infty ij} - 1) / (\varepsilon_{\infty ij} + 2) = P$, $\frac{\varepsilon_{ij}''^2 + \varepsilon_{ij}' + \varepsilon_{ij}''^2 - 2}{(\varepsilon_{ij}' + 2)^2 + \varepsilon_{ij}''^2} = x$

and $3\varepsilon_{ij}'' / \{(\varepsilon_{ij}' + 2)^2 + \varepsilon_{ij}''^2\} = y$, the above Eqs (1.86) and (1.87) can be put into a form :

$$x = P + \left(\frac{1}{\omega\tau}\right) \cdot y \quad (1.88)$$

which is a straight line between x and y whose slope $(1/\omega\tau)$ may be used [53] to get τ of a dipolar solute.

Since $n = \frac{N\rho_{ij}}{M_j} w_j$, the number of dipoles per unit volume, Eq (1.86) reduces to

$$x = P + K\rho_{ij} \cdot w_j \quad (1.89)$$

where $K = \frac{N\mu^2}{9\varepsilon_0 kTM_j} \cdot \frac{1}{1 + \omega^2\tau^2}$.

The Eq (1.89) is evidently a linear equation between the variables x and w_j . The slope $K\rho_{ij}$ may be used [53] to estimate μ_j of a dipolar liquid molecule under hf electric field.

1.17. Eyring's Rate Theory

According to Eyring [54] the dipole rotation is like a chemical rate process in which the dipole rotates from one equilibrium position to the other. The process requires an activation energy sufficient to overcome the energy barrier separating two mean equilibrium positions. The average time required for single rotation involved is known as relaxation time τ given by :

$$\tau = \frac{h}{kT} e^{(\Delta F_{\tau}/RT)} \quad (1.90)$$

where ΔF_{τ} is the free energy of activation. From thermodynamics one gets

$$\Delta F_{\tau} = \Delta H_{\tau} - T\Delta S_{\tau} \quad (1.91)$$

where ΔH_{τ} and ΔS_{τ} are enthalpy and entropy of activation due to dielectric relaxation. So from Eqs (1.90) and (1.91) it is shown that

$$\ln(\tau T) = \ln A' + \frac{\Delta H_{\tau}}{R} \cdot \frac{1}{T} \quad (1.92)$$

where $A' = \frac{h}{k} e^{(-\Delta S_{\tau}/R)}$ (1.93)

(h/k) is the ratio of Plancks' constant to Boltzmann constant and R is gramme molar gas constant. ΔH_{τ} is obtained from the slope of linear equation of $\ln(\tau T)$ against $1/T$. With ΔH_{τ} and known τ , ΔS_{τ} and ΔF_{τ} could, however, be estimated from Eqs (1.93) and (1.91) respectively.

Like dielectric relaxation, the viscous flow of the liquid may be considered as a rate process. Viscous flow is, however, involved with the translational as well as rotational motions of the molecules, with an activation energy to pass over a potential barrier. We can write from Eyring's [54] rate theory :

$$\eta = \frac{hV}{N} e^{(\Delta F_{\eta}/RT)} \quad (1.94)$$

where η and V are the coefficient of viscosity and the molar volume of the liquid respectively. ΔF_{η} , the free energy of activation for viscous flow is :

$$\Delta F_{\eta} = \Delta H_{\eta} - T\Delta S_{\eta} \quad (1.95)$$

The Eq. (1.94) with the help of Eq. (1.95) becomes

$$\eta = \frac{hV}{N} e^{-(\Delta S_{\eta}/R)} \cdot e^{(\Delta H_{\eta}/RT)} \quad (1.96)$$

$$\ln\eta = \ln B + \frac{\Delta H_{\eta}}{R} \cdot \frac{1}{T} \quad (1.97)$$

ΔH_{η} can be obtained from the slope of the linear variation of $\ln\eta$ with $1/T$ of Eq.(1.97). The corresponding ΔS_{η} and ΔF_{η} from Eqs. (1.96) and (1.95) could readily be obtained.

The approximate linearity of $\ln(\tau T)$ against $1/T$ of Eq (1.92) has been used in this thesis in many chapters to estimate the thermodynamic energy parameters of dipolar solutes in nonpolar solvents. Such study provides the information about molecular association in addition to stability or unstability of the molecules.

1.18. Relaxation Time and its Relationship with Viscosity

The torque acting on a dipolar molecule in a nonpolar solvent under electric field [1] is counter balanced by frictional force. This force is proportional to angular velocity of the polar molecule. The torque is given by:

$$M = \xi \frac{dv}{dt} \quad (1.98)$$

where ξ is a frictional coefficient depending on the surrounding medium.

The dipole may be assumed [1] a sphere of radius 'a' immersed in a medium of internal viscosity η_{int} . The frictional coefficient is according to Stokes' formula :

$$\xi = 8\pi\eta_{int} a^3 \quad (1.99)$$

The dipole in liquid state behaves as Brownian particle obeying a relation between τ and ξ :

$$\tau = \frac{\xi}{2kT} \quad (1.100)$$

From Eqs (1.99) and (1.100) it leads

$$\tau = \frac{4\pi a^3}{kT} \cdot \eta_{int} \quad (1.101)$$

Debye [1] further considered the macroscopic viscosity η in place of η_{int} of the medium. So Eq (1.101) becomes :

$$\tau = \frac{4\pi a^3}{kT} \cdot \eta \quad (1.102)$$

From measured τ and η at a certain temperature T , the size of the rotating unit may be estimated from Eq. (1.102) to arrive at the structural concept of a dipolar liquid molecule.

The Eq (1.102) was modified by Perrin [55] for ellipsoidal dipolar molecule. Thus μ has components μ_a , μ_b and μ_c along three principal axes a , b , c of the ellipsoid. The Eq (1.17) becomes.

$$\frac{\epsilon_r^* - 1}{\epsilon_r^* + 2} \cdot \frac{M}{\rho} = \frac{N}{3\epsilon_0} \left[\alpha + \frac{1}{3kT} \left\{ \frac{\mu_a^2}{1+j\omega\tau_a} + \frac{\mu_b^2}{1+j\omega\tau_b} + \frac{\mu_c^2}{1+j\omega\tau_c} \right\} \right] \quad (1.103)$$

where τ_a , τ_b , τ_c are the relaxation times of the dipole along the three axes. Moreover, the dipole may act along one of the ellipsoidal axes. In such case τ is given by Fischer and Frank [56].

$$\tau = \frac{4\pi abcf}{kT} \eta_{int} \quad (1.104)$$

where a , b , c are the semi major axes of the ellipsoid and f is the structure factor.

1.19. Dielectric Relaxation of Polar Liquid Molecules in Nonpolar Solvent under Radio Frequency Electric Field

Under a radio frequency (rf) electric field $E = E_0 e^{j\omega t}$ heat developed in a polar-nonpolar liquid mixture is due to combined effect of dielectric loss and joule heating. But rf conductivity often provides an information of conduction current in polar dielectrics.

Sen and Ghosh [57,58] subsequently put forward a theory of rf conductivity based on the assumption of existence of free ions in polar dielectrics. The conduction current due to free ions plays a prominent role to yield conductivity rather than the displacement current as suggested by Murphy and Morgan [37] in hf electric field. From Murphy - Morgan [37] relation hf conductivity σ' is written as :

$$\sigma' = \frac{1}{4\pi} \frac{\epsilon_s - \epsilon_\infty}{1 + \omega^2 \tau^2} \cdot \omega^2 \tau \quad (1.105)$$

using $\tau = 4\pi\eta a^3 / kT$ from Eq (1.102) we have :

$$\sigma' = \frac{\epsilon_s - \epsilon_\infty}{kT} \cdot \omega^2 a^3 \eta \quad (1.106)$$

The factors $(\epsilon_s - \epsilon_\infty)$ and η/T decrease with temperature and σ' , therefore, should decrease with temperature. But the experimental results show that the rf conductivity, increases with temperature like electrolyte. The conductivity in electrolytes is mainly due to free ions and Walden's rule is valid. This rule states that the product of equivalent conductance at infinite dilution and the viscosity of the solvent is approximately constant. A similar relation is observed in case of polar dielectric liquids where $\sigma' \eta = \text{constant}$.

1.20. A Brief Review of the Previous Works

From 1850 to 1904, a large number of workers [12,13, 59-61] inferred the structural aspects of dipolar gases and liquids from dielectric polarisation study. The observations are found in good agreement of gas kinetic values.

The radii of alcohols, ketones and glycerins were determined by Mizushima [62,63] from the Debye theory. The radii were found to be smaller than the gas kinetic value maintaining the same order. Strathan [64] estimated μ for methyl, ethyl and amyl alcohols in benzene from the intercepts of molar volume against concentration curve. μ 's were found to be independent of temperature in accordance with Debye theory. Debye [1] explained the anomalous dispersion pointed out by Drude [61], under rf electric field by the polarity of the molecules. ϵ'' 's under 4.3 meter wavelength electric field were measured by Fischer and Frank [56] to estimate τ_j of aromatic halides. The shorter τ_j 's were claimed for the rotation of $\text{CH}_2 - \text{X}$ group around their bond ring. But the theory could not explain the behaviour of alcohols for the strong interaction of $-\text{OH}$ groups due to formation of hydrogen bonding. Goss [65] analysed the dielectric polarisation of some polar-nonpolar liquid mixtures to show the solvent effect under anisotropic electric field for non-spherical polar molecules. The study further showed the induction effect related to the dielectric constant of the liquids.

Onsager [66], Plumley [67] and Pao [68] interpreted the origin of conduction in dielectric liquids. Even the purest hydrocarbons such as hexane contain a small number of ions. Ryhel [69] and Eck [70] showed that ionic conduction occurs due to existence of ionic cluster in the liquids. Whiffen and Thomson [71] obtained τ_j of toluene, o-xylene, p-cyanine to predict the size of the molecules. Jackson and Powles [72] estimated τ_j of polar molecules in C_6H_6 and paraffin. The observation showed that τ_j 's depends on the viscosity of solvents. Schallamach [73] studied the relaxation phenomena in polar molecules under rf electric field. The molecular rearrangement takes place in liquid state under single relaxation process. Mecke and Reuter [74] measured

permittivities of normal alcohols, and phenols in C_6H_6 , CCl_4 and cyclohexane at $20^\circ C$ and $40^\circ C$. The molecular associations are inferred from their measured μ 's. The dielectric absorption measurement of aliphatic chlorides and alcohols were performed by Kremmling [75]. It was found difficult to sort out the effects of molecular association and H-bond formation onto change in shape of molecules. Further, the internal rotation, multiple relaxation times etc. could, however, be predicted.

Jaffe and Lemay [76] concluded that dielectric liquids gave conduction current under breakdown voltage. The presence of positive ions are noticed by Green [77] in dielectric liquids due to dissociation of impurity molecules by external cosmic rays. τ 's were found by Curties et al [78] in different solutions and in pure liquids although they have same viscosity. τ_j 's were estimated by Poley [79] from ϵ'' 's measurement for monosubstituted benzenes. The increase of τ_j occurs with molecular size. Müller [80], however, calculated the low molecular radii in comparison to other methods. Dielectric measurements on pure normal propyl to decyl alcohols were carried out by Garg and Smyth [81] to show three different τ_j 's for three distinct dispersive regions. The larger τ_j 's are associated with polymeric clusters formation by the strong H-bonding between -OH groups. The intermediate τ_j 's were attributed to the rotation of free alcohol molecules. A significant contribution to obtain τ_j and μ_j of polar liquid in nonpolar solvent under GHz electric field was made by Gopalakrishna [53]. The main advantage of this method is to know the density of the pure solvent. Schellman [82] studied the associations in saturated dielectric liquids. Srivastava and Vershri [83] explained the variation of ϵ' of binary polar mixtures with concentration c and temperature TK by :

$$\epsilon' = \left(1 + \frac{m}{T}\right) + \left(p + \frac{q}{T^{1/2}}\right) c + zc^2$$

where p , q , l , m and z are constants. The relation was tested for mixtures of water-methyl and water-butyl alcohols.

Hart and Mungali [84] observed the conduction current in chlorobenzene after distillation. Higasi et al [85] analysed the experimental data of n-alkyl bromide in liquid state in terms of distribution of τ 's between two Fröhlich's [7] limiting τ 's. The lower τ_j signifies the internal rotation of $-\text{CH}_2\text{Br}$ group while larger τ 's for whole molecular rotation. Bergmann et al [29] estimated τ_1 (smaller) and τ_2 (larger) by employing a graphical method in complex plane for diphenyl ether, anisol, and o-dimethoxy benzene. The results are interpreted as the intramolecular and molecular rotations of polar molecules respectively. Krishnaji and Mansingh [86] studied the dielectric relaxation process of alkyl cyanides and alkythiols. The τ_j 's increase with the size of the molecules. Froster [87] explained the conduction in aliphatic hydrocarbons by the presence of impurities of trace polar or trapped electrons at the electrode surfaces. Experimental evidence thus showed the electronic nature of conduction in unsaturated hydrocarbons. Sinha et al [88,89] predicted the temperature dependence of τ and μ of some polar molecules in nonpolar solvent. The viscosity dependence of τ_j on T is $\tau_j T / \eta^\gamma = \text{constant}$ is, however, predicted. γ is the ratio of enthalpies of activation of dielectric relaxation and viscous flow. Barbenza [90] studied the dielectric behaviour of methyl alcohol in the temperature range of 5°C to 55°C under the electric fields of wavelengths 5cm to 15cm. The results were explained by single relaxation process. The measurements showed activation energy of 3.4 K cal / mole from rate process [54]. Adamczewski and Jachym [91] concluded that conductivity of organic liquids is a function of temperature. Very low values of σ were also found in nonpolar liquids. Jaiprakash [92] estimated τ_j of five almost spherical polar molecules in nonpolar solvent in good agreement with Gopalakrishna's method [53]. Bhattacharyya et al [30] analysed phenetole, aniline and orthochloro aniline in terms of molecular and intramolecular τ_2 and τ_1 from the equation of Bergmann et al. [29].

Non-rigid molecules having two τ 's and average τ could, however, be obtained by Higasi et al [31] based on single frequency measurement technique.

A crude estimation of τ_1 and τ_2 can be had with a suitable equation derived from Debye model. The existence of natural charge carriers in liquids of two kinds of mobilities μ^+ and μ^- was, however, tested by Loheneysen and Nageral [93]. The direct evidence of ionic conduction in polar dielectrics was found by Gaspared and Gosse [94] when the electrodes were membraned by teflon.

Crossley et al [95] and Glasser et al [96] measured concentration variation of ϵ' and ϵ'' of aliphatic alcohols in n-heptane at 25°C under hf electric fields of different wave lengths. The lower τ_j 's are due to rotation of -OH groups, the intermediate τ_j 's for the monomer or small multimers formed by polar chain, while the shortest τ_j 's in low frequency are associated with H-bonded structure. The ϵ' and ϵ'' of methanol, ethanol, 2-propanol, 1-butanol, 3-methyl-1 butanol in C_6H_6 for different w_j under X-band electric field was measured by Purohit and Sharma [97]. The marked increase of $\tan \delta$ curves against w_j 's in the region $0.03 \leq w_j \leq 0.04$ showed the formation of dimers except for 1-butanol. A similar observation on $\tan \delta$ vs. w_j curve, was, however, carried out by Vyas and Vashisth [98] in case of four aliphatic alcohols and their binary mixtures and the mixtures of alcohols with DMF and 2-fluoroaniline in benzene for different w_j under 3 cm wave length electric field at 30°C. The alcohols + DMF mixtures showed complex formations at a very low concentration. The study of alcohol + 2 fluoro-aniline, however, indicates dissociation effects.

The relaxation parameters of Trifluoroethanol and Trifluoro acetic acid in dilute benzene solution was studied by Purohit et al [99]. The results could, however, be explained by strong H-bonding in the compounds. Hydrogen bonding plays a vital role in n-butylamine - n-butanol and in n-propylamine - n propanol mixtures as observed by Tripathy et al [100]. A number of workers [101-106] estimated τ from the number density 'n' of free ions, radius 'a' of rotating units, activation energy ΔE_τ and thermodynamic energy parameters ΔH_τ , ΔS_τ , ΔF_τ for some straight chain alcohols, anilines, benzyl chloride, acetone under rf electric field at different temperatures. τ_j 's are observed to increase with the number of

C-atom of dipolar molecules. ΔE_τ increases with the size of the molecules. The ratio of activation energies for electronic conduction and viscous flow is greater than unity for associative liquids while reverse is true for non associative liquids. The different ΔF_τ signifies the breaking of the cluster of molecules. It is greatly affected by the addition of impurity such as water. The relaxation parameters from the rf conductivity σ has been used to study the structure of liquids. Other group of workers, [107-111] measured relative permittivities ϵ' and ϵ'' of some substituted toluidines, para compounds, diphenylene oxide, chloral and ethyl trichloro acetate in benzene, dioxane, n-heptane at various w_j 's and $t^\circ\text{C}$ under nearly 3cm wavelength electric field to estimate τ_j , μ_j and thermodynamic energy parameters. The observed results were explained in terms of molecular associations of the polar liquid molecules. Rajyam et al [112] studied the dielectric dispersion of glycerol and diethylene glycol under rf, mw and uhf electric fields at 80°C and confirmed the Cole-Davidson type of dispersion [20,21]. Mulechi et al [113] observed the self association of tertiary butyl alcohol and developed a method for simultaneous determination of three independent values of free energy of self association from experimental data.

Acharyya and Chatterjee [114] and Acharyya et al [115] estimated relaxation parameters τ_j , μ_j , ΔH_τ , ΔS_τ , ΔF_τ of some interesting polar liquid molecules in C_6H_6 and CCl_4 . High concentration σ data of a polar-nonpolar liquid mixture is liable to yield μ_j of dimer formation. σ in low concentration region behaves linearly with w_j and gives μ_j due to monomer formation. They also estimated μ_{theo} 's to study the structural conformations. Agarwal [116] measured ϵ' and ϵ'' of n-butyl chloride, chlorobenzene and tertiary butyl alcohol in C_6H_6 at 32°C under 9.96 GHz electric field to estimate τ_j . It is observed that τ_j is influenced by structural configuration in the following manner :

$$\tau_{\text{linear}} > \tau_{\text{planer}} > \tau_{\text{spherical}}$$

Madan [117] studied the dielectric absorption of thiophene, acetone, benzophenone and their mixtures in mw electric field over a wide range of

temperatures. The experimental and theoretical τ_j 's were found to agree within the experimental error. Gandhi and Sharma [118] determined τ_0 , τ_1 and τ_2 , distribution parameters of isobutyl - methacrylate and allyl-methacrylate and their mixtures in C_6H_6 . The observed results reveal the intramolecular and molecular rotations.

Guided by the work of Acharyya et al [115], Murthy et al [38] added a new dimension in the theoretical formulations by which simultaneous determination of τ_j and μ_j of a polar liquid in nonpolar solvent can be made. Makosz [119] calculated μ of some ellipsoidal shaped dipolar liquids in nonpolar solvents at 25°C from the formula derived from Onsager's equation. Sharma and Sharma [120], Sharma et al [121] estimated ϵ' and ϵ'' of dilute solutions of dimethyl sulphoxide (DMSO) in C_6H_6 , CCl_4 and of DMF + DMSO mixtures in C_6H_6 in temperature range of 25°C to 40°C under 9.174 GHz electric field to estimate τ_j , μ_j , ΔH_τ , ΔS_τ , ΔF_τ of dielectric relaxation and ΔH_η , ΔS_η and ΔF_η for viscous flow. The monomer structure i.e. the solute-solvent association of DMSO in solutions have been inferred. The solute-solute formation between DMF and DMSO increases with the enrichment of DMF in DMSO to a maximum value around 17 mole % of DMSO at all temperatures. A similar study on acetophenone and DMSO and their mixtures in C_6H_6 was done by Singh and Sharma [122] under 9.33 GHz electric field in the temperature range of 20°C to 40°C. Non linear behaviour of τ reveals the presence of solute-solvent and solute-solute molecular associations.

Saha and Acharyya [123] estimated the same parameters of NMA, DMF, DMA in C_6H_6 , dioxane and CCl_4 by using the measured values of ϵ' and ϵ'' [124-128] in a newly developed methodology. The ternary mixtures of DMF + CH_3OH , DMF + acetonitrile, DMF + acetone in C_6H_6 were studied by them [129]. Higher and lower values of μ_j 's arise for the monomer or dimer formations. The high or low concentration σ_{ij} 's with w_j 's, although σ_{ij} 's behave linearly with lower w_j 's yield μ_j 's for dimer or monomer formations. μ_{jk} 's of polar-polar

mixture (jk) in solutions decreases with $t^{\circ}\text{C}$ which is supported by solute-solute molecular association. μ_{theo} 's from the available bond angles and bond moments of substituent polar groups attached to the parent molecules were estimated in agreement with measured hf μ_j 's to shed much light on the inductive and mesomeric moments of polar groups. Puranik et al. [130] measured static ϵ_0 and hf dielectric constants ϵ_{∞} and activation energies of ethanol and ethelene glycol (EG) from 10 MHz to 10 GHz at different temperatures. Activation energy of EG is found to be larger than that of ethanol indicating molecular association due to strong H-bonding in polyhydric alcohols.

Saha et al [32] used the concentration variation of the measured ϵ'_{ij} , ϵ''_{ij} , ϵ_{oiij} , $\epsilon_{\infty ij} = n_{\text{Dij}}^2$ of some disubstituted anilines and benzenes in C_6H_6 and CCl_4 under nearly 3 cm wave length electric field at 35°C [131-133] to estimate τ_1 , τ_2 and μ_1 , μ_2 due to rotation of flexible polar groups attached to the parent molecules and whole molecules themselves. The results are explained on the basis of polarity, size of the molecules and solvent environment around the solute molecules. Difference between μ_{theo} 's and experimental μ 's might be due to non consideration of inductive and mesomeric effects of the substituent polar groups of the molecules. The values of ϵ'_{ij} , ϵ''_{ij} , ϵ_{oiij} and $\epsilon_{\infty ij}$ measured by Srivastava and Chandra [134] of monosubstituted anilines at different ω_j 's at 35°C in C_6H_6 under electric field frequencies of 2.02, 3.86 and 22.06 GHz were used by Sit et al [33] to detect the mono or double relaxation phenomena in them. Elsayed et al [135] estimated the ΔH_{τ} , ΔS_{τ} , ΔF_{τ} from the temperature variation of τ_j 's of solid and liquid phase of Ag Sb Te₂ under 10^6 Hz electric field. The strength of dielectric dispersion $\Delta\epsilon'$ was observed to be proportional to number of dipoles per unit volume. τ_j 's decrease with temperature due to increase of thermal agitations to weaken the intermolecular forces. The dielectric relaxation studies of four pure nicotines and their quartarnary mixtures were made by Jangid et al [136] to draw the sufficient information about intramolecular and intermolecular interactions of solute-solvent (monomer) and solute-solute (dimer) formations. ϵ' , ϵ'' and $\tan \delta$ of CH_3OH , methyl acetate, methyl formate,

ethyl formate and acetone in C_6H_6 under 10.3 GHz electric field measured at 308 K by Varadarajan and Rajagopal [137] established the rotation of — OH group about the whole molecule. They [138] observed dipole-dipole interaction and molecular association of five monoalcohols in benzene.

The measured ϵ' , ϵ'' , n_D^2 of CH_3OH + ketone, methanol + nitrile under 5.70, 9.70 and 32.97 GHz electric fields are used [139] to obtain τ and μ . The molecular shapes, sizes and structures are explained by H-bonding. Vyas and Rana [140] measured ϵ' and ϵ'' of chlorobenzene, nitrobenzene, orthochloro aniline and their mixtures under 9.1 GHz, 10 KHz and optical frequency at 30°C to estimate τ and thermodynamic energy parameters. The study indicates solute-solvent and solute-solute molecular associations. Sengwa and Kaur [141] determined Kirkwood correlation factor g , average τ_0 , ΔF_{τ_0} of orthohydroxybenzaldehyde in C_6H_6 at 10°, 20°, 30°C under 9.83 GHz electric field. Both inter and intramolecular associations about their respective bonds decreases by — CHO and — OH group rotations. The high τ_2 corresponds to group rotation. Molecular associations hinder the intramolecular rotations of — CHO and — OH groups in this compound to affect τ . Temperature variation of dielectric relaxation studies of ethylene glycol (EG) — water (H_2O) mixture were carried out by Saha and Ghosh [142] under 1 MHz electric field. High values of τ_{jk} of EG — H_2O mixture is inferred from polymeric cluster formation by molecular association. Dash et al [143] investigated micro-level molecular dynamics of 1-propanol, 1-butanol, 1-octanol, methyl isobutyl ketones etc in terms of complex formations by H-bonding between two polar molecules in nonpolar solvent. The increase in $\rightarrow O-H$ bond length due to enhancement of the bond moment $\Delta\mu$ may be analysed. The temperature variation of τ_j 's were used by Thakur and Sharma [144] to measure the thermodynamic energy parameters of dielectric relaxation and viscous flow of acetonitrile and DMF in C_6H_6 under 9.40 GHz electric field in order to arrive at the solute-solvent molecular associations.

References

- [1] P. Debye, "*Polar Molecules*" The Chemical Catalogue Company, Inc. (1929)
- [2] L. Onsager, *J Amer Chem. Soc* **58** (1936) 1486.
- [3] J G Kirkwood, *J Amer. Phys* **7** (1939) 911.
- [4] CFJ Bottcher, *Physica* **6** (1939) 59.
- [5] H Fröhlich, *Trans Faraday Soc* **44** (1948) 238.
- [6] J G Powles, *Trans Faraday Soc.* **51** (1955) 377.
- [7] H Fröhlich, "*Theory of Dielectrics*" (Oxford University Press : Oxford 1949).
- [8] C P Smyth "*Dielectric Behaviour and Structure*" (New York : McGraw Hill 1955).
- [9] Nora E. Hill, W.E. Vaughan, A H Price and M. Davies. "*Dielectric Properties and Molecular Behaviour*" (Van Nostrand Reinhold Company : London 1969).
- [10] A K Jonscher, *Physics of Dielectric Solids*, Invited papers edited by CHL Goodman (Canterbury 1980).
- [11] H A Lorentz "*Theory of electrons*" *Ann Physik* **9** (1880) 641 Comm. Acad Amsterdam 1880.
- [12] O F Mosotti *Mem. di Mathem e di fisica in Modena* **24** II (1850) 49.
- [13] R Clausius "*Die mechanische warmetheorie* Vol. II p. 62 Vieweg 1879.
- [14] L Lorentz *Ann. Physik* **11** (1880) 70; *Vidensk, Selsk Skrifter* **8** (1869)205; **10** (1875)485.

- [15] P Langevin *J Phys* (4) **4** (1905) 678; *Ann. Chim. Phys* (8) **5** (1950) 70.
- [16] H Fröhlich and R Sack *Proc. Roy Soc. (London)* **182A** (1944) 388.
- [17] S Acharyya, A K Chatterjee, P Acharyya and I L Saha *Indian J Phys.* **56B** (1982) 291.
- [18] *McGraw Hill Encyclopedia of Science and Technology*, **13** (1997), 269.
- [19] K S Cole and R H Cole *J Chem Phys.* **9** (1941) 341.
- [20] D W Davidson and R H Cole, *J Chem Phys* **18** (1951) 1417.
- [21] D W Davidson and R H Cole, *J Chem Phys* **19** (1951) 1484.
- [22] J G Powles, *J Mol. Liquids* **56** (1993) 35.
- [23] K. W. Yagner *Ann Phys* **40** (1913) 814.
- [24] W.A. Yager. *Physics* **7** (1936) 434.
- [25] J G Kirkwood and R M Fouss *J Chem Phys* **9** (1941) 329.
- [26] R M Fouss and J W Kirkwood, *J Amer. Chem. Soc.* **63** (1941) 385.
- [27] A Matsumoto and K Higasi *J Chem. Phys.* **36** (1962) 1776.
- [28] A Budo *Phys. Z* **39** (1938) 706.
- [29] K Bergmann, D M Roberti and C P Smyth, *J. Phys. Chem.* **64** (1960) 665.
- [30] J Bhattacharyya, A Hasan, S. B. Roy and G. S. Kastha, *J. Phys. Soc. Japan* **28** (1970) 204.
- [31] K Higasi, Y. Koga and M. Nakamura, *Bull Chem. Soc. Japan* **44** (1971) 988.
- [32] U Saha, S K. Sit, R C Basak and S Acharyya *J Phys. D.: Appl. Phys* **27** (1994) 596.

- [33] S K Sit, R C Basak, U Saha and S Acharyya *J Phys. D : Appl. Phys* **27** (1994) 2194.
- [34] S K Sit and S Acharyya, *Indian J Phys* **70B** (1996) 19.
- [35] S K Sit, N Ghosh and S Acharyya *Indian J Pure & Appl. Phys* **35** (1997) 329.
- [36] N Ghosh S K Sit, A K Bothra and S Acharyya, *J Phys. D : Appl. Phys.* (U.K.) **34** (2001) 379.
- [37] F J Murphy and S O Morgan, *Bell.Syst. Tech. J* **18** (1939) 502.
- [38] M B R Murthy, R L Patil and D K Deshpande *Indian J Phys.* **63B** (1989) 491.
- [39] G Z Hedestrand, *J Phys. Chem* **B2** (1929) 428.
- [40] P Cohen Henrique *Ph. D Dissertation* 1935.
- [41] R J W Le Fevre and C P Smyth, *Trans. Faraday Soc* **46** (1950) 812.
- [42] C F J Böttcher "*Theory of Electric Polarisation*" Elsevier Publishing Company New York 1952.
- [43] K Higasi, *Bull. Inst. Phys. Chem. Res. Tokyo* **22** (1943) 805.
- [44] B Krishna and K K Srivastava, *J Chem. Phys.* **27** (1957) 835.
- [45] S C Srivastava and P Chandra, *J Chem. Phys* **30** (1959) 816.
- [46] Jaiprakash *Indian J Pure & Appl. Phys* **11** (1973) 901.
- [47] E A Guggenheim, *Trans. Faraday Soc.* **45** (1949) 714.
- [48] J C Maxwell, *Treatise on Electricity* Vol II Oxford (1881).
- [49] J C Maxwell *Electricity and Magnetism* 3rd Edn P-452 Oxford (1892).
- [50] J W Smith *Trans Faraday Soc.* **46** (1950) 394.

- [51] E A Guggenheim, *Trans. Faraday, Soc.* **47** (1951) 573.
- [52] N Ghosh, A Karmakar, S K Sit and S Acharyya, *Indian J Pure & Appl. Phys.* **38** (2000) 574.
- [53]. K V Gopalakrishna *Trans. Faraday Soc.* **53** (1957) 767.
- [54] H Eyring, S Glasstone and K J Laidler '*The Theory of Rate Process*' (New York : Mc. GrawHill) 1941.
- [55] F Perrin *J Phys. radium* **5** (1931) 497.
- [56] E Fischer and F C Frank, *Physik Z* **40** (1939) 345.
- [57] S N Sen and R Ghosh, *J Phys. Soc. Japan* **33** (1972) 838.
- [58] S N Sen and R Ghosh, *Indian J Pure & Appl. Phys.* **10** (1972) 701.
- [59.] H A Lorentz *Arch. Nerl. Sci* **25** (1892) 363.
- [60] Von helmholtz, *Berlin Ber* (1892) 1093.
- [61] P Drude *Ann. Phys. LPZ* **14** (1904) 667.
- [62] S I Mizushima, *Phys Z* **28** (1926) 418.
- [63] S I Mizushima : *Sci Papers Inst. Phys. Chem. Research* (Tokyo) **5** (1927) 201.
- [64] J D Stranathan, *Phys. Rev* **91** (1928) 653.
- [65] F R Goss, *Chem. Soc. J* (1940) 752.
- [66] L J Onsager, *J Chem. Phys.* **2** (1934) 509.
- [67] H J Plumely, *Phys. Rev* **59** (1941) 200.
- [68] C S Pao, *Phys Rev* **64** (1943) 60.
- [69] F Ryhel, *Z Physik* **44** (1943) 89.

- [70] J L Eck, *Ann Phys* **4** (1949) 12.
- [71] D M Wiffen and H W Thompson, *Trans Faraday Soc.* **24** (1946) 114, 122.
- [72] W Jackson and J W Powles, *Trans Faraday Soc.* **24A** (1946) 101.
- [73] A Schallamach, *Trans. Faraday Soc.* **24A** (1946) 180.
- [74] R Mache and A Reuter, *Z Naturforsch* **4a** (1949) 368.
- [75] G Kremmling, *Z Naturforsch* **5a** (1950) 675.
- [76] G Jaffe and C Z Lemay, *J Chem. Phys* **21** (1953) 920.
- [77] W B Green, *J Appl. Phys.* **26** (1955) 1257.
- [78] A J Curties, P L McGreer, G B Rathmann and C P. Smyth. *J. Amer. Chem. Soc.* **74** (1952) 644.
- [79] J Ph. Poley, *J Appl. Sci. Res* **4** (1955) 337.
- [80] R C Müller and C P Smyth, *J Chem. Phys.* **24** (1956) 814.
- [81] S K Garg and C P Smyth, *J Chem. Phys.* **42** (1956) 1397.
- [82] J A Schellman, *J. Chem. Phys.* **26** (1957) 1225.
- [83] G P Srivastava and V P Vershri, *Physica* **23** (1957) 173.
- [84] J Hart and A G Mungali, *Trans. Am. Inst. Elec. Engrs:* **76** (1957) 1295.
- [85] K Higasi, K Bergmann, and C. P Smyth *J Phys. Chem.* **64** (1960) 880.
- [86] Krishnaji and A Mansingh, *J Chem. Phys.* **41** (1964) 827.
- [87] E O Foster, *Electro Chim Acta* **9** (1964) 1319.
- [88] B Sinha, S B Roy and G S Kastha *Indian J Phys* **40** (1966) 101.
- [89] B Sinha, S. B Roy and G.S. Kastha *Indian J Phys.* **41** (1967) 183.

- [90] G H Berbenza, *J Chem. Phys.* (France) **5** **65** (1968) 906.
- [91] I Adamczewski and B Jachym, *Acta. Phys. Polon* **34** (1968) 1015.
- [92] J Prakash, *Indian J Pure & Appl. Phys.* **8** (1970) 106.
- [93] H V Loheneysen and H Nageral *J Phys D : Appl. Phys* **4** (1971) 1718.
- [94] F Gaspared and J P Gosse, *Electro Chim. Acta* (GB) **15** (1970) 599.
- [95] J Crossley, L Glasser and C P Smyth, *J Chem Phys.* **55** (1971) 2197.
- [96] L Glasser, J Crossley and C P Smyth *J Chem. Phys.* **57** (1972) 3977.
- [97] H D Purohit and H S Sharma, *Indian J Pure & Appl. Phys* **9** (1971) 450.
- [98] A D Vyas and V M Vashisth, *J Mol. Liquids* **38** (1988) 11.
- [99] H D Purohit, H S Sharma and A D Vyas, *Indian J Pure & Appl. Phys* **12** (1974) 273.
- [100] S Tripathy, G S Roy and B B Swain *Indian J Pure & Appl. Phys.* **31** (1993) 828.
- [101] S N Sen and R Ghosh, *J Phys. Soc. Japan* **36** (1974) 743.
- [102] A K Ghosh and S N Sen. *Indian J Pure & Appl. Phys.* **18** (1980) 588.
- [103] A K. Ghosh and S N Sen, *J Phys. Soc. Japan* **48** (1980) 1219.
- [104] R Ghosh and Ira. Chaudhury, *Pramana, J Phys* **16** (1981) 319.
- [105] R Ghosh and Ira Chaudhury, *Indian J Pure & Appl. Phys.* **20** (1982) 717.
- [106] R Ghosh and A K Chatterjee. *Indian J Pure & Appl. Phys* **29** (1991) 650.
- [107] J P Shukla and M C Saxena, *Indian J Pure & Appl. Phys.* **11** (1973) 896.
- [108] R L Dhar, A Mathur, J P Shukla and M C Saxena, *Indian J Pure & Appl. Phys.* **11** (1973) 568.

- [109] Y Koga, H Takahashi and H Higasi, *Bull Chem. Soc. Japan* **46** (1973) 3359.
- [110] S K Srivastava and S L Srivastava, *Indian, J Pure & Appl. Phys* **13** (1975) 179.
- [111] S K S Somevanshi, S B I Misra and N K Mehrotra, *Indian. J Pure & Appl. Phys.* **16** (1978) 57.
- [112] B S Rajyam, C R K Ramasastry and C R K Murthy, *Z Naturforsch A (Germany)* **32A** (1977) 1309.
- [113] S Mulechi, S Balanicka and J Nowak, *J Chem. Soc. Faraday Trans 2 (G.B)* **1** (1980) 42.
- [114] S Acharyya and A K. Chatterjee, *Indian J Pure & Appl. Phys* **23** (1985) 484.
- [115] C R Acharyya, A K Chatterjee, P K Sanyal and S Acharyya, *Indian J Pure & Appl. Phys.* **24** (1986) 234.
- [116] C B Agarwal *Indian J Pure & Appl. Phys.* **24** (1986) 204.
- [117] M P Madan, *J Mol. Liquids (Netherland)* **33** (1987) 203.
- [118] J M Gandhi and G L Sharma, *J Mol. Liquids (Netherland)* **38** (1988) 23.
- [119] J J Makosz *Acta. Phys Polon (Poland)* **A78** (1990) 907.
- [120] Ashok Sharma and D R Sharma, *J. Phys. Soc. Japan* **61** (1992) 1049.
- [121] A Sharma, D R Sharma and M S Chauhan *Indian J Pure & Appl. Phys.* **31** (1993) 841.
- [122] P J Singh and K S Sharma, *Indian J Pure & Appl. Phys.* **34** (1996) 1.
- [123] U Saha and S Acharyya, *Indian J. Pure & Appl. Phys.* **32** (1994) 346.
- [124] J S Dhull and D R Sharma *J Phys D : Appl. Phys* **15** (1982) 2307.

- [125] J S Dhull and D R Sharma *Indian J Pure & Appl. Phys.* **21** (1983) 694.
- [126] A K Sharma and D R Sharma, *J Phys. Soc. Japan* **53** (1984) 4771.
- [127] A K Sharma and D R. Sharma *Indian J Pure & Appl. Phys.* **23** (1985) 418.
- [128] A K Sharma, D R Sharma and D S Gill. *J Phys D : Appl. Phys.* **18** (1985) 1199.
- [129] U Saha and S Acharyya, *Indian J Pure & Appl. Phys.* **31** (1993) 181.
- [130] S M Puranik, A C Kumbharkhane and S C Mehrotra, *Indian J Phys.* **67B** (1993) 9.
- [131] M L Arrawatia, P C Gupta and M L Sisodia *Indian J Pure & Appl. Phys.* **15** (1977) 770.
- [132] P C Gupta, M L Arrawatia and M L Sisodia *Indian J Pure & Appl. Phys.* **16** (1978) 451.
- [133] S M Khameshara and M L Sisodia, *Indian J Pure & Appl. Phys.* **18** (1980) 110.
- [134] S C Srivastava and Suresh Chandra *Indian J Pure & Appl. Phys* **13** (1975) 101.
- [135] S N Elsayed, A Abdelghany, A H Abou El Ela and N H Mousa, *Indian. J Pure & Appl. Phys.* **33** (1995) 185.
- [136] R A Jangid, D Bhatnagar and J M Gandhi *Indian J Pure & Appl. Phys.* **35** (1997) 47.
- [137] R Varadarajan and A Rajagopal *Indian J Pure & Appl. Phys.* **36** (1998) 13.
- [138] R Varadarajan and A Rajagopal *Indian J Pure & Appl. Phys.* **36** (1998) 113.

- [139] V Madhurima, V R K Murthy and J Sobhanadri, *Indian. J Pure & Appl. Phys.* **36** (1998) 85.
- [140] A D Vyas and V A Rana, *Indian J Pure & Appl. Phys* **36** (1998) 21.
- [141] R J Sengwa and Kulvinder Kaur. *Indian J Pure & Appl. Phys.* **37** (1999) 469.
- [142] U Saha and R Ghosh *J Phys D : Appl. Phys.* **32** (1999) 820.
- [143] S K Dash, J K Das and B B Swain, *Indian J. Pure & Appl. Phys.* **38** (2000) 791.
- [144] Nagesh Thakur and D R Sharma. *Indian. J Pure & Appl. Phys.* **38** (2000) 328.

CHAPTER -2

SCOPE AND OBJECTIVE OF THE PRESENT WORK

SCOPE AND OBJECTIVE OF THE PRESENT WORK

2.1. Introduction

Dielectric relaxation phenomena of dielectropolar liquid molecules in nonpolar solvents at a single or different temperatures under hf electric field is of much importance as it provides with a valuable information regarding shape, size and structure of dipolar molecules. Moreover solute-solvent and solute-solute molecular associations can be inferred from such study. The structural and associational aspects of dipolar liquid molecules can be made from the measured dielectric relaxation parameters viz the hf dipole moment μ_j , static or low frequency dipole moment μ_s , double relaxation times τ_1 and τ_2 , theoretical dipole moment μ_{theo} obtained from bond angles and bond moments of substituent polar groups attached to parent polar molecule. Different thermodynamic energy parameters ΔH_τ and ΔH_η due to dielectric relaxation and viscous flow respectively can, however, be measured from the estimated τ_j at different temperatures by a method in Chapter 2. The entropy of activation ΔS_τ , free energy of activation ΔF_τ are then obtained. The main objective of this thesis is to modify the existing theories to get new formulations within the frame work of Debye-Smyth and Hill model. The concrete concept about structural conformation and various associational aspects of dipolar liquid molecules could thus be attempted for.

2.2. Theoretical Formulations to Estimate hf τ_j and μ_j

The real σ_{ij}' and imaginary σ_{ij}'' parts of hf complex conductivity σ_{ij}^* of solution (ij) are related by [1]

$$\sigma_{ij}'' = \sigma_{\infty ij} + \left(\frac{1}{\omega \tau_j} \right) \sigma_{ij}' \quad (2.1)$$

This is a straight line between the variables σ_{ij}'' and σ_{ij}' of different weight fractions w_j 's whose slope $(1/\omega \tau_j)$ is used to estimate τ_j of a dipolar molecule.

But the variation of σ_{ij}'' against σ_{ij}' for highly nonspherical associative polar liquids for different w_j 's at a given temperature does not obey the linear curve (Figure 2.1) as claimed by Murthy et al [1].

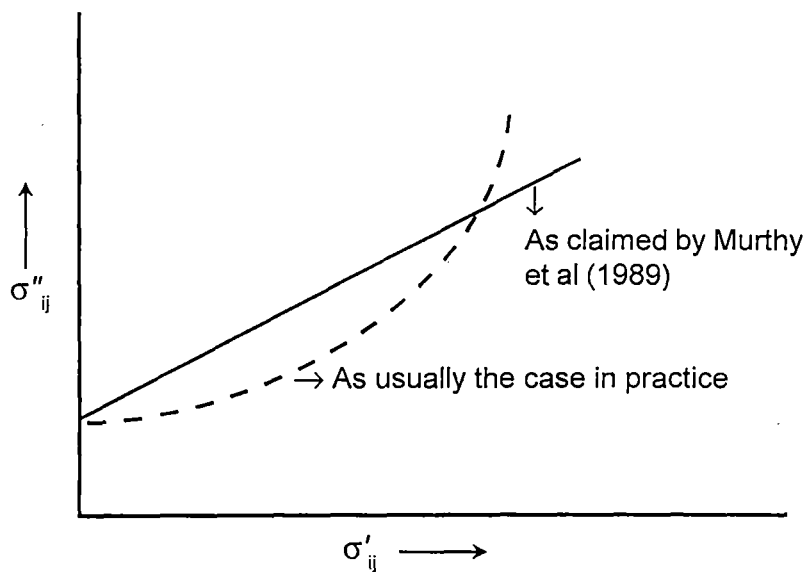


Figure 2.1

For such liquids, the individual variations of σ_{ij}'' and σ_{ij}' with w_j 's of dipolar solute as shown in Figures 2.2 and 2.3 can be used to estimate τ_j [2].

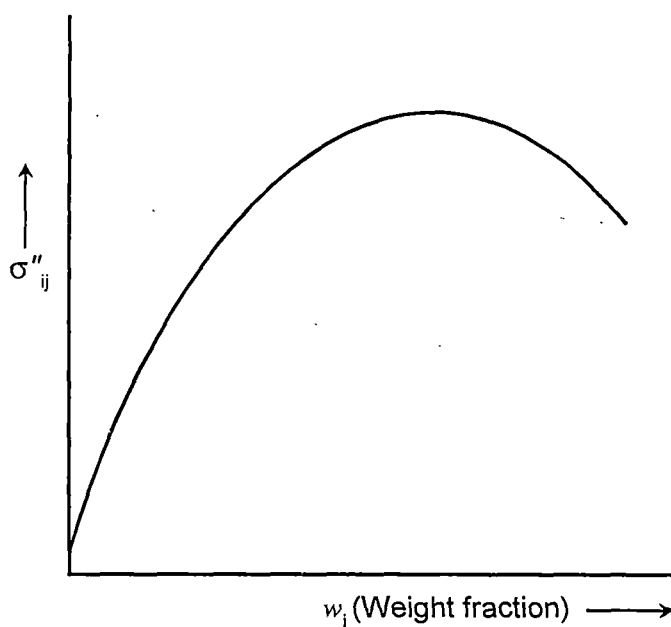


Figure 2.2

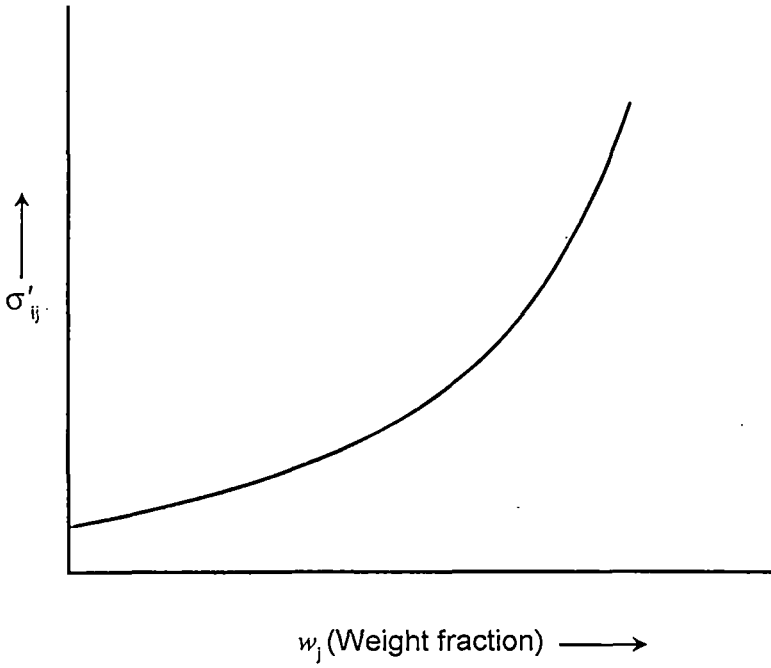


Figure 2.3

$$\frac{(d\sigma_{ij}''/dw_j)w_{j \rightarrow 0}}{(d\sigma_{ij}'/dw_j)w_{j \rightarrow 0}} = \frac{1}{\omega\tau_j} \quad (2.2)$$

The estimated τ_j from Eq (2.2) are in good agreement with Gopalakrishna's formulation [3]. The simple and straight forward theoretical formulation has been used to estimate τ_j 's in Chapters 5 and 6 respectively.

Since the total hf conductivity $\sigma_{ij} = \omega\epsilon_o (\epsilon_{ij}'^2 + \omega_{ij}''^2)^{1/2} \simeq \sigma_{ij}''$, we have from Eq (2.2) $(d\sigma_{ij}'/dw_j)w_{j \rightarrow 0} = \omega\tau_j\beta$ (2.3)

The real part σ_{ij}' of hf complex conductivity σ_{ij}^* is [4,5]

$$\sigma_{ij}' = \frac{N\mu_j^2\rho_{ij}}{27M_jkT} \left(\frac{\omega^2\tau_j}{1+\omega^2\tau_j^2} \right) (\epsilon_{ij} + 2)^2 w_j \quad (2.4)$$

which on differentiation w.r. to w_j and at $w_j \rightarrow 0$ yields that

$$(d\sigma_{ij}'/dw_j)w_{j \rightarrow 0} = \frac{N\mu_j^2\rho_i}{27M_jkT} \left(\frac{\omega^2\tau_j}{1+\omega^2\tau_j^2} \right) (\epsilon_i+2)^2 \quad (2.5)$$

From Eqs. (2.3) and (2.5) one gets.

$$\mu_j = \left[\frac{27 M_j k T \beta}{N \rho_j (\epsilon_j + 2)^2 \omega b} \right]^{1/2} \quad (2.6)$$

where M_j is molecular weight of a polar molecule, k = Boltzmann constant = $1.38 \times 10^{-23} \text{ J mole}^{-1} \cdot \text{K}^{-1}$, N = Avogadro's number = 6.023×10^{23} , ρ_j and ϵ_j are the density and dielectric relative permittivity of solvent used and β is the linear coefficient of $\sigma_{ij} - w_j$ curve in the limit $w_j = 0$. The dimensionless parameter 'b' involved with τ_j is $b = 1/(1 + \omega^2 \tau_j^2)$. We have employed Eq (2.6) to get hf μ_j as given in chapters 5, 6 and 8 of this thesis in terms of measured τ_j 's.

The hf σ_{ij} is, however, involved with the transport of bound molecular charges. A new formulation is, therefore, advanced by introducing χ_{ij} 's where χ_{ij} is the hf dielectric susceptibility of orientational polarisation.

The real ϵ_{ij}' and imaginary ϵ_{ij}'' parts of hf complex ϵ_{ij}^* are related by :

$$\epsilon_{ij}' = \epsilon_{\infty ij} + \left(\frac{1}{\omega \tau} \right) \epsilon_{ij}'' \quad (2.7)$$

In terms of real $\chi_{ij}' = \epsilon_{ij}' - \epsilon_{\infty ij}$ and imaginary $\chi_{ij}'' = \epsilon_{ij}''$ parts of complex χ_{ij}^* we have :

$$\chi_{ij}'' = (\omega \tau) \chi_{ij}' \quad (2.8)$$

variation of χ_{ij}'' with χ_{ij}' is expected to be linear, the slope $(\omega \tau)$ of which could yield τ_j of a polar liquid.

Again, for complicated polar molecules the variations of χ_{ij}'' with χ_{ij}' are not strictly linear unlike Figure 2.1 under such context Eq (2.8) becomes :

$$(d\chi_{ij}'' / dw_j)_{w_j \rightarrow 0} / (d\chi_{ij}' / dw_j)_{w_j \rightarrow 0} = \omega \tau \quad (2.9)$$

to give τ_j 's. The polar-polar interactions are supposed to be fully eliminated to obtain τ_j 's by Eq. (2.9).

The imaginary part χ_{ij}'' of dimensionless complex susceptibility χ_{ij}^* of solution (ij) in S.I. unit is written as [4,6] :

$$\chi_{ij}'' = \frac{N\mu_j^2\rho_{ij}}{27\varepsilon_0M_jkT} \frac{\omega\tau_j}{1+\omega^2\tau_j^2} \cdot (\varepsilon_{ij} + 2)^2 w_j \quad (2.10)$$

$$\text{or, } \left(\frac{d\chi_{ij}''}{dw_j}\right)_{w_j \rightarrow 0} = \frac{N\rho_i\mu_j^2}{27\varepsilon_0M_jkT} \frac{\omega\tau_j}{1+\omega^2\tau_j^2} (\varepsilon_i + 2)^2 \quad (2.11)$$

The approximation $\chi_{ij} \simeq \chi_{ij}''$ like $\sigma_{ij} \simeq \sigma_{ij}''$ was not made in order to obtain μ_j from τ_j in the dielectric susceptibility measurement.

From Eqs. (2.9) and (2.11) one obtains to get hf μ_j 's from :

$$\mu_j = \left[\frac{27\varepsilon_0M_jkT\beta}{N\rho_i(\varepsilon_i + 2)^2 b} \right]^{1/2} \quad (2.12)$$

in terms of the linear coefficient β of $\chi_{ij}' - w_j$ curve in the limit $w_j = 0$.

ε_0 is the permittivity of free space = 8.854×10^{-12} F.m⁻¹ and the other symbols have their usual meanings as stated earlier.

The hf μ_j in chapter 7 of this thesis are computed from Eq. (2.12). But the Eq.(2.6) showed higher μ_j 's in comparison to Eq (2.12). The difference $\Delta\mu_j$ may provide an additional information [7] of bound molecular charges as seen in Chapter 8.

2.3. Static Experimental Parameter X_{ij} and Static μ_s

The Eq (1.77) is :

$$\therefore \frac{\varepsilon_{oij} - 1}{\varepsilon_{oij} + 2} - \frac{\varepsilon_{\infty ij} - 1}{\varepsilon_{\infty ij} + 2} = \frac{\varepsilon_{oi} - 1}{\varepsilon_{oi} + 2} - \frac{\varepsilon_{\infty i} - 1}{\varepsilon_{\infty i} + 2} + \frac{N\mu_s^2}{9\varepsilon_0kT} c_j \quad (2.13)$$

where ε_{oij} and $\varepsilon_{\infty ij}$ are the low and infinite frequency relative permittivities of solution (ij). The molar concentration c_j is $c_j = \rho_{ij} w_j / M_j$, where w_j is the weight

fraction of polar liquid.

$$\frac{\epsilon_{oij} - \epsilon_{\infty ij}}{(\epsilon_{oij} + 2)(\epsilon_{\infty ij} + 2)} = \frac{\epsilon_{oi} - \epsilon_{\infty i}}{(\epsilon_{oi} + 2)(\epsilon_{\infty i} + 2)} + \frac{N\mu_s^2}{27\epsilon_0 kT} \frac{\rho_{ij} w_j}{M_j} \quad (2.14)$$

The weight W_i of volume V_i of a nonpolar solvent is mixed with the weight W_j of a polar solute of volume V_j to make a solution. The solution density ρ_{ij} is :

$$\begin{aligned} \rho_{ij} &= \frac{W_i + W_j}{V_i + V_j} = \frac{W_i + W_j}{W_i/\rho_i + W_j/\rho_j} \\ &= \frac{\rho_i \rho_j}{\left(\frac{W_i}{W_i + W_j}\right) \rho_j + \left(\frac{W_j}{W_i + W_j}\right) \rho_i} \\ &= \frac{\rho_i \rho_j}{w_i \rho_j + w_j \rho_i} = \frac{\rho_i}{1 - \gamma w_j} \end{aligned} \quad (2.15)$$

where $w_i = \frac{W_i}{W_i + W_j}$ and $w_j = \frac{W_j}{W_i + W_j}$ are the weight fractions of solvent and solute respectively such that $w_i + w_j = 1$ and $\gamma = (1 - \rho_i/\rho_j)$, where ρ_i and ρ_j are the densities of pure solvent and solute respectively. Thus Eq. (2.14) becomes :

$$\frac{\epsilon_{oij} - \epsilon_{\infty ij}}{(\epsilon_{oij} + 2)(\epsilon_{\infty ij} + 2)} = \frac{\epsilon_{oi} - \epsilon_{\infty i}}{(\epsilon_{oi} + 2)(\epsilon_{\infty i} + 2)} + \frac{N\mu_s^2 \rho_i (1 - \gamma w_j)^{-1} w_j}{27\epsilon_0 kT M_j} \quad (2.16)$$

$$\text{or } X_{ij} = X_i + \frac{N\mu_s^2 \rho_i}{27\epsilon_0 M_j kT} w_j + \frac{N\mu_s^2 \rho_i}{27\epsilon_0 M_j kT} \gamma w_j^2 + \dots \quad (2.17)$$

$$X_{ij} = a_0 + a_1 w_j + a_2 w_j^2 + \dots \quad (2.18)$$

The static experimental parameter X_{ij} of a solution is thus a function of w_j 's. The Eq (2.17) is highly converging in nature since w_j lies within $0 < w_j < 1$. The

computed error in the regression analysis of Eq. (2.18) shed much light on its functional dependence on estimated μ_s .

Equating the coefficients of equal powers of w_j from both right hand sides of Eqs. (2.17) and (2.18) one gets

$$\mu_s = \left(\frac{27 \epsilon_0 M_j kT}{N \rho_j} a_1 \right)^{1/2} \quad (2.19)$$

and

$$\mu_s = \left(\frac{27 \epsilon_0 M_j kT}{N \rho_j \gamma} a_2 \right)^{1/2} \quad (2.20)$$

to estimate static dipole moment μ_s at any stage of dilution.

The present extrapolation technique on $X_{ij}-w_j$ curve unlike Lefevre [8] and Guggenheim [9] is a single one which seems to be better over the usual procedures where at least two extrapolations are needed to obtain μ_s of a polar liquid. But μ_s from Eq (2.20) is not reliable because the term γ is influenced by the effects of solvent, relative density, solute-solute or, dipole-dipole interaction, internal field, and macroscopic viscosity etc. [5].

This theory has widely been tested [5] on a large number of straight long chain alcohols in chapter 6 of this thesis.

2.4. Double Relaxation Times τ_1, τ_2 and Dipole Moments μ_1, μ_2

The orientational polarisation is however, achieved by introducing the orientational susceptibility χ_{ij} because $\epsilon_{\infty ij}$ which includes the fast polarisation, always appears as a subtracted term in Bergmann et. al. equations. The clumsiness of algebra and the effects of fast polarisation can thus be avoided by the established symbols of dielectric terminologies and parameters $\chi_{ij}' = \epsilon_{ij}' - \epsilon_{\infty ij}$, $\chi_{ij}'' = \epsilon_{ij}''$ and $\chi_{oij} = \epsilon_{oij} - \epsilon_{\infty ij}$ in Bergmann et. al equations [10].

$$\chi_{ij}''/\chi_{oij} = c_1 \frac{1}{1+\omega^2\tau_1^2} + c_2 \frac{1}{1+\omega^2\tau_2^2} \quad (2.21)$$

$$\chi_{ij}''/\chi_{oij} = c_1 \frac{\omega\tau_1}{1+\omega^2\tau_1^2} + c_2 \frac{\omega\tau_2}{1+\omega^2\tau_2^2} \quad (2.22)$$

χ_{ij}' and χ_{ij}'' are the real and imaginary parts of the complex dielectric orientational susceptibility χ_{ij}^* and χ_{oij} is the low frequency susceptibility which is real.

Let $\alpha_1 = \omega\tau_1$ and $\alpha_2 = \omega\tau_2$ Eqs. (2.21) and (2.22) are solved to get.

$$c_1 = \frac{(\chi_{ij}'\alpha_2 - \chi_{ij}'')(1+\alpha_1^2)}{\chi_{oij}(\alpha_2 - \alpha_1)} \quad (2.23)$$

$$c_2 = \frac{(\chi_{ij}'' - \chi_{ij}'\alpha_1)(1+\alpha_2^2)}{\chi_{oij}(\alpha_2 - \alpha_1)} \quad (2.24)$$

which are the relative weight factors for the two separate broad dispersions and $\alpha_2 > \alpha_1$.

Now, adding Eqs. (2.23) and (2.24) since $c_1 + c_2 = 1$ we get.

$$\frac{(\chi_{oij} - \chi_{ij}')}{\chi_{ij}'} = \omega(\tau_2 + \tau_1) \frac{\chi_{ij}''}{\chi_{ij}'} - \omega^2\tau_1\tau_2 \quad (2.25)$$

It is a straight line between the variables $(\chi_{oij} - \chi_{ij}') / \chi_{ij}'$ and χ_{ij}''/χ_{ij}' having slope $\omega(\tau_2 + \tau_1)$ and intercept $-\omega^2\tau_1\tau_2$. It is solved for different ω 's of a polar molecule for a fixed value of angular frequency $\omega (= 2\pi f)$ of the electric field to get τ_1 and τ_2 for the rotations of flexible polar groups attached to the parent molecule and the molecule itself respectively.

The estimated τ_1 and τ_2 can be used to obtain μ_1 and μ_2 from Eqs (2.6) and (2.12) of the flexible part and the whole molecule.

The theoretical values of c_1 and c_2 towards dielectric dispersions are derived from Fröhlich's [11] Eqs. (2.26) and (2.27), with known τ_1 and τ_2 of Eq. (2.25):.

$$\chi_{ij}' / \chi_{oij} = 1 - \frac{1}{2A} \ln \left(\frac{1 + \omega^2 \tau_2^2}{1 + \omega^2 \tau_1^2} \right) \quad (2.26)$$

$$\chi_{ij}'' / \chi_{oij} = \frac{1}{A} [\tan^{-1}(\omega \tau_2) - \tan^{-1}(\omega \tau_1)] \quad (2.27)$$

$A =$ the Fröhlich parameter $= \ln(\tau_2/\tau_1)$.

The experimental c_1 and c_2 are also obtained from Eqs. (2.23) and (2.24) with the known intercepts $(\chi_{ij}' / \chi_{oij})_{w_j \rightarrow 0}$ and $(\chi_{ij}'' / \chi_{oij})_{w_j \rightarrow 0}$ from concentration (w_j) variation of χ_{ij}' / χ_{oij} and χ_{ij}'' / χ_{oij} of Figures. 2.4 and 2.5. The theoretical and experimental c_1 and c_2 satisfy $|c_1 + c_2| \simeq 1$, suggesting the validity [6,7] of the suggested method.

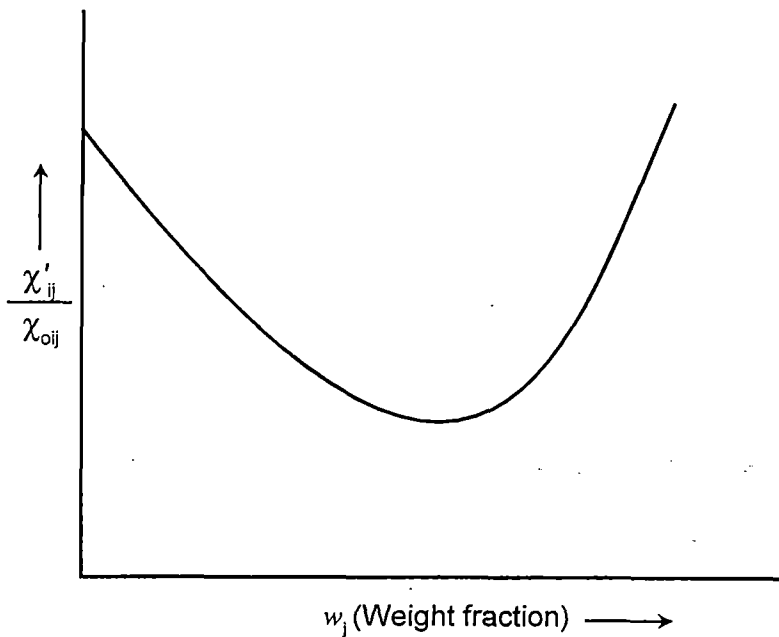


Figure 2.4

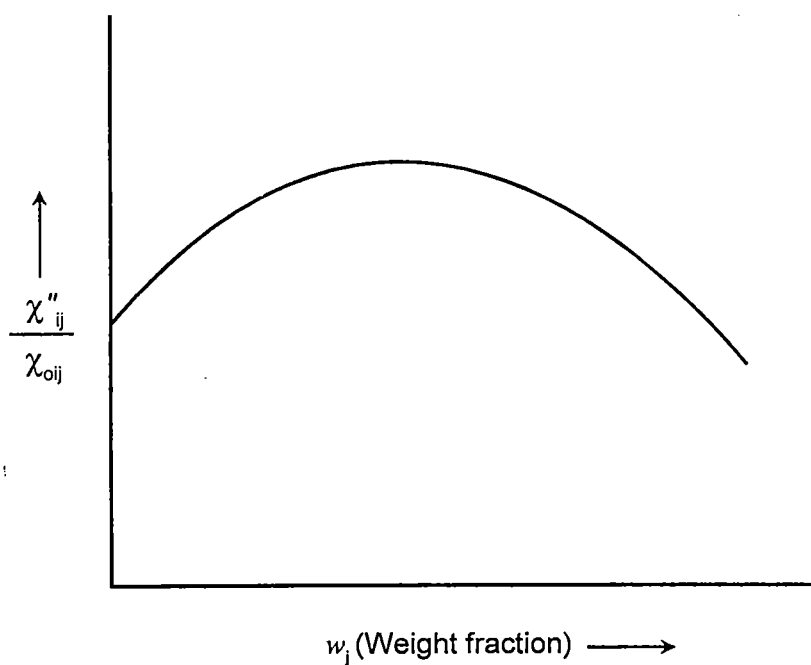


Figure 2.5

The derived theoretical formulations were tested on isomers of anisidine and toluidine and monosubstituted anilines presented in chapter 7 and 8 of this thesis.

2.5. Relaxation Parameters under Rf Electric Field

The rf conductivity of polar - nonpolar liquid mixture is measured by the resonance method. The block diagram of experimental set-up is shown in Figure 2.6a & b. A Hartley oscillator feeds power to the resonant circuit consisting of a coil and a variable air condenser in series with a rf milliammeter. The cylindrical pyrex glass tube of diameter 2cm provided with a pair of stainless steel electrodes of diameter 1.5cm, separated by 1cm is used as a cell. The oscillator is set to the desired frequency. The resonant circuit is tuned with the cell connected in parallel to tuning condenser (c_v) and in series with the rf meter.

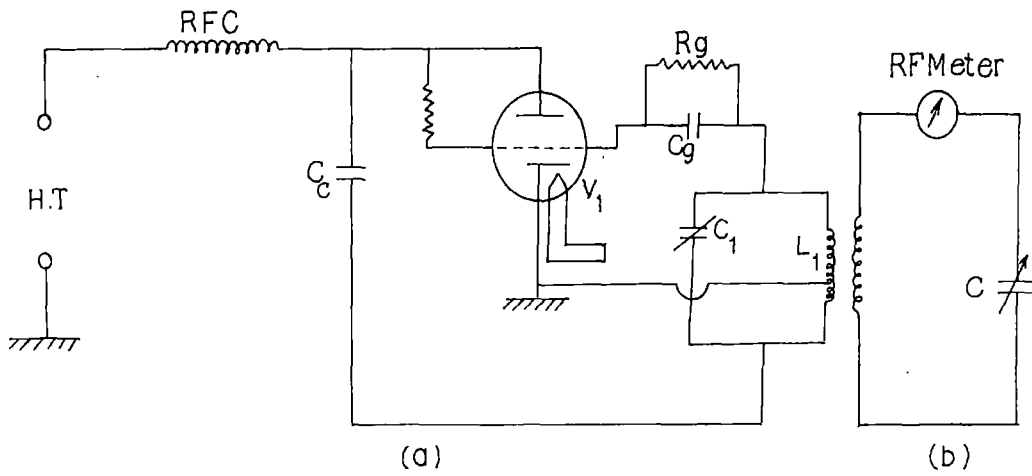


Figure 2.6

- a. Radio Frequency Oscillator
 b. Secondary Tuning Circuit.

LIST OF COMPONENTS

$V_1 = 6L6$
 $R_g = 30K\Omega$
 $C_g = 350\text{pF}$
 $C = 0 - 500\text{pF}$

RFC = Radio Frequency Choke
 RF Meter = Radio Frequency
 Milliammeter
 $C_c = 0.01\mu\text{F}$

2.6. RF Resistance and Conductivity of a Polar Liquid

The resonant currents I_1 and I_2 in the rf milliammeter is measured when the cell is empty and filled up with the dielectric liquid. After the introduction of dielectric cell the secondary circuit is modified as shown in Figure 2.6c and the equivalent circuit is in Figure 2.6d. In case of parallel combination as in Figure (2.6c). let Z_p = equivalent impedance, where

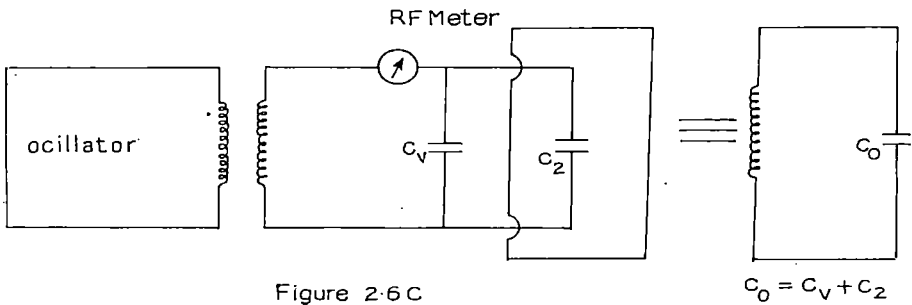


Figure 2-6c
(circuit Arrangement)

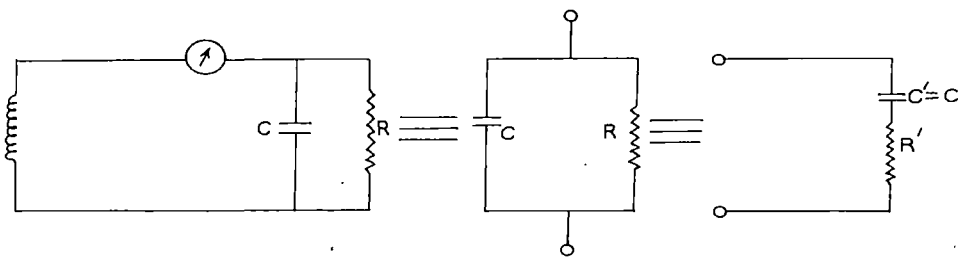


Figure 2-6d
[Equivalent Circuit]

$$Z_p = \frac{R}{1 + j\omega CR} = \frac{R(1 - j\omega CR)}{1 + \omega^2 C^2 R^2} \quad (2.28)$$

In case of series combination as in Figure 2.6d.

$$Z_p = R' + \frac{1}{1 + j\omega CR'} \quad (2.29)$$

Equating the real and imaginary parts of Eqs. (2.28) and (2.29) one obtains :

$$R' = \frac{R}{1 + \omega^2 C^2 R^2} \quad (2.30)$$

further $I_1 = E/R_0$, where R_0 is the rf resistance of the secondary circuit and is given by :

$$R_0 = \frac{C_2 - C_1}{2\omega C_1 C_2} \sqrt{\frac{I_1^2}{I_0^2 - I_1^2}} \quad (2.31)$$

where I_0 and I_1 are the resonant currents in the rf meter without and with the cell, C_1 and C_2 are the capacities for reducing the resonant current I_0 by $1/\sqrt{2}$ where C_0 is the capacity of the tuning condenser for the resonant current I_0 .

$$\text{Again } I_2 = \frac{E}{R_0 + R'} \quad (2.32)$$

$$= \frac{E}{R_0 + \frac{R}{1 + \omega^2 C^2 R^2}} \quad (2.33)$$

Let $I_1/I_2 = \alpha$ we get

$$(\alpha - 1) = \frac{R}{R_0 + \omega^2 C^2 R^2 R_0}$$

$$R = \frac{1 \pm [1 - 4R_0^2 (\alpha - 1)^2 \omega^2 C^2]^{1/2}}{2R_0 (\alpha - 1) \omega^2 C^2}$$

Since $4R_0^2 (\alpha - 1)^2 \omega^2 C^2 \ll 1$ we have rf resistance of a polar liquid.

$$R = \frac{1}{R_0 (\alpha - 1) \omega^2 C^2} \quad (2.34)$$

$$\text{Now } R = \rho \frac{d}{S} \quad (2.35)$$

where ρ is the specific resistance of the liquid, d is the distance between the electrodes of cross-sectional area S .

If σ' is the rf conductivity of the liquid, then

$$\sigma' = \frac{d}{R.S} \quad (2.36)$$

The capacity of the tuning condenser for the resonant current I_0 is given by,

$$C_0 = \frac{S}{4\pi d} \quad (2.37)$$

From Eqs. (2.36) and (2.37) we get the working formula of σ' where

$$\sigma' = \frac{1}{4\pi R C_0} \quad (2.38)$$

2.7. Washing of Dielectric Cell and Purification of Dipolar Liquids

Before filling the cell with experimental liquid, the cell was cleaned with sodium hydroxide and chromic acid, then for several times with pure distilled water and finally with benzene. The cell was then dried by an electric drier.

The liquids under investigation were N, N dimethyl formamide (DMF), dimethyl sulphoxide (DMSO), methanol (CH_3OH), ethanol ($\text{C}_2\text{H}_5\text{OH}$) n-propanol ($\text{C}_3\text{H}_7\text{OH}$) 2-butanol ($\text{C}_4\text{H}_9\text{OH}$) in solvents benzene (C_6H_6) and carbon tetrachloride (CCl_4). They were of Analar grade from Messrs BDH (London) and E. Merck (Germany). The liquids were distilled in vacuum and kept in a

desiccator before use. The temperature of the cell was controlled by a thermostat of accuracy $\pm 0.5^\circ\text{C}$.

2.8. Coefficient of Viscosity of Dipolar Liquids

The coefficient of viscosity η of the dielectric liquids was measured by Ostwald viscometer.

The volumes of distilled water and the experimental liquid flowing through the capillary tube of length l and radius r per unit time are

$$V_1 = \frac{\pi P_1 r^4}{8 \eta_1 l} = \frac{K \pi \rho_1 r^4}{8 \eta_1 l} \quad (2.39)$$

$$V_2 = \frac{\pi P_2 r^4}{8 \eta_2 l} = \frac{K \pi \rho_2 r^4}{8 \eta_2 l} \quad (2.40)$$

Here P_1 and P_2 are the pressure differences between the ends of capillary tube. η_1 and η_2 are the coefficient of viscosities of water and experimental liquid respectively.

Now,

$$\frac{V_1}{V_2} = \frac{\rho_1}{\rho_2} \cdot \frac{\eta_2}{\eta_1} \quad (2.41)$$

and since the times t_1 and t_2 of free fall of two liquids vary inversely as V_1 and V_2

$$\frac{\eta_1}{\eta_2} = \frac{t_1}{t_2} \cdot \frac{\rho_1}{\rho_2} \quad (2.42)$$

with the Known η_1 , ρ_1 , ρ_2 [12], t_1 and t_2 by a digital timer stop watch η_2 's were estimated.

2.9. Formulations for n , τ_j and μ_j Under Rf Electric Field

The equation of motion of a polar molecule through a viscous medium under rf electric field is

$$M \frac{dv}{dt} = eE_0 e^{j\omega t} - 6\pi\eta a v \quad (2.43)$$

It is solved by :

$$v = A e^{j\omega t} \quad (2.44)$$

The drift velocity of ion is

$$v = \frac{eE_0 e^{j\omega t}}{M(\gamma + j\omega)} \quad (2.45)$$

Where $\gamma = 6\pi\eta a/M$ and $j = \sqrt{-1}$, a complex number. Hence

$$v = \frac{eE_0}{M} \left[\frac{\gamma}{\gamma^2 + \omega^2} - j \frac{\omega}{\gamma^2 + \omega^2} \right] e^{j\omega t}$$

and the mobility of ion

$$\mu = \frac{v}{E} = \frac{e}{M} \left[\frac{\gamma}{\gamma^2 + \omega^2} - j \frac{\omega}{\gamma^2 + \omega^2} \right]$$

If n be the number of ions per unit volume, the conduction current is

$$i = \frac{ne^2}{M} \left[\frac{\gamma}{\gamma^2 + \omega^2} - j \frac{\omega}{\gamma^2 + \omega^2} \right] E_0 e^{j\omega t} \quad (2.46)$$

The real part σ'_{ij} of complex hf conductivity σ_{ij}^* is [13]

$$\begin{aligned} \sigma' &= ne\mu = \frac{ne^2}{M} \cdot \frac{\gamma}{\gamma^2 + \omega^2} \\ &= \frac{ne^2}{M} \cdot \frac{6\pi\eta a/M}{(6\pi\eta a/M)^2 + \omega^2} \\ \sigma' &= \frac{ne^2}{6\pi\eta a} \end{aligned} \quad (2.47)$$

as
$$\frac{6\pi\eta a}{M} \gg \omega$$

Again from Murphy – Morgan [14] relation σ_{ij}^* is given by

$$\sigma_{ij}^* = \sigma_{ij}' + j \sigma_{ij}'' \quad (2.48)$$

where $\sigma_{ij}' = \frac{\omega}{4\pi} \epsilon_{ij}''$ and $\sigma_{ij}'' = -\frac{\omega}{4\pi} \epsilon_{ij}'$ are the real and imaginary parts, of hf complex conductivity σ_{ij}^*

From Eqs. (2.47) and (2.48) σ_{ij}' is

$$\sigma_{ij}' = \frac{\omega}{4\pi} \epsilon_{ij}'' + \left(\frac{ne^2}{6\pi a} \right) \cdot \frac{1}{\eta_{ij}} \quad (2.49)$$

Eq. (2.49) with Eq. (1.32) becomes

$$\sigma_{ij}' = \frac{\omega}{4\pi} \left(\frac{\epsilon_{oij} - \epsilon_{\infty ij}}{1 + \omega^2 \tau^2} \right) \omega \tau + \left(\frac{ne^2}{6\pi a} \right) \cdot \frac{1}{\eta_{ij}} \quad (2.50)$$

under rf electric field $\omega^2 \tau^2 \ll 1$, Eq (2.50) becomes :

$$\sigma_{ij}' = \frac{\omega^2 \tau}{4\pi} (\epsilon_{oij} - \epsilon_{\infty ij}) + \left(\frac{ne^2}{6\pi a} \right) \cdot \frac{1}{\eta_{ij}} \quad (2.51)$$

The Eq. (2.51) shows that σ_{ij}' varies linearly with $1/\eta_{ij}$. The slope $(ne^2/6\pi a)$ is used to estimate n.

$$\text{Einstein - Stokes relation [15] is } D\eta/T = \frac{k}{6\pi a} \quad (2.52)$$

where $D = \frac{\mu kT}{e}$, the diffusion coefficient. Eq (2.52) with Eq (1.102) and (2.47) becomes

$$\tau_j = \frac{2na^2 e^2}{3\sigma_{ij}' kT} \quad (2.53)$$

where a = molecular radius, e = electronic charge = 4.803×10^{-10} e.s.u and k = Boltzmann constant = 1.38×10^{-16} erg mole $^{-1}$ K $^{-1}$, T = Temperature in Kelvin.

$$\text{Again } \sigma_{ij}' = \frac{\omega}{4\pi} \epsilon_{ij}'' \quad (2.54)$$

The ϵ_{ij}'' according to Smyth [4] is

$$\epsilon_{ij}'' = \frac{4\pi N d_{ij} w_j \mu_j^2 (\epsilon_{oij} + 2) (n_{Dij}^2 + 2) \omega \tau}{27 M_j kT (1 + \omega^2 \tau^2)} \quad (2.55)$$

In rf electric field $\omega^2 \tau^2 \ll 1$

$$\therefore \sigma_{ij}' = \frac{4\pi^2 f^2 N \tau_j \mu_j^2 d_{ij} (\epsilon_{oij} + 2) (n_{Dij}^2 + 2) w_j}{27 M_j kT} \quad (2.56)$$

which on differentiation with respect to w_j and at $w_j \rightarrow 0$ yields :

$$\left(\frac{d\sigma_{ij}'}{dw_j} \right)_{w_j \rightarrow 0} = \frac{4\pi^2 f^2 N \tau_j \mu_j^2 d_{ij} (\epsilon_{oi} + 2) (n_{Di}^2 + 2)}{27 M_j kT} \quad (2.57)$$

$(d\sigma_{ij}'/dw_j)_{w_j \rightarrow 0} = \beta$ is the linear coefficient of variation of σ_{ij}' with w_j . μ_j is finally given by :

$$\mu_j = \left[\frac{27 M_j kT \beta}{4\pi^2 f^2 N \tau_j d_{ij} (\epsilon_{oi} + 2) (n_{Di}^2 + 2)} \right]^{1/2} \quad (2.58)$$

where

M_j = molecular weight of dipolar liquid

f = frequency of applied electric field

N = Avogadro's number = 6.023×10^{23}

d_{ij} = density of solvent

ϵ_{oi} = relative permittivity of solvent

n_{Di} = refractive index of solvent.

The theoretical formulations thus derived are applied on some alcohols and interesting aprotic polar amides in the 9th and 10th chapter of the thesis.

2.10. Eyrings' Rate Theory

The thermodynamic energy parameters using Eyring's rate theory [16] were attempted from the temperature variation of τ_j under hf electric field. The energy parameters ΔH_τ , the enthalpy of activation, ΔS_τ , the entropy of activation and ΔF_τ , the free energy of activation gives an insight into the stability or unstability [2,17-19] of the systems. However, the aspect of molecular association [2,17,19] could also be inferred from such study.

The radius 'a' of a rotating unit is [20-22].

$$a = \frac{\tau_j T}{\eta^\gamma} \quad (2.59)$$

where $\gamma = \Delta H_\tau / \Delta H_\eta$,

$$\text{or, } \ln \tau_j T = \ln a + \gamma \cdot \ln \eta \quad (2.60)$$

establishing the linear relation between $\ln \tau_j T$ and $\ln \eta$. The slope γ of Eq.(2.60) gives information of solute - solvent and solute-solute associations. If $\gamma > 0.50$ the solute molecule behaves as solid phase rotator[2,17]. This fact has been discussed in the chapters 3, 5 and 10 of this thesis.

2.11. Structural Aspects of Dipolar Molecules From μ_{theo}

Structure of a polar molecule is studied in terms of atomic orbitals which often overlaps to form hybridised orbitals. The phenomenon is known as hybridisation. When two atoms are linked by a covalent bond, the distance between the centre of the two atomic nuclei is called bond length. The bond due to overlap of two S orbitals is called σ - bond. The sidewise overlap of two half filled p-orbitals to have a nodal plane form a π - bond. The bond angle depends on the nature of hybridisation due to size and the electronegativity of atoms or groups attached to a molecule.

Available bond moments of flexible polar groups of a molecule are used to estimate μ_{theo} by simple vector addition rules [2, 5, 6, 17, 23] on the planer molecule. The μ_{theo} 's differ from measured hf μ_j and static μ_s due to inductive, electromeric and mesomeric effects [2, 5, 6] owing to their aromaticity or electronegativity.

Inductive Effect

The different electronegativities of atoms produces a certain degree of polarity in the bond. The more or less electronegative atoms acquire a δ^- or δ^+ charges. Such polarity in the bond is called I-effect. $-\text{NO}_2$, $-\text{OH}$, $-\text{C}_6\text{H}_5$ etc. push electrons while $(\text{CH}_3)\text{C}-$, $(\text{CH}_3)_2\text{CH}-$, CH_3- etc pull electrons away from C – atom are said to have +I and – I effects.

Electromeric Effect

It is a temporary effect involving the complete transfer of a shared pair of π electrons to one or other atoms joined by double or triple bonds. Thus it is a polarisability effect.

Mesomeric (Resonance) Effect

Mesomeric effect refers to the polarity produced in a molecule as a result of interaction between two π bonds or a π bond and lone pair of electrons.

The groups i.e. $-\text{NH}_2$, $-\text{OH}$, $-\text{OCH}_3$ etc. loose electrons towards a C-atom are said to have +M effect. While $-\text{NO}_2$, $-\text{C}\equiv\text{N}$, $-\text{C}=\text{O}$ etc draw electrons away from a C-atom are said to have a – M effect.

All these effects play the vital role in the measured μ_j 's and μ_s 's. These effects possibly may change the experimental parameters : σ_{ij} , χ_{ij} , X_{ij} etc to a certain degree. The agreement of μ_j 's or μ_s 's with μ_{theo} is, however accomplished by multiplying [5] the available bond moments with $\mu_s / \mu_{\text{theo}}$ or $\mu_j / \mu_{\text{theo}}$ as shown in this thesis.

References

- [1] MBR Murthy, R L Patil and D K Deshpande *Indian. J Phys.* **63B** (1989) 491.
- [2] N Ghosh, R C Basak, S K Sit and S Acharyya *J Mol. Liquids* (Germany) **85** (2000) 375.
- [3] K V Gopalakrishna, *Trans Faraday Soc.* **53** (1957) 767.
- [4] C P Smyth '*Dielectric Behaviour and Structure* (New York : McGraw Hill) 1955.
- [5] N Ghosh, A Karmakar, S K Sit and S Acharyya *Indian J. Pure & Appl. Phys.* **38** (2000) 574.
- [6] N Ghosh, S K Sit, A K Bothra and S Acharyya *J Phys D : Appl. Phys.* (U.K.) **34** (2001) 379.
- [7] N Ghosh, S K Sit and S Acharyya, *J Mol. Liquids* (Germany) accepted for publication, 2001.
- [8] R J W Lefevre and C P Smyth. *Trans. Faraday Soc.* **46** (1950) 812.
- [9] E A Guggenheim, *Trans Faraday Soc* **47** (1951) 573.
- [10] K Bergmann, D M Roberti and C P Smyth *J Phys. Chem.* **64** (1960) 665.
- [11] H Fröhlich '*Theory of Dielectrics*' (Oxford University Press : Oxford) 1949.
- [12] *Hand Book of Chemistry and Physics*, C R C Press 58th Edition 1977-78.
- [13] R Ghosh and Ira Chaudhury, *Pramana J Phys.* **16** (1981) 319.
- [14] F J Murphy and S O Morgan '*Bell Syst Tech J* **18** (1939) 502.
- [15] R Ghosh and Ira Chaudhury, *Indian J Pure & Appl. Phys* **18** (1980) 669.

- [16] H Eyring, S Glasstone and K J Laidler '*The Theory of Rate Process*' (New York : McGraw Hill) 1941.
- [17] S K Sit, N Ghosh, U Saha and S Acharyya *Indian J Phys.* **71B** (1997) 533.
- [18] N Ghosh, R Ghosh, R C Basak, K Dutta and S Acharyya, *Pramana J. Phys.* (Communicated) 2002.
- [19] N Ghosh, R Ghosh and S Acharyya *Indian J Pure & Appl. Phys.* (Communicated) 2001.
- [20] B Sinha, S B Roy and G S Kastha *Indian. J Phys.* **40** (1966) 101.
- [21] B Sinha, S B Roy and G S Kastha, *Indian. J. Phys.* **41** (1967) 183.
- [22] U Saha and S Acharyya, *Indian. J Pure & Appl. Phys.* **32** (1994) 346.
- [23] S K Sit, N Ghosh and S Acharyya, *Indian. J Pure & Appl. Phys.* **35** (1997) 329.

CHAPTER-3

**STRUCTURAL AND ASSOCIATIONAL
ASPECTS OF BINARY AND SINGLE POLAR
LIQUIDS IN NONPOLAR SOLVENT UNDER
HIGH FREQUENCY ELECTRIC FIELD**

STRUCTURAL AND ASSOCIATIONAL ASPECTS OF BINARY AND SINGLE POLAR LIQUIDS IN NONPOLAR SOLVENT UNDER HIGH FREQUENCY ELECTRIC FIELD

The dielectric relaxation mechanism of a polar-nonpolar liquid mixture under the microwave electric field is of special interest [1,2] for its inherent ability to predict the associational aspects of polar solutes in nonpolar solvents. An investigation was, however, made on ternary solution of binary polar liquids in which both or even one of them are aprotic [2,3] to study various types of weak molecular associations by polar liquids in nonpolar solvents. We are, therefore, tempted further to consider more mixtures of binary aprotic polar liquids like N, N. dimethyl formamide (DMF) and dimethyl sulphoxide (DMSO) together with a single aprotic polar liquid like N, N. diethyl formamide (DEF) and DMSO in C_6H_6 and CCl_4 [4-6] respectively. DMSO, DMF and DEF are very interesting liquids for their wide application in medicine and industry. They also act as building blocks of proteins and enzymes. The concentration variation of the measured real ϵ'_{ijk} , ϵ'_{ij} or ϵ'_{ik} and imaginary ϵ''_{ijk} , ϵ''_{ij} or ϵ''_{ik} parts of hf complex dielectric constants ϵ^*_{ijk} , ϵ^*_{ij} or ϵ^*_{ik} of jk , j or k polar solutes in nonpolar solvents are used to detect the weak molecular interactions among the molecules [7] at a single or different temperatures under nearly 3cm wavelength electric field. The τ_{jk} of jk polar mixtures as well as τ_j 's or τ_k 's of j or k polar solutes in a nonpolar solvent were estimated from :

$$K''_{ijk} = K_{\infty ij k} + \frac{1}{\omega \tau_{jk}} K'_{ijk} \quad (3.1)$$

where $K''_{ijk} = \frac{\omega}{4\pi} \epsilon''_{ijk}$ and $K'_{ijk} = \frac{\omega}{4\pi} \epsilon'_{ijk}$ are the imaginary and real parts of complex hf conductivity K^*_{ijk} [8]. The other terms carry usual significance as presented elsewhere [2]. The τ_{jk} 's are estimated from the slopes of the

linear variations of K''_{ijk} against K'_{ijk} of Eq. (3.1). The linearity of Eq. (3.1) is tested by the correlation coefficients and the errors involved in the measurement of τ 's are within 5%. τ_{jk} 's are then plotted with different mole fractions x_k 's of DMSO at various experimental temperatures as shown in Figure 3.1.

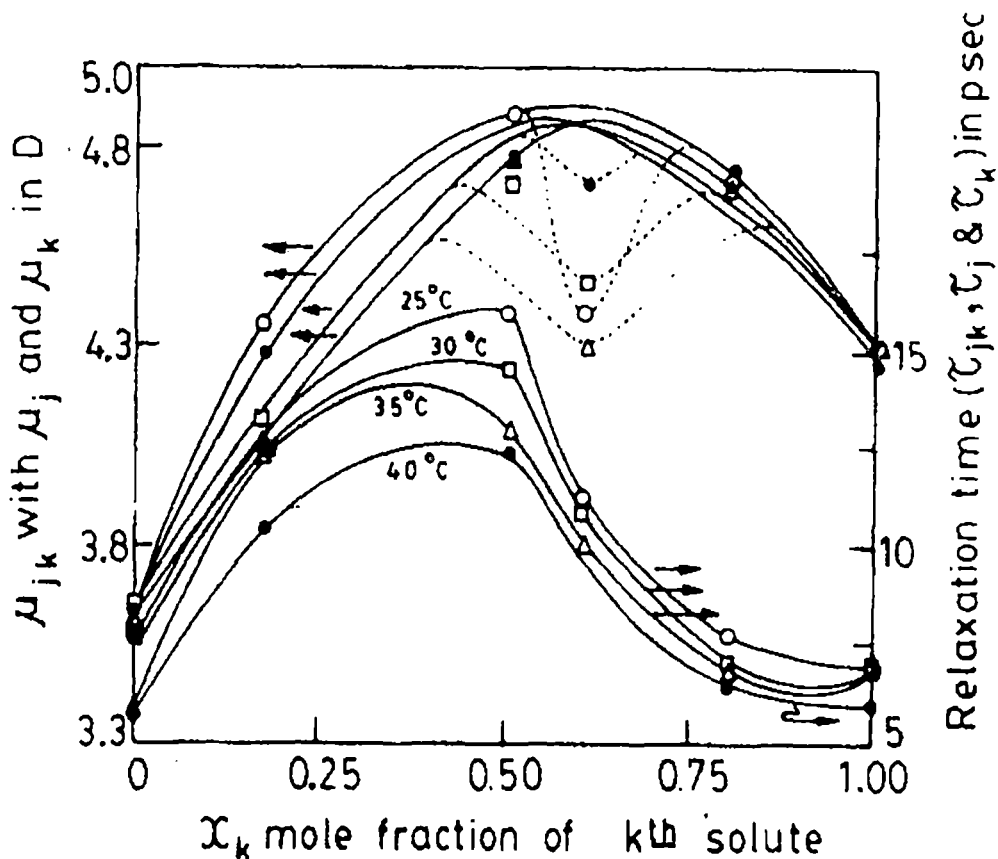


Figure 3.1 : Variation of τ_{jk} and μ_{jk} of DMF-DMSO mixture in C_6H_6 against mole fraction x_k of DMSO with τ_j and τ_k and μ_j and μ_k of DMF and DMSO respectively at different temperatures : (O) at 25°C, (□) at 30°C, (Δ) at 35°C and (●) at 40°C

The formation of dimer is responsible for the gradual rise of τ_{jk} from τ_j of DMF at $x_k = 0$ to $x_k = 0.5$ and then its rapid fall to τ_k due to rupture of dimerisation and self association [4]. The estimated τ 's are slightly larger than those of Gopalakrishna's method [9]. But τ 's from conductivity measurement are much more reliable as they provide microscopic relaxation times [10].

The energy parameters due to dielectric relaxation process were then obtained in terms of measured τ from the rate process equation of Eyring *et al* [11] :

$$\tau_s = \frac{A}{T} e^{(\Delta F_\tau/RT)}$$

$$\text{or } \ln(\tau_s T) = \ln A' + \frac{\Delta H_\tau}{RT} \quad (3.2)$$

where $A' = Ae^{-\Delta S_\tau/R}$.

Eq. (3.2) is a straight line of $\ln(\tau_s T)$ against $1/T$ as seen in Figure 3.2 having intercepts and slopes to yield the entropy of activation ΔS_τ enthalpy of activation ΔH_τ and free energy of activation ΔF_τ due to dielectric relaxation.

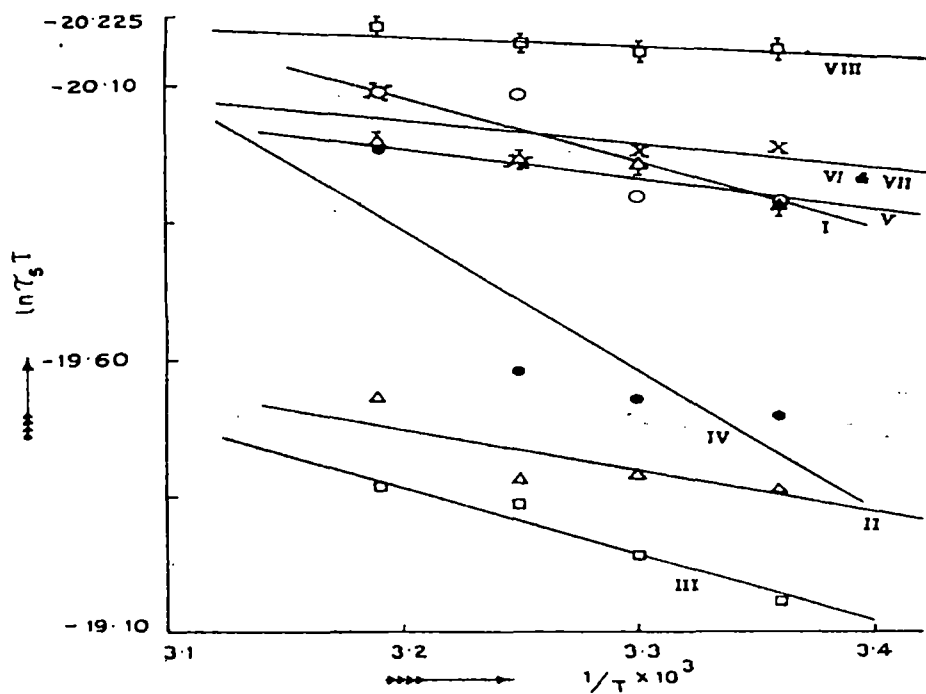


Figure 3.2: Variation of $\ln(\tau_s T)$ against $\frac{1}{T}$ of binary and single polar solutes in nonpolar solvent. I-DMF + 0 mole% DMSO in C_6H_6 (O), II-DMF + 17 mole% DMSO in C_6H_6 (Δ), III-DMF + 50 mole% DMSO in C_6H_6 (\square), IV-DMF + 60 mole% DMSO in C_6H_6 (\bullet), V-DMF + 80 mole% DMSO in C_6H_6 (∇), VI-DMF + 100 mole% DMSO in C_6H_6 (X), VII-DMF + 100 mole% DMSO in C_6H_6 (X), VIII-DMSO in CCl_4 (\odot).

The values of $\gamma (= \Delta H_\tau / \Delta H_\eta)$ for all the liquids except DMSO in CCl_4 are greater than 0.55, as obtained from the slope of the linear relation of $\ln(\tau_s T)$ with $\ln \eta$ indicating them as solid phase rotators in solvent environment. η is the coefficient of viscosity of solvent. ΔH_η due to viscous flow of the solvent is obtained from slope of $\ln(\tau_s T)$ against $1/T$ and known γ . Again, ΔH_η are greater than ΔH_τ for all the mixtures except 0,50 and 60 mole % DMSO in DMF and C_6H_6 . The difference in ΔH_τ and ΔH_η is due to the involvement of various types of bondings which are either formed or broken to some extent, depending on the temperature and concentration of the system. The negative values of ΔS_τ 's for all the system except 0 and 60 mole% DMSO in DMF and C_6H_6 indicate the existence of cooperative orientation of the molecules arising out of steric forces to yield more ordered states while the reverse is true for positive ΔS_τ 's. Although, ΔF_τ 's in all cases are almost constant at all temperatures, they increase with x_k of DMSO from $x_k = 0.0$ to $x_k = 0.5$ and then decrease gradually to $x_k = 1.0$ signifying the maximum dimerisation of DMF-DMSO mixture around $x_k = 0.5$. The formation of dimer causes larger molecular size and hence, the energy needed for rotation in the relaxation process is higher.

The hf conductivity K_{ijk} as a function of weight fraction w_{jk} is given by

$$K_{ijk} = \frac{\omega}{4\pi} (\epsilon'_{ijk} + \epsilon''_{ijk})^{1/2} \quad (3.3)$$

Since $\epsilon'_{ijk} \gg \epsilon''_{ijk}$ Eq. (3.1) can be written as

$$K_{ijk} = K_{\infty ij k} + \frac{1}{\omega \tau_{jk}} K'_{ijk}$$

or
$$\left(\frac{dK'_{ijk}}{dw_{jk}} \right) w_{jk} \rightarrow 0 = \omega \tau_{jk} \beta \quad (3.4)$$

Here β 's are the slopes of $K_{ijk} - w_{jk}$, $K_{ij} - w_j$ or $K_{ik} - w_k$ curves respectively, which are linear with almost identical intercepts probably due to same polarity

of the molecules [2]. The real part of *hf* conductivity, K'_{ijk} is again related to w_{jk} of *jk* polar solute dissolved in a nonpolar solvent (i) at temperature TK [12] as

$$K'_{ijk} = \frac{\mu_{jk}^2 N \rho_{ijk} F_{ijk}}{3M_{jk} kT} \left(\frac{\omega^2 \tau_{jk}}{1 + \omega^2 \tau_{jk}^2} \right) w_{jk} \quad (3.5)$$

Differentiating Eq. (3.5) with respect to w_{jk} and comparing the result at $w_{jk} \rightarrow 0$ to Eq. (3.4), one obtains the following relation

$$\mu_{jk} = \left[\frac{27M_{jk} kT}{N \rho_i (\epsilon_i + 2)^2} \cdot \frac{\beta}{\omega b} \right]^{1/2} \quad (3.6)$$

to estimate μ_{jk} , μ_j or μ_k of the respective solutes. b is a dimensionless parameter in terms of estimated τ_{jk} , τ_j or τ_k given by :

$$b = \frac{1}{1 + \omega^2 \tau_{jk}^2} \quad (3.7)$$

The other terms in Eq. (3.6) carry usual significance [2]. All the μ 's are then plotted against different x_k 's of DMSO at each temperature as shown in Figure 3.1. It shows the gradual rise of μ_{jk} in the range $0 < x_k \leq 0.5$. It then decreases slowly in order to exhibit the convex nature of each curve with an abnormally low value of μ_{jk} around $x_k = 0.6$. This sort of behaviours of $\mu_{jk} - x_k$ curves (Figure 3.1) is explained by the fact that dimers are being formed from $x_k \geq 0$ to $x_k = 0.6$, causing increase of μ . The rupture of dimerisation *i.e.* self association occurs in higher concentrations in the range $0.6 \leq x_k < 1.0$ to yield lower values of μ 's. But around $x_k = 0.6$ all μ_{jk} 's are minimum indicating the possible occurrence of double relaxation phenomena in such mixtures. μ_{jk} together with μ_j and μ_k for each mixture of a fixed concentration are shown graphically only to observe their temperature dependence like $\mu_{jk} = a + bt + ct^2$ with coefficients a , b and c as seen in Figure 3.3. The variation is concave with maximum depression at 17 mole% DMSO in DMF mixture. The depression gradually decreases upto $x_k = 0.6$ of DMSO in DMF and C_6H_6

probably due to solute-solute molecular association in the range $0 < x_k < 0.6$. The maximum dimerisation is, however, inferred from low μ 's because of the larger molecular sizes as confirmed by high values of $\tau_s T / \eta'$ (being proportional to volume of the rotating unit) for 60 mole% DMSO in DMF and C_6H_6 . As temperature increases the dipole-dipole interaction is weakened and the absorption of hf electric energy increases resulting in the rupture of dimer to yield high μ 's for smaller molecular species [10]. The slight convex nature of curves for 0 mole% DMSO in DMF and C_6H_6 and DMSO in C_6H_6 along with almost straight line variation of 100 mole% DMSO in DMF and C_6H_6 and DMSO in CCl_4 (Figure 3.3) is probably due to solute-solvent molecular interaction of either DMF with C_6H_6 or DMSO with C_6H_6 and CCl_4

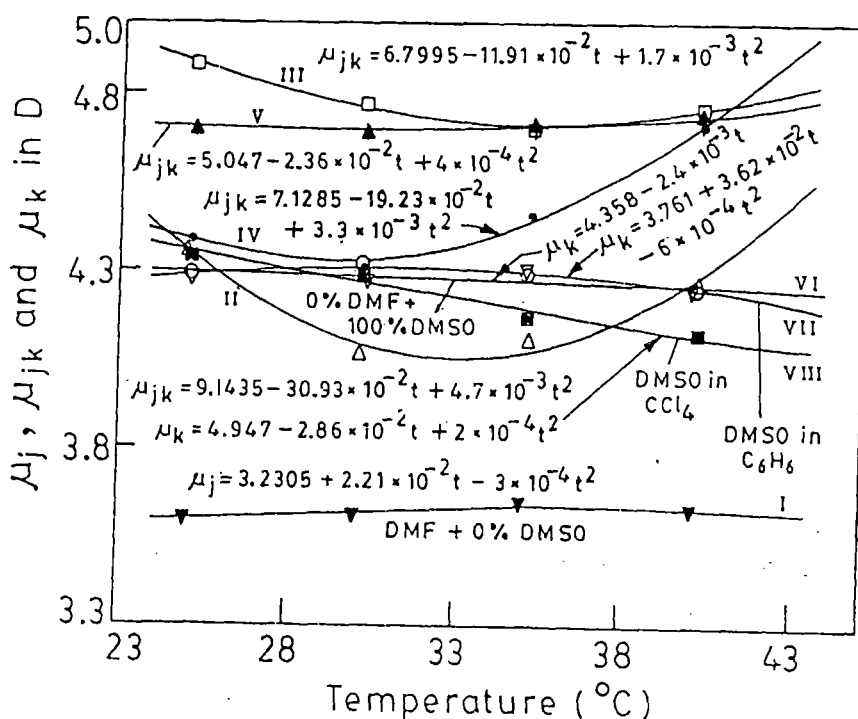


Figure 3.3 : Variation of μ_j , μ_{jk} and μ_k of binary and single polar solutes in nonpolar solvent with temperature t in $^{\circ}C$.

I-DMF + 0 mole% DMSO in C_6H_6 (\blacktriangledown), II-DMF+17 mole % DMSO in C_6H_6 (Δ), III-DMF+50 mole % DMSO in C_6H_6 (\square), IV-DMF +60 mole % DMSO in C_6H_6 (\bullet), V-DMF+80 mole % DMSO in C_6H_6 (\blacktriangle), VI-DMF+100 mole % DMSO in C_6H_6 (∇), VII-DMSO in C_6H_6 (\circ), VIII-DMSO in CCl_4 (\blacksquare).

respectively as illustrated in Figure 3.4. The associations of DMF, DEF and DMSO in C_6H_6 can arise due to interactions of fractional positive charges of N and S atoms of the molecules with the π delocalised electron cloud of C_6H_6 ring as seen in Figure 3.4 (i), (iii) and (iia) respectively. Again, one of C-Cl dipoles of CCl_4 , owing to more -ve charge on Cl atom, interacts with the

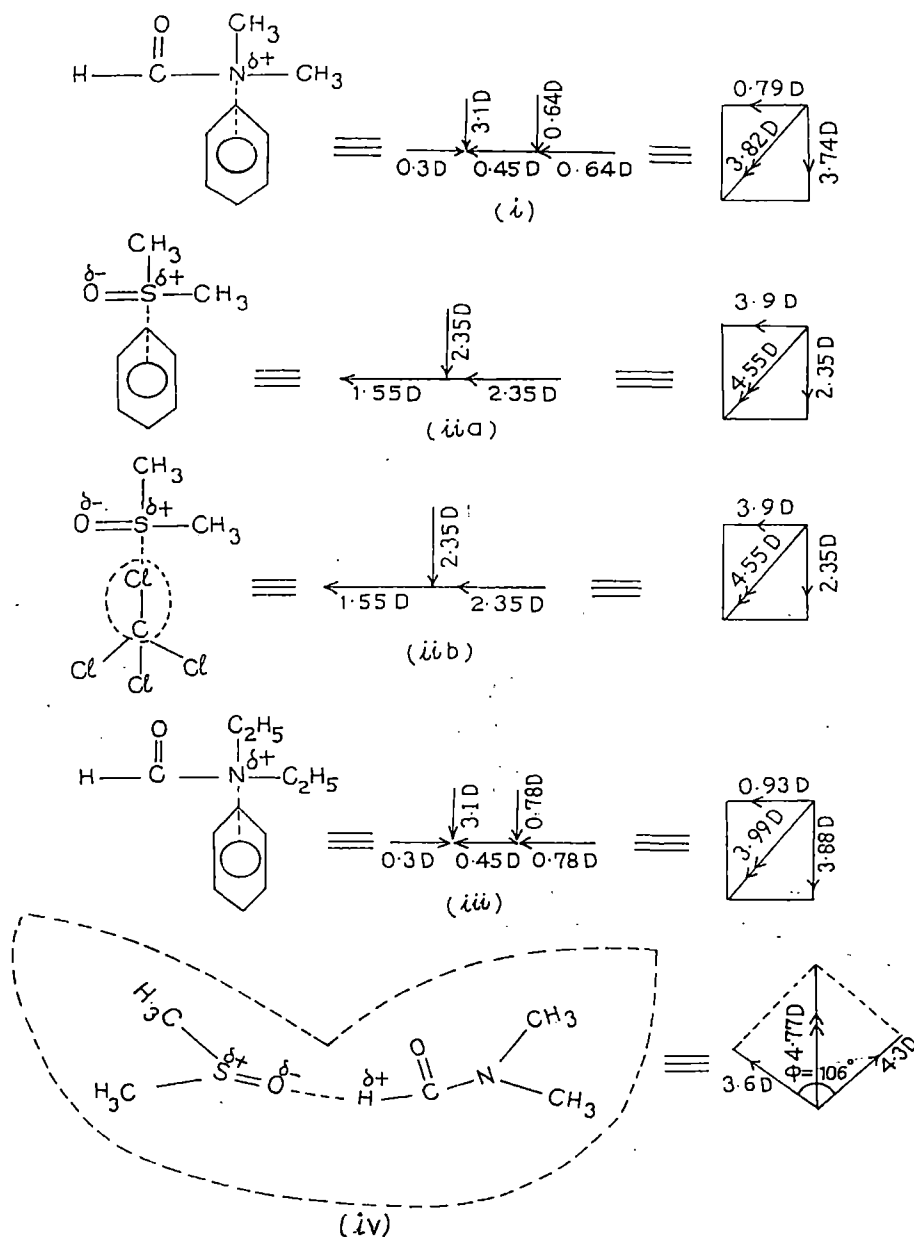


Figure 3.4 : Conformational structures along with solute-solvent and solute-solute interaction of molecules. (i) DMF in C_6H_6 , (iia) DMSO in C_6H_6 (iib) DMSO in CCl_4 , (iii) DEF in C_6H_6 , (iv) DMSO-DMF dimer.

fractional +ve charge of S-atom of DMSO (Figure 3.4 (iib)). The $\mu_{\text{theo}} = 4.55$ D of DMSO is, however, computed from available bond moments of 2.35 D and 1.55 D for $\text{S} \leftarrow \text{CH}_3$ and $\text{O} = \text{S}$ respectively, assuming the molecule to be planer one. The major contributions to μ_{theo} for DMF and DEF are due to 0.64 D and 0.78 D for $\text{N} \leftarrow \text{CH}_3$ and $\text{N} \leftarrow \text{C}_2\text{H}_5$ since the other common bond moments in them are the same with values of 0.3 D, 0.45 D and 3.10D for $\text{C} \leftarrow \text{H}$, $\text{C} \leftarrow \text{N}$ and $\text{C} \leftarrow \text{O}$ respectively. Figure 3.4 (iv), however, shows a certain angle $\phi (= 106^\circ)$ between monomeric μ 's of DMF and DMSO to have $\mu_{\text{theo}} = 4.77$ D of dimer below $x_k = 0.6$.

The slight deviations of the μ 's from the μ_{theo} 's occur probably due to the presence of inductive and mesomeric moments of such molecules. This is also observed elsewhere [13]. The corrected μ 's obtained from the reduced bond moments of the substituent groups by factors $\mu_{\text{cal}} / \mu_{\text{theo}}$ establish the above facts at different temperatures, too. Thus the dielectric relaxation parameters from *hf* conductivity measurements offer a useful tool to arrive at the structural and associational aspects of the non-spherical polar liquids.

References

- [1] C R. Acharyya, A.K. Chatterjee, P K Sanyal and S Acharyya *Indian J. Pure & Appl. Phys.* **24** (1986). 234.
- [2] A K Chatterjee, U Saha, N Nandi, R C Basak and S Acharyya *Indian J. Phys.* **66B** (1992) 291.
- [3] U Saha and S Acharyya *Indian J. Pure & Appl. Phys.* **3** (1993), 181.
- [4] A Sharma D R Sharma and M S Chauhan *Indian J. Pure & Appl. Phys.* **31**(1993) 841.
- [5] A Sharma and D R Sharma *J. Phys. Soc. Japan.* **61** (1992),1049.
- [6] A R Saksena *Indian J. Pure & Appl. Phys.* **16** (1978).1079.
- [7] U Saha and S Acharyya *Indian J. Pure & Appl. Phys.* **32** (1994).346.
- [8] F J Murphy and S O Morgan *Bell. Syst. Tech. J.* **18** (1939).502.
- [9] K V. Gopalakrishna *Trans. Faraday Soc.* **53** (1957):767.

- [10] S K Sit and S Acharyya *Indian J. Phys.* **70B** (1996), 19
- [11] H Eyring, S Glasstone and K J Laidler *The Theory of Rate Process* (New York : McGraw Hill) (1941).
- [12] C P Smyth *Dielectric Behaviour and Structure* (New York : McGraw Hill) (1955).
- [13] R C Basak, S K Sit, N Nandi and S Acharyya *Indian J. Phys.* **70B** (1996), 37.

CHAPTER -4

DOUBLE RELAXATIONS OF SOME ISOMERIC OCTYL ALCOHOLS BY HIGH FREQUENCY ABSORPTION IN NONPOLAR SOLVENT

DOUBLE RELAXATIONS OF SOME ISOMERIC OCTYL ALCOHOLS BY HIGH FREQUENCY ABSORPTION IN NON-POLAR SOLVENT

4.1. Introduction

The dielectric relaxation mechanism of a polar-nonpolar liquid mixture is a very convenient and useful tool in ascertaining the shape, size and structure of a polar molecule [1]. The process is generally involved with the estimation of dipole moment μ in terms of the relaxation time τ for a polar molecule in a nonpolar solvent under different high frequency (*hf*) electric field of gigahertz (GHz) range at a fixed or different temperatures. There exist several methods[2] to estimate τ of a polar liquid in a nonpolar solvent. They offer a deep insight into the intrinsic properties of a polar molecule because of the absence of dipole-dipole interactions in polar-nonpolar liquid mixtures.

Highly non-spherical polar molecules, on the other hand, possess more than one τ in the electric field of GHz range for the rotations of different substituent groups attached to the parent molecule and the whole molecule itself. Budo[3], however, proposed that complex dielectric constant ϵ^* , of a polar liquid may be represented as the sum of a number of non-interacting Debye type dispersions each with a characteristic τ . The method was then made simpler by Bergmann *et al.* [4] by assuming that the dielectric relaxation is the sum of two Debye type dispersions characterised by the intramolecular and molecular τ_1 and τ_2 respectively. The corresponding relative contributions c_1 and c_2 towards dielectric relaxations could then be estimated. They used a graphical analysis which consists of plotting normalised values of $(\epsilon' - \epsilon_\infty)/(\epsilon_0 - \epsilon_\infty)$ against $\epsilon''/(\epsilon_0 - \epsilon_\infty)$ on a complex plane in terms of the measured real ϵ' , imaginary ϵ'' parts of ϵ^* , static dielectric constant ϵ_0 and high frequency dielectric constant ϵ_∞ of a polar liquid for different frequencies of the electric field. A number of chords were then drawn through the points on the curve until a set of parameters was found out in consistency with all the experimental points. Bhattacharyya

et al. [5] subsequently modified the above procedure to get τ_1 , τ_2 and c_2, c_2 for a polar liquid from the relaxation data measured at least at two different frequencies of the electric fields.

A procedure was devised [6] to get τ_1 and τ_2 from the slope and intercept of a derived straight line equation involved with the single frequency measurements of the dielectric relaxation parameters like ϵ_{oij} , $\epsilon_{\infty ij}$, ϵ'_{ij} and ϵ''_{ij} for different weight fractions w_j 's of a polar solute (j) in a nonpolar solvent (i) at a given temperature. The technique had already been applied on disubstituted benzenes and anilines [6] at 9.945 GHz electric field as well as monosubstituted anilines[7] at 22.06, 3.86, 2.02 GHz electric fields respectively. All these investigations reveal that they often showed the double relaxation behaviour at certain frequency of the electric field.

The aliphatic alcohols are long straight chain, hydrogen bonded polymer type molecules having possibility of their bending, twisting and rotation under *hf* electric field each with a characteristic τ , besides the average macroscopic distribution of τ . The alcohols have high dipole moments owing to their strong intermolecular forces exerted by them like polymers in solution. Onsager's equation may be a better choice for such associative liquids, but it is not so simple like Debye's equation because of the presence of quadratic term ϵ^*_{ij} . The relaxation behaviour of aliphatic alcohols is very interesting because they show more than two τ 's in pure state, but for a polar-nonpolar liquid mixture *hf* process becomes increasingly important on dilution [8,9]. An extensive study to detect the frequency dependence of double relaxation behaviour of four long chain normal aliphatic alcohols like 1-butanol, 1-hexanol, 1-heptanol, 1-decanol in solvent n-heptane [10] including methanol and ethanol at 9.84 GHz in benzene [11,12] at 25°C was already made [13]. All the alcohols showed τ_1 and τ_2 at all frequencies of the electric field except methanol which is a simple molecule to possess the expected τ_2 only.

The method [6] was applied on six isomeric octyl alcohols like 2-methyl-3-heptanol, 3-methyl-3-heptanol, 4-methyl-3-heptanol, 5-methyl-3-heptanol, 4-octanol and 2-octanol at 24.33, 9.25 and 3.00 GHz electric fields, as reported in Tables 1-3 respectively, because of the availability of ϵ'_{ij} , ϵ''_{ij} , ϵ_{0ij} and $\epsilon_{\infty ij}$ measured by Crossley *et al.* [14] in n-heptane at 25°C. The straight line equations between $(\epsilon_{0ij} - \epsilon'_{ij}) / (\epsilon'_{ij} - \epsilon_{\infty ij})$ and $\epsilon''_{ij} / (\epsilon'_{ij} - \epsilon_{\infty ij})$ for all the octyl alcohols at different w_j 's are linear as shown in Figure 4.1 only to establish the applicability of Debye model in such isomeric alcohols like normal alcohols [13] once again. Moreover, all the long chain octyl alcohols are structural isomers with the molecular formula $C_8H_{18}O$ having greater number of C-atoms in their structures. They are, therefore, expected to possess two relaxation processes at audio and radio frequencies of electric field at low temperature in pure state [14].

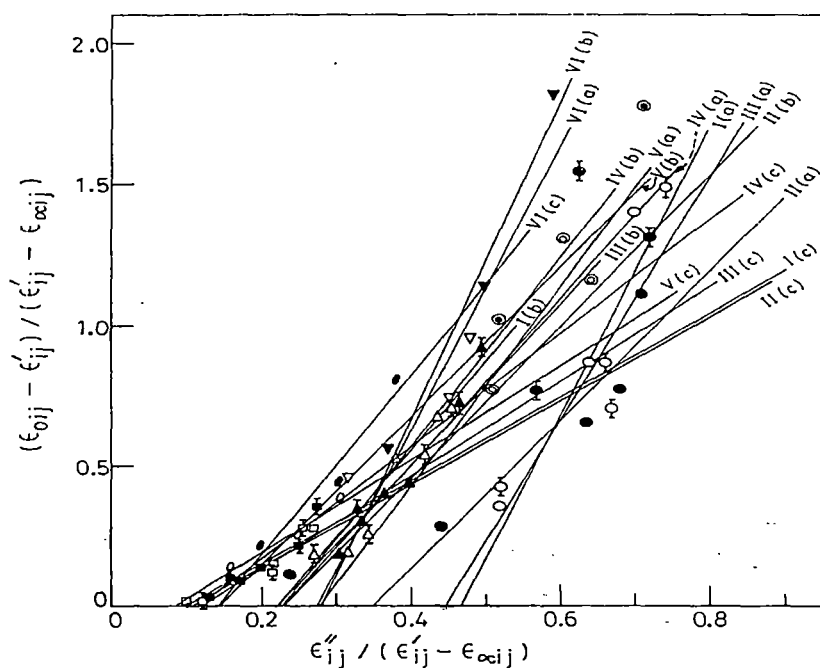


Figure 4.1 : Plot of $(\epsilon_{0ij} - \epsilon'_{ij}) / (\epsilon'_{ij} - \epsilon_{\infty ij})$ against $\epsilon''_{ij} / (\epsilon'_{ij} - \epsilon_{\infty ij})$ of some isomeric octyl alcohols in n-heptane at 25°C.

Ia, Ib, Ic for 2 methyl 3 heptanol at 24.33, 9.25 and 3.00 GHz (O, Δ , \square)
 IIa, IIb, IIc for 3 methyl 3 heptanol at 24.33, 9.25 and 3.00 GHz (\bullet , \blacktriangle , \blacksquare)
 IIIa, IIIb, IIIc for 4 methyl 3 heptanol at 24.33, 9.25 and 3.00 GHz (\circ , \triangle , \square)
 IVa, IVb, IVc for 5 methyl 3 heptanol at 24.33, 9.25, and 3.00 GHz (\odot , \blacktriangle , \blacksquare)
 Va, Vb, Vc for 4 octanol at 24.33, 9.25 and 3.00 GHz (\ominus , ∇ , \circ)
 VIa, VIb, VIc for 2 octanol at 24.33, 9.25 and 3.00 GHz (\odot , \blacktriangledown , \bullet)

Table 4.1 : The estimated relaxation times τ_2 and τ_1 from the slopes and the intercepts of straight line Eq. (4.8) with % of errors and correlation coefficients (r) together with measured τ_s from $K''_{ij}-K'_{ij}$ curve and most probable relaxation time $\tau_0 = \sqrt{\tau_1\tau_2}$ for six isomeric octyl alcohols at 25°C under different frequencies of electric fields.

System with Sl. No.&Mol.wt.M _i	Frequency in GHz	Intercept & slope of Eq.(4.8)		Correlation coefficient (r)	% Error in regression technique	Estimated value of τ_2 & τ_1 in p. Sec.		Measured τ_s in p. Sec.	Most probable relaxation time $\tau_0 = \sqrt{\tau_1\tau_2}$
I 2-methyl-3-heptanol(a) in n-heptane M _i =130gm	24.33	2.3718	5.0952	0.9011	6.34	29.96	3.39	1.84	10.08
	9.25	0.6871	3.1205	0.9700	1.90	49.61	4.10	3.58	14.26
	3.00	0.1408	1.4830	0.9771	1.50	73.31	5.41	6.74	19.91
II 3-methyl-3-heptanol(a) in n-heptane M _i =130gm	24.33	0.9087	2.6282	0.9294	4.59	14.52	2.68	2.19	6.24
	9.25	0.6389	2.7714	0.9709	1.93	43.34	4.37	3.70	13.76
	3.00	0.1611	1.5018	0.9985	0.10	73.55	6.17	5.58	21.30
III 4-methyl-3-heptanol(a) in n-heptane M _i =130gm	24.33	1.9653	4.3873	0.8851	7.30	25.40	3.31	1.90	9.17
	9.25	0.6411	2.8636	0.9682	2.11	45.08	4.21	4.13	13.78
	3.00	0.2008	1.7153	0.9206	5.14	84.34	6.71	11.98	23.79
IV 5-methyl-3-heptanol(a) in n-heptane M _i =130gm	24.33	0.6929	2.9788	0.5684	26.36	17.83	1.66	1.71	5.44
	9.25	0.7445	3.2866	0.9846	1.19	52.36	4.21	5.39	14.85
	3.00	0.2362	2.0308	0.9371	4.74	101.22	6.58	13.11	25.81
V 4-octanol in n-heptane M _i =130gm	24.33	0.9572	3.4750	0.8569	10.34	20.77	1.97	1.83	5.40
	9.25	0.3810	2.6361	0.9470	4.02	42.74	2.64	5.46	10.62
	3.00	0.1428	1.6929	0.9846	1.18	85.13	4.72	12.76	20.05
VI 2-octanol in n-heptane M _i =130 gm.	24.33	1.3664	5.0208	0.6336	23.30	30.97	1.89	1.83	7.65
	9.25	1.5853	5.6407	0.9888	0.86	92.00	5.11	6.26	21.68
	3.00	0.4458	3.1697	0.9780	1.69	160.41	7.83	18.70	35.44

Table 4.2 : Fröhlich parameter A, relative contributions c_1 and c_2 due to τ_1 and τ_2 , theoretical values of x and y from Fröhlich's Eqs(4.9) and (4.10) and from graphical extrapolation technique at $\omega_j \rightarrow 0$.

System with Sl. No.	Frequency, GHz	Fröhlich parameter A = ln(τ_1/τ_2)	Theoretical values of x & y from Eqs. (4.9) and (4.10)		Theoretical values of c_1 & c_2		Estimated values of x & y at $\omega_j \rightarrow 0$		Estimated values of c_1 and c_2	
I 2-methyl-3-heptanol in n-heptane	(a) 24.33	2.1790	0.3457	0.4028	0.3686	1.2101	0.795	0.366	1.0226	-0.2476
	(b) 9.25	2.4932	0.5637	0.4023	0.4886	0.9434	1.075	0.19	1.1624	-0.2324
	(c) 3.00	2.6063	0.7973	0.3232	0.6144	0.5500	1.075	0.074	1.1143	-0.0808
II 3-methyl-3-heptanol(a) in n-heptane	24.33	1.6997	0.5195	0.4490	0.4542	0.7733	0.865	0.32	1.0321	-0.1120
	(b) 9.25	2.2943	0.5792	0.4115	0.4922	0.8573	0.91	0.256	0.9569	0.0810
	(c) 3.00	2.4781	0.7865	0.3349	0.6028	0.5600	1.025	0.094	1.0589	-0.0579
III 4-methyl-3-heptanol(a) in n-heptane	24.33	2.0378	0.3747	0.4173	0.3857	1.0842	0.78	0.35	0.9961	-0.2117
	(b) 9.25	2.3710	0.5775	0.4075	0.4932	0.8812	0.95	0.208	1.0177	-0.0805
	(c) 3.00	2.5313	0.7543	0.3490	0.5902	0.6112	1.015	0.094	1.0551	-0.0827
IV 5-methyl-3-heptanol(a) in n-heptane	24.33	2.3741	0.5644	0.4088	0.4862	0.9057	0.645	0.274	0.6389	0.3763
	(b) 9.25	7.5207	0.5499	0.4020	0.4814	0.9805	0.95	0.172	1.0297	-0.2211
	(c) 3.00	2.7332	0.7222	0.3529	0.5833	0.6848	1.065	0.042	1.1326	-0.2341
V 4-octanol in n-heptane	(a) 24.33	2.3555	0.5080	0.4131	0.4553	1.0030	0.72	0.22	0.7840	0.0126
	(b) 9.25	2.7833	0.6506	0.8720	0.5463	0.8372	0.895	0.116	0.9254	-0.0654
	(c) 3.00	2.8924	0.7813	0.3197	0.6210	0.5900	0.99	0.052	1.0218	-0.0850
VI 2-octanol in n-heptane	(a) 24.33	2.7964	0.4507	0.3867	0.4257	1.3507	0.67	0.208	0.7223	0.0764
	(b) 9.25	2.3925	0.4292	0.3795	0.4124	1.4780	0.895	0.214	0.9850	-0.3026
	(c) 3.00	3.0198	0.6201	0.3658	0.5361	0.9672	1.04	0.102	1.0810	-0.1813

The paper presents the frequency dependence of τ_1 and τ_2 at all frequencies of 24.33, 9.25 and 3.00 GHz electric field for all the octyl alcohols like normal alcohols too. The measured τ_s from the slope of the linear equation of imaginary

K''_{ij} and real K'_{ij} part of the total complex hf conductivity K^*_{ij} and the most probable relaxation time τ_0 from $\tau_0 = \sqrt{\tau_1\tau_2}$ are placed in Table 4.1 together with the estimated τ_1 and τ_2 in order to see their trends with frequency of the applied electric field. The relative contributions c_1 and c_2 towards dielectric relaxations in terms of intramolecular relaxation time τ_1 and molecular relaxation time τ_2 are then estimated from Fröhlich's equations [15] as well as the graphical method of Figures 4.2 and 4.3. The estimated c_1 and c_2 are placed in Table 4.2.

The dipole moments μ_1 and μ_2 due to flexible parts as well as the whole molecules in terms of the estimated τ_1 and τ_2 and the slopes β of the linear variation of hf conductivity K_{ij} with w_j are shown in Table 4.3.

Table 4.3 : Estimated intercept and slope of $K_{ij}-w_j$ equation, dimensionless parameters b_1, b_2 Eq.(4.16), estimated dipole moments μ_2, μ_1 Eq.(4.15), μ_{theo} from bond angles and bond moments together with μ_1 from $\mu_1 = \mu_2 (c_1/c_2)^{1/2}$ in Debye.

System with Sl. No. & Mol wt.	Frequency GHz	Intercept & slope of of $K_{ij}-w_j$ equation		Dimensionless parameter		Estimated dipole moments (In Debye)		μ_{theo} in D	Estimated μ_1 in D from $\mu_1 = \mu_2(c_1/c_2)^{1/2}$
		$\alpha \times 10^{-18}$	$\beta \times 10^{-10}$	b_1	b_2	μ_2	μ_1		
I 2-methyl-3-heptanol(a) in n-heptane $M_1 = 130\text{gm}$	24.33	2.3632	0.6974	0.0455	0.7885	4.80	1.15	1.76	2.65
	(b) 9.25	0.8998	0.3126	0.1075	0.9463	3.39	1.14		2.44
	(c) 3.00	0.2911	0.1224	0.3439	0.9897	2.08	1.23		2.20
II 3-methyl-3-heptanol(a) in n-heptane $M_1 = 130\text{gm}$	24.33	2.3630	0.7490	0.1689	0.8564	2.58	1.15	1.76	1.98
	(b) 9.25	0.8959	0.3554	0.1363	0.9395	3.21	1.22		2.43
	(c) 3.00	0.2910	0.1330	0.3425	0.2867	2.18	1.29		2.26
III 4-methyl-3-heptanol(a) in n-heptane $M_1 = 130\text{gm}$	24.33	2.3635	0.7213	0.6230	0.7963	4.17	1.17	1.76	2.49
	(b) 9.25	0.8984	0.3278	0.1273	0.9436	3.19	1.17		2.39
	(c) 3.00	0.2911	0.1283	0.2837	0.9843	2.35	1.26		2.31
IV 5-methyl-3-heptanol(a) in n-heptane $M_1 = 130\text{gm}$	24.33	2.3646	0.6415	0.1187	0.9396	2.85	1.01	1.76	2.09
	(b) 9.25	0.9021	0.2771	0.0975	0.9436	3.35	1.08		2.35
	(c) 3.00	0.2922	0.1138	0.2157	0.9849	2.54	1.19		2.34
V 4-octanol in n-heptane $M_1 = 130\text{gm}$	(a) 24.33	2.3561	0.6492	0.0903	0.9169	3.29	1.03	1.08	2.22
	(b) 9.25	0.8965	0.2618	0.1396	0.9770	2.72	1.03		2.20
	(c) 3.00	0.2919	0.1044	0.2799	0.9922	2.13	1.13		2.19
VI 2-octanol in n-heptane $M_1 = 130\text{ gm.}$	(a) 24.33	2.3533	0.6572	0.9428	0.9230	4.80	1.03	1.08	2.69
	(b) 9.25	0.8980	0.2753	0.0338	0.9190	5.67	1.09		3.00
	(c) 3.00	0.2897	0.1221	0.0887	0.9787	3.88	1.23		2.89

The slopes β and the intercepts α of the linear variation of K_{ij} with w_j , as placed in Table 4.3, at each frequency for all isomers in n-heptane are almost the same probably due to their same polarity [16]. This fact is also supported by their conformations as shown in Figure 4.4. It was, therefore, very difficult to plot K_{ij} against w_j . The computed μ_2 's for most of the isomeric alcohols show larger

values at 24.33 GHz and gradually decrease with lower frequencies unlike μ_1 . In order to compare μ_2 and μ_1 with theoretical dipole moments μ_{theo} , a special attention is to be paid on the conformational structure of each isomer from the available bond angles and bond moment. They are shown in Figure 4.4. Using the usual C—C bond moment of 0.09 D from methanol and ethanol [13] μ_{theo} for four methyl substituted octanols are found to show slightly larger values (see Figure 4.4 and Table 4.3) than 1-heptanol [13] except the desired values for 2-octanol and 4-octanol perhaps due to bond moments of C—H₃ and —O—H groups in their structures. The calculated value of μ_1 from $\mu_1 = \mu_2 (c_1/c_2)^{1/2}$ assuming two relaxation processes are equally probable, are also placed in the last column of Table 4.3 with all the estimated μ 's for comparison.

4.2. Theoretical Formulations to Estimate Relaxation Parameters

The complex dielectric constant ϵ_{ij}^* of a polar-nonpolar liquid mixture can be represented as the sum of a number of non-interacting Debye type dispersions in accordance with Budo's [3] relation.

$$\frac{\epsilon_{ij}^* - \epsilon_{\infty ij}}{\epsilon_{0ij} - \epsilon_{\infty ij}} = \sum \frac{c_k}{1 + j\omega\tau_k} \quad (4.1)$$

Where $j = \sqrt{-1}$ is complex number and $\sum c_k = 1$. The term c_k is the relative contribution for the k th type of relaxation processes. When ϵ_{ij}^* consists of two Debye type dispersions, Budo's relation reduces to Bergmann's equations [4].

$$\frac{\epsilon'_{ij} - \epsilon_{\infty ij}}{\epsilon_{0ij} - \epsilon_{\infty ij}} = \frac{c_1}{1 + \omega^2\tau_1^2} + \frac{c_2}{1 + \omega^2\tau_2^2} \quad (4.2)$$

and

$$\frac{\epsilon''_{ij}}{\epsilon_{0ij} - \epsilon_{\infty ij}} = c_1 \frac{\omega\tau_1}{1 + \omega^2\tau_1^2} + c_2 \frac{\omega\tau_2}{1 + \omega^2\tau_2^2} \quad (4.3)$$

such that $c_1 + c_2 = 1$. Now with

$$\frac{\varepsilon'_{ij} - \varepsilon_{\infty ij}}{\varepsilon_{0ij} - \varepsilon_{\infty ij}} = x, \quad \frac{\varepsilon''_{ij}}{\varepsilon_{0ij} - \varepsilon_{\infty ij}} = y$$

$\omega\tau = \alpha$ and using $a = (1/1+\alpha^2)$ $b = \alpha/(1+\alpha^2)$ the Eqs (4.2) and (4.3) can be written as;

$$x = c_1 a_1 + c_2 a_2 \quad (4.4)$$

$$y = c_1 b_1 + c_2 b_2 \quad (4.5)$$

where suffixes 1 and 2 with a and b are related to τ_1 and τ_2 respectively. From Eqs (4.4) and (4.5), since $\alpha_2 - \alpha_1 \neq 0$ and $\alpha_2 > \alpha_1$ we have

$$c_1 = \frac{(x\alpha_2 - y)(1 + \alpha_1^2)}{\alpha_2 - \alpha_1} \quad (4.6)$$

$$c_2 = \frac{(y - x\alpha_1)(1 + \alpha_2^2)}{\alpha_2 - \alpha_1} \quad (4.7)$$

Since $c_1 + c_2 = 1$, we get the following equation with the help of Eqs (4.6) and (4.7):

$$\frac{1-x}{y} = (\alpha_1 + \alpha_2) - \frac{x}{y} \alpha_1 \alpha_2$$

which on substitution of the values x , y and α yields :

$$\frac{\varepsilon_{0ij} - \varepsilon'_{ij}}{\varepsilon'_{ij} - \varepsilon_{\infty ij}} = \omega(\tau_1 + \tau_2) \frac{\varepsilon''_{ij}}{\varepsilon'_{ij} - \varepsilon_{\infty ij}} - \omega^2 \tau_1 \tau_2 \quad (4.8)$$

Eq. (4.8) is thus a straight line equation between $(\varepsilon_{0ij} - \varepsilon'_{ij}) / (\varepsilon'_{ij} - \varepsilon_{\infty ij})$ and $\varepsilon''_{ij} / (\varepsilon'_{ij} - \varepsilon_{\infty ij})$ with slope $\omega(\tau_1 + \tau_2)$ and intercept $-\omega^2 \tau_1 \tau_2$ respectively, where ω is the angular frequency of the applied electric field of frequency f in GHz. With the measured dielectric relaxation data of ε'_{ij} , ε''_{ij} , ε_{0ij} and $\varepsilon_{\infty ij}$ for different weight fractions w_j 's of each octyl alcohol in n-heptane at 25°C under 24.33, 9.25 and 3.00 GHz electric field [14] we get slope and intercept of Eq. (4.8) to yield τ_1 and τ_2 as shown in Table 4.1.

The relative contributions, c_1 and c_2 towards the dielectric relaxations in terms of x , y and τ_1 , τ_2 for each octyl alcohol are found out and placed in Table 4.2. The theoretical values [15] of x and y are, however, calculated from Fröhlich's Eqs:

$$x = \frac{\epsilon'_{ij} - \epsilon_{\infty ij}}{\epsilon_{0ij} - \epsilon_{\infty ij}} = 1 - \frac{1}{2A} \ln \left(\frac{e^{2A} \omega^2 \tau_1^2 + 1}{1 + \omega^2 \tau_1^2} \right) \quad (4.9)$$

$$y = \frac{\epsilon''_{ij}}{\epsilon_{0ij} - \epsilon_{\infty ij}} = \frac{1}{A} [\tan^{-1}(e^A \omega \tau_1) - \tan^{-1}(\omega \tau_1)] \quad (4.10)$$

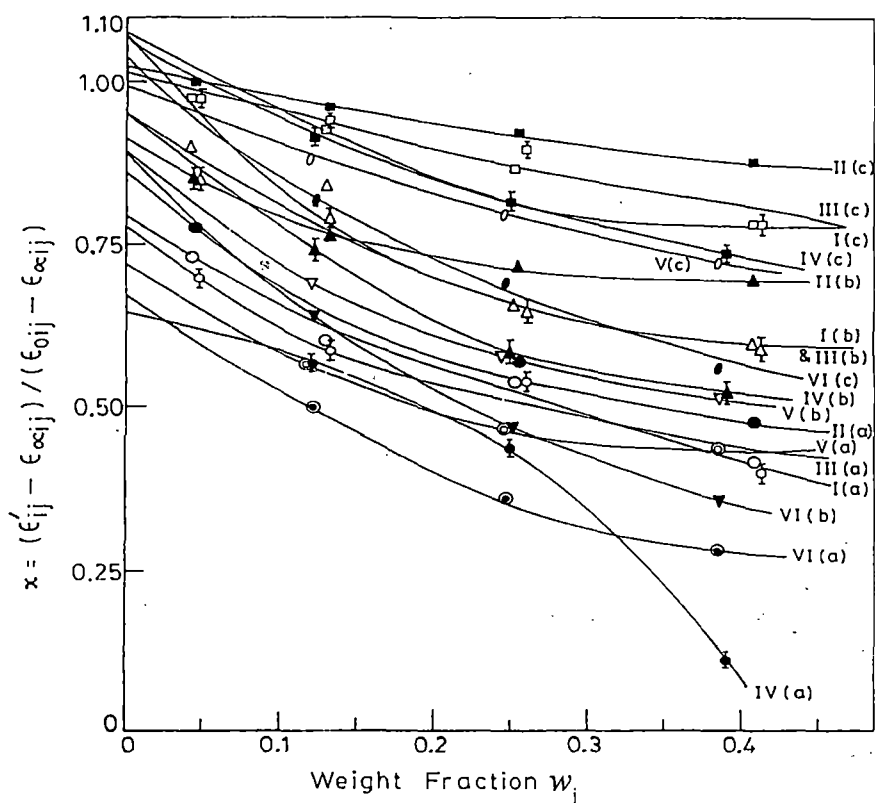


Figure 4.2 : Plot of $(\epsilon'_{ij} - \epsilon_{\infty ij}) / (\epsilon_{0ij} - \epsilon_{\infty ij})$ against weight fraction w_j of some isomeric octyl alcohols in n-heptane at 25°C.

Ia, Ib, Ic for 2 methyl 3 heptanol at 24.33, 9.25 and 3.00 GHz (O, Δ , \square)

Ila, Ilb, Ilc for 3 methyl 3 heptanol at 24.33, 9.25 and 3.00 GHz (\bullet , \blacktriangle , \blacksquare)

IIIa, IIIb, IIIc for 4 methyl 3 heptanol at 24.33, 9.25 and 3.00 GHz (\circ , Δ , \square)

IVa, IVb, IVc for 5 methyl 3 heptanol at 24.33, 9.25, and 3.00 GHz (\diamond , \blacktriangle , \blacksquare)

Va, Vb, Vc for 4 octanol at 24.33, 9.25 and 3.00 GHz (\odot , ∇ , \circ)

VIa, VIb, VIc for 2 octanol at 24.33, 9.25 and 3.00 GHz (\odot , \blacktriangledown , \bullet)

where $A = \text{Fröhlich parameter} = \ln(\tau_2/\tau_1)$ and τ_1 is called the small limiting relaxation time as obtained from the double relaxation method. A simple graphical extrapolation technique, on the other hand, was considered to get the values of x and y at $w_j \rightarrow 0$ from Figures 4.2 and 4.3 respectively. This is really in accordance with Bergmann's Eqs (4.2) and (4.3) when the once estimated τ_1 and τ_2 from Eq. (4.8) are substituted in the right hand sides of above Eqs (4.2) and (4.3).

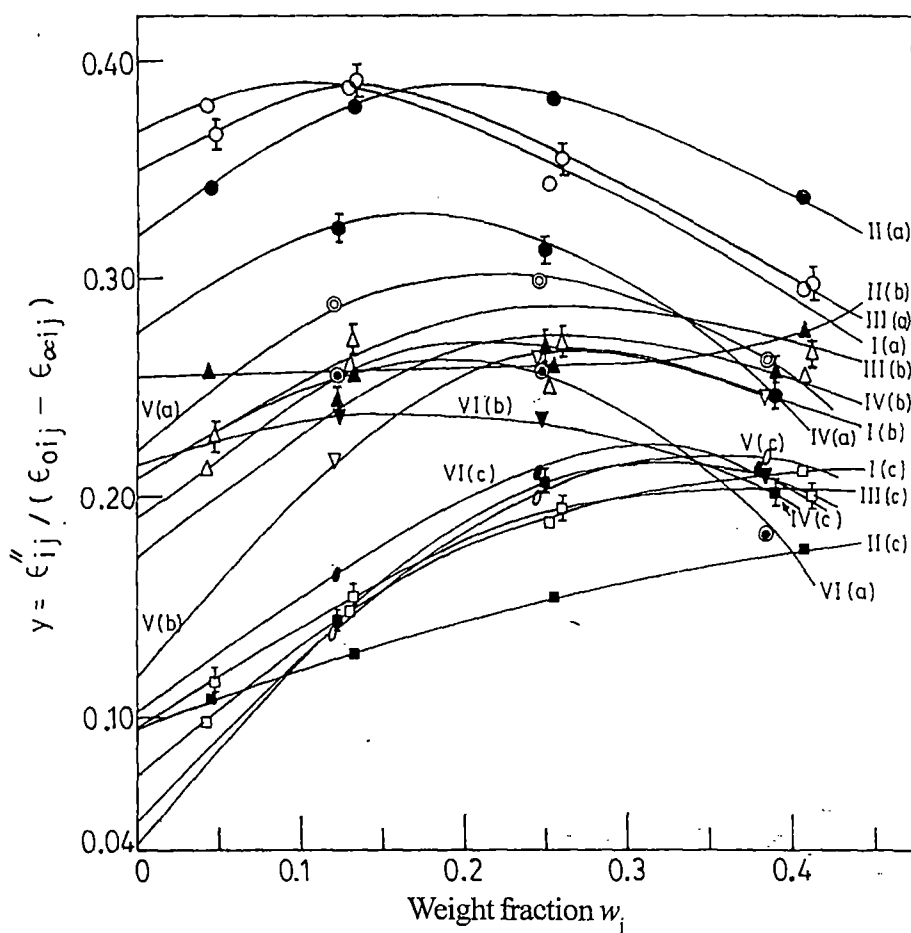


Figure 4.3 : Plot of $\epsilon''_{ij}/(\epsilon_{0ij}-\epsilon_{\infty ij})$ against weight fraction w_j of some isomeric octyl alcohols in n-heptane at 25°C.

Ia, Ib, Ic for 2 methyl 3 heptanol at 24.33, 9.25 and 3.00 GHz (O, Δ , \square)

Ila, IIb, IIc for 3 methyl 3 heptanol at 24.33, 9.25 and 3.00 GHz (\bullet , \blacktriangle , \blacksquare)

IIIa, IIIb, IIIc for 4 methyl 3 heptanol at 24.33, 9.25 and 3.00 GHz (\odot , \triangleleft , \square)

IVa, IVb, IVc for 5 methyl 3 heptanol at 24.33, 9.25, and 3.00 GHz (\odot , \blacktriangle , \blacksquare)

Va, Vb, Vc for 4 octanol at 24.33, 9.25 and 3.00 GHz (\odot , ∇ , \circ)

VIa, VIb, VIc for 2 octanol at 24.33, 9.25 and 3.00 GHz (\odot , \blacktriangledown , \bullet)

The values of μ_1 and μ_2 of octyl alcohols in terms of τ_1 , τ_2 and slope β of the concentration variation of the experimental *hf* conductivity K_{ij} were then estimated. The *hf* conductivity K_{ij} is, however, given by Murphy and Morgan [17]:

$$K_{ij} = \frac{\omega}{4\pi} (\epsilon''_{ij}{}^2 + \epsilon'_{ij}{}^2)^{1/2} \quad (4.11)$$

as a function w_j of polar solute. Since $\epsilon''_{ij} \ll \epsilon'_{ij}$ in the *hf* electric field, the term ϵ''_{ij} offers resistance of polarisation. Thus the real K'_{ij} of the *hf* K^*_{ij} of a polar-nonpolar liquid mixture at TK can be written according to Smyth [18] as :

$$K'_{ij} = \frac{\mu_j^2 N \rho_{ij} F_{ij}}{3M_j kT} \left(\frac{\omega^2 \tau}{1 + \omega^2 \tau^2} \right) w_j \quad (4.12)$$

which on differentiation with respect to w_j and for $w_j \rightarrow 0$ yields that :

$$\left(\frac{dK'_{ij}}{dw_j} \right)_{w_j \rightarrow 0} = \frac{\mu_j^2 N \rho_i F_i}{3M_j kT} \left(\frac{\omega^2 \tau}{1 + \omega^2 \tau^2} \right) \quad (4.13)$$

where M_j is the molecular weight of a polar solute, N the Avogadro number, k the Boltzmann constant, the local field $F_{ij} = 1/9 (\epsilon_{ij} + 2)^2$ becomes $F_i = 1/9 (\epsilon_i + 2)^2$ and the density $\rho_{ij} \rightarrow \rho_i$ the density of solvent at $w_j \rightarrow 0$.

Again, the total *hf* conductivity $K_{ij} = (\omega/4\pi)\epsilon_{ij}$ can be written as :

$$K_{ij} = K_{\infty ij} + \frac{1}{\omega\tau} K'_{ij}$$

or

$$\left(\frac{dK'_{ij}}{dw_j} \right)_{w_j \rightarrow 0} = \omega\tau \left(\frac{dK_{ij}}{dw_j} \right)_{w_j \rightarrow 0} = \omega\tau\beta \quad (4.14)$$

where β is the slope of $K_{ij} - w_j$ curve at infinite dilution. From Eqs. (4.13) and (4.14) we get :

$$\mu_j = \left[\frac{27M_j kT}{N\rho_j (\epsilon_j + 2)^2} \cdot \frac{\beta}{\omega b} \right]^{1/2} \quad (4.15)$$

as the dipole moment of each octyl alcohol in terms of b , where b is a dimensionless parameter given by :

$$b = \frac{1}{1 + \omega^2 \tau^2} \quad (4.16)$$

The computed μ_1 and μ_2 together with b_1 , b_2 and β of $k_{ij}-w_j$ equations for all the octyl alcohols are placed in Table 4.3.

4.3. Results and Discussion

The least square fitted straight line equations of $(\epsilon_{0ij} - \epsilon'_{ij}) / (\epsilon'_{ij} - \epsilon_{\infty ij})$ against $\epsilon''_{ij} / (\epsilon'_{ij} - \epsilon_{\infty ij})$ for six isomeric octyl alcohols like 2-methyl-3-heptanol, 3-methyl-3-heptanol, 4-methyl-3-heptanol, 5-methyl-3-heptanol, 4-octanol and 2-octanol in solvent n-heptane at 25°C under 24.33, 9.25 and 3.00 GHz electric field at different w_j 's of polar solutes are shown in Figure 4.1 together with the experimental points on them. w_j 's are, however, calculated from the mole fractions x_i and x_j of solvent and solute with molecular weights M_i and M_j respectively according to the relation [19].

$$w_j = \frac{x_j M_j}{x_i M_i + x_j M_j}$$

All the straight line equations are almost perfectly linear as evident from the correlation coefficients r lying in the range 0.9985-0.5684. The corresponding % of errors in terms of r in getting the slopes and intercepts of all the straight lines are placed in the 6th and 5th columns of Table 4.1. The errors are, however, large at 24.33 GHz indicating departure from the linear behaviour as evident from low values of r perhaps due to inherent uncertainty in measured data for such higher frequency [13].

The estimated values of τ_2 and τ_1 for all the isomeric octyl alcohols from the slopes and the intercepts of straight line equations are of smaller magnitude at 24.33 GHz and increase gradually to attain maximum value at 3.00 GHz under the present investigation. This may be due to the fact that at higher frequency the rate of hydrogen bond rupture in long chain alcohols is the maximum thereby reducing τ for each rotating unit [13]. τ_2 and τ_1 are then compared with the measured τ_s from the relation :

$$K''_{ij} = K'_{\infty ij} + \frac{1}{\omega\tau_s} K'_{ij}$$

and τ_0 where $\tau_0 = \sqrt{\tau_1\tau_2}$. As evident from Table 4.1 although $\tau_0 > \tau_1$; τ_s agrees well with τ_1 for most of the solutes except slight disagreement at 3.00 GHz for 4-methyl-3-heptanol, 5-methyl-3-heptanol, 4-octanol and 2-octanol. This is explained on the basis of the fact that conductivity measurement may be applicable in higher frequency in yielding microscopic τ only whereas the double relaxation method offers a better understanding of molecular relaxation phenomena showing microscopic as well as macroscopic τ as observed elsewhere [13]. Unlike normal aliphatic alcohols, -OH groups are screened by the substituted -CH₃ group, broad dispersion characterised by relatively short relaxation times were thus observed [14]. The respective positions of -CH₃ and -OH groups also greatly affect the static dielectric constant, correlation factor, their temperature dependence and type of hydrogen bonding in them.

The relative contributions c_1 and c_2 towards dielectric relaxations are also estimated in terms of $(\epsilon'_{ij} - \epsilon_{\infty ij}) / (\epsilon_{0ij} - \epsilon_{\infty ij})$, $\epsilon''_{ij} / (\epsilon_{0ij} - \epsilon_{\infty ij})$ with the estimated, τ_1, τ_2 as shown in Table 4.2 by Fröhlich and graphical methods. $x = (\epsilon'_{ij} - \epsilon_{\infty ij}) / (\epsilon_{0ij} - \epsilon_{\infty ij})$ and $y = \epsilon''_{ij} / (\epsilon_{0ij} - \epsilon_{\infty ij})$ were, however, evaluated from Fröhlich's Eqs.(4.9) and (4.10) in the first case. The usual variations of $(\epsilon'_{ij} - \epsilon_{\infty ij}) / (\epsilon_{0ij} - \epsilon_{\infty ij})$ and $\epsilon''_{ij} / (\epsilon_{0ij} - \epsilon_{\infty ij})$ with ω_j are concave and convex as found in Figures 4.2 and

4.3 in accordance with Bergmann Eqs. (4.2) and (4.3), except 5-methyl-3-heptanol at 24.33 GHz whose $[(\epsilon'_{ij} - \epsilon_{\infty ij}) / (\epsilon_{0ij} - \epsilon_{\infty ij})]$ curves is convex in nature due to its non-accurate ϵ_{0ij} and $\epsilon_{\infty ij}$ values like ethanol as observed elsewhere [13]. x and y were also obtained graphically from Figures 4.2 and 4.3 in the limit $w_j = 0$.

In Fröhlich method c_1 and c_2 are all positive as evident from 6th columns of Table 4.2 with $c_2 > c_1$. In graphical method $c_1 > c_2$ with negative c_2 for most of the systems probably due to inertia of the flexible parts under hf electric field, as shown in 10th and 11th columns of same Table 4.2. c_2 are, however, positive for the systems 5-methyl-3-heptanol, 4-octanol and 2-octanol at 24.33 GHz as well as 3-methyl-3-heptanol at 9.25 GHz. Both the methods in most cases, yield $|c_2 + c_1| \geq 1$, signifying thus the possibility of occurrence of more than two relaxation processes in them [13].

The dipole moments μ_1 and μ_2 of all the isomeric alcohols due to their flexible parts and the whole molecules are estimated in terms of dimensionless parameters b_1 , b_2 and slope β of $K_{ij} - w_j$ curves by using Eq. (4.15). The variations of K_{ij} with w_j are all linear having almost the same intercepts α and slopes β at each frequency of electric field. It was, therefore, difficult to plot them as they almost coincide. The values of α and β of K_{ij} 's are little different and comparatively large at 24.33 GHz (Table 4.3). This sort of behaviour is perhaps due to same dipole moments [16] possessed by the polar molecules under investigation as evident from μ_2 and μ_1 placed in 7th and 8th columns of Table 4.3. μ_2 for most of the polar molecules shows high values at 24.33 GHz and decrease gradually with lower frequencies except 3-methyl-3-heptanol, 5-methyl-3-heptanol and 2-octanol whose μ_2 's are found greater at 9.25 GHz electric field. This type of behaviour may be explained on the basis of the fact that such alcohols behaving almost like the polymer molecules have long chain of C-atoms and tend to break up in nonpolar solvent in order to reduce or even eliminate the absorption under hf electric field. The proportion of smaller molecular

species having comparatively small number of C-atoms and their corresponding absorption will increase thereby [10]. The values of μ_1 's on the other hand, are almost constant exhibiting a trend to increase a little towards low frequency. They are finally compared with bond moments of 1.5 D of O-H group making an angle 105° with the -C-O- bond axis according to the preferred conformations of all the isomers as sketched in Figure 4.4.

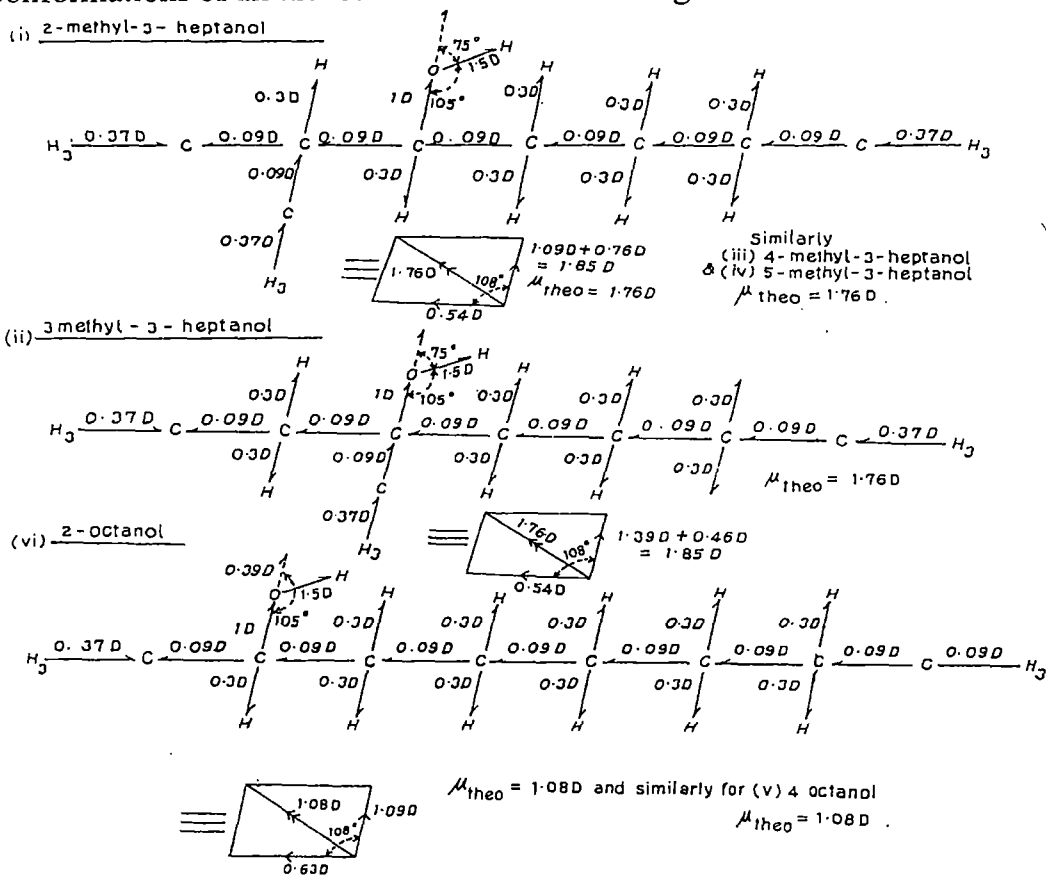


Figure 4.4: Conformations of some isomeric octyl alcohols

This confirms that μ_1 arises due to the rotation of -OH group around C-O bond in the long chain alcohols studied so far [13]. The slight difference is due to difference in steric hindrances as a result of structural configurations at different frequencies. μ_1 also estimated from $\mu_1 = \mu_2 (c_1 / c_2)^{1/2}$ assuming two relaxation processes are equally probable as shown in the last column of Table 4.3. The other bond moments 0.47, 0.3, 1.0 and 0.09 D for C-H₃, C-H, C-O

and C–C bonds are also involved to justify their conformations. The resultant of all these bonds by vector addition method yields μ_{theo} of 1.76 D and 1.08 D for four methyl substituted heptanols and two octanols respectively. The derived result should decrease with increase in the number of C-atoms and μ_{theo} for them should be less than that for 1-heptanol [13]. But for μ_{theo} in Figure 4.4 three isomers are only displayed due to typical positions of $-\text{CH}_3$ and $-\text{OH}$ groups. This may probably be the reason of having slightly larger values of μ_{theo} from 1-heptanol as observed elsewhere [13].

4.4 Conclusions

The methodology so far advanced for the double broad dispersions of the polar-nonpolar liquid mixtures based on Debye's model seems to be much simpler, straightforward and significant one to detect the very existence of τ_1 and τ_2 of a polar liquid in a nonpolar solvent. The correlation coefficients between the desired dielectric relaxation parameters involved in the derived equations of Eq. (4.8) could, however, be estimated to find out % of errors entered in the estimated τ_1 and τ_2 of a polar liquid, because τ is claimed to be accurate within $\pm 10\%$. The isomeric octyl alcohols like normal aliphatic alcohols are found to yield both τ_1 and τ_2 at all frequencies of the electric field of GHz range. The corresponding μ_1 and μ_2 can then be estimated from Eq. (4.15) in terms of b_1 and b_2 which are, however, involved with τ_1 and τ_2 as estimated, to arrive at their preferred conformations as shown in Figure 4.4.

References

- [1] U Saha & S Acharyya, *Indian J Pure & Appl Phys.* **32**(1994) 346.
- [2] KV Gopalakrishna, *Trans Faraday Soc.* **53** (1957) 767.
- [3] A Budo, *Phys Z*, **39** (1938) 706.
- [4] K. Bergmann, D.M. Roberti & C.P. Smyth, *J Phys Chem*, **64** (1960) 665.

- [5] J. Bhattacharyya, A. Hasan, S.B. Roy & G.S. Kastha *J Phys Soc Japan*, **28** (1970) 204.
- [6] U Saha, S. K. Sit, R.C. Basak & S Acharyya, *J Phys D : Appl Phys*, **27** (1994) 596.
- [7] S. K. Sit, R.C. Basak, U Saha, & S Acharyya, *J Phys D. : Appl Phys*, **27** (1994) 2194.
- [8] D J Denney & J W Ring, *J Chem Phys*, **39** (1963) 1268.
- [9] M Moriamez & A Lebrun, *Arch Soi (Geneva)*, **13** (1960) 40.
- [10] L Glasser, J Crossley & C P Smyth, *J Chem Phys*, **57** (1972) 3977.
- [11] H D Purohit & H S Sharma, *Indian J Pure & Appl Phys*, **8** (1970) 10.
- [12] A K Ghosh , Ph D Dissertation (NBU), 1981.
- [13] S K Sit & S Acharyya, *Indian J Phys* **70B** (1996) 19.
- [14] J Crossley. L Glasser & C P Smyth, *J Chem Phys*, **55** (1971) 2197.
- [15] H Fröhlich, *Theory of dielectrics* (Oxford University Press, Oxford) 1949.
- [16] A K Chatterjee, U Saha, N Nandi, R C Basak & S Acharyya. *Indian J Phys*. **66B** (1992) 291.
- [17] F J Murphy & S O Morgan, *Bell Syst Tech J*, **18** (1939) 502.
- [18] C P Smyth, *Dielectric behaviour and structure*, (New York: McGraw Hill) 1955.
- [19] A K Ghosh & S Acharyya , *Indian J Phys*, **52B** (1978) 129.

CHAPTER-5

DIELECTRIC RELAXATION OF PARA POLAR LIQUIDS UNDER HIGH FREQUENCY ELECTRIC FIELD

DIELECTRIC RELAXATION OF PARA POLAR LIQUIDS UNDER HIGH FREQUENCY ELECTRIC FIELD

5.1. Introduction

The dielectric relaxation phenomena of a polar liquid in nonpolar solvent have already gained much attention of a large number of workers [1-3]. The process is thought to be a sensitive tool to investigate the molecular size, shape and structure of a polar liquid. The structural and associational aspects of the polar liquid can thus be inferred in terms of their measured relaxation time τ and hence dipole moment μ at different experimental temperatures in $^{\circ}\text{C}$. The subsequent use of the temperature dependence of τ 's usually yields different thermodynamic energy parameters of a polar unit. The polar liquids having substituted polar groups in their para positions deserve to be specially investigated. The μ 's of such para liquids are usually found to be zero [4], due to symmetrical distribution of bond moments of the substituted polar groups in a plane. Sometimes they show a resultant μ when the dipolar and free groups are out of plane with the parent ring.

Earlier investigations [5] were made on substituted hydroxy and methoxy benzaldehydes in benzene to reveal that τ is generally governed by both molecular and intra-molecular rotations. However, no such study on the long chain substituted parabenzaldehydes and phenones have been made so far. Dhar et al [6] and Some vanshi et al [7] have recently measured real ϵ'_{ij} and imaginary ϵ''_{ij} parts of complex dielectric constant ϵ_{ij}^* of p-hydroxypropiofenone, p-chloropropiofenone, p-acetamidobenzaldehyde, p-benzyloxybenzaldehyde in dioxane and p-anisidine, p-phenitidine, o-chloroparanitroaniline and p-bromonitro benzene in benzene respectively under 3 cm. wave length electric field at different experimental temperatures. The purpose of their study was only to observe the molecular and intra-molecular group rotations in the molecules. Non spherical molecular liquids of such type also are known to be strongly non-Debye in their relaxation behaviour. We, therefore, concentrate

our attention to these molecules [6,7] to study dielectric relaxation phenomena by conductivity measurement technique [8] based on the internationally accepted symbols of dielectric terminology and parameters. The phenones together with other di- or tri-substituted benzenes having rigid and free dipolar groups at their para positions are included in the present investigation to compare the dielectric relaxation properties with the benzaldehyde groups. Moreover, our aim is to observe how τ 's and μ 's vary with respect to sizes, shapes and structures of the molecules and to get an idea of molecular environment of such polar liquids too, in solvents. For most of the polar liquids the imaginary part σ''_{ij} varies linearly [8] with the real part σ'_{ij} of hf complex conductivity σ_{ij}^* for different w_j 's of a solute. But in the present polar - nonpolar liquid mixtures the variation of σ''_{ij} with σ'_{ij} was not linear [9] to yield τ_j . The ratio of the individual slopes of σ''_{ij} and σ'_{ij} against w_j 's curves at $w_j \rightarrow 0$, on the other hand, is used to get τ_j 's of these p - polar liquids in order to report them in Table 5.1.

Table 5.1 : The ratio of slopes of concentration variation of imaginary σ''_{ij} and real σ'_{ij} parts of high frequency complex conductivity σ_{ij}^* at $w_j \rightarrow 0$ estimated and reported τ_j in pico second, dimensionless parameter $b [=1/(1+\omega^2\tau_j^2)]$, coefficients α, β, γ , of equation : $\sigma_{ij} = \alpha + \beta w_j + \gamma w_j^2$, estimated and reported dipole moment μ_j in Coulomb-metre at different experimental temperatures in $^{\circ}\text{C}$ and the theoretical dipole moment μ_{theo} in Coulomb-metre from bond angles and bond moments for different para compounds.

System with Sl. No. and Molecular weight M_j	Temp. in $^{\circ}\text{C}$	Ratio of slopes of σ''_{ij} & σ'_{ij} with w_j ($d\sigma''_{ij}/dw_j$) $x/y = \frac{d\sigma''_{ij}/dw_j}{d\sigma'_{ij}/dw_j}$	Estimated τ_j in p.sec	Reported τ_j in p.sec	Dimensionless parameter $b = 1/(1+\omega^2\tau^2)$	Coefficients in the equation $\sigma_{ij} = \alpha + \beta w_j + \gamma w_j^2$			Estimated $\mu_j \times 10^{30}$ in Coulomb metre	Reported $\mu_j \times 10^{30}$ in Coulomb metre	Dipole moments $\mu_{\text{theo}} \times 10^{30}$ from bond angles and bond moments
						α	β	$\gamma \times 10^{-1}$			
i. Para hydroxy-propiofenone $M_j=0.150\text{kg}$.	17	0.8287	19.86	-	0.4070	1.1390	-4.4450	3.7653	0.00		
	23	0.7451	22.08	25.40	0.3571	1.1409	0.1812	1.2713	2.36	10.20	8.27
	30	0.7028	23.41	24.20	0.3307	1.1626	-2.1708	2.1640	0.00		
ii. Para-chloropropiophenone $M_j = 0.1685\text{kg}$	19	0.7427	22.15	20.80	0.3556	1.1177	1.1648	1.9445	9.43		
	25	0.8261	19.92	19.70	0.4056	1.1457	-1.3627	1.4874	0.00	9.84	9.73
	31	0.7272	22.63	18.20	0.3458	1.1420	1.2634	0.0199	10.31		
iii. Para acetamidobenzaldehyde $M_j = 0.163\text{kg}$.	17	0.5756	28.58	21.80	0.2490	1.1506	0.6998	1.6243	8.55		
	23	0.7736	21.27	20.80	0.3744	1.1564	2.2621	-0.6401	12.75	10.37	13.12
	30	0.7260	22.66	19.00	0.3453	1.1427	5.1761	-1.5843	20.51		
iv. Para benzyloxybenzaldehyde $M_j = 0.212\text{kg}$.	17	1.0111	16.27	18.60	0.5056	1.1234	12.3384	-4.4758	26.62		
	20	0.5865	28.06	20.00	0.2259	1.1503	1.1738	-0.3428	12.56		
	25	0.6247	26.34	19.40	0.2807	1.1620	0.9386	-	10.87		
v. Paraanisidine $M_j=0.123\text{kg}$	30	1.2238	13.44	16.90	0.5998	1.1822	0.7957	-	7.04		
	20	2.2120	7.43	3.89	0.8306	1.1377	5.4655	-1.4819	12.23	5.20	
	30	2.4152	6.81	3.67	0.8537	1.1621	1.6783	-	6.87	10.33	6.28
vi. Paraphenitidine $M_j=0.137\text{kg}$.	40	3.4952	4.71	3.17	0.9243	1.1675	1.6843	-	6.79	8.87	
	20	1.5288	10.76	11.08	0.7005	1.1792	4.8244	-	13.21	7.47	15.04
	30	1.9049	8.64	10.63	0.7839	1.1308	12.4534	-2.1671	20.61	9.27	
vii. Ortho-chloro-paranitroaniline $M_j=0.1725\text{kg}$	40	2.1036	7.82	9.95	0.8158	1.2066	3.4959	0.2012	10.98	10.47	
	20	1.5124	10.88	10.57	0.6958	1.0930	1.1354	-0.0829	7.21	8.13	
	30	1.9522	8.43	9.89	0.7921	1.1270	0.1559	-	2.57	10.93	15.93
viii. Para-bromonitrobenzene $M_j=0.202\text{kg}$.	40	2.2126	7.44	9.18	0.8302	1.1402	0.0820	-	1.85	13.10	
	20	1.6446	10.01	-	0.7299	1.1823	0.6118	0.0189	5.59	-	
	30	1.7818	9.24	-	0.7603	1.2166	-0.6123	0.2231	0.00	-	8.40
	40	1.9503	8.44	-	0.7917	1.2299	-0.4882	0.2188	0.00	-	

The intercepts and slopes of linear relationship of $\ln(\tau_j T)$ against $1/T$ as shown in Table 5.2, could, however, be used to obtain thermodynamic energy parameters like enthalpy of activation ΔH_τ , entropy of activation ΔS_τ and free energy of activation ΔF_τ of dielectric relaxation process of the rate theory of Eyring et al [10]. The enthalpy of activation ΔH_η due to viscous flow was, however, obtained from the slope γ of the linear relationship of $\ln(\tau_j T)$ against $\ln \eta$, where η is the coefficient of viscosity of the solvent to test the behaviour of solutes in solvents.

The values of ΔS_τ , ΔH_τ and ΔF_τ of Table 5.2 give an insight into molecular dynamics of the systems. The estimated Debye factor $(\tau_j T/\eta)$ and Kalman factor $(\tau_j T/\eta^\gamma)$ in Table 5.2 signify the applicability of the required relaxation model for such p – liquids.

Table 5.2 : The intercepts and slopes of $\ln \tau_j T$ against $1/T$ curves, energy parameters like enthalpy of activation ΔH_τ in Kilo Joule mole⁻¹, the entropy of activation ΔS_τ in Joule mole⁻¹ K⁻¹, free energy of activation ΔF_τ in Kilo-Joule-mole⁻¹ for dielectric relaxation process, enthalpy of activation ΔH_η in Kilo Joule mole⁻¹ due to viscous flow, γ as the ratio of ΔH_τ and ΔH_η , Kalman factor $(\tau_j T/\eta^\gamma)$, Debye factor $(\tau_j T/\eta)$ at different experimental temperatures in °C and the coefficients of μ_j -t equations $\mu_j = a + bt + ct^2$ of different para compounds.

System with Sl. No.	Temp. in °C	Intercept & slope of $\ln \tau_j T$ Vs $1/T$ Curve		ΔH_τ in KJ mole ⁻¹	ΔS_τ in J mole ⁻¹ K ⁻¹	ΔF_τ in KJ mole ⁻¹	$\gamma = (\Delta H_\tau / \Delta H_\eta)$	ΔH_η in KJ mole ⁻¹	Kalman factor $\tau_j T/\eta^\gamma$	Debye factor $\tau_j T/\eta$ x10 ⁶	Coefficients in the equation $\mu_j \times 10^{10} = a + bt + ct^2$		
		Intercept	slope								a	b	c
i. Para hydroxy-propiofenone	17	-21.36	724.41	6.02	-19.02	11.53	0.54	11.15	19.75x10 ⁻⁸	4.0135	35.4250	-3.2286	0.0716
	23				-20.49	12.08			23.64x10 ⁻⁸	5.0274			
	30				-21.64	12.58			27.55x10 ⁻⁸	6.2221			
	37				-18.51	11.76			19.36x10 ⁻⁸	4.6767			
ii. Para-chloropropiophenone	19	-33.17	4227.52	35.13	79.57	11.90	2.63	13.36	0.2112	4.6531	92.9880	-7.1216	0.1407
	25				77.86	11.93			0.2535	4.7300			
	31				74.30	12.54			0.2938	6.1424			
	37				81.03	10.01			0.1890	2.3761			
iii. Para acetamido-benzaldehyde	17	-24.76	1770.09	14.71	7.92	12.41	1.10	13.37	11.12x10 ⁻⁶	5.7757	-4.2996	0.6554	0.0050
	23				9.17	11.99			9.41x10 ⁻⁶	4.8430			
	30				7.31	12.49			11.86x10 ⁻⁶	6.0228			
	37				8.77	11.99			10.23x10 ⁻⁶	5.1205			
iv. Para benzyloxy benzaldehyde	20	-32.27	4022.34	33.43	71.34	12.52	1.89	17.68	19.57x10 ⁻⁴	5.7293	9.0620	0.4582	0.0146
	25				69.81	12.62			22.42x10 ⁻⁴	6.0379			
	30				70.24	12.14			22.09x10 ⁻⁴	5.2333			
	35				71.49	11.41			20.70x10 ⁻⁴	4.2025			
v. Paraanisidine	20	-25.94	1771.20	14.71	18.54	9.29	1.62	9.08	3.20x10 ⁻⁴	3.3647	38.7900	-1.8560	0.0264
	30				17.33	9.47			3.82x10 ⁻⁴	3.6781			
	40				18.57	8.91			3.07x10 ⁻⁴	2.8188			
vi. Paraphenitidine	20	-23.58	1167.25	9.70	-1.67	10.19	1.21	8.02	22.87x10 ⁻⁶	4.8728	-52.6800	4.9975	-0.0851
	30				-1.22	10.07			22.49x10 ⁻⁶	4.6665			
	40				-1.68	10.22			22.87x10 ⁻⁶	4.6800			
vii. Ortho-chloro-paranitroaniline	20	-24.52	1447.51	12.03	6.19	10.22	1.49	8.07	17.99x10 ⁻⁵	4.9271	28.2500	-1.4440	0.0196
	30				6.88	10.00			17.86x10 ⁻⁵	4.5531			
	40				6.18	10.09			18.05x10 ⁻⁵	4.4526			
viii. Para-bromo-nitrobenzene	20	-21.28	479.23	3.98	-20.58	10.01	0.47	8.47	9.25x10 ⁻⁸	4.5331	33.5400	-1.9565	0.0280
	30				-20.64	10.24			9.44x10 ⁻⁸	4.9906			
	40				-20.58	10.42			9.21x10 ⁻⁸	5.0511			

The dipole moments μ_j 's of all the liquids were finally worked out from the slopes β 's of hf conductivities σ_{ij} 's with w_j 's and dimensionless parameters b 's with the estimated τ_j at all the temperatures. All the μ_j 's as placed in Table 5.1, are found, to be temperature dependent quantities. The coefficients a , b and c of $\mu_j - t$ curves of Figure 5.2, are, however, placed in Table 5.2, in order to compare with the reported μ 's as well as theoretical μ_{theo} 's, obtained from bond angles and bond moments of substituent polar groups attached with the parent ones of Figure 5.3. The disagreement of the measured μ_j 's with μ_{theo} 's as obtained from Figure 5.3, for these compounds establishes the fact that the inductive moments combined with the mesomeric moments of the substituent polar groups with the parent molecules is a function of temperature.

5.2. Theoretical Formulations

Under the hf electric field the dimensionless complex dielectric constant ϵ_{ij}^* is :

$$\epsilon_{ij}^* = \epsilon'_{ij} - j\epsilon''_{ij} \quad (5.1)$$

where ϵ'_{ij} is the real part of dielectric constant and ϵ''_{ij} is the dielectric loss factor. Hence Murphy - Morgan relation [11] for the complex hf conductivity σ_{ij}^* of a solution of polar-nonpolar liquid mixture is

$$\sigma_{ij}^* = \omega\epsilon_0\epsilon''_{ij} + j\omega\epsilon_0\epsilon'_{ij} \quad (5.2)$$

where $\sigma_{ij}' (= \omega\epsilon_0\epsilon''_{ij})$ and $\sigma_{ij}'' (= \omega\epsilon_0\epsilon'_{ij})$ are the real and imaginary parts of complex hf conductivity, $\epsilon_0 =$ permittivity of free space $= 8.854 \times 10^{-12} \text{ F m}^{-1}$, j is a complex number $= \sqrt{-1}$, $\omega = 2\pi f$, f being frequency of applied electric field.

The total hf conductivity σ_{ij} is, however, obtained from.

$$\sigma_{ij} = \omega \epsilon_0 \sqrt{\epsilon''_{ij}{}^2 + \epsilon'_{ij}{}^2} \quad (5.3)$$

The imaginary part of hf conductivity σ_{ij}'' is related to the real part of hf conductivity σ_{ij}' by

$$\sigma_{ij}'' = \sigma_{\infty ij} + \left(\frac{1}{\omega \tau} \right) \sigma_{ij}' \quad (5.4)$$

where $\sigma_{\infty ij}$ is the constant conductivity at $w_j = 0$ and τ is the relaxation time of a polar unit = τ_j . Eq (5.4) on differentiation with respect to σ_{ij}' becomes.

$$\frac{d\sigma_{ij}''}{d\sigma_{ij}'} = \frac{1}{\omega \tau_j} \quad (5.5)$$

to yield τ_j of a polar solute. It is often better to use the ratio of the individual slopes of variations of σ_{ij}'' and σ_{ij}' with w_j at $w_j \rightarrow 0$ to avoid the effect of polar-polar interactions in a liquid mixture to get τ_j from :

$$(d\sigma_{ij}''/dw_j)_{w_j \rightarrow 0} / (d\sigma_{ij}'/dw_j)_{w_j \rightarrow 0} = \frac{1}{\omega \tau_j}$$

$$\text{or, } x/y = 1/\omega \tau_j \quad (5.6)$$

Again, it is observed experimentally that σ_{ij}'' is nearly equal to σ_{ij} of Eq (5.3) under hf alternating electric field. Hence Eq (5.4) becomes :

$$\sigma_{ij} = \sigma_{\infty ij} + \left(\frac{1}{\omega \tau_j} \right) \sigma_{ij}'$$

$$\text{or } (d\sigma_{ij}'/dw_j)_{w_j \rightarrow 0} = \omega \tau_j \beta \quad (5.7)$$

where $\beta = (d\sigma_{ij}'/dw_j)$ the slope of $\sigma_{ij}' - w_j$ curve at $w_j \rightarrow 0$.

All the β 's are however, presented in Table 5.1 for all the liquids. The real part of hf conductivity [9,12] σ_{ij}' at T K of a given solution of w_j is :

$$\sigma_{ij}' = \left(\frac{N \rho_{ij} \mu_j^2}{27 k_B M_j T} \right) \left(\frac{\omega^2 \tau_j}{1 + \omega^2 \tau_j^2} \right) (\epsilon'_{ij} + 2)^2 w_j \quad (5.8)$$

which on differentiation with respect to w_j and at $w_j \rightarrow 0$, yields :

$$(d\sigma_{ij}'/dw_j)_{w_j \rightarrow 0} = \frac{N\mu_j^2 \rho_i}{27M_j k_B T} \frac{\omega^2 \tau_j}{(1+\omega^2 \tau_j^2)} (\epsilon_i + 2)^2 \quad (5.9)$$

where

N = Avogadro's Number

ρ_i = density of solvent

ϵ_i = dielectric relative permittivity of the solvent

M_j = molecular weight of solute and

k_B = Boltzmann Constant.

All the symbols stated above are expressed in S.I. unit. From Eqs (5.7) and (5.9) one gets μ_j in Coulomb metre under hf electric field as :

$$\mu_j = \left[\frac{27 M_j k_B T}{N \rho_i (\epsilon_i + 2)^2} \frac{\beta}{\omega b} \right]^{1/2} \quad (5.10)$$

in terms of a dimensionless parameter 'b'

$$b = 1/(1 + \omega^2 \tau_j^2) \quad (5.11)$$

with the measured τ_j of the liquid.

All the measured μ_j 's in terms of β 's and b's of Eqs (5.10) and (5.11) are, however, placed in Table 5.1 and compared with the reported μ 's and μ_{theo} 's the latter ones are obtained from bond angles and bond moments of the substituted groups of the molecules as shown in Figure 5.3.

5.3. Results and Discussion

The relaxation time τ_j 's of the para polar liquids as reported in Table 5.1 in dioxane and benzene respectively were estimated from the ratio of the individual slopes of both the imaginary σ_{ij}'' and real σ_{ij}' parts of high frequency

conductivity σ_{ij}^* with weight fraction w_j of polar solutes at different experimental temperatures in $^{\circ}\text{C}$ under 3 cm. wave length electric field. τ_j 's of these liquids could not be obtained directly from the slope of Eq (5.5) of σ_{ij}'' with σ_{ij}' because of the non linear character [8]. Thus the individual slopes of $\sigma_{ij}'' - w_j$ and $\sigma_{ij}' - w_j$ curves at $w_j \rightarrow 0$ were used to get τ 's of these para polar liquids from Eq. (5.6) in order to minimize the effects of dipole-dipole interactions, macroscopic viscosity, internal field etc.

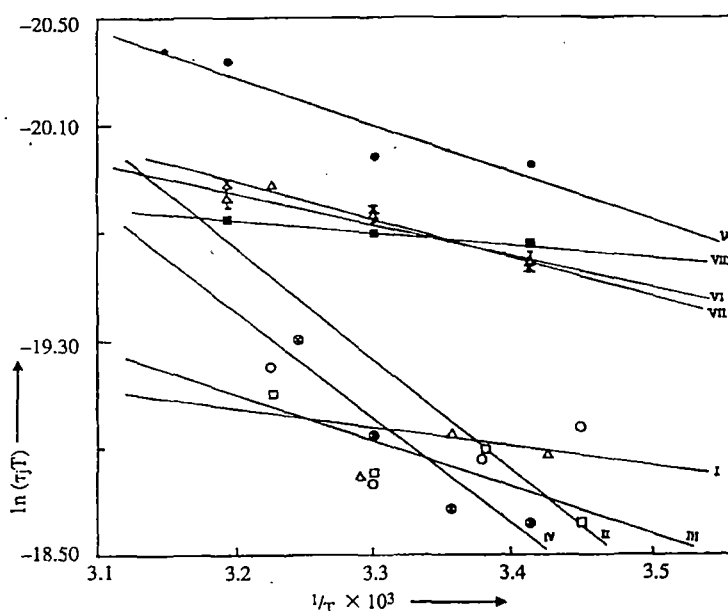


Figure 5.1. Straight line plots of $\ln(\tau_j T)$ against $1/T$. (I) parahydroxypropiophenone ($-\circ-$), (II) parachloropropiophenone ($-\triangle-$), (III) paraacetamidobenzaldehyde ($-\square-$), (IV) parabenzyloxybenzaldehyde ($-\otimes-$), (V) paraanisidine ($-\bullet-$), (VI) paraphenitidine ($-\times-$), (VII) orthochloroparanitroaniline ($-\circ-$) and (VIII) parabromonitrobenzene ($-\blacksquare-$)

The estimated ratio of the individual slopes of σ_{ij}'' and σ_{ij}' curves with w_j 's together with estimated and reported τ_j 's are placed in the 3rd, 4th and 5th columns of Table 5.1. The τ_j 's thus obtained agree well with the reported τ 's where such are available [6,7] based on Gopalakrishna's method [13]. As observed in Table 5.1, the τ 's of molecules having phenone and benzaldehyde groups are higher in comparison to other di- and tri-substituted para polar molecules. This is probably due to larger sizes of the rotating units. It is also interesting to note that variation of τ of such molecules as presented in Table 5.1 are irregular in disagreement with the Debye model of relaxation as observed elsewhere [4].

This may be explained by the fact that stretching of bond angles and bond moments of polar groups with temperature and the distribution of bond moments around the parent molecules leads to either symmetric or asymmetric shape of the molecules. The rest of the molecules show the lower values of τ decreasing with increase of temperature in agreement with the Debye relaxation in spite of the fact that they are nonspherical.

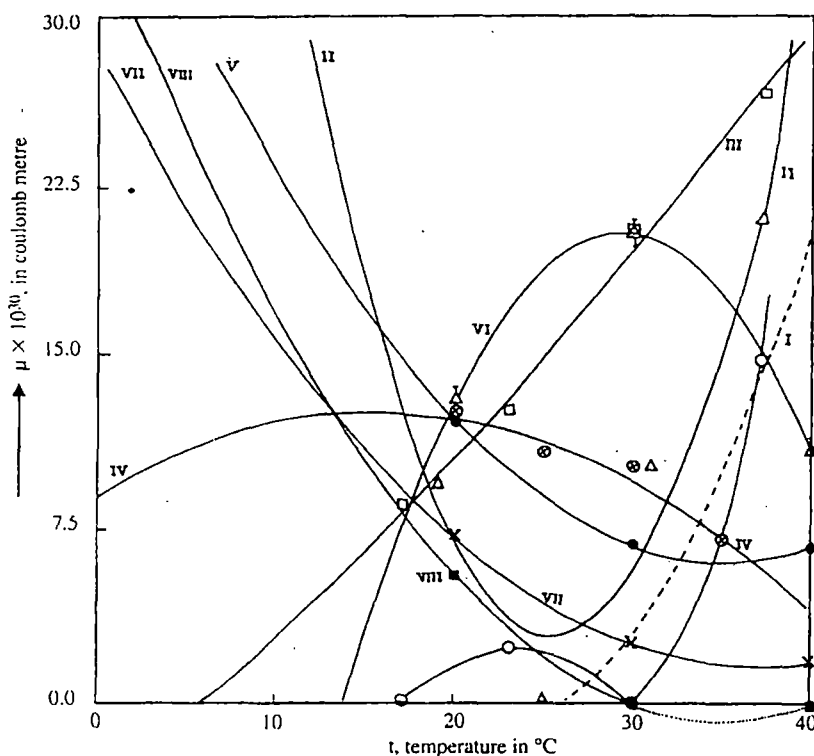


Figure 5.2. Variation of dipole moments $\mu_j \times 10^{30}$ in Coulomb metre against t in $^{\circ}\text{C}$. (I) parahydroxypropio-phenone ($-\circ-$), (II) parachloropropio-phenone ($-\triangle-$), (III) paraaceta-midobenzaldehyde ($-\square-$), (IV) parabenzyloxybenzaldehyde ($-\otimes-$), (V) paraanisidine ($-\bullet-$), (VI) paraphenitidine ($-\frac{1}{2}-$), (VII) ortho-chloroparanitroaniline ($-x-$) and (VIII) parabromonitrobenzene ($-\blacksquare-$).

The process of rotation of the rotating dipoles requires an activation energy sufficient to overcome the energy barrier between two equilibrium positions, one can write according to Eyring et al [10] with the known τ_j by :

$$\tau_j = (A/T)e^{\Delta F_{\tau}^{\ddagger}/RT} \quad (\Delta F_{\tau}^{\ddagger} = \Delta H_{\tau}^{\ddagger} - T \Delta S_{\tau}^{\ddagger})$$

$$\text{or, } \ln(\tau_j T) = \ln(Ae^{-\Delta S_{\tau}^{\ddagger}/R}) + (\Delta H_{\tau}^{\ddagger}/RT)$$

$$= \ln A' + (\Delta H_{\tau}^{\ddagger}/R) \cdot (1/T) \quad (5.12)$$

Eq (5.12) is a straight line of $\ln(\tau_j T)$ against $1/T$ having intercept and slope to measure the thermodynamic energy parameters like enthalpy of activation (ΔH_τ), entropy of activation (ΔS_τ) and free energy of activation (ΔF_τ) of dielectric relaxation process of the molecules. The intercepts and slopes of the least squares fitted $\ln(\tau_j T)$ against $1/T$ curves as illustrated graphically in Figure 5.1, were accurately obtained and placed in the 3rd and 4th columns of Table 5.2. The variation of $\ln \tau_j T$ against $1/T$ are linear for almost all the liquids with the available experimental data. The enthalpy of activation ΔH_η due to viscous flow of the solvent was, however, estimated from the slope of the linear equation of $\ln(\tau_j T)$ against $\ln \eta$ at different experimental temperatures. As evident from Table 5.2, the values of $\gamma (= \Delta H_\tau / \Delta H_\eta) > 0.50$ for all the liquids except para bromonitrobenzene exhibit the solvent environment around the solute molecules which behave as solid phase rotators. The low value of γ , on the other hand, for p-bromonitrobenzene may indicate the weak molecular interaction of such dipole with benzene. The values of ΔS_τ 's for the system like p-hydroxypropiophenone, p-phenitidine and p-bromonitrobenzene are negative. This is due to the fact that activated states are more ordered than the normal states unlike other molecules. The high values of ΔS_τ and ΔH_τ of p-chloropropiophenone and p-benzyloxybenzaldehyde indicate the activated states are not stable probably due to internal resistance suffered by larger dipole rotations. The rest of the molecules possess ΔH_τ of nearly the same magnitude. The ΔF_τ 's between the activated and unactivated states of all the systems are, however, the same as the activation is accomplished by rupture of bonds of dipolar groups in the same degree of freedom [6,7]. Unlike Kalman factor $(\tau_j T / \eta^\gamma)$ at different temperatures, the Debye factor $(\tau_j T / \eta)$ is almost constant signifying the applicability of Debye model of relaxation behaviour for such para liquids [14]. The μ_j 's from Eq. (5.10) of all the p-liquids were obtained from slopes β 's of $\sigma_{ij} - w_j$ curves and dimensionless parameters b's of Eq (5.11) involved with measured τ_j 's of Eq.(5.6). The slopes and intercepts of σ_{ij} against w_j as presented in Table 5.1 were obtained by careful regression technique and are found to be almost constant at all the experimental temperatures under 3 cm. wave length electric field perhaps for their same polarity. Thus σ_{ij}' , σ_{ij}'' and σ_{ij} with w_j 's could not be shown

graphically. Parahydroxypropiophenone (curve 1) and p-acetamidobenzaldehyde (curve III) showed the monotonic increase of μ_j with temperature (Figure 5.2) for their increasing molecular asymmetry at higher temperatures. The μ_j -t curves of p-benzyloxybenzaldehyde (curve IV) and p-phenitidine (curve VI) are convex in nature [15] showing zero values at lower and higher temperatures unlike the other four assuming minimum values at different temperatures as seen in Figure 5.2. The least squares fitted μ_j -t curve for p-bromonitrobenzene which showed 5.59×10^{-30} C.m at 20°C but zero values of μ_j at 30°C and 40°C for its strong symmetry attained at those temperatures was, however, obtained. Like curves II, V and VII of other p-compounds it (curve VIII) also showed minimum having -ve μ_j between 30°C to 40°C , shown by dotted line to satisfy the continuous curve. The usual variation of μ_j against $t^\circ\text{C}$ for p-hydroxypropiophenone (curve I) is shown by least squares fitted dotted line together with the solid line drawn through the estimated μ_j 's. The above nature of μ_j -t curves are explained by the rupture of solute-solvent (monomer) and solute-solute (dimer) association due to stretching of bond angles and bond moments of substituted polar groups at different temperatures.

The theoretical dipole moments μ_{theo} 's of all the p - liquids were also calculated from the vector addition of the available bond moments 4.67, 10.33, 4.40, 4.40, 1.00, 8.00, 5.63, 1.50, 14.10 and 5.70 multiples of 10^{-30} Coulomb metre (C.m.) for C \rightarrow OH, C \rightarrow CHO, C \rightarrow OCH₃ and C \rightarrow NH₂ bonds making angles 62° , 55° , 57° , 142° and 0° for the rest C \rightarrow H, C \Rightarrow O, C \rightarrow Cl, C \rightarrow N, C \rightarrow NO₂ and C \rightarrow Br bonds respectively with C atom of the parent molecules which are assumed to be planer structures, as shown in Figure 5.3, The μ_{theo} 's thus obtained are finally placed in the 12th column of Table 5.1. The slight disagreement between measured μ_j 's and μ_{theo} 's reveals the presence of inductive and mesomeric moments of the substituent polar groups due to their aromaticity. In p-acetamidobenzaldehyde, p-phenitidine, orthochloro para nitro aniline and p-bromonitrobenzene, the μ_{theo} 's are larger while for others μ_{theo} 's are smaller than the measured values. This fact at once predicts that the

substituent polar groups in former molecules push the electrons towards the electro negative atoms and there by inductive effect is less than in latter systems where they pull the electrons. The electromeric effect is also prominent in the system containing $C \Rightarrow O$ groups.

5.4. Conclusions

A very convenient method to evaluate τ_j 's from the ratio of the individual slopes of $\sigma_{ij}'' - w_j$ and $\sigma_{ij}' - w_j$ curves at $w_j \rightarrow 0$ and the corresponding μ_j 's in SI unit of several chain like para liquids at different experimental temperatures is suggested in order to avoid polar - polar interactions. The slopes of $\sigma_{ij}'' - \sigma_{ij}'$ curves are very often not linear in almost all liquids and hence could not be used to obtain τ_j 's. Both τ_j 's and hence μ_j 's within the accuracy of 10% and 5% are now reliable. Para - hydroxypropiophenone and p - chloropropiophenone show zero values of μ at certain temperatures owing to their symmetry gained at that temperatures. The variation of μ with temperature in $^{\circ}C$ is not a new concept, but for p-liquids, the convex, concave or gradual increase occur probably due to association or dissociation of solute - solute and solute - solvent molecular associations and stretching of bond moments of the substituent polar groups at different temperatures. Different thermodynamic energy parameters, could therefore, be estimated from the stand point of Eyring's rate theory [15,16] to infer molecular dynamics of the nonspherical liquids. μ_{theo} 's of the molecules could, however, be found out from the available bond angles and bond moments of the substituent polar groups attached to the parent molecules. They are usually found to differ from the measured μ_j 's indicating the existence of mesomeric and inductive effects in polar liquids due to their aromaticity.

References

- [1] G S Kastha, J Dutta, J Bhattacharyya and S.B. Roy *Indian J Phys* **43B**, (1965) 14.
- [2] C R Acharyya, A K Chatterjee, P K Sanyal and S. Acharyya, *Indian J Pure & Appl Phys*, **24** (1986) 234.
- [3] U Saha and S. Acharyya, *Indian J. pure & Appl Phys* **31** (1993) 181.
- [4] S Acharyya, A K Chatterjee, P Acharyya and I L Saha, *Indian J. Phys.* **56B** (1982) 291.
- [5] J P Shukla, S I Ahmed, D D Shukla & M C Saxena, *J. Phys. Chem* **72** (1968) 1013.
- [6] R L Dhar, A Mathur, J P Shukla and M C Saxena *Indian J. Pure & Appl Phys.* **11**, (1973) 568.
- [7] S K S Somevanshi, S B I Misra & N K Mehrotra, *Indian J Pure & Appl Phys* **16** (1978) 57.
- [8] M B R Murthy, R L Patil and D K Deshpande, *Indian J. Phys.* **63B** (1989) 491.
- [9] R C Basak, A Karmakar, S K Sit and S Acharyya, *Indian J. Pure & Appl Phys.* **37** (1999) 224.
- [10] H Eyring, S Glasstone and K J Laidler, *The theory of rate process* (Mc Graw Hill: New York), 1941.
- [11] F J Murphy and S O Morgan, *Bell Syst Tech J* **18** (1939) 502.
- [12] C P Smyth, *Dielectric behaviour and structure* (Mc Graw Hill: New York) 1955.
- [13] K V Gopalakrishna *Trans Faraday Soc.* **53** (1957) 767.
- [14] K Dutta, S K Sit and S Acharyya, *J Mol. Liquids* **92** (2001) 263.
- [15] H Eyring, *J Chem Phys.* **4** (1936) 283
- [16]. W Kauzmann : *Rev. mod. Phys.* **14** (1942) 12.

CHAPTER -6

STRUCTURAL AND ASSOCIATIONAL ASPECTS OF DIELECTROPOLAR STRAIGHT CHAIN ALCOHOLS FROM RELAXATION PHENOMENA

STRUCTURAL AND ASSOCIATIONAL ASPECTS OF DIELECTROPOLAR STRAIGHT CHAIN ALCOHOLS FROM RELAXATION PHENOMENA

6.1. Introduction

The relaxation phenomena of a dielectropolar liquid in a nonpolar solvent has attracted the attention of a large number of workers [1-3] as it is a very sensitive and useful tool to ascertain the shape, size and structure of a polar molecule. The technique provides one with much information about the stability [4] of the system undergoing relaxation phenomena. It also offers valuable insight into the solute-solute i.e. dimer and solute — solvent i.e. monomer formations [4]. Structural and associational aspects of a polar liquid in a non polar solvent can, however, be gained by measured static dipole moment μ_s and high frequency (hf) dipole moment μ_j in terms of relaxation time τ_j with weight fraction w_j .

Alcohols behaving like almost polymers have α, β, γ etc. dispersion regions. The strong dipole of —OH group rotates about $\equiv \text{C}-\text{O}$ —bond without disturbing CH_3 or CH_2 groups and thus they have possibility to exhibit intramolecular as well as intermolecular rotations. Sit and Acharyya [5] and Sit et al [6] studied the straight long chain alcohols like 1-butanol, 1-hexanol, 1-heptanol, 1-decanol in *n*-heptane [7] ethanol and methanol in benzene [8] (9.84 GHz) and 2-methyl —3 heptanol, 3—methyl —3heptanol, 4-methyl-3 heptanol, 5-methyl —3heptanol, 4 octanol and 2 octanol in *n*-heptane [9] at 25°C to observe that all the alcohols except methanol showed the double relaxation times, τ_1 and τ_2 at all the frequencies in GHz range. The alcohols were again expected to exhibit the triple relaxation phenomena [7] for different frequencies of electric field in GHz range. Such long chain liquids under investigation have wide applications in the fields of biological research, medicine and industry. Moreover, the study of alcohols in terms of modern internationally accepted units and symbols appears

to be superior for the unified, coherent and rationalised nature of the SI unit used.

The μ_s of all the associated dielectropolar molecules under static electric field was derived from static experimental parameter X_{ij} . X_{ij} is again involved with dimensionless static and high frequency relative permittivities ϵ_{0ij} and $\epsilon_{\infty ij}$ of Table 6.1 based on Debye model [10]. The linear coefficient of the expected non-linear experimental X_{ij} curves against w_j graphically shown in Figure 6.1 of alcohols were conveniently used to estimate μ_s at a given temperature.

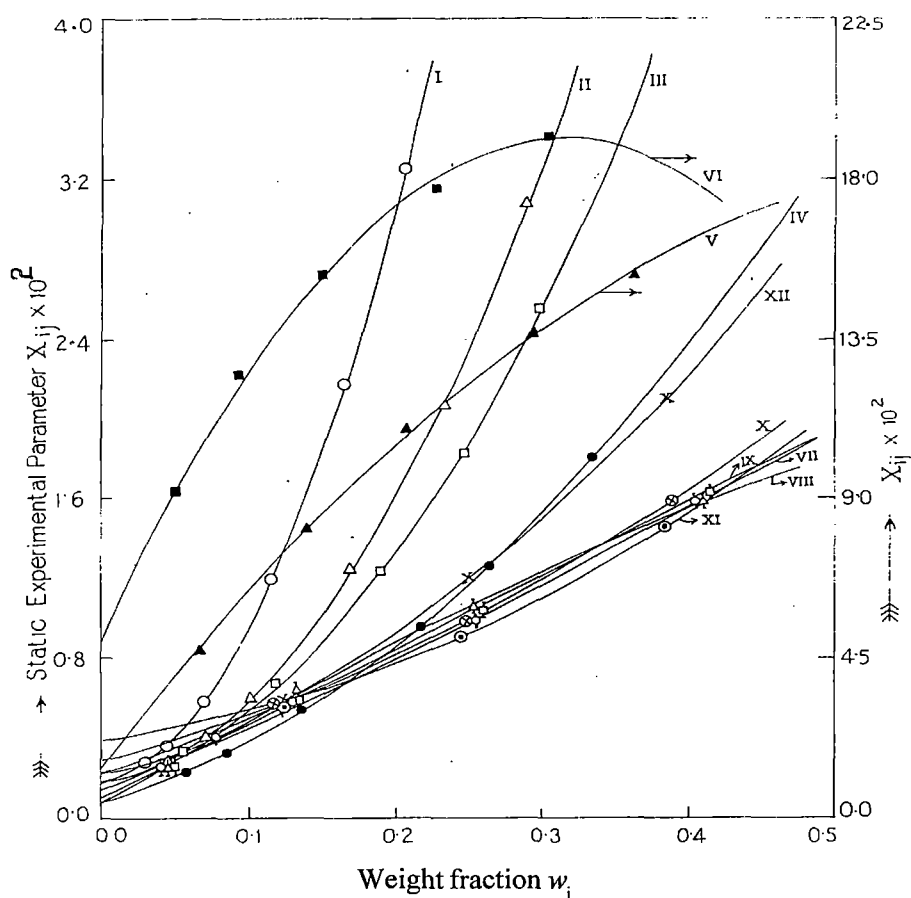


Figure 6.1 : Variation of static experimental parameter (X_{ij}) against weight fraction w_j of solute at 25°C under nearly 24 GHz electric field [ethanol and methanol at 9.84 GHz]

(I) 1-butanol (—○—), (II) 1-hexanol (—△—), (III) 1-heptanol (—□—), (IV) 1-decanol (—●—), (V) ethanol (—▲—), (VI) methanol (—■—), (VII) 2-methyl - 3 heptanol (—⊙—), (VIII) 3-methyl-3 heptanol (—⊔—), (IX) 4-methyl - 3 heptanol (—⊕—), (X) 5-methyl - 3 heptanol (—⊗—), (XI) 4-octanol (—⊖—), (XII) 2-octanol (—x—)

The τ_j of all the alcohols were, however, estimated from the slope of linear variation of imaginary σ_{ij}'' against real σ_{ij}' parts [11] of hf complex conductivity σ_{ij}^* for different weight fractions w_j s as seen in Figure 6.2. The hf σ_{ij}'' did not vary linearly with hf σ_{ij}' at higher or even lower concentrations [12]. It is therefore, better to use the ratio of slopes of individual variations of σ_{ij}'' and σ_{ij}' both in $\Omega^{-1} \text{m}^{-1}$ with w_j 's of Figures 6.3 and 6.4 to get the exact and accurate value of $d\sigma_{ij}''/d\sigma_{ij}'$ in the limit $w_j = 0$ to evaluate τ_j [13,14]. τ_j 's thus obtained by both the methods are placed in Table 6.3 to see how far they are close in agreements. τ_j 's of such dielectropolar alcohols were, however, estimated at 1.233 cm. for molecules like 1-butanol, 1-hexanol, 1-decanol, 2-methyl-3 heptanol, 3-methyl-3heptanol, 4-methyl-3heptanol, 5-methyl-3heptanol, 4-octanol, 2-octanol and at 1.249cm wave length electric field for 1-heptanol at which measured ϵ_{ij}'' of a given w_j of the solute when were graphically plotted against the electric field frequency "f" showed peak indicating the most effective dispersive region for such liquids.

The formulation to measure μ_j 's of all the alcohols involves with the slopes β 's of the expected $\sigma_{ij}-w_j$ non linear curves of Figure 6.5 and dimensionless parameter 'b' in terms of τ_j 's obtained by both the methods as τ_j 's were not found to agree excellently in Table 6.3. The σ_{ij}'' and σ_{ij}' in $\Omega^{-1} \text{m}^{-1}$ are not linear with w_j as evident from Figures 6.3 and 6.4. μ_j 's thus obtained are finally compared with μ_{theo} 's from available bond angles and bond moments of the substituent polar groups attached to parent ones. The slight disagreement between the measured μ_j 's and μ_s from μ_{theo} 's indicates the existence of inductive and mesomeric moments of different substituent polar groups present in such dielectropolar molecules in addition to strong hydrogen bonding in them as displayed by the molecular conformation of Figure 6.6.

The solvent C_6H_6 unlike n-heptane is a cyclic compound with three double bonds and six p-electrons on six carbon atoms. Hence π - π interaction or resonance effect combined with inductive effect known as mesomeric effect

is expected to play an important role in the measured μ_j under hf electric field. A special attention is to be paid to have the conformational structures of the alcohols to evaluate μ_{theo} as seen in Figure 6.6 and Table 6.2 from the reduction of the available bond moments [5,6] of different substituent polar groups by the ratio of $\mu_s / \mu_{\text{theo}}$. This takes into account of H-bonding in addition to inductive effect in them. Thus the conclusion regarding the molecular association of such long chain associated aliphatic alcohols may also be the reason to yield higher dipole moments.

6.2. Static Relaxation Parameter and Static dipole moment μ_s

Under static electric field μ_s of a dielectropolar molecule (j) in a non polar solvent (i) may be obtained from the following equation [10]

$$\frac{\epsilon_{\text{oj}}-1}{\epsilon_{\text{oj}}+2} - \frac{\epsilon_{\infty\text{ij}}-1}{\epsilon_{\infty\text{ij}}+2} = \frac{\epsilon_{\text{oi}}-1}{\epsilon_{\text{oi}}+2} - \frac{\epsilon_{\infty\text{i}}-1}{\epsilon_{\infty\text{i}}+2} + \frac{N\mu_s^2 c_j}{9\epsilon_0 k_B T} \quad (6.1)$$

where ϵ_{oj} and $\epsilon_{\infty\text{ij}}$ are the dimensionless low and infinite frequency relative permittivities of solution (ij). ϵ_0 is the permittivity of free space = 8.854×10^{-12} F.m⁻¹. c_j is the molar concentration of the solute, where $c_j = (\rho_{\text{ij}} w_j) / M_j$ and the other symbols carry usual meanings.

A polar liquid of weight W_j and volume V_j is mixed with a nonpolar solvent of weight W_i and volume V_i to get the solution density ρ_{ij} where

$$\begin{aligned} \rho_{\text{ij}} &= \frac{W_i + W_j}{V_i + V_j} = \frac{W_i + W_j}{W_i/\rho_i + W_j/\rho_j} \\ \rho_{\text{ij}} &= \frac{\rho_i \rho_j}{\rho_j W_i / (W_i + W_j) + \rho_i W_j / (W_i + W_j)} \\ &= \frac{\rho_i \rho_j}{\rho_j w_i + \rho_i w_j} = \rho_i (1 - \gamma w_j)^{-1} \end{aligned} \quad (6.2)$$

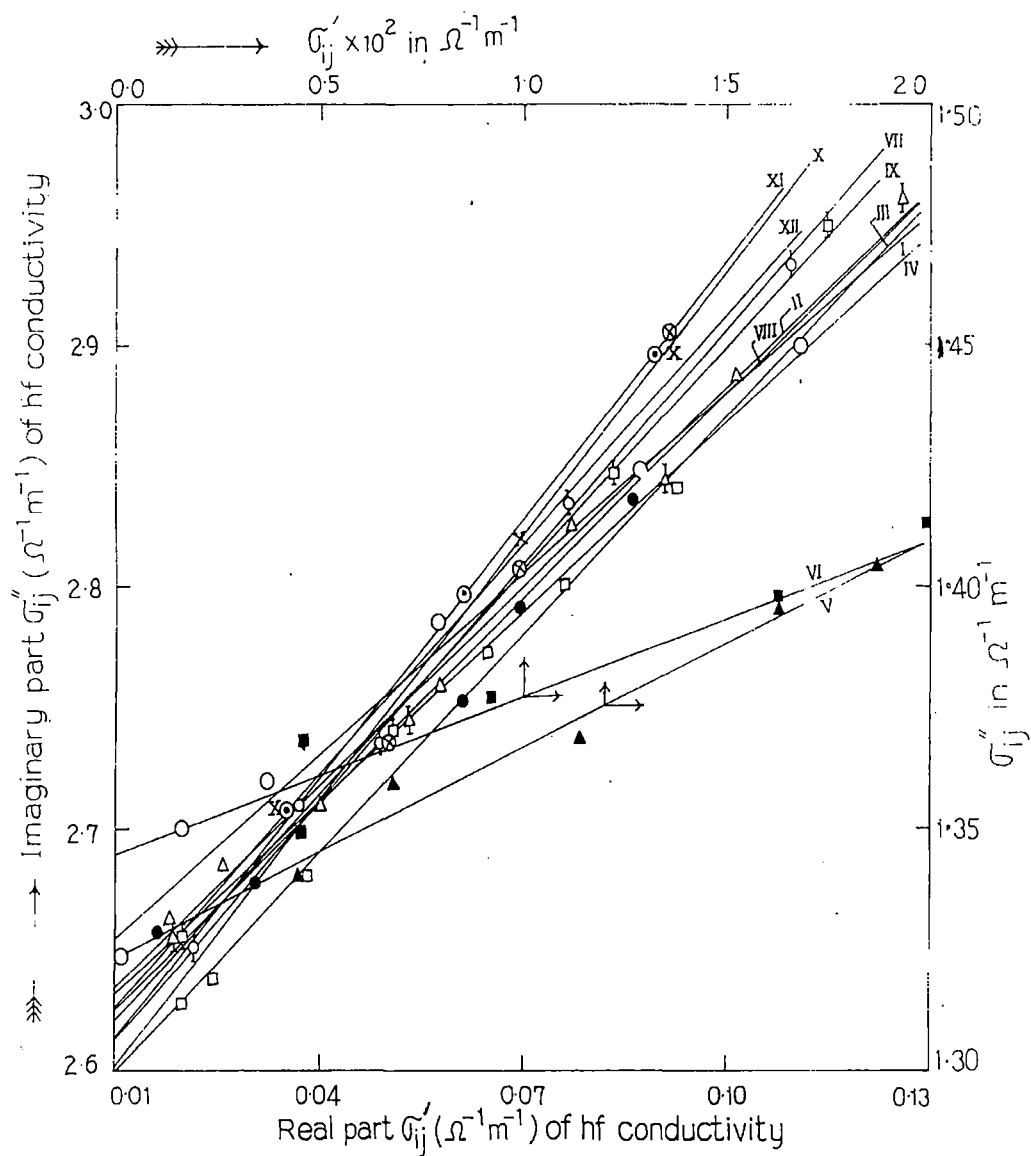


Figure 6.2 : Variation of imaginary part of hf conductivity (σ''_{ij}) against real part (σ'_{ij}) of some alcohols at 25°C under nearly 24 GHz electric field [ethanol and methanol at 9.84 GHz]

- (I) 1-butanol (—○—),
- (II) 1-hexanol (—△—),
- (III) 1-heptanol (—□—), (IV) 1-decanol (—●—),
- (V) ethanol (—▲—), (VI) methanol (—■—),
- (VII) 2-methyl-3 heptanol (—○—),
- (VIII) 3-methyl-3 heptanol (—△—),
- (IX) 4-methyl-3 heptanol (—□—),
- (X) 5-methyl-3 heptanol (—⊗—),
- (XI) 4-octanol (—⊙—),
- (XII) 2-octanol (—x—)

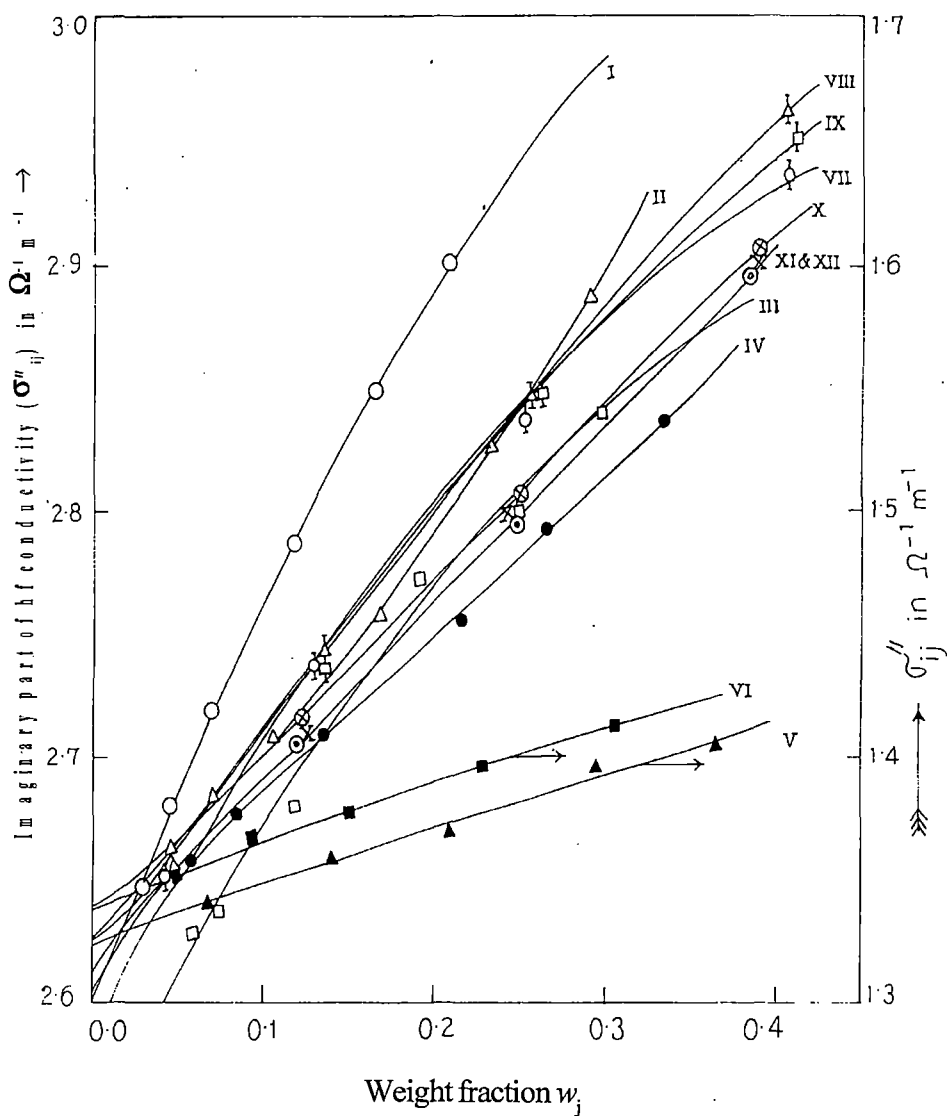


Figure 6.3 : Plot of imaginary part of hf conductivity (σ''_{ij}) in $\Omega^{-1} m^{-1}$ against weight fraction w_j of solute at 25°C under nearly 24 GHz electric field [ethanol and methanol at 9.84 GHz]

- (I) 1-butanol (—○—),
- (II) 1-hexanol (—△—),
- (III) 1-heptanol (—□—), (IV) 1-decanol (—●—),
- (V) ethanol (—▲—), (VI) methanol (—■—),
- (VII) 2-methyl - 3 heptanol (—⊙—),
- (VIII) 3-methyl-3 heptanol (—△̇—),
- (IX) 4-methyl - 3 heptanol (—□̇—),
- (X) 5-methyl - 3 heptanol (—⊗—),
- (XI) 4-octanol (—⊖—),
- (XII) 2-octanol (—x—)

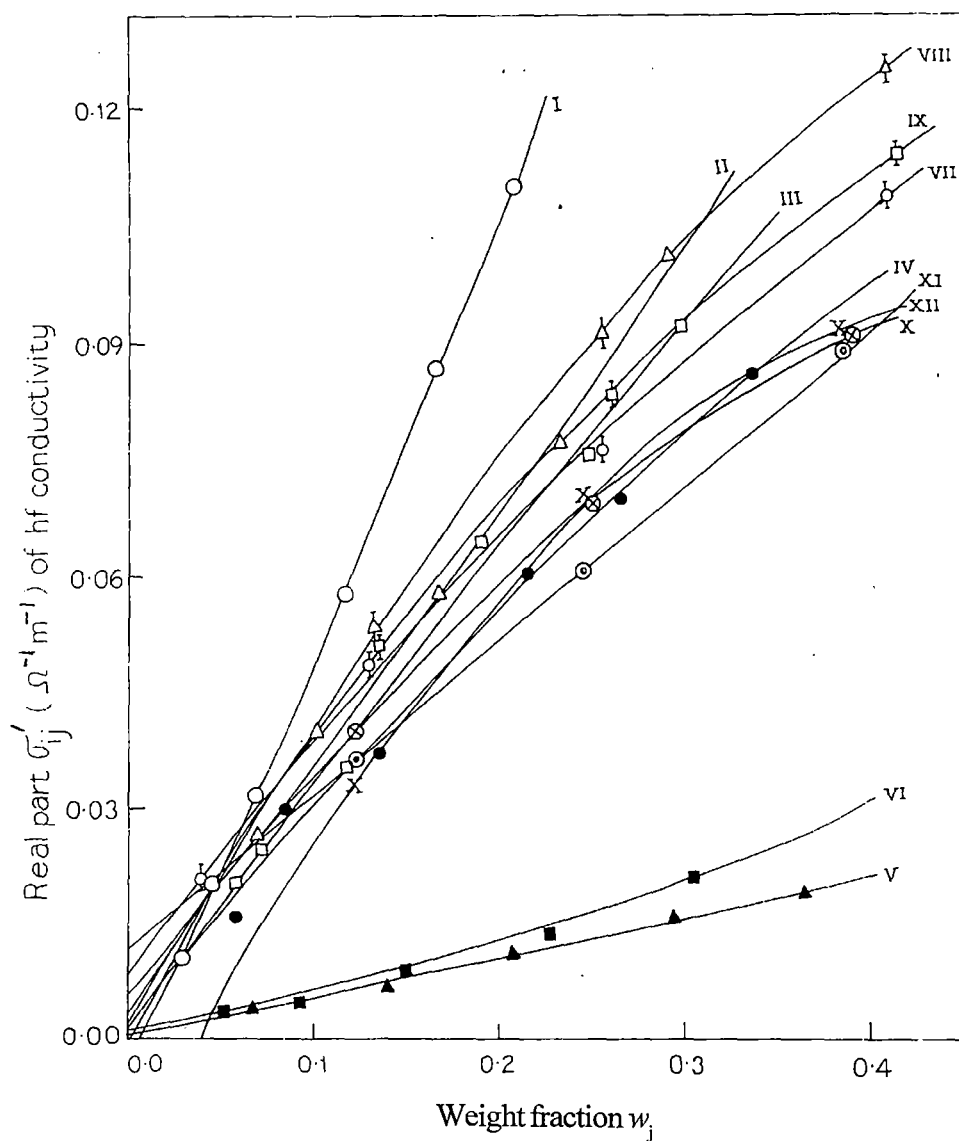


Figure 6.4 : Plot of real part of hf conductivity (σ'_{ij}) in $\Omega^{-1} m^{-1}$ against weight fraction w_j of solute at 25°C under nearly 24 GHz electric field [ethanol and methanol at 9.84 GHz]

- (I) 1-butanol (—○—),
- (II) 1-hexanol (—△—),
- (III) 1-heptanol (—□—), (IV) 1-decanol (—●—),
- (V) ethanol (—▲—), (VI) methanol (—■—),
- (VII) 2-methyl - 3 heptanol (—◊—),
- (VIII) 3-methyl-3 heptanol (—⋈—),
- (IX) 4-methyl - 3 heptanol (—◻—),
- (X) 5-methyl - 3 heptanol (—⊗—),
- (XI) 4-octanol (—⊙—),
- (XII) 2-octanol (—x—)

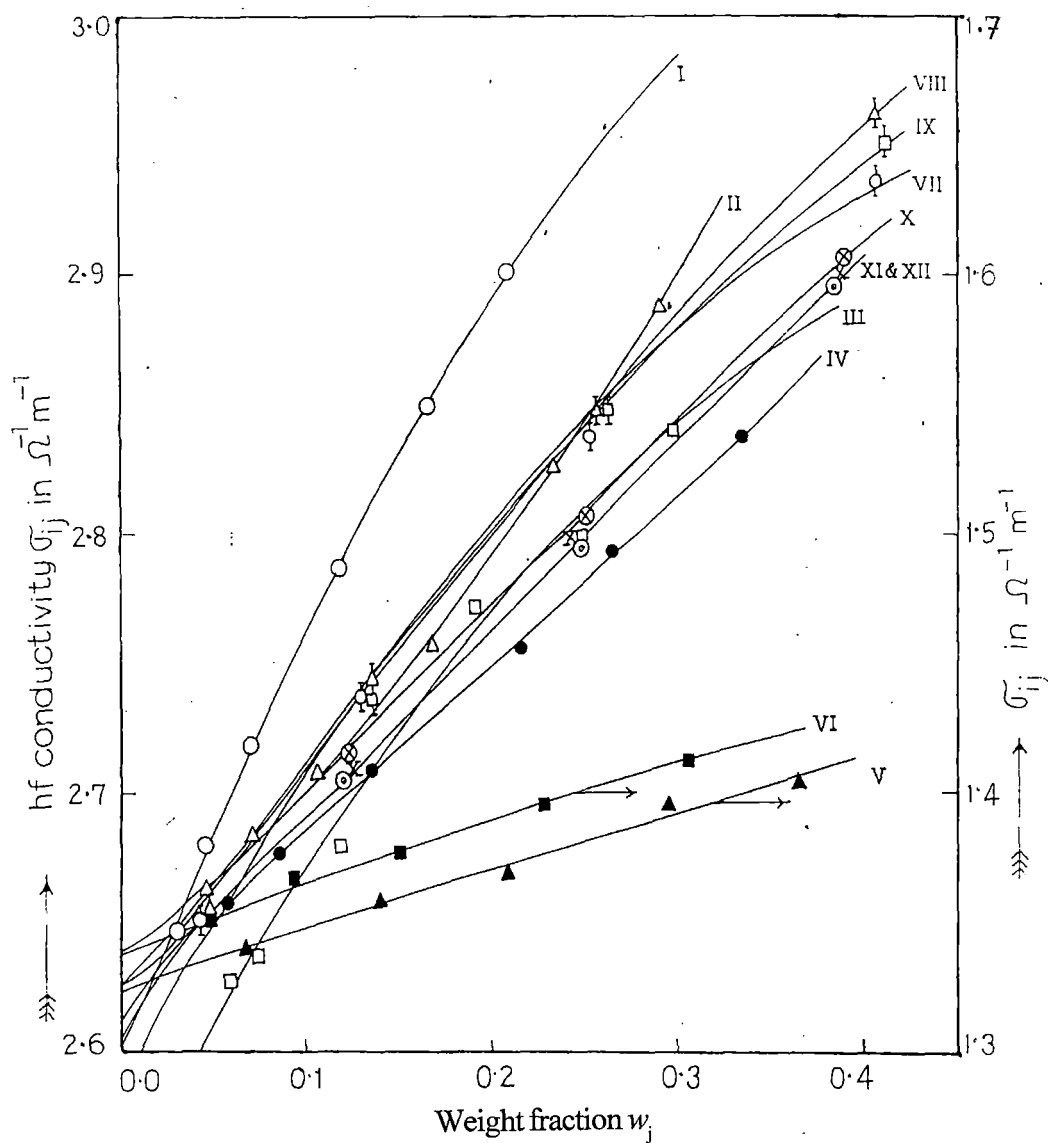


Figure 6.5 : Plot of total hf conductivity (σ_{ij}) in $\Omega^{-1} \text{ m}^{-1}$ against weight fraction w_j of solute at 25°C under nearly 24 GHz electric field [ethanol and methanol at 9.84 GHz]

- (I) 1-butanol (—O—),
- (II) 1-hexanol (— Δ —),
- (III) 1-heptanol (— \square —), (IV) 1-decanol (— \bullet —),
- (V) ethanol (— \blacktriangle —), (VI) methanol (— \blacksquare —),
- (VII) 2-methyl-3 heptanol (— \odot —),
- (VIII) 3-methyl-3 heptanol (— \triangle —),
- (IX) 4-methyl-3 heptanol (— \square —),
- (X) 5-methyl-3 heptanol (— \otimes —),
- (XI) 4-octanol (— \odot —),
- (XII) 2-octanol (—x—)

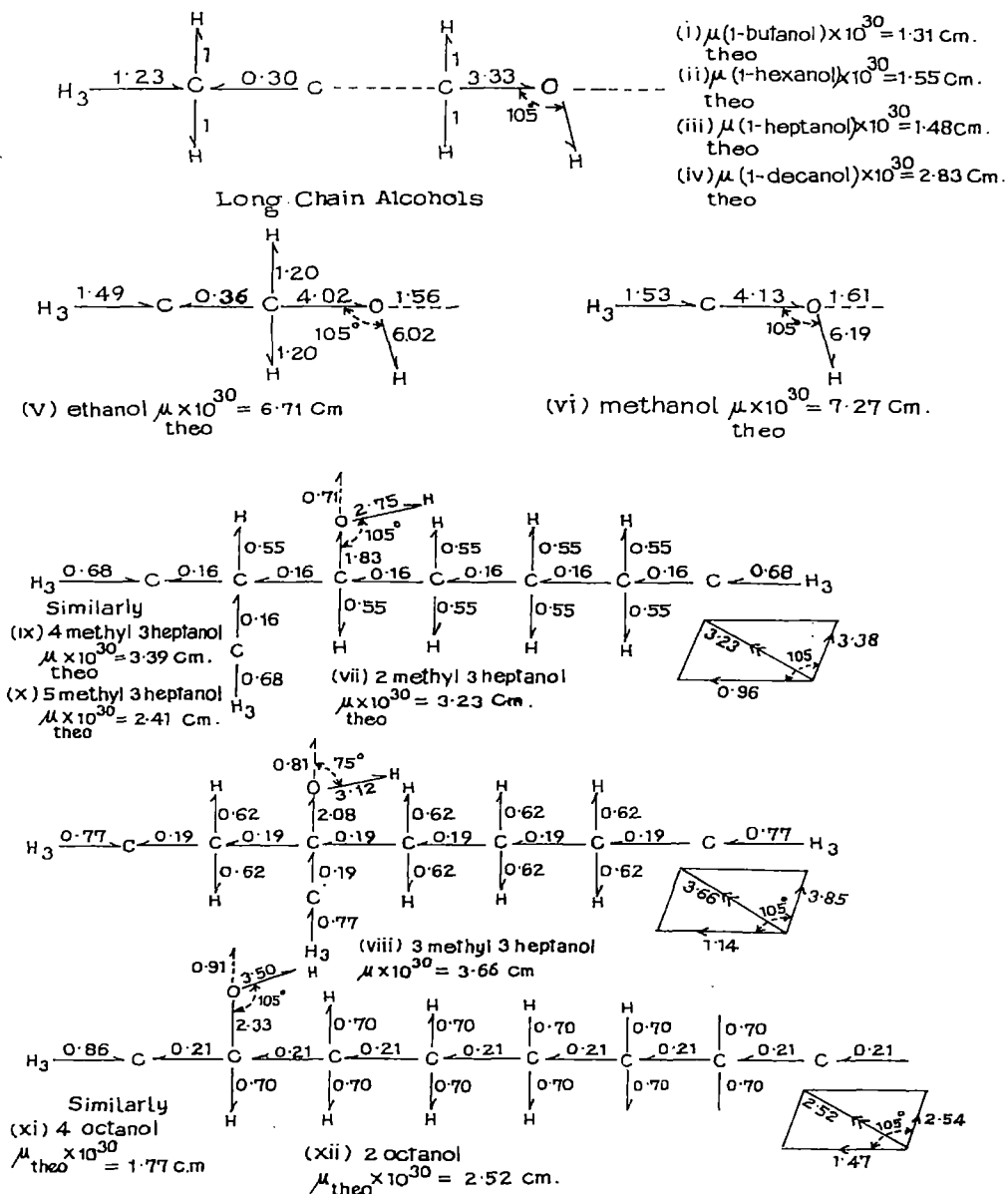


Figure 6.6 : Conformational structures of dielectropolar alcohols [Bond moment $\times 10^{30}$ Coulomb-metre (C.m.) given in figures]

The weight fractions w_j and w_i of solute and solvent are given by

$$w_j = \frac{W_j}{W_i + W_j} \text{ and } w_i = \frac{W_i}{W_i + W_j} \text{ such that } w_i + w_j = 1$$

and $\gamma = (1 - \rho_i/\rho_j)$, ρ_i and ρ_j are densities of pure solvent and solute respectively.

Now Eq. (6.1) may be written as

$$\frac{\epsilon_{oij} - \epsilon_{\infty ij}}{(\epsilon_{oij} + 2)(\epsilon_{\infty ij} + 2)} = \frac{\epsilon_{oi} - \epsilon_{\infty i}}{(\epsilon_{oi} + 2)(\epsilon_{\infty i} + 2)} + \frac{N\rho_i\mu_s^2}{27\epsilon_0 M_j k_B T} w_j (1 - \gamma w_j)^{-1}$$

$$X_{ij} = X_i + \frac{N\rho_i\mu_s^2}{27\epsilon_0 M_j k_B T} w_j + \frac{N\rho_i\mu_s^2}{27\epsilon_0 M_j k_B T} \gamma w_j^2 + \dots \quad (6.3)$$

The right hand side of Eq. (6.3) is obviously a polynomial equation of w_j like

$$X_{ij} = a_0 + a_1 w_j + a_2 w_j^2 + \dots \quad (6.4)$$

Now comparing the linear coefficients of Eqs. (6.3) and (6.4) one gets μ_s from:

$$\mu_s = \left(\frac{27\epsilon_0 M_j k_B T}{N\rho_i} a_1 \right)^{1/2} \quad (6.5)$$

where a_1 is the linear coefficient of $X_{ij}-w_j$ curve of Figure 6.1. But μ_s from higher coefficients of Eqs. (6.3) and (6.4) are not reliable as they are involved with the various effects of solvent, relative density, solute-solute association, internal field, macroscopic viscosity etc. μ_s from Eq. (6.5) along with a_1 are placed in Table 6.2 to compare with hf μ_j 's presented in Table 6.4.

Table 6.1 : Measured dielectric relative permittivities ϵ'_{ij} , ϵ''_{ij} , ϵ_{oij} and $\epsilon_{\infty ij}$ of some dielectropolar alcohols in nonpolar solvent at 25°C under different weight fractions w_j .

Systems with Sl. no. & molecular weight	Weight fraction w_j of alcohols	Measured dielectric relative permittivities			
		ϵ'_{ij}	ϵ''_{ij}	ϵ_{oij}	$\epsilon_{\infty ij}$
(i) 1-butanol in n-heptane $M_j=0.074$ kg.	0.0291	1.957	0.0079	1.971	1.928
	0.0451	1.981	0.0147	2.000	1.945
	0.0697	2.011	0.0236	2.050	1.958
	0.1163	2.060	0.0425	2.175	2.978
	0.1652	2.105	0.0644	2.381	2.000
	0.2072	2.144	0.0818	2.621	2.020
(ii) 1-hexanol in n-heptane $M_j=0.102$ kg.	0.0458	1.968	0.0131	1.988	1.944
	0.0703	1.984	0.0190	2.015	1.952
	0.1028	2.001	0.0296	2.064	1.970
	0.1687	2.037	0.0425	2.196	1.989
	0.2335	2.088	0.0569	2.360	2.002
	0.2901	2.134	0.0748	2.580	2.018
(iii) 1-heptanol in n-heptane $M_j=0.116$ kg.	0.0564	1.968	0.0147	1.985	1.932
	0.0735	1.975	0.0182	2.008	1.945
	0.1175	2.007	0.0265	2.066	1.957
	0.1909	2.076	0.0482	2.195	1.989
	0.2465	2.097	0.0567	2.315	2.002
	0.2970	2.126	0.0693	2.464	2.008
(iv) 1-decanol in n-heptane $M_j=0.158$ kg.	0.0572	1.965	0.0120	1.976	1.940
	0.0857	1.979	0.0223	2.003	1.952
	0.1351	2.003	0.0273	2.050	1.964
	0.2140	2.036	0.0449	2.147	1.990
	0.2640	2.064	0.0513	2.220	2.008
	0.3353	2.097	0.0637	2.346	2.030
(v) ethanol in benzene $M_j=0.046$ kg.	0.0664	2.450	0.0082	3.300	2.262
	0.1393	2.483	0.0124	4.300	2.190
	0.2077	2.500	0.0208	5.400	2.120
	0.2953	2.550	0.0297	7.000	2.062
	0.3638	2.567	0.0342	8.200	2.016
	(vi) methanol in benzene $M_j=0.032$ kg.	0.0514	2.467	0.0082	4.800
0.0930		2.500	0.0083	6.500	2.155
0.1495		2.517	0.0168	8.600	2.085
0.2266		2.550	0.0298	11.400	2.016
0.3049		2.583	0.0387	13.700	1.960

Contd...

Systems with Sl. no. & molecular weight	Weight fraction w_j of alcohols	Measured dielectric relative permittivities			
		ϵ'_{ij}	ϵ''_{ij}	ϵ_{oij}	$\epsilon_{\infty ij}$
(vii) 2-methyl	0.0437	1.960	0.0156	1.971	1.930
3-heptanol in	0.1299	2.022	0.0361	2.059	1.966
n-heptane	0.2522	2.095	0.0565	2.172	2.007
$M_j=0.130$ kg	0.4081	2.169	0.0809	2.330	2.054
(viii) 3-methyl	0.0450	1.965	0.0137	1.974	1.934
3-heptanol in	0.1334	2.028	0.0393	2.069	1.966
n-heptane	0.2538	2.103	0.0674	2.180	2.004
$M_j=0.130$ kg	0.4085	2.188	0.0928	2.334	2.057
(ix) 4-methyl	0.0466	1.964	0.0146	1.976	1.936
3-heptanol in	0.1326	2.025	0.0375	2.065	1.969
n-heptane	0.2590	2.104	0.0616	2.185	2.011
$M_j=0.130$ kg.	0.4124	2.180	0.0849	2.352	2.065
(x) 5-methyl	0.1228	2.008	0.0296	2.048	1.956
3-heptanol in	0.2489	2.075	0.0511	2.168	2.004
n-heptane	0.3898	2.148	0.0676	2.315	2.040
$M_j=0.130$ kg.					
(xi) 4-octanol in	0.1201	2.000	0.0265	2.040	1.948
n-heptane	0.2445	2.067	0.0449	2.148	1.997
$M_j=0.130$ kg.	0.3838	2.140	0.0659	2.282	2.031
(xii) 2-octanol in	0.1236	2.001	0.0245	2.049	1.954
n-heptane	0.2479	2.068	0.0513	2.195	1.996
$M_j=0.130$ kg.	0.3844	2.141	0.0680	2.410	2.036

Table 6.2 : Coefficients a_0, a_1, a_2 of $X_{ij} - w_j$ fitted curve of Figure 6.1, correlation coefficient (r), % of error in getting X_{ij} , static or low frequency dipole moment $\mu_s \times 10^{30}$ Coulomb-metre, theoretical dipole moments $\mu_{\text{theo}} \times 10^{30}$ in Coulomb-metre from reduced bond moments by μ_s/μ_{theo} and μ_1, μ_2 , by double relaxation method.

Systems with sl. no. & molecular weight M_j	Coefficients $a_0, a_1,$ and a_2 in Eq. $X_{ij} = a_0 + a_1 w_j + a_2 w_j^2$			Correlation coefficient (r)	% of error in fitting technique	$\mu_s \times 10^{30}$ in Coulomb-metre from Eq. (6.5)	Corrected $\mu_{\text{theo}} \times 10^{30}$ in Coulomb-metre from bond angle & reduced bond moments	μ_1 and μ_2 in Coulomb-meter from double relaxation method	
	$a_0 \times 10^3$	$a_1 \times 10^3$	a_2					$\mu_1 \times 10^{30}$ in C.m.	$\mu_2 \times 10^{30}$ in C.m.
(i) 1-butanol in n-heptane $M_j = 0.074$ kg.	1.8126	9.6141	0.6665	0.9826	0.95	1.31	4.97x0.2636 =1.31	3.63	29.17
(ii) 1-hexanol in n-heptane $M_j = 0.102$ kg.	1.7060	9.8358	0.3075	0.9847	0.83	1.55	4.37x0.3547 = 1.55	3.43	21.20
(iii) 1-heptanol in n-heptane $M_j = 0.116$ kg.	2.2603	7.9095	0.2345	0.9872	0.70	1.48	4.07x0.3636 = 1.48	3.73	27.00
(iv) 1-decanol in n-heptane $M_j = 0.158$ kg.	0.7973	21.0951	0.0901	0.9922	0.43	2.83	3.17x0.8927 = 2.83	3.83	17.24
(v) ethanol in benzene $M_j = 0.046$ kg	14.2833	524.0612	-0.3980	0.9915	0.51	6.71	5.57x1.2047 = 6.71	1.70	490.73

Systems with sl. no. & molecular weight M_j	Coefficients $a_0, a_1,$ and a_2 in Eq. $X_{ij} = a_0 + a_1 w_j + a_2 w_j^2$			Correlation coefficient (r)	% of error in fitting technique	$\mu_j \times 10^{30}$ in Coulomb-metre from Eq. (6.5)	Corrected $\mu_{\text{theo}} \times 10^{30}$ in Coulomb-metre from bond angle & reduced bond moments	μ_1 and μ_2 in Coulomb-metre from double relaxation method	
	$a_0 \times 10^3$	$a_1 \times 10^3$	a_2					$\mu_1 \times 10^{30}$ in C.m.	$\mu_2 \times 10^{30}$ in C.m.
(vi) methanol in benzene $M_j = 0.032$ kg.	49.8741	883.7091	-1.4159	0.9668	1.97	7.27	$5.87 \times 1.2385 = 7.27$	—	293.96
(vii) 2-methyl 3-heptanol in n-heptane $M_j = 0.130$ kg.	1.2160	33.4337	0.0050	0.9998	0.01	3.23	$5.87 \times 0.5503 = 3.23$	3.83	16.00
(viii) 3-methyl 3-heptanol in n-heptane $M_j = 0.130$ kg.	0.7339	43.0349	-0.0155	0.9986	0.19	3.66	$5.87 \times 0.6235 = 3.66$	3.83	8.60
(ix) 4-methyl 3-heptanol in n-heptane $M_j = 0.130$ kg.	0.9118	36.7395	0.0008	0.9996	0.03	3.36	$5.87 \times 0.5775 = 3.39$	3.90	13.90
(x) 5-methyl 3-heptanol in n-heptane $M_j = 0.130$ kg.	2.8971	18.6631	0.0369	0.9968	0.25	2.41	$5.87 \times 0.4106 = 2.41$	3.37	9.50
(xi) 4-octanol in n-heptane $M_j = 0.130$ kg.	2.5834	10.0231	0.0639	0.9946	0.42	1.77	$3.60 \times 0.4917 = 1.77$	3.43	10.97
(xii) 2-octanol in n-heptane $M_j = 0.130$ kg.	2.2868	20.4032	0.0737	0.9956	0.34	2.52	$3.60 \times 0.700 = 2.52$	3.43	16.00

Table 6.3 : Intercept (c) and slope (m) of $\sigma''_{ij} - \sigma'_{ij}$ equation (Figure 6.2), correlation coefficient (r), percentage of error, relaxation time τ_j in p-sec from Eq. (6.10), ratio of slopes of σ''_{ij} and σ'_{ij} with w_j ($=x/y$), relaxation time τ_j in p-sec from Eq. (6.11), calculated relaxation time τ_j in p-sec from Gopalakrishnas' method for some dielectropolar alcohols under nearly 24 GHz electric field (Q-band microwave) at 25°C.

System with SI.No and molecular weight	Intercept & slope of $\sigma''_{ij} - \sigma'_{ij}$ fitted equation		Correlation coefficient (r)	% of error	Estimated relaxation time τ_j in p-sec from Eq (6.10)	Ratio of slopes of σ''_{ij} & σ'_{ij} with w_j $x/y = (d\sigma''_{ij}/dw_j) / (d\sigma'_{ij}/dw_j)$	Estimated relaxation time τ_j in p-sec from Eq. (6.11)	Relaxation time τ_j in p-sec estimated from Gopalakrishnas method
	Intercept (c)	slope (m)						
(i) 1-butanol in n-heptane $M_j = 0.074$ kg.	2.3624	2.4816	0.9959	0.22	2.64	3.6206	1.81	2.47
(ii) 1-hexanol in n-heptane $M_j = 0.102$ kg.	2.6082	2.7315	0.9959	0.22	2.40	1.7857	3.66	2.25
(iii) 1-heptanol in n-heptane $M_j = 0.116$ kg.	2.5711	2.9898	0.9973	0.15	2.22	4.0081	1.65	2.07
(iv) 1-decanol in n-heptane $M_j = 0.158$ kg.	2.6089	2.5881	0.9926	0.41	2.53	2.0160	3.25	2.39
(v) ethanol in benzene $M_j = 0.046$ kg	1.3239	4.2872	0.9881	0.72	3.77	4.5418	3.56	3.62

Contd.....

System with Sl.No and molecular weight	Intercept & slope of $\sigma''_{ij} - \sigma'_{ij}$ fitted equation		Correlation coefficient (r)	% of error	Estimated relaxation time τ_i in p-sec from Eq (6.10)	Ratio of slopes of σ''_{ij} & σ'_{ij} with $w_i x/y = (d\sigma''_{ij}/dw_i)$	Estimated relaxation time τ_i in p-sec from Eq. (6.11)	Relaxation time τ_i in p-sec estimated from Gopalakrishnas method
	Intercept (c)	slope (m)						
(vi) methanol in benzene $M_j = 0.032$ kg	1.3448	3.2089	0.9633	2.17	5.04	6.6999	2.41	4.87
(vii) 2-methyl 3-heptanol in n-heptane $M_j = 0.130$ kg.	2.5820	3.2340	0.9995	0.04	2.02	3.3250	1.97	1.86
(viii) 3-methyl 3-heptanol in n-heptane $M_j = 0.130$ kg.	2.5997	2.8021	0.9976	0.16	2.34	2.2682	2.89	2.26
(ix) 4-methyl 3-heptanol in n-heptane $M_j = 0.130$ kg.	2.5901	3.0947	0.9989	0.07	2.11	2.7665	2.37	1.95
(x) 5-methyl 3-heptanol in n-heptane $M_j = 0.130$ kg.	2.5653	3.6562	0.9949	0.39	1.79	2.2437	2.92	1.63
(xi) 4-octanol in n-heptane $M_j = 0.130$ kg.	2.5791	3.5515	0.9999	0.01	1.84	3.8814	1.69	1.68
(xii) 2-octanol in n-heptane $M_j = 0.130$ kg.	2.5960	3.1511	0.9875	0.96	2.08	1.5636	4.19	1.93

Table 6.4 : Coefficients α, β, γ , of hf σ_{ij} against w_j curves (Figure 6.5) correlation coefficient (r), percentage of error, dimensionless parameter b using τ_j from Eq. (6.10) and (6.11), computed $\mu_j \times 10^{30}$ in Coulomb metre from Eqs. (6.10) and (6.16) and Eqs. (6.11) and (6.16) estimated $\mu_j \times 10^{30}$ in Coulomb metre from Gopalakrishna's method for some dielectropolar alcohols under nearly 24 GHz electric field (Q-band microwave) at 25°C.

Systems with Sl. no. & molecular weight	Coefficient of $\sigma_{ij} - w_j$ fitted equation			Correlation coefficient (r)	% of error	Dimension less parameter using τ_j from Eq. (6.10) $b=1/(1+\omega^2\tau_j^2)$	Dimension less parameter using τ_j from Eq. (6.11) $b=1/(1+\omega^2\tau_j^2)$	Computed $\mu_j \times 10^{30}$ in Coulomb metre		Estimated $\mu_j \times 10^{30}$ in Coulomb metre from Gopalakrishna's method
	$\sigma_{ij} = \alpha + \beta w_j + \gamma w_j^2$							hfmethod of Eqs. (6.10)&(6.16)	hfmethod of Eqs. (6.11)&(6.16)	
	α	β	γ							
(i) 1-butanol in n-heptane $M_j = 0.074$ kg.	2.5987	1.8394	-1.8413	0.9975	0.14	0.8601	0.9290	4.28	4.16	3.58
(ii) 1-hexanol in n-heptane $M_j = 0.102$ kg.	2.6391	0.5176	1.1817	0.9962	0.21	0.8815	0.7618	2.63	2.83	3.35
(iii) 1-heptanol in n-heptane $M_j = 0.116$ kg.	2.5500	1.3385	-1.2079	0.9932	0.37	0.8992	0.9417	4.50	4.39	3.59
(iv) 1-decanol in n-heptane $M_j = 0.158$ kg.	2.6242	0.6046	0.0962	0.9992	0.05	0.8700	0.8022	3.57	3.71	3.55
(v) ethanol in benzene $M_j = 0.046$ kg.	1.3255	0.2288	-0.0206	0.9924	0.46	0.9485	0.9538	1.44	1.43	1.33

Contd.....

Systems with Sl. no. & molecular weight	Coefficient of $\sigma_{ij} - w_j$ fitted equation			Correlation coefficient (r)	% of error	Dimension less parameter using τ from Eq. (6.10) $b=1/(1+\omega^2\tau_j^2)$	Dimension less parameter using τ from Eq. (6.11) $b=1/(1+\omega^2\tau_j^2)$	Computed $\mu_j \times 10^{30}$ in Coulomb metre		Estimated $\mu_j \times 10^{30}$ in Coulomb metre from Gopalakrishna's method
	$\sigma_{ij} = \alpha + \beta w_j + \gamma w_j^2$							hf method of Eqs. (6.10)&(6.16)	hf method of Eqs. (6.11)&(6.16)	
	α	β	γ							
(vi) methanol in benzene $M_j = 0.034$ kg	1.3367	0.3049	-0.1812	0.9930	0.42	0.9116	0.9783	1.41	1.36	1.18
(vii) 2-methyl 3-heptanol in n-heptane $M_j = 0.130$ kg.	2.5885	1.3064	-1.1371	0.9958	0.28	0.9130	0.9169	4.64	4.63	3.42
(viii) 3-methyl 3-heptanol in n-heptane $M_j = 0.130$ kg.	2.6133	1.0310	-0.4311	0.9984	0.10	0.8867	0.8368	4.18	4.30	3.54
(ix) 4-methyl 3-heptanol in n-heptane $M_j = 0.130$ kg.	2.6079	1.0777	-0.5929	0.9968	0.22	0.9058	0.8841	4.23	4.28	3.48
(x) 5-methyl 3-heptanol in n-heptane $M_j = 0.130$ kg.	2.6259	0.7479	-0.0668	0.9996	0.03	0.9304	0.8340	3.47	3.67	3.24
(xi) 4-octanol in n-heptane $M_j = 0.130$ kg.	2.6160	0.7566	-0.0677	0.9999	0.01	0.9268	0.9375	3.50	3.48	3.27
(xii) 2-octanol in n-heptane $M_j = 0.130$ kg.	2.6157	0.7437	-0.0249	0.9999	0.01	0.9083	0.7093	3.51	3.97	3.32

6.3. High Frequency Dipole moment μ_j and Relaxation time τ_j

Under hf electric field of GHz range the dimensionless complex dielectric relative permittivity ϵ_{ij}^* of solution (ij) is written as

$$\epsilon_{ij}^* = \epsilon_{ij}' + j \epsilon_{ij}'' \quad (6.6)$$

where ϵ_{ij}' and ϵ_{ij}'' are the real and imaginary parts of hf complex permittivity ϵ_{ij}^* . The hf complex conductivity σ_{ij}^* of a polar-nonpolar liquid mixture [15] of weight fraction w_j is :

$$\sigma_{ij}^* = \sigma_{ij}' + j \sigma_{ij}'' \quad (6.7)$$

where $\sigma_{ij}' = \omega \epsilon_0 \epsilon_{ij}''$ and $\sigma_{ij}'' = \omega \epsilon_0 \epsilon_{ij}'$ are real and imaginary parts of complex conductivity σ_{ij}^* and j is a complex number $= (-1)^{1/2}$.

The total hf conductivity σ_{ij} , is, however, obtained from

$$\sigma_{ij} = \omega \epsilon_0 (\epsilon_{ij}'^2 + \epsilon_{ij}''^2)^{1/2} \quad (6.8)$$

σ_{ij}'' is related to σ_{ij}' by [11]

$$\sigma_{ij}'' = \sigma_{\infty ij} + \left(\frac{1}{\omega \tau_j} \right) \sigma_{ij}' \quad (6.9)$$

where $\sigma_{\infty ij}$ is the constant conductivity at $w_j \rightarrow 0$ and τ_j is the relaxation time of a polar liquid molecule.

Eq. (6.9) on differentiation with respect to σ_{ij}' becomes

$$d\sigma_{ij}'' / d\sigma_{ij}' = \frac{1}{\omega \tau_j} \quad (6.10)$$

It is often better to use the ratio of slopes of individual variations of σ_{ij}'' and σ_{ij}' with w_j at $w_j \rightarrow 0$ to avoid polar-polar interaction in a given solvent to get τ_j from :

$$(d\sigma_{ij}''/dw_j) / (d\sigma_{ij}'/dw_j) = 1/\omega \tau_j$$

$$\text{or, } x/y = 1/\omega \tau_j \quad (6.11)$$

where $\omega = 2\pi f$, f being the frequency of alternating electric field.

In hf region of GHz range, it is often observed that $\sigma_{ij}'' \simeq \sigma_{ij}$ and Eq. (6.9) becomes

$$\sigma_{ij} = \sigma_{\infty ij} + (1/\omega\tau_j) \sigma_{ij}' \quad (6.12)$$

$$\text{or} \quad \beta = (1/\omega\tau_j) (d\sigma_{ij}'/dw_j) \quad (6.13)$$

where $\beta = (d\sigma_{ij}'/dw_j)$, is the slope of $\sigma_{ij} - w_j$ curve at $w_j \rightarrow 0$

The σ_{ij}' of a solution of weight fraction w_j of a polar molecule at T K is given by Smyth [14,16] as :

$$\sigma_{ij}' = \frac{N\rho_i\mu_j^2}{27M_jk_B T} \left(\frac{\omega^2\tau_j}{1+\omega^2\tau_j^2} \right) (\epsilon_{ij}' + 2) w_j \quad (6.14)$$

Eq. (6.14) on differentiation with respect to w_j and at $w_j \rightarrow 0$ yields

$$(d\sigma_{ij}'/dw_j)_{w_j \rightarrow 0} = \frac{N\rho_i\mu_j^2}{27M_jk_B T} \left(\frac{\omega^2\tau_j}{1+\omega^2\tau_j^2} \right) (\epsilon_i + 2)^2 \quad (6.15)$$

Where $N =$ Avogadro's number = 6.023×10^{23}

$\rho_i =$ density of solvent

$M_j =$ molecular weight of solute

$k_B =$ Boltzmann constant = 1.38×10^{-23} joule mole⁻¹K⁻¹.

From Eqs. (6.13) and (6.15) one gets hf μ_j as:

$$\mu_j = \left[\frac{27M_jk_B T}{N\rho_i (\epsilon_i + 2)^2} \cdot \frac{\beta}{\omega b} \right]^{1/2} \quad (6.16)$$

$$\text{where } b = \frac{1}{1+\omega^2\tau_j^2} \quad (6.17)$$

is a dimensionless parameter involved with estimated τ_j from Eqs. (6.10) and (6.11). All the computed hf μ_j 's in terms of slopes β 's and b 's are placed in Table

6.4 in order to compare with μ_{theo} 's, μ_s and μ_1, μ_2 of the flexible part and end-over-end rotation of the whole molecule [5,6] presented in Table 6.2.

6.4. Results and Discussion

The dimensionless real ϵ'_{ij} and imaginary ϵ''_{ij} parts of hf complex relative permittivity ϵ^*_{ij} along with static and infinite frequency relative permittivities ϵ_{oij} and $\epsilon_{\infty ij}$ of solution (ij) for different w_j of alcohols in different solvents at 25°C are presented in Table 6.1. The static experimental solution parameter X_{ij} 's involved with ϵ_{oij} and $\epsilon_{\infty ij}$ of Table 6.1 are shown in Figure 6.1 for different w_j of alcohols. The nature of variation of X_{ij} with w_j 's are parabolic in nature satisfying a polynomial equation $X_{ij} = a_0 + a_1 w_j + a_2 w_j^2$. The coefficients of $X_{ij}-w_j$ curves i.e. a_0, a_1 and a_2 are placed in 2nd, 3rd and 4th columns of Table 6.2. As evident from Figure 6.1, the $X_{ij}-w_j$ curves for methanol, ethanol and 3 methyl 3 heptanol are convex in nature as their coefficients of quadratic terms in Table 6.2 are negative. The remaining X_{ij} 's on the other hand, showed a gradual increase with w_j 's for all the coefficients of the curves are positive as seen in Table 6.2. The anomalous behaviour of $X_{ij}-w_j$ curves from linearity for all the alcohols in different solvents at a given temperature in °C may rouse an interesting relaxation mechanism in such long chain associated liquids. In comparison to octyl alcohols, the curves of normal alcohols in higher concentrations are highly concave having a tendency to meet at a common point on the X_{ij} axis at $w_j \rightarrow 0$. This sort of behaviour of $X_{ij}-w_j$ curves of Figure 6.1 arises either due to solute-solute i.e. dimer or solute-solvent i.e. monomer formations in comparatively high concentrations. The convex shape of ethanol and methanol occurs for the probable experimental uncertainty in their ϵ_{oij} and $\epsilon_{\infty ij}$ measurements. The identical nature of variation of all the octyl alcohols have almost the same slope, but of different intercepts as a result of solvation effect. Their X_{ij} 's have tendency to become closer within $0.1 \leq w_j \leq 0.2$ indicating various molecular association in them.

In case of non-associated liquids a_2 's were found to be vanishingly small in comparison to a_0 and a_1 to yield almost linear variation of X_{ij} against w_j . The estimated correlation coefficient (r) and the percentage of error (%) entered in 5th and 6th columns of Table 6.2 for all the alcohols are such that one may rely on the linear terms of $X_{ij}-w_j$ curve to compute μ_s 's from Eq. (6.5). μ_s 's thus computed are placed in the 7th column of Table 6.2 to compare with μ_{theo} 's obtained from bond angles and bond moments of the substituent polar groups, as presented in Figure 6.6 and μ_1 and μ_2 of the flexible part and the whole molecule by the double relaxation method [5,6] at nearly 24 GHz electric field. The smaller and larger deviations of X_{ij} 's from linearity with w_j 's as seen in Figure 6.1 confirm the molecular association of such associated dielectropolar liquids in different solvents.

The relaxation times τ_j 's are, however, derived from the slopes of linear [11] variation of σ_{ij}'' with σ_{ij}' of Figure 6.2 for all the alcohols. Although, the experimental data, on the other hand, did not strictly fall on the fitted linear curves of σ_{ij}'' and σ_{ij}' both in $\Omega^{-1}\text{m}^{-1}$ as drawn in Figure 6.2, the slope of σ_{ij}'' against σ_{ij}' of Figure 6.2 was however, used to obtain τ_j from Eq. (6.10). The 2nd, 3rd and 6th columns of Table 6.3 contain all the estimated intercepts and slopes together with the measured τ_j 's. The linearity of σ_{ij}'' against σ_{ij}' curves as shown graphically in Figure 6.2 is again tested by correlation coefficient r 's and % of errors. They are entered in the 4th and 5th columns of Table 6.3 only to see how far σ_{ij}'' and σ_{ij}' are correlated to each other. But it is often better to use the ratio of the individual slopes of variation of σ_{ij}'' and σ_{ij}' with w_j at $w_j \rightarrow 0$ to get τ_j . τ_j 's by using Eq.(6.11) are not in close agreement with those obtained from Eq.(6.10) and by freshly calculated Gopalakrishna's method as seen in Table 6.3. Figures 6.3 and 6.4 showed that both σ_{ij}'' and σ_{ij}' vary nonlinearly with w_j . The nonlinear behaviour of σ_{ij}'' and σ_{ij}' as seen in Figures 6.3 and 6.4 with w_j 's invites the associational and structural aspects of such long chain dielectropolar associated molecules. The latter method to measure τ_j 's thus

appears to be a significant improvement [12,13] over the former one [11] as it eliminates the polar-polar interaction in a given solvent.

The hf μ_j 's from Eq. (6.16) was obtained from the slope β of the nonlinear variation of σ_{ij} in $\Omega^{-1}\text{m}^{-1}$ with w_j 's of Figure 6.5 and dimensionless parameter 'b' of Eq. (6.17) in terms of τ_j obtained by both the methods. The intercept α and slope β of hf σ_{ij} with w_j curves of Figure 6.5 are entered in the 2nd and 3rd columns of Table 6.3. It is interesting to note that the curves of $\sigma_{ij}-w_j$ variation of Figure 6.5 are almost identical with $\sigma_{ij}''-w_j$ curves of Figure 6.3. This fact at once confirms the applicability of the approximation $\sigma_{ij}'' \simeq \sigma_{ij}$ as done in Eqs. (6.9) and (6.12). The imaginary σ_{ij}'' and total hf σ_{ij} in case of normal alcohols in Figures 6.3 and 6.5 decreases gradually with w_j 's of 1-butanol to methanol except ethanol. This can be explained on the basis of the fact that the polarity of the molecules decrease from 1-butanol to methanol. Both σ_{ij}'' 's and σ_{ij} 's in Figures 6.3 and 6.5 of all the octyl alcohols are found to be closer only to show their nearly same polarity. The almost coincident curves of 4 octanol ($\text{---}\odot\text{---}$) and 2-octanol ($\text{---}\text{X}\text{---}$) arise due to their identical polarity as estimated in Figure 6.6.

The estimated μ_s 's and μ_j 's in Table 6.2 and 6.4 are then compared with μ_1 and μ_2 in Table 6.2 by double relaxation method [5,6] and those by freshly calculated Gopalakrishna's method. For all the octyl alcohols μ_j 's and μ_s 's are in excellent agreement with Gopalakrishna's μ_j 's (reported data) and μ_1 . The estimated μ_j 's for normal alcohols agree with reported μ 's and μ_1 . All these discussions made above establish the fact that a part of the molecule is rotating under GHz electric field. Slight disagreement in μ 's and the reported ones arises due to steric hindrances of the substituent polar units of their structural configurations of Figure 6.6 and the existence of associated nature for their hydrogen bonding. Unlike methanol and ethanol μ_s 's are always lower than μ_j 's and μ_1 's for all the alcohols. This at once reveals that under static electric field the possible formation of dimers which undergo to rupture into the solute solvent association i.e. monomer in the hf electric field to increase μ 's. It is

also evident that dimer formation is favourable in octyl alcohols than normal alcohols due to existence of strong inductive effect for their –OH groups at the end of molecular chains.

The theoretical dipole moments μ_{theo} 's of all the alcohols under study were calculated from the available bond angles and bond moments of the substituent polar groups like $\text{H}_3\text{-C}$, C-H , C-O , O-H ($<105^\circ$) and C-C of 1.23×10^{-30} , 1.0×10^{-30} , 3.33×10^{-30} , 1.30×10^{-30} and 0.3×10^{-30} Coulomb-metre (C.m) as presented elsewhere [5,6]. The values thus estimated are then made closer with the measured static μ_s 's or even μ_j 's by reducing the available bond moments by a factor μ_s/μ_{theo} which takes into account of the inductive and mesomeric effects of the substituent polar groups as shown in Figure 6.6. An inductive effect of polar unit acts along the chain of molecular axis of the normal alcohols to make them strongly polar due to presence of –OH group at their end of the axis. The comparatively higher μ_{theo} 's in octyl alcohols is probably due to screening effect of their –OH groups by other polar groups like $\text{H}_3\text{-C}$, C-H which favour the dimer formation of these alcohols through H-bonding to make their μ_s 's and μ_j 's higher than the normal alcohols as seen in Figure 6.6.

6.5. Conclusions

The modern internationally accepted symbols of dielectric terminologies and parameters in SI units are conveniently used to obtain the static and hf dipole moments μ_s and μ_j in terms of relaxation time τ_j of a polar molecule. τ_j 's measured from the slope of imaginary σ_{ij}'' and real σ_{ij}' of complex hf conductivity σ_{ij}^* for different ω_j are not in agreement with those measured from the ratio of the individual slopes of $\sigma_{ij}''-\omega_j$ and $\sigma_{ij}'-\omega_j$ curves at $\omega_j \rightarrow 0$ indicating the applicability of the latter method in long chain dielectropolar alcohols. This method of determination of τ_j is a significant improvement over the previous one as it eliminates polar-polar interactions in a given solvent. The comparison of μ_j 's and μ_s 's with μ_1 and μ_2 of the flexible part and the whole molecule by

double relaxation method and μ_{theo} 's from bond angles and bond moments seems to be an interesting phenomenon to have deep insight into relaxation mechanism of dielectropolar alcohols.

The results indicate that a part of the molecule is rotating under GHz electric field. The slight departure among the measured μ_s , μ_j and μ_{theo} reveals different associational aspects of dielectropolar alcohols in different solvents through the frequency dependence of relaxation parameters. It also shows the strong polar nature of normal alcohols which favour solute solvent association due to presence of $-\text{OH}$ group at the end of their bond axis. But the comparatively higher values of μ_j 's in octyl alcohols indicates the solute-solute association due to $-\text{H}$ bonding supported by the fact that $-\text{OH}$ being screened by $-\text{CH}_3$ and a large number of $>\text{CH}_2$ polar groups. The μ_s/μ_{theo} 's are almost constant for all the alcohols to take into account of all these facts in addition to their material property of the system. This study further supports the rotation of $-\text{OH}$ group along the $\equiv \text{C}-\text{O}-$ bond of all the alcohols under static and hf electric fields. Moreover, the methodology so far developed within the framework of Debye and Smyth model appears to be sound, simple, straightforward and useful to arrive at associational and structural aspects of alcohols which are thought to be non-Debye in relaxation behaviour.

References

- [1] KV Gopalakrishna, *Trans Faraday Soc.* **53** (1957) 767.
- [2] G S Kastha, J Dutta, J Bhattacharyya and S B Roy *Indian J Phys.* **43** (1969) 14.
- [3] S K Dutta, C R Acharyya and S Acharyya *Indian J Phys.* **55B** (1981) 140.
- [4] S K Sit, N Ghosh, U Saha and S Acharyya *Indian J Phys.* **71B** (1997) 533.

- [5] S K Sit and S Acharyya *Indian J Phys.* **70B** (1996) 19.
- [6] S K Sit, N Ghosh and S Acharyya *Indian J Pure & Appl. Phys.* **35** (1997) 329.
- [7] L Glasser, J Crossley and C P Smyth *J Chem Phys.* **57** (1972) 3977.
- [8] A K Ghosh *Ph D Dissertation* (N.B.U) 1981.
- [9] J Crossley, L Glasser and C P. Smyth *J Chem Phys.* **55** (1971) 2197.
- [10] P Debye '*Polar Molecules*' (Chemical Catalogue) 1929.
- [11] MBR Murthy, RL Patil and D K Deshpande *Indian J Phys.* **63B** (1989) 491.
- [12] N Ghosh, R C Basak, S K Sit and S Acharyya *J Mol Liquids* (Germany) **85** (2000) 375.
- [13] R C Basak, S K Sit, N Nandi and S Acharyya *Indian J Phys.* **70B** (1996) 37.
- [14] R C Basak, A Karmakar, S K Sit and S Acharyya, *Indian J Pure & Appl. Phys.* **37** (1999) 224.
- [15] F J Murphy and S O Morgan *Bell Syst Tech J* **18** (1939) 502.
- [16] C P Smyth '*Dielectric Behaviour and Structure*' (McGraw Hill : New York) 1955.

CHAPTER -7

STRUCTURAL AND ASSOCIATIONAL ASPECTS OF ISOMERS OF ANISIDINE AND TOLUIDINE UNDER A GIGAHERTZ ELECTRIC FIELD

STRUCTURAL AND ASSOCIATIONAL ASPECTS OF ISOMERS OF ANISIDINE AND TOLUIDINE UNDER A GIGAHERTZ ELECTRIC FIELD

7.1. Introduction

The dielectric relaxation of a polar liquid molecule in a nonpolar solvent under static and high frequency (hf) electric fields provides one with valuable information on various types of molecular associations [1,2] and the structural configuration of the polar molecule from relaxation parameters such as the relaxation time τ and dipole moment μ , measured by any standard method [3,4]. μ_j 's determined by concentration variation of the real part of the hf dielectric susceptibility are concerned with the orientational polarization and are further used to shed more light on the structural and associational aspects of a polar molecule [5].

Srivastava and Chandra [6] measured the real ϵ'_{ij} and imaginary ϵ''_{ij} parts of the relative complex permittivity, ϵ^*_{ij} and the static and infinitely hf relative permittivities, ϵ_{oij} and $\epsilon_{\infty ij}$ of isomers of anisidines and toluidines in C_6H_6 under 2.02, 3.86 and 22.06 GHz electric fields at 35°C. The purpose of such study was to observe the solute-solvent and solute-solute molecular associations, besides the possible existence of either double or single relaxation behaviour of anisidines and toluidines.

Nowadays, the usual practice is to study dielectric relaxation phenomena by dimensionless complex hf dielectric orientational susceptibility χ^*_{ij} [5] rather than the relative hf permittivity ϵ^*_{ij} or hf conductivity σ^*_{ij} . The ϵ^*_{ij} includes within it all types of polarizations while σ^*_{ij} is concerned with the transport of bound charges. Hence it is better to work with χ_{ij} for its more direct link with orientational polarization. Moreover, the present system of study in the modern concept of internationally accepted symbols of dielectric terminology and

parameters in SI units is interesting because of its rationalized, coherent and unified nature.

Under such a context we derived a linear equation (7.5) in terms of the real $\chi'_{ij} = (\epsilon'_{ij} - \epsilon_{\infty ij})$ and imaginary $\chi''_{ij} = \epsilon''_{ij}$ parts of the complex $hf \chi^*_{ij}$ and low-frequency dielectric susceptibility $\chi_{0ij} = (\epsilon_{0ij} - \epsilon_{\infty ij})$, which is real as presented in Table 7.1 under 9.945 GHz electric field, to obtain τ_1 and τ_2 of the flexible parts and the whole molecules in C_6H_6 at 35°C.

The electric field frequency of $f=9.945$ GHz was claimed to be the most effective dispersive region for such molecules [7]. When χ''_{ij} 's were plotted against frequency (f) they showed a peak in the neighbourhood of 9.945 GHz, at which point the dielectric orientation processes of polar molecules [8,9] are invariably maximum. At this frequency χ'_{ij} , χ''_{ij} and χ_{0ij} were again adjusted by a careful graphical interpolation technique [7]. One could make a strong conclusion of double relaxation phenomena of a polar molecule in a nonpolar solvent based on single-frequency measurement of the relaxation parameters, provided the accurate value of χ_{0ij} involved with ϵ_{0ij} and $\epsilon_{\infty ij}$ is available. The use of n^2_{Dij} for $\epsilon_{\infty ij}$ [6] may often introduce additional error into the calculation. Nevertheless, the data are accurate up to 5% for χ''_{ij} and 2% for χ'_{ij} and χ_{0ij} . The liquid molecules at this f absorb electric energy much more strongly to exhibit reasonable τ_1 and τ_2 for all the chemical systems under identical environments. τ_1 and τ_2 are, however, measured from the intercept and slope of the derived straight-line equation (see equation (7.5) of $(\chi_{0ij} - \chi'_{ij}) / \chi'_{ij}$ against χ''_{ij} / χ'_{ij} of Figure 7.1 for different weight fractions w_j 's of polar solute at the single frequency $\omega (= 2\pi f)$, signifying the material property of the systems. The correlation coefficients r and minimum chisquare values to test the linearity of the curves of Figure 7.1, along with the estimated τ_1 and τ_2 , are given in Table 7.2. In absence of reliable τ , the ratio of the individual slopes of variation of χ''_{ij} and χ'_{ij} with w_j 's at $w_j \rightarrow 0$, as seen in Figures 7.2 and 7.3, were conveniently used to evaluate τ_j to compare with those of Murthy *et al* [10] of Figure 7.4 and Gopalakrishna's method [11].

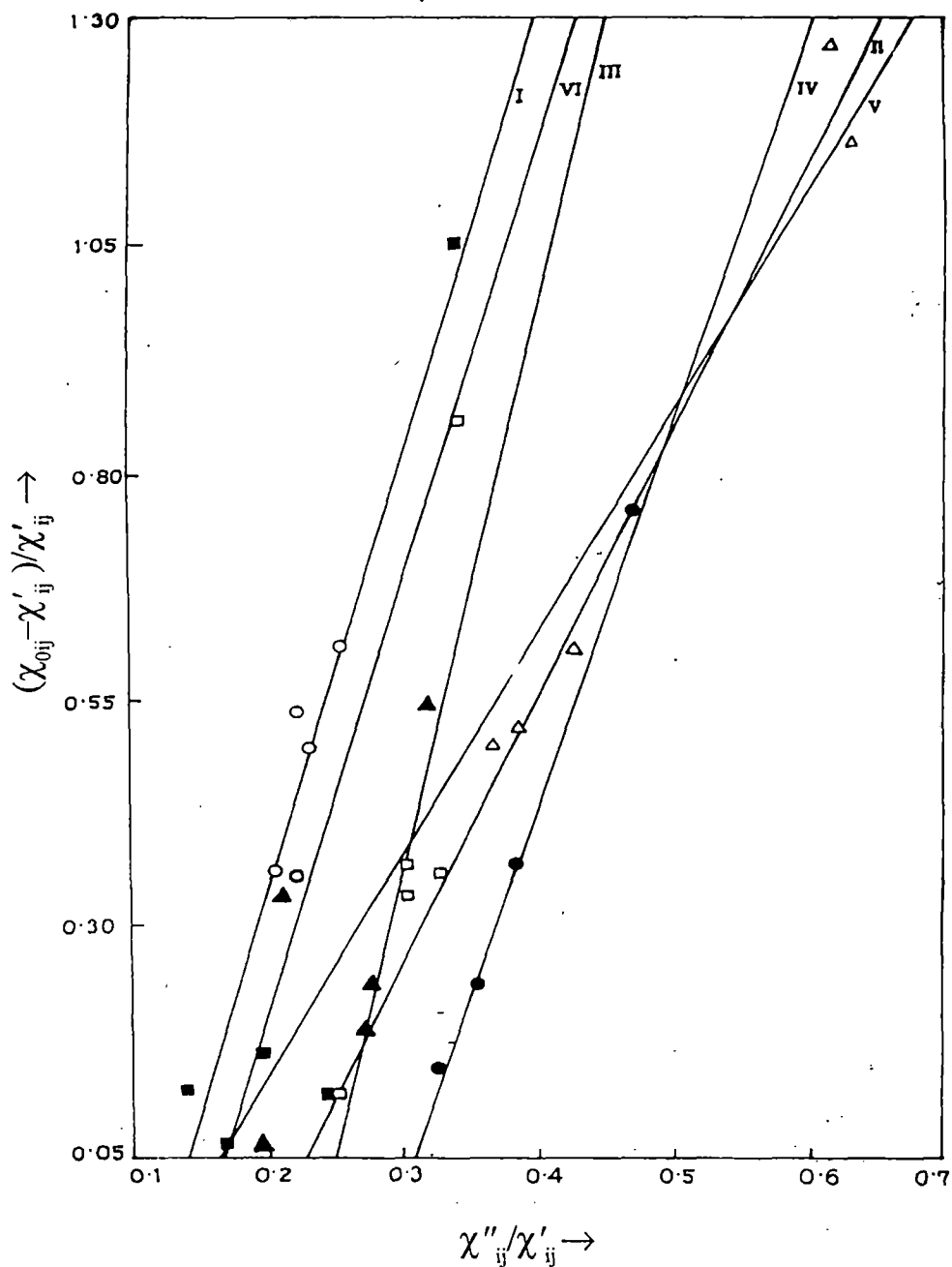


Figure 7.1. Linear variation of $(\chi_{0ij} - \chi'_{ij}) / \chi'_{ij}$ against χ''_{ij} / χ'_{ij} of isomers of anisidine and toluidine in benzene at 35°C under a 9.945 GHz electric field. ((I) o-anisidine (—○—), (II) m-anisidine (—△—), (III) p-anisidine (—□—), (IV) o-toluidine (—●—), (V) m-toluidine (—▲—) and (VI) p-toluidine (—■—)).

The theoretical weighted contributions c_1 and c_2 due to the estimated τ_1 and τ_2 presented in Table 7.3, towards dielectric dispersions, were calculated from Fröhlich's equations [12] in order to compare with the experimental contributions by the graphical extrapolation technique of Figures 7.5 and 7.6 at $w_j \rightarrow 0$. The symmetric and asymmetric distributions parameters γ and δ were, however, worked out from the variation of χ'_{ij}/χ_{0ij} and χ''_{ij}/χ_{0ij} with w_j in the limit $w_j = 0$ to conclude the symmetric distribution behaviour obeyed by such molecules. The characteristic relaxation time τ_{cs} from δ and ϕ of Figure 7.7 along with the symmetric relaxation time τ_s in terms of γ are found out to compare with τ_1 , τ_2 and τ_j in Table 7.2. The dipole moments μ_1 , μ_2 , and μ_0 in Coulomb metres (C m), in terms of b_1 , b_2 and b_0 involved with τ_1 , τ_2 , and τ_0 , where τ_0 is the most probable relaxation time ($=\sqrt{\tau_1\tau_2}$) and linear coefficient β 's of χ'_{ij} against w_j curves of Figure 7.3 were determined in order to place them in Table 7.4. The comparison, however, indicates that the flexible parts of the molecules rotate under X-band gigahertz electric fields. They are compared with μ_{theo} 's obtained from available bond angles and bond moments of the substituent polar groups attached to the parent molecules, as displayed in Figure 7.8, and μ_j by freshly calculated Gopalakrishna's method of Table 7.4. The slight disagreement between the measured μ 's and μ_{theo} 's invites the existence of inductive and mesomeric effects of substituent polar groups.

7.2. Theoretical formulations for τ_1 , τ_2 and τ_0

Bergmann *et al's* equations [13] are concerned with molecular orientational polarization processes. We therefore introduce χ_{ij} 's to avoid clumsiness of algebra as $\epsilon_{\infty ij}$ includes a fast polarization process and frequently appears as a subtracted term in the equations. Thus, with the established symbols of parameters of dielectric terminology like $\chi'_{ij} = (\epsilon'_{ij} - \epsilon_{\infty ij})$, $\chi''_{ij} = \epsilon''_{ij}$ and $\chi_{0ij} = (\epsilon_{0ij} - \epsilon_{\infty ij})$ of Table 7.1, Bergmann *et al's*

Table 7.1 : Concentration variations of the measured real ϵ'_{ij} and imaginary ϵ''_{ij} parts of the hf complex relative permittivity under a 9.945 GHz electric field, the static and hf relative permittivities ϵ_{0ij} and $\epsilon_{\infty ij}$ along with the real χ'_{ij} and imaginary χ''_{ij} parts of the complex dimensionless dielectric orientational susceptibility χ^*_{ij} and the low-frequency susceptibility χ_{0ij} which is real for isomers of anisidine and toluidine in benzene at 35°C.

System with Serial number and molecular weight (M_j)	Weight fraction, w_j , of solute	Measured dielectric relative permittivities				Dimensionless dielectric orientational susceptibilities		
		ϵ'_{ij}	ϵ''_{ij}	ϵ_{0ij}	$\epsilon_{\infty ij}$	χ'_{ij}	χ''_{ij}	χ_{0ij}
(i) o-anisidine $M_j = 0.123$ kg.	0.0326	2.3104	0.0148	2.336	2.239	0.0714	0.0148	0.097
	0.0604	2.3520	0.0244	2.404	2.247	0.1050	0.0244	0.157
	0.0884	2.4064	0.0340	2.459	2.255	0.1514	0.0340	0.204
	0.1135	2.4416	0.0400	2.538	2.262	0.1796	0.0400	0.276
	0.1361	2.4672	0.0512	2.588	2.267	0.2002	0.0512	0.321
(ii) m-anisidine $M_j = 0.123$ kg.	0.0160	2.2720	0.0234	2.315	2.235	0.0370	0.0234	0.080
	0.0336	2.3040	0.0390	2.384	2.241	0.0630	0.0390	0.143
	0.0579	2.3904	0.0618	2.477	2.246	0.1444	0.0618	0.231
	0.0823	2.4544	0.0744	2.553	2.253	0.2014	0.0744	0.300
	0.1109	2.5344	0.1056	2.675	2.261	0.2734	0.1056	0.414
(iii) p-anisidine $M_j = 0.123$ kg.	0.0319	2.3104	0.0252	2.373	2.237	0.0734	0.0252	0.136
	0.0597	2.3904	0.0474	2.442	2.246	0.1444	0.0474	0.196
	0.0848	2.5088	0.0642	2.539	2.250	0.2588	0.0642	0.289
	0.1106	2.5376	0.0840	2.638	2.262	0.2756	0.0840	0.376
	0.1396	2.6272	0.1086	2.745	2.269	0.3582	0.1086	0.476
(iv) o-toluidine $M_j = 0.107$ kg.	0.0137	2.2752	0.0162	2.301	2.241	0.0342	0.0162	0.060
	0.0459	2.3648	0.0408	2.392	2.250	0.1148	0.0408	0.142
	0.0622	2.4032	0.0570	2.457	2.255	0.1482	0.0570	0.202
	0.1048	2.5376	0.0900	2.577	2.264	0.2736	0.0900	0.313
(v) m-toluidine $M_j = 0.107$ kg.	0.0264	2.3136	0.0150	2.337	2.243	0.0706	0.0150	0.094
	0.0538	2.3552	0.0342	2.413	2.248	0.1072	0.0342	0.165
	0.0781	2.4576	0.0402	2.470	2.252	0.2056	0.0402	0.218
	0.1015	2.4840	0.0618	2.526	2.258	0.2260	0.0618	0.268
	0.1225	2.5280	0.0732	2.591	2.262	0.2660	0.0732	0.329
(vi) p-toluidine $M_j = 0.107$ kg.	0.0213	2.3100	0.0102	2.319	2.237	0.0730	0.0102	0.082
	0.0428	2.3040	0.0204	2.367	2.244	0.0600	0.0204	0.123
	0.0616	2.3904	0.0276	2.413	2.249	0.1414	0.0276	0.164
	0.0916	2.4704	0.0384	2.483	2.254	0.2164	0.0384	0.229
	0.1048	2.4960	0.0582	2.523	2.260	0.2360	0.0582	0.263

equations become

$$\frac{\chi'_{ij}}{\chi_{0ij}} = c_1 \frac{1}{1 + \omega^2 \tau_1^2} + c_2 \frac{1}{1 + \omega^2 \tau_2^2} \quad (7.1)$$

and

$$\frac{\chi''_{ij}}{\chi_{0ij}} = c_1 \frac{\omega \tau_1}{1 + \omega^2 \tau_1^2} + c_2 \frac{\omega \tau_2}{1 + \omega^2 \tau_2^2} \quad (7.2)$$

assuming the molecules possess two separate broad dispersions for which the relative weight factors c_1 and c_2 are such that $c_1 + c_2 = 1$. χ'_{ij} and χ''_{ij} are the real and imaginary parts of the hf complex susceptibility χ^*_{ij} and χ_{0ij} is the static or low-frequency susceptibility which is real.

Let $\alpha_1 = \omega\tau_1$ and $\alpha_2 = \omega\tau_2$, Eqs (7.1) and (7.2) are solved to obtain

$$c_1 = \frac{(\chi'_{ij}\alpha_2 - \chi''_{ij})(1 + \alpha_1^2)}{\chi_{0ij}(\alpha_2 - \alpha_1)} \quad (7.3)$$

and

$$c_2 = \frac{(\chi''_{ij} - \chi'_{ij}\alpha_1)(1 + \alpha_2^2)}{\chi_{0ij}(\alpha_2 - \alpha_1)} \quad (7.4)$$

provided $\alpha_2 > \alpha_1$. Now adding Eqs. (7.3) and (7.4), since $c_1 + c_2 = 1$, one obtains

$$\frac{\chi_{0ij} - \chi'_{ij}}{\chi'_{ij}} = \omega(\tau_1 + \tau_2) \frac{\chi''_{ij}}{\chi'_{ij}} - \omega^2\tau_1\tau_2. \quad (7.5)$$

Eq. (7.5) gives a straight line between the variables $(\chi_{0ij} - \chi'_{ij})/\chi'_{ij}$ and χ''_{ij}/χ'_{ij} having intercept $-\omega^2\tau_1\tau_2$ and slope $\omega(\tau_1 + \tau_2)$. It was solved for different concentrations w_j 's of each of the polar molecules of Table 7.1 for a given fixed value of the angular frequency $\omega (= 2\pi f)$ of the applied electric field at 35°C, where $f = 9.945$ GHz. The values of τ_1 and τ_2 from the intercept and slope of Eq. (7.5) are found as shown in Table 7.2.

The theoretical values of c_1 and c_2 towards dielectric relaxations were obtained from Eqs. (7.3) and (7.4) using values of χ'_{ij}/χ_{0ij} and χ''_{ij}/χ_{0ij} of Fröhlich's [12] following equations (7.6) and (7.7), in terms of the estimated τ_1 and τ_2 of Table 7.2 from the intercepts and slopes of Eq. (7.5):

$$\chi'_{ij}/\chi_{0ij} = 1 - \frac{1}{2A} \ln \left(\frac{1 + \omega^2\tau_2^2}{1 + \omega^2\tau_1^2} \right) \quad (7.6)$$

$$\chi''_{ij}/\chi_{0ij} = \frac{1}{A} [\tan^{-1}(\omega\tau_2) - \tan^{-1}(\omega\tau_1)] \quad (7.7)$$

The theoretical c_1 and c_2 are given in Table 7.3 in order to compare them with the experimental values obtained by graphically extrapolated values of χ'_{ij}/χ_{0ij} and χ''_{ij}/χ_{0ij} in the limit $w_j = 0$ in Figures 7.5 and 7.6 and Eqs. (7.3) and (7.4). The Fröhlich's parameter A where $A = \ln(\tau_2/\tau_1)$ is given in Table 7.3 for each compound.

Table 7.2 : Slope and intercept of the linear equation of $(\chi_{0ij} - \chi'_{ij})/\chi'_{ij}$ against χ''_{ij}/χ'_{ij} , correlation coefficient (r), minimum chisquare values, relaxation time τ_1 and τ_2 of the flexible part as well as the whole molecules, measured τ from Eq. (7.9) and (7.10), reported τ (Gopalakrishna) and most probable relaxation time τ_0 , together with symmetric τ_s and characteristic τ_{cs} from symmetric and asymmetric distribution parameters γ and δ of some monosubstituted anilines at 35°C under a 9.945 GHz (X-band microwave) electric field.

System with serial number and molecular weight (M_j)	Intercept and slope from Eq.(7.5) for $(\chi_{0ij} - \chi'_{ij})/\chi'_{ij}$ against χ''_{ij}/χ'_{ij}		Correlation Coefficient (r)	Chisquare Value ($\times 10^2$)	Estimated Relaxation times τ_1 and τ_2 (ps)	Most probable relaxation time $\tau_0 = \sqrt{\tau_1 \tau_2}$	Measured τ (ps) ^a	Ratio of slopes of χ''_{ij} and χ'_{ij} with w_j of Eq. (7.10)	
	Intercept (c)	Slope (m)						$(d\chi''_{ij}/dw_j)_{w_j \rightarrow 0}$	$(d\chi'_{ij}/dw_j)_{w_j \rightarrow 0}$
(i) o-anisidine $M_j = 0.123$ kg	0.6373	4.8390	0.7743	4.36	2.17	75.31	12.78	4.18	0.1560
(ii) m-anisidine $M_j = 0.123$ kg	0.6075	2.9047	0.9888	1.22	3.63	42.88	12.48	5.20	0.3033
(iii) p-anisidine $M_j = 0.123$ kg	1.4948	6.2149	0.8310	24.77	4.01	95.50	19.57	4.47	0.1824
(iv) o-toluidine $M_j = 0.107$ kg	1.2684	4.2603	0.9986	0.13	5.15	63.06	18.02	4.95	0.4025
(v) m-toluidine $M_j = 0.107$ kg	0.3501	2.4337	0.6864	30.10	2.46	36.51	9.48	4.18	0.1605
(vi) p-toluidine $M_j = 0.107$ kg	0.7348	4.7136	0.8687	-23.25	2.58	72.89	13.71	3.36	0.1755

System with serial number and molecular weight (M_j)	Relaxation times			
	τ (ps) ^b	τ (ps) ^c	τ (ps) ^d	τ (ps) ^e
(i) o-anisidine $M_j = 0.123$ kg	2.50	3.29	2.46	130.40
(ii) m-anisidine $M_j = 0.123$ kg	4.86	4.28	3.02	64.22
(iii) p-anisidine $M_j = 0.123$ kg	2.92	3.70	140.19	305.52
(iv) o-toluidine $M_j = 0.107$ kg	6.44	4.15	16.05	82.37
(v) m-toluidine $M_j = 0.107$ kg	2.57	4.01	5.85	458.51
(vi) p-toluidine $M_j = 0.107$ kg	2.81	3.34	1.38	12.07

^a Measured by the slope of χ''_{ij} against χ'_{ij} using the straight-line equation (7.9).

^b From the ratio of individual slopes. ^c By Gopalakrishna's method [11] ^d From the symmetric distribution parameter γ of Eq.(7.17).

^e From the asymmetric distribution parameter of Eq. (7.19).

7.3 Theoretical formulation for the dipole moment

The real ϵ'_{ij} and imaginary ϵ''_{ij} parts of the hf complex relative permittivity are written as

$$\epsilon'_{ij} = \epsilon_{\infty ij} + (1/\omega\tau)\epsilon''_{ij}$$

or
$$\epsilon'_{ij} - \epsilon_{\infty ij} = (1/\omega\tau)\epsilon''_{ij}$$

or
$$\chi'_{ij} = (1/\omega\tau)\chi''_{ij} \quad (7.8)$$

and
$$(d\chi''_{ij}/d\chi'_{ij}) = \omega\tau_j \quad (7.9)$$

The variation of susceptibility χ''_{ij} with χ'_{ij} Eq. (7.9) is caused by variation in concentrations, w_j 's, of the polar liquids under the fixed frequency of the electric field. As χ''_{ij} is, however, claimed to vary linearly with χ'_{ij} [10] of different concentrations and the frequency is fixed, the slope of χ''_{ij} with χ'_{ij} can conveniently be used to obtain τ_j from Eq. (7.9).

However, in case of monosubstituted anilines the variations of χ''_{ij} with χ'_{ij} , as seen in Figure 7.4, are not strictly linear. The ratio of individual slopes from the variations of χ''_{ij} and χ'_{ij} with w_j 's in Figures 7.2 and 7.3 is, however, thought to be a better representation of Eq. (7.9) to obtain τ_j where polar-polar interactions are supposed to be fully avoided.

Table 7.3 : Fröhlich's parameter A, relative contributions c_1 and c_2 due to theoretical τ_1 and τ_2 values of χ'_{ij}/χ_{0ij} and χ''_{ij}/χ_{0ij} of Fröhlich's equations, (7.6) and (7.7), and those by the graphical method at $w_j \rightarrow 0$, symmetric γ and asymmetric distribution parameters δ of some monosubstituted anilines at 35°C under a 9.945 GHz (X-band microwave) electric field.

System with serial number	Fröhlich's parameter A = ln (τ_1/τ_2)	Estimated values of χ'_{ij}/χ_{0ij} and χ''_{ij}/χ_{0ij} of Fröhlich's equations (7.6) and (7.7)		Weighted contributions c_1 and c_2 from Eq.(7.3) and (7.4)		Estimated values of χ'_{ij}/χ_{0ij} and χ''_{ij}/χ_{0ij} from Figures 7.5 & 7.6 at $w_j \rightarrow 0$		Weighted contribution c_1 and c_2 from the graphical technique		Symmetric distribution parameter γ	Asymmetric distribution parameter δ
		c_1	c_2	c_1	c_2	c_1	c_2	γ	δ		
(i) O-anisidine	3.5469	0.5598	0.3458	0.5099	1.3664	0.7100	0.1470	0.7117	0.2570	0.5716	0.1360
(ii) m-anisidine	2.4692	0.5848	0.4011	0.4997	0.8952	0.3339	0.3094	0.2508	0.7791	0.2475	0.5671
(iii) p-anisidine	3.1703	0.4419	0.3656	0.4222	1.6317	0.2114	0.1523	0.2062	0.6360	0.4813	0.4111
(iv) o-toluidine	2.5051	0.4600	0.4035	0.4296	1.1665	0.4995	0.2638	0.5197	0.4708	0.3821	0.3524
(v) m-toluidine	2.6974	0.6661	0.3726	0.5517	0.7879	0.5894	0.1308	0.5839	0.1173	0.6650	0.1422
(vi) p-toluidine	3.3412	0.5432	0.3576	0.4818	1.3361	0.9550	0.1148	0.9889	-0.1933	0.1617	0.1853

Thus

$$\left(\frac{d\chi''_{ij}}{dw_j}\right)_{w_j \rightarrow 0} \cdot \left[\left(\frac{d\chi'_{ij}}{dw_j}\right)_{w_j \rightarrow 0}\right]^{-1} = \omega\tau_j \quad (7.10)$$

The imaginary part χ''_{ij} of χ^*_{ij} is [14,15]

$$\chi''_{ij} = \frac{N\rho_{ij}\mu_j^2}{27\varepsilon_0 M_j k_B T} \left(\frac{\omega\tau}{1+\omega^2\tau^2}\right) (\varepsilon_{ij} + 2)^2 w_j \quad (7.11)$$

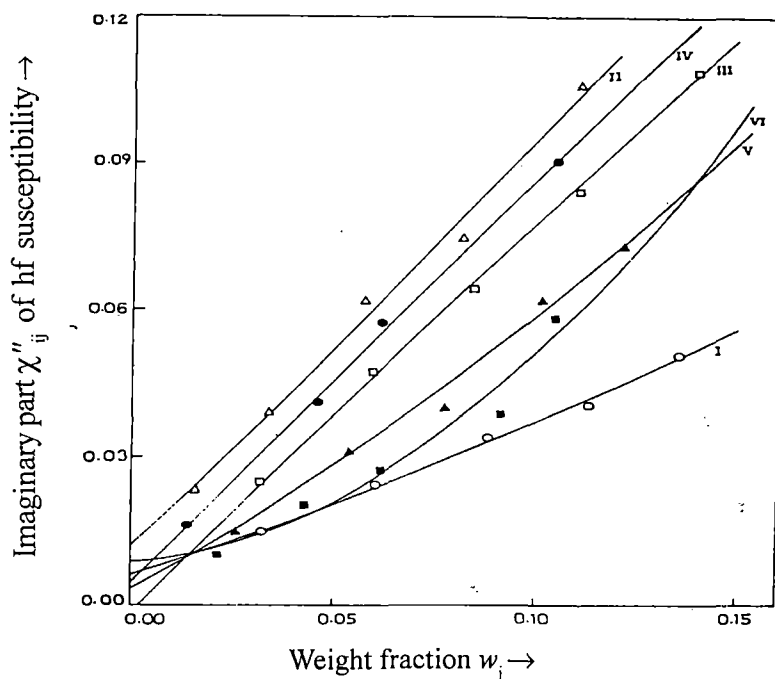


Figure 7.2. Variation of the imaginary part χ''_{ij} of the hf susceptibility against the weight fraction w_j of solute in benzene at 35°C under a 9.945 GHz electric field: (I) o-anisidine (—○—), (II) m-anisidine (—△—), (III) p-anisidine (—□—), (IV) o-toluidine (—●—), (V) m-toluidine (—▲—) and (VI) p-toluidine (—■—).

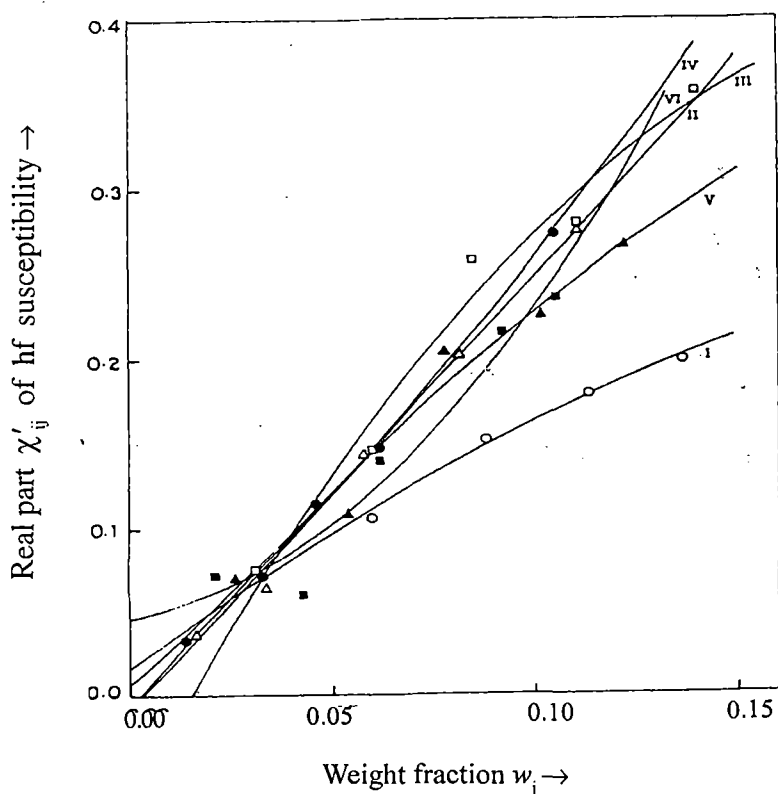


Figure 7.3. Variation of the real part χ'_{ij} of the hf susceptibility against the weight fraction w_j of solute in benzene at 35°C under a 9.945 GHz electric field: (I) o-anisidine (—○—), (II) m-anisidine (—△—), (III) p-anisidine (—□—), (IV) o-toluidine (—●—), (V) m-toluidine (—▲—) and (VI) p-toluidine (—■—).

Eq. (7.11), when differentiated with respect to w_j and at $w_j \rightarrow 0$ yields

$$\left(\frac{d\chi''_{ij}}{dw_j}\right)_{w_j \rightarrow 0} = \frac{N\rho_i\mu_j^2}{27\varepsilon_0 M_j k_B T} \left(\frac{\omega\tau}{1+\omega^2\tau^2}\right) (\varepsilon_i + 2)^2 \quad (7.12)$$

At $w_j \rightarrow 0$, the density of solution ρ_{ij} and $(\varepsilon_{ij} + 2)^2$ tends to ρ_i and $(\varepsilon_i + 2)^2$ where ρ_i and ε_i are the density and relative permittivity of solvent i , respectively.

In comparison to earlier works presented elsewhere [15,16] the approximation that $\chi_{ij} \simeq \chi''_{ij}$, as $\sigma_{ij} \simeq \sigma''_{ij}$, is not necessary to obtain the μ_j 's from the τ_j 's where σ''_{ij} is the imaginary part of the complex hf conductivity and σ_{ij} is the total hf conductivity of the polar-nonpolar liquid mixture.

From Eqs. (7.10) and (7.12) one obtains

$$\omega\tau_j \left(\frac{d\chi'_{ij}}{dw_j}\right)_{w_j \rightarrow 0} = \frac{N\rho_i\mu_j^2}{27\varepsilon_0 M_j k_B T} \left(\frac{\omega\tau}{1+\omega^2\tau^2}\right) (\varepsilon_i + 2)^2$$

or

$$\mu_j = \left[\frac{27\varepsilon_0 M_j k_B T \beta}{N\rho_i (\varepsilon_i + 2)^2 b} \right]^{1/2} \quad (7.13)$$

where τ_j and μ_j are the relaxation time and the dipole moment of the j th solute and ε_0 is the permittivity of free space, $8.854 \times 10^{-12} \text{ Fm}^{-1}$. Here N is the Avogadro number, 6.023×10^{23} ; ρ_i is the density of the solvent, 865 kg m^{-3} ; k_B is the Boltzmann constant, $1.38 \times 10^{-23} \text{ J mol}^{-1} \text{ K}^{-1}$; ε_i is the dielectric relative permittivity of the solvent, benzene, 2.253; M_j is the molecular weight of the solute in kilogrammes; β is the linear coefficient of the $\chi'_{ij}-w_j$ curve at $w_j \rightarrow 0$; and $b = 1/(1+\omega^2\tau^2)$ is a dimensionless parameter involved with the measured τ_j .

Table 7.4 : Coefficients α, β and γ of the $\chi'_{ij}-w_j$ curve (Figure 7.3) with correlation coefficients and percentage of errors, dimensionless parameter b , estimated μ_j 's where μ is from $\mu_1 = \mu_2(c_1/c_2)^{1/2}$ and theoretical μ from bond angles and bond moments together with reported μ (Gopalakrishna [11]) of some monosubstituted anilines in benzene at 35°C under a 9.945 GHz (X-band microwave) electric field.

System with serial number and molecular weight (M_j)	Coefficients of the equation $\chi'_{ij} = \alpha + \beta w_j + \gamma w_j^2$			Correlation coefficient of $\chi'_{ij}-w_j$ equation	% of error involved in $\chi'_{ij}-w_j$ equation	Dimensionless parameters			Estimated dipole moments μ ($\times 10^{30}$ Cm)		
	α	β	γ			b_0^a	b_1^b	b_2^c	μ_0	μ_1	μ_2
(i) o-anisidine $M_j = 0.123$ kg	0.0149	1.7546	-2.8056	0.9960	0.24	0.6108	0.9820	0.0432	6.17	4.87	23.21
(ii) m-anisidine $M_j = 0.123$ kg	-0.0094	2.5108	0.4641	0.9968	0.19	0.6221	0.9511	0.1224	7.31	5.91	16.49
(iii) p-anisidine $M_j = 0.123$ kg	-0.0634	4.4003	-10.2107	0.9962	0.23	0.4010	0.9410	0.0273	12.06	7.87	46.23
(iv) o-toluidine $M_j = 0.107$ kg	0.0063	2.0495	4.7368	0.9979	0.14	0.4412	0.9062	0.0606	7.32	5.11	19.75
(v) m-toluidine $M_j = 0.107$ kg	-0.0078	2.8140	-4.6071	0.9782	1.30	0.7404	0.9769	0.1613	6.62	5.76	14.19
(vi) p-toluidine $M_j = 0.107$ kg.	0.0464	0.3863	14.5432	0.9593	2.41	0.5770	0.9747	0.0460	2.78	2.14	9.84

Systems with serial number and molecular weight (M_j)	Dipole moments		
	Estimated μ ($\times 10^{30}$ Cm) ^a	Theoretical μ ($\times 10^{30}$ Cm) ^c	μ ($\times 10^{30}$ Cm) ^f
(i) o-anisidine $M_j = 0.123$ kg	14.18	3.40	4.50
(ii) m-anisidine $M_j = 0.123$ kg	12.32	5.50	6.17
(iii) p-anisidine $M_j = 0.123$ kg	23.51	6.30	6.53
(iv) o-toluidine $M_j = 0.107$ kg	11.98	4.63	5.77
(v) m-toluidine $M_j = 0.107$ kg	11.87	3.43	5.17
(vi) p-toluidine $M_j = 0.107$ kg	5.91	5.13	5.30

$$^a b_0 = \frac{I}{1 + \omega^2 \tau_0^2}$$

^c From bond angles and bond moments.

^f From Gopalakrishna's method [11].

$$^b b_1 = \frac{I}{1 + \omega^2 \tau_1^2}$$

$$^c b_2 = \frac{I}{1 + \omega^2 \tau_2^2}$$

$$^d \text{From } \mu_1 = \mu_2 \left(\frac{c_1}{c_2} \right)^{1/2}$$

The μ_1, μ_2 and μ_0 in terms of b_1, b_2 and b_0 involved with τ_1, τ_2 and τ_0 , respectively, were then computed with the knowledge of β of $\chi'_{ij}-w_j$ curves of Figure 7.3. The μ 's thus obtained from Eq. (7.13) are given in Table 7.4 in order to compare with those of Gopalakrishna [11] and μ_{theo} 's obtained from bond angles and bond moments of the substituent polar groups of the molecules of Figure 7.8.

7.4. Symmetric and characteristic relaxation times τ_s and τ_{cs}

The symmetric and asymmetric distribution parameters γ and δ appear in the following equations :

$$\chi_{ij}^*/\chi_{0ij} = \frac{1}{1+(j\omega\tau_s)^{1-\gamma}} \quad (7.14)$$

$$\chi_{ij}^*/\chi_{0ij} = \frac{1}{(1+j\omega\tau_{cs})^\delta} \quad (7.15)$$

Although the left-hand side of Eqs. (7.14) and (7.15) are identical, the former is associated with the symmetric relaxation time τ_s and latter with the characteristic relaxation time τ_{cs} . Separating the real and imaginary parts of Eqs.(7.14) and (7.15) and rearranging them in terms of $(\chi'_{ij}/\chi_{0ij})_{\omega j \rightarrow 0}$ and $(\chi''_{ij}/\chi_{0ij})_{\omega j \rightarrow 0}$ obtained from Figures 7.5 and 7.6 the γ and τ_s were found using.

$$\gamma = \frac{2}{\pi} \tan^{-1} \left[\left(1 - \frac{\chi'_{ij}}{\chi_{0ij}}\right) \frac{\chi'_{ij}}{\chi''_{ij}} - \frac{\chi''_{ij}}{\chi_{0ij}} \right] \quad (7.16)$$

and

$$\tau_s = \frac{1}{\omega} \left[\frac{1}{(\chi'_{ij}/\chi''_{ij}) \cos(\gamma\pi/2) - \sin(\gamma\pi/2)} \right]^{1/(1-\gamma)} \quad (7.17)$$

Again δ and τ_{cs} can be obtained from Eq. (7.15)

$$\tan(\phi\delta) = \frac{\chi''_{ij}}{\chi'_{ij}} \quad (7.18)$$

and

$$\tan \phi = \omega\tau_{cs} \quad (7.19)$$

As ϕ cannot be evaluated directly, an arbitrary theoretical curve between $(1/\phi) \log(\cos\phi)$ against ϕ in degrees was drawn in Figure 7.7, from which

$$\frac{1}{\phi} \log (\cos \phi) = \frac{\log \left[\left(\chi'_{ij} / \chi_{0ij} \right) / \cos (\phi \delta) \right]}{\phi \delta} \quad (7.20)$$

can be found. The known value of $(1/\phi) \log (\cos \phi)$ is used to obtain ϕ . With known ϕ and δ , τ_{cs} were found out from Eqs. (7.18) and (7.19). τ_s and τ_{cs} so evaluated are given in Table 7.2 in order to compare with values of τ by Murthy *et al* [10], Gopalakrishna [11] and τ_1 and τ_2 determined by double relaxation methods. The estimated values of γ and δ are however, given in Table 7.3.

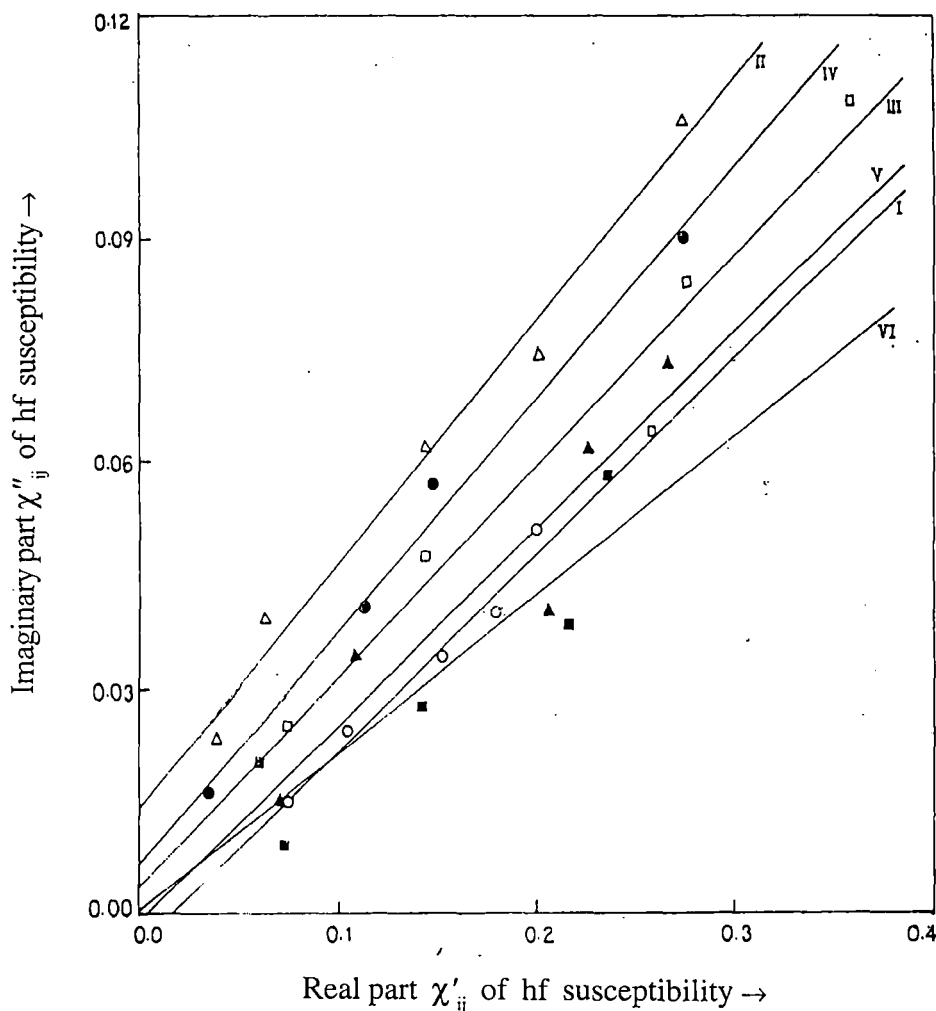


Figure 7.4. Linear plot of Imaginary part χ''_{ij} of the hf susceptibility against the real part χ'_{ij} of anisidine and toluidine in benzene at 35°C under a 9.945 GHz electric field: (I) o-anisidine (—o—), (II) m-anisidine (—Δ—), (III) p-anisidine (—□—), (IV) o-toluidine (—●—), (V) m-toluidine (—▲—) and (VI) p-toluidine (—■—).

7.5. Results and discussion

The least-squares fitted linear equations of $(\chi_{0ij} - \chi'_{ij})/\chi'_{ij}$ against χ''_{ij}/χ'_{ij} for different weight fractions w_j 's of the monosubstituted anilines in benzene at 35°C under a 9.945 GHz electric field are shown graphically in Figure 7.1, with the symbols denoting the experimental points. The experimental points are found to satisfy Eq. (7.5). χ'_{ij} and χ''_{ij} are the real and imaginary parts of the complex dielectric orientational susceptibility χ^*_{ij} and χ_{0ij} is the low-frequency dielectric susceptibility which is real. They are, however, derived from the measured relative permittivities [7] ϵ'_{ij} , ϵ''_{ij} , ϵ_{0ij} and $\epsilon_{\infty ij}$ of Table 7.1. The linearity of all the curves of Figure 7.1 are confirmed by correlation coefficients, r 's lying in the range 0.6894-0.9986. The chisquare test of all the curves were again made to support their linearity. The slopes and intercepts of all the linear curves of Figure 7.1 are placed in the second and third columns of Table 7.2. The chisquare values are, however, large for *o*-anisidine, *p*-anisidine and *m*-toluidine probably because of the large errors introduced in the ϵ'_{ij} , ϵ''_{ij} , ϵ_{0ij} and $\epsilon_{\infty ij}$ measurements for the molecules. In order to find the existence of double relaxation phenomena, accurate measurements of ϵ_{0ij} and $\epsilon_{\infty ij}$ are necessary. The refractive index n^2_{Dij} measured by Abbe's refractometer yields $\epsilon_{\infty ij} = n^2_{Dij}$ [6], although Cole-Cole [3,4] plot often gives $\epsilon_{\infty ij}$ as 1-1.15 times n^2_{Dij} .

The slope and intercept of each straight-line equation (7.5), obtained from χ'_{ij} , χ''_{ij} and χ_{0ij} of different w_j 's of Table 7.1 by least-squares fitting are used to determine τ_1 and τ_2 for each compound, as seen in the sixth and seventh columns of Table 7.2. τ_2 's are found to increase gradually from the *meta* to the *ortho* and to the *para* forms for all the anisidines and toluidines, probably due to the presence of the C→NH₂ group in them. The electric field of nearly 3 cm wavelength greatly influences the C→NH₂ group. On the other hand, τ_1 increases from *ortho* to *para* for the anisidines, while the reverse is true for the toluidines. The increase in the τ_1 values indicates that the flexible parts of the molecules

are more loosely bound to the parent molecules [17,18], which signifies that the material property of the system is undergoing relaxation.

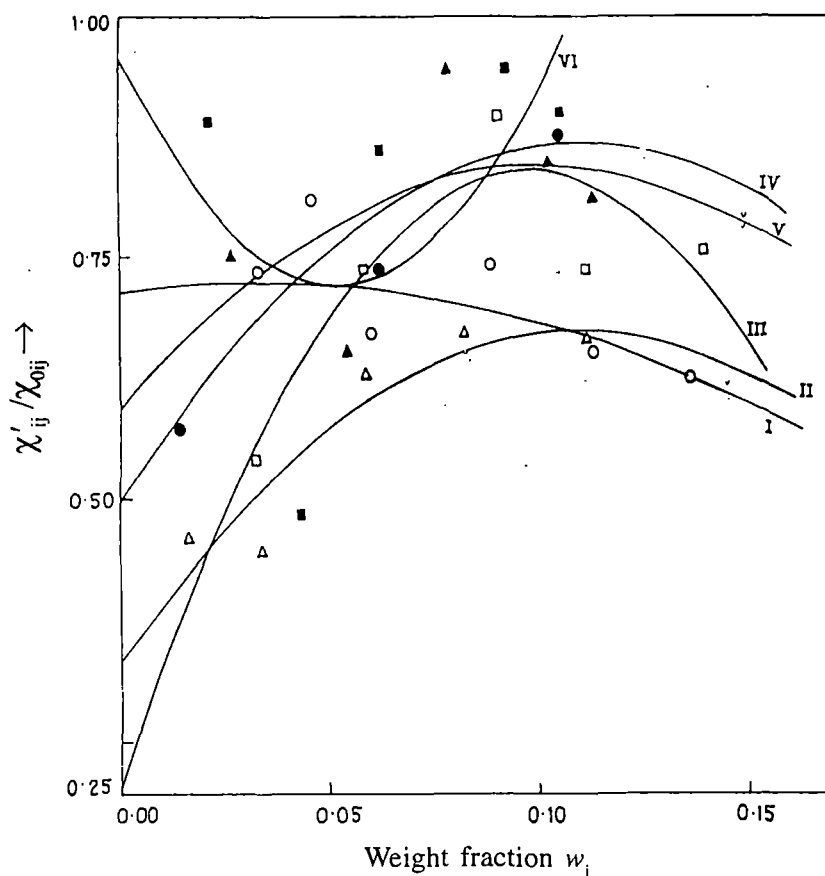


Figure 7.5. Plot of χ''_{ij}/χ'_{0ij} against the weight fraction w_j of isomers of anisidine and toluidine in benzene at 35°C under a 9.945 GHz electric field : (I) o-anisidine (—○—), (II) m-anisidine (—△—), (III) p-anisidine (—□—), (IV) o-toluidine (—●—), (V) m-toluidine (—▲—) and (VI) p-toluidine (—■—).

In the absence of a reliable τ_j under a hf electric field we tried to calculate τ_j 's from the slopes of the least-squares fitted straight-line equation of χ''_{ij} against χ'_{ij} as claimed by Murthy *et al* [10], and give them in the ninth column of Table 7.2. The available experimental points were found to deviate from linearity as illustrated in Figure 7.4. The individual plots of χ''_{ij} and χ'_{ij} against the w_j 's of the isomers of the anisidines and toluidines are not strictly linear as observed in Figures 7.2 and 7.3. This at once prompted us to use the ratio of the individual slopes of variations of χ''_{ij} and χ'_{ij} with the w_j 's at $w_j \rightarrow 0$ of Figures 7.2 and 7.3

to obtain τ_j 's. The τ_j 's thus obtained agree well with τ_1 from double relaxation and Gopalakrishna's [11] methods. This confirms the basic soundness of the latter method to determine τ_j where polar-polar interactions are fully avoided. Moreover, it shows that the hf dielectric susceptibility measurement yields a microscopic relaxation time whereas the double relaxation method gives both microscopic and macroscopic τ_1 and τ_2 , as observed elsewhere [19].

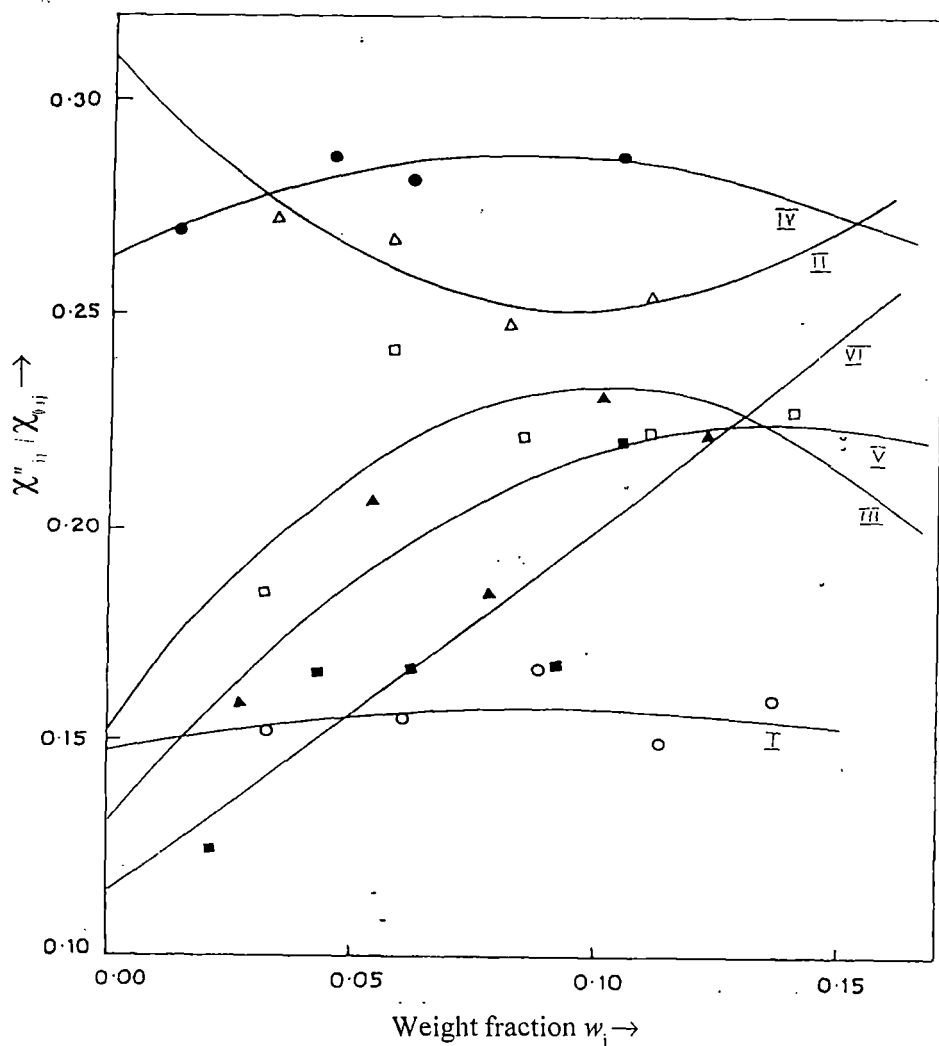


Figure 7.6. Plot of χ''_{ij}/χ'_{0ij} against the weight fraction w_j of isomers of anisidine and toluidine in benzene at 35°C under a 9.945 GHz electric field : (I) o-anisidine (—○—), (II) m-anisidine (—△—), (III) p-anisidine (—□—), (IV) o-toluidine (—●—), (V) m-toluidine (—▲—) and (VI) p-toluidine (—■—).

Large τ_2 's signify the larger sizes of the rotating units of solute-solvent, i.e. monomer formation under a hf electric field. The existence of a distribution of τ 's between τ_2 and τ_1 helps us to test the symmetric and asymmetric distribution parameters γ and δ of such compounds. These are calculated from Eqs. (7.16) and (7.18) with the values of χ'_{ij}/χ_{0ij} and χ''_{ij}/χ_{0ij} at $w_j \rightarrow 0$ of Figures 7.5 and 7.6. The values of $(1/\phi) \log(\cos\phi)$ against ϕ in degrees as shown in Figure 7.7 is essential to obtain δ . Knowing ϕ from the curve of Figure 7.7, δ 's were obtained. γ and δ so obtained are seen in the 11th and 12th columns of Table 7.3. The values of γ establishes the non-rigid behaviour of the molecules in benzene in a 9.945 GHz electric field. They obey symmetric relaxation phenomena as δ 's are found to be low.

The symmetric relaxation time τ_s from Eq. (7.17) agrees with the τ_1 's and τ 's due to Gopalakrishna's method [11] indicating symmetric relaxation behaviour for such molecules; but in case of p-anisidine the agreement is poor. It may probably be due to the experimental uncertainty or the presence of two flexible polar units in a line. The characteristic relaxation time τ_{cs} obtained from δ gives high values. They thus rule out the applicability of asymmetric relaxation behaviour for such polar molecules in benzene.

We find the relative contributions c_1 and c_2 towards dielectric dispersions for each polar compound, reported in tables and figures from Eqs. (7.3) and (7.4) for fixed τ_1 and τ_2 of Eq. (7.5) and χ'_{ij}/χ_{0ij} and χ''_{ij}/χ_{0ij} of Fröhlich's equations, (7.6) and (7.7). The same could, however, be obtained by a graphical technique. The c_1 and c_2 by both the methods are given in Table 7.3. The Fröhlich's parameter, A , which predicts the temperature variation of the width of the distribution of τ . A is equal to $\ln(\tau_2/\tau_1)$. c_1 and c_2 obtained with χ'_{ij}/χ_{0ij} and χ''_{ij}/χ_{0ij} of Fröhlich's equations and the least-squares fitted graphically estimated values from Figures 7.5 and 7.6 satisfy $c_1 + c_2 \simeq 1$. The variation of χ'_{ij}/χ_{0ij} and χ''_{ij}/χ_{0ij} with w_j usually do not obey Bergmann *et al's* [13] equation (7.1) and (7.2), as observed elsewhere [17, 18]. For p-toluidine c_2 becomes negative as seen in the tenth column of

Table 7.3. This arises due to the inertia of the whole molecule with respect to its flexible part under nearly 10 GHz electric field [7,19].

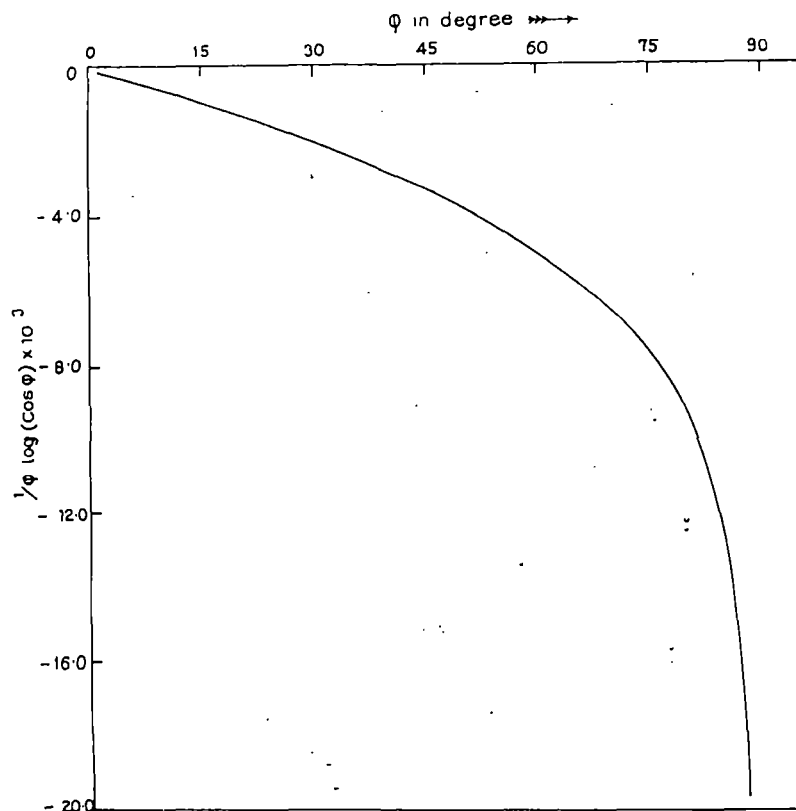


Figure 7.7. Variation of $1/\phi \log(\cos \phi) \times 10^3$ against ϕ in degree

The dipole moments μ_1 and μ_2 of the flexible parts and whole molecules of all the compounds under investigation were obtained in terms of the dimensionless parameters b_1 and b_2 related to τ_1 and τ_2 and the linear coefficient β of the $\chi'_{ij}-w_j$ curve of Figure 7.3. They are placed in the 11th and 12th columns of Table 7.4 together with μ_0 in terms of b_0 related to τ_0 , where τ_0 is the most probable relaxation time ($=\sqrt{\tau_1\tau_2}$) for the distribution of τ 's between two fixed values. The correlation coefficients, r 's, of the $\chi'_{ij}-w_j$ curves were also estimated and are entered in the fifth column of Table 7.4, but only to show how far the χ'_{ij} 's are correlated with the w_j 's. The corresponding percentage of error in terms of r are entered in the sixth column of Table 7.4. The variation of the χ'_{ij} 's with the w_j 's gives a reliable slope of β to yield reliable μ_1 , μ_2 and μ_0 values. Almost

all $\chi'_{ij}-w_j$ curves in Figure 7.3 show a tendency to be closer in the region $0.00 \leq w_j \leq 0.03$, indicating an almost identical polarity of the solute molecules in addition to solute-solvent (monomer) and solute-solute (dimer) formations [9].

The solvent, benzene, is a cyclic compound with three double bonds and six p-electrons on six carbon atoms. Hence the $\pi - \pi$ interaction or resonance effect combined with an inductive effect, known as the mesomeric effect, is expected to play an important role in the measured hf μ_j . Special attention is therefore, paid to obtain the conformational structures of the isomers of anisidine and toluidine from the available bond angles and bond moments of the substituent polar groups. The polar groups C—NH₂ ($\angle 142^\circ$) C—OCH₃ ($\angle 57^\circ$) and C—CH₃ ($\angle 180^\circ$) having bond moments of 3.90×10^{-30} , 2.40×10^{-30} and 1.23×10^{-30} Cm, respectively, are used to obtain the theoretical μ_{theo} of Figure 7.8. In the case of the anisidines, the amino group, —NH₂, exhibits a mesomeric effect by pushing the electrons towards the C atom of the benzene ring, but the inductive effect is more prominent in the —OCH₃ group rather than mesomeric effect; so the latter pulls the electrons from the C atom of the ring. Hence the resultant μ_{theo} increases from the *para* to the *ortho* and to the *meta* forms, as seen in Table 7.4. In the case of the methyl group, —CH₃, in toluidines the inductive effect is important as the sp² hybridized C atom of benzene is more electronegative than the C atom of the —CH₃ group, which is sp³ hybridized. Thus the direction of the bond moment is towards the benzene ring. For the —NH₂ group the mesomeric and inductive effects act oppositely, but as the mesomeric effect is more pronounced so resultant bond moment is toward the C₆H₆ ring. In the *ortho*, *meta* and *para* toluidines, the angle between the —CH₃ and —NH₂ groups are 60°, 120° and 180°, respectively. Hence there is an increment in μ_{theo} from the *ortho* to the *meta* and to the *para* forms (Table 7.4).

In the absence of reliable μ_j values of these compounds Gopalakrishna's method [11] was employed to obtain hf μ_j 's (reported data). The close agreement between the reported μ_j (Gopalakrishna), μ_1 and μ_{theo} as seen in Table 7.4

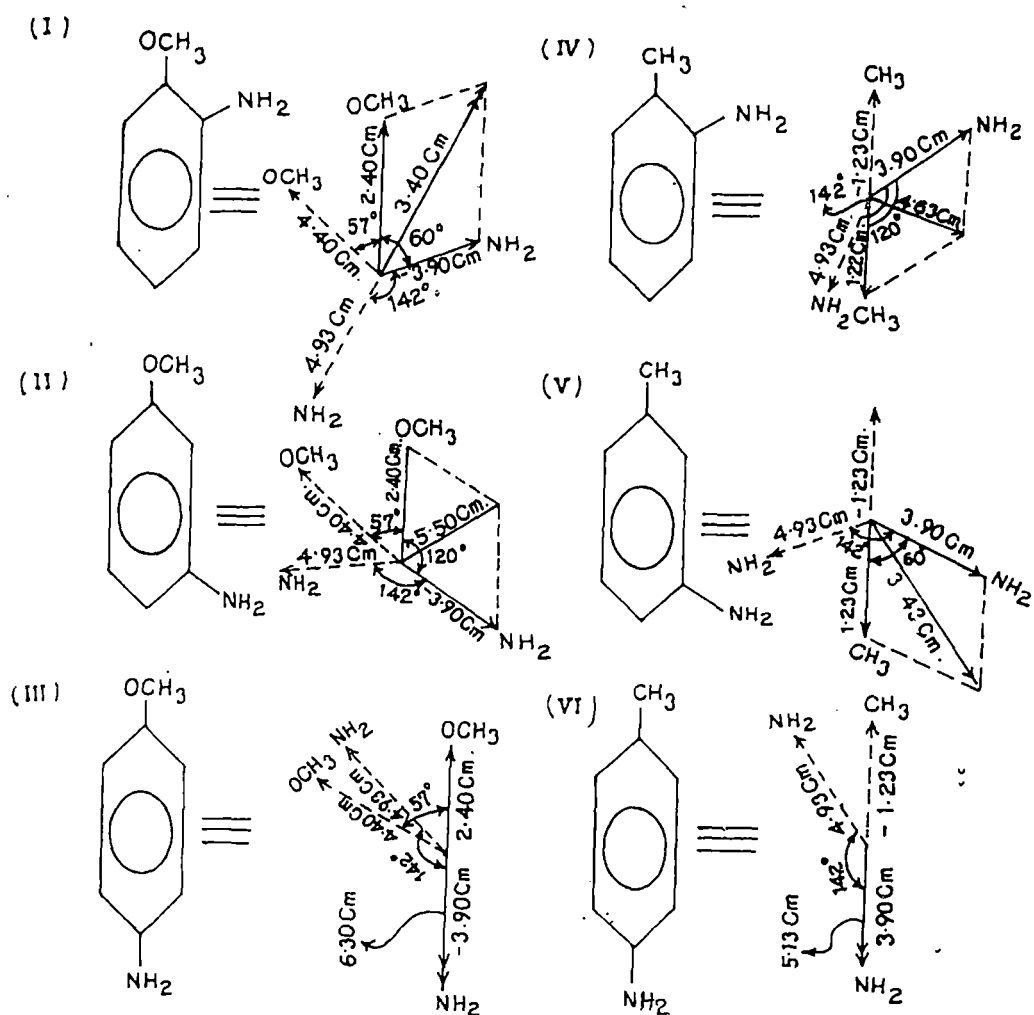


Figure 7.8: Conformational structures of isomers of anisidine and toluidine : (i) ortho anisidine, (ii) meta anisidine, (iii) para anisidine, (iv) orthotoluidine, (v) meta toluidine, (vi) para toluidine.

[Bond moment $\times 10^{30}$ Coulomb metre (C.m) given in figures]

establishes the basic soundness of the method prescribed for obtaining $hf\mu_j$. It also confirms the fact that a part of the molecule is rotating under a nearly 3 cm wavelength electric field.

7.6 Conclusions

The theoretical consideration for the effective utilization of the established symbols of the dielectric susceptibilities, χ_{ij} 's, from the dielectric relative permittivities ϵ_{ij} 's appear to be sound to study the dielectric relaxation mechanism as χ_{ij} 's are directly concerned with orientational polarization. The significant equations in terms of the χ_{ij} 's help one to grasp new physical insight into polar-polar and polar-nonpolar molecular interactions in solution. The single-frequency measurement of the relaxation parameters thus provides a unique method to obtain macroscopic and microscopic relaxation times and hence dipole moments of the whole and the flexible parts of the molecules. The estimation of τ from the linear equation (7.5) is a very simple, straightforward and significant one to obtain μ from equation (7.13) in terms of linear coefficient β of the familiar $\chi'_{ij}-w_j$ curve. The correlation coefficient r and the chisquare values signify the minimum error introduced into the desired parameters. The molecules under identical states show interesting phenomena of a double or, often, a single relaxation mechanism depending upon the solvent used. The probability of showing the double relaxation phenomena of monosubstituted anilines in benzene depends upon the electric field frequency of nearly 10 GHz. Various types of molecular associations, such as solute – solute and solute – solvent interactions, are thus inferred from the usual departure of graphically fitted plots of χ'_{ij}/χ_{0ij} and χ''_{ij}/χ_{0ij} with w_j following Bergmann's equations [13]. Non-rigid characteristics of the molecules are ascertained by estimation of symmetric and asymmetric distribution parameters in benzene. The molecular associations are also supported by the conformational structures of the molecules in which the mesomeric, inductive and electromeric effects play prominent roles.

References

- [1] A Sharma and D R. Sharma *J. Phys. Soc. Japan* **61** (1992), 1049.
- [2] S K Sit, N Ghosh, U Saha and S Acharyya *Indian J. Phys.* **71B** (1997),533.
- [3] K S Cole and R H Cole *J. Chem. Phys.* **9** (1941), 341.
- [4] D W Davidson and R H Cole *J. Chem. Phys.* **19** (1951) 1484.
- [5] A K Jonscher *Physics of Dielectric Solids, Invited Papers* ed. C.H.L. Goodman (1980) Canterbury.
- [6] S C Srivastava and S Chandra *Indian J. Pure & Appl Phys.* **13** (1975) 101.
- [7] S K Sit and S Acharyya *Indian J. Pure & Appl. Phys.* **34** (1996) 255.
- [8] A K. Jonscher *Inst. Phys. Conference (Canterbury)* ed. CHL Goodman (1980).
- [9] N Ghosh, A Karmakar, S K Sit and S Acharyya *Indian J. Pure & Appl. Phys.* **38** (2000) 574.
- [10] M B R Murthy, R L Patil and D K Deshpande *Indian J.Phys.* **63B** (1989) 491.
- [11] K V Gopalakrishna *Trans. Faraday Soc.* **53** (1957) 767.
- [12] H Fröhlich *Theory of Dielectrics* (Oxford : Oxford University Press) 1949.
- [13] K Bergmann, D M Roberti and C P Smyth *J. Phys. Chem.* **64**(1960) 665.
- [14] C P Smyth *Dielectric Behaviour and Structure* (New York :McGraw-Hill).(1955)
- [15] K Dutta, S K Sit and S Acharyya *Pramana : J. Phys.* **57** (2001), 775.

- [16] N Ghosh, R C Basak, S K Sit and S Acharyya *J. Mol. Liquids* **85** (2000)375.
- [17] U Saha, S K Sit, R C Basak and S Acharyya *J. Phys. D : Appl. Phys.* **27** (1994) 596.
- [18] S K Sit, R C Basak, U Saha and S Acharyya *J. Phys. D: Appl. Phys.* **27** (1994), 2194.
- [19] S K Sit, N Ghosh and S Acharyya *Indian J. Pure. & Appl. Phys.* **35** (1997)329.

CHAPTER -8

DOUBLE RELAXATION PHENOMENA OF MONOSUBSTITUTED ANILINES IN BENZENE UNDER HIGH FREQUENCY ELECTRIC FIELD

DOUBLE RELAXATION PHENOMENA OF MONO-SUBSTITUTED ANILINES IN BENZENE UNDER HIGH FREQUENCY ELECTRIC FIELD

8.1. Introduction

In recent years, single or double relaxation phenomenon of polar liquid molecules in nonpolar solvents under high frequency (hf) electric field attracted the attention of a large number of workers [1,2]. The study often provides the valuable information on the shape, size and structure, in addition to solute — solvent or solute — solute molecular associations in terms of relaxation time τ and dipole moment μ estimated by any conventional method [3,4]. The stability or unstability [5] of the molecules towards dielectric relaxations, is, however, inferred from such study. τ_1 and τ_2 of the double relaxation method, τ_j from the ratio of slopes of the individual variations of χ''_{ij} and χ'_{ij} with weight fractions w_j 's in the limit $w_j = 0$. and μ_j 's from the linear coefficient β 's of either $\chi'_{ij}-w_j$ or hf conductivity $\sigma_{ij}-w_j$ curves shed more light on the structural aspects of such dielectropolar liquid molecules [6].

The real ϵ'_{ij} and imaginary ϵ''_{ij} parts of hf complex relative permittivity ϵ^*_{ij} together with the low frequency or static and optical frequency relative permittivities ϵ_{oij} and $\epsilon_{\infty ij}$ of isomers of methoxy substituted anilines (anisidines) and methyl substituted anilines (toluidines) in benzene under 2.02, 3.86 and 22.06 GHz electric field for different w_j 's were measured by Srivastava and Chandra [7] at 35°C. The analytical grade ortho-, para toluidines and para-anisidines were supplied by M/S. Riedel (Germany) and the others were of M/S. BDH (London). The liquids were further purified by repeated fractional distillations and their physical constants like density ρ . viscosity η and refractive indices n_{Dij} were carefully checked in agreement with the literature values before use. The purpose of the study [7] was to detect the possible existence of solute — solvent (monomer) and solute – solute (dimer) molecular associations in the mixtures of various concentrations.

Nowadays, the usual trend is to study the dielectric relaxation processes in terms of hf complex dielectric orientational susceptibility χ_{ij}^* rather than hf complex conductivity σ_{ij}^* or hf relative permittivity ϵ_{ij}^* . ϵ_{ij}^* includes within it all types of polarisations while σ_{ij}^* is associated with transport of bound molecular charges. Hence it is more reasonable to work with χ_{ij} 's as they have direct link with the orientational polarisations [8]. Moreover, the present method of study in S.I unit is superior because of its unified, coherent and rationalised nature.

The dielectric susceptibilities like real $\chi'_{ij} = (\epsilon'_{ij} - \epsilon_{\infty ij})$, imaginary $\chi''_{ij} = \epsilon''_{ij}$ parts of complex susceptibility $\chi_{ij}^* = (\epsilon_{ij}^* - \epsilon_{\infty ij})$ and the low frequency susceptibility $\chi_{oij} = (\epsilon_{oij} - \epsilon_{\infty ij})$ which is real, were derived from the measured relative permittivities ϵ'_{ij} , ϵ''_{ij} , ϵ_{oij} and $\epsilon_{\infty ij}$ in each system for different ω_j 's of the respective solute [7]. The experimental results of χ_{ij} 's for different ω_j 's thus collected together are placed in Table 8.1 for use. One could make a strong conclusion of double relaxation phenomena of a polar molecule in a nonpolar solvent based on single frequency measurement of the relaxation parameters provided the accurate value of χ_{oij} involved with ϵ_{oij} and $\epsilon_{\infty ij}$ is available. The use of n_{Dij}^2 for $\epsilon_{\infty ij}$ [7] may often introduce additional error in the calculation. Nevertheless the data presented in Table 8.1 are accurate upto 5% for χ''_{ij} and 2% for χ'_{ij} and χ_{oij} respectively.

The polar liquids like monosubstituted anilines often possess two or more τ 's in GHz electric field for the rotation of their flexible polar groups to the parent molecules and the whole molecule itself [9]. Bergmann et al [10] devised a graphical method to obtain double relaxation times τ_1 and τ_2 and hence weighted contributions c_1 and c_2 towards dielectric dispersions for some complex polar liquid molecules. The method is based on plotting the measured values of ϵ' , ϵ'' , ϵ_0 and ϵ_∞ at various frequencies ω on a semicircle in a complex plane. A point was then selected on the chord through two fixed points on the semicircle drawn in consistency with the experimental data. Bhattacharyya et al [11], subsequently modified the above procedure to get the same with the

experimental values measured only at two different frequencies of GHz range.

Thus the object of the present paper is to detect the double relaxation times τ_1 and τ_2 due to rotations of the flexible parts and the whole molecules using χ_{ij} 's based on a single frequency measurement technique [7,12-13]. The aniline derivatives are thought to absorb electric energy strongly nearly at 10 GHz electric field. The parameters measured at 2.02, 3.86 and 22.06 GHz electric field may yield considerable τ_1 and τ_2 in comparison to 10 GHz electric field. Moreover, the present system of study in terms of new physical parameters, like χ_{ij} 's seems to yield a better insight into the relaxation phenomena of polar liquid molecules in nonpolar solvents. This study further tempted us to see how far χ_{ij} 's and σ_{ij} 's with w_j measurement yield the μ 's. The aspect of molecular orientational polarisation, is, however, achieved by introducing χ_{ij} 's because $\epsilon_{\infty ij}$ which includes the fast polarisation always appears as a subtracted term in Bergmann's equations [10]. Thus in order to exclude the fast polarisation processes and to avoid the clumsiness of algebra the established symbols of dielectric terminologies and parameters like $\chi'_{ij} = (\epsilon'_{ij} - \epsilon_{\infty ij})$, $\chi''_{ij} = \epsilon''_{ij}$ and $\chi_{oij} = (\epsilon_{oij} - \epsilon_{\infty oij})$ of Table 8.1 are used to write the Bergmann's equations [10].

$$\chi'_{ij} / \chi_{oij} = \frac{c_1}{1 + \omega^2 \tau_1^2} + \frac{c_2}{1 + \omega^2 \tau_2^2} \quad (8.1)$$

$$\chi''_{ij} / \chi_{oij} = c_1 \frac{\omega \tau_1}{1 + \omega^2 \tau_1^2} + c_2 \frac{\omega \tau_2}{1 + \omega^2 \tau_2^2} \quad (8.2)$$

assuming two separate broad dispersions for which the sum of c_1 and c_2 is unity. Eq. (8.1) and (8.2) are now solved to get.

$$\frac{\chi_{oij} - \chi'_{ij}}{\chi'_{ij}} = \omega (\tau_1 + \tau_2) \frac{\chi''_{ij}}{\chi'_{ij}} - \omega^2 \tau_1 \tau_2 \quad (8.3)$$

when the variables $(\chi_{oij} - \chi'_{ij}) / \chi'_{ij}$ and χ''_{ij} / χ'_{ij} of Eq. (8.3) are plotted for

different w_j 's of a polar liquid at any given frequency ω of the applied electric field, a straight line results with intercept $-\omega^2\tau_1\tau_2$ and slope $\omega(\tau_1+\tau_2)$, as shown in Figure 8.1. The intercept and slope of Eq.(8.3) are, however, obtained by linear regression analysis made on the measured susceptibilities of different w_j 's of the monosubstituted anilines in C_6H_6 of Table 8.1 to get τ_1 and τ_2 as shown in the 7th and 8th columns of Table 8.2 extracted from the data of Table 8.1. The reliability of the data are checked through chisquares values. In absence of reliable τ_j values, the ratio of individual slopes of variation of χ''_{ij} and χ'_{ij} with w_j 's at $w_j \rightarrow 0$, as seen in Figures 8.2 and 8.3; were conveniently used to evaluate τ_j to compare with those of Murthy et al [14] of Figure 8.4 and Gopalakrishna's method [15].

The theoretical weighted contributions c_1 and c_2 due to estimated τ_1 and τ_2 from Eq. (8.3) were worked out from Fröhlich's equations [16] and are placed in Table 8.3 in order to compare them with the experimental ones from the intercept of the least squares fitted curves of χ'_{ij}/χ_{oij} and χ''_{ij}/χ_{oij} against w_j from Figures 8.5 and 8.6 in the limit $w_j = 0$. The values of χ'_{ij}/χ_{oij} and χ''_{ij}/χ_{oij} at $w_j = 0$ together with arbitrary curve of $1/\phi \log(\cos \phi)$ against ϕ in degrees shown elsewhere [17] are further used to obtain symmetric and asymmetric distribution parameters γ and δ as seen in Table 8.3 to conclude the symmetric relaxation behaviour of such molecules. Symmetric relaxation time τ_s from γ and characteristic relaxation time τ_{cs} from δ and ϕ are further estimated in order to compare both τ_s and τ_{cs} with τ_1 , τ_2 and τ_j in Table 8.2.

The dipole moments μ_1 and μ_2 by both hf susceptibility and conductivity measurement techniques are, however, worked out from linear coefficient β 's of $\chi'_{ij} - w_j$ and $\sigma_{ij} - w_j$ curves of Figures 8.3 and 8.7 in terms of b_1 , b_2 involved with the estimated τ_1 , τ_2 by double relaxation method. The μ_1 and μ_2 thus obtained are placed in Table 8.4 to see how far they are affected by the orientational polarisation and bound molecular charge in connection with χ_{ij} 's and σ_{ij} 's respectively. The estimated μ_1 and μ_2 by both the methods are finally

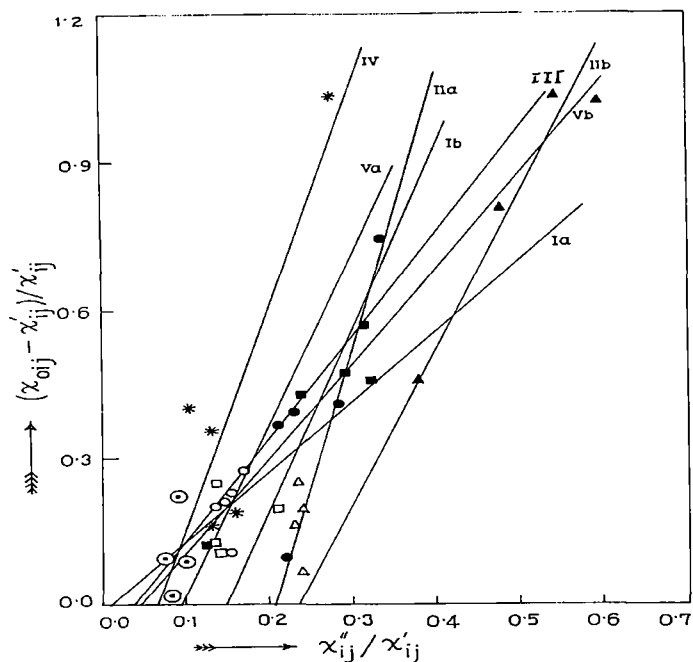


Figure 8.1: Linear variation of $(\chi'_{0ij} - \chi'_{ij})/\chi'_{ij}$ against χ''_{ij}/χ'_{ij} of monosubstituted anilines in benzene at 35° C under GHz electric field.

(Ia) o-anisidine at 3.86 GHz (—○—), (Ib) o-anisidine at 22.06 GHz (—●—),
 (IIa) m-anisidine at 3.86 GHz (—△—), (IIb) m-anisidine at 22.06 GHz (—▲—),
 (III) o-toluidine at 2.02 GHz (—⊙—), (IV) m-toluidine at 3.86 GHz (—*—),
 (Va) p-toluidine at 3.86 GHz (—□—) and (Vb) p-toluidine at 22.06 GHz (—■—) respectively.

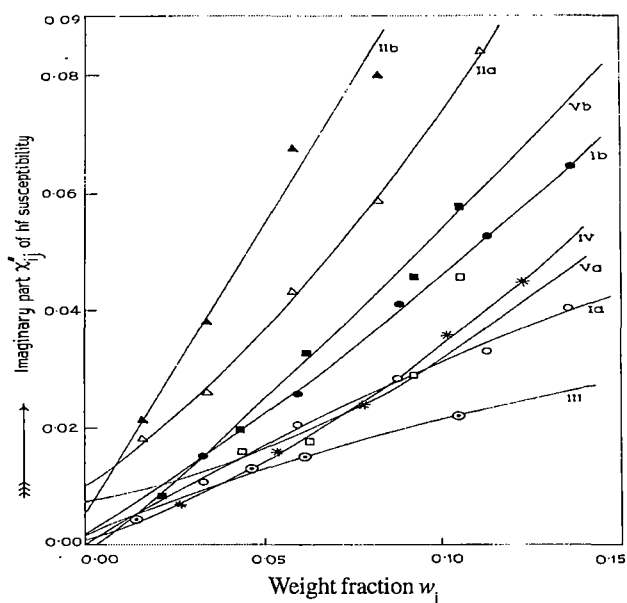


Figure 8.2: Variation of imaginary part of hf susceptibility χ''_{ij} against weight fraction w_j of monosubstituted anilines in benzene at 35° C under GHz electric field.

(Ia) o-anisidine at 3.86 GHz (—○—), (Ib) o-anisidine at 22.06 GHz (—●—),
 (IIa) m-anisidine at 3.86 GHz (—△—), (IIb) m-anisidine at 22.06 GHz (—▲—),
 (III) o-toluidine at 2.02 GHz (—⊙—), (IV) m-toluidine at 3.86 GHz (—*—),
 (Va) p-toluidine at 3.86 GHz (—□—) and (Vb) p-toluidine at 22.06 GHz (—■—) respectively.

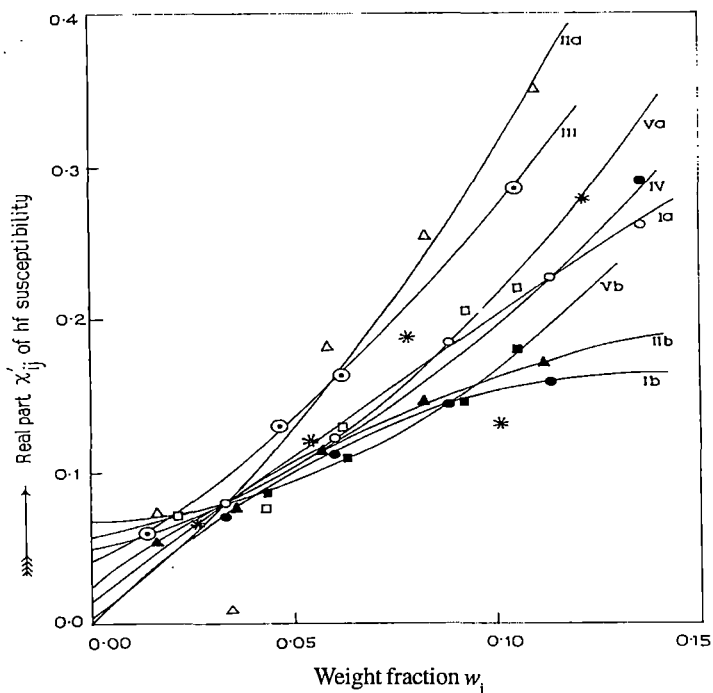


Figure 8.3: Variation of real part of hf susceptibility χ'_{ij} against weight fraction w_j of monosubstituted anilines in benzene at 35^o C under GHz electric field.

(Ia) o-anisidine at 3.86 GHz (—○—), (Ib) o-anisidine at 22.06 GHz (—●—),
 (IIa) m-anisidine at 3.86 GHz (—△—), (IIb) m-anisidine at 22.06 GHz (—▲—),
 (III) o-toluidine at 2.02 GHz (—⊙—), (IV) m-toluidine at 3.86 GHz (—*—),
 (Va) p-toluidine at 3.86 GHz (—□—) and (Vb) p-toluidine at 22.06 GHz (—■—) respectively.

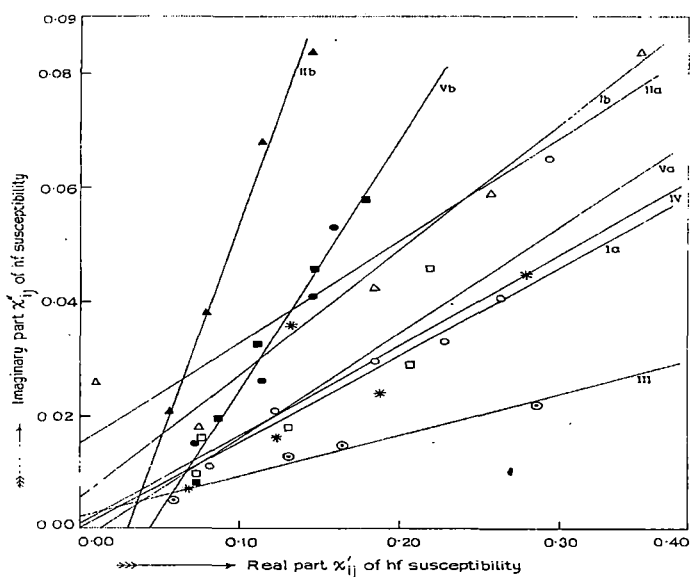


Figure 8.4: Linear plot of imaginary part of hf susceptibility χ''_{ij} against real part χ'_{ij} of monosubstituted anilines in benzene at 35^o C under GHz electric field.

(Ia) o-anisidine at 3.86 GHz (—○—), (Ib) o-anisidine at 22.06 GHz (—●—),
 (IIa) m-anisidine at 3.86 GHz (—△—), (IIb) m-anisidine at 22.06 GHz (—▲—),
 (III) o-toluidine at 2.02 GHz (—⊙—), (IV) m-toluidine at 3.86 GHz (—*—),
 (Va) p-toluidine at 3.86 GHz (—□—) and (Vb) p-toluidine at 22.06 GHz (—■—) respectively.

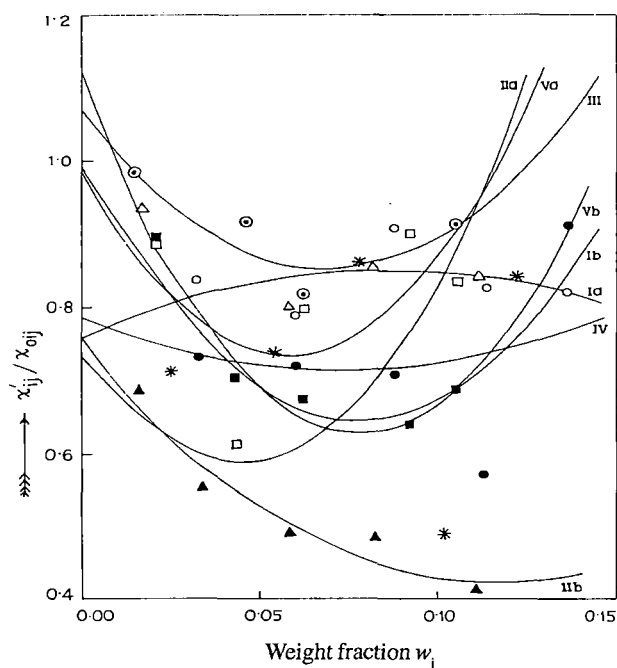


Figure 8.5: Plot of χ''_{ij}/χ_{0ij} against weight fraction w_j of monosubstituted anilines in benzene at 35° C under GHz electric field.

(Ia) o-anisidine at 3.86 GHz (—○—), (Ib) o-anisidine at 22.06 GHz (—●—),
 (IIa) m-anisidine at 3.86 GHz (—△—), (IIb) m-anisidine at 22.06 GHz (—▲—),
 (III) o-toluidine at 2.02 GHz (—⊙—), (IV) m-toluidine at 3.86 GHz (—*—),
 (Va) p-toluidine at 3.86 GHz (—□—) and (Vb) p-toluidine at 22.06 GHz (—■—) respectively.

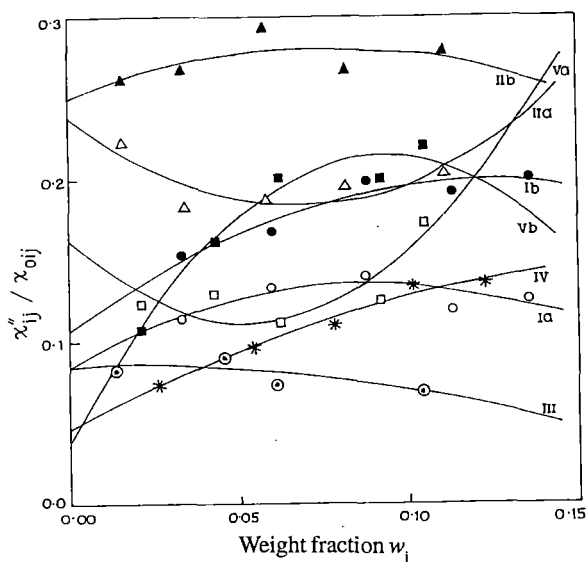


Figure 8.6: Plot of χ'_{ij}/χ_{0ij} against weight fraction w_j of monosubstituted anilines in benzene at 35° C under GHz electric field.

(Ia) o-anisidine at 3.86 GHz (—○—), (Ib) o-anisidine at 22.06 GHz (—●—),
 (IIa) m-anisidine at 3.86 GHz (—△—), (IIb) m-anisidine at 22.06 GHz (—▲—),
 (III) o-toluidine at 2.02 GHz (—⊙—), (IV) m-toluidine at 3.86 GHz (—*—),
 (Va) p-toluidine at 3.86 GHz (—□—) and (Vb) p-toluidine at 22.06 GHz (—■—) respectively.

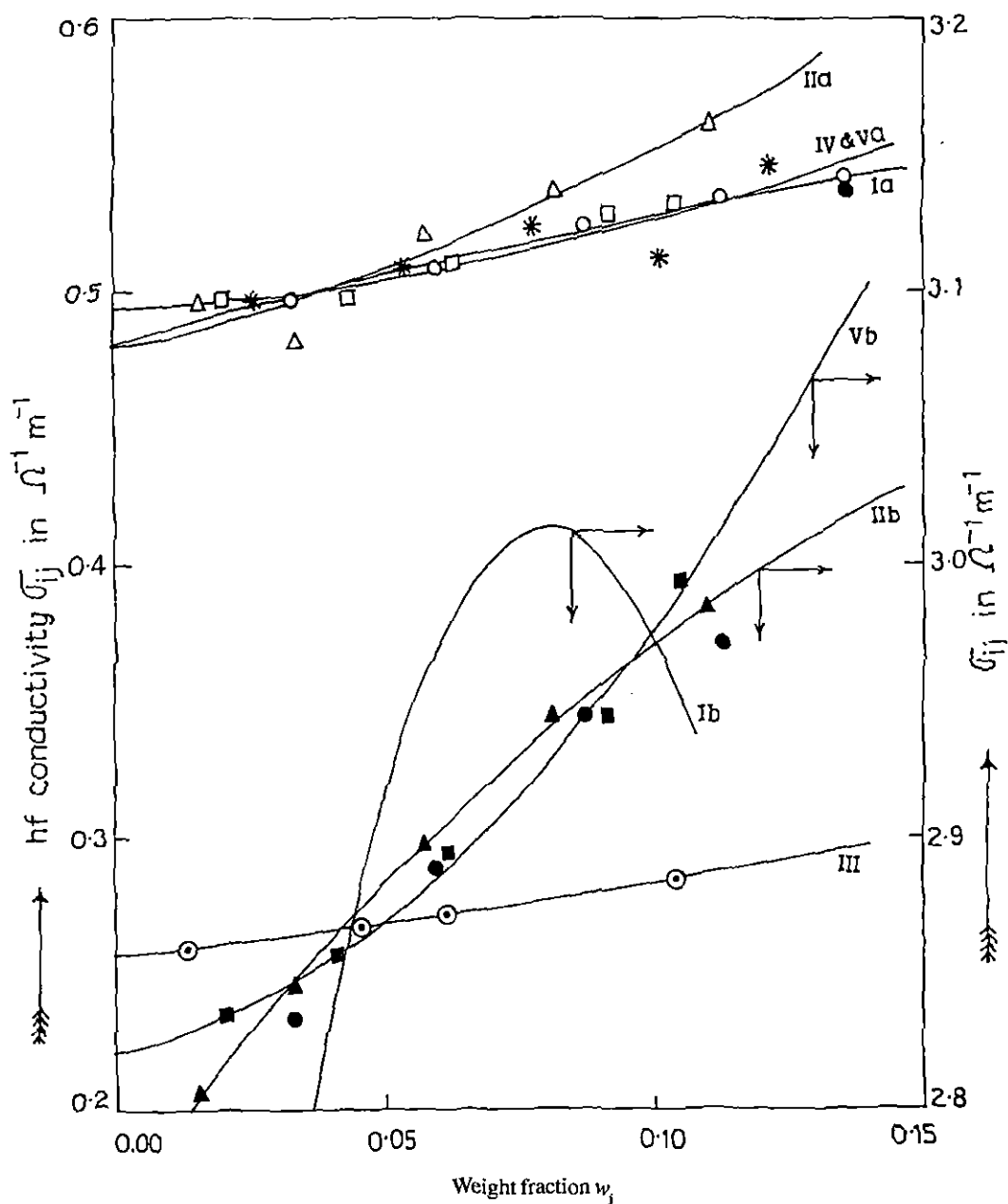


Figure 8.7: Plot of total hf conductivity σ_j against weight fraction w_j of monosubstituted anilines in benzene at 35° C under GHz electric field.

(Ia) o-anisidine at 3.86 GHz (—○—), (Ib) o-anisidine at 22.06 GHz (—●—),
 (IIa) m-anisidine at 3.86 GHz (—△—), (IIb) m-anisidine at 22.06 GHz (—▲—),
 (III) o-toluidine at 2.02 GHz (—⊙—), (IV) m-toluidine at 3.86 GHz (—*—),
 (Va) p-toluidine at 3.86 GHz (—□—) and (Vb) p-toluidine at 22.06 GHz (—■—) respectively.

Table 8.1 : Real ϵ'_{ij} and imaginary ϵ''_{ij} parts of hf complex relative permittivity ϵ^*_{ij} , static and optical frequency hf relative permittivities ϵ_{oij} and $\epsilon_{\infty ij}$ together with real χ'_{ij} and imaginary χ''_{ij} parts of hf complex dielectric orientational susceptibility χ^*_{ij} along with low frequency susceptibility χ_{oij} which is real for some monosubstituted anilines in benzene under different electric field frequencies at 35° C for various concentrations.

Systems with serial number & molecular weight M_j	Frequency (f) in GHz	Weight fraction w_j of solute	Measured dielectric relative permittivities				Dimensionless dielectric orientational susceptibilities		
			ϵ'_{ij}	ϵ''_{ij}	ϵ_{oij}	$\epsilon_{\infty ij}$	χ'_{ij}	χ''_{ij}	χ_{oij}
	(a) 3.86	0.0326	2.32	0.011	2.336	2.239	0.081	0.011	0.097
		0.0604	2.37	0.021	2.404	2.247	0.123	0.021	0.157
		0.0884	2.44	0.029	2.459	2.255	0.185	0.029	0.204
		0.1135	2.49	0.033	2.538	2.262	0.228	0.033	0.276
		0.1361	2.53	0.041	2.588	2.267	0.263	0.041	0.321
II o-anisidine in benzene $M_j = 0.123$ kg	(b) 22.06	0.0326	2.31	0.015	2.336	2.239	0.071	0.015	0.097
		0.0604	2.36	0.026	2.404	2.247	0.113	0.026	0.157
		0.0884	2.40	0.041	2.459	2.255	0.145	0.041	0.204
		0.1135	2.42	0.053	2.538	2.262	0.158	0.053	0.276
		0.1361	2.56	0.065	2.588	2.267	0.293	0.065	0.321
II	(a) 3.86	0.0160	2.31	0.018	2.315	2.235	0.075	0.018	0.080
		0.0336	2.25	0.026	2.384	2.241	0.009	0.026	0.143
		0.0579	2.43	0.043	2.477	2.246	0.184	0.043	0.231
		0.0823	2.51	0.059	2.553	2.253	0.257	0.059	0.300
		0.1109	2.61	0.084	2.675	2.261	0.349	0.084	0.414
m-anisidine in benzene $M_j = 0.123$ kg	(b) 22.06	0.0160	2.29	0.021	2.315	2.235	0.055	0.021	0.080
		0.0336	2.32	0.038	2.384	2.241	0.079	0.038	0.143
		0.0579	2.36	0.068	2.477	2.246	0.114	0.068	0.231
		0.0823	2.40	0.080	2.553	2.253	0.147	0.080	0.300
		0.1109	2.43	0.115	2.675	2.261	0.169	0.115	0.414

Contd...

Systems with serial number & molecular weight M_j	Frequency (f) in GHz	Weight fraction w_j of solute	Measured dielectric relative permittivities				Dimensionless dielectric orientational susceptibilities		
			ϵ'_{ij}	ϵ''_{ij}	ϵ_{nij}	$\epsilon_{\infty ij}$	χ'_{ij}	χ''_{ij}	χ_{nij}
III	2.02	0.0137	2.30	0.005	2.301	2.241	0.059	0.005	0.060
o-toluidine		0.0459	2.38	0.013	2.392	2.250	0.130	0.013	0.142
in benzene		0.0622	2.42	0.015	2.457	2.255	0.165	0.015	0.202
$M_j = 0.107$ kg		0.1048	2.55	0.022	2.577	2.264	0.286	0.022	0.313
IV	3.86	0.0264	2.31	0.007	2.337	2.243	0.067	0.007	0.094
m-toluidine		0.0538	2.37	0.016	2.413	2.248	0.122	0.016	0.165
in benzene		0.0781	2.44	0.024	2.470	2.252	0.188	0.024	0.218
$M_j = 0.107$ kg.		0.1015	2.39	0.036	2.526	2.258	0.132	0.036	0.268
	(a) 3.86	0.1225	2.54	0.045	2.591	2.262	0.278	0.045	0.329
		0.0213	2.31	0.010	2.319	2.237	0.073	0.010	0.082
		0.0428	2.32	0.016	2.367	2.244	0.076	0.016	0.123
		0.0616	2.38	0.018	2.413	2.249	0.131	0.018	0.164
V	(b) 22.06	0.0916	2.46	0.029	2.483	2.254	0.206	0.029	0.229
p-toluidine in benzene		0.1048	2.48	0.046	2.523	2.260	0.220	0.046	0.263
$M_j = 0.107$ kg		0.0213	2.31	0.009	2.319	2.237	0.073	0.009	0.082
		0.0428	2.33	0.020	2.367	2.244	0.086	0.020	0.123
	(b) 22.06	0.0616	2.36	0.033	2.413	2.249	0.111	0.033	0.164
		0.0916	2.40	0.046	2.483	2.254	0.146	0.046	0.229
		0.1048	2.44	0.058	2.523	2.260	0.180	0.058	0.263

Table 8.2 : Intercept and slope of linear equation of $(\chi_{oij}'' - \chi_{ij}') / \chi_{ij}'$ against χ_{ij}'' / χ_{ij}' , correlation coefficient (r) and chisquare values, estimated relaxation times τ_1 and τ_2 due to rotation of flexible polar group and whole molecule, measured τ_j from Eq (8.16) and (8.17), reported τ (Gopalakrishna) symmetric and characteristic relaxation times τ_s and τ_{es} of Eq. (8.11) and (8.13), of some monosubstituted anilines in benzene at 35°C under different GHz electric field frequencies.

Systems with serial number & Molecular weight (M_j)	Frequency (f) in GHz	Intercept and slope of Eq. (8.3)		Correlation coefficient (r) and chisquares values involved in Eq. (8.3)		Estimated relaxation times τ_1 and τ_2 in p.sec		Measured τ (ps) ^a	Ratio of slopes of $\chi_{ij}'' - w_j$ & $\chi_{ij}' - w_j$ curves at $w_j \rightarrow 0$	Relaxation times			
		Intercept (c)	Slope (m)	(r)Chisquares		τ (ps) ^b	τ (ps) ^c			τ_s (ps)	τ_{es} (ps)		
				(r)	Chisquares								
I. o-anisidine in benzene $M_j = 0.123$ kg	(a) 3.86	0.0179	1.4360	0.3032	0.07	0.52	58.73	6.29	0.1891	7.80	5.25	0.92	471.52
	(b) 22.06	0.5406	3.6741	0.8277	0.23	1.11	25.41	1.59	0.1601	1.15	1.56	0.90	—
II. m-anisidine in benzene $M_j = 0.123$ kg	(a) 3.86	1.1404	5.5485	0.9999	0.15	8.82	220.07	7.61	0.2188	9.02	8.05	12.30	90.52
	(b) 22.06	0.7318	3.1447	0.9803	0.02	1.83	20.87	5.55	0.5413	3.91	4.41	2.33	14.80
III. o-toluidine in benzene $M_j = 0.107$ kg	2.02	0.0773	2.0910	0.2402	0.02	2.97	161.86	5.70	0.1536	12.11	4.97	17.06	—

^aMeasured by the slope of χ_{ij}'' against χ_{ij}' using Eq. (8.16).

^b From the ratio of individual slopes.

^cBy Gopalakrishna's method [15]

Contd...

Systems with serial number & Molecular weight (M_j)	Frequency (f) in GHz	Intercept and slope of Eq. (8.3)		Correlation coefficient (r) and chisquares values involved in Eq. (8.3)		Estimated relax- ation times τ_1 and τ_2 in p.sec		Measured τ (ps) ^a	Ratio of slopes of $\chi''_{ij}-w_j$ & $\chi'_{ij}-w_j$ curves at $w_j \rightarrow 0$	Relaxation times				
		Intercept (c)	Slope (m)			(r)Chisquares					τ	τ	τ_s	τ_{cs}
											(ps) ^b	(ps) ^c	(ps)	(ps)
(IV) m-toluidine in benzene $M_j=0.107$ kg	3.86	0.2938	4.5092	0.8469	0.51	2.73	183.29	6.53	0.3792	15.64	7.05	2.23	1181.3	
(V) p-toluidine in benzene $M_j = 0.107$ kg	(a) 3.86	0.3149	3.4446	0.6480	0.30	3.88	138.22	7.64	0.2116	8.73	7.65	8.15	—	
	(b) 22.06	0.0821	1.9151	0.9408	0.03	0.32	13.51	3.19	46.1743	333.30	5.53	2.11	—	

^aMeasured by the slope of χ''_{ij} against χ'_{ij} using Eq. (8.16).

^b From the ratio of individual slopes.

^cBy Gopalakrishna's method [15]

Table 8.3 : Frohlich's parameter A, χ'_{ij}/χ_{oij} and χ''_{ij}/χ_{oij} values estimated from Frohlich's equations (8.6) and (8.7) with estimated τ_1 and τ_2 and those obtained from Figures 8.5 and 8.6 at $w_j \rightarrow 0$, weighted contributions c_1 and c_2 from Frohlich's method and those by graphical technique together with symmetric and asymmetric distribution parameters γ and δ of some monosubstituted anilines in benzene at 35°C under different electric field frequencies in GHz range.

Systems with serial number	Frequency (f) in GHz	Frohlich parameter (A)	Estimated values of χ'_{ij}/χ_{oij} & χ''_{ij}/χ_{oij} of Frohlich's equations (8.6) and (8.7)		Weighted contributions c_1 & c_2 from Eqs. (8.4) and (8.5)		Estimated values of χ'_{ij}/χ_{oij} & χ''_{ij}/χ_{oij} from Figures 8.5 and 8.6 at $w_j \rightarrow 0$		Weighted contributions c_1 and c_2 from graphical technique		Symmetric distribution parameter γ	Asymmetric distribution parameter δ	
I. o-anisidine in C_6H_6	(a) 3.86	4.7269	0.8829	0.2001	0.7491	0.4053	0.7613	0.0859	0.7073	0.1637	0.7089	0.0757	
	(b) 22.06	3.1308	0.5893	0.3646	0.5200	1.0893	1.0006	0.1086	1.0380	-0.1801	-0.0724	—	
II. m-anisidine in C_6H_6	(a) 3.86	3.2169	0.4811	0.3650	0.4496	1.5081	0.7527	0.2389	0.7712	0.4485	0.3155	0.2688	
	(b) 22.06	2.4340	0.5534	0.4063	0.4816	0.9439	0.7468	0.2508	0.7699	0.2181	0.2969	0.2910	
III. o-toluidine in C_6H_6	2.02	3.9982	0.7936	0.2699	0.6755	0.6212	1.0700	0.0841	1.0498	0.1133	-0.4921	—	
IV m-toluidine in C_6H_6	3.86	4.2068	0.6401	0.3049	0.5826	1.2450	0.7858	0.0475	0.7903	-0.0213	0.8230	0.0393	
V p-toluidine in C_6H_6	(a) 3.86	3.5730	0.6509	0.3320	0.5727	1.0167	0.9901	0.1639	0.9769	0.2657	-0.0661	—	
	(b) 22.06	3.7429	0.7992	0.2766	0.6685	0.5943	1.1134	0.0399	1.1208	-0.0233	-0.8078	—	

Table 8.4 : Linear coefficient 'β's, correlation coefficient (r) and % of error of $\chi'_{ij} - w_j$ and $\sigma_{ij} - w_j$ curves of Figure 8.3 and 8.7, estimated dipole moments μ_1 and μ_2 for rotations of flexible polar groups and whole molecule by susceptibility and conductivity measurement techniques, dimensionless parameters b_1 and b_2 together with theoretical dipole moment μ_{theo} obtained from bond angles and bond moments, reported μ (Gopalakrishna) of some monosubstituted anilines in benzene at 35° C under different electric field frequencies.

Systems with serial number and molecular weight (M_j) in kg.	Frequency (f) in GHz	Linear coefficient of $\chi'_{ij} - w_j$ & $\sigma_{ij} - w_j$ curves of Figs. 8.3 and 8.7	Correlation coefficient (r) and % of errors involved in $\chi'_{ij} - w_j$ and $\sigma_{ij} - w_j$ curves		Dimensionless parameters		Estimated dipole moment $\mu \times 10^{30}$ C.m from hf susceptibility and conductivity measurement		Theoretical $\mu \times 10^{30}$ in C.m from bond angles and bond moments	$\mu \times 10^{30}$ in C.m from Gopalakrishnas method.
			(r)	% of error	b_1	b_2	μ_1	μ_2		
					$\frac{1}{1+\omega^2\tau_1^2}$	$\frac{1}{1+\omega^2\tau_2^2}$				
I. o-anisidine in C_6H_6 $M_j = 0.123$	(a) 3.86	1.9358 0.4890	0.9980 0.9984	0.12 0.10	0.9998	0.3304	5.07 5.50	8.81 9.56	3.40	5.03
	(b) 22.06	2.4031 17.3978	0.9102 0.9316	5.18 5.98	0.9769	0.0747	5.71 13.88	20.66 50.19		
II. m-anisidine in C_6H_6 $M_j = 0.123$	(a) 3.86	1.8788 0.4623	0.9417 0.9508	3.41 2.89	0.9563	0.0339	5.10 5.46	27.10 29.01	5.50	6.33
	(b) 22.06	1.8214 2.5571	0.9934 0.9963	0.40 0.22	0.9396	0.1068	5.07 5.42	15.03 16.08		
III. o-toluidine in C_6H_6 $M_j = 0.107$	2.02	1.4840	0.9966	0.23	0.9986	0.1917	4.14	9.45	4.63	5.37
		0.1981	0.9981	0.13			4.51	10.30		

Contd...

Systems with serial number and molecular weight (M_j) in kg.	Frequency (f) in GHz	Linear coefficient of $\chi'_{ij}-w_j$ & $\sigma_{ij}-w_j$ curves of Figs. 8.3 and 8.7	Correlation coefficient (r) and % of errors involved in $\chi'_{ij}-w_j$ and $\sigma_{ij}-w_j$ curves		Dimensionless parameters		Estimated dipole moment $\mu \times 10^{30}$ C.m from hf susceptibility and conductivity measurement		Theoretical $\mu \times 10^{30}$ in C.m from bond angles and bond moments	$\mu \times 10^{30}$ in C.m from Gopalakrishnas method.
			(r)	% of error	b_1	b_2	μ_1	μ_2		
					$\frac{1}{1+\omega^2\tau_1^2}$	$\frac{1}{1+\omega^2\tau_2^2}$				
IV. m-toluidine in C_6H_6 $M_j=0.107$	3.86	0.5720	0.8479	8.48			2.57	11.69	3.43	4.90
		0.1265	0.8732	7.16	0.9956	0.0482	2.61	11.87		
V. p-toluidine in C_6H_6 $M_j=0.107$	(a) 3.86	0.4791	0.9755	1.46			2.36	8.22	5.13	5.00
		0.1638	0.9825	1.04	0.9912	0.0818	2.98	10.38		
	(b) 22.06	0.0109	0.9819	1.08			0.35	0.75		
		0.3762	0.9864	0.81	0.9980	0.2221	1.88	3.99		

compared with reported μ 's (Gopalakrishna) and μ_{theo} 's from bond angles and bond moments of polar groups of the parent polar molecules to support their conformations. The slight disagreement between measured μ_j 's and μ_{theo} 's invites the existence of inductive, mesomeric and electromeric effects suffered by polar groups, in addition to weak molecular associations between the polar molecules.

8.2. Weighted contributions c_1 and c_2 for τ_1 and τ_2

By putting $\alpha_1 = \omega\tau_1$ and $\alpha_2 = \omega\tau_2$ the Eqs. (8.1) and (8.2) are solved to get

$$c_1 = \frac{(\chi'_{ij}\alpha_2 - \chi''_{ij})(1 + \alpha_1^2)}{\chi_{oij}(\alpha_2 - \alpha_1)} \quad (8.4)$$

and

$$c_2 = \frac{(\chi''_{ij} - \chi'_{ij}\alpha_1)(1 + \alpha_2^2)}{\chi_{oij}(\alpha_2 - \alpha_1)} \quad (8.5)$$

provided $\alpha_2 > \alpha_1$. The theoretical values of c_1 and c_2 towards dielectric relaxations were, however, obtained from Eqs. (8.4) and (8.5) with the help of Fröhlich's following theoretical equations [16].

$$\chi'_{ij}/\chi_{oij} = 1 - \frac{1}{2A} \ln \left(\frac{1 + \omega^2\tau_2^2}{1 + \omega^2\tau_1^2} \right) \quad (8.6)$$

$$\chi''_{ij}/\chi_{oij} = \frac{1}{A} [\tan^{-1}(\omega\tau_2) - \tan^{-1}(\omega\tau_1)] \quad (8.7)$$

in terms of the measured τ_1 and τ_2 as presented in Table 8.2 from Eq. (8.3) of double relaxation method.

The theoretical c_1 and c_2 as entered in Table 8.3 are compared with the experimental ones obtained from the intercept of fitted parabolic curves of χ'_{ij}/χ_{oij} and χ''_{ij}/χ_{oij} against w_j of Figures 8.5 and 8.6 in the limit $w_j=0$ and Eqs. (8.4)

and (8.5). The curves in Figures 8.5 and 8.6 drawn by the regression analysis of polynomial fitting, are thought to yield the accurate values of χ' / χ_{oj} and $\chi''_{ij} / \chi_{\text{oj}}$ in the limit $w_j = 0$ in comparison to earlier study of graphical extrapolation technique based on personal judgement. The Fröhlich parameter $A = \ln(\tau_2/\tau_1)$ are placed in Table 8.3 for each compound at different frequencies.

8.3. Symmetric and characteristic relaxation times τ_s and τ_{cs}

The molecules under present investigation appear to behave like nonrigid ones at 2.02, 3.86 and 22.06 GHz electric field having either symmetric or asymmetric distribution parameters γ and δ involved in the Eqs. (8.8) and (8.9)

$$\frac{\chi^*_{ij}}{\chi_{\text{oj}}} = \frac{1}{1+(j\omega\tau_s)^{1-\gamma}} \quad (8.8)$$

$$\frac{\chi^*_{ij}}{\chi_{\text{oj}}} = \frac{1}{(1+j\omega\tau_{cs})^\delta} \quad (8.9)$$

The former one (Eq. 8.8) is associated with symmetric relaxation time τ_s and the latter one (Eq. 8.9) with characteristic relaxation time τ_{cs} . Separating the real and imaginary parts of Eqs. (8.8) and (8.9) and rearranging them in terms of $\chi'_{ij} / \chi_{\text{oj}}$ and $\chi''_{ij} / \chi_{\text{oj}}$ at $w_j \rightarrow 0$ of Figures 8.5 and 8.6 γ and τ_s were obtained from :

$$\gamma = \frac{2}{\pi} \tan^{-1} \left[(1 - \chi'_{ij} / \chi_{\text{oj}}) \frac{\chi'_{ij}}{\chi''_{ij}} - \frac{\chi''_{ij}}{\chi_{\text{oj}}} \right] \quad (8.10)$$

and

$$\tau_s = \frac{1}{\omega} \left[\frac{1}{(\chi'_{ij} / \chi''_{ij}) \cos\left(\frac{\gamma\pi}{2}\right) - \sin\left(\frac{\gamma\pi}{2}\right)} \right]^{1/(1-\gamma)} \quad (8.11)$$

Similarly δ and τ_{cs} can be had from Eq. (8.9):

$$\tan(\varphi\delta) = \frac{(\chi''_{ij} / \chi_{oij})w_j \rightarrow 0}{(\chi'_{ij} / \chi_{oij})w_j \rightarrow 0} \quad (8.12)$$

$$\text{and } \tan \varphi = \omega\tau_{cs} \quad (8.13)$$

As φ can not be evaluated directly an arbitrary theoretical curve between $1/\varphi \log(\text{Cos } \varphi)$ against φ in degrees was drawn elsewhere [17] from which

$$\frac{1}{\varphi} \log(\text{Cos } \varphi) = \log \left[\frac{\chi'_{ij} / \chi_{oij}}{\text{Cos } \varphi\delta} \right] / \varphi\delta \quad (8.14)$$

can be known. The known values of $(1/\varphi) \log(\text{Cos } \varphi)$, is used to know φ from $1/\varphi \log(\text{Cos } \varphi) - \varphi$ curve. With known φ Eqs. (8.12) and (8.13) were used to obtain δ and τ_{cs} respectively. τ_s and τ_{cs} so evaluated are entered in Table 8.2 to compare with τ_j 's by Murthy et al [14], freshly calculated Gopalakrishna [15] and τ_1, τ_2 by double relaxation methods. Estimated γ and δ are shown in Table 8.3.

8.4. Theoretical Formulation to obtain hf dipole moment μ_j :

(A) hf susceptibility method

The real ϵ'_{ij} and imaginary ϵ''_{ij} parts of hf complex relative permittivity ϵ^*_{ij} are related by :

$$\epsilon'_{ij} = \epsilon_{\infty ij} + \left(\frac{1}{\omega\tau} \right) \epsilon''_{ij}$$

$$\epsilon'_{ij} - \epsilon_{\infty ij} = \left(\frac{1}{\omega\tau} \right) \epsilon''_{ij}$$

$$\chi'_{ij} = \left(\frac{1}{\omega\tau} \right) \chi''_{ij} \quad (8.15)$$

$$\text{and } (d\chi''_{ij} / d\chi'_{ij}) = \omega\tau \quad (8.16)$$

χ''_{ij} 's are expected to vary linearly with χ'_{ij} [14] as seen in Figure 8.4. The slope of linear equation of χ''_{ij} and χ'_{ij} was used to get τ_j from Eq. (8.16).

But the variations of χ''_{ij} with χ'_{ij} in Figure 8.4 are not strictly linear, the ratio of individual slopes of variations of χ''_{ij} and χ'_{ij} with w_j 's in Figures 8.2 and 8.3 is a better representation of Eq. (8.16) to get τ_j where the polar-polar interactions are supposed to be eliminated. Thus

$$\left(\frac{d\chi''_{ij}}{dw_j}\right)_{w_j \rightarrow 0} / \left(\frac{d\chi'_{ij}}{dw_j}\right)_{w_j \rightarrow 0} = \omega\tau_j \quad (8.17)$$

The imaginary part χ''_{ij} of χ^*_{ij} is [17-19]

$$\chi''_{ij} = \frac{N\rho_{ij}\mu_j^2}{27\varepsilon_0 M_j k_B T} \left(\frac{\omega\tau}{1+\omega^2\tau^2}\right) (\varepsilon_{ij} + 2)^2 w_j \quad (8.18)$$

which on differentiation with respect to w_j and at $w_j \rightarrow 0$ yields that

$$\left(\frac{d\chi''_{ij}}{dw_j}\right)_{w_j \rightarrow 0} = \frac{N\rho_{ij}\mu_j^2}{27\varepsilon_0 M_j k_B T} \cdot \left(\frac{\omega\tau}{1+\omega^2\tau^2}\right) (\varepsilon_{ij} + 2)^2 \quad (8.19)$$

From Eqs. (8.17) and (8.19) one obtains

$$\omega\tau \left(\frac{d\chi'_{ij}}{dw_j}\right)_{w_j \rightarrow 0} = \frac{N\rho_{ij}\mu_j^2}{27\varepsilon_0 M_j k_B T} \left(\frac{\omega\tau}{1+\omega^2\tau^2}\right) (\varepsilon_{ij} + 2)^2$$

$$\mu_j = \left[\frac{27\varepsilon_0 M_j k_B T \beta}{N\rho_{ij}(\varepsilon_{ij} + 2)^2 b} \right]^{1/2} \quad (8.20)$$

where ε_0 is the permittivity of free space = 8.854×10^{-12} F.m⁻¹

β = linear coefficient of $\chi'_{ij} - w_j$ curves of Figure 8.3 at $w_j \rightarrow 0$

B. hf conductivity method

According to Murphy and Morgan [20] the real and imaginary parts of hf conductivity are related by :

$$\sigma_{ij}'' = \sigma_{\infty ij} + \frac{1}{\omega\tau} \sigma_{ij}' \quad (8.21)$$

where $\sigma_{ij}' = \omega\epsilon_0 \epsilon_{ij}''$ and $\sigma_{ij}'' = \omega\epsilon_0 \epsilon_{ij}'$ are the real and imaginary parts of hf complex conductivity σ_{ij}^* . $\omega = 2\pi f$ and f is the frequency of applied electric field in GHz range.

$$(d\sigma_{ij}''/dw_j)w_{j \rightarrow 0} = \left(\frac{1}{\omega\tau}\right) (d\sigma_{ij}'/dw_j)w_{j \rightarrow 0}$$

Since $\sigma_{ij}'' \simeq \sigma_{ij}$ where σ_{ij} the total hf conductivity $= \omega\epsilon_0(\epsilon_{ij}'^2 + \epsilon_{ij}''^2)^{1/2}$

$$\text{One has } (d\sigma_{ij}'/dw_j)w_{j \rightarrow 0} = \omega\tau\beta \quad (8.22)$$

where β is the linear coefficient of $\sigma_{ij}-w_j$ curve of Figure 8.7 in the limit $w_j = 0$.

Again, the real σ_{ij}' of hf complex conductivity σ_{ij}^* is [18,22]

$$\sigma_{ij}' = \frac{N\mu_j^2 \rho_{ij}}{27M_j k_B T} \left(\frac{\omega^2 \tau}{1+\omega^2 \tau^2}\right) (\epsilon_{ij} + 2) w_j \quad (8.23)$$

which on differentiation w.r. to w_j and at $w_j \rightarrow 0$ yields that

$$\left(\frac{d\sigma_{ij}'}{dw_j}\right)w_{j \rightarrow 0} = \frac{N\mu_j^2 \rho_{ij}}{27M_j k_B T} \left(\frac{\omega^2 \tau}{1+\omega^2 \tau^2}\right) (\epsilon_{ij} + 2)^2 \quad (8.24)$$

From Eqs. (8.22) and (8.24) one gets

$$\mu_j = \left[\frac{27M_j k_B T \beta}{N \rho_{ij} (\epsilon_{ij} + 2)^2 \omega \tau} \right]^{1/2} \quad (8.25)$$

where β = linear coefficient of $\sigma_{ij} - w_j$ curve of Figure 8.7 at $w_j \rightarrow 0$. In both the Eqs. (8.20) and (8.25) we have

$$N = \text{Avogadro's number} = 6.023 \times 10^{23}$$

$$\rho_i = \text{density of solvent (C}_6\text{H}_6) = 865 \text{ kg. m}^{-3}$$

$$\epsilon_i = \text{relative permittivity of solvent C}_6\text{H}_6 = 2.253$$

$$M_j = \text{molecular weight of solute in kg.}$$

$$k_B = \text{Boltzmann constant} = 1.38 \times 10^{-23} \text{ J.mole}^{-1} \text{ K}^{-1}$$

$$b = \frac{1}{1 + \omega^2 \tau^2} = \text{dimensionless parameter involved with measured } \tau.$$

Dipole moment μ_1, μ_2 in terms of b_1, b_2 involved with estimated τ_1, τ_2 were computed from both the Eqs. (8.20) and (8.25) as well with the linear coefficient β 's of both, $\chi'_{ij} - w_j$ and $\sigma_{ij} - w_j$ curves of Figures 8.3 and 8.7. All μ_j 's are placed in Table 8.4 together with μ_{theo} 's and reported μ_j 's (Gopalakrishna) for comparison.

8.5. Results and Discussion

The least squares fitted straight line equations in terms of χ'_{ij}, χ''_{ij} and χ_{oij} of Table 8.1 were worked out for each system as shown graphically in Figure 8.1 at different w_j of solute in solvent benzene at 35°C under GHz electric field with the experimental points placed upon them. χ'_{ij} and χ''_{ij} are real and imaginary parts of hf complex dimensionless dielectric orientational susceptibility χ^*_{ij} and χ_{oij} is the static or low frequency real dielectric susceptibility. They are, however, derived from measured [7] relative permittivities $\epsilon'_{ij}, \epsilon''_{ij}, \epsilon_{oij}$, and $\epsilon_{\infty ij}$ of Table 8.1. The correlation coefficients (r) and chisquare values placed in the 5th and 6th columns of Table 8.2 are estimated to show how far the variables $(\chi_{oij} - \chi'_{ij})/\chi'_{ij}$ and χ''_{ij}/χ'_{ij} of Eq (8.3) are correlated.

It is seen that r is low for o-anisidine at 3.86 GHz and o-toluidine at 2.02 GHz possibly for errors introduced in the measurement of ϵ'_{ij} , ϵ''_{ij} , ϵ_{oij} and $\epsilon_{\infty ij}$. This fact is also confirmed by remarkable deviations of experimental data from linear curves of Figure 8.1. In order to locate the double relaxation phenomena accurate measurements of ϵ_{oij} and $\epsilon_{\infty ij}$ are essential. The refractive index n_{Dij} measured by Abbe's refractometer often yields $\epsilon_{\infty ij} = n_{Dij}^2$ [7] although Cole-Cole [3] and Cole-Davidson [21] plots give $\epsilon_{\infty ij}$ (1.0–1.15) times of n_{Dij}^2 . The intercepts and slopes of linear curves of Figure 8.1 are seen in the 3rd and 4th columns of Table 8.2, to get τ_1 and τ_2 due to rotation of flexible polar groups and end over end rotations of the whole molecules. τ_1 and τ_2 thus measured are presented in the 7th and 8th columns of Table 8.2 τ_2 's in Table 8.2 increases gradually from meta to ortho for anisidines at 22.06 GHz while the reverse is true at 3.86 GHz. But in case of toluidines τ_2 increases from para to ortho and to meta forms. This behaviour is, however, explained by the fact that C — NH₂ group is significantly influenced by GHz electric field. On the other hand τ_1 increases from ortho to meta forms for anisidines while it increases from meta to ortho and to para forms for toluidines. This behaviour, however, indicates that flexible parts of the molecules are loosely bound to the parent molecules [12, 13].

In absence of reliable τ_j 's of monosubstituted anilines the slopes of the least squares fitted straight line curves of χ''_{ij} against χ'_{ij} of Figure 8.4 as claimed by Murthy et al [14] were used to get τ_j from Eq. (8.16). They are placed in the 9th column of Table 8.2. The experimental points of Table 8.1 are found to deviate from linearity of Figure 8.4 due to solute - solute molecular interactions. The individual variations of χ''_{ij} and χ'_{ij} with w_j are not strictly linear as seen in Figures 8.2 and 8.3. This fact at once prompted one to use the ratio of slopes of the individual variations of χ''_{ij} and χ'_{ij} with w_j 's [17] entered in 10th column of Table 8.2 to evaluate τ_j from Eq. (8.17) at $w_j \rightarrow 0$. τ_j 's thus obtained are in close agreement with τ_1 from double relaxation and Gopalakrishna's [15] method and are placed in the 11th column of Table 8.2. τ_j for p-toluidine at 22.06

GHz shows large value probably for error introduced in ϵ'_{ij} , ϵ''_{ij} , ϵ_{oij} and $\epsilon_{\infty ij}$ measurements. The basic soundness of the latter method in getting τ_j is thus confirmed because the polar - polar interactions are fully avoided [22]. Moreover, it shows that hf susceptibility measurement yields microscopic τ where as double relaxation method gives both microscopic and macroscopic τ_1 and τ_2 as observed elsewhere [23].

Large τ_2 arises for the bigger size of rotating unit ($\tau_j T/\eta^j$) due to solvent environment around solute molecules. The distribution of τ between two extreme τ_1 and τ_2 values yields the symmetric and asymmetric distribution parameters γ and δ . They are, however, obtained from Eqs. (8.10) and (8.12) with $(\chi'_{ij}/\chi_{oij})_{\omega_j \rightarrow 0}$ and $(\chi''_{ij}/\chi_{oij})_{\omega_j \rightarrow 0}$ of Figures 8.5 and 8.6. The value of $(1/\phi) \log (\cos \phi)$ against ϕ in degree as shown elsewhere [17] is essential to know δ . Knowing ϕ , δ 's were obtained. γ and δ are entered in 12th and 13th column of Table 8.3.

The symmetric relaxation times τ_s from Eq. (8.11) in terms of γ of Eq. (8.10) are presented in the 13th column of Table 8.3. The close agreement of τ_s 's with τ_1 's and reported τ 's by freshly calculated from Gopalakrishna's method, indicates symmetric relaxation behaviour of such molecules in C_6H_6 . The agreement is however, poor in case of o-toluidine. The characteristic relaxation times τ_{cs} obtained from Eq. (8.13) for o-anisidine at 3.86 GHz, m-anisidine at 3.86 and 22.06 GHz and m-toluidine at 3.86 GHz as seen in 14th column of Table 8.2 shows high values as δ 's are found to be low. For other systems τ_{cs} and δ could not be found out as $(1/\phi) \log (\cos \phi)$ for them are positive. This fact rules out the applicability of asymmetric relaxation behaviour for such compounds.

The theoretical weighted contributions of c_1 and c_2 towards dielectric relaxations were obtained from Eqs. (8.4) and (8.5) by the measured τ_1 and τ_2 of Eq. (8.3) and χ'_{ij}/χ_{oij} and χ''_{ij}/χ_{oij} of Fröhlich's equations (8.6) and (8.7). The

6th and 7th columns of Table 8.3 contain c_1 and c_2 . The experimental c_1 and c_2 values were also obtained from $(\chi'_{ij} / \chi_{oij})w_{j \rightarrow 0}$ and $(\chi''_{ij} / \chi_{oij})w_{j \rightarrow 0}$ of the concentration variations of χ'_{ij} / χ_{oij} and χ''_{ij} / χ_{oij} of Figures 8.5 and 8.6 by using Eqs. (8.4) and (8.5). They are presented in the 10th and 11th columns of Table 8.3 for comparison with the theoretical ones. Fröhlich's equations (8.6) and (8.7) are related to Fröhlich parameter A , where $A = \ln(\tau_2/\tau_1)$. Both the theoretical and experimental c_1 and c_2 as seen in Table 8.3 showed that $|c_1 + c_2| \simeq 1$ establishing the validity of Eq. (8.3). It is interesting to note that experimental c_2 's are negative in case of o-anisidine and p-toluidine at 22.06 GHz and m-toluidine for the inertia of the flexible parts [23]. In Figures 8.5 and 8.6 it is also seen that the experimental points often do not lie on the smooth fitted curves probably due to solute - solute or solute-solvent molecular associations.

The dipole moments μ_1 and μ_2 of the flexible parts and the whole molecules were estimated from the linear coefficients β 's in the 3rd column of Table 8.4 of both $\chi'_{ij}-w_j$ and $\sigma_{ij}-w_j$ curves of Figures 8.3 and 8.7 and dimensionless parameters b_1 and b_2 involved with measured τ_1 and τ_2 from Eq. (8.3). The μ_1 and μ_2 thus obtained from Eqs. (8.20) and (8.25) are placed in the 8th and 9th columns of Table 8.4 for comparison. Correlation coefficients r 's and % of errors involved in the regression analysis in the 4th and 5th columns of Table 8.4 were made only to show how far χ'_{ij} 's and σ_{ij} 's are correlated with w_j 's. Both the χ'_{ij} 's and σ_{ij} 's with w_j in Figures 8.3 and 8.7 give reliable β to yield accurate μ_1 and μ_2 . It is seen in Figures 8.3 and 8.7 that almost all the curves show a tendency to be closer within the region $0.00 \leq w_j \leq 0.03$ indicating the same polarity of the molecules, in addition to solute-solvent (monomer) or solute-solute (dimer) molecular associations [6,22]. μ_1 and μ_2 in Table 8.4 from $\chi'_{ij}-w_j$ curves of Figure 8.3 are always smaller in magnitude than $\sigma_{ij}-w_j$ curves of Figure 8.7 as χ_{ij} 's are associated with orientational polarisation while σ_{ij} is more linked with the bound molecular charges. Theoretical dipole moments μ_{theo} 's of monosubstituted anilines as estimated elsewhere [17] in terms of available bond angles and bond

moments of polar groups $C \rightarrow NH_2$, $C \rightarrow OCH_3$, $C \rightarrow CH_3$ are entered in the 10th column of Table 8.4 to compare with the experimental μ_j 's. The contribution of inductive, mesomeric and electromeric moments of the substituent polar groups of the molecules towards the hf μ_j 's are, however, explained by the factor $\mu_j(\text{expt})/\mu_{j,\text{theo}}$ of values 1.49, 1.68, 0.93, 0.92, 0.89, 0.75, 0.46 and 0.07 of Ia, Ib, IIa, IIb, III, IV, Va and Vb respectively. The amount of bound molecular charge is judged from the difference $\Delta\mu_j$ between μ_j 's of hf σ_{ij} and χ'_{ij} respectively to contribute to hf σ_{ij} [8].

In absence of reliable μ_j 's Gopalakrishna's method [15] were reemployed. The close agreement between reported μ_j 's (Gopalakrishna) μ_1 and μ_{theo} 's confirms the basic soundness of the methods prescribed in getting hf μ_j in addition to the fact that a part of the molecule is rotating under GHz electric field.

8.6. Conclusions

The methodology so far presented in SI units with internationally accepted symbols of dielectric terminologies and parameters appears to be more topical, simple, straightforward and unique one to predict relaxation parameters as χ_{ij} 's are directly linked with molecular orientational polarisation. The significant and interesting equations to evaluate τ_j 's and μ_j 's in terms of χ_{ij} helps one to shed more light on the relaxation phenomena of complicated molecules. The simple straight line equation (8.3) provides with microscopic and macroscopic τ 's i.e. τ_1 and τ_2 . The method to evaluate τ_j from the ratio of slopes of individual variations of χ''_{ij} and χ'_{ij} with ω_j is a better representation of the earlier method of Murthy et al as it eliminates polar-polar interactions in solution. The relative weight factors c_1 and c_2 by Fröhlich's and graphical method shows $|c_1 + c_2| \simeq 1$ confirming the applicability of the linear equation (8.3) to estimate τ_1 and τ_2 respectively for monosubstituted anilines. The close agreement of τ_j , τ_1 and τ_2 confirms the nonrigid character of the molecules under hf electric field in C_6H_6 .

μ_1 and μ_2 by hf susceptibility and conductivity methods establish the fact that different types of polarisations are associated with χ'_{ij} 's and σ_{ij} 's. The theoretical reasons of evaluating τ_1 's and μ_1 's in agreement of τ_j 's and μ_j 's from freshly calculated Gopalakrishna's method is really sound. Various types of molecular associations are inferred from usual departure of graphically fitted plots of χ'_{ij} / χ_{oij} and χ''_{ij} / χ_{oij} with w_j 's and conformational structure of the molecules in which the effect of inductive, mesomeric and electromeric moments of the polar groups of the molecule plays the prominent role.

References

- [1] A Sharma, D R Sharma and M S Chauhan *Indian J Pure & Appl. Phys.* **31** (1993) 841.
- [2] K Higasi, Y Koga and M Nakamura *Bull Chem Soc. Japan* **44** (1971) 988.
- [3] K S Cole and R H Cole *J Chem Phys* **9** (1941) 341.
- [4] E A Guggenheim *Trans Faraday Soc.* **45** (1949) 714.
- [5] S K Sit, N Ghosh U Saha and S Acharyya *Indian J Phys.* **71B** (1997) 533.
- [6] N Ghosh, A Karmakar, S K Sit and S Acharyya *Indian J Pure. & Appl. Phys.* **38** (2000) 574.
- [7] S. C Srivastava and S Chandra *Indian J Pure & Appl. Phys* **13** (1975) 101.
- [8] A K Jonscher *Physics of Dielectric Solids, invited papers* ed CHL Goodman 1980. (Canterbury).
- [9] A Budo *Phys Z* **39** (1938) 706.

- [10] K Bergmann, D M Roberti and C P Smyth *J Phys Chem* **64** (1960) 665.
- [11] J Bhattacharyya, A Hasan, S B Roy and G S Kastha *J Phys. Soc. Japan* **28** (1970) 204.
- [12] U Saha, S K Sit, R C Basak and S Acharyya *J Phys D : Appl. Phys* **27** (1994) 596.
- [13] S K Sit, R C Basak, U Saha and S Acharyya *J Phys D : Appl. Phys* **27** (1994) 2194.
- [14] M B R Murthy, R L Patil and D K Deshpande *Indian J Phys.* **63B** (1989) 491.
- [15] K V Gopalakrishna *Trans. Faraday Soc.* **53** (1957) 767.
- [16] H Fröhlich, *'Theory of Dielectric's* (Oxford University Press : Oxford) 1949.
- [17] N Ghosh, S K Sit, A K Bothra and S Acharyya *J Phys D : Appl. Phys* **34** (2001) 379.
- [18] C P Smyth *Dielectric Behaviour and Structure* (New York : McGraw Hill) 1955.
- [19] K Dutta, S K Sit and S Acharyya *Pramana J. Phys.* **57** (2001) 775.
- [20] F J Murphy and S O Morgan, *Bell Syst. Tech. J* **18** (1939) 502.
- [21] D W Davidson and R H Cole *J. Chem Phys* **19** (1951) 1484.
- [22] N Ghosh, R C Basak, S K Sit and S Acharyya *J Mol. Liquids* **85** (2000) 375.
- [23] S K Sit, N Ghosh and S Acharyya *Indian J Pure & Appl. Phys.* **35** (1997) 329.

CHAPTER -9

**STRUCTURAL CONFORMATION AND
ASSOCIATIONAL ASPECTS OF SOME
NORMAL ALCOHOLS IN BENZENE AND
THEIR MIXTURES UNDER RF ELECTRIC
FIELD AT SINGLE AND DIFFERENT
TEMPERATURES**

STRUCTURAL CONFORMATION AND ASSOCIATIONAL ASPECTS OF SOME NORMAL ALCOHOLS IN BENZENE AND THEIR MIXTURES UNDER RF ELECTRIC FIELD AT SINGLE AND DIFFERENT TEMPERATURES

9.1. Introduction

The experimental determination of rf conductivity σ'_{ij} or σ'_{jk} of polar-nonpolar, or polar-polar liquid mixtures is of considerable interest to many workers [1-4] as it provides an useful tool to estimate the free ion density n , relaxation time τ_j or τ_{jk} , dipole moment μ_j , various thermodynamic energy parameters including activation energy ΔE_{jk} . Rf measurement technique gives an insight into the properties of the polar groups, intermolecular field and structural aspects of dipolar liquid molecules.

According to Murphy and Morgan [5] the displacement current alone is the factor to yield hf conductivity in dielectric liquids. But most of the polar liquid dielectrics specially long chain alcohols display electrical conduction due to the combined effects of displacement and ionic currents. The evidence of existence of free ions and electrons in polar liquids was shown by many workers [6-8]. These substances may be considered to be semiconducting liquids. In microwave electric field, however, the dependence of conductivity on the conduction current is unimportant, but below 20 MHz the dielectric loss ϵ'' for the transport of free ions becomes important. The generation of free ions or electrons in both pure polar and polar-nonpolar liquid mixtures has been attributed to many reasons. Cosmic rays, natural radioactivity, thermal dissociation etc. in the insulating dielectrics are the main sources of the presence of such ions and electrons. But no specific reasons have not yet been reached for such formation of free ions and electrons in dielectric liquids.

Assuming the existence of displacement current and conduction current in polar dielectrics Sen and Ghosh [9] derived a simple formulation of rf

conductivity σ'_{ij} and solution viscosity η_{ij} . We thought to apply this formulation on some simple aliphatic alcohols like methanol, ethanol, n-propanol and 2-butanol in benzene and their mixtures like 2 butanol + n propanol; n propanol + ethanol and 2 butanol + ethanol. The slope of the linear relation between σ'_{ij} and $1/\eta_{ij}$ as seen by straight line curves of Figure 9.1 for polar-nonpolar liquid mixture is used to estimate number density of free ions 'n' in terms of molecular radius 'a' from gas kinetic theory. The intercepts and slopes along with the estimated n are, however, placed in Table 9.1. Einstein-Stokes relation [10] helps one to estimate τ_j of a polar unit. and τ_{jk} of polar-polar mixture. τ_j at infinite dilution is, however, obtained from graphical extrapolation of $\tau_j - w_j$ curve at $w_j = 0$ of Figure 9.2. The linear coefficient β of $\sigma'_{ij} - w_j$ curve of Figure 9.3 is further used to estimate rf dipole moment μ_j of a polar molecule from Smyths' relation [11]. Estimated μ_j 's along with μ_{theo} 's of Figure 9.4 are placed in Table 9.1 for comparison. The comparison of μ_{theo} 's with measured μ_j 's shed more light on their structural conformations.

The $\ln \sigma'_{jk}$ of polar-polar mixtures of 2 butanol + n propanol, n propanol + ethanol and 2 butanol + ethanol are plotted in Figure 9.5 as a function of $1/T$, where T is the temperature in Kelvin. The slopes of the fitted straight line curves of Figure 9.5 were used to estimate semi-conduction activation energy ΔE_{jk} of binary polar-polar liquid mixtures as seen in Table 9.2. The variation of τ_{jk} with temperature are helpful to estimate different thermodynamic energy parameters $\Delta H_{\tau_{jk}}$, $\Delta S_{\tau_{jk}}$, $\Delta F_{\tau_{jk}}$ from Eyrings rate theory [12]. The linear curves of Figure 9.6 are used to estimate the energy parameters. They are entered in Table 9.3 to conclude about the stability or unstability [13,14] of the binary mixtures undergoing relaxation phenomena. The corresponding τ_{jk} 's at different temperatures are shown in Figure 9.7 as a function of mole fraction of the jth solute in jk mixture.

All the relaxation parameters hence estimated are placed in different Table of 9.1 to 9.4 for comparison with the available data of Ghosh and Sen

[15]. The main purpose of the present study on some interesting dielectropolar alcohols is to test the adequacy or otherwise of mathematical formulation so far derived [9,16] and new formulation presented in the 2nd chapter of this thesis to arrive at a concrete concept on their structural conformation and various associational aspects under rf electric field. It is also observed that almost all the alcohols except methanol showed the double relaxation behaviour showing τ_1 and τ_2 for the rotation of their flexible polar groups and whole molecular rotation under GHz electric field [17]. Such long chain, hydrogen bonded polymer type liquids have wide applications in the fields of biological research, medicine and industry.

9.2. Rf Experimental Details

The block diagram of the experimental arrangement and the theoretical formulation to estimate rf conductivity and other physical parameters of binary polar-nonpolar (ij) and polar-polar (jk) liquid mixture have been described in detail in chapter 2. The dielectric cell used was a cylindrical glass tube of diameter 2 cm fitted with a pair of stainless steel circular electrodes of diameter 1.5 cm and separated by 1 cm. The Analar grade methanol, ethanol, n-propanol, 2-butanol and benzene are obtained from M/S BDH (London) and E.Merck (Germany). They were distilled in vacuum and kept in a desiccator before use. The viscosity of the liquids were measured by an Ostwald viscometer where highly pure distilled water was used as a reference liquid. The temperature of the experiment was controlled by a good thermostat whose accuracy was $\pm 0.5^\circ\text{C}$. Other essential physical parameters like density ρ , static relative permittivity ϵ_0 and refractive index n_D are checked in agreement with literature values [18] before use.

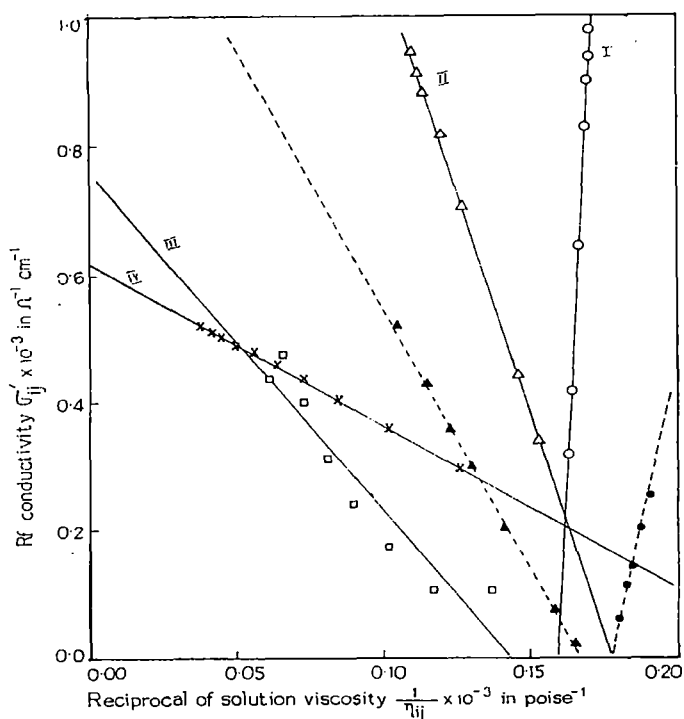


Figure 9.1: Linear variation of rf conductivity σ'_{ij} in $\Omega^{-1}\text{cm}^{-1}$ against reciprocal of solution viscosity $1/\eta_{ij}$ in poise^{-1} of some normal alcohols in benzene at 25°C under 1 MHz electric field. (I) methanol (—○—), (II) ethanol (—△—), (III) n-propanol (—□—), (IV) 2-butanol (—X—), methanol (—●—), ethanol (—▲—)

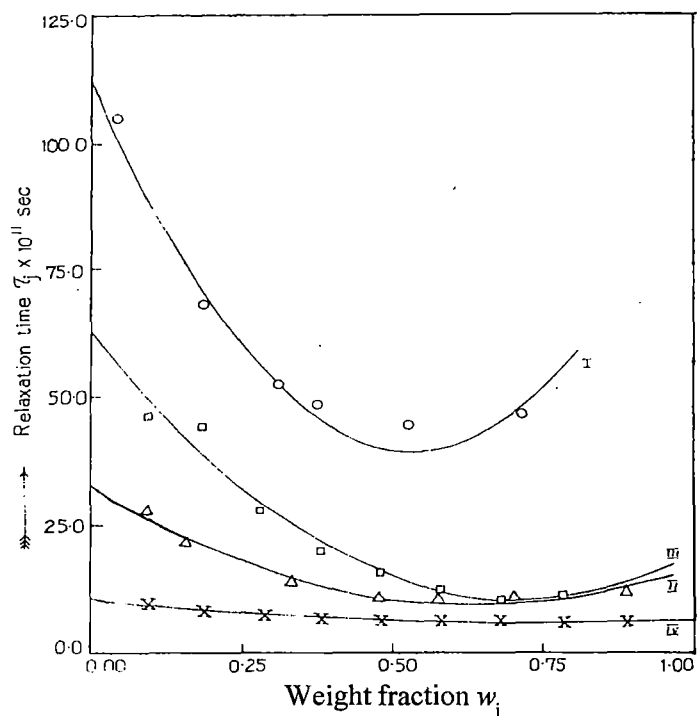


Figure 9.2: Non linear plot of relaxation time τ_j against weight fraction w_j of some normal alcohols in benzene at 25°C under 1 MHz electric field. (I) methanol (—○—), (II) ethanol (—△—), (III) n-propanol (—□—), (IV) 2-butanol (—X—),

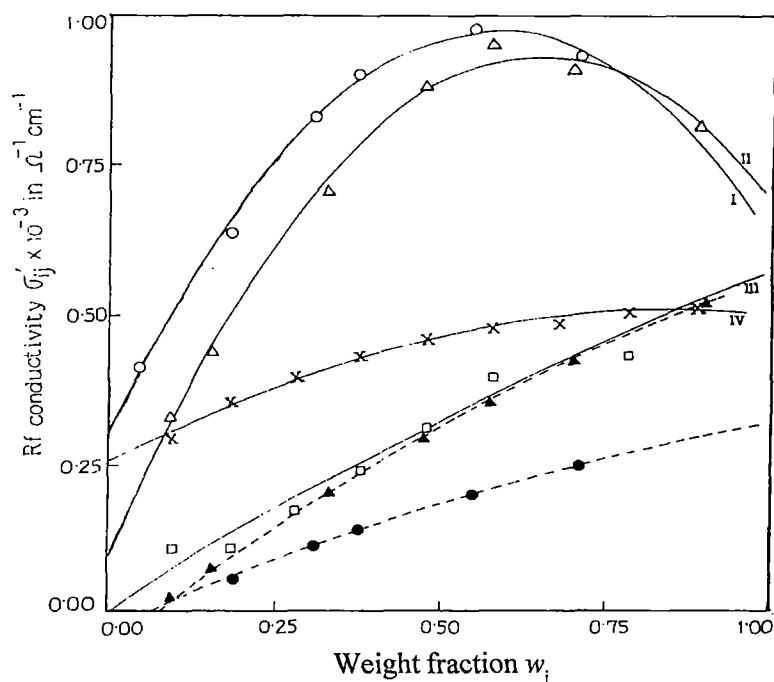


Figure 9.3: Variation of rf conductivity σ'_{ij} in $\Omega^{-1}\text{cm}^{-1}$ against weight fraction w_j of some normal alcohols in benzene at 25°C under 1MHz electric field.

(I) methanol (—O—), (II) ethanol (— Δ —), (III) n-propanol (— \square —), (IV) 2-butanol (—X—), methanol (—●—), ethanol (— \blacktriangle —)

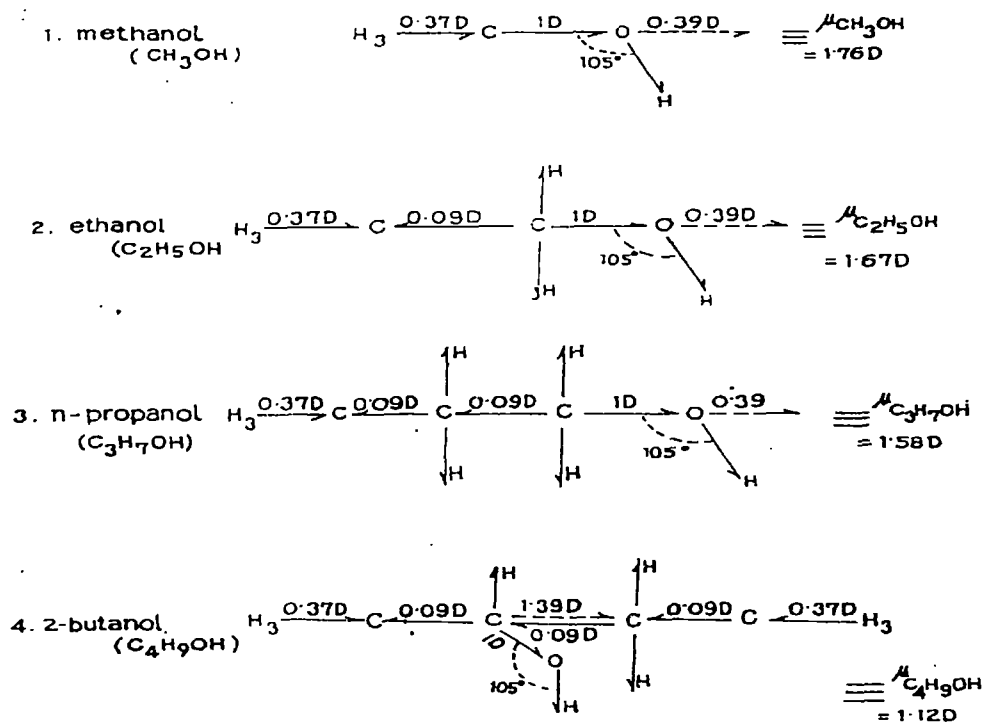


Figure 9.4: Conformational structure of some alcohols.

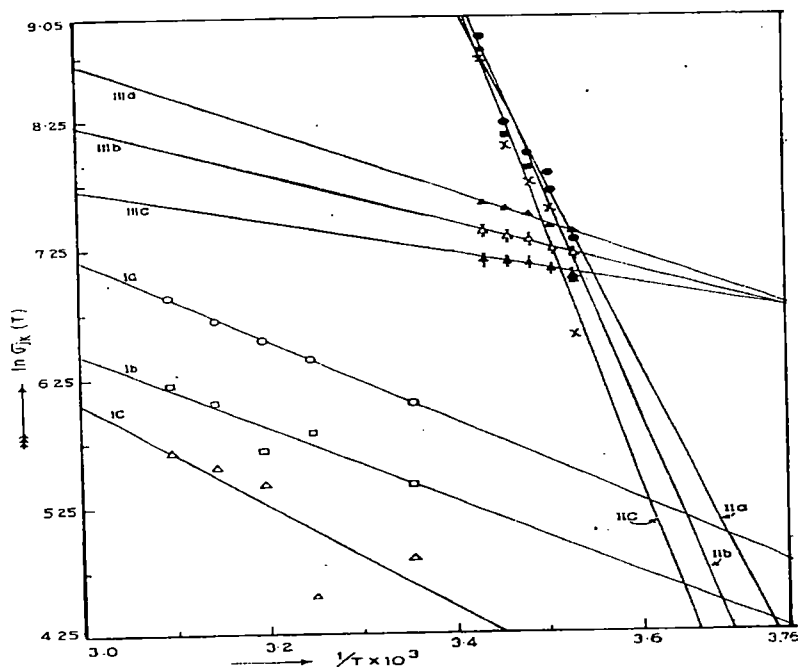


Figure 9.5: Plot of $\ln \sigma'_{jk}(T)$ against $1/T$ of polar-polar mixtures at different concentrations (x_j) of solute under 1 MHz electric field.

(I) 2 butanol + n-propanol (Ia) $x_j = 0.1690$ (—○—), (Ib) $x_j = 0.4486$ (—□—), (Ic) $x_j = 0.7649$ (—△—)
 (II) n-propanol + ethanol (IIa) $x_j = 0.3349$ (—●—), (IIb) $x_j = 0.4302$ (—■—), (IIc) $x_j = 0.5311$ (—X—)
 (III) 2 butanol + ethanol (IIIa) $x_j = 0.2905$ (—▲—), (IIIb) $x_j = 0.3805$ (—⬇—), (IIIc) $x_j = 0.4795$ (—⬆—)

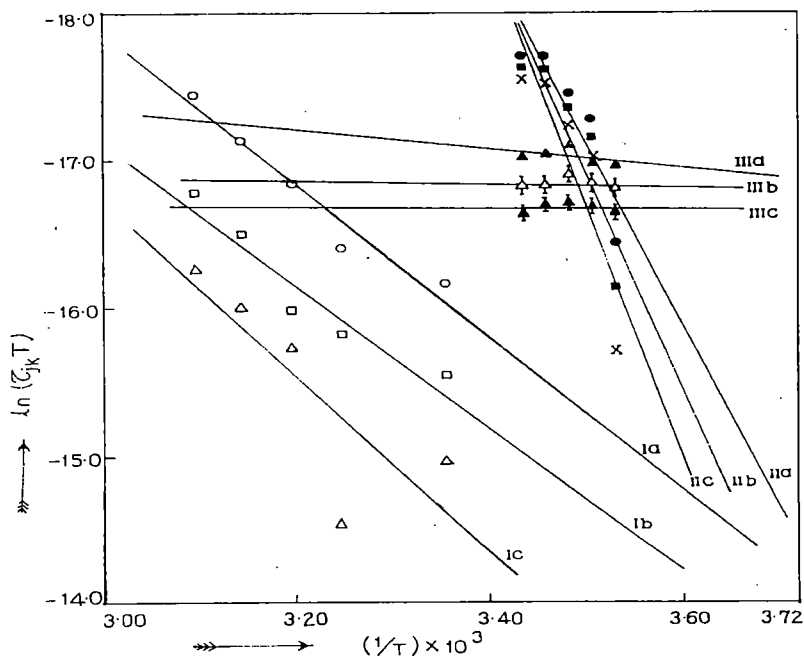


Figure 9.6: Plot of $\ln (\tau_{jk} T)$ against $1/T$ of polar-polar mixtures at different concentrations (x_j) of solute under 1 MHz electric field.

(I) 2 butanol + n-propanol (Ia) $x_j = 0.1690$ (—○—), (Ib) $x_j = 0.4486$ (—□—), (Ic) $x_j = 0.7649$ (—△—)
 (II) n-propanol + ethanol (IIa) $x_j = 0.3349$ (—●—), (IIb) $x_j = 0.4302$ (—■—), (IIc) $x_j = 0.5311$ (—X—)
 (III) 2 butanol + ethanol (IIIa) $x_j = 0.2905$ (—▲—), (IIIb) $x_j = 0.3805$ (—⬇—), (IIIc) $x_j = 0.4795$ (—⬆—)

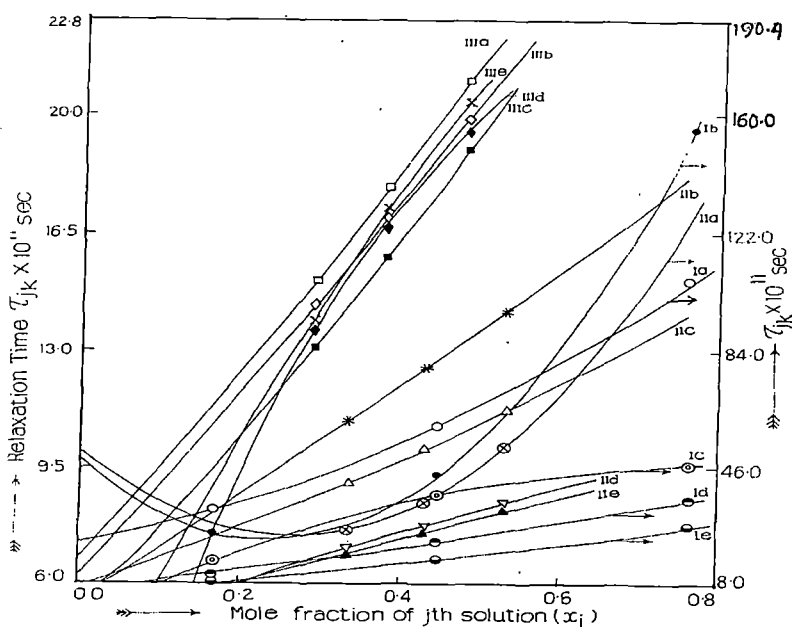


Figure 9.7: Variation of relaxation time τ_{jk} against mole fraction of j th solute (x_j) of polar-polar liquid mixtures under 1MHz electric field at different temperatures in Kelvin.

(I) 2 butanol + n-propanol mixture, (Ia) $T = 298\text{K}$ ($\text{---}\circ\text{---}$), (Ib) $T = 308\text{K}$ ($\text{---}\bullet\text{---}$), (Ic) $T = 313\text{K}$ ($\text{---}\odot\text{---}$), (Id) $T = 318\text{K}$ ($\text{---}\ominus\text{---}$), (Ie) $T = 323\text{K}$ ($\text{---}\ominus\text{---}$),

(II) n-propanol + ethanol mixture, (IIa) $T = 283\text{K}$ ($\text{---}\oplus\text{---}$), (IIb) $T = 285\text{K}$ ($\text{---}\ast\text{---}$), (IIc) $T = 287\text{K}$ ($\text{---}\triangle\text{---}$), (IId) $T = 289\text{K}$ ($\text{---}\nabla\text{---}$), (IIe) $T = 291\text{K}$ ($\text{---}\blacktriangle\text{---}$).

(III) 2 butanol + ethanol mixture, (IIIa) $T = 283\text{K}$ ($\text{---}\square\text{---}$), (IIIb) $T = 285\text{K}$ ($\text{---}\diamond\text{---}$), (IIIc) $T = 287\text{K}$ ($\text{---}\blacksquare\text{---}$), (IIId) $T = 289\text{K}$ ($\text{---}\blacklozenge\text{---}$), (IIIe) $T = 291\text{K}$ ($\text{---}\times\text{---}$)

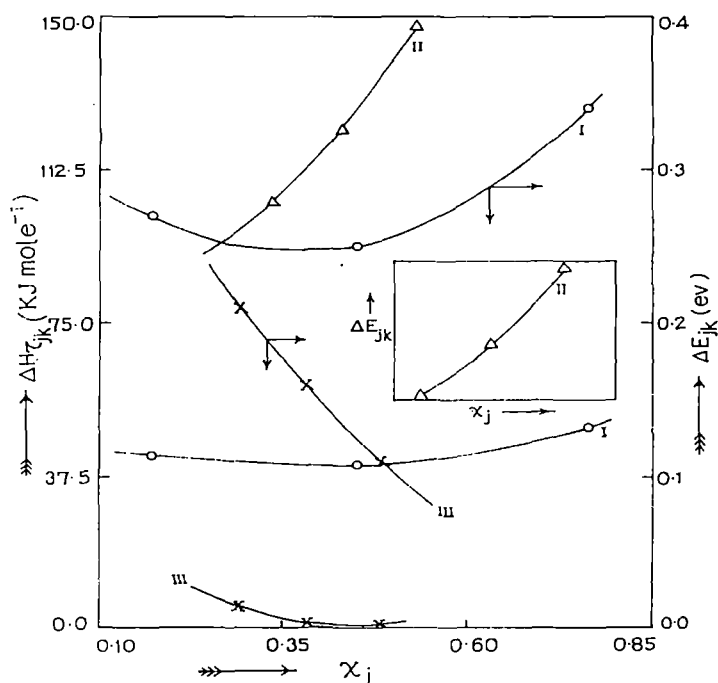


Figure 9.8: Variation of enthalpy of activation ΔH_{jk} and activation energy ΔE_{jk} with mole fraction of j th solute (x_j) of polar-polar liquid mixtures.

(I) 2 butanol + n-propanol ($\text{---}\circ\text{---}$), (II) n-propanol + ethanol ($\text{---}\triangle\text{---}$), (III) 2 butanol + ethanol ($\text{---}\times\text{---}$)

9.3. Results and Discussion

(A) Dielectric behaviour of polar-nonpolar liquid mixture :

The dependence of σ'_{ij} of polar-nonpolar liquid mixture on η_{ij} are, however, shown by least squares fitted linear curves of Figure 9.1 by solid lines with symbols showing the experimental points. The data measured by Ghosh and Sen [15] for methanol, and ethanol in benzene at 30°C under 800KHz electric field was shown simultaneously by the dotted lines of Figure 9.1. It is evident that both our σ'_{ij} for methanol, ethanol, n-propanol, 2 butanol and those of Ghosh and Sen [15] shows excellent linear dependence on the reciprocal of solution viscosity (η_{ij}). The intercepts and slopes of fitted straight line equations of Figure 9.1 are placed in the 5th and 6th columns of Table 9.1. The slope of the following linear equation of

$$\sigma'_{ij} = \left(\frac{\epsilon_{oij} - \epsilon_{\infty ij}}{4\pi} \right) \cdot \omega^2 \tau + \left(\frac{ne^2}{6\pi a} \right) \cdot \frac{1}{\eta_{ij}} \quad (9.1)$$

and of Figure 9.1 has been used to estimate 'n' with the knowledge of 'a' from the gas kinetic theory to see them in the 7th column of Table 9.1 along with reported [15] ones.

The estimated 'n' helps to compute τ_j at various concentrations w_j 's by the following relation [10].

$$\tau_j = \frac{2}{3} \frac{a^2 e}{\mu k_B T} \quad (9.2)$$

where a = molecular radius, e = electronic charge = 4.803×10^{-10} e.s.u., μ = mobility of free ions, k_B = Boltzmann constant = 1.38×10^{-16} erg mole⁻¹, K⁻¹, T = Temperature in Kelvin.

Again mobility of free ions is related to σ'_{ij} by [19]:

$$\mu = \sigma'_{ij} / ne \quad (9.3)$$

From Eqs. (9.2) and (9.3) one obtains

$$\tau_j = \frac{2na^2e^2}{3\sigma'_{ij} k_B T} \quad (9.4)$$

Both n and τ_j at different concentrations are entered in 7th and 8th columns of Table 9.1 together with measured data of Ghosh and Sen [15] as seen in the 7th and 9th columns.

Figure 9.1 shows that σ'_{ij} decreases with the increase of $1/\eta_{ij}$ exhibiting the negative slope of all the systems except for methanol. This sort of behaviour as observed elsewhere [15] may be explained on the basis of the fact that methanol is less viscous than solvent benzene in comparison to other alcohols.

Table 9.1 shows that estimated τ_j 's together with those of Ghosh and Sen [15] shows non linear dependence on weight fraction w_j of solute probably due to solute-solute or solute-solvent molecular association. A simple extrapolation curve between τ_j and w_j as seen in Figure 9.2 is, however, made to estimate τ_j of a polar unit at $w_j = 0$. τ_j so obtained is, however, placed in the 10th column of Table 9.1 which is supposed to be free from polar-polar interaction.

According to Smyth [11] the hf σ'_{ij} is written as

$$\sigma'_{ij} = \frac{4\pi^2 f^2 N \tau_j d_{ij} \mu_j^2 (\epsilon_{oij} + 2) (n_{Dij}^2 + 2) w_j}{27 M_j k_B T} \quad (9.5)$$

which gives the rf dipole moment μ_j as

$$\mu_j = \left[\frac{27 M_j k_B T \beta}{4\pi^2 f^2 N \tau_j d_{ij} (\epsilon_{oi} + 2) (n_{Di}^2 + 2)} \right]^{1/2} \quad (9.6)$$

where

- M_j = molecular weight of solute
 f = frequency of applied electric field
 d_i = density of solvent
 N = Avogadro's number = 6.023×10^{23}
 ϵ_{oi} = Static relative permittivity of solvent
 n_{Di} = refractive index of solvent.

It is seen in Figure 9.3 that σ'_{ij} for all the systems except n-propanol increases gradually with w_j attaining a maximum value at $w_j = 0.5$ indicating thereby a change of phase beyond a certain concentration. n-propanol may show its change of phase at higher concentration. The variation of σ'_{ij} with w_j as observed by Ghosh and Sen [15] for methanol and ethanol in benzene at 30°C under 800 KHz electric field are shown by dotted curves with the symbols showing the experimental points. The variation of σ'_{ij} with w_j may be represented by best fitted polynomial equation of $\sigma'_{ij} = \alpha + \beta w_j + \gamma w_j^2$ whose linear coefficient $\beta = (d\sigma'_{ij}/dw_j)_{w_j \rightarrow 0}$ is obtained by least squares fitting technique. It is used to get the rf dipole moment μ_j of a polar molecule from Eq (9.6).

Theoretical dipole moment μ_{theo} as seen in 15th column of Table 9.1 are estimated from available bond angles and bond moments of flexible polar groups by simple vector addition method considering the molecules to be planer sketched in Figure 9.4. Estimated and reported μ_j [15] are placed in 14th column of Table 9.1 in order to compare them with μ_{theo} to throw much light on their structural conformation. It is evident that μ_j 's are lower than μ_{theo} 's probably due to the fact that under rf electric field, the inter ionic forces between the molecules forming polymeric clusters hinder the rotation of dipoles which may be the main factor to yield lower μ_j 's.

Table 9.1 : Estimated values of rf conductivity (σ'_{ij}), reciprocal of solution viscosity ($1/\eta_{ij}$) and relaxation times (τ_j) at different concentrations, intercepts and slopes of linear curves of Figure 9.1, number density of free ions (n), relaxation time at infinite dilution, coefficients α, β, γ of fitted curves of Figure 9.3, estimated and theoretical dipole moments along with reported n, τ_j and μ_j of some normal alcohols in benzene at 25°C under 1MHz electric field.

Systems with serial number and molecular weight (M_j)	Weight fraction w_j of solute	Rf conductivity $\sigma'_j \times 10^{-3}$ in $\Omega^{-1}cm^{-1}$	Reciprocal of solution viscosity $(1/\eta_j) \times 10^{-3}$ in $poise^{-1}$	Intercept (A) & slope(B) of σ'_j vs. $1/\eta_j$ fitted curves of Figure 9.1		Number density $n \times 10^{13}$ of free ions	Estimated relaxation time $\tau_j \times 10^{11}$ see at different w_j	Reported relaxation time $\tau'_j \times 10^{11}$ at different w_j	Estimated relaxation time $\tau_j \times 10^{11}$ at $w_j = 0$	Coefficients α, β, γ of the equation $\sigma_j \times 10^{-3} = \alpha + \beta w_j + \gamma w_j^2$ of Figure 9.3			Estimated dipole moment in Debye	Theoretical dipole moment μ_{theo} in Debye			
				Intercept (A)	Slope (B)					α	β	γ					
(I) Methanol in benzene $M_j=32gm$	0.0452	0.417	0.1644	- 14.1709	88.6940	18.3029	104.80	—	112.59	0.3106	2.2847	- 1.9667	0.44	1.76			
	0.1836	0.642	0.1670				68.07	175.50									
	0.3103	0.830	0.1690				4.3024*	52.65							91.97	135.96*	0.23*
	0.3749	0.900	0.1700				48.56	74.86									
	0.5501	0.981	0.1708				44.55	50.95									
	0.7101	0.935	0.1704				46.74	40.48									
(II) Ethanol in benzene $M_j=46gm.$	0.0906	0.337	0.1540	2.4491	- 13.7305	3.1618	27.89	282.68	32.56	0.1034	2.5549	- 1.9735	1.03	1.67			
	0.1551	0.439	0.1462				21.41	78.94									
	0.3302	0.704	0.1271				13.35	27.99									
	0.4729	0.880	0.1135				10.68	18.99							157.41*	0.34*	
	0.5737	0.948	0.1099				9.92	15.71									
	0.7012	0.911	0.1120				10.32	13.10									
0.8898	0.812	0.1195	11.58	10.79													

Contd..

Systems with serial number and molecular weight (M_j)	Weight fraction w_j of solute	Rf conductivity $\sigma'_j \times 10^{-3}$ in $\Omega^{-1}\text{cm}^{-1}$	Reciprocal of solution viscosity $(1/\eta_j) \times 10^{-3}$ in poise $^{-1}$	Intercept (A) & slope (B) of σ'_j vs. $1/\eta_j$ fitted curves of Figure 9.1		Number density $n \times 10^{-13}$ of free ions	Estimated relaxation time $\tau_j \times 10^{11}$ see at different w_j	Reported relaxation time $\tau'_j \times 10^{11}$ at different w_j	Estimated relaxation time $\tau_j \times 10^{11}$ at $w_j = 0$	Coefficients α, β, γ of the equation $\sigma_j \times 10^{-3} = \alpha + \beta w_j + \gamma w_j^2$ of Figure 9.3			Estimated dipole moment in Debye	Theoretical dipole moment μ_{theo} in Debye
				Intercept (A)	Slope (B)					α	β	γ		
(III) n-propanol in benzene $M_j=60\text{gm}$	0.0925	0.103	0.1374				46.44	—						
	0.1865	0.105	0.1173				45.56	—						
	0.2821	0.171	0.1022				27.97	—						
	0.3794	0.238	0.0903	0.7599	-5.2762	1.3342	20.09	—	62.86	0.0023	0.7229	-0.1489	0.45	1.58
	0.4783	0.313	0.0807				15.28	—						
	0.5790	0.399	0.0729				11.99	—						
	0.6815	0.476	0.0663				10.05	—						
0.7857	0.434	0.0608				11.02	—							
(IV) 2-butanol in benzene $M_j=74\text{gm}$	0.0927	0.295	0.1261				9.64	—						
	0.1870	0.360	0.1016				7.90	—						
	0.2827	0.402	0.0849				7.08	—						
	0.3801	0.436	0.0727				6.52	—						
	0.4791	0.460	0.0635	0.6189	-2.5520	0.6913	6.18	—	10.17	0.2585	0.5648	-0.3125	1.10	1.12
	0.5798	0.478	0.0562				5.95	—						
	0.6822	0.486	0.0503				5.85	—						
	0.7863	0.504	0.0455				5.64	—						
0.8922	0.514	0.0415				5.53	—							
1.0000	0.518	0.0380				5.49	—							

* A. K. Ghosh and S. N. Sen J Phys. Soc. Japan 48 (1980) 1219.

Table 9.2 : Temperature variation of rf conductivity $\sigma'_{jk} \times 10^{-3} \Omega^{-1} \text{ cm}^{-1}$ at different mole fractions, intercept and slope of $\ln \sigma'_{jk}(T)$ against $1/T$ curves and activation energies ΔE_{jk} in eV of binary polar mixture of different alcohols of different concentration.

Systems with Serial No.	Mole fraction of j th solute (x _j)	Temperature in Kelvin (T)	Rf-conductivity of jk polar mixtures $\sigma'_{jk} \times 10^{-3}$ in $\Omega^{-1} \text{ cm}^{-1}$	Intercept & slope of $\ln \sigma'_{jk}(T)$ vs $1/T$ fitted equation		Activation energy ΔE_{jk} of jk polar mixtures in eV
				Intercept (c)	Slope $m \times 10^{-3}$	
I (a)	2-butanol* (5.2c.c) + n propanol (20.8c.c) 0.1690	298	0.4310	16.69	- 3.168	0.27
		308	0.6058			
		313	0.7016			
		318	0.8266			
		323	0.9923			
I (b)	2 butanol* (12.5 c.c) + n propanol (12.5 c.c) 0.4486	298	0.2300	14.97	- 2.845	0.25
		308	0.3400			
		313	0.2933			
		318	0.4310			
		323	0.4999			
I (c)	2 butanol* (19.2 c.c) + n propanol (4.8 c.c.) 0.7649	298	0.1290	17.81	- 3.925	0.34
		308	0.0950			
		313	0.2278			
		318	0.2627			
		323	0.2974			

* j th solute.

Systems with Serial No.	Mole fraction of j th solute (x _j)	Temperature in Kelvin (T)	Rf-conductivity of jk polar mixtures $\sigma'_{jk} \times 10^{-3}$ in $\Omega^{-1} \text{ cm}^{-1}$	Intercept & slope of $\ln \sigma'_{jk}(T)$ vs $1/T$ fitted equation		Activation energy ΔE_{jk} of jk polar mixtures in eV
				Intercept (c)	Slope $m \times 10^{-3}$	
II (a)	n propanol* (9.6 c.c.) + ethanol (14.4 c.c.) 0.3349	283	1.4875	59.67	- 14.815	1.28
		285	2.4981			
		287	2.9075			
		289	3.7521			
		291	7.3546			
II (b)	n propanol* (14.4 c.c.) + ethanol (14.4 c.c.) 0.4302	283	1.0800	66.93	- 16.941	1.46
		285	2.1800			
		287	2.6100			
		289	3.4193			
		291	6.7572			
II (c)	n propanol* (14.4 c.c.) + ethanol (9.6 c.c.) 0.5311	283	0.7089	77.19	- 19.93	1.72
		285	1.9160			
		287	2.3401			
		289	3.1408			
		291	6.2266			

* j th solute.

Systems with Serial No.	Mole fraction of j th solute (x _j)	Temperature in Kelvin (T)	Rf-conductivity of jk polar mixtures $\sigma'_{jk} \times 10^{-3}$ in $\Omega^{-1} \text{ cm}^{-1}$	Intercept & slope of $\ln \sigma'_{jk}(T)$ vs $1/T$ fitted equation		Activation energy ΔE_{jk} of jk polar mixtures in eV
				Intercept (c)	Slope $m \times 10^{-3}$	
III (a) 2-butanol* (9.6 c.c.) + ethanol (14.4 c.c.)	0.2905	283	1.5795	16.01	- 2.45	0.21
		285	1.6415			
		287	1.8147			
		289	1.8970			
		291	1.9779			
III (b) 2 butanol* (12 c.c.) + ethanol (12 c.c.)	0.3805	283	1.3350	13.82	- 1.87	0.16
		285	1.3900			
		287	1.5000			
		289	1.5250			
		291	1.6000			
III (c) 2 butanol* (14.4 c.c.) + ethanol (9.6 c.c.)	0.4795	283	1.1352	11.47	- 1.25	0.11
		285	1.1864			
		287	1.2508			
		289	1.2617			
		291	1.2813			

* j th solute.

Table 9.3 : Ion density 'n' from rf conductivity σ'_{jk} , relaxation time τ_{jk} , intercept & slope of $\ln \tau_{jk} T$ against $1/T$, enthalpy of activation ΔH_{τ} in K J mole⁻¹, entropy of activation ΔS_{τ} in J mole⁻¹ K⁻¹, free energy of activation ΔF_{τ} in K J mole⁻¹ at different temperatures.

Systems with serial Number	Mole fraction of jth solute x_j	Temp. in Kelvin (T)	Rf conductivity of jk polar mixtures $\sigma'_{jk} \times 10^{-3} \Omega^{-1} cm^{-1}$	Ion density $n \times 10^{-13}$ per c.c.	Relaxation time $\tau_{jk} \times 10^{11}$ in sec.	Intercept & slope of $\ln(\tau_{jk} T)$ vs $1/T$ fitted equation.		Enthalpy of activation ΔH_{τ} in KJ mole ⁻¹	Entropy of activation ΔS_{τ} in J mole ⁻¹ k ⁻¹	Free energy of activation ΔF_{τ} in KJ mole ⁻¹
						Intercept (C)	Slope $m \times 10^{-3}$			
I (a) 2-butanol* (5.2 c.c.) + n-propanol (20.8 c.c.)	0.1690	298	0.4310	6.9682	31.98	- 33.41	5.178	43.028	81.29	18.80
		308	0.6058	7.7167	24.38					
		313	0.7016	5.7003	15.30					
		318	0.8266	5.0327	11.29					
		323	0.9923	4.3949	8.08					
I (b) 2-butanol* (12.5 c.c.) + n-propanol (12.5 c.c.)	0.4486	298	0.2300	6.9682	59.93	- 31.68	4.850	40.299	66.91	20.36
		308	0.3400	7.7167	43.44					
		313	0.2933	5.7003	36.60					
		318	0.4310	5.0327	21.65					
		323	0.4999	4.3949	16.05					
I (c) 2-butanol* (19.2 c.c.) + n-propanol (4.8 c.c.)	0.7649	298	0.1290	6.9682	106.86	- 34.55	5.940	49.365	92.53	21.79
		308	0.0950	7.7167	155.47					
		313	0.2278	5.7003	47.13					
		318	0.2627	5.0327	35.52					
		323	0.2974	4.3949	26.97					
II (a) n-propanol* (9.6 c.c.) + ethanol (14.4 c.c.)	0.3349	283	1.4875	20.7080	25.34	- 60.99	12.531	104.132	307.22	17.19
		285	2.4981	15.0410	10.88					
		287	2.9075	14.6480	9.04					
		289	3.7521	14.9240	7.09					
		291	7.3546	28.6660	6.90					

* jth solute

Systems with serial Number	Mole fraction of jth solute x_j	Temp. in Kelvin (T)	Rf conductivity of jk polar mixtures $\sigma'_{jk} \times 10^{-3} \Omega^{-1} \text{cm}^{-1}$	Ion density $n \times 10^{-13}$ per c.c.	Relaxation time $\tau_{jk} \times 10^{11}$ in sec.	Intercept & slope of $\ln(\tau_{jk} T)$ vs $1/T$ fitted equation.		Enthalpy of activation ΔH in KJ mole ⁻¹	Entropy of activation ΔS in J mole ⁻¹ k ⁻¹	Free energy of activation ΔF in KJ mole ⁻¹
						Intercept (C)	Slope $m \times 10^{-3}$			
II (b) n-propanol* (14.4 c.c.) + ethanol (14.4 c.c.)	0.4302	283	1.0800	20.7080	34.90				368.57	17.94
		285	2.1800	15.0410	12.47				374.03	15.65
		287	2.6100	14.6480	10.07	-68.44	14.711	122.246	374.90	14.65
		289	3.4193	14.9240	7.78				371.90	14.77
		291	6.7572	28.6660	7.51				369.23	14.80
II (c) n-propanol* (14.4 c.c.) + ethanol (9.6 c.c.)	0.5311	283	0.7089	20.7080	53.17				455.06	18.93
		285	1.9160	15.0410	14.19				462.32	15.95
		287	2.3401	14.6480	11.23	-78.95	17.775	147.714	460.59	15.52
		289	3.1408	14.9240	8.47				459.32	14.97
		291	6.2266	28.6660	8.15				456.07	15.00
III (a) 2-butanol* (9.6 c.c.) + ethanol (14.4 c.c.)	0.2905	283	1.5795	11.4337	15.08				-37.21	15.97
		285	1.6415	11.4018	14.37				-37.01	15.98
		287	1.8147	11.5411	13.06	-19.31	0.6542	5.44	-36.40	15.88
		289	1.8970	12.6766	13.63				-36.95	16.11
		291	1.9779	13.5238	13.85				-37.27	16.28
III (b) 2-butanol* (12 c.c.) + ethanol (12 c.c.)	0.3805	283	1.3350	11.4337	17.84				-55.96	16.36
		285	1.3900	11.4018	16.97				-55.62	16.47
		287	1.5000	11.5411	15.80	-17.26	0.0633	0.53	-55.09	16.34
		289	1.5250	12.6766	16.96				-55.75	16.64
		291	1.6000	13.5238	17.12				-55.90	16.79
III (c) 2-butanol* (14.4 c.c.) + ethanol (9.6 c.c.)	0.4795	283	1.1352	11.4337	20.98				-57.93	16.74
		285	1.1864	11.4018	19.88				-57.55	16.75
		287	1.2508	11.5411	18.95	-16.82	0.0421	0.35	-57.22	16.77
		289	1.2617	12.6766	19.49				-57.22	16.97
		291	1.2813	13.5238	20.38				-57.96	17.21

* jth solute

Table 9.4 : Relaxation time $\tau_k \times 10^{11}$ sec and $\tau_j \times 10^{11}$ sec of k th and j-th solute at different experimental temperature from $\tau_{jk} - x_j$ fitted equation of Figure 9.7 at $x_j=0$ and $x_j=1$, relaxation time for the mixture as obtained from mixing rule $\tau_{jk} = x_j\tau_j + x_k\tau_k$ and from equation (9.8).

Systems with Sl. Nos.	Temperature in Kelvin	Value of Relaxation Time in Sec. obtained from ($\tau_{jk} - x_j$) curves for $x_j = 0$ for $x_j = 1$ $\tau_k \times 10^{11}$ $\tau_j \times 10^{11}$		Mole fraction		Relaxation time obtained from mixing rule $\tau_{jk} = x_j\tau_j + x_k\tau_k$	Experimental Relaxation Time in Sec. $\tau_{jk} \times 10^{11}$ (from equation (9.8))
		x_j	x_k				
(I) 2 butanol + n-propanol	Ia 298	21.244	152.272	0.1690	0.8310	43.39	31.98
				0.4486	0.5514	80.02	59.93
				0.7649	0.2351	121.47	106.86
	Ib 308	49.264	300.977	0.1690*	0.8310	91.80	24.38
				0.4486	0.5514	162.18	43.44
				0.7649	0.2351	241.80	155.47
	Ic 313	-3.030	45.628	0.1690	0.8310	5.244	15.30
				0.4486	0.5514	18.80	36.60
				0.7649	0.2351	34.19	47.13
	Id 318	5.893	47.308	0.1690	0.8310	12.89	11.29
				0.4486	0.5514	24.47	21.65
				0.7649	0.2351	37.57	35.52
	Ie 323	3.747	34.694	0.1690	0.8310	8.98	8.08
				0.4486	0.5514	17.63	16.05
				0.7649	0.2351	27.42	26.97

Systems with Sl. Nos.	Temperature in Kelvin	Value of Relaxation Time in Sec. obtained from ($\tau_{jk} - x_j$) curves for $x_j = 0$ for $x_j = 1$ $\tau_k \times 10^{11}$ $\tau_j \times 10^{11}$		Mole fraction x_j x_k		Relaxation time obtained from mixing rule $\tau_{jk} = x_j \tau_j + x_k \tau_k$	Experimental Relaxation Time in Sec. $\tau_{jk} \times 10^{11}$ (from equation (9.8))
(II) n propanol + ethanol	IIa 283	51.272	248.436	0.3349	0.6651	117.30	25.34
				0.4302	0.5698	136.09	34.90
				0.5311	0.4689	155.98	53.17
	IIb 285	5.558	22.676	0.3349	0.6651	11.29	10.88
				0.4302	0.5698	12.92	12.47
				0.5311	0.4689	14.65	14.19
	IIc 287	5.927	17.56	0.3349	0.6651	9.82	9.04
				0.4302	0.5698	10.93	10.07
				0.5311	0.4689	12.10	11.23
	IIId 289	4.369	11.127	0.3349	0.6651	6.63	7.09
				0.4302	0.5698	7.28	7.78
				0.5311	0.4689	7.96	8.47
	IIe 291	5.368	11.699	0.3349	0.6651	7.49	6.90
				0.4302	0.5698	8.09	7.51
				0.5311	0.4689	8.73	8.15

Systems with Sl. Nos.	Temperature in Kelvin	Value of Relaxation Time in Sec. obtained from ($\tau_{jk} - x_j$) curves for $x_j = 0$ for $x_j = 1$ $\tau_k \times 10^{11}$ $\tau_j \times 10^{11}$		Mole fraction x_j x_k		Relaxation time obtained from mixing rule $\tau_{jk} = x_j \tau_j + x_k \tau_k$	Experimental Relaxation Time in Sec. $\tau_{jk} \times 10^{11}$ (from equation (9.8))
(III) 2 butanol + ethanol	IIIa 283	6.781	39.269	0.2905	0.7095	16.22	15.08
				0.3805	0.6195	19.14	17.84
				0.4795	0.5205	22.36	20.98
	IIIb 285	6.268	36.028	0.2905	0.7095	14.91	14.37
				0.3805	0.6195	17.59	16.97
				0.4795	0.5205	20.54	19.88
	IIIc 287	5.015	37.845	0.2905	0.7095	14.55	13.06
				0.3805	0.6195	17.51	15.80
				0.4795	0.5205	20.76	18.95
	IIId 289	-3.85	13.168	0.2905	0.7095	1.09	13.63
				0.3805	0.6195	2.62	16.96
				0.4795	0.5205	4.31	19.49
	IIIe 291	1.286	31.666	0.2905	0.7095	10.11	13.85
				0.3805	0.6195	12.84	17.12
				0.4795	0.5205	15.85	20.38

B. Dielectric relaxation behaviour of polar-polar mixture

The conduction that arises due to mobility of free ions and electrons in an insulating dielectric liquid under rf electric field is an additional term to the dielectric loss ϵ'' . It is expressed as real part of rf conductivity [10] σ'_{jk} . σ'_{jk} of polar-polar mixtures (jk) of 2-butanol + n-propanol, n-propanol + ethanol and 2-butanol + ethanol, at various concentration of the j-th component are entered in the 4th column of Table 9.2 in the temperature range 283 K to 323K under 1MHz electric field. The temperature dependence of $\sigma'_{jk}(T)$ may be expressed as [19,20].

$$\sigma'_{jk}(T) = \sigma'_1 \exp. \left(-\frac{\Delta E_{jk}}{k_B T} \right) \quad (9.7)$$

which is obviously a straight line between $\ln \sigma'_{jk}(T)$ and $1/T$ as seen graphically in Figure 9.5, satisfied by experimental points for different systems under investigation. Here σ'_1 is the pre exponential factor which is assumed to be constant for a given liquid mixture. The slope of the linear variation as placed in the 6th column of Table 9.2 is however, utilised to get activation energy ΔE_{jk} of the polar-polar mixtures as seen in the 7th column at different mole fractions x_j 's. Again, it is seen that the extrapolation of linear curves of $\ln \sigma'_{jk}(T)$ vs. $1/T$ in K^{-1} of Figure 9.5 for each system have a tendency to meet in the neighbourhood of certain values of $1/T$ depending upon the nature of the mixtures. Non linear variation of ΔE_{jk} with x_j 's as seen in Figure 9.8 arises probably due to polar-polar molecular associations.

The dielectric relaxation time τ_{jk} of polar-polar mixtures at different experimental temperatures were also estimated from [10]:

$$\tau_{jk} = \frac{2na^2e^2}{3\sigma'_{jk} k_B T} \quad (9.8)$$

where a is the radius of rotating unit which is of the order of 10^{-8} cm, n is the

free ion density calculated from the slope of linear fitted curve of σ'_{jk} against $1/\eta_{jk}$. Estimated n 's are entered in the 5th column of Table 9.3 at different temperatures for all the systems. The estimated τ_{jk} for different mole fraction x_j 's of the j th solute and at different temperatures are placed in the 6th column of Table 9.3. In order to get an idea about the variation of τ_{jk} with x_j , plots are drawn for three binary polar-polar mixtures keeping temperature constant as shown in Figure 9.7 with the following fitted equations.

(I) For 2-butanol + n-propanol. mixture

$$\text{Ia. } \tau_{jk} \times 10^{11} = 21.244 + 49.794 x_j + 81.234 x_j^2 \text{ at } 298 \text{ K}$$

$$\text{Ib. } \tau_{jk} \times 10^{11} = 49.264 - 228.255 x_j + 479.968 x_j^2 \text{ at } 308 \text{ K}$$

$$\text{Ic. } \tau_{jk} \times 10^{11} = -3.030 + 120.628 x_j - 71.970 x_j^2 \text{ at } 313 \text{ K}$$

$$\text{Id. } \tau_{jk} \times 10^{11} = 5.893 + 30.007 x_j + 11.408 x_j^2 \text{ at } 318 \text{ K}$$

$$\text{Ie. } \tau_{jk} \times 10^{11} = 3.747 + 24.560 x_j + 6.387 x_j^2 \text{ at } 323 \text{ K}$$

(II) For n-propanol + ethanol mixture

$$\text{IIa. } \tau_{jk} \times 10^{11} = 51.272 - 215.683 x_j + 412.847 x_j^2 \text{ at } 283 \text{ K}$$

$$\text{IIb. } \tau_{jk} \times 10^{11} = 5.558 + 15.273 x_j + 1.845 x_j^2 \text{ at } 285 \text{ K}$$

$$\text{IIc. } \tau_{jk} \times 10^{11} = 5.927 + 8.119 x_j + 3.514 x_j^2 \text{ at } 287 \text{ K}$$

$$\text{IId. } \tau_{jk} \times 10^{11} = 4.369 + 8.813 x_j - 2.055 x_j^2 \text{ at } 289 \text{ K}$$

$$\text{IIe. } \tau_{jk} \times 10^{11} = 4.714 + 6.627 x_j - 0.296 x_j^2 \text{ at } 291 \text{ K}$$

(III) For 2-butanol + ethanol mixture

$$\text{IIIa. } \tau_{jk} \times 10^{11} = 6.781 + 26.962 x_j + 5.526 x_j^2 \text{ at } 283 \text{ K}$$

$$\text{IIIb. } \tau_{jk} \times 10^{11} = 6.268 + 27.124 x_j + 2.636 x_j^2 \text{ at } 285 \text{ K}$$

$$\text{IIIc. } \tau_{jk} \times 10^{11} = 5.015 + 25.590 x_j + 7.240 x_j^2 \text{ at } 287 \text{ K}$$

$$\text{IIId. } \tau_{jk} \times 10^{11} = -3.850 + 77.389 x_j - 60.821 x_j^2 \text{ at } 289 \text{ K}$$

$$\text{IIIe. } \tau_{jk} \times 10^{11} = 1.286 + 48.518 x_j - 18.138 x_j^2 \text{ at } 291 \text{ K}$$

The results shows that τ_{jk} increases monotonically with x_j at all temperature [21]. It is found that τ_{jk} 's are of constant values when $x_j < 0.325$ for all the systems. The individual τ_j or τ_k of the j th and k th solute for all the systems at different temperatures can be obtained by graphical extrapolation of $(\tau_{jk} - x_j)$ curves at $x_j = 0$ and $x_j = 1.0$ and the values so obtained are entered in the 3rd and the 4th columns of Table 9.4. τ_k 's were found to be negative for the systems 2-butanol + n-propanol and 2-butanol+ethanol at 313k and 289k respectively. τ_{jk} as seen in 7th column of Table 9.4 calculated from mixing rule were also compared with the experimental relaxation time entered in 8th column as estimated from Eq. (9.8). Experimental τ_{jk} 's are found to well agree with the values calculated from simple mixing rule for 2 butanol + n propanol (System I) for $x_j = 0.1690, 0.4486$ and 0.7649 at 318K and 323K respectively; for n-propanol + ethanol(system II) of $x_j = 0.3349, 0.4302$ and 0.5311 at temperatures 285 K, 287 K, 289 K, 291 K and for system 2 butanol + ethanol (System III) of $x_j = 0.2905, 0.3805,$ and 0.4795 at temperatures 283K, 285K and 287 K which indicates that the systems obey colligative property at all these experimental temperatures. Experimental relaxation times are found to differ highly for system I at 298K, 308K and 313K, for system II at 283 K and for system III at temperature 289 K and 291 K which shows that the systems do not obey colligative property at those temperature. Comparatively high values of τ_{jk} arises probably due to formation of polymeric clusters by molecular association whereas low values of τ_{jk} indicate low association between j th and k th polar unit. This sort of behaviour indicates that intermolecular interaction among the binary polar species in higher concentration occurs to increase τ_{jk} . This behaviour also invites further study to see the value of τ_{jk} for 1:1 binary mixture.

It is seen in Table 9.3 that τ_{jk} of the liquid mixtures decreases with temperature although a small discrepancy has been observed for 2 butanol + ethanol mixture probably due to experimental uncertainty in the rf conductivity measurement. Thermodynamic energy parameters ($\Delta F_\tau, \Delta H_\tau, \Delta S_\tau$) for dielectric

relaxation process are related to relaxation time and temperature T K by [12]

$$\tau = \frac{h}{k_B T} \exp (\Delta F_\tau / RT) \quad (9.9)$$

$$\Delta F_\tau = \Delta H_\tau - T \Delta S_\tau \quad (9.10)$$

$$\text{or } \ln (\tau T) = \ln A' + \left(\frac{\Delta H_\tau}{R} \right) \cdot \frac{1}{T} \quad (9.11)$$

The slopes of the linear equation between $\ln (\tau_{jk} T)$ and $1/T$ shown graphically in Figure 9.6 satisfied by experimental points are used to estimate $\Delta H_{\tau_{jk}}$. Estimated $\Delta H_{\tau_{jk}}$, $\Delta S_{\tau_{jk}}$ and $\Delta F_{\tau_{jk}}$ are placed in 9th, 10th and 11th column of Table 9.3. The concentration x_j dependence of $\Delta H_{\tau_{jk}}$ are shown in Figure 9.8. It indicates that addition of j th component of the mixture causes a decrease in the height of the activation energy barrier encountered by the rotating unit [16]. The reverse is true for 2 butanol + ethanol (system III) mixture. It is also confirmed by the exactly similar variation of ΔE_{jk} with x_j . The high positive value of $\Delta S_{\tau_{jk}}$ for system I and II suggests that configuration involved in dipolar association has an activated state which is less ordered than the normal state.

9.4. Conclusions

Relaxation parameters n , τ_j , μ_j for polar solutes in nonpolar solvent C_6H_6 at $25^\circ C$ and ΔE_{jk} , τ_{jk} , thermodynamic energy parameters ΔH_τ , ΔS_τ , ΔF_τ for polar polar binary mixtures at different experimental temperatures under rf electric field of 1 MHz frequency shows close agreement with the values estimated by previous workers [15,16]. This fact establishes the validity of the theoretical formulation so far achieved within the frame work of Debye-Smyth [11,22] model. The linear curves of Figures 9.1, 9.5 and 9.6, satisfied by experimental points, suggests that polar-nonpolar and polar-polar mixtures of alcohols strictly obey equations (9.1), (9.7) and (9.11). Thermodynamic energy parameters $\Delta H_{\tau_{jk}}$,

$\Delta S_{\tau_{jk}}$ and $\Delta F_{\tau_{jk}}$ provides the important information regarding the stability or unstability of the systems undergoing relaxation behaviours. The non linear variation of the relaxation parameters τ_j , τ_{jk} , ΔE_{jk} and $\Delta H_{\tau_{jk}}$ with concentration as seen in Figures 9.2, 9.7 and 9.8 shows the probable existence of polar-nonpolar and polar-polar molecular associations. Study of theoretical dipole moments μ_{theo} gives a deep insight into the distribution of bond moments of different — CH_3 — and — OH groups of the molecules under rf electric field. This study invariably gives valuable information of the structural aspects of the alcohols under investigation.

References

- [1] S N Sen and R Ghosh, *J Phys. Soc. Japan* **33** (1972) 838.
- [2] A K Ghosh and S N Sen. *Indian J Pure & Appl. Phys* **18** (1989) 588.
- [3] R Ghosh and Ira Chaudhury. *Indian J Pure & Appl. Phys.* **20** (1982) 717.
- [4] R Ghosh and A K Chatterjee *Indian J Pure & Appl. Phys* **29** (1991) 650.
- [5] F J Murphy and S O Morgan, *Bell. Syst. Tech J* **18** (1939) 502.
- [6] H V Loheneysen and H Nageral *J Phys D : Appl. Phys* **4** (1971) 1718.
- [7] P Standhammer and W F Seyer, *J Appl. Phys* **28** (1957) 405.
- [8] I. Adamczewski and B Jachym, *Acta Phys. Polon (Poland)* **34** (1968) 1015.
- [9] S N Sen and R Ghosh. *Indian J Pure & Appl. Phys.* **10** (1972) 701.
- [10] R Ghosh and Ira Chaudhury. *Indian J Pure & Appl. Phys.* **18** (1980) 669.
- [11] C P Smyth, '*Dielectric Behaviour and Structure* (New York : McGraw Hill 1955).

- [12] H Eyring, S Glasstone and K J Laidler *'The Theory of Rate Process'* (New York : McGraw Hill) 1941.
- [13] S K Sit, N Ghosh, U Saha and S Acharyya *Indian J Phys* **71B** (1997) 533.
- [14] N Ghosh, R C Basak, S K Sit and S Acharyya *J Mol. Liquids.* **85** (2000) 375.
- [15] A K Ghosh and S N Sen, *J Phys. Soc. Japan* **48** (1980) 1219.
- [16] U Saha and R Ghosh *J Phys. D : Appl. Phys* **32** (1999) 820.
- [17] N Ghosh, A Karmakar, S K Sit and S Acharyya *Indian J Pure & Appl. Phys.* **38** (2000) 574.
- [18] *'Hand Book of Chemistry and Physics'* CRC Press, 58 Edition 1977-78.
- [19] R Ghosh and Ira Chaudhury, *Pramana J Phys.* **16** (1981) 319.
- [20] Manisha Gupta and J P Shukla *Indian J Pure & Appl. Phys.* **31** (1993) 786.
- [21] U Saha, *Ph.D Dissertation* (N.B.U) India 1993.
- [22] P Debye *'Polar Molecules'* (Chemical Catalogue)1929.

CHAPTER -10

RELAXATION PHENOMENA OF APROTIC POLAR LIQUID MOLECULES UNDER A KILOHERTZ ELECTRIC FIELD

RELAXATION PHENOMENA OF APROTIC POLAR LIQUID MOLECULES UNDER A KILOHERTZ ELECTRIC FIELD

10.1. Introduction

The experimental determination of radio frequency (rf) conductivity σ'_{ij} of polar-nonpolar liquid mixture is of special interest as it provides an information of various relaxation parameters like free ion density 'n', relaxation time τ_j , dipole moment μ_j and thermodynamic energy parameters including the activation energy ΔE_j of a polar solute. These measured parameters helps one to ascertain shape, size and structure of a polar molecule, in addition to solute-solvent (monomer) and solute-solute (dimer) molecular associations.

According to Murphy and Morgan [1] displacement current is the only factor to yield electrical conduction in a pure polar dielectric liquid. But for almost all the insulating dipolar liquids electrical conduction arises due to the combined effects of displacement current and ohmic current arising out of actual charge transfer [2-4]. In microwave (mw) electric field the mobility of free charge carriers ceases, but in rf electric field below 20 MHz the dielectric loss ϵ'' for the free charge transfer in dielectropolar liquids gives a significant contribution to rf conductivity σ'_{ij} . Cosmic rays, natural radioactivity, thermal dissociation etc. are supposed to be the main sources of the presence of free ions and electrons in liquid dielectrics. But no concrete conclusion have not yet been reached so far regarding such ion formation in a dipolar liquid.

Sen and Ghosh [5,6] took into account of such type of electrical conduction in rf electric field and showed that σ'_{ij} is a linear function of reciprocal of solution viscosity η_{ij} . We applied this formulation on two aprotic polar liquids : N, N dimethyl formamide (DMF) and dimethyl sulphoxide (DMSO) in both C_6H_6 and CCl_4 in the temperature range of 30°C to 60°C under 500KHz electric field. The slope of the linear relation between σ'_{ij} and $1/\eta_{ij}$

(Eq 10.1) as shown by the straight line curves of Figure 10.1 is used to estimate free ion density 'n' in terms of molecular radius 'a' obtained from gas kinetic theory. The estimated slope and hence n are placed in Table 10.2. Einstein-Stokes relation [7] is further employed to get τ_j at different concentrations w_j 's and at different temperatures as seen in Table 10.1. τ_j at infinite dilution is, however, obtained from $\tau_j - w_j$ fitted equations to get dipole moment under rf electric field at different temperatures by Smyths' relation [8] in terms of linear coefficient β of $\sigma'_{ij} - w_j$ fitted curves, in order to place them in Table 10.2. The theoretical dipole moment μ_{theo} obtained from available bond angles and bond moments of flexible polar groups attached to parent molecule as seen elsewhere [9] are then compared with these measured μ_j 's. The comparison, however, showed that the structural conformations of such liquids are correct. The variation of μ_j with temperature in $^{\circ}\text{C}$ as seen in Figure 10.2 further provides a valuable information regarding molecular association.

It is evident from Figure 10.3 that $\ln \sigma'_{ij}$ displays a linear relationship with $1/T$, where T is temperature in Kelvin. The slope of the least squares fitted straight line curves of Figure 10.3 has conveniently been used to estimate the semiconduction activation energy ΔE_j at different concentrations. The measured ΔE_j are entered in the 7th column of Table 10.3. The variation of τ_j with temperature prompted us to obtain thermodynamic energy parameters ΔH_{τ} , ΔS_{τ} and ΔF_{τ} from Eyrings rate theory [10]. The dimensionless parameter $\gamma (= \Delta H_{\tau} / \Delta H_{\eta})$ was estimated from linear relationship between $\ln \tau_j T$ and $\ln \eta$. γ was used to get the energy of activation ΔH_{η} due to viscous flow. It finally indicates the solvent environment around solute molecules [11]. The estimated energy parameters along with γ are entered in Table 10.4 to conclude about either stability or unstability [9, 11, 12] of polar-nonpolar liquid mixtures under rf electric field. The Debye and Kalman factors $\tau_j T / \eta$ and $\tau_j T / \eta^{\gamma}$, as seen in the 8th and 9th columns of Table 10.3 were computed to suggest that measured data of such aprotic polar liquids obey Debye relaxation behaviour.

The purpose of the present paper is to test the adequacy or otherwise of the theoretical formulation so far derived [5,6] and the modified formulations presented in the chapter 2 of this thesis. A clear concept about structural conformation and molecular associations of the said polar liquids could, however, be attained. In addition this paper also provides an experimental verification of the results obtained in case of DMF + DMSO in C_6H_6 under GHz electric field of chapter 3 of this thesis. Although dielectric relaxation studies have been carried out on several dipolar liquids under rf electric field by many workers [13-16], but rf σ'_{ij} measurement for such aprotic polar liquids have not yet been made.

10.2. Rf Experimental details

The block diagram of the experimental set up and the theoretical formulation to estimate σ'_{ij} and other physical parameters of a polar-nonpolar (ij) liquid mixture have been presented in detail in chapter 2. A cylindrical glass tube made up of pyrex glass of diameter 2 cm is used as a dielectric cell which is fitted with a pair of stainless steel electrodes of diameter 1.5 cm and separated by 1cm. The Analar grade N, N dimethyl formamide (DMF), dimethyl sulphoxide (DMSO), benzene C_6H_6 , carbon tetrachloride CCl_4 were obtained from E. Merck (Germany). They were distilled in vacuum and kept in a dessicator before use. The viscosity of the experimental liquids were measured at different temperatures by an Ostwald viscometer with highly pure distilled water as a reference fluid. The temperature of all the experiments were controlled by a highly sensitive thermostat whose accuracy was $\pm 0.5^\circ C$. Other physical constants like density ρ , static relative permittivity ϵ_0 and refractive index n_D were carefully checked in agreement with literature values [17].

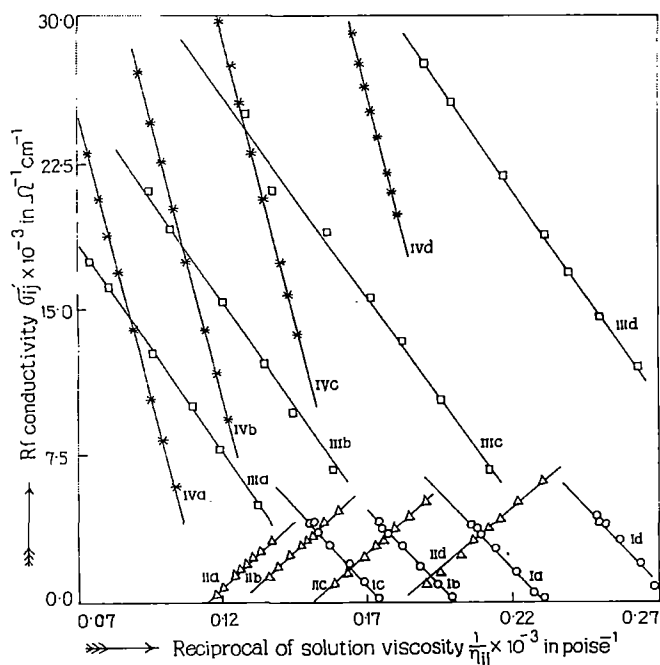


Figure 10.1: Linear variation of rf conductivity σ'_{ij} against reciprocal of solution viscosity $1/\eta_{ij}$ of aprotic polar liquids in benzene and carbon tetrachloride at different experimental temperatures under 500 KHz electric field.

(I) DMF in C_6H_6 (—○—), (Ia) at 30°C, (Ib) at 40°C, (Ic) at 50°C, (Id) at 60°C.

(II) DMF in CCl_4 (—△—), (IIa) at 30°C, (IIb) at 40°C, (IIc) at 50°C, (IIId) at 60°C.

(III) DMSO in C_6H_6 (—□—), (IIIa) at 30°C, (IIIb) at 40°C, (IIIc) at 50°C, (IIId) at 60°C.

(IV) DMSO in CCl_4 (—*—), (IVa) at 30°C, (IVb) at 40°C, (IVc) at 50°C, (IVd) at 60°C.

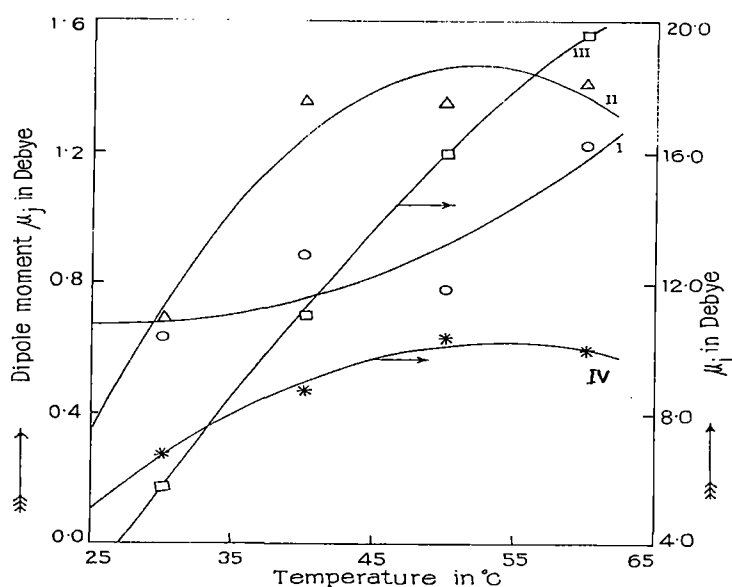


Figure 10.2: Plot of dipole moment μ_j in Debye against temperature in °C of aprotic polar liquids in C_6H_6 and CCl_4 under 500KHz electric field.

(I) DMF in C_6H_6 (—○—), (II) DMF in CCl_4 (—△—), (III) DMSO in C_6H_6 (—□—),

(IV) DMSO in CCl_4 (—*—)

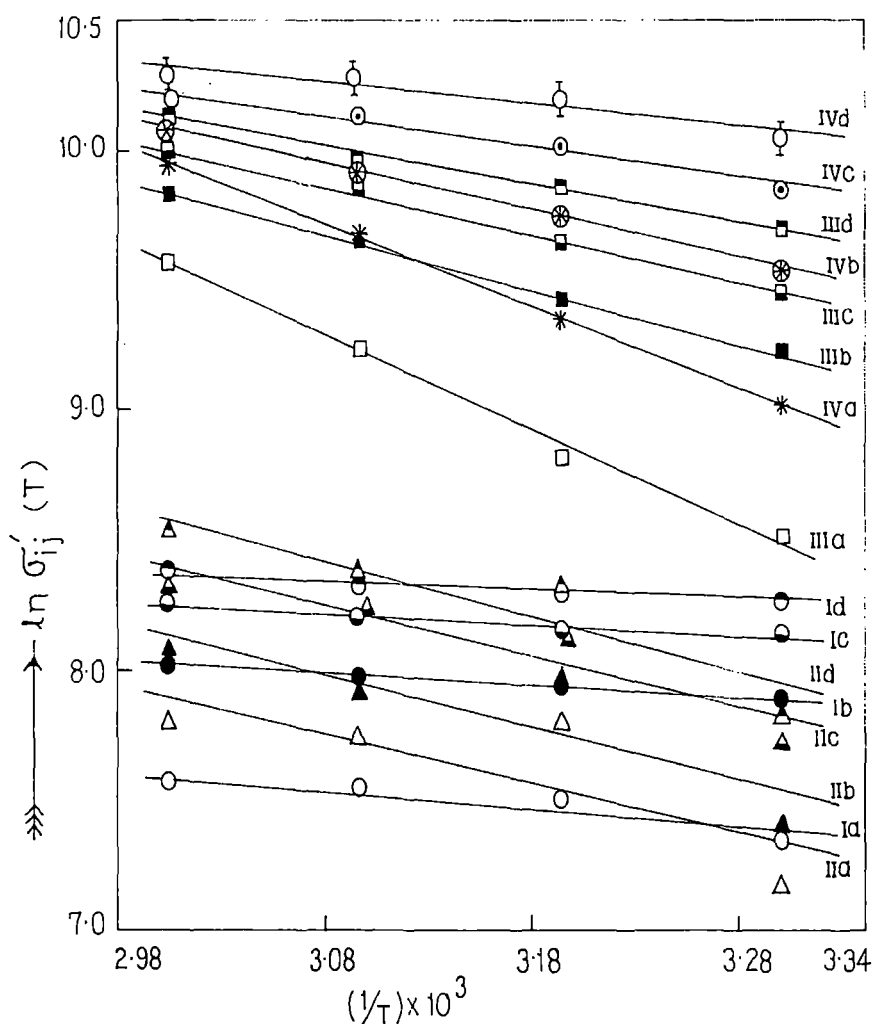


Figure 10.3: Plot of $\ln \sigma'_{ij} (T)$ against $1/T$ of aprotic polar liquids in C_6H_6 and CCl_4 at different weight fractions (w_j) of solute under 500 KHz electric field.

(I) DMF in C_6H_6

(Ia) $w_j = 0.3520$ (—○—), (Ib) $w_j = 0.5218$ (—●—)

(Ic) $w_j = 0.6563$ (—●—), (Id) $w_j = 0.7500$ (—●—)

(II) DMF in CCl_4

(IIa) $w_j = 0.3772$ (—△—), (IIb) $w_j = 0.4760$ (—▲—),

(IIc) $w_j = 0.6248$ (—▲—), (IId) $w_j = 0.7316$ (—▲—)

(III) DMSO in C_6H_6

(IIIa) $w_j = 0.1124$ (—□—), (IIIb) $w_j = 0.2021$ (—■—),

(IIIc) $w_j = 0.2754$ (—■—), (IIId) $w_j = 0.3878$ (—■—),

(IV) DMSO in CCl_4

(IVa) $w_j = 0.0954$ (—*—), (IVb) $w_j = 0.1742$ (—⊗—),

(IVc) $w_j = 0.2601$ (—○—), (IVd) $w_j = 0.3453$ (—○—)

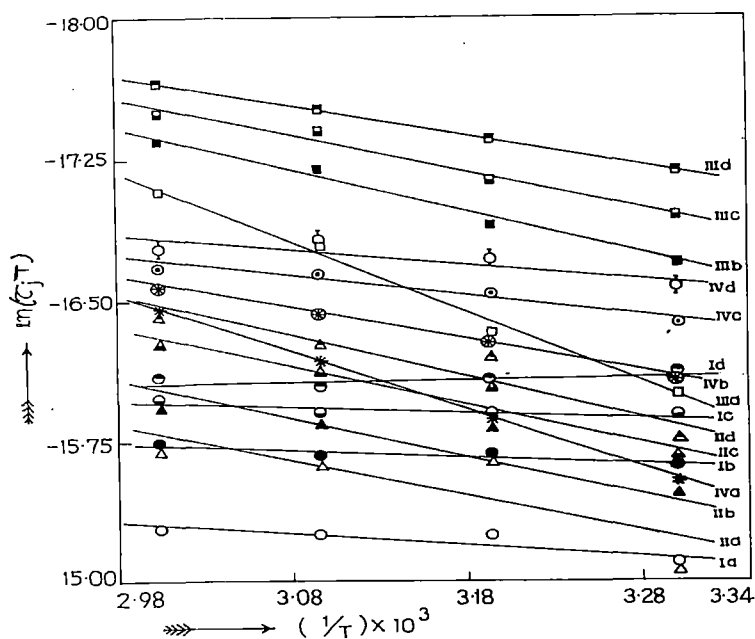


Figure 10.4: Plot of $\ln(\tau_j T)$ against $1/T$ of aprotic polar liquids in C_6H_6 and CCl_4 at different weight fractions (w_j) of solute under 500 KHz electric field.

(I) DMF in C_6H_6

(Ia) $w_j = 0.3520$ (—○—), (Ib) $w_j = 0.5218$ (—●—) (Ic) $w_j = 0.6563$ (—◐—), (Id) $w_j = 0.7500$ (—◑—)

(II) DMF in CCl_4

(IIa) $w_j = 0.3772$ (—△—), (IIb) $w_j = 0.4760$ (—▲—), (IIc) $w_j = 0.6248$ (—◀—), (IId) $w_j = 0.7316$ (—◁—)

(III) DMSO in C_6H_6

(IIIa) $w_j = 0.1124$ (—□—), (IIIb) $w_j = 0.2021$ (—■—), (IIIc) $w_j = 0.2754$ (—◓—), (IIId) $w_j = 0.3878$ (—◔—),

(IV) DMSO in CCl_4 (IVa) $w_j = 0.0954$ (—*—), (IVb) $w_j = 0.1742$ (—⊗—), (IVc) $w_j = 0.2601$ (—⊙—),

(IVd) $w_j = 0.3453$ (—⊚—)

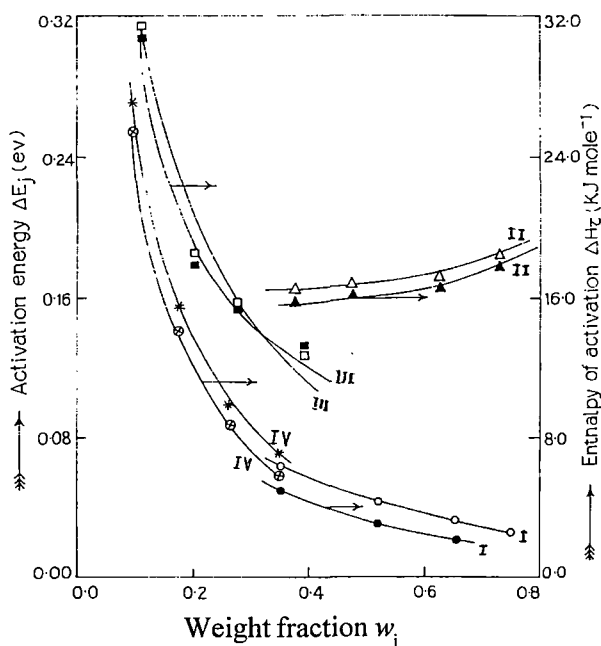


Figure 10.5: Variation of semiconduction activation energy (ΔE_j) and enthalpy of activation due to dielectric relaxation (ΔH_τ) against weight fraction of solute w_j of aprotic polar liquids in benzene and carbon tetrachloride under 500 KHz electric field.

$\Delta E_j - w_j$ variation

(I) DMF in C_6H_6 (—○—),

(II) DMF in CCl_4 (—△—),

(III) DMSO in C_6H_6 (—□—),

(IV) DMSO in CCl_4 (—*—),

$\Delta H_\tau - w_j$ variation

(I) DMF in C_6H_6 (—●—),

(II) DMF in CCl_4 (—▲—),

(III) DMSO in C_6H_6 (—■—),

(IV) DMSO in CCl_4 (—⊗—)

10.3. Results and Discussion

The linear dependence of σ'_{ij} on $1/\eta_{ij}$ is obtained graphically by applying regression analysis on the data. As a result curves of Figure 10.1 with proper symbols of the experimental data are worked out. It is seen in Figure 10.1 that σ'_{ij} shows excellent linear dependence on $1/\eta_{ij}$ for both DMF and DMSO in C_6H_6 and CCl_4 at different experimental temperatures. The slope of the linear equation:

$$\sigma'_{ij} = \left(\frac{\epsilon_{oij} - \epsilon_{\infty ij}}{4\pi} \right) \omega^2 \tau + \left(\frac{ne^2}{6\pi a} \right) \frac{1}{\eta_{ij}} \quad (10.1)$$

of Figure 10.1 are placed in the 4th column of Table 10.2. They were used to obtain 'n' with the knowledge of molecular radius 'a' of the gas kinetic values. The estimated 'n' are shown in the 5th column of Table 10.2 at different experimental temperatures for each system.

Figure 10.1 shows that σ'_{ij} decreases with rise of $1/\eta_{ij}$ having negative slope for all the systems at all temperatures except for DMF in CCl_4 which showed positive slope. This happens probably due to the fact that DMF is less viscous [12,14] than CCl_4 .

The values of 'n' then used to obtain τ_j at different concentrations and temperatures from [7] :

$$\tau_j = \frac{2na^2e^2}{3\sigma'_{ij}k_B T} \quad (10.2)$$

τ_j 's at different temperatures and concentrations w_j 's are entered in Table 10.1. A simple extrapolation technique is, however employed on the measured τ_j 's of Eq (10.2) and the following polynomial equations between τ_j and w_j were worked out. It is evident when $w_j = 0$ one gets τ_j at infinite dilution.

I. DMF in C₆H₆

$$\tau_j \times 10^{10} = 119.48 - 430.95 w_j + 377.71 w_j^2 \text{ at } 30^\circ\text{C}$$

$$\tau_j \times 10^{10} = 74.52 - 275.72 w_j + 248.67 w_j^2 \text{ at } 40^\circ\text{C}$$

$$\tau_j \times 10^{10} = 90.67 - 347.83 w_j + 318.50 w_j^2 \text{ at } 50^\circ\text{C}$$

$$\tau_j \times 10^{10} = 44.08 - 144.54 w_j + 122.71 w_j^2 \text{ at } 60^\circ\text{C}$$

II. DMF in CCl₄

$$\tau_j \times 10^{10} = 37.59 - 97.26 w_j + 69.63 w_j^2 \text{ at } 30^\circ\text{C}$$

$$\tau_j \times 10^{10} = 10.62 - 18.56 w_j + 10.89 w_j^2 \text{ at } 40^\circ\text{C}$$

$$\tau_j \times 10^{10} = 15.92 - 36.78 w_j + 24.89 w_j^2 \text{ at } 50^\circ\text{C}$$

$$\tau_j \times 10^{10} = 15.10 - 35.87 w_j + 24.28 w_j^2 \text{ at } 60^\circ\text{C}$$

III. DMSO in C₆H₆

$$\tau_j \times 10^{10} = 22.68 - 153.63 w_j + 242.52 w_j^2 \text{ at } 30^\circ\text{C}$$

$$\tau_j \times 10^{10} = 5.99 - 31.36 w_j + 45.44 w_j^2 \text{ at } 40^\circ\text{C}$$

$$\tau_j \times 10^{10} = 2.94 - 12.86 w_{jj} + 17.82 w_j^2 \text{ at } 50^\circ\text{C}$$

$$\tau_j \times 10^{10} = 1.62 - 4.78 w_{jj} + 5.68 w_j^2 \text{ at } 60^\circ\text{C}$$

IV. DMSO in CCl₄

$$\tau_j \times 10^{10} = 11.37 - 63.92 w_j + 100.12 w_j^2 \text{ at } 30^\circ\text{C}$$

$$\tau_j \times 10^{10} = 6.68 - 31.12 w_j + 49.81 w_j^2 \text{ at } 40^\circ\text{C}$$

$$\tau_j \times 10^{10} = 4.21 - 14.93 w_j + 21.20 w_j^2 \text{ at } 50^\circ\text{C}$$

$$\tau_j \times 10^{10} = 2.49 - 4.16 w_j + 4.32 w_j^2 \text{ at } 60^\circ\text{C}.$$

τ_j 's so estimated are presented in the 6th column of Table 10.2. They are supposed to be free from polar-polar interaction [11,18].

According to Smyth [8] real part σ'_{ij} of complex hf σ_{ij}^* is written as

$$\sigma'_{ij} = \frac{4\pi^2 f^2 N \tau_j d_i \mu_j^2 (\epsilon_{oij} + 2) (n_{Di}^2 + 2)}{27 M_j k_B T} w_j \quad (10.3)$$

Eq. (10.3) on differentiation w.r. to w_j and at $w_j \rightarrow 0$ yields

$$\mu_j = \left[\frac{27 M_j k_B T \beta}{4\pi^2 f^2 N \tau_j d_i (\epsilon_{oi} + 2) (n_{Di}^2 + 2)} \right]^{1/2} \quad (10.4)$$

where

- M_j = molecular weight of solute
- f = frequency of applied electric field
- k_B = Boltzmann constant = 1.38×10^{-16} erg mole⁻¹ K⁻¹
- N = Avogadro's number = 6.023×10^{23}
- d_i = density of solvent
- ϵ_{oi} = static relative permittivity of solvent
- n_{Di} = refractive index of solvent.

The linear coefficient $\beta = (d\sigma'_{ij}/dw_j)_{w_j \rightarrow 0}$ of $\sigma'_{ij} - w_j$ curves of $\sigma'_{ij} = \alpha + \beta w_j + \gamma w_j^2$ as seen in the 8th column of Table 10.2 was used to estimate μ_j from Eq. (10.4).

The μ_{theo} 's obtained by vector addition of group moments [9] of planer molecules are placed in 11th column together with the estimated μ_j 's in the 10th column of Table 10.2. It is seen that for DMF μ_j 's $< \mu_{\text{theo}}$'s probably due to

the fact that under rf electric field the greater inter ionic forces hinders the dipolar rotation [12] for lower μ_j 's. But for DMSO inter ionic forces are weaker giving μ_j 's $>$ μ_{theo} 's.

μ_j 's are plotted against $t^\circ\text{C}$ in Figure 10.2. The variation of μ_j 's with respect to t in $^\circ\text{C}$ are, however, represented by the following equations :

I. DMF in C_6H_6

$$\mu_j = 0.988 - 0.0239 t + 0.0005t^2$$

II. DMF in CCl_4

$$\mu_j = -2.622 + 0.1566t - 0.0015t^2$$

III. DMSO in C_6H_6

$$\mu_j = -15.5795 + 0.8343t - 0.0041t^2$$

IV. DMSO in CCl_4

$$\mu_j = -7.773 + 0.6649t - 0.0061t^2$$

Curve I for DMF in C_6H_6 showed monotonic increase of μ_j with $t^\circ\text{C}$ for its increasing molecular asymmetry attained at higher temperature. Other curves on the other hand are convex in nature showing $\mu_j = 0$ both at lower and higher temperatures due to symmetry [11] gained by the molecules. The above nature of $\mu_j - t$ curves are interpreted by the rupture of monomer and dimer formations due to stretching of bond moments of flexible polar groups attached to molecules by thermal agitation.

The ionic conduction due to mobility of free charges in an insulating dipolar liquid occurs for ϵ'' . Rf $\sigma'_{ij}(T)$ can be expressed by [19,20]:

$$\sigma'_{ij}(T) = \sigma'_i \exp(-\Delta E_j/k_B T) \quad (10.5)$$

$$\ln \sigma'_{ij}(T) = \ln \sigma'_i - \left(\frac{\Delta E_j}{k_B}\right) \cdot \frac{1}{T} \quad (10.6)$$

Table 10.1 : Radio frequency conductivity (σ'_{ij}), reciprocal of solution viscosity ($1/\eta_{ij}$) and estimated relaxation times (τ_j) of aprotic polar liquids in benzene (C_6H_6) and carbontetrachloride (CCl_4) at different concentrations (w_j) and temperatures under 500 KHz electric field.

Systems with serial number & Molecular weight (M_j)	Weight fraction w_j of solute	Rf conductivity $\sigma'_{ij} \times 10^{-3}$ in $\Omega^{-1} \text{ cm}^{-1}$				Reciprocal of solution viscosity $1/\eta_{ij} \times 10^{-3}$ in poise ⁻¹				Estimated Relaxation times $\tau_j \times 10^{10}$ sec.			
		30°C	40°C	50°C	60°C	30°C	40°C	50°C	60°C	30°C	40°C	50°C	60°C
(I) DMF in C_6H_6 $M_j=73$ gm.	0.0984	0.1620	0.2400	0.2000	0.4069	0.2315	0.1985	0.1739	0.2743	88.18	57.05	69.67	32.86
	0.2143	0.4064	0.9000	0.9800	0.8159	0.2265	0.1936	0.1690	0.2694	35.15	15.21	14.22	16.39
	0.3520	1.5400	1.8000	1.9000	1.9203	0.2208	0.1881	0.1635	0.2637	9.28	7.61	7.33	6.96
	0.5218	2.6400	2.8000	2.9000	3.0761	0.2141	0.1818	0.1572	0.2570	5.41	4.89	4.80	4.35
	0.6563	3.4600	3.4200	3.6200	3.8630	0.2091	0.1770	0.1526	0.2520	4.13	4.00	3.85	3.46
	0.7105	3.7600	3.8200	4.0000	4.1221	0.2071	0.1752	0.1508	0.2500	3.79	3.58	3.48	3.24
	0.7500	3.9800	3.0400	4.1200	4.3547	0.2058	0.1739	0.1495	0.2486	3.34	3.39	3.38	3.07
(II) DMF in CCl_4 $M_j=73$ gm.	0.1315	0.4186	1.4100	0.9446	0.9600	0.1176	0.1360	0.1593	0.1901	28.98	8.56	12.25	11.47
	0.2324	0.8094	1.8000	1.4626	1.5000	0.1199	0.1389	0.1630	0.1948	14.99	6.71	7.91	7.34
	0.3772	1.2900	2.4300	2.3100	2.4300	0.1236	0.1433	0.1685	0.2019	9.40	4.97	5.01	4.53
	0.4760	1.6500	2.8500	2.8500	3.1200	0.1261	0.1465	0.1725	0.2071	7.35	4.24	4.06	3.53
	0.5478	1.9500	3.1800	3.2100	3.6900	0.1281	0.1489	0.1755	0.2111	6.22	3.80	3.61	2.98
	0.6248	2.2500	3.5100	3.7500	4.2300	0.1303	0.1551	0.1789	0.2155	5.39	3.44	3.09	2.60
	0.7316	2.5766	4.0539	4.3296	5.0659	0.1334	0.1554	0.1838	0.2219	4.71	2.98	2.67	2.16
0.8583	3.0927	4.7072	5.1506	6.1785	0.1373	0.1602	0.1899	0.2301	3.92	2.57	2.25	1.78	

Contd...

Systems with serial number & Molecular weight (M_j)	Weight fraction w_i of solute	Rf conductivity $\sigma'_{ij} \times 10^{-3}$ in $\Omega^{-1} \text{ cm}^{-1}$				Reciprocal of solution viscosity $1/\eta_{ij} \times 10^{-3}$ in poise^{-1}				Estimated Relaxation times $\tau_j \times 10^{10}$ sec.			
		30°C	40°C	50°C	60°C	30°C	40°C	50°C	60°C	30°C	40°C	50°C	60°C
(III) DMSO in C_6H_6 $M_j = 78\text{gm}$	0.0596	1.0020	3.7500	6.8003	12.0001	0.1505	0.1763	0.2122	0.2626	18.39	4.71	2.40	1.39
	0.1124	5.0064	6.7504	10.4001	14.600	0.1322	0.1579	0.1949	0.2498	3.67	2.62	1.57	1.14
	0.1597	7.8003	9.7506	13.4020	16.9021	0.1192	0.1444	0.1815	0.2394	2.36	1.81	1.22	0.98
	0.2021	10.1095	12.1500	15.6000	18.9000	0.1096	0.1342	0.1711	0.2307	1.82	1.46	1.05	0.88
	0.2754	12.8031	15.4500	19.0002	21.8906	0.0962	0.1195	0.1555	0.2172	1.44	1.14	0.86	0.76
	0.3878	16.2001	19.2001	21.2000	25.6003	0.0810	0.1023	0.1366	0.1992	1.14	0.92	0.77	0.65
	0.4516	17.6000	21.1500	25.1000	27.6000	0.0743	0.0946	0.1277	0.1903	1.05	0.84	0.65	0.60
(IV) DMSO in CCl_4 $M_j = 78\text{gm}$	0.0657	5.8200	9.3001	13.6000	19.9600	0.1035	0.1219	0.1463	0.1802	8.28	5.07	3.40	2.25
	0.0954	8.2436	11.7000	15.7010	21.1601	0.0991	0.1177	0.1427	0.1784	5.84	4.03	2.94	2.13
	0.1233	10.3700	13.9021	17.5012	22.1200	0.0954	0.1140	0.1395	0.1768	4.65	3.40	2.64	2.03
	0.1742	13.9450	17.5003	20.7004	23.8003	0.0892	0.1078	0.1341	0.1739	3.46	2.70	2.23	1.89
	0.2195	17.0024	20.2011	23.1509	25.2400	0.0843	0.1029	0.1296	0.1714	2.83	2.34	1.99	1.78
	0.2601	18.9500	22.6000	25.6000	26.4407	0.0804	0.0988	0.1258	0.1692	2.54	2.09	1.80	1.70
	0.2967	20.7720	24.6004	27.5005	27.6400	0.0772	0.0954	0.1225	0.1673	2.32	1.92	1.68	1.68
	0.3453	23.0450	27.1000	29.8000	29.0800	0.0732	0.0912	0.1185	0.1648	2.09	1.74	1.55	1.55

Table 10.2 : Intercept and slope of fitted linear curves of Figure 10.1, number density of free ions (n), relaxation time τ_j at $w_j=0$, coefficients α , β , γ , of $\sigma_{ij} - w_j$ fitted equations together with estimated and theoretical dipole moments μ 's of aprotic polar liquids in C_6H_6 and CCl_4 at different temperatures under 500 KHz electric field.

Systems with serial number and molecular weight	Temperature in $^{\circ}C$	Intercept & slope of $\sigma_{ij} \times 10^{-3}$ vs. $(1/\eta_{ij}) \times 10^{-3}$ fitted curves of Fig.10.1		Number density of free ions $n \times 10^{-14}$ per c.c.	Relaxation time $\tau_j \times 10^{10}$ sec. at $w_j = 0$	Coefficients α, β, γ , of the fitted equation $\sigma'_{ij} = \alpha + \beta w_j + \gamma w_j^2$			Estimated dipole moment μ_j in Debye	Theoretical dipole moment in μ_{theo} in Debye
		intercept (A)	slope $B \times 10^{-3}$			$\alpha \times 10^{-3}$	$\beta \times 10^{-3}$	$\gamma \times 10^{-3}$		
(i) DMF in benzene $M_j = 73$ gm	30	35.9890	-0.1558	3.9774	119.48	-0.5278	5.4103	0.9083	0.63	3.82
	40	30.8290	-0.1543	3.9384	74.52	-0.4028	6.4416	-0.7380	0.89	
	50	28.3775	-0.1620	4.1355	90.67	-0.5082	7.3149	-1.4802	0.78	
	60	44.2220	-0.1603	4.0917	44.08	-0.3509	6.4678	-0.1793	1.22	
(ii) DMF in carbon tetrachloride $M_j = 73$ gm	30	-15.0763	0.1323	3.3772	37.59	-0.0043	3.5322	0.1259	0.69	3.82
	40	-17.0963	0.1361	3.4734	10.62	0.9225	3.5938	0.9405	1.35	
	50	-20.4090	0.1346	3.4350	15.92	0.2598	5.0935	0.6902	135	
	60	-24.1995	0.1320	3.3692	15.10	0.2471	4.9702	2.2676	1.41	
(iii) DMSO in benzene $M_j = 78$ gm.	30	33.8410	-0.2180	5.4128	22.68	-3.2997	80.9619	-77.7434	5.80	4.55
	40	41.3407	-0.2165	5.3747	5.99	-0.5318	73.3962	-56.7150	11.01	
	50	50.6499	-0.2061	5.1153	2.94	2.9616	72.5886	-56.3693	16.01	
	60	68.8253	-0.2166	5.3779	1.62	8.6837	57.0748	-33.9152	19.57	
(iv) DMSO in carbon tetrachloride $M_j = 78$ gm.	30	64.9110	-0.5719	14.1790	11.37	-0.0014	94.2025	-80.0827	6.72	4.55
	40	79.7491	-0.5779	14.3473	6.68	3.8179	88.6445	-62.0821	8.74	
	50	98.9472	-0.5836	14.4872	4.21	8.9490	74.0356	-39.3454	10.34	
	60	125.6921	-0.5862	14.5513	2.49	17.6255	37.6434	-13.2139	9.90	

Table 10.3 : Intercepts and slopes of $\ln \sigma'_{ij}(T) - 1/T$ fitted linear curves of Figure 10.3, activation energies (ΔE_j), Debye and Kalman factors of dipolar aprotic polar liquids in benzene under 500 KHz electric field at different concentrations.

Systems with serial number	Weight fraction of solute (w_j)	Temperature in Kelvin (T)	R.f. conductivity $\sigma'_{ij} \times 10^{-3}$ in $\Omega^{-1} \text{ cm}^{-1}$	Intercept & slope of $\ln \sigma'_{ij}(T)$ vs. $1/T$ fitted equation		Activation energy ΔE_j of solute in eV	Debye factor $(\tau_j T/\eta) \times 10^6$	Kalman factor $(\tau_j T/\eta^2) \times 10^8$
				Intercept (C)	Slope $m \times 10^{-3}$			
(I) DMF in benzene (C_6H_6)	0.3520	303	1.5400	9.7897	-0.7316	0.0631	50.1003	197.9447
		313	1.8000				48.3058	176.0617
		323	1.9000				55.8926	185.3988
		333	1.9203				64.6249	193.2359
	0.5218	303	2.6400	9.5227	-0.4979	0.0429	29.2252	56.8518
		313	2.8000				31.0523	54.7470
		323	2.9000				36.6164	57.5515
		333	3.0761				40.3453	55.8763
	0.6563	303	3.4600	9.3993	-0.3857	0.0332	22.3010	31.1670
		313	3.4200				25.4261	31.9406
		323	3.6200				29.3373	32.5396
		333	3.8630				32.1222	31.0626
0.7500	303	3.9800	9.2352	-0.2894	0.0249	18.0558	8.6841	
	313	3.0400				21.5207	9.0592	
	323	4.1200				25.7778	9.2876	
	333	4.3547				28.5025	8.6517	

Contd...

Systems with serial number	Weight fraction of solute (w_j)	Temperature in Kelvin (T)	R.f. conductivity $\sigma'_{ij} \times 10^{-3}$ in $\Omega^{-1} \text{ cm}^{-1}$	Intercept & slope of $\ln \sigma'_{ij} (T)$ vs. $1/T$ fitted equation		Activation energy ΔE_j of solute in eV	Debye factor $(\tau_j T / \eta) \times 10^6$	Kalman factor $(\tau_j T / \eta^2) \times 10^8$
				Intercept (C)	Slope $m \times 10^{-3}$			
(II) DMF in Carbon tetrachloride (CCl_4)	0.3772	303	1.2900	13.6151	-0.1903	0.1640	32.6481	6570.2763
		313	2.4300				20.5863	4231.8254
		323	2.3100				25.0546	5270.9757
		333	2.4300				27.8021	6001.1005
	0.4760	303	1.6500	14.0027	-0.1957	0.1687	25.5234	6394.3492
		313	2.8500				17.5502	4521.1758
		323	2.8500				20.3088	5393.3334
		333	3.1200				21.6539	5947.7380
	0.6248	303	2.2500	14.4049	-0.1998	0.1722	18.7181	5633.8900
		313	3.5100				14.2531	4435.9495
		323	3.7500				15.4329	4981.5824
		333	4.2300				15.9720	5368.4248
0.7316	303	2.5766	15.0325	-0.2149	0.1852	16.3432	7798.8866	
	313	4.0539				12.3394	6174.4696	
	323	4.3296				13.3675	7044.0690	
	333	5.0959				13.2599	7399.9411	

Contd...

Systems with serial number	Weight fraction of solute (w_j)	Temperature in Kelvin (T)	R.f. conductivity $\sigma'_{ij} \times 10^{-3}$ in $\Omega^{-1} \text{cm}^{-1}$	Intercept & slope of $\ln \sigma'_{ij}(T)$ vs. $1/T$ fitted equation		Activation energy ΔE_j of solute in eV	Debye factor $(\tau_j T / \eta) \times 10^6$	Kalman factor $(\tau_j T / \eta^2) \times 10^8$
				Intercept (C)	Slope $m \times 10^{-3}$			
(III) DMSO in benzene (C_6H_6)	0.1124	303	5.0064	20.6028	- 3.6714	0.3164	19.8435	High value
		313	6.7504				16.6311	
		323	10.4001				11.9514	
		333	14.6000				10.5713	
	0.2021	303	10.1094	16.2840	- 2.1445	0.1848	9.8245	10827.861
		313	12.1500				9.2395	10811.879
		323	15.6000				7.9651	9996.0246
		333	18.9000				9.1674	11071.221
	0.2754	303	12.8031	15.5148	- 1.8350	0.1582	7.7613	2846.2402
		313	15.4500				7.2646	2751.927
		323	19.0002				6.5397	2572.9898
		333	21.8906				7.0537	2893.4703
0.3878	303	16.2001	14.5869	- 1.4833	0.1278	6.1302	706.9345	
	313	19.2001				5.8485	676.8529	
	323	21.2000				5.8614	681.1654	
	333	25.6003				6.0235	703.2188	

Contd...

Systems with serial number	Weight fraction of solute (w_j)	Temperature in Kelvin (T)	R.f. conductivity $\sigma'_{ij} \times 10^{-3}$ in $\Omega^{-1} \text{ cm}^{-1}$	Intercept & slope of $\ln \sigma'_{ij} (T)$ vs. $1/T$ fitted equation		Activation energy ΔE_j of solute in eV	Debye factor $(\tau_j T / \eta) \times 10^6$	Kalman factor $(\tau_j T / \eta^2) \times 10^8$
				Intercept (C)	Slope $m \times 10^{-3}$			
(IV) DMSO in carbon tetrachloride (CCl_4)	0.0954	303	8.2436	19.4253	- 3.1519	0.2717	20.2944	153513.13
		313	11.7000				16.7094	144138.42
		323	15.7010				14.7127	146457.23
		333	21.1601				13.0451	152207.23
	0.1742	303	13.9450	15.4750	- 1.7923	0.1545	11.9961	1581.5724
		313	17.5003				11.1713	1485.2464
		323	20.7004				11.1571	1496.9883
		333	23.8003				11.5970	1571.8872
	0.2601	303	18.9500	13.6495	- 1.1426	0.0985	8.8296	164.3480
		313	22.6000				8.6488	152.9701
		323	25.6000				9.0217	150.9270
		333	26.4407				10.4434	164.2551
0.3453	303	23.0450	12.7630	- 0.8114	0.0699	7.2602	49.7633	
	313	27.1000				7.2156	45.5918	
	323	29.8000				7.7514	44.8189	
	333	29.0800				9.4924	49.7418	

Contd...

Table 10.4 : Intercepts and slopes of fitted linear curves of Figure 10.4, enthalpy of activation ΔH_τ in KJ mole⁻¹, entropy of activation ΔS_τ in J mole⁻¹ K⁻¹, free energy of activation ΔF_τ in KJ mole⁻¹, dimensionless parameter $\gamma (= \Delta H_\tau / \Delta H_\eta)$ of dipolar aprotic polar liquids in benzene and carbon tetrachloride at different concentrations under 500 KHz electric field.

Systems with Serial number	Weight fraction of solute (w_j)	Temperature in Kelvin	Intercept & slope of $\ln(\tau_j T)$ vs. $(1/T)$ fitted equation		Enthalpy of activation ΔH_τ in KJ mole ⁻¹	$\gamma = \frac{\Delta H_\tau}{\Delta H_\eta}$	Enthalpy of activation ΔH_η in KJ mole ⁻¹ due to viscous flow	Entropy of activation ΔS_τ in J mole ⁻¹ K ⁻¹	Free energy of activation ΔF_τ in KJ mole ⁻¹
			Intercept (c)	Slope $m \times 10^{-3}$					
(I) DMF in benzene (C ₆ H ₆)	0.3520	303						- 55.7322	21.8449
		313	- 17.0955	0.5966	4.9580	0.3766	13.1326	- 54.8765	22.1343
		323						- 55.3234	22.8274
		333						- 55.6075	23.4753
	0.5218	303						- 57.6571	20.4877
		313	- 16.8291	0.3631	3.0176	0.2399	12.5785	- 57.4038	20.9850
		323						- 57.8162	21.6922
		333						- 57.5194	22.1716
	0.6563	303						- 58.4739	19.8068*
		313	- 16.7073	0.2514	2.0892	0.1761	11.8637	- 58.7086	20.4650
		323						- 58.8485	21.0973
		333						- 58.4131	21.5408
	0.7500	303						- 65.4166	19.2752
		313	- 15.8656	0.0066	- 0.5460	- 0.0297	18.3540	- 65.7424	20.0314
		323						- 65.9326	20.7502
		333						- 65.3336	21.2101

Contd...

Systems with Serial number	Weight fraction of solute (w_j)	Temperature in Kelvin	Intercept & slope of $\ln(\tau_j T)$ vs. $(1/T)$ fitted equation		Enthalpy of activation ΔH_τ in KJ mole ⁻¹	$\gamma = \frac{\Delta H_\tau}{\Delta H_\eta}$	Enthalpy of activation ΔH_η in KJ mole ⁻¹ due to viscous flow	Entropy of activation ΔS_τ in J mole ⁻¹ K ⁻¹	Free energy of activation ΔF_τ in KJ mole ⁻¹
			Intercept (c)	Slope $m \times 10^{-3}$					
(II) DMF in Carbon tetrachloride CCl_4	0.3772	303						-19.5998	21.8790
		313						-16.2519	21.0271
		323	-21.5622	1.9182	15.9403	1.1475	13.8912	-18.1566	21.8049
		333						-19.0568	22.2862
	0.4760	303						-16.0755	21.2593
		313	-21.9484	1.9721	16.3884	1.1937	13.7290	-13.4947	20.6122
		323						-15.0245	21.2413
		333						-15.6347	21.5947
	0.6248	303						-12.3714	20.4784
		313	-22.3520	2.0132	16.7299	1.2324	13.5750	-10.6743	20.0710
		323						-11.6856	20.5044
		333						-12.0799	20.7525
	0.7316	303						-7.1320	20.1368
		313	-22.9765	2.1631	17.9758	1.3296	13.5197	-5.4958	19.6960
		323						-6.6344	20.1187
		333						-6.7921	20.2376

Contd...

Systems with Serial number	Weight fraction of solute (w_1)	Temperature in Kelvin	Intercept & slope of $\ln(\tau_1 T)$ vs. $(1/T)$ fitted equation		Enthalpy of activation ΔH_τ in KJ mole ⁻¹	$\gamma = \frac{\Delta H_\tau}{\Delta H_\eta}$	Enthalpy of activation ΔH_η in KJ mole ⁻¹ due to viscous flow	Entropy of activation ΔS_τ in J mole ⁻¹ K ⁻¹	Free energy of activation ΔF_τ in KJ mole ⁻¹
			Intercept (c)	Slope $m \times 10^{-3}$					
		303						38.2853	19.5129
		313						37.5476	19.3609
	0.1124	323	- 28.3417	3.7441	31.1133	2.4796	12.5477	38.4717	18.6869
		333						37.9820	18.4653
	0.2021	303						1.2812	17.7428
		313	- 23.9116	2.1818	18.1310	1.4630	12.3932	0.9551	17.8321
		323						1.6509	17.5978
		333						1.1399	17.7514
(III) DMSO in benzene (C_6H_6)	0.2754	303						- 4.3130	17.1493
		313	- 23.2495	1.9064	15.8424	1.2507	12.6665	- 4.3584	17.2066
		323						- 3.7961	17.0685
		333						- 4.5145	17.3457
	0.3878	303						- 11.9094	16.5553
		313	- 22.3323	1.5579	12.9467	1.0275	12.6007	- 11.8082	16.6427
		323						- 11.8513	16.7747
		333						- 11.8985	16.9089

Contd...

Systems with Serial number	Weight fraction of solute (w_j)	Temperature in Kelvin	Intercept & slope of $\ln(\tau_j T)$ vs. $(1/T)$ fitted equation		Enthalpy of activation ΔH_τ in KJ mole ⁻¹	$\gamma = \frac{\Delta H_\tau}{\Delta H_\eta}$	Enthalpy of activation ΔH_η in KJ mole ⁻¹ due to viscous flow	Entropy of activation ΔS_τ in J mole ⁻¹ K ⁻¹	Free energy of activation ΔF_τ in KJ mole ⁻¹
			Intercept (c)	Slope $m \times 10^{-3}$					
		303						15.7630	20.6820
	0.0954	313	-25.6616	3.0636	25.4582	1.9124	13.3122	15.8904	20.4845
		323						15.7341	20.7361
		333						15.8134	20.1924
		303						-17.1520	19.3582
	0.1742	313	-21.7120	1.7041	14.1611	1.0583	13.3810	-16.8568	19.4373
		323						-16.9425	19.6335
		333						-17.1341	19.8667
(IV) DMSO in Carbon tetra chloride (CCl ₄)	0.2601	303						-32.4419	18.5865
		313	-19.8843	1.0537	8.7566	0.6454	13.5677	-31.9969	18.7716
		323						-31.9094	19.0633
		333						-32.4933	19.5769
		303						-39.8743	18.0937
	0.3453	313	-19.0003	0.7234	6.0118	0.4347	13.8298	-39.2606	18.3004
		323						-39.1461	18.6560
		333						-39.9423	19.3126

Which shows that $\ln \sigma'_{ij}(T)$ is a linear function of $1/T$ as displayed in Figure 10.3. The experimental points were found to satisfy the curves of Figure 10.3. σ'_1 is the pre exponential factor which is constant for a given liquid mixture. The slope of the linear curves of Figure 10.3 as seen in the 6th column of Table 10.3 were utilised to get ΔE_j in order to place them in the 7th column of the same table at different concentrations w_j 's. Non linear variation of ΔE_j with w_j of Figure 10.5 shows probable existence of solute-solvent molecular associations [12].

The rotating dipoles under rf electric field requires an free energy of activation ΔF_τ to overcome the potential energy barrier between two equilibrium positions. ΔF_τ is, however, related to measured τ_j by [10].

$$\tau_j = A/T \exp(\Delta F_\tau/RT) \quad (10.7)$$

$$\text{where} \quad \Delta F_\tau = \Delta H_\tau - T \Delta S_\tau \quad (10.8)$$

$$\text{or} \quad \ln(\tau_j T) = \ln A' + \left(\frac{\Delta H_\tau}{R}\right) \cdot \frac{1}{T} \quad (10.9)$$

$$\text{where} \quad A' = A e^{-\Delta S_\tau/R} \text{ and } A = h/k_B$$

The intercepts and slopes of Eq (10.9) as shown graphically in Figure 10.4 were accurately estimated in order to place them in 4th and 5th columns of Table 10.4. They were used to compute the thermodynamic energy parameters ΔH_τ , ΔS_τ and ΔF_τ (Table 10.4) due to dielectric relaxation. The variation of ΔH_τ with w_j of Figure 10.5 are non linear except for DMF in C_6H_6 probably due to solute-solvent molecular associations [12]. The 9th column of Table 10.4 showed positive ΔS_τ for DMSO in C_6H_6 (System III) at $w_j = 0.1124$ and 0.2021 and for DMSO in CCl_4 (System IV) at $w_j = 0.0954$. This fact suggests that configuration involved in dipolar association has an activated state which is less ordered than the normal state [12,16]. For system III and IV ΔS_τ passes over from positive to negative values beyond a certain concentration suggesting the fact that the systems becomes more ordered with increase in w_j 's due to solute-solvent and

solute-solute molecular association. This fact is also confirmed by the sharp fall of both ΔE_j and ΔH_τ with w_j as found in Figure 10.5. The enthalpy of activation due to viscous flow was obtained from the slope of the linear equation of $\ln(\tau_j T)$ against $\ln \eta$ at different concentrations for each system. It is evident from the 7th column of Table 10.4 that $\gamma = (\Delta H_\tau / \Delta H_\eta) > 0.50$ for all the systems except DMF in C_6H_6 showing solvent environment around the solute molecule. It behaves as solid phase rotators [11]. The non associative behaviour of DMF in C_6H_6 is, however, confirmed by the linear variation of both ΔE_j and ΔH_τ with w_j as displayed in Figure 10.5. The -Ve value of γ and ΔH_τ for DMF in C_6H_6 at $w_j = 0.7500$ arises probably due to experimental uncertainty. The Debye ($\tau_j T / \eta$) and Kalman ($\tau_j T / \eta^\gamma$) factors in 8th and 9th columns of Table 10.4 showed almost the constant value at all concentrations for each system. It, therefore, indicates the applicability of Debye — Smyth model [8,21] of dielectric relaxation for aprotic polar liquids too.

10.4. Conclusions

The accurate experimental τ_j 's can be estimated in the limit $w_j = 0$ from the best fitted polynomial equations between the measured τ 's at different weight fractions w_j 's. The reliability of the method is due to the fact that the polar-polar interactions [11,18] are fully avoided. The comparison of the measured rf μ_j 's in terms of τ_j 's at $w_j = 0$ with the theoretical μ_{theo} 's provides a better insight into the structural aspect of dipolar molecules. The role of short range ionic forces in the measured μ_j 's is thus be studied. The nature of μ_j -t curves as seen in the figures establishes the breaking of the dimer into monomer due to thermal agitation [11]. This type of molecular association is further confirmed by non-linear variation of relaxation parameter ΔE_j and ΔH_τ with w_j 's. The curves of $\sigma'_{ij} - 1/\eta_{ij}$, $\ln \sigma'_{ij}(T) - 1/T$ and $\ln(\tau_j T) - 1/T$ are, however, satisfied by the experimental points for aprotic polar liquids to show the validity of the formulation so far derived. The almost constant values of Debye and Kalman factor $\tau_j T / \eta$ and $\tau_j T / \eta^\gamma$ reflects the applicability of Debye-Smyth model of dielectric relaxation on such polar liquid molecules.

References

- [1] F.J. Murphy and S O Morgan, *Bell Syst. Tech J* **18** (1939) 502.
- [2] P Standhammer and W F Seyer, *J Appl. Phys.* **28** (1957) 405.
- [3] I. Adamczewski and B Jachym, *Acta Phys Polon (Poland)* **34** (1968) 1015.
- [4] H V Loheneysen and H Nageral, *J Phys D : Appl Phys (UK)* **4** (1971) 1718.
- [5] S N Sen and R Ghosh, *Indian J Pure & Appl. Phys.* **10** (1972) 701.
- [6] S N Sen and R Ghosh, *J Phys Soc Japan* **33** (1972) 838.
- [7] R Ghosh and Ira Chaudhury, *Indian J Pure & Appl. Phys.* **18** (1980) 669.
- [8] C P Smyth '*Dielectric Behaviour and Structure*' (New York : McGraw Hill 1955).
- [9] S K Sit, N Ghosh, U Saha and S Acharyya *Indian J Phys.* **71B** (1997) 533.
- [10] H Eyring, S Glasstone and K J Laidler '*The Theory of Rate Process*' (New York : McGraw Hill 1941).
- [11] N Ghosh, R C Basak, S K Sit and S Acharyya *J Mol Liquids (Germany)* **85** (2000) 375.
- [12] N Ghosh, R Ghosh, R C Basak, K. Dutta and S Acharyya *Pramana J. Phys.* Communicated 2002.
- [13] A K Ghosh and S N Sen, *J Phys Soc Japan* **48** (1980) 1219.
- [14] R Ghosh and Ira Chaudhury. *Indian J Pure & Appl Phys* **20** (1982) 717.
- [15] R Ghosh and A K Chatterjee. *Indian J Pure & Appl. Phys.* **29** (1991) 650.

- [16] U Saha and R Ghosh *J Phys D : Appl Phys (UK)* **32** (1999) 820.
- [17] '*Hand Book of Chemistry and Physics*' CRC Press 58th Edition 1977-78.
- [18] N Ghosh, A Karmakar, S K Sit and S Acharyya, *Indian J Pure & Appl. Phys* **38** (2000) 574.
- [19] R Ghosh and Ira Chaudhury, *Pramana J Phys* **18** (1981) 319.
- [20] Manisha Gupta and J P Shukla, *Indian J Pure & Appl Phys* **31** (1993) 786.
- [21] P Debye '*Polar Molecules*' (Chemical catalogue) 1929.

CHAPTER -11

SUMMARY AND CONCLUSION

SUMMARY AND CONCLUSION

The subject matter of the thesis has been divided in several chapters. All the chapters are highly informative to analyse the structural and associational aspects of dielectropolar liquid molecules under low and high frequency (hf) electric fields.

A brief account of the dielectric terminologies and parameters in terms of relative permittivities under the static and hf electric fields has been made in **Chapter 1**. Different fundamental theories of polar dielectrics in nonpolar solvents have been well discussed to represent the chronological development of the subject. The theoretical equations had been used by previous experimental workers in terms of various plots, tables and figures to estimate the relaxation parameters. Short review on the experimental and theoretical technique has been included in this chapter to support different molecular associations. At the end, an extensive reference list of dielectric theories on liquids and solids has been added to acquire an overall knowledge.

In **Chapter 2** the derived theoretical formulations to estimate relaxation time τ_j , static dipole moment μ_s , double relaxation times τ_1 & τ_2 and dipole moments μ_1 & μ_2 under low and hf electric field of GHz range is presented. The block diagram of the experimental set up of radio frequency (rf) oscillator along with the theoretical formulations to estimate rf conductivity σ'_{ij} , τ_j and μ_j under rf electric field has been shown and well discussed. The overall outcome of **Chapter 2** is aimed at to conclude on the structural and associational aspects of polar liquid molecules in nonpolar solvents, under hf electric fields. The theories are based on Debye, Smyth and Hill model of dielectropolar liquids. The concept of structural and associational aspects of polar molecules in nonpolar solvents are, however, achieved through the study of thermodynamic energy parameters like enthalpy of activation ΔH_τ , entropy of activation ΔS_τ and free energy of activation ΔF_τ of dielectric relaxation of a polar molecule. The variation of τ

and μ with temperature and concentration helps one to estimate energy parameters from the rate theory of Eyring et. al. The theoretical formulations so far derived are tested by experimental measurements in the rf electric field signifying the applicability of the method.

The structural and associational aspects of binary (jk) polar-polar mixtures of N, N dimethyl formamide (DMF) and dimethyl sulphoxide (DMSO) together with a single (j or k) N, N diethyl formamide (DEF) and DMSO in nonpolar solvent (i) are studied in terms of relaxation times τ_j , τ_k or τ_{jk} and dipole moments μ_j , μ_k or μ_{jk} of the jth, kth or jk polar mixture of the solutes under GHz electric field at various experimental temperatures for different weight fractions w_{jk} 's of polar solutes in **Chapter 3**. The variation of τ_{jk} with mole fractions x_k 's of DMSO in DMF and C_6H_6 reveals the probable solute-solute molecular associations around $x_k = 0.5$ of DMSO. The solute-solvent molecular associations begin at and around 50 mole % of DMSO in DMF and continue upto 100 mole % of DMSO. The concentration and temperature variation of τ_{jk} of such aprotic liquids are in excellent agreement with the variation of τ_{jk} of jk polar mixture with x_k 's of DMSO. Thermodynamic energy parameters are, however, obtained from Eyrings' rate process equation with the estimated τ 's to support the molecular association. The slight disagreement between the theoretical dipole moments μ_{theo} 's from the bond angles and bond moments is noticed with the measured μ 's to indicate the temperature dependence of mesomeric and inductive effects of different substituent polar groups of the molecules.

The **Chapter 4**, however, reports the double relaxation behaviour of some isomeric octyl alcohols in n-heptane at 25°C under 24.33, 9.25 and 3.00 GHz electric fields. τ_1 and τ_2 for the flexible parts and the whole molecules are measured by a single frequency measurement of dielectric relaxation parameters. The alcohols are long straight chain hydrogen bonded polymer having methyl and hydroxyl groups attached to the — C — atoms which may bend, twist or

rotate internally each with a characteristic τ . The relative contributions c_1 and c_2 are estimated from Fröhlich's equations and graphical technique. τ_1 and τ_2 decreases with frequency (f) due to rupture of H-bonding in long chain alcohols causing self or solute-solvent association of molecules. μ_1 and μ_2 in terms of τ_1 and τ_2 are again found out for the rotation of their $-\text{OH}$ groups about $-\text{C}-\text{O}-$ bonds only. μ_1 and μ_2 are finally compared with μ_{theo} 's arising out of structural aspects of the bond angles and bond moments of the substituent polar groups of the molecules.

The structural and associational aspects of nonspherical para polar liquids (j) in nonpolar solvents (i) are studied through hf conductivities σ_{ij} 's of solutions in **Chapter 5**. These liquids are widely used in pharmaceuticals, dyes, fragrances, agrochemicals, explosives and plastics. τ 's of the associative liquids under 3 cm wavelength electric field at different experimental temperatures in $^{\circ}\text{C}$, are estimated from the ratio of slopes of the individual variations of real σ'_{ij} and imaginary σ''_{ij} parts of hf complex conductivity σ^*_{ij} with w_j 's of polar liquids. The variation of τ with temperature for comparatively larger nonspherical para molecules in dioxane is not strictly obeyed by Debye model unlike other simpler para di or tri-substituted benzenes in C_6H_6 . The thermodynamic energy parameters ΔH_{τ} , ΔS_{τ} and ΔF_{τ} are obtained from Eyrings' rate process equation with the estimated τ 's in order to get solvent environment around the solute. The value of $\gamma (= \Delta H_{\tau} / \Delta H_{\eta}) > 0.50$ for all p-liquids except for p-bromonitrobenzene indicating solvent environment around solute molecules. The higher values of γ are due to solid phase rotators for the liquids. The estimated Kalman and Debye factors $\tau_j T / \eta^{\gamma}$ and $\tau_j T / \eta$ establish the Debye relaxation mechanism for almost all the para molecules. The obtained μ_j 's with the estimated τ_j 's are then compared with the reported μ 's and μ_{theo} 's. The temperature variation of μ_j explains the rupture of solute-solute association to form solute-solvent association due to stretching of bond angles and bond moments of polar molecules. The non associative nature of p-bromonitrobenzene in C_6H_6 is also confirmed by typical

nature of μ_j -t curve. Association or non-association of polar solutes in C_6H_6 and dioxane is, however, established from negative and positive ΔS_τ 's of Table 5.2. μ_j 's of some para molecules are often zero indicating the symmetric shape of the molecules. At other temperatures some p-molecules show the net moments. The slight disagreement between the measured and theoretical μ 's reveals the presence of inductive and mesomeric effects of the substituent polar groups in molecules at different experimental temperatures.

In **Chapter 6** the structural and associational aspects of some straight chain aliphatic alcohols are inferred from their static μ_s 's and hf μ_j 's in terms of τ_j 's under effective dispersive region of nearly 24 GHz electric field. Since dielectric dispersion is governed by frequency domain of AC spectroscopy, the dipolar liquids of normal and octyl alcohols absorb electric energy much more strongly at 24 GHz to yield accurate relative permittivities. Taking this fact into account the study of dielectric relaxation was carried out on such dielectropolar liquids. τ_j 's are estimated from the slope of linear variation of the imaginary part σ''_{ij} with the real part σ'_{ij} of hf complex conductivity σ_{ij}^* for different w_j 's in order to compare with those obtained from the ratio of individual slopes of σ''_{ij} and σ'_{ij} with w_j 's of solute. Non linear variation of both σ''_{ij} and σ'_{ij} with w_j indicates various types of molecular association in long chain dielectropolar alcohols. The linear coefficient a_1 of static experimental parameter X_{ij} with w_j is used to obtain μ_s . The $X_{ij}-w_j$ curves are closer within the region $0.1 \leq w_j \leq 0.2$ indicating same polarity of the molecules arising out of solute-solvent molecular associations. The slopes β of $\sigma_{ij}-w_j$ curves are employed to get hf μ_j 's in terms of τ_j 's obtained by two methods only to see how far they agree with μ_1 and μ_2 from double relaxation method. Unlike methanol and ethanol μ_s 's are lower than μ_j 's and μ_1 's for all the alcohols. This at once reveals the possible formation of monomers and dimers in the static and hf electric field. The dimer formation is favourable in octyl alcohols than the normal alcohols due to existence of strong inductive effect for their - OH groups at the end of molecular chains. It is,

however, observed that — OH groups of alcohols rotates about — C — O — bond under GHz electric field. The slight disagreement of μ_{theo} 's with μ_j 's and μ_s 's suggest the strong hydrogen bonding in them, in addition to mesomeric and inductive effects of the substituent polar groups attached to the parent molecules. Comparatively higher values of both μ_{theo} 's and μ_j 's in octyl alcohols indicates the solute-solvent association due to strong hydrogen bonding supported by the fact that — OH groups being screened by —CH₃ and a large number of >CH₂ groups.

τ_1 and τ_2 for isomers of anisidine and toluidine in C₆H₆ under 9.945 GHz electric field are predicted from the slope and intercept of a derived linear equation of $(\chi_{\text{ojj}} - \chi'_{\text{ij}}) / \chi'_{\text{ij}}$ against $\chi''_{\text{ij}} / \chi'_{\text{ij}}$ for different w_j 's solute at 35°C. χ'_{ij} and χ''_{ij} are the real and imaginary parts of hf complex orientational susceptibility χ^*_{ij} and χ_{ojj} is the low frequency real dielectric susceptibility. Larger values of τ_2 occur due to larger size of rotating units governed by solute-solvent i.e. monomer formation under hf electric field. Highly dispersive region is again established by the isomers of anisidine and toluidine which absorbed electric energy much more strongly at 9.945 GHz electric field to show reasonable τ_1 and τ_2 . The τ 's, dimensionless parameter b 's and the linear coefficients β 's of $\chi'_{\text{ij}} - w_j$ curves are used to obtain μ_1 and μ_2 of the molecules. Almost all $\chi'_{\text{ij}} - w_j$ curves have a tendency to be closer within the region $0.00 \leq w_j \leq 0.03$ showing the possible formation of monomers and dimers. c_1 and c_2 due to τ_1 and τ_2 from Fröhlich's equations are compared with the experimental ones by concentration variation of $\chi'_{\text{ij}} / \chi_{\text{ojj}}$ and $\chi''_{\text{ij}} / \chi_{\text{ojj}}$ curves at $w_j \rightarrow 0$. Theoretical and experimental values of c_1 and c_2 showed $|c_2 + c_2| \simeq 1$ establishing the validity of the linear equation in such liquids also. The estimated τ 's from the ratio of the individual slopes of variations of χ''_{ij} and χ'_{ij} with w_j at $w_j \rightarrow 0$ are compared with the existing methods. The symmetric and characteristic τ_s and τ_{cs} by symmetric and asymmetric distribution parameters γ and δ suggest the symmetric relaxation behaviour of the molecules. The measured μ_1 and μ_2 by double relaxation method

and reported μ suggest that a part of the molecule is rotating under GHz electric field. The slight disagreement between μ_{theo} and measured μ_1 demands the inductive and mesomeric effects of the substituted polar groups in addition to structural and associational aspects of such molecules. All these findings are beautifully presented in **Chapter 7**.

The linear equation $(\chi_{\text{oij}} - \chi'_{\text{ij}}) / \chi'_{\text{ij}} = \omega(\tau_1 + \tau_2) (\chi''_{\text{ij}} / \chi'_{\text{ij}}) - \omega^2 \tau_1 \tau_2$ for different ω_j 's of monosubstituted anilines (j) in C_6H_6 at 35°C under electric field frequencies of 2.02, 3.86 and 22.06 GHz are plotted graphically in **Chapter 8** to yield τ_1 and τ_2 . Larger τ_2 signify the monomer associations. τ 's from the ratio of the individual slopes of χ''_{ij} and χ'_{ij} with ω_j at $\omega_j \rightarrow 0$ are compared with the existing methods. Theoretical c_1 and c_2 for τ_1 and τ_2 from Fröhlich's equations and the experimental ones from graphically extrapolated values of the fitted curves of $\chi'_{\text{ij}} / \chi_{\text{oij}}$ and $\chi''_{\text{ij}} / \chi_{\text{oij}}$ with ω_j at $\omega_j \rightarrow 0$ are also compared. The findings reveals that $|c_1 + c_2| \simeq 1$. The applicability of derived linear equation is thereby established. The latters are employed to get γ and δ to yield τ_s and τ_{cs} in order to establish that monosubstituted anilines obey symmetric relaxation behaviour. μ_1 and μ_2 from τ_1 and τ_2 and linear coefficient β of variations of χ'_{ij} and σ_{ij} with ω_j are estimated. Higher μ 's from $\sigma_{\text{ij}} - \omega_j$ curves arise due to all types of polarisations involved with σ_{ij} 's while χ_{ij} 's is concerned with orientational polarisation. The difference $\Delta\mu_j$ between μ_j 's from $\sigma_{\text{ij}} - \omega_j$ and $\chi'_{\text{ij}} - \omega_j$ curves provides one to infer the bound charges of the molecules due to σ_{ij} measurements. μ_1 and μ_2 are compared with reported μ 's and μ_{theo} 's. The slight disagreement of measured μ_j 's from μ_{theo} 's is explained by inductive, mesomeric and electromeric effects.

The **Chapter 9 and 10** present the results of the rf conductivity σ' (real part) measurements to arrive at the structural and associational aspects of some normal alcohols in C_6H_6 only, aprotic polar liquids in C_6H_6 and CCl_4 and pure polar-polar liquid mixtures at single and different temperatures. The slope of σ' and $1/\eta$ is used to get number density 'n' of free ions of the liquid. τ_j 's and τ_{jk} 's

are, however, obtained in terms of measured 'n' from Einstein - Stokes relation with the values of gas kinetic molecular radius 'a'. Non linear variation of τ_j with w_j arises probably due to solute-solvent interactions. Higher τ_{jk} is due to formation of polymeric clusters by molecular association between j and k polar solutes. τ_j thus measured together with slopes β of $\sigma'_{ij}-w_j$ curves, yields rf μ_j from Smyth's relation to compare them with μ_{theo} 's. σ_{ij} 's for normal alcohols increases gradually with w_j to attain the maximum value at $w_j=0.5$, except for n-propanol, indicating a change of phase, arising out of solute-solvent molecular association. The μ_{theo} 's, on the other hand, gives an insight into the distribution of bond moments of different $-CH_3$ and $-OH$ groups to yield important information on structure of alcohols. The convex and concave nature of μ_j-t curves for aprotic polar liquids are interpreted by rupture of monomer and dimer associations due to stretching of bond moments of the substituent polar groups by thermal agitation. The disagreement between rf μ_j and μ_{theo} arises due to short range ionic forces influencing the whole dipolar rotations. Temperature variation of τ_j again helps one to obtain $\Delta H_\tau, \Delta S_\tau, \Delta F_\tau$ and $\gamma (= \Delta H_\tau / \Delta H_\eta)$ from Eyrings' rate process equation to conclude the stability or instability of the chemical systems and solvent environment around solute molecules. Debye and Kalman factors $\tau_j T / \eta$ and $\tau_j T / \eta^\gamma$ showed the molecules obeyed Debye relaxation. The semiconduction activation energies ΔE_j or ΔE_{jk} are obtained from temperature variation of rf σ' . They are finally compared with the literature values only to arrive at the structural and associational aspects of such molecules under 1 MHz and 500KHz rf electric field respectively.

In **Chapters 3 to 7 and 9** μ_{theo} 's of a large number of dipolar molecules under investigation have been obtained in terms of available bond angles and bond moments of substituent polar groups of parent molecules by vector addition method. This study invariably gives an important information of structures of the molecules concerned. The disagreement between μ_{theo} 's and estimated μ_j 's at once indicates the existence of inductive, mesomeric and electromeric effects

of substituent polar groups of the molecules, in addition to short range ionic forces.

In some chapters the dielectric theories are presented in SI units because of its unified, coherent and rationalised nature. The curves with the available experimental points in several figures of different chapters show the validity of the derived theoretical formulations. These are supported by the correlation coefficients r 's, % of errors and minimum chisquare testing on the data of polar-nonpolar liquid mixture of different w_j 's of solute in various nonpolar solvents at given experimental temperature. Many theories of dielectric relaxations have been formulated in terms of relative permittivities ϵ_{ij} 's. Measurement of τ_j 's and μ_j 's were carried out in terms of hf conductivity σ_{ij} which is concerned with bound molecular charges of polar molecules.

Nowadays, the study of dielectric relaxation phenomena is preferred in terms of dielectric orientational susceptibilities χ_{ij} 's in SI units as seen in **Chapter 7 and 8** of the thesis. χ_{ij} 's are supposed to be involved only with orientational polarisation of molecules. But the dielectric relaxation phenomena can recently be studied by Thermally Stimulated Depolarisation Current (TSDC) density and Isothermal Frequency Domain of AC Spectroscopy. These may give a firm answer to the problem of polar-nonpolar liquid mixtures including polymer and liquid crystal about which the present author is involved. But the latter two methods are very lengthy and often needs the tedious computer simulation technique unlike σ_{ij} and χ_{ij} measurements. The latter appear to be simple, straight forward and easy to arrive at the expected conclusion. Moreover, the polar-nonpolar liquid mixtures can be studied by taking into account of the concept of other models like Onsager, Kirkwood, Fröhlich etc. But the latter methods are not so simple like Debye - Smyth and Hill model used in this thesis. Further work can be carried out to predict the relaxation phenomena by assuming moment of inertia of the polar molecules under ultra high frequency (uhf) electric field. Numerical calculation on relaxation parameters of polar molecules in nonpolar

solvents may be carried out on the basis of Newton Raphson method to arrive at the results.

The discussion made above on the thesis entitled 'Structural and associational aspects of some dielectropolar liquid molecules in nonpolar solvents from relaxation phenomena' thus summarised ultimately provides the future workers in this field of liquid dielectrics to open a new and vast scope to work further in the investigation of structural and associational aspects of interesting dielectropolar liquids in nonpolar solvents like benzene, n-hexane, n-heptane, para-xylene, carbon tetrachloride, dioxane etc. under hf electric field. It can thus be concluded that the study of highly nonspherical polar liquid molecules in nonpolar solvents is, however, explained by the Debye-Smyth model which was supposed to be applicable to the nearly spherical molecules of simpler configuration in different nonpolar solvents.

**LIST OF PUBLISHED
AND COMMUNICATED PAPERS**

The subject matter of the thesis presented in several chapters has been published and communicated to different indian and foreign journals of international repute.

1. Structural and associational aspects of binary and single polar liquids in nonpolar solvent under high frequency electric field : S.K. Sit, N. Ghosh, U. Saha and S. Acharyya *Indian J Phys* **71B** (1997) 533.
2. Double relaxations of some isomeric octyl alcohols by high frequency absorption in nonpolar solvent : S.K. Sit, N. Ghosh and S. Acharyya *Indian J. Pure & Appl. Phys* **35** (1997) 329.
3. Dielectric relaxation of para polar liquids under high frequency electric field : N. Ghosh, R.C. Basak, S.K. Sit and S. Acharyya, *J. Mol. Liquids* (Germany) **85** (2000) 375.
4. Structural and associational aspects of dielectropolar straight chain alcohols from relaxation phenomena : N. Ghosh, A. Karmakar, S.K. Sit and S. Acharyya, *Indian J. Pure & Appl. Phys.* **38** (2000) 574.
5. Structural and associational aspects of isomers of anisidine and toluidine under a gigahertz electric field : N. Ghosh, S.K. Sit, A.K. Bothra and S. Acharyya. *J. Phys. D : Appl Phys* (U.K) **34** (2001) 379.
6. Double relaxation phenomena of monosubstituted anilines in benzene under high frequency electric field : N. Ghosh, S.K. Sit and S. Acharyya, *J. Mol. Liquids* (Germany) Accepted for publication 2001.
7. Structural conformation and associational aspects of some normal alcohols in benzene and their mixtures under rf electric field at single and different temperatures : N. Ghosh, R. Ghosh, R.C. Basak, K. Dutta and S. Acharyya *Pramana J Phys* communicated 2002.
8. Relaxation phenomena of aprotic polar liquid molecules under a kilohertz electric field : N. Ghosh, R. Ghosh and S. Acharyya *Indian J Pure & Appl. Phys.* Communicated 2001.

Structural and associational aspects of binary and single polar liquids in non polar solvent under high frequency electric field

S K Sit, N Ghosh, U Saha and S Acharyya

Department of Physics, Raiganj College, Raiganj, Uttar Dinajpur-733 134,
West Bengal, India

Received 17 April 1996, accepted 19 December 1996

Abstract : The structural and associational aspects of binary (jk) polar mixtures of N,N dimethyl formamide (DMF) and dimethyl sulphoxide (DMSO) together with a single (j or k) N, N diethyl formamide (DEF) and DMSO in nonpolar solvents (i) are studied in terms of their high frequency (hf) conductivities. The relaxation times τ 's and dipole moments μ 's of the solutes under Giga hertz electric field at various temperatures are estimated from the measured real and imaginary parts of hf dielectric constants at different weight fractions of polar solutes. The variation of τ_{jk} 's with mole fractions x_k 's of DMSO in DMF and C_6H_6 reveals the probable solute-solute molecular association around $x_k = 0.5$ of DMSO. The solute-solvent molecular association begins at and around 50 mole% DMSO in DMF and continues upto 100 mole% DMSO. The concentration and temperature variations of τ_{jk} of these protic liquids are in accord with the information of variation of τ_{jk} of jk polar mixtures with x_k 's of DMSO. Thermodynamic energy parameters are also obtained from Eyring's rate process equation with the estimated τ 's to support the molecular associations. The slight disagreement between the theoretical dipole moments μ_{theo} 's from the bond angles and bond moments is noticed with the measured μ 's in terms of slopes of concentration variation of hf conductivity curves at infinite dilutions and τ 's. This indicates the temperature dependence of mesomeric and inductive moments of different substituent groups of the molecules.

Keywords : Dipole moment, relaxation time, associational aspects.

PACS Nos. : 31.70.Dk, 33.15.Kr

The dielectric relaxation mechanism of a polar-nonpolar liquid mixture under the microwave electric field is of special interest [1,2] for its inherent ability to predict the associational aspects of polar solutes in nonpolar solvents. An investigation was, however, made on ternary solution of binary polar liquids in which both or even one of them are aprotic [2,3] to study various types of weak molecular associations by polar liquids in

nonpolar solvents. We are, therefore, tempted further to consider more mixtures of binary aprotic polar liquids like N,N dimethyl formamide (DMF) and dimethyl sulphoxide (DMSO) together with a single aprotic polar liquid like N,N diethyl formamide (DEF) and DMSO in C_6H_6 and CCl_4 [4–6] respectively. DMSO, DMF and DEF are very interesting liquids for their wide application in medicine and industry. They also act as building blocks of proteins and enzymes. The concentration variation of the measured real ϵ'_{ijk} , ϵ'_{ij} or ϵ'_{ik} and imaginary ϵ''_{ijk} , ϵ''_{ij} or ϵ''_{ik} parts of hf complex dielectric constants ϵ^*_{ijk} , ϵ^*_{ij} or ϵ^*_{ik} of jk , j or k polar solutes in nonpolar solvents are used to detect the weak molecular interactions among the molecules [7] at a single or different temperatures under nearly 3 cm wavelength electric field. The τ_{jk} of jk polar mixtures as well as τ_j 's or τ_k 's of j or k polar solutes in a nonpolar solvent were estimated from :

$$K''_{ijk} = K_{\infty ij k} + \frac{1}{\omega\tau_{jk}} K'_{ijk}, \quad (1)$$

where $K''_{ijk} = \frac{\omega}{4\pi} \epsilon''_{ijk}$ and $K'_{ijk} = \frac{\omega}{4\pi} \epsilon'_{ijk}$ are the imaginary and real parts of complex hf conductivity K^*_{ijk} [8]. The other terms carry usual significance as presented elsewhere [2]. The τ_{jk} 's are estimated from the slopes of the linear variations of K''_{ijk} against K'_{ijk} of eq. (1). The linearity of eq. (1) is tested by the correlation coefficients and the errors involved in the measurement of τ 's are within 5%. τ_{jk} 's are then plotted with different mole fractions x_k 's of DMSO at various experimental temperatures as shown in Figure 1.

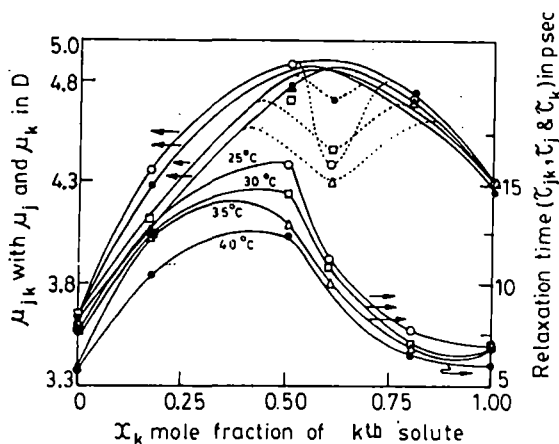


Figure 1. Variation of τ_{jk} and μ_{jk} of DMF–DMSO mixture in C_6H_6 against mole fraction x_k of DMSO with τ_j and τ_k and μ_j and μ_k of DMF and DMSO respectively at different temperatures : (○) at 25°C, (□) at 30°C, (Δ) at 35°C and (●) at 40°C.

The formation of dimer is responsible for the gradual rise of τ_{jk} from τ_j of DMF at $x_k = 0$ to $x_k = 0.5$ and then its rapid fall to τ_k due to rupture of dimerisation and self association [4]. The estimated τ 's are slightly larger than those of Gopalakrishna's method [9]. But τ 's from conductivity measurement are much more reliable as they provide microscopic relaxation times [10].

The energy parameters due to dielectric relaxation process were then obtained in terms of measured τ from the rate process equation of Eyring *et al* [11] :

$$\tau_s = \frac{A}{T} e^{\Delta F_r / RT}$$

$$\text{or } \ln(\tau_s T) = \ln A' + \frac{\Delta H_r}{RT} \tag{2}$$

where $A' = Ae^{-\Delta S_r / R}$.

Eq. (2) is a straight line of $\ln(\tau_s T)$ against $\frac{1}{T}$ as seen in Figure 2 having intercepts and slopes to yield the entropy of activation ΔS_r , enthalpy of activation ΔH_r and free energy of activation ΔF_r due to dielectric relaxation. The values of $\gamma \left(= \frac{\Delta H_r}{\Delta H_\eta} \right)$ for all the liquids

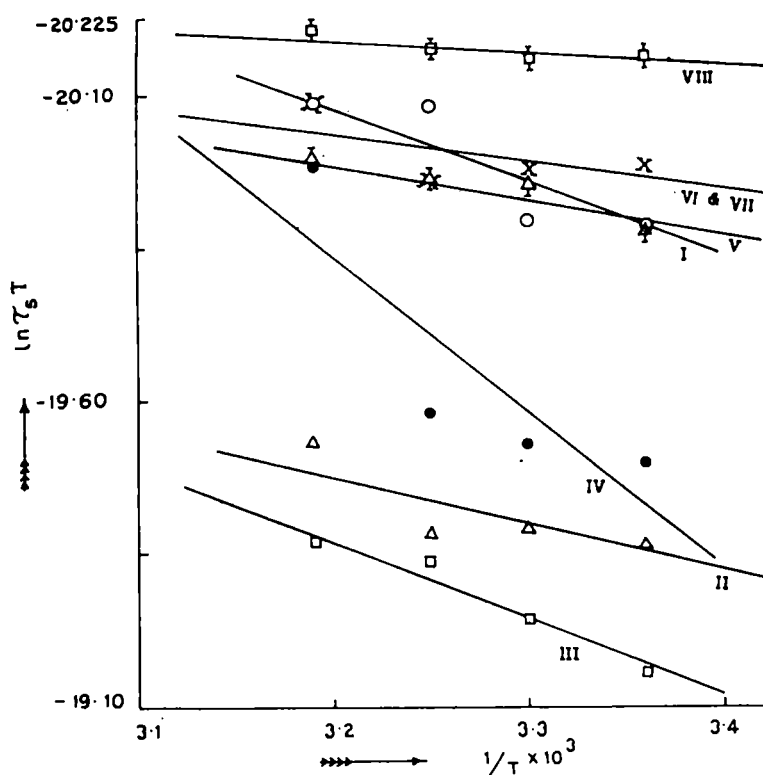


Figure 2. Variation of $\ln(\tau_s T)$ against $\frac{1}{T}$ of binary and single polar solutes in nonpolar solvent. I-DMF + 0 mole% DMSO in C_6H_6 (O), II-DMF + 17 mole% DMSO in C_6H_6 (Δ), III-DMF + 50 mole% DMSO in C_6H_6 (\square), IV-DMF + 60 mole% DMSO in C_6H_6 (\bullet), V-DMF + 80 mole% DMSO in C_6H_6 (\blacktriangle), VI-DMF + 100 mole% DMSO in C_6H_6 (X), VII-DMF + 100 mole% DMSO in C_6H_6 (X), VIII-DMSO in CCl_4 (\oplus).

except DMSO in CCl_4 are greater than 0.55, as obtained from the slope of the linear relation of $\ln(\tau_s T)$ with $\ln \eta$ indicating them as solid phase rotators in solvent environment. η is the

coefficient of viscosity of solvent. ΔH_η due to viscous flow of the solvent is obtained from slope of $\ln(\tau_r T)$ against $\frac{1}{T}$ and known γ . Again, ΔH_η are greater than ΔH_τ for all the mixtures except 0, 50 and 60 mole% DMSO in DMF and C_6H_6 . The difference in ΔH_τ and ΔH_η is due to the involvement of various types of bondings which are either formed or broken to some extent, depending on the temperature and concentration of the system. The negative values of ΔS_τ 's for all the systems except 0 and 60 mole% DMSO in DMF and C_6H_6 indicate the existence of cooperative orientation of the molecules arising out of steric forces to yield more ordered states while the reverse is true for positive ΔS_τ 's. Although, ΔF_τ 's in all cases are almost constant at all temperatures, they increase with x_k of DMSO from $x_k = 0.0$ to $x_k = 0.5$ and then decrease gradually to $x_k = 1.0$ signifying the maximum dimerisation of DMF-DMSO mixture around $x_k = 0.5$. The formation of dimer causes larger molecular size and hence, the energy needed for rotation in the relaxation process is higher.

The hf conductivity K_{ijk} as a function of weight fraction W_{jk} is given by

$$K_{ijk} = \frac{\omega}{4\pi} (\epsilon'_{ijk}{}^2 + \epsilon''_{ijk}{}^2)^{\frac{1}{2}} \quad (3)$$

Since $\epsilon'_{ijk} \gg \epsilon''_{ijk}$ eq. (1) can be written as

$$K_{ijk} = K_{\infty ij k} + \frac{1}{\omega \tau_{jk}} K'_{ijk}$$

$$\text{or} \quad \left(\frac{dK'_{ijk}}{dW_{jk}} \right)_{W_{jk} \rightarrow 0} = \omega \tau_{jk} \beta \quad (4)$$

Here, β 's are the slopes of $K_{ijk} - W_{jk}$, $K_{ij} - W_j$ or $K_{ik} - W_k$ curves respectively, which are linear with almost identical intercepts probably due to same polarity of the molecules [2]. The real part of hf conductivity, K'_{ijk} is again related to W_{jk} of jk polar solute dissolved in a nonpolar solvent (i) at temperature T°K [12] as

$$K'_{ijk} = \frac{\mu_{jk}^2 N \rho_{ijk} F_{ijk}}{3 M_{jk} k T} \left(\frac{\omega^2 \tau_{jk}}{1 + \omega^2 \tau_{jk}^2} \right) W_{jk} \quad (5)$$

Differentiating eq. (5) with respect to W_{jk} and comparing the result at $W_{jk} \rightarrow 0$ to eq. (4), one obtains the following relation

$$\mu_{jk} = \left[\frac{27 M_{jk} k T}{N \rho_i (\epsilon_i + 2)^2} \cdot \frac{\beta}{\omega b} \right]^{1/2} \quad (6)$$

to estimate μ_{jk} , μ_j or μ_k of the respective solutes. b is a dimensionless parameter in terms of estimated τ_{jk} , τ_j or τ_k given by :

$$b = \frac{1}{1 + \omega^2 \tau_{jk}^2} \quad (7)$$

The other terms in eq. (6) carry usual significance [2]. All the μ 's are then plotted against different x_k 's of DMSO at each temperature as shown in Figure 1. It shows the gradual rise of μ_{jk} in the range $0 < x_k \leq 0.5$. It then decreases slowly in order to exhibit the convex nature of each curve with an abnormally low value of μ_{jk} around $x_k = 0.6$. This sort of behaviours of $\mu_{jk} - x_k$ curves (Figure 1) is explained by the fact that dimers are being formed from $x_k \geq 0$ to $x_k = 0.6$ causing increase of μ . The rupture of dimerisation *i.e.* self association occurs in higher concentrations in the range $0.6 \leq x_k < 1.0$ to yield lower values of μ 's. But around $x_k = 0.6$, all μ_{jk} 's are minimum indicating the possible occurrence of double relaxation phenomena in such mixtures to be studied later on. μ_{jk} together with μ_j and μ_k for each mixture of a fixed concentration are shown graphically only to observe their temperature dependence like $\mu_{jk} = a + bt + ct^2$ with coefficients a , b and c as seen in Figure 3. The variation is concave with maximum depression at 17 mole% DMSO in DMF mixture. The depression gradually decreases upto $x_k = 0.6$ of DMSO in DMF and C_6H_6 probably due to solute-solute molecular association in the range $0 < x_k < 0.6$. The maximum

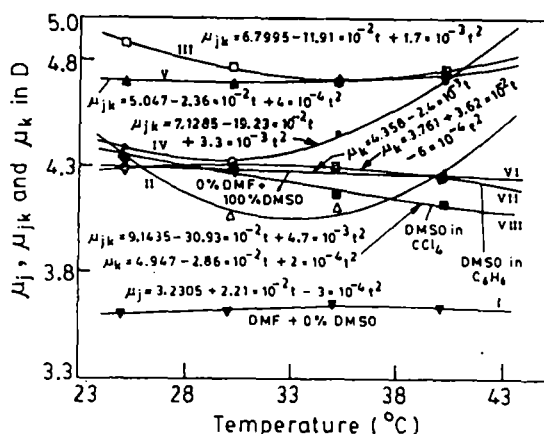


Figure 3. Variation of μ_j , μ_{jk} and μ_k of binary and single polar solutes in nonpolar solvent with temperature t in $^{\circ}C$.

I—DMF + 0 mole% DMSO in C_6H_6 (\blacktriangledown), II—DMF + 17 mole% DMSO in C_6H_6 (Δ), III—DMF + 50 mole% DMSO in C_6H_6 (\square), IV—DMF + 60 mole% DMSO in C_6H_6 (\bullet), V—DMF + 80 mole% DMSO in C_6H_6 (\blacktriangle), VI—DMF + 100 mole% DMSO in C_6H_6 (∇), VII—DMSO in C_6H_6 (\circ), VIII—DMSO in CCl_4 (\blacksquare).

dimerisation is, however, inferred from low μ 's because of the larger molecular sizes as confirmed by high values of $\tau_r T / \eta'$ (being proportional to volume of the rotating unit) for 60 mole% DMSO in DMF and C_6H_6 . As temperature increases the dipole-dipole interaction is weakened and the absorption of hf electric energy increases resulting in the rupture of dimer to yield high μ 's for smaller molecular species [10]. The slight convex nature of curves for 0 mole% DMSO in DMF and C_6H_6 and DMSO in C_6H_6 , along with almost straight line variation of 100 mole% DMSO in DMF and C_6H_6 and DMSO in CCl_4 (Figure 3) is probably due to solute-solvent molecular interaction of either DMF with C_6H_6 or DMSO with C_6H_6 and CCl_4 respectively as illustrated in Figure 4. The associations of DMF, DEF and DMSO in C_6H_6 can arise due to interactions of fractional positive charges of N and S atoms of the molecules with the π delocalised electron cloud of C_6H_6 ring as seen in Figure 4(i), (iii) and (iia) respectively. Again, one C—Cl dipoles of CCl_4 , owing to more -ve charge on Cl atom, interacts with the fractional

+ve charge of S-atom of DMSO (Figure 4 (iib)). The $\mu_{\text{theo}} = 4.55$ D of DMSO is, however, computed from available bond moments of 2.35 D and 1.55 D for $\text{S} \leftarrow \text{CH}_3$ and $\text{O} = \text{S}$ respectively, assuming the molecule to be planar one. The major contributions to μ_{theo} for DMF and DEF are due to 0.64 D and 0.78 D for $\text{N} \leftarrow \text{CH}_3$ and $\text{N} \leftarrow \text{C}_2\text{H}_5$ since the other common bond moments in them are the same with values of 0.3 D, 0.45 D and 3.10 D for $\text{C} \leftarrow \text{H}$, $\text{C} \leftarrow \text{N}$ and $\text{C} = \text{O}$ respectively. Figure 4 (iv), however, shows a certain angle $\phi (= 106^\circ)$ between monomeric μ 's of DMF and DMSO to have $\mu_{\text{theo}} = 4.77$ D of dimer below $x_k = 0.6$.

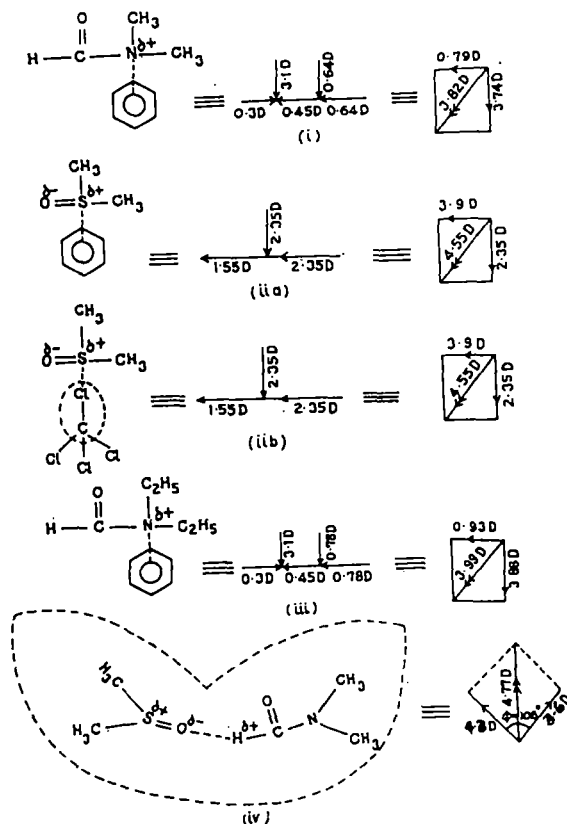


Figure 4. Conformational structures along with solute-solvent and solute-solute interaction of molecules. (i) DMF in C_6H_6 , (ii a) DMSO in C_6H_6 , (ii b) DMSO in CCl_4 (iii) DEF in C_6H_6 , (iv) DMSO-DMF dimer.

The slight deviations of the μ 's from the μ_{theo} 's occur probably due to the presence of inductive and mesomeric moments of such molecules. This is also observed elsewhere [13]. The corrected μ 's obtained from the reduced bond moments of the substituent groups by factors $\mu_{\text{cal}}/\mu_{\text{theo}}$ establish the above facts at different temperatures, too. Thus the dielectric relaxation parameters from hf conductivity measurements offer a useful tool to arrive at the structural and associational aspects of the non-spherical polar liquids.

Acknowledgment

The authors are thankful to Sri R C Basak for his interest in this work.

References

- [1] C R Acharyya, A K Chatterjee, P K Sanyal and S Acharyya *Indian J. Pure Appl. Phys.* **24** 234 (1986)
- [2] A K Chatterjee, U Saha, N Nandi, R C Basak and S Acharyya *Indian J. Phys.* **66B** 291 (1992)
- [3] U Saha and S Acharyya *Indian J. Pure Appl. Phys.* **31** 181 (1993)
- [4] A Sharma, D R Sharma and M S Chauhan *Indian J. Pure Appl. Phys.* **31** 841 (1993)
- [5] A Sharma and D R Sharma *J. Phys. Soc. Jpn.* **61** 1049 (1992)
- [6] A R Saksena *Indian J. Pure Appl. Phys.* **16** 1079 (1978)
- [7] U Saha and S Acharyya *Indian J. Pure Appl. Phys.* **32** 346 (1994)
- [8] F J Murphy and S O Morgan *Bull. Syst. Tech. J.* **18** 502 (1939)
- [9] K V Gopalakrishna *Trans. Faraday Soc.* **53** 767 (1957)
- [10] S K Sit and S Acharyya *Indian J. Phys.* **70B** 19 (1996)
- [11] H Eyring, S Glasstone and K J Laidler *The Theory of Rate Process* (New York : McGraw-Hill) (1941)
- [12] C P Smyth *Dielectric Behaviour and Structure* (New York : McGraw Hill) (1955)
- [13] R C Basak, S K Sit, N Nandi and S Acharyya *Indian J. Phys.* **70B** 37 (1996)

Double relaxations of some isomeric octyl alcohols by high frequency absorption in non-polar solvent

S K Sit, N Ghosh & S Acharyya

Department of Physics, University College, P O Raiganj, Dist Uttar Dinajpur, 733 134, W Bengal

Received 29 March 1996; revised 18 June 1996; accepted 7 November 1996

The double relaxation behaviour of some isomeric octyl alcohols in n-heptane at 25°C under the electric field frequencies of 24.33, 9.25 and 3.00 GHz is studied to get the relaxation times τ_1 and τ_2 for their flexible parts and whole molecules by a method of single frequency measurements of dielectric relaxation parameters. The isomers are long, straight chain, hydrogen bonded, polymer type molecules having methyl and hydroxyl groups attached to their C-atoms which may bend, twist or rotate internally under hf electric field each with a characteristic τ . The relative contributions, c_1 and c_2 towards dielectric relaxations due to τ_1 and τ_2 are also estimated by using Fröhlich's equations and the graphical technique. The dipole moments μ_1 and μ_2 in terms of τ_1 and τ_2 of flexible part and the whole molecules are again found out from slope β of the total hf conductivity K_{ij} as a function of weight fractions ω_j 's of the solute indicating μ_1 for the rotation of their -OH groups about C-C bonds only. μ_1 and μ_2 are finally compared with the theoretical dipole moments μ_{theo} arising out of the structures with bond-angles and bond-moments of their substituent groups to establish the conformations of these isomers are justified like normal alcohols observed earlier.

1 Introduction

The dielectric relaxation mechanism of a polar-non-polar liquid mixture is a very convenient and useful tool in ascertaining the shape, size and structure of a polar molecule¹. The process is generally involved with the estimation of dipole moment μ in terms of the relaxation time τ for a polar molecule in a non-polar solvent under different high frequency (hf) electric field of giga hertz (GHz) range at a fixed or different temperatures. There exist several methods² to estimate τ of a polar liquid in a non-polar solvent. They offer a deep insight into the intrinsic properties of a polar molecule because of the absence of dipole-dipole interactions in polar-non-polar liquid mixtures.

Highly non-spherical polar molecules, on the other hand, possess more than one τ in the electric field of GHz range for the rotations of different substituent groups attached to the parent molecule and the whole molecule itself. Budo³, however, proposed that complex dielectric constant ϵ^* of a polar liquid may be represented as the sum of a number of non-interacting Debye type dispersions each with a characteristic τ . The method was then made simpler by Bergmann *et al.*⁴ by assuming that the dielectric relaxation is the sum of two Debye type dispersions characterised

by the intramolecular and molecular τ_1 and τ_2 respectively. The corresponding relative contributions c_1 and c_2 towards dielectric relaxations could then be estimated. They used a graphical analysis which consists of plotting normalised values of $(\epsilon' - \epsilon_\infty)/(\epsilon_0 - \epsilon_\infty)$ against $\epsilon''/(\epsilon_0 - \epsilon_\infty)$ on a complex plane in terms of the measured real ϵ' , imaginary ϵ'' parts of ϵ^* , static dielectric constant ϵ_0 and high frequency dielectric constant ϵ_∞ of a polar liquid for different frequencies of the electric field. A number of chords were then drawn through the points on the curve until a set of parameters was found out in consistency with all the experimental points. Bhattacharyya *et al.*⁵ subsequently modified the above procedure to get τ_1 , τ_2 and c_1 , c_2 for a polar liquid from the relaxation data measured at least at two different frequencies of the electric fields.

A procedure was devised⁶ to get τ_1 and τ_2 from the slope and intercept of a derived straight line equation involved with the single frequency measurements of the dielectric relaxation parameters like $\epsilon_{\alpha ij}$, $\epsilon_{\beta ij}$, ϵ'_{ij} and ϵ''_{ij} for different weight fractions ω_j 's of a polar solute (j) in a non-polar solvent (i) at a given temperature. The technique had already been applied on disubstituted benzenes and anilines⁶ at 9.945 GHz electric field as well as mono-substituted anilines⁷ at 22.06, 3.86,

2.02 GHz electric fields respectively. All these investigations reveal that they often showed the double relaxation behaviour at certain frequency of the electric field.

The aliphatic alcohols are long straight chain, hydrogen bonded polymer type molecules having possibility of their bending, twisting and rotation under hf electric field each with a characteristic τ , besides the average macroscopic distribution of τ . The alcohols have high dipole moments owing to their strong intermolecular forces exerted by them like polymers in solution. Onsager's equation may be a better choice for such associative liquids, but it is not so simple like Debye's equation because of the presence of quadratic term ϵ_{ij}^* . The relaxation behaviour of aliphatic alcohols is very interesting because they show more than two τ 's in pure state, but for a polar-non-polar liquid mixture hf process becomes increasingly important on dilution^{8,9}. An extensive study to detect the frequency dependence of double relaxation behaviour of four long chain normal aliphatic alcohols

like 1-butanol, 1-hexanol, 1-heptanol, 1-decanol in solvent n-heptane¹⁰ including methanol and ethanol at 9.84 GHz in benzene^{11,12} at 25°C was already made¹³. All the alcohols showed τ_1 and τ_2 at all frequencies of the electric field except methanol which is a simple molecule to possess the expected τ_2 only.

The method⁶ was applied on six isomeric octyl alcohols like 2-methyl-3-heptanol, 3-methyl-3-heptanol, 4-methyl-3-heptanol, 5-methyl-3-heptanol, 4-octanol and 2-octanol at 24.33, 9.25 and 3.00 GHz electric fields, as reported in Tables 1-3 respectively, because of the availability of ϵ'_{ij} , ϵ''_{ij} , ϵ_{0ij} and $\epsilon_{\infty ij}$ measured by Crossley *et al.*¹⁴ in n-heptane at 25°C. The straight line equations between $(\epsilon_{0ij} - \epsilon'_{ij})/(\epsilon'_{ij} - \epsilon_{\infty ij})$ and ϵ''_{ij}/c $\epsilon'_{ij} - \epsilon_{\infty ij}$ for all the octyl alcohols at different ω_j 's are linear as shown in Fig. 1 only to establish the applicability of Debye model in such isomeric alcohols like normal alcohols¹³ once again. Moreover, all the long chain octyl alcohols are structural isomers with the molecular formula $C_8H_{18}O$ having greater

Table 1—The estimated relaxation times τ_2 and τ_1 from the slopes and the intercept of straight line Eq. (8) with errors and correlations (r) together with measured τ_s from $K''_{ij} - K'_{ij}$ curve and most probable relaxation time $\tau_0 = \sqrt{\tau_1 \tau_2}$ for six isomeric octyl alcohols at 25°C under different frequencies of electric fields

System with Sl. No. & Mol. wt M_j	Frequency in GHz	Intercept & slope of Eq.(8)		Correlation coefficient (r)	% Error in regression technique	Estimated values of τ_2 & τ_1 , in p Sec.		Measured τ_s , in p Sec.	Most probable relaxation time $\tau_0 = \sqrt{\tau_1 \tau_2}$
I 2-methyl-3-heptanol in n-heptane $M_j = 130$ gm	(a) 24.33	2.3718	5.0952	0.9011	6.34	29.96	3.39	1.84	10.08
	(b) 9.25	0.6871	3.1205	0.9700	1.90	49.61	4.10	3.58	14.26
	(c) 3.00	0.1408	1.4830	0.9771	1.50	73.31	5.41	6.74	19.91
II 3-methyl-3-heptanol in n-heptane $M_j = 130$ gm	(a) 24.33	0.9087	2.6282	0.9294	4.59	14.52	2.68	2.19	6.24
	(b) 9.25	0.6389	2.7714	0.9709	1.93	43.34	4.37	3.70	13.76
	(c) 3.00	0.1611	1.5018	0.9985	0.10	73.55	6.17	5.58	21.30
III 4-methyl-3-heptanol in n-heptane $M_j = 130$ gm	(a) 24.33	1.9653	4.3873	0.8851	7.30	25.40	3.31	1.90	9.17
	(b) 9.25	0.6411	2.8636	0.9682	2.11	45.08	4.21	4.13	13.78
	(c) 3.00	0.2008	1.7153	0.9206	5.14	84.34	6.71	11.98	23.79
IV 5-methyl-3-heptanol in n-heptane $M_j = 130$ gm	(a) 24.33	0.6929	2.9788	0.5684	26.36	17.83	1.66	1.71	5.44
	(b) 9.25	0.7445	3.2866	0.9846	1.19	52.36	4.21	5.39	14.85
	(c) 3.00	0.2362	2.0308	0.9371	4.74	101.22	6.58	13.11	25.81
V 4-octanol in n-heptane $M_j = 130$ gm	(a) 24.33	0.9572	3.4750	0.8569	10.34	20.77	1.97	1.83	5.40
	(b) 9.25	0.3810	2.6361	0.9470	4.02	42.74	2.64	5.46	10.62
	(c) 3.00	0.1428	1.6929	0.9846	1.18	85.13	4.72	12.76	20.05
VI 2-octanol in n-heptane $M_j = 130$ gm	(a) 24.33	1.3664	5.0208	0.6336	23.30	30.97	1.89	1.83	7.65
	(b) 9.25	1.5853	5.6407	0.9888	0.86	92.00	5.11	6.26	21.68
	(c) 3.00	0.4458	3.1697	0.9780	1.69	160.41	7.83	18.70	35.44

Table 2—Fröhlich parameter A , relative contributions c_1 and c_2 due to τ_1 and τ_2 , theoretical values of x and y from Fröhlich's Eqs (9) and (10) and from graphical extrapolation technique at $\omega_1 \rightarrow 0$

System with Sl. No.	Frequency, GHz	Fröhlich parameter $\Delta = \ln(\tau_2/\tau_1)$	Theoretical values of x & y from Eqs (9) and (10)		Theoretical values of c_1 & c_2		Estimated values of x & y at $\omega_1 \rightarrow 0$		Estimated values of c_1 and c_2	
			x	y	c_1	c_2	x	y	c_1	c_2
I 2-methyl-3-heptanol in n-heptane	(a) 24.33	2.1790	0.3457	0.4028	0.3686	1.2101	0.795	0.366	1.0226	-0.2476
	(b) 9.25	2.4932	0.5637	0.4023	0.4886	0.9434	1.075	0.19	1.1624	-0.2324
	(c) 3.00	2.6063	0.7973	0.3232	0.6144	0.5500	1.075	0.074	1.1143	-0.0808
II 3-methyl-3-heptanol in n-heptane	(a) 24.33	1.6997	0.5195	0.4490	0.4542	0.7733	0.865	0.32	1.0321	-0.1120
	(b) 9.25	2.2943	0.5792	0.4115	0.4922	0.8573	0.91	0.256	0.9569	0.0810
	(c) 3.00	2.4781	0.7865	0.3349	0.6028	0.5600	1.025	0.094	1.0589	-0.0579
III 4-methyl-3-heptanol in n-heptane	(a) 24.33	2.0378	0.3747	0.4173	0.3857	1.0842	0.78	0.35	0.9961	-0.2117
	(b) 9.25	2.3710	0.5775	0.4075	0.4932	0.8812	0.95	0.208	1.0177	-0.0805
	(c) 3.00	2.5313	0.7543	0.3490	0.5902	0.6112	1.015	0.094	1.0551	-0.0827
VI 5-methyl-3-heptanol in n-heptane	(a) 24.33	2.3741	0.5644	0.4088	0.4862	0.9057	0.645	0.274	0.6389	0.3763
	(b) 9.25	7.5207	0.5499	0.4020	0.4814	0.9805	0.95	0.172	1.0297	-0.2211
	(c) 3.00	2.7332	0.7222	0.3529	0.5833	0.6848	1.065	0.042	1.1326	-0.2341
V 4-octanol in n-heptane	(a) 24.33	2.3555	0.5080	0.4131	0.4553	1.0030	0.72	0.22	0.7840	0.0126
	(b) 9.25	2.7833	0.6506	0.8720	0.5463	0.8372	0.895	0.116	0.9254	-0.0654
	(c) 3.00	2.8924	0.7813	0.3197	0.6210	0.5900	0.99	0.052	1.0218	-0.0850
VI 2-octanol in n-heptane	(a) 24.33	2.7964	0.4507	0.3867	0.4257	1.3507	0.67	0.208	0.7223	0.0764
	(b) 9.25	2.3925	0.4292	0.3795	0.4124	1.4780	0.895	0.214	0.9850	-0.3026
	(c) 3.00	3.0198	0.6201	0.3658	0.5361	0.9672	1.04	0.102	1.0810	-0.1813

Table 3—Estimated intercept and slope of $K_{ij} - \omega_j$ equation, dimensionless parameters b_2 , b_1 (eq. (16)), estimated dipole moments μ_2 , μ_1 (eq. (15)), μ_{theo} from bond angles and bond moments together with μ_1 from $\mu_1 = \mu_2(c_1/c_2)^{1/2}$ in Debye

System with Sl. No. Mol wt.	Frequency GHz	Intercept & slope or of $K_{ij} = \omega_j$ equation		Dimensionless parameter		Estimated dipole moments (in Debye)		μ_{theo} in D	Estimated μ_1 in D from $\mu_1 = \mu_2(c_1/c_2)^{1/2}$
		$\alpha \times 10^{-10}$	$\beta \times 10^{-10}$	b_1	b_2	μ_2	μ_1		
I 2-methyl-3-heptanol in n-heptane $M_j = 130$ gm	(a) 24.33	2.3632	0.6974	0.0455	0.7885	4.80	1.15	1.76	2.65
	(b) 9.25	0.8998	0.3126	0.1075	0.9463	3.39	1.14		2.44
	(c) 3.00	0.2911	0.1224	0.3439	0.9897	2.08	1.23		2.20
II 3-methyl-3-heptanol in n-heptane $M = 130$ gm	(a) 24.33	2.3630	0.7490	0.1689	0.8564	2.58	1.15	1.76	1.98
	(b) 9.25	0.8959	0.3554	0.1363	0.9395	3.21	1.22		2.43
	(c) 3.00	0.2910	0.1330	0.3425	0.2867	2.18	1.29		2.26
III 4-methyl-3-heptanol in n-heptane $M_j = 130$ gm	(a) 24.33	2.3635	0.7213	0.623	0.7963	4.17	1.17	1.76	2.49
	(b) 9.25	0.8984	0.3278	0.1273	0.9436	3.19	1.17		2.39
	(c) 3.00	0.2911	0.1283	0.2837	0.9843	2.35	1.26		2.31
IV 5-methyl-3-heptanol in n-heptane $M_j = 130$ gm	(a) 24.33	2.3646	0.6415	0.1187	0.9396	2.85	1.01	1.76	2.09
	(b) 9.25	0.9021	0.2771	0.0975	0.9436	3.35	1.08		2.35
	(c) 3.00	0.2922	0.1138	0.2157	0.9849	2.54	1.19		2.34
V 4-octanol in n-heptane $M_j = 130$ gm	(a) 24.33	2.3561	0.6492	0.0903	0.9169	3.29	1.03	1.08	2.22
	(b) 9.25	0.8965	0.2618	0.1396	0.9770	2.72	1.03		2.20
	(c) 3.00	0.2919	0.1044	0.2799	0.9922	2.13	1.13		2.19
VI 2-octanol in heptane $M_j = 130$ gm	(a) 24.33	2.3533	0.6572	0.9428	0.9230	4.80	1.03	1.08	2.69
	(b) 9.25	0.8980	0.2753	0.0338	0.9190	5.67	1.09		3.00
	(c) 3.00	0.2897	0.1221	0.0887	0.9787	3.88	1.23		2.89

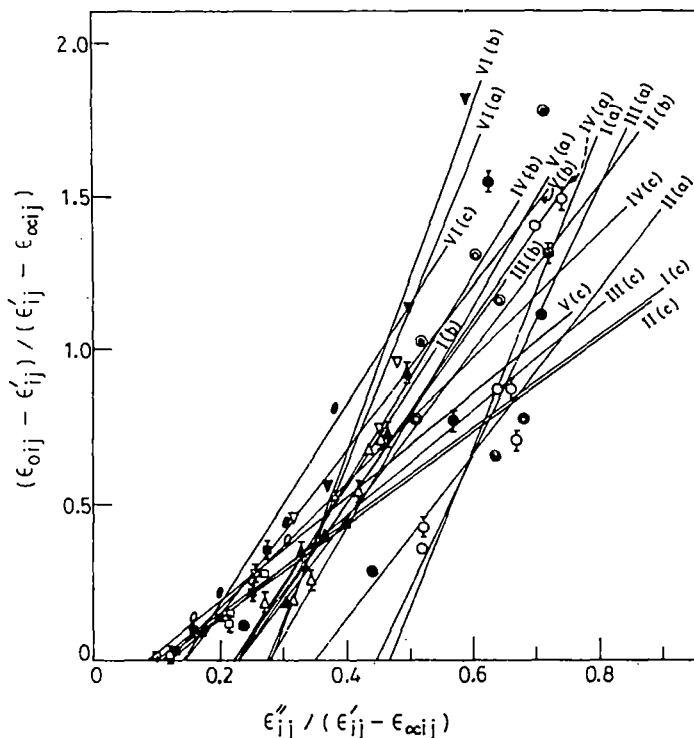


Fig. 1—Plot of $(\epsilon'_{0ij} - \epsilon'_{ij}) / (\epsilon'_{ij} - \epsilon_{\infty ij})$ against $\epsilon''_{ij} / (\epsilon'_{ij} - \epsilon_{\infty ij})$ of some isomeric octyl alcohols in n-heptane at 25°C. Curves of I (a); I (b), I (c) for 2-methyl-3-heptanol at 24.33, 9.25 and 3.00 GHz (\circ , Δ , \square). Curves of II (a), II (b), II (c) for 3-methyl-3-heptanol at 24.33, 9.25 and 3.00 GHz (\bullet , \blacktriangle , \blacksquare). Curves of III (a), III (b), III (c) for 4-methyl-3-heptanol at 24.33, 9.25 and 3.00 GHz (\circ , Δ , \square). Curves of IV(a), IV (b), IV (c) for 5-methyl-3-heptanol at 24.33, 9.25, 3.00 GHz (\bullet , \blacktriangle , \blacksquare). Curves of V (a), V (b), V (c) for 4-octanol at 24.33, 9.25 and 3.00 GHz (\circ , ∇ , \diamond). Curves of VI (a), VI (b), VI (c) for 2-octanol at 24.33, 9.25 and 3.00 GHz (\bullet , \blacktriangledown , \bullet).

number of C-atoms in their structures. They are, therefore, expected to possess two relaxation processes at audio and radio frequencies of electric field at low temperature in pure state¹⁴.

The paper presents the frequency dependence of τ_1 and τ_2 at all frequencies of 24.33, 9.25 and 3.00 GHz electric field for all the octyl alcohols like normal alcohols too. The measured τ_s from the slope of the linear equation of imaginary K''_{ij} and real K'_{ij} parts of the total complex hf conductivity K^*_{ij} and the most probable relaxation time τ_0 from $\tau_0 = \sqrt{\tau_1 \tau_2}$ are placed in Table 1 together with the estimated τ_1 and τ_2 in order to see their trends with frequency of the applied electric field. The relative contributions c_1 and c_2 towards dielectric relaxations in terms of intramolecular relaxation time τ_1 and molecular relaxation time τ_2 are then estimated from Fröhlich's equations¹⁵ as well as the graphical method of Figs 2 and 3. The estimated c_1 and c_2 are placed in Table 2.

The dipole moments μ_1 and μ_2 due to flexible parts as well as the whole molecules in terms of

the estimated τ_1 and τ_2 and the slopes β of the linear variation of hf conductivity K_{ij} with ω_j are shown in Table 3. The slopes β and the intercepts α of the linear variation of K_{ij} with ω_j , as placed in Table 3, at each frequency for all the isomers in n-heptane are almost the same probably due to their same polarity¹⁶. This fact is also supported by their conformations as shown in Fig. 4. It was, therefore, very difficult to plot K_{ij} against ω_j . The computed μ_2 's for most of the isomeric alcohols show larger values at 24.33 GHz and gradually decrease with lower frequencies unlike μ_1 . In order to compare μ_2 and μ_1 with theoretical dipole moments μ_{theo} , a special attention is to be paid on the conformational structure of each isomer from the available bond angles and bond moment. They are shown in Fig. 4. Using the usual C—C bond moment of 0.09 D from methanol and ethanol¹³ μ_{theo} for four methyl substituted octanols are found to show slightly larger values (see Fig. 4 and Table 3) than 1-heptanol¹³ except the desired values for 2-octanol and 4-octanol perhaps due to

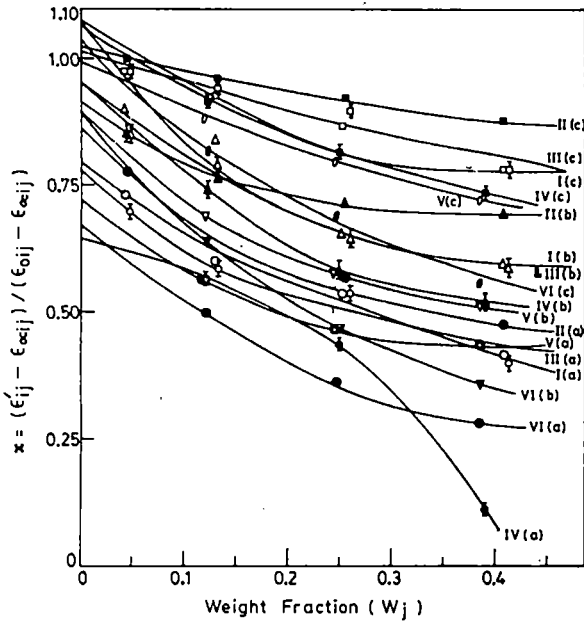


Fig. 2—Plot of $(\epsilon'_{ij} - \epsilon_{\infty ij})/(\epsilon'_{ij} - \epsilon_{\infty ij})$ against weight fraction ω_j of some isomeric octyl alcohols in n-heptane at 25°C. Curves of I (a), I (b), I (c) for 2-methyl-3-heptanol at 24.33, 9.25 and 3.00 GHz. (O, Δ , \square). Curves of II (a), II (b), II (c) for 3-methyl-3-heptanol at 24.33, 9.25 and 3.00 GHz (\bullet , \blacktriangle , \blacksquare). Curves of III (a), III (b), III (c) for 4-methyl-3-heptanol at 24.33, 9.25 and 3.00 GHz (\circ , \triangle , \square). Curves of IV(a), IV (b), IV (c) for 5-methyl-3-heptanol at 24.33, 9.25, 3.00 GHz (\blacklozenge , \blacktriangledown , \blacklozenge). Curves of V (a), V (b), V (c) for 4-octanol at 24.33, 9.25 and 3.00 GHz (O, ∇ , \diamond). Curves of VI (a), VI (b), VI (c) for 2-octanol at 24.33, 9.25 and 3.00 GHz (\ominus , \blacktriangledown , \bullet).

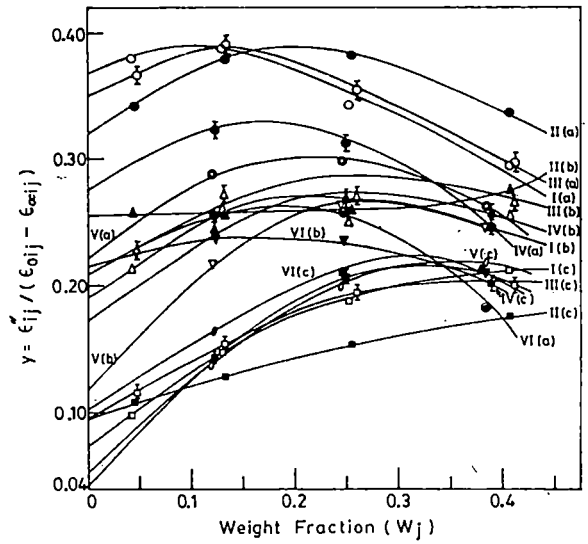


Fig. 3—Plot of $\epsilon''_{ij}/(\epsilon_{0ij} - \epsilon_{\infty ij})$ against weight fraction ω_j of some isomeric octyl alcohols in n-heptane at 25°C. Curves of I (a), I (b), I (c) for 2-methyl-3-heptanol at 24.33, 9.25 and 3.00 GHz. (O, Δ , \square). Curves of II (a), II (b), II (c) for 3-methyl-3-heptanol at 24.33, 9.25 and 3.00 GHz (\bullet , \blacktriangle , \blacksquare). Curves of III (a), III (b), III (c) for 4-methyl-3-heptanol at 24.33, 9.25 and 3.00 GHz (\circ , \triangle , \square). Curves of IV(a), IV (b), IV (c) for 5-methyl-3-heptanol at 24.33, 9.25, 3.00 GHz (\blacklozenge , \blacktriangledown , \blacklozenge). Curves of V (a), V (b), V (c) for 4-octanol at 24.33, 9.25 and 3.00 GHz (O, ∇ , \diamond). Curves of VI (a), VI (b), VI (c) for 2-octanol at 24.33, 9.25 and 3.00 GHz (\ominus , \blacktriangledown , \bullet).

bond moments of C—H₃ and —O—H groups in their structures. The calculated value of μ_1 from $\mu_1 = \mu_2(c_1/c_2)^{1/2}$ assuming two relaxation processes are equally probable, are also placed in the last column of Table 3 with all the estimated μ 's for comparison.

2 Theoretical Formulations to Estimate Relaxation Parameters

The complex dielectric constant ϵ^*_{ij} of a polar-non-polar liquid mixture can be represented as the sum of a number of non-interacting Debye type dispersions in accordance with Budo's³ relation.

$$\frac{\epsilon^*_{ij} - \epsilon_{\infty ij}}{\epsilon_{0ij} - \epsilon_{\infty ij}} = \sum \frac{c_k}{1 + j\omega\tau_k} \quad \dots (1)$$

where $j = \sqrt{-1}$ is a complex number and $\sum c_k = 1$. The term c_k is the relative contribution for the k th type of relaxation processes. When ϵ^*_{ij} con-

sists of two Debye type dispersions, Budo's relation reduces to Bergmann's equations⁴:

$$\frac{\epsilon'_{ij} - \epsilon_{\infty ij}}{\epsilon_{0ij} - \epsilon_{\infty ij}} = \frac{c_1}{1 + \omega^2\tau_1^2} + \frac{c_2}{1 + \omega^2\tau_2^2} \quad \dots (2)$$

and

$$\frac{\epsilon''_{ij}}{\epsilon_{0ij} - \epsilon_{\infty ij}} = c_1 \frac{\omega\tau_1}{1 + \omega^2\tau_1^2} + c_2 \frac{\omega\tau_2}{1 + \omega^2\tau_2^2} \quad \dots (3)$$

such that $c_1 + c_2 = 1$. Now with

$$\frac{\epsilon'_{ij} - \epsilon_{\infty ij}}{\epsilon_{0ij} - \epsilon_{\infty ij}} = x, \quad \frac{\epsilon''_{ij}}{\epsilon_{0ij}\epsilon_{\infty ij}} = y$$

$\omega\tau = \alpha$ and using $a = (1/1 + \alpha^2)$ and $b = \alpha/(1 + \alpha^2)$ the Eqs (2) and (3) can be written as;

$$x = c_1 a_1 + c_2 a_2 \quad \dots (4)$$

$$y = c_1 b_1 + c_2 b_2 \quad \dots (5)$$

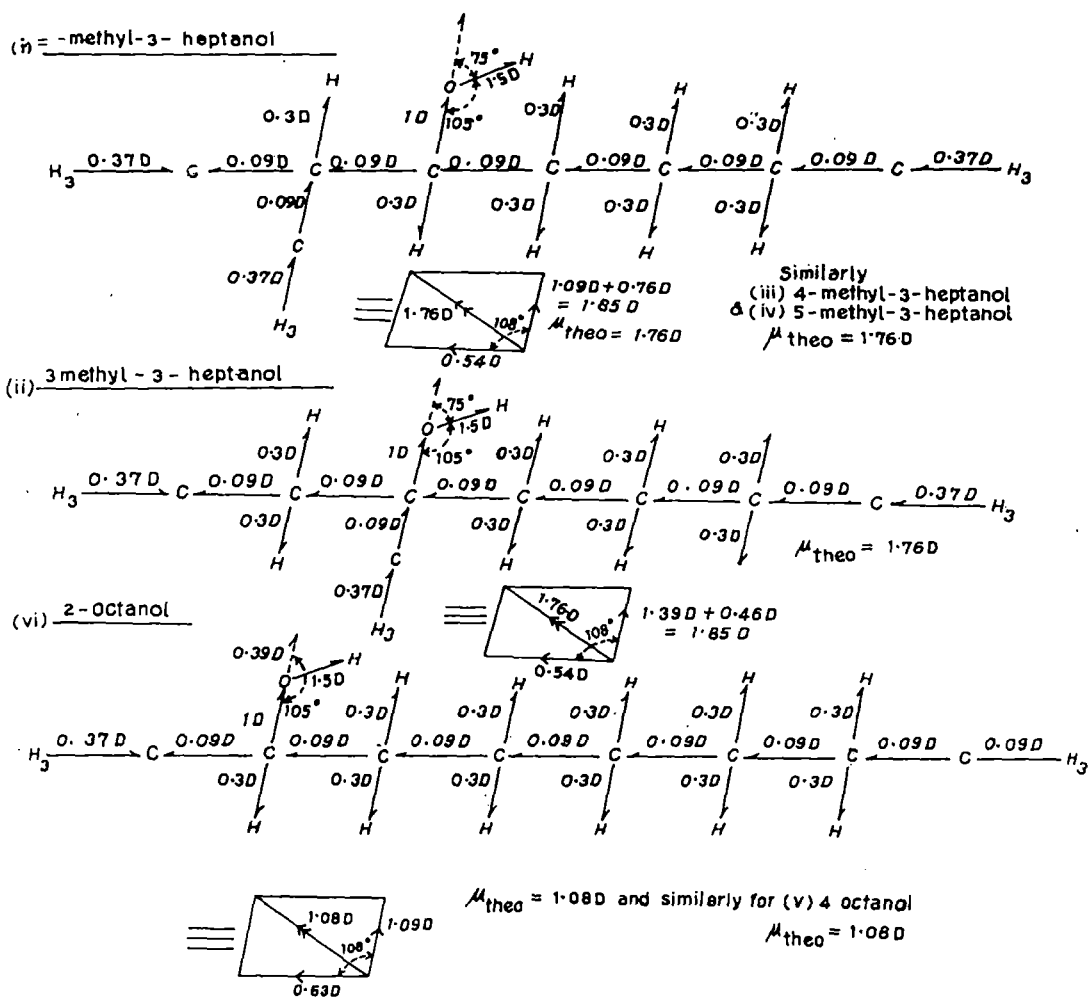


Fig. 4—Conformations of some isomeric octyl alcohols

where suffixes 1 and 2 with a and b are related to τ_1 and τ_2 respectively. From Eqs (4) and (5), since $\alpha_2 - \alpha_1 \neq 0$ and $\alpha_2 > \alpha_1$ we have

$$c_1 = \frac{(x\alpha_2 - y)(1 + \alpha_1^2)}{\alpha_2 - \alpha_1} \dots (6)$$

$$c_2 = \frac{(y - x\alpha_1)(1 + \alpha_2^2)}{\alpha_2 - \alpha_1} \dots (7)$$

Since $c_1 + c_2 = 1$, we get the following equation with the help of Eqs (6) and (7):

$$\frac{1-x}{y} = (\alpha_1 + \alpha_2) - \frac{x}{y} \alpha_1 \alpha_2$$

which on substitution of the values x , y and α yields:

$$\frac{\epsilon_{0ij} - \epsilon'_{ij}}{\epsilon'_{ij} - \epsilon_{\infty ij}} = \omega(\tau_1 + \tau_2) \frac{\epsilon''_{ij}}{\epsilon'_{ij} - \epsilon_{\infty ij}} - \omega^2 \tau_1 \tau_2 \dots (8)$$

Eq. (8) is thus a straight line equation between $(\epsilon_{0ij} - \epsilon'_{ij})/(\epsilon'_{ij} - \epsilon_{\infty ij})$ and $\epsilon''_{ij}/(\epsilon'_{ij} - \epsilon_{\infty ij})$ with slope $\omega(\tau_1 + \tau_2)$ and intercept $-\omega^2 \tau_1 \tau_2$ respectively, where ω is the angular frequency of the applied electric field of frequency f in GHz. With the measured dielectric relaxation data of ϵ'_{ij} , ϵ''_{ij} , ϵ_{0ij} and $\epsilon_{\infty ij}$ for different weight fractions ω_j 's of each octyl alcohol in n-heptane at 25°C under 24.33, 9.25 and 3.00 GHz electric fields¹⁴ we get slope and intercept of Eq. (8) to yield τ_1 and τ_2 as shown in Table 1.

The relative contributions, c_1 and c_2 towards the dielectric relaxations in terms of x , y and τ_1 , τ_2 for each octyl alcohol are found out and placed in Table 2. The theoretical values¹⁵ of x and y are, however, calculated from Fröhlich's Eqs:

$$x = \frac{\epsilon'_{ij} - \epsilon_{\infty ij}}{\epsilon_{0ij} - \epsilon_{\infty ij}} = 1 - \frac{1}{2A} \ln \left(\frac{e^{2A} \omega^2 \tau_1^2 + 1}{1 + \omega^2 \tau_1^2} \right) \quad \dots (9)$$

$$y = \frac{\epsilon''_{ij}}{\epsilon_{0ij} - \epsilon_{\infty ij}} = \frac{1}{A} [\tan^{-1}(e^A \omega \epsilon_1) - \tan^{-1}(\omega \tau_1)] \dots (10)$$

where $A = \text{Fröhlich parameter} = \ln(\tau_2/\tau_1)$ and τ_1 is called the small limiting relaxation time as obtained from the double relaxation method. A simple graphical extrapolation technique, on the other hand, was considered to get the values of x and y at $\omega_j \rightarrow 0$ from Figs 2 and 3 respectively. This is really in accordance with Bergmann's Eqs (2) and (3) when the once estimated τ_1 and τ_2 from Eq. (8) are substituted in the right hand sides of above Eqs (2) and (3).

The values of μ_1 and μ_2 of octyl alcohols in terms of τ_1 , τ_2 and slope β of the concentration variation of the experimental hf conductivity K_{ij} were then estimated. The hf conductivity K_{ij} is, however, given by Murphy and Morgan¹⁷:

$$K_{ij} = \frac{\omega}{4\pi} (\epsilon''_{ij} + \epsilon'^2_{ij})^{1/2} \quad \dots (11)$$

as a function of ω_j of polar solute. Since $\epsilon''_{ij} \ll \epsilon'_{ij}$ in the hf electric field, the term ϵ''_{ij} offers resistance of polarisation. Thus the real part K'_{ij} of the $hf K_{ij}$ of a polar-non-polar liquid mixture at TK can be written according to Smyth¹⁸ as:

$$K'_{ij} = \frac{\mu_j^2 N \rho_{ij} F_{ij}}{3 M_j k T} \left(\frac{\omega^2 \tau}{1 + \omega^2 \tau^2} \right) \omega_j \quad \dots (12)$$

which on differentiation with respect to ω_j and for $\omega_j \rightarrow 0$ yields that:

$$\left(\frac{dK'_{ij}}{d\omega_j} \right)_{\omega_j \rightarrow 0} = \frac{\mu_j^2 N \rho_{ij} F_{ij}}{3 M_j k T} \left(\frac{\omega^2 \tau}{1 + \omega^2 \tau^2} \right) \quad \dots (13)$$

where M_j is the molecular weight of a polar solute, N the Avogadro number, k the Boltzmann constant, the local field $F_{ij} = 1/9 (\epsilon_{ij} + 2)^2$ between $F_i = 1/9 (\epsilon_i + 2)^2$ and the density $\rho_{ij} \rightarrow \rho_i$ the density of solvent at $\omega_j \rightarrow 0$.

Again, the total hf conductivity $K_{ij} = \omega/4\pi \epsilon_{ij}$

can be written as:

$$K_{ij} = K_{ij\infty} + \frac{1}{\omega \tau} K'_{ij}$$

or

$$\left(\frac{dK'_{ij}}{d\omega_j} \right)_{\omega_j \rightarrow 0} = \omega \tau \left(\frac{dK_{ij}}{d\omega_j} \right)_{\omega_j \rightarrow 0} = \omega \tau \beta \quad \dots (14)$$

where β is the slope of $K_{ij} - \omega_j$ curve at infinite dilution. From Eqs (13) and (14) we get:

$$\mu_j = \left[\frac{27 M_j k T}{N \rho_i (\epsilon_i + 2)^2} \cdot \frac{\beta}{\omega b} \right]^{1/2} \quad \dots (15)$$

as the dipole moment of each octyl alcohol in terms of b , where b is a dimensionless parameter given by:

$$b = \frac{1}{1 + \omega^2 \tau^2} \quad \dots (16)$$

The computed μ_1 and μ_2 together with b , b_2 and β of $K_{ij} - \omega_j$ equations for all the octyl alcohols are placed in Table 3.

3 Results and Discussion

The least square fitted straight line equations of $(\epsilon_{0ij} - \epsilon'_{ij})/(\epsilon'_{ij} - \epsilon_{\infty ij})$ against $\epsilon''_{ij}/(\epsilon'_{ij} - \epsilon_{\infty ij})$ for six isomeric octyl alcohols like 2-methyl-3-heptanol, 3-methyl-3-heptanol, 4-methyl-3-heptanol, 5-methyl-1,3-heptanol, 4-octanol and 2-octanol in solvent *n*-heptane at 25°C under 24.33, 9.25 and 3.00 GHz electric field at different ω_j 's of polar solutes are shown in Fig. 1 together with the experimental points on them. ω_j 's are, however, calculated from the mole fractions x_i and x_j of solvent and solute with molecular weights M_i and M_j respectively according to the relation¹⁹:

$$\omega_j = \frac{x_j M_j}{x_i M_i + x_j M_j}$$

All the straight line equations are almost perfectly linear as evident from the correlation coefficients r lying in the range 0.9985-0.5684. The corresponding % of errors in terms of r in getting the slopes and intercepts of all the straight lines are placed in the 6th and 5th columns of Table 1. The errors are, however, large at 24.33 GHz indicating departure from the linear behaviour as evi-

dent from low values of r perhaps due to inherent uncertainty in measured data for such higher frequency¹³.

The estimated values of τ_2 and τ_1 for all the isomeric octyl alcohols from the slopes and the intercepts of straight line equations are of smaller magnitude at 24.33 GHz and increase gradually to attain maximum value at 3.00 GHz under the present investigation. This may be due to the fact that at higher frequency the rate of hydrogen bond rupture in long chain alcohols is the maximum thereby reducing τ for each rotating unit¹³. τ_2 and τ_1 are then compared with the measured τ_s from the relation:

$$K''_{ij} = K_{ij\infty} + \frac{1}{\omega \tau_s} K'_{ij}$$

and τ_0 where $\tau_0 = \sqrt{\tau_1 \tau_2}$. As evident from Table 1 although $\tau_0 > \tau_1$; τ_s agrees well with τ_1 for most of the solutes except slight disagreement at 3.00 GHz for 4-methyl-3-heptanol, 5-methyl-3-heptanol, 4-octanol and 2-octanol. This is explained on the basis of the fact that conductivity measurement may be applicable in higher frequency in yielding microscopic τ only whereas the double relaxation method offers a better understanding of molecular relaxation phenomena showing microscopic as well as macroscopic τ as observed earlier¹³. Unlike normal aliphatic alcohols, -OH groups are screened by the substituted -CH₃ group, broad dispersion characterised by relatively short relaxation times were thus observed¹⁴. The respective positions of -CH₃ and -OH groups also greatly affect the static dielectric constant, correlation factor, their temperature dependence and type of hydrogen bonding in them.

The relative contributions c_1 and c_2 towards dielectric relaxations are also estimated in terms of $(\epsilon'_{ij} - \epsilon_{\infty ij}) / (\epsilon_{0ij} - \epsilon_{\infty ij})$, $\epsilon''_{ij} / (\epsilon_{0ij} - \epsilon_{\infty ij})$ with the estimated, τ_1 , τ_2 as shown in Table 2 by Fröhlich and graphical methods. $x = (\epsilon'_{ij} - \epsilon_{\infty ij}) / (\epsilon_{0ij} - \epsilon_{\infty ij})$ and $y = \epsilon''_{ij} / (\epsilon_{0ij} - \epsilon_{\infty ij})$ were, however, evaluated from Fröhlich's Eqs (9) and (10) in the first case. The usual variations of $(\epsilon'_{ij} - \epsilon_{\infty ij}) / (\epsilon_{0ij} - \epsilon_{\infty ij})$ and $\epsilon''_{ij} / (\epsilon_{0ij} - \epsilon_{\infty ij})$ with ω_j are concave and convex as found in Figs 2 and 3 in accordance with Bergmann Eqs (2) and (3), except 5-methyl-3-heptanol at 24.33 GHz whose $\{(\epsilon'_{ij} - \epsilon_{\infty ij}) / (\epsilon_{0ij} - \epsilon_{\infty ij})\}$ curves is convex in nature due to its non-accurate ϵ_{0ij} and $\epsilon_{\infty ij}$ values like ethanol as observed earlier¹³. x and y were also obtained graphically from Figs (2) and (3) in the limit $\omega_j = 0$.

In Fröhlich-method c_1 and c_2 are all positive as

evident from 6th and 7th columns of Table 2 with $c_2 > c_1$. In graphical method $c_1 > c_2$ with negative c_2 for most of the systems probably due to inertia of the flexible parts under hf electric field, as shown in 10th and 11th columns of same Table 2. c_2 are, however, positive for the systems 5-methyl-3-heptanol, 4-octanol and 2-octanol at 24.33 GHz as well as 3-methyl-3-heptanol at 9.25 GHz. Both the methods in most cases, yield $|c_1 + c_2| \geq 1$, signifying thus the possibility of occurrence of more than two relaxation processes in them¹³.

The dipole moments μ_1 and μ_2 of all the isomeric alcohols due to their flexible parts and the whole molecules are estimated in terms of dimensionless parameters b_1 , b_2 and slope β of $K_{ij} - \omega_j$ curves by using Eq. (15). The variations of K_{ij} with ω_j are all linear having almost the same intercepts α and slopes β at each frequency of electric field. It was, therefore, difficult to plot them as they almost coincide. The values of α and β of K_{ij} 's are little different and comparatively large, at 24.33 GHz (Table 3). This sort of behaviour is perhaps due to same dipole moments¹⁶ possessed by the polar molecules under investigation as evident from μ_2 and μ_1 placed in 7th and 8th columns of Table 3. μ_2 for most of the polar molecules shows high values at 24.33 GHz and decrease gradually with lower frequencies except 3-methyl-3-heptanol, 5-methyl-3-heptanol and 2-octanol whose μ_2 's are found greater at 9.25 GHz electric field. This type of behaviour may be explained on the basis of the fact that such alcohols behaving almost like the polymer molecules have long chain of C-atoms and tend to break up in a non-polar solvent in order to reduce or even eliminate the absorption under hf electric field. The proportion of smaller molecular species having comparatively small number of C-atoms and their corresponding absorption will increase thereby¹⁰. The values of μ_1 's on the other hand, are almost constant exhibiting a trend to increase a little towards low frequency. They are finally compared with bond moments of 1.5 D of -O-H group making an angle 105° with the -C-O- bond axis according to the preferred conformations of all the isomers as sketched in Fig. 4. This confirms that μ_1 arises due to the rotation of -OH group around C-O bond in the long chain alcohols studied so far¹³. The slight difference is due to difference in steric hindrances as a result of structural configurations at different frequencies. μ_1 also estimated from $\mu_1 = \mu_2 (c_1/c_2)^{1/2}$ assuming two relaxation processes are equally probable as shown in the last column of Table 3. The other bond moments 0.47, 0.3, 1.0 and 0.09 D for

C—H₃, C—H, C—O and C—C bonds are also involved to justify their conformations. The resultant of all these bonds by vector addition method yields μ_{theo} of 1.76 D and 1.08 D for four methyl substituted heptanols and two octanols respectively. The derived result should decrease with increase in the number of C-atoms and μ_{theo} for them should be less than that for 1-heptanol¹³. But for μ_{theo} in Fig. 4 three isomers are only displayed due to typical positions of —CH₃ and —OH groups. This may probably be the reason of having slightly larger values of μ_{theo} from 1-heptanol as observed earlier¹³.

4 Conclusion

The methodology so far advanced for the double broad dispersions of the polar-non-polar liquid mixtures based on Debye's model seems to be much simpler, straightforward and significant one to detect the very existence of τ_1 and τ_2 of a polar liquid in a non-polar solvent. The correlation coefficients between the desired dielectric relaxation parameters involved in the derived equations of Eq. (8) could, however, be estimated to find out % of errors entered in the estimated τ_1 and τ_2 of a polar liquid, because τ is claimed to be accurate within $\pm 10\%$. The isomeric octyl alcohols like normal aliphatic alcohols are found to yield both τ_1 and τ_2 at all frequencies of the electric field of GHz range. The corresponding μ_1 and μ_2 can then be estimated from Eq. (15) in terms of b_1 and b_2 which are, however, involved with τ_1 and τ_2 as estimated, to arrive at their preferred conformations as shown in Fig. 4.

Acknowledgement

The authors are thankful to Mr A R Sit, BE (Electrical) for his interest in this work.

References

- 1 Saha U & Acharyya S, *Indian J Pure & Appl Phys*, 32(1994) 346.
- 2 Gopalakrishna KV, *Trans Faraday Soc*, 53 (1957) 767.
- 3 Budo A, *Phys Z*, 39 (1938) 706.
- 4 Bergmann K, Roberti D M & Smyth C P, *J Phys Chem*, 64 (1960) 665.
- 5 Bhattacharyya J, Hasan A, Roy S B & Kastha G S, *J Phys Soc Japan*, 28 (1970) 204.
- 6 Saha U, Sit S K, Basak R C & Acharyya S, *J Phys D Appl Phys*, 27 (1994) 596.
- 7 Sit S K, Basak R C, Saha U & Acharyya S, *J Phys D: Appl Phys*, 27 (1994) 2194.
- 8 Denney D J & Ring J W, *J Chem Phys*, 39 (1963) 1268.
- 9 Moriametz M & Lebrun A, *Arch Soi (Geneva)*, 13 (1960) 40.
- 10 Glasser L, Crossley J & Smyth C P, *J Chem Phys*, 57 (1972) 3977.
- 11 Purohit H D & Sharma H S, *Indian J Pure & Appl Phys*, 8 (1970) 10.
- 12 Ghosh A K, PhD Dissertation (NBU), 1981.
- 13 Sit S K & Acharyya S, *Indian J Phys B*, 70 (1996) 19.
- 14 Crossley J, Glasser L & Smyth C P, *J Chem Phys*, 55 (1971) 2197.
- 15 Fröhlich H, *Theory of dielectrics* (Oxford University Press, Oxford) 1949.
- 16 Chatterjee A K, Saha U, Nandi N, Basak R C & Acharyya S, *Indian J Phys*, 668 (1992) 291.
- 17 Murphy F J & Morgan S D, *Bull Syst Techn J*, 18 (1939) 502.
- 18 Smyth C P, *Dielectric behaviour and structure*, (McGraw-Hill, New York) 1955.
- 19 Ghosh A K & Acharyya S, *Indian J Phys*, 528 (1978) 129.

Reprinted from

journal of
**MOLECULAR
LIQUIDS**

Journal of Molecular Liquids 85 (2000) 375–385

Dielectric relaxation of para polar liquids
under high frequency electric field

N Ghosh, RC Basak, SK Sit, S Acharyya

*Department of Physics, Raiganj College (University College) P.O. Raiganj, Dist. Uttar Dinajpur,
Pin-733134 (W.B), India.*



ELSEVIER



Dielectric relaxation of para polar liquids under high frequency electric field

N Ghosh, RC Basak, SK Sit, S Acharyya

Department of Physics, Raiganj College (University College) P.O. Raiganj, Dist. Uttar Dinajpur, Pin-733134 (W.B), India.

Abstract

The structural and associational aspects of nonspherical para polar liquids (j) in nonpolar solvents (i) are studied through high frequency conductivities σ_{ij} 's of solutions. The relaxation time τ of the respective liquids under 3cm. wavelength electric field at various experimental temperatures in °C are estimated from the slope of individual variations of real σ'_{ij} and imaginary σ''_{ij} parts of hf complex conductivity σ^*_{ij} with weight fractions w_j 's of polar liquid. The temperature variation of τ for comparatively larger nonspherical para molecules in dioxane are not strictly obeyed by the Debye model unlike other simpler para di- or tri-substituted benzene in benzene. Thermodynamic energy parameters ΔH_τ , ΔS_τ and ΔF_τ are obtained from Eyring's rate process equation with the estimated τ 's in order to get information on the solvent environment around them. The higher values of γ obtained from $\ln\tau_j T$ against $\ln\eta$ equation indicate the solid phase rotators for the liquids. The estimated Kalman and Debye factors $\tau_j T/\eta^\gamma$ and $\tau_j T/\eta$ establish the Debye relaxation mechanism for almost all the para-molecules. The obtained dipole moments μ_j 's in terms of slope β of σ_{ij} - w_j curve and dimensionless parameter 'b' involved with estimated τ are then compared with the reported μ and μ_{theo} obtained from bond angles and bond moments. The μ_j 's of para liquids are often zero but at other temperatures they show net moments. The slight disagreement between the measured and theoretical μ 's reveals the presence of the inductive and mesomeric moments of substituted polar groups in molecules at different temperatures. © 2000 Elsevier Science B.V. All rights reserved.

1. INTRODUCTION

The dielectric relaxation phenomena of a polar liquid in nonpolar solvent have already gained much attention from a large number of workers [1–3]. The process is thought to be a sensitive tool to investigate the molecular size, shape and structure of a polar liquid. The structural and associational aspects of the polar liquid can thus be inferred in terms of their measured relaxation time τ and hence dipole moment μ at different experimental temperatures in °C. The subsequent use of the temperature dependence of τ 's usually yields different thermodynamic energy parameters of a polar unit. The polar liquids having substituted polar groups in their para positions deserve to be specially investigated. The μ 's of such para liquids are usually found to be zero [4] due to symmetrical distribution of bond moments of the substituted polar groups in a plane. Sometimes they show a resultant μ when the dipolar and free groups are out of plane with the parent ring.

Earlier investigations [5] were made on substituted hydroxy and methoxybenzaldehydes in

benzene, to reveal that τ is generally governed by both molecular and intra-molecular rotations. However, no such study on the long chain substituted parabenzaldehydes and phenones have been made so far. Dhar et al [6] and Somevanshi et al [7] have recently measured real ϵ'_{ij} and imaginary ϵ''_{ij} parts of complex dielectric constant ϵ^*_{ij} of p-hydroxy-propiofenone, p-chloropropiofenone, p-acetamidobenzaldehyde, p-benzyloxybenzaldehyde in dioxane and p-anisidine, p-phenitidine, o-chloroparanitroaniline and p-bromonitrobenzene in benzene respectively under 3 cm. wavelength electric field at different experimental temperatures. The purpose of their study was only to observe the molecular and intra-molecular group rotations in the molecules. Nonspherical molecular liquids of such type also are known to be strongly non-Debye in their relaxation behaviour. We, therefore, concentrate our attention to these molecules [6,7] to study dielectric relaxation phenomena by conductivity measurement technique [8] based on the internationally accepted symbols of dielectric terminology and parameters. The phenones together with other di- or tri-substituted benzenes having rigid and free dipolar groups at their para positions are included in the present investigation to compare the dielectric relaxation properties with the benzaldehyde groups. Moreover, our aim is to observe how τ 's and μ 's vary with respect to sizes, shapes and structures of the molecules and to get an idea of molecular environment of such polar liquids too, in solvents. For most of the polar liquids the imaginary part σ''_{ij} varies linearly [8] with the real part σ'_{ij} of hf complex conductivity σ^*_{ij} for different w_j 's of a solute. But in the present polar-nonpolar liquid mixtures the variation of σ''_{ij} with σ'_{ij} was not linear [9] to yield τ_j . The ratio of the individual slopes of σ''_{ij} and σ'_{ij} against w_j 's curves at $w_j \rightarrow 0$, on the other hand, is used to get τ_j 's of these p-polar liquids in order to report them in Table 1.

The intercepts and slopes of linear relationship of $\ln(\tau_j T)$ against $1/T$ as shown in Table 2, could, however, be used to obtain thermodynamic energy parameters like enthalpy of activation ΔH_r , entropy of activation ΔS_r and free energy of activation ΔF_r of dielectric

Table 1

The ratio of slopes of concentration variation of imaginary σ''_{ij} and real σ'_{ij} parts of high frequency complex conductivity σ^*_{ij} at $w_j \rightarrow 0$ estimated and reported τ_j in pico second, dimensionless parameter b [$= 1/(1 + \omega^2 \tau_j^2)$], coefficients α, β, γ , of equation: $\sigma_{ij} = \alpha + \beta w_j + \gamma w_j^2$, estimated and reported dipole moment μ_j in Coulomb-metre at different experimental temperatures in $^\circ\text{C}$ and the theoretical dipole moment μ_{theo} in Coulomb-metre from bond angles and bond moments for different para compounds.^a

System with Sl. No. and Molecular weight M_j	Temp. in $^\circ\text{C}$	Ratio of slopes of σ''_{ij} & σ'_{ij} with w_j ($d\sigma''_{ij}/dw_j$) $x/y = \frac{(d\sigma''_{ij}/dw_j)}{(d\sigma'_{ij}/dw_j)}$	Estimated τ_j in p.sec	Reported τ_j in p.sec	Dimen- sionless para- meter $b = 1/$ $(1 + \omega^2 \tau_j^2)$	Coefficients in the equation $\sigma_{ij} = \alpha + \beta w_j + \gamma w_j^2$			Estimated $\mu_j \times 10^{30}$ in Coulomb metre	Reported $\mu_j \times 10^{30}$ in Coulomb metre	Dipole moments $\mu_{\text{theo}} \times 10^{30}$ from bond angles and bond moments
						$\alpha \times 10^{-10}$	$\beta \times 10^{-11}$	$\gamma \times 10^{-12}$			
1. Para hydroxy- propiofenone $M_j = 0.150\text{kg}$	17	0.8287	19.86	-	0.4070	12.8647	-5.0205	42.5270	0.00		
	23	0.7451	22.08	25.40	0.3571	12.8887	0.0919	15.2643	2.36	10.20	8.27
	30	0.7028	23.41	24.20	0.3307	13.5236	-2.4503	-24.4312	0.00		
2. Para - chloropro- piofenone $M_j = 0.1685\text{kg}$	37	1.1073	14.86	23.10	0.5508	12.9387	-19.9001	5.2591	15.03		
	19	0.7427	22.15	20.80	0.3556	12.7486	-1.3145	6.8967	9.43	9.84	9.73
	25	0.8261	19.92	19.70	0.4056	12.9382	-1.5409	16.8094	0.00		
3. Para acetamido- benzaldehyde $M_j = 0.163\text{kg}$	31	0.7272	22.63	18.20	0.3458	12.8983	1.4290	0.2140	10.31		
	37	2.1799	7.55	17.10	0.8261	12.5003	13.8819	-64.5742	21.14		
	17	0.5756	28.58	21.80	0.2490	13.0577	0.7906	6.5180	8.55	10.37	13.12
4. Para benzyloxy benzaldehyde $M_j = 0.212\text{kg}$	23	0.7736	21.27	20.80	0.3744	13.0602	2.5550	-7.2309	12.75		
	30	0.7260	22.66	19.00	0.3453	12.9053	5.8673	17.9855	20.51		
	37	1.0111	16.27	18.60	0.5056	12.6908	13.9352	-50.5510	26.62		
	20	0.5865	28.06	20.00	0.2259	12.9919	1.3256	-3.8704	12.56		
	25	0.6247	26.34	19.40	0.2807	13.1236	1.0601	-	10.87	10.63	6.23
	30	0.8358	19.69	18.00	0.4112	13.2032	1.3264	-	10.19		
	35	1.2238	13.44	16.90	0.5998	13.3518	0.8984	-	7.04		

System with Sl. No. and Molecular weight M_j	Temp. in $^{\circ}\text{C}$	Ratio of slopes of σ'_{ij} & σ''_{ij} with w_j ($d\sigma'_{ij}/dw_j$) $x/y = \frac{d\sigma'_{ij}/dw_j}{d\sigma''_{ij}/dw_j}$	Estimated τ_j in p. sec	Reported τ_j in p. sec	Dimensionless parameter $h = 1/(1 + \sigma_j^2)^2$ $\alpha \times 10^{-10}$	Coefficients in the equation $\sigma_{ij} = \alpha + \beta w_j + \gamma w_j^2$ $\beta \times 10^{-11}$ $\gamma \times 10^{-12}$			Estimated $\mu_j \times 10^{30}$ in Coulomb metre	Reported $\mu_j \times 10^{30}$ in Coulomb metre	Dipole moments from bond angles and bond moments $\mu_{\text{obs}} \times 10^{30}$
5. Paraanisidine $M_j = 0.123$ kg	20	2,2120	7.43	3.89	0.8306	12.8499	6.1740	-16.7410	12.23	5.20	6.28
	30	2,4152	6.81	3.67	0.8537	13.1252	1.8955	-	6.87	10.33	
	40	3,4952	4.71	3.17	0.9243	13.1862	1.9022	-	6.79	8.87	
6. Paraphenitidine $M_j = 0.137$ kg	20	1,5288	10.76	11.08	0.7005	13.3177	5.4487	-	13.21	7.47	15.04
	30	1,9049	8.64	10.63	0.7839	12.7717	14.0691	-24.4860	20.61	9.27	
	40	2,1036	7.82	9.95	0.8158	13.6273	3.9487	-	2.744	10.98	
7. Ortho-chloro-paranitroaniline $M_j = 0.1725$ kg	20	1,5124	10.88	10.57	0.6958	12.3443	1.2822	-0.9397	7.21	8.13	15.93
	30	1,9522	8.43	9.89	0.7921	12.7291	0.1756	-	2.57	10.93	
	40	2,2126	7.44	9.18	0.8302	12.8787	0.0908	-	1.85	13.10	
8. Para-bromo-nitrobenzene $M_j = 0.202$ kg	20	1,6446	10.01	-	0.7299	13.3533	0.6908	0.2145	5.59	-	8.40
	30	1,7818	9.24	-	0.7603	13.7402	-0.6908	2.5184	0.00	-	
	40	1,9503	8.44	-0.7917	13.8959	-0.5847	2.5301	0.00	-	-	

relaxation process of the rate theory of Eyring et al [10]. The enthalpy of activation ΔH_{η} due to viscous flow was, however, obtained from the slope γ of the linear relationship in $\ln(\tau_j T)$ against $\ln \eta$, where η is the coefficient of viscosity of the solvent to test the behaviour of solutes in solvents.

The value of ΔS_{τ} , and ΔH_{τ} and ΔF_{τ} , of Table 2 give an insight into the molecular dynamics of the systems. The estimated Debye factor $\tau_j T / \eta$ and Kalman factor $\tau_j T / \eta^{\gamma}$ in Table 2 signify the applicability of the required relaxation model for such p-liquids.

Table 2

The intercepts and slopes of $\ln \tau_j T$ against $1/T$ curves, energy parameters like enthalpy of activation ΔH_{τ} in Kilo Joule mole $^{-1}$, the entropy of activation ΔS_{τ} in Joule mole $^{-1}$ K $^{-1}$, free energy of activation ΔF_{τ} in Kilo-Joule-mole $^{-1}$ for dielectric relaxation process, enthalpy of activation ΔH_{η} in Kilo Joule mole $^{-1}$ due to viscous flow, γ as the ratio of ΔH_{τ} and ΔH_{η} , Kalman factor ($\tau_j T / \eta^{\gamma}$), Debye factor ($\tau_j T / \eta$) at different experimental temperatures in $^{\circ}\text{C}$ and the coefficients of μ_j -t equations $\mu_j = a + bt + ct^2$ of different para compounds

System with Sl. No.	Temp. in $^{\circ}\text{C}$	Intercept & slope of $\ln \tau_j T$ vs $1/T$ Curve Intercept slope		ΔH_{τ} in KJ mole $^{-1}$	ΔS_{τ} in J mole $^{-1}$ K $^{-1}$	ΔF_{τ} in KJ mole $^{-1}$	$\gamma = (\Delta H_{\tau} / \Delta H_{\eta})$	ΔH_{η} in KJ mole $^{-1}$	Kalman Factor $\tau_j T / \eta^{\gamma}$	Debye Factor $\tau_j T / \eta$ $\times 10^6$	Coefficients in the equation $\mu_j \times 10^{30} = a + bt + ct^2$		
											a	b	c
1. Para hydroxy propiophenone	17				-19.02	11.53			19.75×10^{-8}	4.0135	35.4250	-3.2286	0.0716
	23	-21.36	-724.41	6.02	-20.49	12.08	0.54	11.15	23.64×10^{-8}	5.0274			
	30				-21.64	12.58			27.55×10^{-8}	6.2221			
2. Para chloro-propiophenone	19				79.57	11.90			0.2112	4.6531	92.9880	-7.1216	0.1407
	25	-33.17	4227.52	35.13	77.86	11.93	2.63	13.36	0.2535	4.7300			
	31				74.30	12.54			0.2938	6.1424			
	37				81.03	10.01			0.1890	2.3761			
3. Para acetamido benzaldehyde	17				7.92						-4.2996	0.6554	0.0050
	23	-24.76	1770.09	14.71	9.17	12.41	1.10	13.37	11.12×10^{-6}	5.7757			
	30				7.31	11.99			9.41×10^{-6}	4.8430			
	37				8.77	12.49			11.86×10^{-6}	6.0228			
4. Para benzyloxy benzaldehyde	20				71.34	12.52			19.57×10^{-4}	5.7293	9.0620	0.4582	0.0146
	25	-32.27	4022.34	33.43	69.81	12.62	1.89	17.68	22.42×10^{-4}	6.0379			
	30				70.24	12.14			22.09×10^{-4}	5.2333			
	35				71.49	11.41			20.70×10^{-4}	4.2025			

System with SI. No.	Temp. in °C	Intercept & slope of $\ln \tau_j T$ Vs $1/T$ Curve Intercept slope	ΔH_τ in KJ mole ⁻¹	ΔS_τ in J mole ⁻¹ K ⁻¹	ΔF_τ in KJ mole ⁻¹	$\gamma = (\Delta H_\tau / \Delta H_n)$	ΔH_n in KJ mole ⁻¹	Kalman Factor $\tau_j T / \eta^2$	Debye Factor $(\tau_j T / \eta) \times 10^6$	Coefficients in the equation $\mu_j \times 10^{30} = a + bt + ct^2$			
		a	b	c									
5. Paraanisidine	20			18.54	9.29			3.20×10^{-4}	3.3647	38.7900	-1.8560	0.0264	
	30	-25.94	1771.20	14.71	17.33	9.47	1.62	9.08	3.82×10^{-4}				3.6781
	40				18.57	8.91			3.07×10^{-4}				2.8188
6. Paraaphentidine	20	-23.58	1167.25	9.70	-1.67	10.19			22.87×10^{-6}	4.8728	-52.6800	4.9975	-0.0851
	30				-1.22	10.07	1.21	8.02	22.49×10^{-6}	4.6665			
	40				-1.68	10.22			22.87×10^{-6}	4.6800			
7. Ortho chloro-para nitroaniine	20				6.19	10.22			17.99×10^{-5}	4.9271	28.2500	-1.4440	0.0196
	30	-24.52	1447.51	12.03	6.88	10.00	1.49	8.07	17.86×10^{-5}	4.5531			
	40				6.18	10.09			18.05×10^{-5}	4.4526			
8. Para bromo-nitrobenzene	20				-20.58	10.01			9.25×10^{-8}	4.5331	33.5400	-1.9565	0.0280
	30	-21.28	479.23	3.98	-20.64	10.24	0.47	8.47	9.44×10^{-8}	4.9906			
	40				-20.58	10.42			9.21×10^{-8}	5.0511			

The dipole moments μ_j 's of all the liquids were finally worked out from the slopes β 's of hf conductivities σ_{ij} 's with w_j 's and dimensionless parameters b 's with the estimated τ_j at all the temperatures. All the μ_j 's placed in Table 1 are found to be temperature dependent quantities. The coefficients a , b and c of μ_j - t curves of Figure 2, are, however, placed in Table 2, in order to compare with the reported μ 's as well as theoretical μ_{theo} 's, obtained from bond angles and bond moments of substituent polar groups attached with the parent ones of Figure 3. The disagreement of the measured μ_j 's with μ_{theo} 's as obtained from Figure 3, for these compounds establishes the fact that the inductive moments combined with the mesomeric moments of the substituent polar groups with the parent molecules is a function of temperature.

2. THEORETICAL FORMULATIONS

Under the hf electric field the dimensionless complex dielectric constant k_{ij}^* is:

$$k_{ij}^* = k'_{ij} - jk''_{ij} \quad (1)$$

where $k'_{ij} = \epsilon'_{ij} / \epsilon_0 =$ real part of dielectric constant and $k''_{ij} = \epsilon''_{ij} / \epsilon_0 =$ dielectric loss factor, respectively. ϵ'_{ij} and ϵ''_{ij} are real and imaginary parts of complex permittivity ϵ_{ij}^* having dimension of Farad meter⁻¹ (F.m⁻¹) and $\epsilon_0 =$ permittivity of free space = 8.854×10^{-12} F.m⁻¹. Hence Murphy-Morgan relation for the complex hf conductivity σ_{ij}^* of a solution of a polar-nonpolar liquid mixture of weight fraction w_j is:

$$\sigma_{ij}^* = \omega \epsilon_0 k_{ij}'' + j \omega \epsilon_0 k_{ij}' \quad (2)$$

where $\sigma'_{ij} (= \omega \epsilon_0 k''_{ij})$ and $\sigma''_{ij} (= \omega \epsilon_0 k'_{ij})$ are the real and imaginary parts of complex conductivity and j is a complex number = $\sqrt{-1}$.

The hf conductivity σ_{ij} is however obtained from:

$$\sigma_{ij} = \omega \epsilon_0 \sqrt{k''_{ij}{}^2 + k'_{ij}{}^2} \quad (3)$$

The imaginary part of hf conductivity σ''_{ij} is related to the real part of hf conductivity σ'_{ij} by

$$\sigma''_{ij} = \sigma_{\alpha ij} + (1/\omega\tau)\sigma'_{ij} \quad (4)$$

where $\sigma_{\alpha ij}$ is the constant conductivity at $w_j = 0$ and τ is the relaxation time of a polar unit = τ_j . Equation (4) on differentiation with respect to σ'_{ij} becomes.

$$(d\sigma''_{ij}/d\sigma'_{ij}) = (1/\omega\tau_j) \quad (5)$$

to yield τ_j of a polar solute. It is often better to use the ratio of the individual slopes of variations of σ''_{ij} and σ'_{ij} with w_j at $w_j \rightarrow 0$ to avoid the effect of polar-polar interactions in a liquid mixture to get τ_j from:

$$(d\sigma''_{ij}/dw_j)_{w_j \rightarrow 0} / (d\sigma'_{ij}/dw_j)_{w_j \rightarrow 0} = 1/\omega\tau_j$$

$$\text{or, } x/y = 1/\omega\tau_j \quad (6)$$

Again, it is observed experimentally that σ''_{ij} is nearly equal to σ_{ij} of equation (3) under hf alternating electric field, hence equation (4) becomes :

$$\sigma_{ij} = \sigma_{\alpha ij} + (1/\omega\tau_j)\sigma'_{ij}$$

$$\text{or } (d\sigma'_{ij}/dw_j) = \omega\tau_j\beta \quad (7)$$

where $\beta = (d\sigma_{ij}/dw_j)$ = the slope of σ_{ij} - w_j curve at $w_j \rightarrow 0$.

All the β 's are however, presented in Table 1 for all the liquids. The real part of hf conductivity [9-12], σ'_{ij} at T K of a given solution of w_j is :

$$\sigma'_{ij} = (N\rho_{ij}\mu_j^2/27\varepsilon_0k_B M_j T)(\omega^2\tau/1 + \omega^2\tau^2)(\varepsilon_0k_{\alpha ij} + 2)(\varepsilon_0k_{\alpha ij} + 2)w_j \quad (8)$$

which on differentiation with respect to w_j and at $w_j \rightarrow 0$ yields :

$$(d\sigma'_{ij}/dw_j)_{w_j \rightarrow 0} = (N\rho_{ij}\mu_j^2/3\varepsilon_0k_B T M_j) \left(\frac{\varepsilon_i + 2}{3} \right)^2 (\omega^2\tau/1 + \omega^2\tau^2) \quad (9)$$

where N = Avogadro's Number, ρ_i = density of solvent, ε_i = dielectric permittivity of the solvent, M_j = molecular weight of solute and k_B = Boltzmann constant. All the symbols stated above are expressed in SI units. From equations (7) and (9) one gets μ_j in Coulomb meter under hf electric field as

$$\mu_j = \left[\frac{27\varepsilon_0k_B T M_j \beta}{N\rho_i(\varepsilon_i + 2)^2 \omega b} \right]^{1/2} \quad (10)$$

in terms of a dimensionless parameter 'b'

$$b = 1/(1 + \omega^2 \tau_j^2) \quad (11)$$

with the measured τ_j of the liquid.

All the measured τ_j 's in terms of β 's and b 's of equations (10) and (11) are, however, placed in Table 1 and compared with the reported μ 's and μ_{theo} 's the latter ones are obtained from bond angles and bond moments of the substituted groups of the molecules as shown in Figure 3.

3. RESULTS AND DISCUSSIONS

The relaxation time τ_j 's of the para polar liquids as reported in Table 1 in dioxane and benzene respectively were estimated from the ratio of the individual slopes of both the imaginary σ''_{ij} and real σ'_{ij} parts of high frequency conductivity σ^*_{ij} with weight fraction w_j of polar solutes at different experimental temperatures in °C under 3 cm. wavelength electric field. τ_j 's of these liquids could not be obtained directly from the slope of equation (5) of σ''_{ij} with σ'_{ij} because of the non-linear character [8]. Thus the ratio of the individual slopes of $\sigma''_{ij}-w_j$ and $\sigma'_{ij}-w_j$ curves at $w_j \rightarrow 0$ was used to get τ_j 's of these para polar liquids

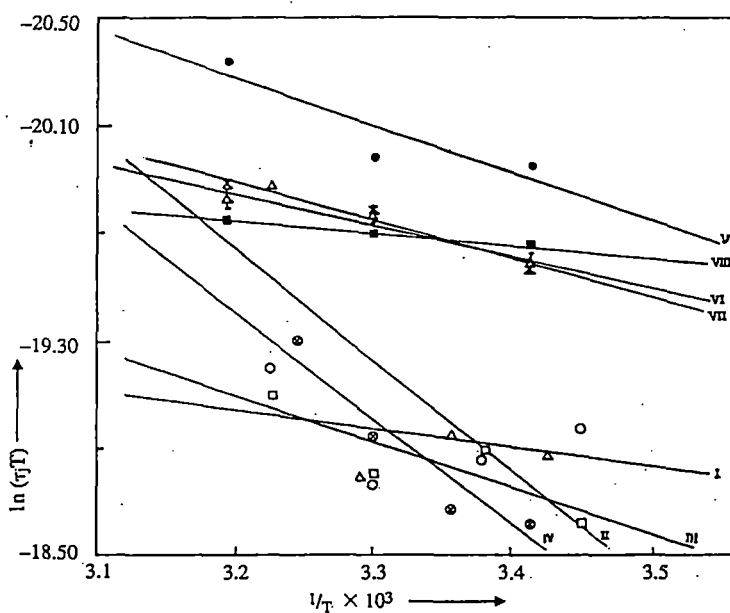


Figure 1. Straight line plots of $\ln(\tau_j T)$ against $1/T$. (I) parahydroxypropiophenone ($-\circ-$), (II) parachloropropiophenone ($-\triangle-$), (III) paracetamidobenzaldehyde ($-\square-$), (IV) parabenzoyloxybenzaldehyde ($-\odot-$), (V) paraanisidine ($-\bullet-$) (VI) parafenitidine ($-\triangle\cdot-$), (VII) orthochloroparanitroaniline ($-\times-$) and (VIII) parabromonitrobenzene ($-\blacksquare-$)

from equation (6) in order to minimize the effects of dipole-dipole interactions, macroscopic viscosity, internal field etc.

The estimated ratio of the individual slopes of σ''_{ij} and σ'_{ij} curves with w_i 's together with estimated and reported τ 's are placed in the 3rd, 4th and 5th columns of Table 1. The τ_j 's thus obtained agree well with the reported τ_j 's where such are available [6,7] based on Gopalakrishna's method [13]. As observed in Table 1, the τ_j 's of molecules having phenone and benzaldehyde groups are higher in comparison to other di- and tri-substituted para polar molecules. This is probably due to larger sizes of the rotating units. It is also interesting to note that variation of τ_j of such molecules as presented in Table 1 are irregular in disagreement with the Debye model of relaxation as observed elsewhere [4]. This may be explained by the fact that stretching of bond angles and bond moments of polar groups with temperature and the distribution of bond moments around the parent molecules leads to either symmetric or asymmetric shape of the molecules. The rest of the molecules show the lower values of τ decreasing with increase of temperature in agreement with the Debye relaxation in spite of the fact that they are nonspherical.

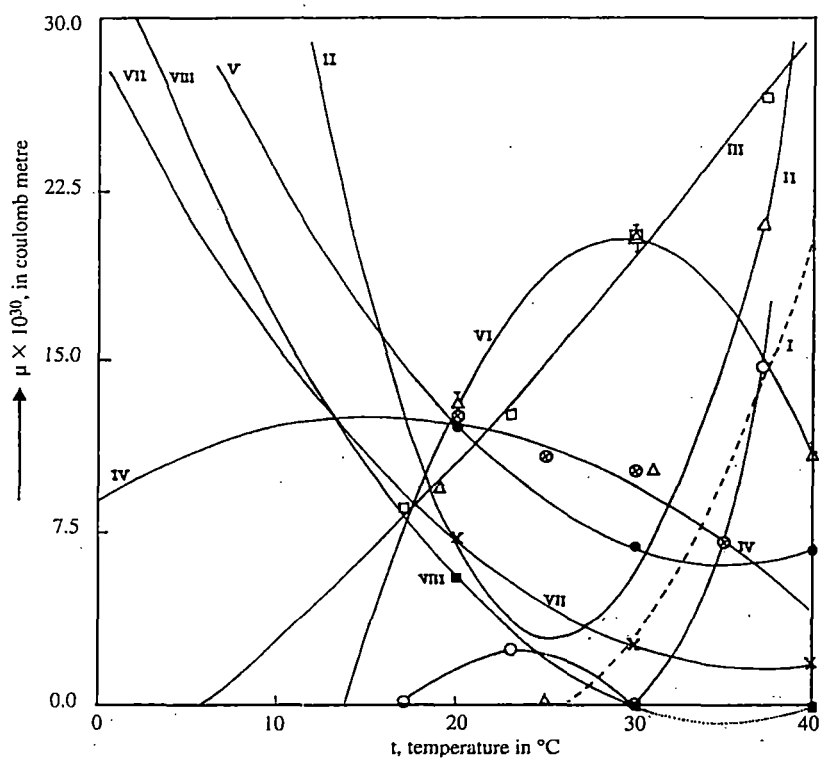


Figure 2. Variation of dipolemoments $\mu_i \times 10^{30}$ in Coulomb metre against t in $^{\circ}\text{C}$, (I) parahydroxypropio-phenone ($-\text{O}-$), (II) parachloropropiophenone ($-\Delta-$), (III) paraaceta-midobenzaldehyde ($-\square-$), (IV) parabenzoyloxybenzaldehyde ($-\otimes-$), (V) paraanisidine ($-\bullet-$), (VI) paraphenitidine ($-\frac{1}{2}-$), (VII) ortho-chloroparanitroaniline ($-\times-$) and (VIII) parabromonitrobenzene ($-\blacksquare-$).

The process of rotation of the rotating dipoles requires an activation energy sufficient to overcome the energy barrier, between two equilibrium positions, one can write according to Eyring et al [10] with the known τ_i by:

$$\begin{aligned}\tau_j &= (A/T)e^{\Delta F_r/RT} \quad (\Delta F_r = \Delta H_r - T\Delta S_r) \\ \text{or, } \ln(\tau_j T) &= \ln(Ae^{-\Delta S_r/R}) + (\Delta H_r/RT) \\ &= \ln A' + (\Delta H_r/R) \cdot (1/T)\end{aligned}\quad (12)$$

Equation (12) is a straight line of $\ln(\tau_j T)$ against $1/T$ having intercept and slope to measure the thermodynamic energy parameters like enthalpy of activation (ΔH_r), entropy of activation (ΔS_r) and free energy of activation (ΔF_r) of dielectric relaxation process of the molecules. The intercepts and slopes of the least squares fitted $\ln(\tau_j T)$ against $1/T$ curves as illustrated graphically in Figure 1, were accurately obtained and placed in the 3rd and 4th column of Table 2. The variation of $\ln \tau_j T$ against $1/T$ are linear for almost all the liquids with the available experimental data. The enthalpy of activation ΔH_r due to viscous flow of the solvent was, however, estimated from the slope of the linear equation of $\ln(\tau_j T)$ against $\ln \eta$ at different experimental temperatures. As evident from Table 2, the values of γ ($= \Delta H_r/\Delta H_\eta$) > 0.50 for all the liquids except parabromonitrobenzene exhibit the solvent environment around the solute molecules which behave as solid phase rotators. The low value of γ , on the other hand, for p-bromonitrobenzene may indicate the weak molecular interaction of such dipole with benzene. The values of ΔS_r 's for the system like p-hydroxypropiofenone, p-phenitidine and p-bromonitrobenzene are negative. This is due to the fact that activated states are more ordered than the normal states unlike other molecules. The high values of ΔS_r and ΔH_r of p-chloropropiofenone and p-benzyloxybenzaldehyde indicate the activated states are not stable probably due to internal resistance suffered by larger dipole rotations. The rest of the molecules possess ΔH_r of nearly the same magnitude. The ΔF_r 's between the activated and unactivated states of all the systems are, however, the same as the activation that is accomplished by the rupture of bonds of dipolar groups in the same degree of freedom [6,7]. Unlike the Kalman factor $\tau_j T/\eta^\gamma$ at different temperatures the Debye factor $\tau_j T/\eta$ is almost constant signifying the applicability of Debye model of relaxation behaviour for such para liquids [14]. The μ_j 's from equation (10) of all the p-liquids were obtained from slopes β 's of $\sigma_{ij}-w_j$ curves and dimensionless parameters b 's of equation (11) involved with measured τ_j 's of equation (6). The slopes and intercepts of σ_{ij} against w_j as presented in Table 1 were obtained by careful regression technique and are found to be almost constant ($\sim 10^{-12} \Omega^{-1} m^{-1}$) at all the experimental temperatures under 3 cm. wavelength electric field perhaps for their same polarity. Thus σ'_{ij} , σ''_{ij} and σ_{ij} with w_j 's could not be shown graphically. Parahydroxypropiofenone (curve I) and p-acetamidobenzaldehyde (curve III) showed the monotonic increase of μ_j with temperature (Figure 2) for their increasing molecular asymmetry at higher temperatures. The μ_j-t curves of p-benzyloxybenzaldehyde (curve IV) and p-phenitidine (curve VI) are convex in nature [15] showing zero values at lower and higher temperatures unlike the other four assuming minimum values at different temperatures as seen in Figure 2. (The least squares fitted μ_j-t curve for p-bromonitrobenzene which showed 5.59×10^{-30} C.m at 20°C but zero values of μ_j at 30°C and 40°C for its strong symmetry attained at those temperatures was, however, obtained. Like curves II, V and VII of other p-compounds it (curve VIII) also showed minimum having-ve μ_j between 30°C to 40°C, shown by dotted line to satisfy the continuous curve. The usual variation of μ_j against t°C for p-hydroxypropiofenone (curve I) is shown by least squares fitted dotted line together with the solid line drawn through the estimated

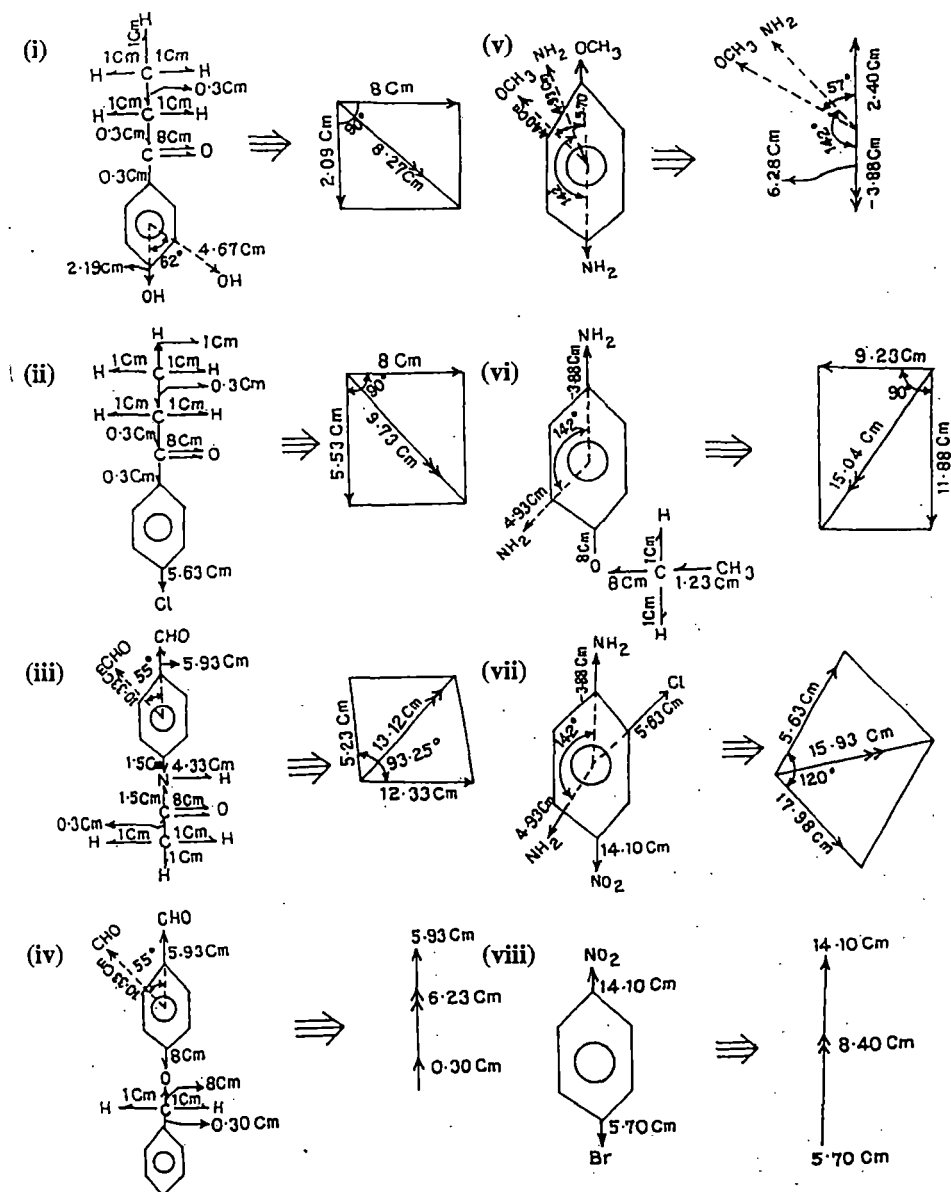


Figure 3. Conformational structures from available bond moments and bond angles of para compounds : (i) para-hydroxypropiophenone (ii) para-chloropropiophenone (iii) para-acetamidobenzaldehyde (iv) para-benzyl-oxybenzaldehyde (v) para-anisidine (vi) para-phenitidine (vii) ortho-chloroparanitroaniline and (viii) para-bromonitrobenzene.

μ_j 's.) The above nature of μ_j -t curves are explained by the rupture of solute-solvent (monomer) and solute-solute (dimer) associations due to stretching of bond angles and bond moments of substituted polar groups at different temperatures.

The theoretical dipole moments μ_{theo} 's of all the p-liquids were also calculated from the vector addition of the available bond moments 4.67, 10.33, -1.40, 4.40, 1.00, 8.00, 5.63, 1.50, 14.10 and 5.70 multiples of 10^{-30} Coulomb metre (C.m) for C \rightarrow OH, C \rightarrow CHO, C \rightarrow OCH₃ and C \rightarrow NH₂ bonds making angles 62°, 55°, 57°, 142° and 0° for the rest C \rightarrow H, C \rightleftharpoons O, C \rightarrow Cl, C \rightarrow N, C \rightarrow NO₂ and C \rightarrow Br bonds respectively with C atom of the parent molecules which are assumed to be planar structures, as shown in Figure 3. The μ_{theo} 's thus obtained are finally placed in the 12th column of Table 1. The slight disagreement between measured μ_j 's and μ_{theo} 's reveals the presence of inductive and mesomeric moments of the substituent polar groups due to their aromaticity. In p-acetamidobenzaldehyde, p-phenetidine, orthochloroparanitroaniline and p-bromonitrobenzene, the μ_{theo} 's are larger while for others μ_{theo} 's are smaller than the measured values. This fact at once predicts that the substituent polar groups in former molecules push the electrons towards the electro-negative atoms and thereby inductive effect is less than in latter system where they pull the electrons. The electromeric effect is also prominent in the system containing C \rightleftharpoons O groups.

4. CONCLUSION

A very convenient method to evaluate τ_j 's from the ratio of the individual slopes of σ''_{ij-w_j} and σ'_{ij-w_j} curves at $w_j \rightarrow 0$ and the corresponding μ_j 's in SI units of several chain like para liquids at different experimental temperatures is suggested in order to avoid polar-polar interactions. The slopes of σ''_{ij-w_j} - σ'_{ij-w_j} curves are very often not linear in almost all liquids and hence could not be used to obtain τ_j 's. Both τ_j 's and hence μ_j 's within the accuracy of 10% and 5% are now reliable. Para-hydroxypropiophenone, and p-chloropropiophenone show zero values of μ at certain temperatures owing to their symmetry gained at that temperatures. The variation of μ with temperature in °C is not a new concept, but for p-liquids the convex, concave or gradual increase occur probably due to association or dissociation of solute-solute and solute-solvent molecular associations and stretching, of bond moments of the substituent polar groups at different temperatures. Different thermodynamic energy parameters could, therefore, be estimated from the stand point of Eyring's rate theory [15,16] to infer the molecular dynamics of the nonspherical liquids. μ_{theo} 's of the molecules could, however, be found out from the available bond angles and bond moments of the substituent polar groups attached to the parent molecules. They are usually found to differ from the measured μ_j 's indicating the existence of mesomeric and inductive effects in polar liquids due to their aromaticity.

References

- [1] G S Kastha, J Dutta, J Bhattacharyya and S B Roy, Ind J Phys 43 B (1965) 14.
- [2] C R Acharyya, A K Chatterjee, P K. Sanyal and S Acharyya, Ind. J. Pure & Appl. Phys. 24 (1986) 234.
- [3] U. Saha and S Acharyya Ind. J. Pure & Appl. Phys 31 (1993) 181.
- [4] S Acharyya, A K Chatterjee, P Acharyya and I L Saha, Ind. J Phys. 56 (1982) 291.
- [5] J P Shukla, S I Ahmed, D D Shukla and M C Saxena, J Phys. Chem 72 (1968) 1013.
- [6] R L Dhar, A Mathur, J P Shukla and M C Saxena, Ind. J. Pure. & Appl Phys. 11 (1973) 568.

- [7] S K S Somevanshi, S B I Misra and N K Mehrotra, *Ind. J Pure and Appl Phys.* **16** (1978) 57.
- [8] M B R Murthy, R L Patil and D K Deshpande, *Ind. J. Phys.* **63 B** (1989) 491.
- [9] R C Basak, A Karmakar, S K Sit and S Acharyya, *Ind. J Pure & Appl. Phys.* **37** (1999) 224.
- [10] H Eyring, S Glasstone, and K J Laidler, *The theory of rate process* (Mc Graw Hill NY) 1941.
- [11] F J Murphy and S O Morgan, *Bell. Syst. Tech. J* **18** (1939) 502.
- [12] C P Smyth, *Dielectric behaviour and structure* (Mc Graw Hill New York) 1955.
- [13] K V Gopala krishna, *Trans. Faraday Soc.* **53** (1957) 767.
- [14] K Dutta, S K Sit and S Acharyya, *Ind. J Pure & Appl Phys.* Communicated 1999.
- [15] H Eyring, *J Chem Phys.* **4** (1936) 283.
- [16] W Kauzmann, *Rev. mod. Phys.* **14** (1942) 12.

INFORMATION FOR AUTHORS

Both review papers and original work will be published. Those intending to write a review are invited to get in touch with the Editor for a preliminary discussion of scope. There is no limitation on length, but it would be convenient if some idea could be given of the probable length of the contribution in pages of camera-ready copy.

Submission of papers

Authors are requested to submit three copies of their manuscript to:

Professor Josef Barthel, Institut für Physikalische und Theoretische Chemie, Universität Regensburg, D-93040 Regensburg, Germany. Fax +49.941.943.4532.

Submission of an article is understood to imply that the article is original and unpublished and is not being considered for publication elsewhere. Upon acceptance of an article by the journal, author(s) will be asked to transfer the copyright of the article to the publisher. This transfer will ensure the widest dissemination of information.

Reprints

Fifty reprints will be supplied free of charge. Additional reprints can be ordered at prices shown on the reprint order form which will be sent after the Editor's acknowledgement of acceptance of the paper.

Instructions for the preparation of a camera-ready paper

The points mentioned below give a summary of the absolute minimum technical requirements to which your contribution should adhere. All text material and illustrations will be photographically reduced by 20–25%.

1. Format

21 cm x 16 cm (8.25" 8 x 6.25"): text dimensions (length and width) for opening page.

23 cm x 16 cm (9.00" 8 x 6.25"): text dimensions (length and width) for all subsequent pages.

Deviations from this text area are not acceptable.

Spacing: 1.0 (single line) spacing

2. Typefonts

Laser/jet printers:

Recommended fonts: 12 point 'Times Roman' (use this font wherever possible), 'Helvetica', 'Bookman Light', and 'New Century Schoolbook'.

Text length: equivalent to approximately 48 single-spaced lines.

Electric typewriter/daisywheel printer:

Recommended fonts: 10 pitch 'Courier', 12 pitch 'Letter Gothic'/'Prestige Elite'. Text width: can be translated into 63 or 76 characters per line using 10 and 12 pitch typing fonts, respectively.

Text length: equivalent to approximately 50 single-spaced lines.

Do not use small font sizes for footnotes. (Remember text reduction to 75–80%.)

3. Printout

Printout must be an original copy. Photocopies are not acceptable.

Paper: print onto either Elsevier camera-ready sheets, A4, or US Letter Paper format. If Elsevier's paper is not used, the paper must be plain white, high quality, and smooth. Print on only one side of the sheet.

Positioning of printout on paper: not critical provided approximately 3 cm (1") of space is left free above the first text line.

Quality of printout: must have uniform contrast over whole text page, be dark and sharp. Printout which is streaked, has lighting variations at the margins, is grey, fuzzy, broken or flecked is not acceptable.

Mathematical symbols and equations must be typed or drawn accurately; handwritten characters are unacceptable.

4. Illustrations

Illustrations must be original drawings or sharp black and white prints. Attach them on/near the page where they are first described with a few spots of suitable glue. Do not use transparent adhesive tape. All notations and details must be legible after reduction. Photocopies, colour plates, screened photographs, and slides are not generally acceptable.

5. Language

Use good, explicit English. Consult a native speaker and/or dictionary where necessary. Authors in Japan please note: Upon request, Elsevier Science Japan will provide authors with a list of people who can check and improve the English of their paper (before submission). Please contact our Tokyo office: Elsevier Science Japan, 1-9-15 Higashi-Azabu, Minato-ku, Tokyo 106-0044; Tel. (03)-5561-5033; Fax (03)-5561-5047.

6. Layout

The tables and illustrations must appear in the appropriate positions in the text with about 1 cm of space above and below. If illustrations need to be reduced they must fit in the available space left in the text. Tables and figures with legends must be incorporated in the text at the appropriate places; it is not acceptable to collect these on separate pages for later placement. The reference list should run on from the end of the text.

7. Miscellaneous

Text must be proof-read and checked for completeness. Label pages with your name and numerical order on their reverse side.

Structural and associational aspects of dielectropolar straight chain alcohols from relaxation phenomena

N Ghosh, A Karmakar, S K Sit & S Acharyya

Department of Physics, Raiganj College (University College), PO Raiganj, Dist Uttar Dinajpur, 733 134 (West Bengal)

Received 15 November 1999; revised 27 March 2000; accepted 6 June 2000

The structural and associational aspects of some straight chain aliphatic alcohols are inferred from their static dipole moments μ_s 's and high frequency (hf) dipole moments μ_j 's in terms of relaxation times τ_j 's under effective dispersive region of nearly 24 GHz electric field. τ_j 's are estimated from the slope of the linear variation of imaginary part σ''_{ij} with real part σ'_{ij} of hf complex conductivity σ^*_{ij} for different weight fractions w_j in order to compare with those obtained from the ratio of the individual slopes of σ'_{ij} and σ''_{ij} with w_j 's of solutes. The linear coefficients of the static experimental parameter X_{ij} with w_j are used to obtain μ_s . The slopes β 's of σ_{ij} with w_j 's are employed to get hf μ_j in terms of τ_j 's obtained by two methods only to see how far they agree with μ_1 and μ_2 from double relaxation method (Sit & Acharyya, 1996 and Sit *et al.*, 1997). It is observed that -OH bond of alcohols about $\equiv C-O-$ bond rotates under GHz electric field. The slight disagreement of theoretical dipole moments μ_{theo} 's from available bond angles and bond moments with μ_j 's and μ_s 's suggest the strong hydrogen bonding in them, in addition to mesomeric and inductive moments of the substituent polar groups attached to the parent molecule.

1 Introduction

The relaxation phenomenon of a dielectropolar liquid in a solvent has attracted the attention of a large number of workers¹⁻³ as it is a very sensitive and useful tool to ascertain the shape, size and structure of a polar molecule. The technique provides one with much information about the stability⁴ of the system undergoing relaxation phenomena. It also offers valuable insight into the solute-solute i.e. dimer and solute-solvent i.e. monomer formations⁴. Structural and associational aspects of a polar liquid in a nonpolar solvent can, however, be gained by measured static dipole moment μ_s and high frequency (hf) dipole moment μ_j in terms of relaxation time τ_j and slope β of hf conductivity σ_{ij} with weight fraction w_j .

Alcohols behaving like almost polymers have α , β and γ etc. dispersion regions. The strong dipole of -OH group rotates about $\equiv C-O-$ bond without disturbing CH_3 or CH_2 groups and thus they have possibility to exhibit intramolecular as well as intermolecular rotations. Sit and Acharyya⁵ and Sit *et al.*⁶ studied the straight long chain alcohols like 1-butanol, 1-hexanol, 1-heptanol, 1-decanol in *n*-heptane⁷, ethanol and methanol in benzene⁸ (9.84GHz) and 2-methyl-3-heptanol, 3-methyl-3-heptanol, 4-methyl-3 heptanol, 5-methyl-3-heptanol, 4-octanol and 2-octanol, in *n*-heptane⁹ at 25°C

to observe that all the alcohols except methanol showed the double relaxation times τ_1 and τ_2 at all the frequencies in GHz range. The alcohols were again expected to exhibit the triple relaxation phenomena⁷ for different frequencies of electric field in GHz range. Such long chain liquids under investigation have wide applications in the fields of biological research, medicine and industry. Moreover, the study of alcohols in terms of modern internationally accepted units and symbols appears to be superior for the unified, coherent and rationalized nature of the SI unit used.

The μ_s of all the associated dielectropolar molecules under static electric field was derived from static experimental parameter X_{ij} . X_{ij} is again involved with the dimensionless dielectric constants k_{0ij} and $k_{\infty ij}$ of Table 1. from the measured relaxation permittivities static ϵ_{0ij} and hf $\epsilon_{\infty ij}$ of dimensions Farad metre⁻¹ (F.m.⁻¹) based on Debye model¹⁰. The linear coefficients of the expected nonlinear experimental X_{ij} curves against w_j graphically shown in Fig. 1, of alcohols were conveniently used to estimate μ_s at a given temperature.

The τ_j of all the alcohols were, however, estimated from the slope of linear variation of imaginary σ''_{ij} against real σ'_{ij} parts¹¹ of hf complex conductivity σ^*_{ij} for different w_j 's as seen in Fig. 2. The hf σ''_{ij} did not vary linearly with hf σ'_{ij} at higher or even lower concen-

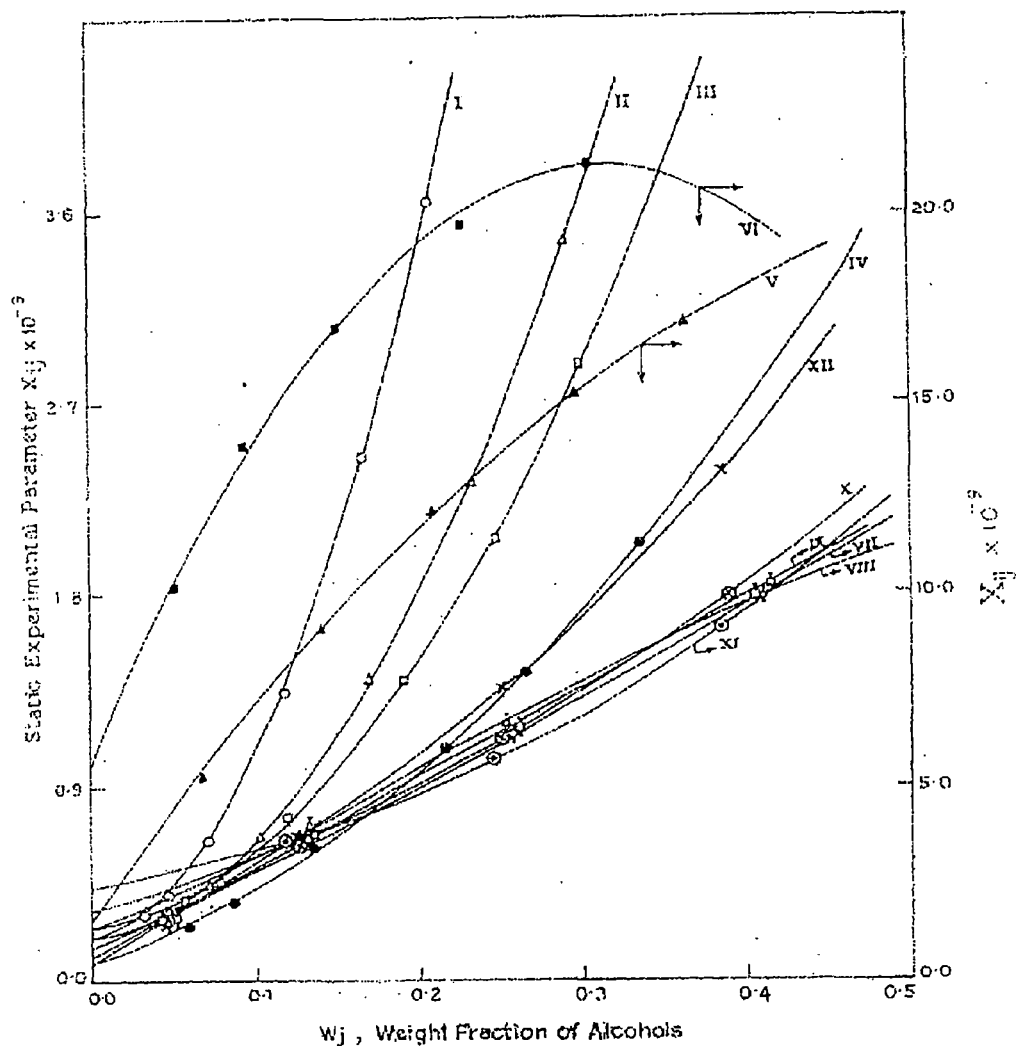


Fig. 1 — Variation of static experimental parameter ($X_{ij} \times 10^{-3}$) against weight fraction w_j of solute at 25°C under nearly 24 GHz electric field [ethanol and methanol at 9.84 GHz]

- | | |
|---|--|
| System - I 1-butanol (— O — O —): | System - VII 2-methyl - 3 heptanol (— Φ — Φ —): |
| System - II 1-hexanol (— Δ — Δ —): | System - VIII 3-methyl - 3 heptanol (— Λ — Λ —): |
| System - III 1-heptanol (— \square — \square —): | System - IX 4-methyl - 3 heptanol (— Γ — Γ —): |
| System - IV 1-decanol (— \bullet — \bullet —): | System - X 5-methyl - 3 heptanol (— \otimes — \otimes —): |
| System - V ethanol (— \blacktriangle — \blacktriangle —): | System - XI 4-Octanol (— \ominus — \ominus —): |
| System - VI methanol (— \blacksquare — \blacksquare —): | System - XII 2-Octanol (— x — x —) |

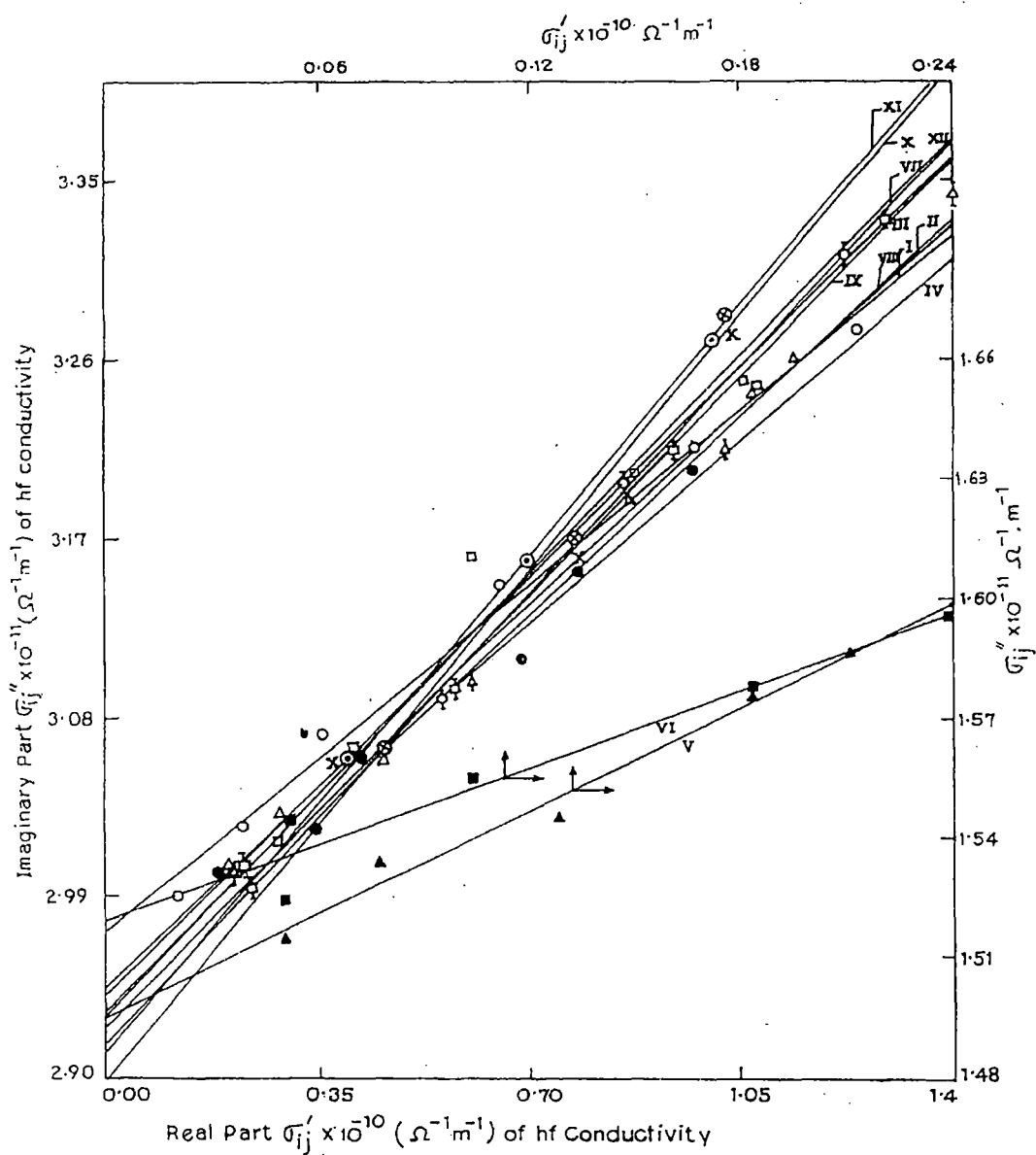


Fig. 2 — Variation of imaginary part of conductivity $\sigma''_{ij} \times 10^{-11}$ in $\Omega^{-1} \text{m}^{-1}$ against real part of conductivity $\sigma'_{ij} \times 10^{-10}$ in $\Omega^{-1} \text{m}^{-1}$

System - I 1-butanol (—○—○—):

System - II 1-hexanol (—△—△—):

System - III 1-heptanol (—□—□—):

System - IV 1-decanol (—●—●—):

System - V ethanol (—▲—▲—):

System - VI methanol (—■—■—):

System - VII 2-methyl - 3 heptanol (—⊖—⊖—):

System - VIII 3-methyl - 3 heptanol (—⊕—⊕—):

System - IX 4-methyl - 3 heptanol (—⊖—⊖—):

System - X 5-methyl - 3 heptanol (—⊗—⊗—):

System - XI 4-Octanol (—⊖—⊖—):

System - XII 2-Octanol (—x—x—)

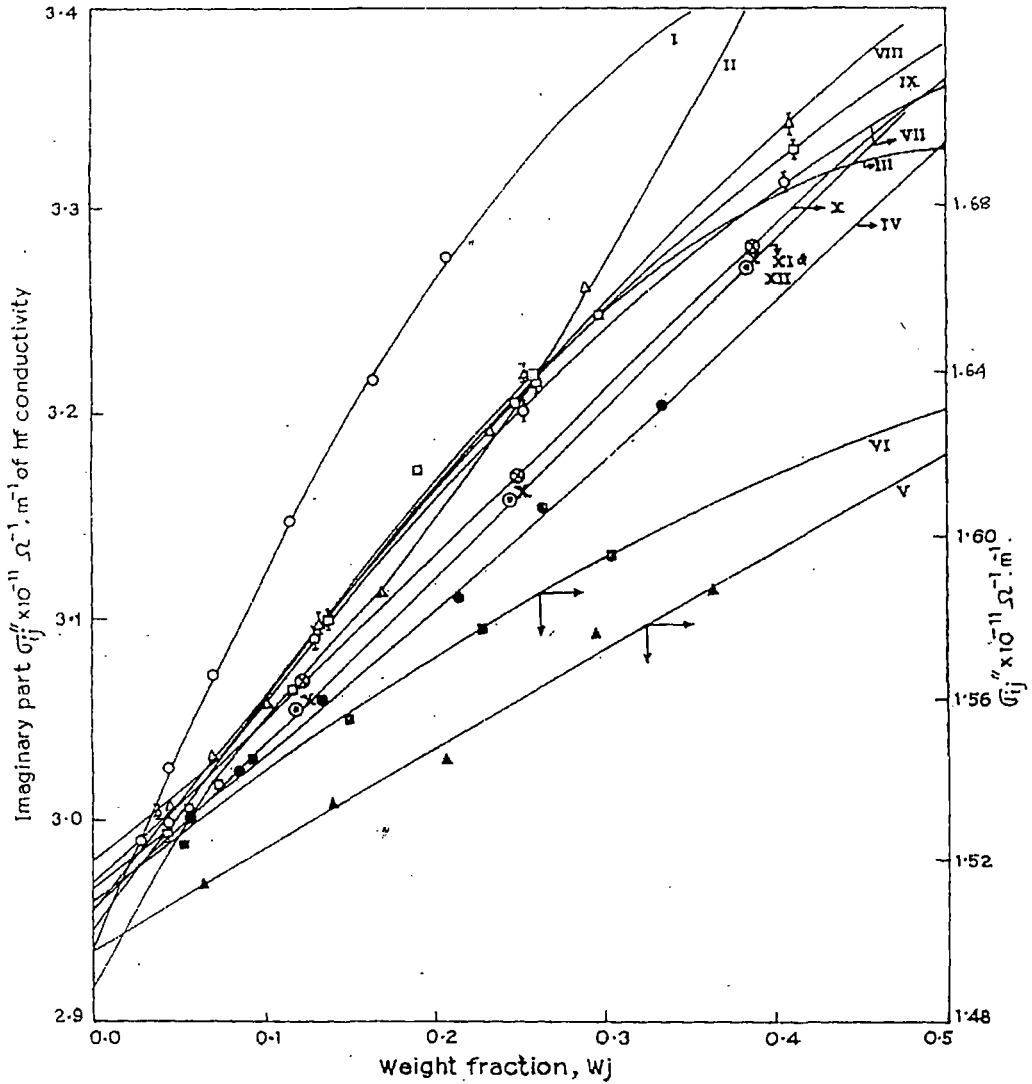


Fig. 3 — Plot of imaginary part of conductivity $\sigma''_{ij} \times 10^{-11}$ in $\Omega^{-1} m^{-1}$ against weight fraction w_j of solute at 25°C under nearly 24 GHz electric field. [ethanol and methanol at 9.84 GHz.]

- | | |
|----------------------------------|---|
| System - I 1-butanol (—○—○—); | System - VII 2-methyl - 3 heptanol (—⊖—⊖—); |
| System - II 1-hexanol (—△—△—); | System - VIII 3-methyl -3 heptanol (—⊖—⊖—); |
| System - III 1-heptanol (—□—□—); | System - IX 4-methyl - 3 heptanol (—⊖—⊖—); |
| System - IV 1-decanol (—⊙—●—); | System - X 5-methyl - 3 heptanol (—⊗—⊗—); |
| System - V ethanol (—▲—▲—); | System - XI 4-Octanol (—⊙—⊙—); |
| System - VI methanol (—■—■—); | System - XII 2-Octanol (—x—x—) |

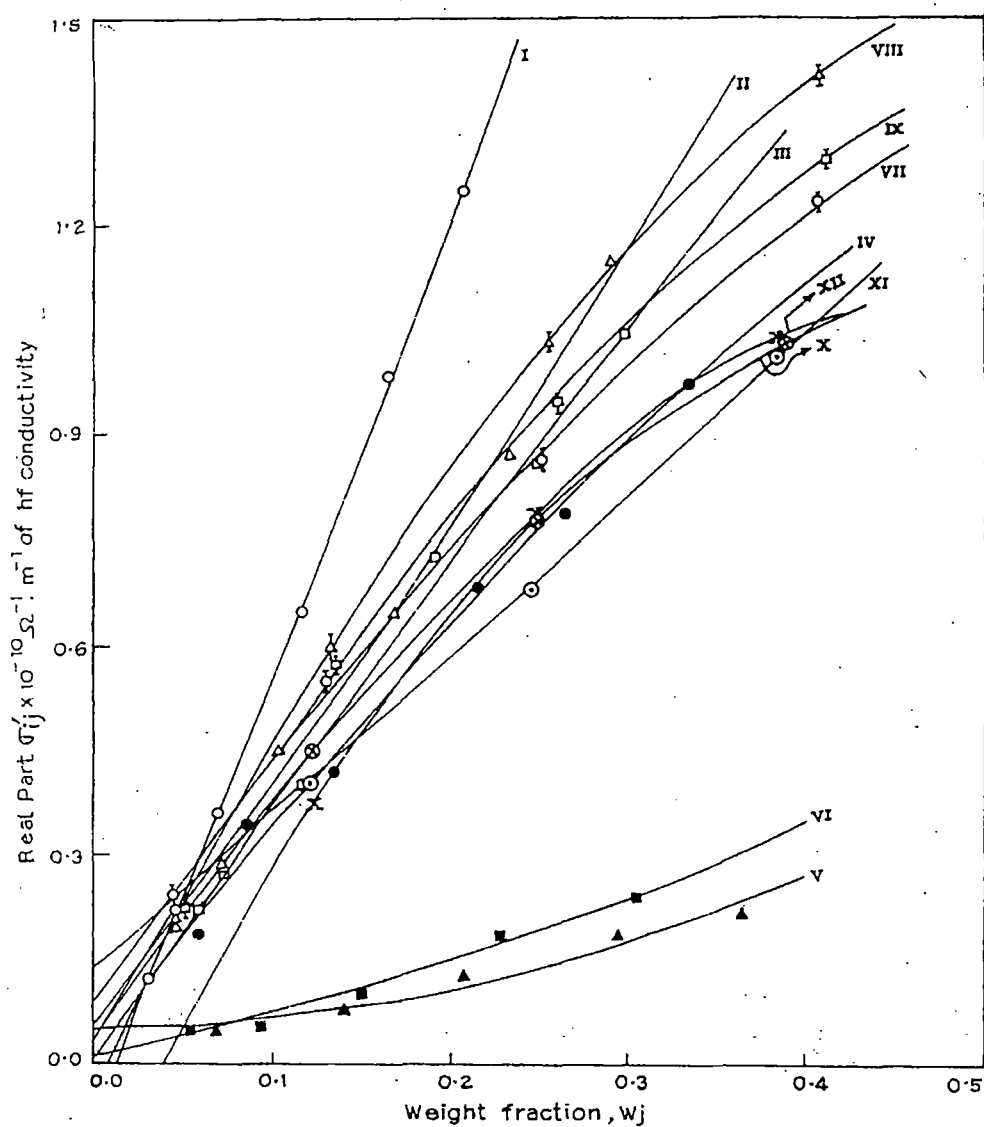


Fig. 4 — Plot of real part of conductivity $\sigma'_{ij} \times 10^{-10}$ in $\Omega^{-1} \text{m}^{-1}$ against weight fraction w_j of solute at 25°C under nearly 24 GHz electric field [ethanol and methanol at 9.84 GHz]

System - I 1-butanol (— O — O —);

System - II 1-hexanol (— Δ — Δ —);

System - III 1-heptanol (— \square — \square —);

System - IV 1-decanol (— \bullet — \bullet —);

System - V ethanol (— \blacktriangle — \blacktriangle —);

System - VI methanol (— \blacksquare — \blacksquare —);

System - VII 2-methyl - 3 heptanol (— Φ — Φ —);

System - VIII 3-methyl - 3 heptanol (— Ψ — Ψ —);

System - IX 4-methyl - 3 heptanol (— Γ — Γ —);

System - X 5-methyl - 3 heptanol (— \otimes — \otimes —);

System - XI 4-Octanol (— \ominus — \ominus —);

System - XII 2-Octanol (— x — x —)

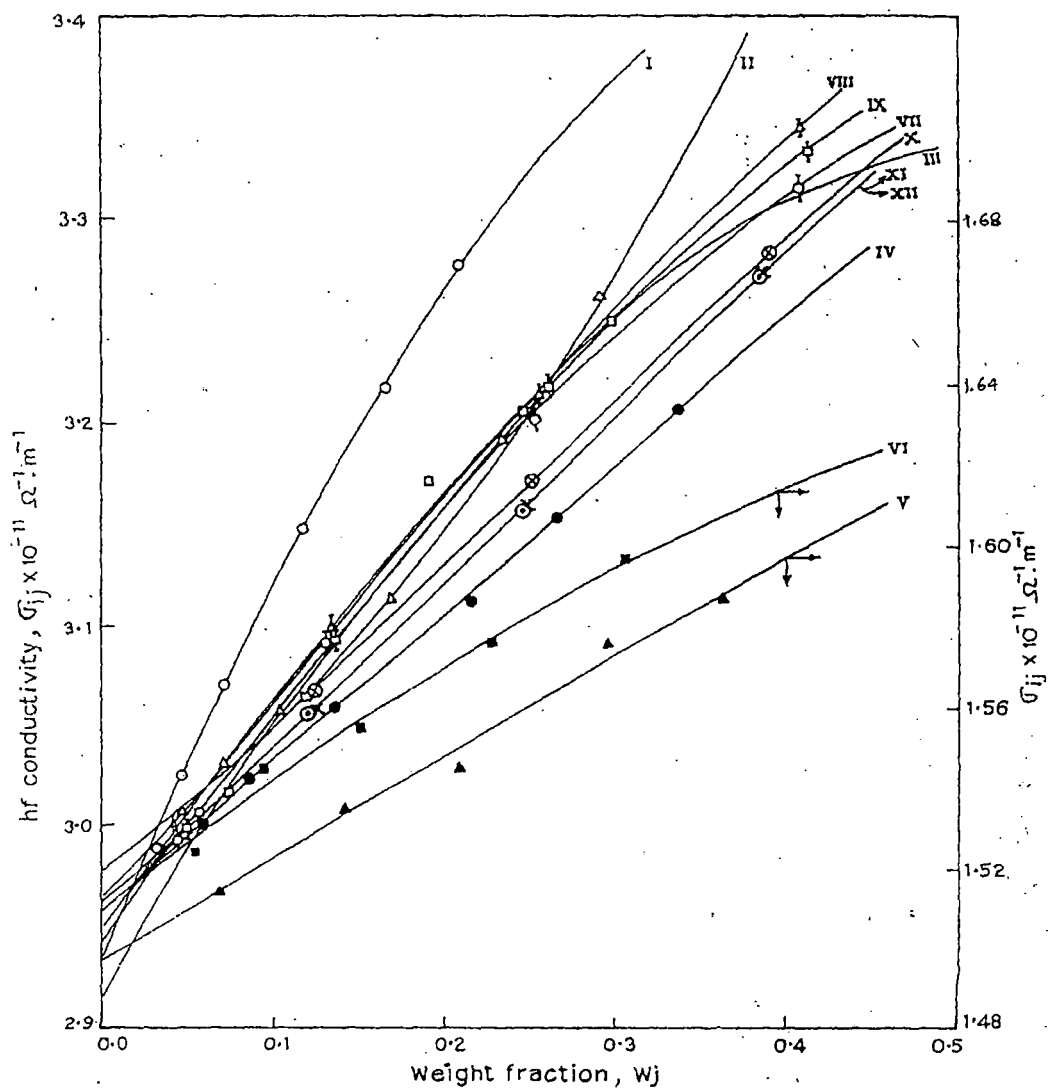


Fig. 5 — Variation of total hf conductivity $\sigma_{ij} \times 10^{-11}$ in $\Omega^{-1} m^{-1}$ against weight fraction w_j of solute at 25°C under nearly 24 GHz electric field [ethanol and methanol at 9.84 GHz]

- | | |
|----------------------------------|--|
| System - I 1-butanol (—O—O—); | System - VII 2-methyl - 3 heptanol (—Φ—Φ—); |
| System - II 1-hexanol (—Δ—Δ—); | System - VIII 3-methyl - 3 heptanol (—A—A—); |
| System - III 1-heptanol (—□—□—); | System - IX 4-methyl - 3 heptanol (—I—I—); |
| System - IV 1-decanol (—●—●—); | System - X 5-methyl - 3 heptanol (—⊗—⊗—); |
| System - V ethanol (—▲—▲—); | System - XI 4-Octanol (—⊖—⊖—); |
| System - VI methanol (—■—■—); | System - XII 2-Octanol (—x—x—) |

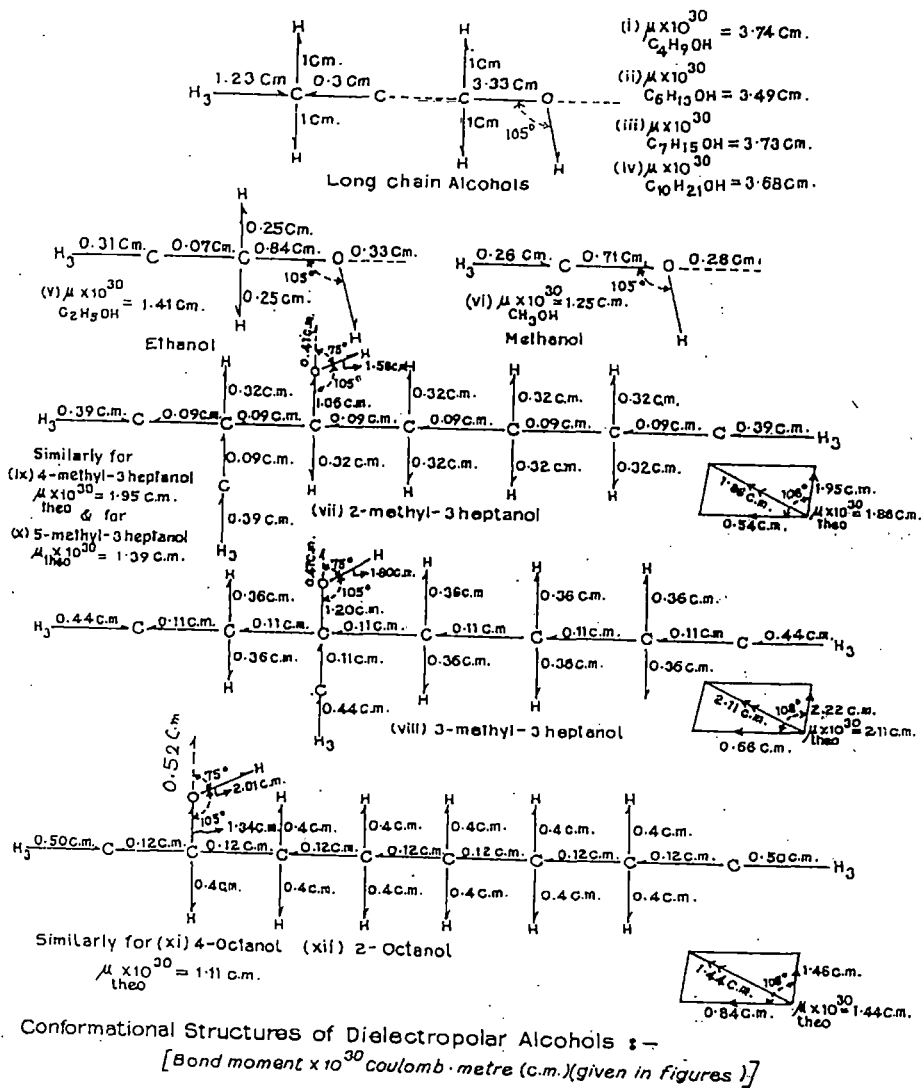


Fig. 6— Conformational structures of dielectropolar alcohols (theoretical dipole moments μ_{theo} from bond angles and reduced bond moments)

trations¹². It is therefore, better to use the ratio of slopes of individual variations of σ''_{ij} and σ'_{ij} both in $\Omega^{-1} \text{ m}^{-1}$ with w_j 's of Figs 3 and 4 to get the exact and accurate value of $d\sigma''_{ij}/d\sigma'_{ij}$ in the limit $w_j = 0$ to evaluate τ_j ^{13,14}. τ_j 's thus obtained by both the methods are placed in Table 3 to see how far they are close in agreements. τ_j 's of such dielectropolar molecules were, however, estimated at 1.233 cm for molecules like 1-butanol, 1-hexanol, 1-decanol, 2-methyl 3-heptanol, 3-methyl 3-

heptanol, 4-methyl-3-heptanol, 5-methyl 3-heptanol, 4-octanol, 2-octanol and at 1.249 cm wavelength electric field for 1- heptanol at which measured ϵ''_{ij} of a given w_j of the solute when were graphically plotted against the electric field frequency "f" showed peak indicating the most effective dispersive region for such liquids.

The formulation to measure μ_j 's of all the alcohols involves with the slopes β 's of the expected $\sigma_{ij}-w_j$ nonlinear curves of Fig. 5 and dimensionless parameter

Table I — Measured dielectric permittivities ϵ'_{ij} , ϵ''_{ij} , ϵ_{0ij} , $\epsilon_{\infty ij}$ in farad metre⁻¹ and dimensionless dielectric constants k'_{ij} , k''_{ij} , k_{0ij} , $k_{\infty ij}$ of some dielectropolar alcohols at 25°C. of different weight fractions w_j

Systems with molecular weight M_j in kg	Weight Fraction w_j	ϵ'_{ij} in F.m ⁻¹	ϵ''_{ij} in F.m ⁻¹	ϵ_{0ij} in F.m ⁻¹	$\epsilon_{\infty ij}$ in F.m ⁻¹	Dimensionless dielectric constants			
						$k'_{ij} \times 10^{-11}$	$k''_{ij} \times 10^{-9}$	$k_{0ij} \times 10^{-11}$	$k_{\infty ij} \times 10^{-11}$
(i) 1-butanol $M_j = 0.074$	0.0291	1.957	0.0079	1.971	1.928	2.2103	0.8922	2.2261	2.1775
	0.0451	1.981	0.0147	2.000	1.945	2.2374	1.6603	2.2589	2.1967
	0.0697	2.011	0.0236	2.050	1.958	2.2713	2.6655	2.3153	2.2114
	0.1163	2.060	0.0425	2.175	1.978	2.3266	4.8001	2.4565	2.2340
	0.1652	2.105	0.0644	2.381	2.000	2.3774	7.2735	2.6892	2.2589
	0.2072	2.144	0.0813	2.621	2.020	2.4215	9.2388	2.9602	2.2814
(ii) 1-hexanol $M_j = 0.102$	0.0458	1.968	0.0131	1.988	1.944	2.2227	1.4795	2.2453	2.1956
	0.0703	1.984	0.0190	2.015	1.952	2.2408	2.1459	2.2758	2.2046
	0.1028	2.001	0.0296	2.064	1.970	2.2600	3.3431	2.3311	2.2250
	0.1687	2.037	0.0425	2.196	1.989	2.3006	4.8001	2.4802	2.2464
	0.2335	2.088	0.0569	2.360	2.002	2.3582	6.4265	2.6655	2.2611
	0.2901	2.134	0.0748	2.580	2.018	2.4102	8.4481	2.9139	2.2792
(iii) 1-heptanol $M_j = 0.116$	0.0564	1.968	0.0147	1.985	1.932	2.2227	1.6603	2.2419	2.1821
	0.0735	1.975	0.0182	2.008	1.945	2.2306	2.0556	2.2679	2.1967
	0.1175	2.007	0.0265	2.066	1.957	2.2668	2.9930	2.3334	2.2103
	0.1909	2.076	0.0482	2.195	1.989	2.3447	5.4439	2.4791	2.2464
	0.2465	2.097	0.0567	2.315	2.002	2.3684	6.4039	2.6146	2.2611
	0.2970	2.126	0.0693	2.464	2.008	2.4012	7.8270	2.7829	2.2679
(iv) 1-decanol $M_j = 0.158$	0.0572	1.965	0.0120	1.976	1.940	2.2193	1.3553	2.2317	2.1911
	0.0857	1.979	0.0223	2.003	1.952	2.2351	2.5186	2.2622	2.2046
	0.1351	2.003	0.0273	2.050	1.964	2.2622	3.0833	2.3153	2.2182
	0.2140	2.036	0.0449	2.147	1.990	2.2995	5.0711	2.4249	2.2476
	0.2640	2.064	0.0513	2.220	2.008	2.3311	5.7940	2.5073	2.2679
	0.3353	2.097	0.0637	2.346	2.030	2.3684	7.1945	2.6496	2.2927
(v) ethanol $M_j = 0.046$	0.0664	2.450	0.0082	3.300	2.262	2.7671	0.9223	3.7271	2.5548
	0.1393	2.483	0.0124	4.300	2.190	2.8047	1.4023	4.8566	2.4734
	0.2077	2.500	0.0208	5.400	2.120	2.8236	2.3529	6.0989	2.3944
	0.2953	2.550	0.0297	7.000	2.062	2.8800	3.3600	7.9060	2.3289
	0.3638	2.567	0.0342	8.200	2.016	2.8988	3.8641	9.2613	2.2769
	0.0514	2.467	0.0082	4.800	2.214	2.7858	0.9284	5.4213	2.5006
(vi) methanol $M_j = 0.032$	0.0930	2.500	0.0083	6.500	2.155	2.8236	0.9408	7.3413	2.4339
	0.1495	2.517	0.0168	8.600	2.085	2.8423	1.8940	9.7131	2.3549
	0.2266	2.550	0.0298	11.400	2.016	2.8800	3.3601	12.8755	2.2769
	0.3049	2.583	0.0387	13.700	1.960	2.9177	4.3765	15.4732	2.2137
	0.0437	1.960	0.0156	1.971	1.930	2.2137	1.7619	2.2261	2.1798
	0.1299	2.022	0.0361	2.059	1.966	2.2847	4.0772	2.3255	2.2205
(vii) 2-methyl 3-heptanol $M_j = 0.130$	0.2522	2.095	0.0565	2.172	2.007	2.3661	6.3813	2.4531	2.2667
	0.4081	2.169	0.0809	2.330	2.054	2.4497	9.1371	2.6316	2.3198
	0.0450	1.965	0.0137	1.974	1.934	2.2193	1.5473	2.2295	2.1843
	0.1334	2.028	0.0393	2.069	1.966	2.2905	4.4387	2.3368	2.2205
	0.2538	2.103	0.0674	2.180	2.004	2.3752	7.6124	2.4622	2.2634
	0.4085	2.188	0.0928	2.334	2.057	2.4712	10.4811	2.6361	2.3232
(viii) 3-methyl 3-heptanol $M_j = 0.130$	0.0466	1.964	0.0146	1.976	1.936	2.2182	1.6490	2.2317	2.1866
	0.1326	2.025	0.0375	2.065	1.969	2.2871	4.2354	2.3323	2.2238
	0.2590	2.104	0.0616	2.185	2.011	2.3763	6.9573	2.4678	2.2713
	0.4124	2.180	0.0849	2.352	2.065	2.4622	9.5889	2.6564	2.3323
	0.1228	2.008	0.0296	2.048	1.956	2.2679	3.3431	2.3131	2.2092
	0.2489	2.075	0.0511	2.168	2.004	2.3436	5.7714	2.4486	2.3634
(ix) 3-heptanol $M_j = 0.130$	0.3898	2.148	0.0676	2.315	2.040	2.4260	7.6350	2.6146	2.3040
	0.1201	2.000	0.0265	2.040	1.948	2.2589	2.9930	2.3040	2.2001
	0.2445	2.067	0.0449	2.148	1.997	2.3345	5.0711	2.4260	2.2555
	0.3838	2.146	0.0659	2.282	2.031	2.4170	7.4430	2.5764	2.2939
	0.1236	2.001	0.0245	2.049	1.954	2.2600	2.7671	2.3142	2.2069
	0.2479	2.068	0.0513	2.195	1.996	2.3357	5.7940	2.4791	2.2543
(x) 2-octanol $M_j = 0.130$	0.3844	2.141	0.0680	2.410	2.036	2.4181	7.6801	2.7219	2.2995

Table 2 — Coefficients a_0 , a_1 and a_2 of static experimental parameter $X_{ij} = a_0 + a_1 w_j + a_2 w_j^2$ correlation coefficients (r), % of errors in getting X_{ij} , static or low frequency dipole-moments $\mu_s \times 10^{30}$ in Coulomb-metre, theoretical dipole-moments $\mu_{theo} \times 10^{30}$ in Coulomb-metre from reduced bond moments by μ_s/μ_{theo} and μ_1 , μ_2 by double relaxation method

Systems with sl. no. & molecular weight M_j	Coefficients a_0 , a_1 and a_2 in Eq. $X_{ij} \times 10^{-9} = a_0 + a_1 w_j + a_2 w_j^2$			Correlation coefficient (r)	% of error in fitting technique	$\mu_s \times 10^{30}$ in Coulomb-metre from Eq. (5)	Corrected $\mu_{theo} \times 10^{30}$ in Coulomb metre from bond angle & reduced bond moments	μ_1 and μ_2 in Coulomb metre from double relaxation method	
	a_0	a_1	a_2					$\mu_1 \times 10^{30}$ in Coulomb metre	$\mu_2 \times 10^{30}$ in Coulomb metre
(i) 1-butanol in <i>n</i> -heptane $M_j = 0.074$ kg	0.2047	1.0852	75.2840	0.9824	0.96	3.74	$4.97 \times 0.7525 = 3.74$	3.63	29.17
(ii) 1-hexanol in <i>n</i> -heptane $M_j = 0.102$ kg	0.1951	1.0710	34.8550	0.9896	0.57	3.49	$4.37 \times 0.7986 = 3.49$	3.43	21.20
(iii) 1-heptanol in <i>n</i> -heptane $M_j = 0.116$ kg	0.2553	0.8932	26.4890	0.9867	0.73	3.73	$4.07 \times 0.9165 = 3.73$	3.73	27.00
(iv) 1-decanol in <i>n</i> -heptane $M_j = 0.158$ kg.	0.0901	2.3826	10.1760	0.9924	0.42	3.68	$3.17 \times 1.1609 = 3.68$	3.83	17.24
(v) ethanol in benzene $M_j = 0.046$ kg	1.6141	59.1892	-44.9614	0.9919	0.49	1.41	$5.57 \times 0.2531 = 1.41$	1.70	490.73
(vi) methanol in benzene $M_j = 0.032$ kg.	5.6331	99.8090	-159.9120	0.9672	1.94	1.25	$5.87 \times 0.2129 = 1.25$	—	293.96
(vii) 2-methyl 3-heptanol in <i>n</i> -heptane $M_j = 0.130$ kg.	0.1372	3.7778	0.5639	0.9997	0.02	1.86	$5.87 \times 0.3168 = 1.86$	3.83	16.00
(viii) 3-methyl 3-heptanol in <i>n</i> -heptane $M_j = 0.130$ kg.	0.0830	4.8577	-1.7495	0.9986	0.09	2.11	$5.87 \times 0.3594 = 2.11$	3.83	8.60
(ix) 4-methyl 3-heptanol in <i>n</i> -heptane $M_j = 0.130$ kg.	0.1032	4.1481	0.0885	0.9998	0.01	1.95	$5.87 \times 0.3322 = 1.95$	3.90	13.90
(x) 5-methyl 3-heptanol in <i>n</i> -heptane $M_j = 0.130$ kg.	0.3270	2.1113	4.1567	0.9972	0.22	1.39	$5.87 \times 0.2368 = 1.39$	3.37	9.50
(xi) 4-octanol in <i>n</i> -heptane $M_j = 0.130$ kg.	0.4402	1.1341	5.2073	0.9946	0.42	1.11	$3.60 \times 0.3083 = 1.11$	3.43	10.97
(xii) 2-octanol in <i>n</i> -heptane $M_j = 0.130$ kg.	0.2591	2.2977	8.3285	0.9955	0.35	1.45	$3.60 \times 0.4028 = 1.45$	3.43	16.00

Table 3 — Intercept (c) and slope (m) of $\sigma''_{ij} - \sigma'_{ij}$ equation (Fig. 2), correlation coefficient (r), percentage of error (%), relaxation time τ_j in psec Eq. (10), ratio of slopes of σ''_{ij} and σ'_{ij} with w_j ($= x/y$), relaxation time τ_j in psec from (Eq. 11), calculated relaxation time τ_j in psec from Gopalakrishana's method for some dielectropolar alcohols under nearly 24 GHz electric field (Q-Band Microwave) at 25 °C

System with sl. no. and molecular weight	Intercept & slope of $\sigma''_{ij} - \sigma'_{ij}$ fitted Equation $c \times 10^{-11}$ m		Correlation coefficient (r)	% of error	Estimated relaxation time τ_j in psec from Eq. (10)	Ratio of the slopes of σ''_{ij} & σ'_{ij} with w_j $x/y = (d\sigma''_{ij}/dw_j)/(d\sigma'_{ij}/dw_j)$	Estimated relaxation time τ_j in psec from Eq (11)	Relaxation time τ_j in psec estimated from Gopalakrishana's method
(i) 1-butanol in <i>n</i> -heptane $M_j = 0.074$ kg.	2.9731	2.4816	0.9959	0.22	2.64	$\frac{2.0789 \times 10^{11}}{5.7404 \times 10^{10}}$ $= 3.6215$	1.81	2.47
(ii) 1-hexanol in <i>n</i> -heptane $M_j = 0.102$ kg.	2.9457	2.7315	0.9959	0.22	2.40	$\frac{5.8541 \times 10^{10}}{3.2779 \times 10^{10}}$ $= 1.7859$	3.66	2.25
(iii) 1-heptanol in <i>n</i> -heptane $M_j = 0.116$ kg.	2.9414	2.9898	0.9973	0.15	2.19	$\frac{1.5295 \times 10^{11}}{3.8161 \times 10^{10}}$ $= 4.0080$	1.65	2.07
(iv) 1-decanol in <i>n</i> -heptane $M_j = 0.158$ kg.	2.9465	2.5881	0.9925	0.41	2.53	$\frac{6.8315 \times 10^{10}}{3.3881 \times 10^{10}}$ $= 2.0163$	3.24	2.39
(v) ethanol in benzene $M_j = 0.046$ kg.	1.4952	4.2872	0.9880	0.72	3.77	$\frac{2.5827 \times 10^{10}}{5.6872 \times 10^9}$ $= 4.5412$	3.56	3.62
(vi) methanol in benzene $M_j = 0.032$ kg.	1.5188	3.2088	0.9633	2.17	5.04	$\frac{3.4467 \times 10^{10}}{5.1439 \times 10^9}$ $= 6.7005$	2.41	4.87
(vii) 2-methyl 3-heptanol in <i>n</i> -heptane $M_j = 0.130$ kg.	2.9162	3.2340	0.9994	0.04	2.02	$\frac{1.2112 \times 10^{11}}{3.6429 \times 10^{10}}$ $= 3.3248$	1.97	1.86
(viii) 3-methyl 3-heptanol in <i>n</i> -heptane $M_j = 0.130$ kg.	2.9361	2.8021	0.9976	0.16	2.33	$\frac{1.1146 \times 10^{11}}{5.1067 \times 10^{10}}$ $= 2.1826$	3.00	2.26
(ix) 4-methyl 3-heptanol in <i>n</i> -heptane $M_j = 0.130$ kg.	2.9254	3.0946	0.9988	0.08	2.11	$\frac{1.2125 \times 10^{11}}{4.3826 \times 10^{10}}$ $= 2.7666$	2.36	1.95
(x) 5-methyl 3-heptanol in <i>n</i> -heptane $M_j = 0.130$ kg.	2.8973	3.6562	0.9949	0.40	1.79	$\frac{8.3993 \times 10^{10}}{3.7395 \times 10^{10}}$ $= 2.2461$	2.91	1.63
(xi) 4-octanol in <i>n</i> -heptane $M_j = 0.130$ kg.	2.9129	3.5515	0.9999	0.01	1.84	$\frac{8.5252 \times 10^{10}}{2.1993 \times 10^{10}}$ $= 3.8763$	1.69	1.68
(xii) 2-octanol in <i>n</i> -heptane $M_j = 0.130$ kg.	2.9320	3.1511	0.9875	0.97	2.08	$\frac{8.3278 \times 10^{10}}{5.3226 \times 10^{10}}$ $= 1.5646$	4.18	1.93

Table 4 — Coefficients α , β , γ of hf σ_{ij} against ω_j curves (Fig. 5) correlation coefficients (r) percentage of error, dimensionless parameter b using τ_j from Eq. (10) and (11), computed $\mu_j \times 10^{30}$ in Coulomb metre from Eqs (10) and (16) and Eqs (11) and (16) estimated $\mu_j \times 10^{30}$ in Coulomb metre from Gopalakrishna's method for some dielectropolar alcohols under nearly 24 GHz electric field (Q-Band micro wave) at 25 °C

System with sl. no. & molecular weight	Coefficients of σ_{ij} - ω_j fitted Equation			Correlation coefficient (r)	% of error	Dimensionless parameter using τ_j from Eq. (10) $b = 1/(1 + \omega^2\tau_j^2)$	Dimensionless parameter using τ_j from Eq. (11) $b = 1/(1 + \omega^2\tau_j^2)$	Computed $\mu_j \times 10^{30}$ in Coulomb metre		Estimated $\mu_j \times 10^{30}$ in Coulomb metre from Gopalakrishna's method
	$\alpha \times 10^{-11}$	$\beta \times 10^{-11}$	$\gamma \times 10^{-11}$					hf method of Eqs (10) & (16)	hf method of Eqs (11) & (16)	
(i) 1-butanol in <i>n</i> -heptane $M_j = 0.074$ kg.	2.9351	2.0769	-2.0776	0.9978	0.12	0.8601	0.9289	4.28	4.11	3.58
(ii) 1-hexanol in <i>n</i> -heptane $M_j = 0.102$ kg.	2.9807	0.5846	-1.3346	0.9961	0.21	0.8815	0.7618	2.63	2.83	3.35
(iii) 1-heptanol in <i>n</i> -heptane $M_j = 0.116$ kg.	2.9173	1.5312	-1.3817	0.9928	0.39	0.9016	0.9417	4.52	4.42	3.59
(iv) 1-decanol in <i>n</i> -heptane $M_j = 0.158$ kg.	2.9639	0.6848	0.1087	0.9995	0.03	0.8699	0.8032	3.57	3.71	3.55
(v) ethanol in benzene $M_j = 0.046$ kg.	1.4970	0.2584	-0.0233	0.9927	0.44	0.9485	0.9538	1.44	1.43	1.33
(vi) methanol in benzene $M_j = 0.032$ kg.	1.5098	0.3444	-0.2046	0.9928	0.43	0.9116	0.9783	1.41	1.36	1.18
(vii) 2-methyl 3-heptanol in <i>n</i> -heptane $M_j = 0.130$ kg.	2.9437	1.2203	-0.7548	0.9958	0.28	0.9130	0.9169	4.22	4.21	3.42
(viii) 3-methyl 3-heptanol in <i>n</i> -heptane $M_j = 0.130$ kg.	2.9515	1.1644	-0.4868	0.9985	0.10	0.8875	0.8264	4.18	4.33	3.54
(ix) 4-methyl 3-heptanol in <i>n</i> -heptane $M_j = 0.130$ kg.	2.9454	1.2172	-0.6697	0.9970	0.02	0.9058	0.8849	4.23	4.28	3.48
(x) 5-methyl 3-heptanol in <i>n</i> -heptane $M_j = 0.130$ kg.	2.9658	0.8446	-0.0754	0.9999	0.01	0.9304	0.8349	3.47	3.67	3.24
(xi) 4-octanol in <i>n</i> -heptane $M_j = 0.130$ kg.	2.9546	0.8544	-0.0762	0.9999	0.01	0.9267	0.9375	3.56	3.48	3.27
(xii) 2-octanol in <i>n</i> -heptane $M_j = 0.130$ kg.	2.9542	0.8399	-0.0280	0.9999	0.01	0.9083	0.7103	3.51	3.97	3.32

b in terms of τ_i 's obtained by both the methods as τ_i 's were not found to agree excellently in Table 3. The σ''_{ij} and σ'_{ij} in $\Omega^{-1} \text{ m}^{-1}$ are not linear with w_j as evident from Figs 3 and 4. μ_j 's thus obtained are finally compared with μ_{theo} 's from available bond angles and bond moments of the substituent polar groups attached to parent ones. The slight disagreement between the measured μ_j 's and μ_x 's from μ_{theo} 's indicates the existence of inductive and mesomeric moments of different substituent polar groups present in such dielectropolar molecules in addition to strong hydrogen bonding in them as displayed by the molecular conformations of Fig 6.

The solvent C_6H_6 unlike n -heptane is a cyclic compound with three double bonds and six p -electrons on six carbon atoms. Hence π - π interaction or resonance effect combined with inductive effect known as mesomeric effect is expected to play an important role in the measured μ_j 's under hf electric field. A special attention is to be paid to have the conformational structures of the alcohols to evaluate μ_{theo} 's as seen in Fig 6 and Table 2 from the reduction of the available bond moments^{5,6} of different substituent polar groups by the ratio of μ_x/μ_{theo} . This takes into account of H-bonding, in addition to inductive effect in them. Thus the conclusion regarding the molecular association of such long chain associated aliphatic alcohols may also be the reason to yield higher dipole moments.

2 Static Relaxation Parameter X_{ij} and Static Dipole Moment μ_s

Under static electric field μ_x of a dielectropolar molecule (j) in a non polar solvent (i) may be obtained from the following equation¹⁰.

$$\frac{(\epsilon_0 k_{0ij} - 1)}{(\epsilon_0 k_{0ij} + 2)} - \frac{(\epsilon_0 k_{\infty ij} - 1)}{(\epsilon_0 k_{\infty ij} + 2)} = \frac{(\epsilon_0 k_{0i} - 1)}{(\epsilon_0 k_{0i} + 2)} - \frac{(\epsilon_0 k_{\infty i} - 1)}{(\epsilon_0 k_{\infty i} + 2)} + \frac{N \mu_s^2}{3 \epsilon_0 k_B T} c_j \quad \dots(1)$$

where $k_{0ij} = \epsilon_{0ij}/\epsilon_0$ and $k_{\infty ij} = \epsilon_{\infty ij}/\epsilon_0$ are the dimensionless static and infinite frequency dielectric constants of solution (ij). ϵ_0 is the permittivity of free space $= 8.854 \times 10^{-12} \text{ F.m}^{-1}$, c_j is the molar concentration of the solute where $c_j = \rho_j w_j / M_j$ and the other symbols carry usual meanings.

A polar liquid of weight W_j and volume V_j is mixed with a nonpolar solvent of weight W_i and volume V_i to get the solution density ρ_{ij} where

$$\rho_{ij} = \frac{W_i + W_j}{V_i + V_j} = \frac{W_i + W_j}{W_i/\rho_i + W_j/\rho_j} = \frac{\rho_i \rho_j}{\rho_j W_i / (W_i + W_j) + \rho_i W_j / (W_i + W_j)} = \frac{\rho_i \rho_j}{\rho_j w_i + \rho_i w_j} = \rho_i (1 - \gamma w_j)^{-1} \quad \dots(2)$$

The weight fractions w_j and w_i of solute and solvent are given by :

$$w_j = \frac{W_j}{W_i + W_j} \text{ and } w_i = \frac{W_i}{W_i + W_j} \text{ such that } w_i + w_j = 1$$

and $\gamma = (1 - \rho_i/\rho_j)$, ρ_i and ρ_j are densities of pure solvent and solute respectively.

Now, Eq. (1) may be written as:

$$\frac{k_{0ij} - k_{\infty ij}}{(\epsilon_0 k_{0ij} + 2)(\epsilon_0 k_{\infty ij} + 2)} = \frac{k_{0i} - k_{\infty i}}{(\epsilon_0 k_{0i} + 2)(\epsilon_0 k_{\infty i} + 2)} + \frac{N \rho_i \mu_s^2}{9 \epsilon_0^2 M_j k_B T} w_j (1 - \gamma w_j)^{-1} X_{ij} = X_i + \frac{N \rho_i \mu_s^2}{9 \epsilon_0^2 M_j k_B T} w_j + \frac{N \rho_i \mu_s^2}{9 \epsilon_0^2 M_j k_B T} \gamma w_j^2 + \dots \quad \dots(3)$$

The right hand side of Eq. (3) is obviously a polynomial equation of w_j like

$$X_{ij} = a_0 + a_1 w_j + a_2 w_j^2 + \dots \quad \dots(4)$$

Now, comparing the linear coefficients of Eqs (3) and (4) one gets μ_s from:

$$\mu_s = \left(\frac{9 \epsilon_0^2 M_j k_B T}{N \rho_i} a_1 \right)^{1/2} \quad \dots(5)$$

where a_1 is the slope of X_{ij} - w_j curve of Fig. 1. But μ_s from higher coefficients of Eqs (3) or (4) are not reliable as they are involved with various effects of solvent, relative density, solute-solute association, internal field, macroscopic viscosity etc. μ_s 's from Eq. (5) along with a_1 are placed in Table 2 to compare with hf μ_j 's presented in Table 4.

3 High Frequency Dipole Moment μ_j and Relaxation Time τ_j

Under hf electric field of GHz range the dimensionless complex dielectric constant k_{ij}^* is:

$$k_{ij}^* = k'_{ij} - j k''_{ij} \quad \dots(6)$$

where $k'_{ij} = \epsilon'_{ij}/\epsilon_0$ and $k''_{ij} = \epsilon''_{ij}/\epsilon_0$ are the real and imaginary parts of complex dielectric constant. ϵ'_{ij} and ϵ''_{ij} are the real and imaginary parts of complex permittivity ϵ^*_{ij} in F.m.⁻¹ and $\epsilon_0 =$ permittivity of free space = 8.854×10^{-12} F.m.⁻¹. The hf complex conductivity σ^*_{ij} of a polar-nonpolar liquid mixture of¹⁵ weight fraction w_j is:

$$\sigma^*_{ij} = \omega \epsilon_0 k''_{ij} + j \omega_0 \epsilon_0 k'_{ij} \quad \dots(7)$$

where $\sigma'_{ij} = \omega \epsilon_0 k''_{ij}$ and $\sigma''_{ij} = \omega \epsilon_0 k'_{ij}$ are real and imaginary parts of complex conductivity and j is a complex number = $(-1)^{1/2}$

The hf conductivity σ_{ij} is, however, obtained from :

$$\sigma_{ij} = \omega \epsilon_0 (k''_{ij}{}^2 + k'_{ij}{}^2)^{1/2} \quad \dots(8)$$

σ''_{ij} is related to σ'_{ij} by

$$\sigma''_{ij} = \sigma_{\infty ij} + (1/\omega \tau_j) \sigma'_{ij} \quad \dots(9)$$

where $\sigma_{\infty ij}$ is the constant conductivity at $w_j \rightarrow 0$ and τ_j is the relaxation time of a polar molecule.

Eq. (9) on differentiation with respect to σ'_{ij} becomes¹¹

$$d\sigma''_{ij}/d\sigma'_{ij} = 1/\omega \tau_j \quad \dots(10)$$

to yield τ_j

It is often better to use the ratio of slopes of individual variation of σ''_{ij} and σ'_{ij} with w_j at $w_j \rightarrow 0$ to avoid polar-polar interaction in a given solvent to get τ_j from: $(d\sigma''_{ij}/dw_j)/(d\sigma'_{ij}/dw_j) = 1/\omega \tau_j$

$$\text{or } x/y = 1/\omega \tau_j \quad \dots(11)$$

where $\omega = 2\pi f$, f being the frequency of alternating electric field.

In hf region of GHz range, it is often observed that $\sigma''_{ij} \cong \sigma_{ij}$ and Eq. (9) becomes:

$$\sigma_{ij} = \sigma_{\infty ij} + (1/\omega \tau_j) \sigma'_{ij} \quad \dots(12)$$

$$\beta = 1/\omega \tau_j (d\sigma'_{ij}/dw_j) \quad \dots(13)$$

where $\beta - (d\sigma'_{ij}/dw_j)$ is the slope of $\sigma_{ij}-w_j$ curve at $w_j \rightarrow 0$

The σ'_{ij} of a solution of weight fraction w_j of a polar molecule at T K is given by Smyth^{14,16} as:

$$\sigma'_{ij} = \frac{N \rho_{ij} \mu_j^2}{27 \epsilon_0 M_j k_B T} \left(\frac{\omega^2 \tau}{1 + \omega^2 \tau^2} \right) (\epsilon_0 k_{0ij} + 2)(\epsilon_0 k_{\infty ij} + 2) w_j \quad \dots(14)$$

Eq. (14) on differentiation with respect to w_j and at $w_j \rightarrow 0$ yields:

$$(d\sigma'_{ij}/dw_j)_{w_j \rightarrow 0} = \frac{N \rho_{ij} \mu_j^2}{3 \epsilon_0 M_j k_B T} \left(\frac{\epsilon_i + 2}{3} \right)^2 \left(\frac{\omega^2 \tau}{1 + \omega^2 \tau^2} \right) \quad \dots(15)$$

where $N =$ Avogadro's number, $\rho_i =$ density of solvent

$\epsilon_i =$ permittivity of solvent;

$M_j =$ Molecular weight of solute and

$k_B =$ Boltzmann constant.

From Eqs (13) and (15) one gets hf μ_j as:

$$\mu_j = \left[\frac{27 \epsilon_0 M_j k_B T}{N \rho_i (\epsilon_i + 2)^2} \frac{\beta}{\omega b} \right]^{1/2} \quad \dots(16)$$

$$\text{where } b = 1/(1 + \omega^2 \tau_j^2) \quad \dots(17)$$

is a dimensionless parameter involved with estimated τ_j from Eqs (10) and (11). All the computed hf μ_j 's in terms of slopes β 's and b 's are placed in Table 4 in order to compare with μ_{theo} 's, μ_x and μ_1, μ_2 of the flexible part and end-over-end rotation of the whole molecule^{5,6} presented in Table 2.

4 Results and Discussions

The dimensionless real k'_{ij} and imaginary k''_{ij} of the complex dielectric constants k^*_{ij} as well as the static k_{0ij} and infinite frequency $k_{\infty ij}$ of dielectric constants were obtained from the measured relaxation permittivities $\epsilon'_{ij}, \epsilon''_{ij}, \epsilon_{0ij}$ and $\epsilon_{\infty ij}$ in F.m.⁻¹ for different w_j 's of alcohols in different solvents at 25°C. The data thus obtained are placed in Table 1. The static experimental solution parameters X_{ij} 's involved with k_{0ij} and $k_{\infty ij}$ of Table 1 are shown in Fig. 1; for different w_j of alcohols. The nature of variation of X_{ij} with w_j 's are parabolic in nature satisfying a polynomial equation: $X_{ij} = a_0 + a_1 w_j + a_2 w_j^2$. The coefficients of $X_{ij}-w_j$ curves i.e. a_0, a_1 and a_2 are placed in the 2nd, 3rd and 4th columns of Table 2. As evident from Fig. 1, the $X_{ij}-w_j$ curves for methanol, ethanol and 3-methyl-3-heptanol are convex in nature as their coefficients of quadratic terms in Table 2 are negative. The remaining X_{ij} 's on the other hand, showed a gradual increase with w_j 's for all the coefficients of the curves are positive as seen in Table 2. The anomalous behaviour of $X_{ij}-w_j$ curves from linearity for all the alcohols in different solvents at a given temperature in °C may rouse an interesting relaxation mechanism in such long chain associated liquids. In comparison to octyl alcohols, the curves of normal alcohols in higher concentrations are highly concave hav-

ing a tendency to meet at a common point on the X_{ij} axis at $w_j \rightarrow 0$. This sort of behaviour of $X_{ij}-w_j$ curves of Fig. 1 arises either due to solute-solute i.e. dimer or solute-solvent i.e. monomer formations in comparatively high concentrations. The convex shape of ethanol and methanol occurs for the probable experimental uncertainty in their ϵ_{0ij} and $\epsilon_{\infty ij}$ measurements. The identical nature of variations of all the octyl alcohols have almost the same slope, but of different intercepts as a result of solvation effect. Their X_{ij} 's have tendency to become closer within $0.1 \leq w_j \leq 0.2$ indicating various molecular association in them.

In case of non-associated liquids a_2 's were found to be vanishingly small in comparison to a_n and a_1 to yield almost linear variation of X_{ij} against w_j . The estimated correlation coefficient (r) and the percentage of error (%) entered in 5th and 6th columns of Table 2 for all the alcohols are such that one may rely on the linear term of $X_{ij}-w_j$ curve to compute μ_s 's from Eq. (5). μ_s 's thus computed are placed in the 7th column of Table 2 to compare with μ_{thco} 's obtained from bond angles and bond moments of the substituent polar groups, as presented in Fig. 6 and μ_1 and μ_2 of the flexible part and the whole molecule by the double relaxation method^{5,6} at nearly 24 GHz electric field. The smaller and larger deviations of X_{ij} 's from linearity with w_j 's as seen in Fig. 1, confirm the molecular associations of such associated dielectropolar liquids in different solvents.

The relaxation times τ_j 's are, however, derived from the slope of linear¹¹ variation of σ''_{ij} with σ'_{ij} of Fig. 2 for all the alcohols. Although, the experimental data, on the other hand, did not strictly fall on the fitted linear curves of σ''_{ij} and σ'_{ij} both in $\Omega^{-1} m^{-1}$ as drawn in Fig. 2, the slope of σ''_{ij} against σ'_{ij} of Fig. 2 was, however, used to obtain τ_j from Eq. (10). The 2nd, 3rd and 6th columns of Table 3 contain all the estimated intercepts and slopes together with the measured τ_j 's. The linearity of σ''_{ij} curves against σ'_{ij} as shown graphically in Fig. 2 is again tested by correlation coefficients r 's and % of errors. They are entered in the 4th and 5th columns of Table 3 only to see how far σ''_{ij} and σ'_{ij} are correlated to each other. But it is often better to use the ratio of the individual slopes of variation of σ''_{ij} and σ'_{ij} with w_j at $w_j \rightarrow 0$ to get τ_j . τ_j 's by using Eq. (11) are not in close agreement with those obtained from Eq. (10) and by freshly calculated Gopalakrishna's method, as seen in Table 3. Figs (3) and (4) showed that both σ''_{ij} and σ'_{ij} vary nonlinearly with w_j . The nonlinear behaviour of σ''_{ij}

and σ'_{ij} as seen in Figs 3 and 4 with w_j 's invites the associational and structural aspects of such long chain dielectropolar associated molecules. The latter method to measure τ_j 's thus appears to be a significant improvement^{12,13} over the former one¹¹ as it eliminates the polar-polar interaction in a given solvent.

The hf μ_j from Eq. (16) was obtained from the slope β of the nonlinear variation of σ_{ij} in $\Omega^{-1} m^{-1}$ with w_j 's of Fig. 5 and dimensionless parameter b of Eq. (17) in terms of τ_j obtained by both the methods. The intercept α and slope β of hf σ_{ij} with w_j curves of Fig. 5 are entered in the 2nd and 3rd columns of Table 3. It is interesting to note that the curves of $\sigma_{ij}-w_j$ variation of Fig. 5 are almost identical with $\sigma''_{ij}-w_j$ curves of Fig. 3. This fact at once confirms the applicability of the approximation that $\sigma''_{ij} \cong \sigma_{ij}$ as done in Eqs (9) and (12). The imaginary σ''_{ij} and total hf σ_{ij} in case of normal alcohols in Figs 3 and 5 decrease gradually with w_j 's of 1-butanol to methanol except ethanol. This can be explained on the basis of the fact that the polarity of the molecules decreases from 1-butanol to methanol. Both σ''_{ij} 's and σ_{ij} 's in Figs 3 and 5 of all the octyl alcohols are found to be closer only to show their nearly same polarity. The almost coincident curves of 4-octanol ($-\Theta-$) and 2-octanol ($-X-$) arise due to their identical polarity as estimated in Fig. 6.

The estimated μ_s 's and μ_j 's in Table 2 and 4 are then compared with the μ_1 and μ_2 in Table 2 by double relaxation method^{5,6} and those by freshly calculated Gopalakrishna's method. For all the normal alcohols μ_j 's and μ_s 's are in excellent agreement with Gopalakrishna's μ_j 's (reported data) and μ_1 . The estimated μ_j 's for octyl alcohols agree with reported μ_j 's and μ_1 . All these discussions made above establish the fact that a part of the molecule is rotating under GHz electric field. Slight disagreement in μ 's and the reported ones arises due to steric hindrances of the substituent polar units of their structural configurations of Fig. 6 and the existence of associative nature for their hydrogen bonding. Unlike normal alcohols, μ_s 's are always lower than μ_j 's and μ_1 's for octyl alcohols. This at once reveals under static electric field the possible formation of dimers which undergo to rupture into the solute solvent association i.e. monomer in the hf electric field to increase μ 's. It is also evident that dimer formation is favourable in octyl alcohols than normal alcohols due to existence of strong

inductive effect for their $-OH$ groups at the end of the molecular chains.

The theoretical dipole moments μ_{theo} 's of all the alcohols under study were calculated from the available bond angles and bond moments of the substituent polar groups like H_3-C , $C-H$, $C-O$, $O-H$ ($\angle 105^\circ$) and $C-C$ of 1.23×10^{-30} , 1.0×10^{-30} , 3.33×10^{-30} , 1.30×10^{-30} and 0.3×10^{-30} Coulomb-meter (C.m.) as presented elsewhere^{5,6}. The values thus estimated are then made closer with the measured static μ_s 's or even μ_j 's by reducing the available bond moments by a factor μ_s/μ_{theo} which takes into account of the inductive and mesomeric effects of the substituent polar groups-as shown in Fig. 6. An inductive effect of polar unit acts along the chain of the molecular axis of the normal alcohols to make them strongly polar due to presence of $-OH$ group at their ends of the axis. The comparatively lower μ_{theo} 's in octyl alcohols is probably due to screening effect of their $-OH$ groups by other polar groups, like H_3-C , $C-H$ which favour the dimer formation of these alcohols through H-bonding to make their μ_s 's and μ_j 's lower than the normal alcohol as seen in Fig. 6.

5 Conclusion

The modern internationally accepted symbols of dielectric terminologies and parameters in SI unit are conveniently used to obtain static and hf dipole moments μ_s and μ_j in terms of relaxation time τ_j of a polar molecule. τ_j 's measured from the slope of imaginary σ''_{ij} against real σ'_{ij} of complex hf conductivity σ^*_{ij} for different ω_j are not in agreement with those measured from the ratio of the individual slopes of $\sigma''_{ij} - \omega_j$ and $\sigma'_{ij} - \omega_j$ curves at $\omega_j \rightarrow 0$ indicating the applicability of the latter method in long chain dielectropolar alcohols. This method of determination of τ_j is a significant improvement over the previous one as it eliminates polar-polar interactions in a given solvent. The comparison of μ_j 's and μ_s 's with μ_1 and μ_2 of the flexible part and the whole molecule by double relaxation method and μ_{theo} 's from bond angles and bond moments seems to be an interesting phenomenon to have deep insight into relaxation mechanism of dielectropolar alcohols.

The results indicate that a part of the molecule is rotating under GHz electric field. The slight departure among the measured μ_s , μ_j and μ_{theo} reveals different associational aspects of dielectropolar alcohols in dif-

ferent solvents through the frequency dependence of relaxation parameters. It also shows the strong polar nature of normal alcohols which favour solute-solvent association due to the presence of $-OH$ group at the end of their bond axis. But the comparatively lower values of μ_j 's in octyl alcohols indicates the solute-solute association due to $-H$ bonding supported by the fact that $-OH$ being screened by $-CH_3$ and a large number of $>CH_2$ polar groups. The μ_s/μ_{theo} 's are almost constant for all the alcohols to take into account of all these facts in addition to their material property of the system. This study further supports the rotation of $-OH$ group along the $\equiv C-O-$ bond of all the alcohols under static and hf electric fields. Moreover, the methodology so far developed within the frame work of Debye and Smyth model appears to be sound, simple, straightforward and useful to arrive at associational and structural aspects of alcohols which are thought to be non-Debye in relaxation behaviour.

References

- Gopalakrishna K V, *Trans Farad Soc*, 33 (1957) 767.
- Kastha G S, Dutta J, Bhattacharyya J & Roy S B, *Indian J Phys*, 43 (1969) 14.
- Dutta S K, Acharyya C R & Acharyya S, *Indian J Phys*, 55B (1981) 140.
- Sit S K, Ghosh N, Saha U & Acharyya S, *Indian J Phys*, 71B (1997) 533.
- Sit S K & Acharyya S, *Indian J Phys*, 70B (1996) 19.
- Sit S K, Ghosh N & Acharyya S, *Indian J Pure & Appl Phys*, 35 (1997) 329.
- Glasser L, Crossley J & Smyth C P, *J Chem Phys*, 57 (1972) 3977.
- Ghosh A K, PhD Dissertation, N B U, (1981).
- Crossley J, Glasser L & Smyth C P, *J Chem Phys*, 55 (1971) 2197.
- Debye P, *Polar Molecules* (Chemical Catalogue), 1929.
- Murthy M B R, Patil R L & Deshpande D K, *Indian J Phys*, B63 (1989) 491.
- Ghosh N, Basak R C, Sit S K & Acharyya S, *J Mol Liq*, Germany, (Accepted for publication), 2000.
- Basak R C, Sit S K, Nandi N & Acharyya S, *Indian J Phys*, B70 (1996) 37.
- Basak R C, Karmakar A, Sit S K & Acharyya S, *Indian J Pure & Appl Phys*, 37 (1999) 224.
- Murphy F J & Morgan S O, *Bell Syst Tech J*, 18 (1939) 502.
- Smyth C P, *Dielectric behaviour and structure*, (McGraw-Hill, New York), 1955.

Structural and associational aspects of isomers of anisidine and toluidine under a gigahertz electric field

N Ghosh, S K Sit, A K Bothra and S Acharyya

Department of Physics, Raiganj College (University College), P.O. Raiganj, District Uttar Dinajpur, PIN - 733134, (WB), India

Received 25 October 2000

Abstract

The relaxation times τ_1 and τ_2 for rotations of the flexible parts and the whole molecules of the isomers of anisidine and toluidine (j) in benzene (i) under a 9.945 GHz electric field are predicted from the slope and intercept of a linear equation of $(\chi_{0ij} - \chi'_{ij})/\chi'_{ij}$ against χ''_{ij}/χ'_{ij} for different weight fractions w_j 's of solute at 35 °C. χ'_{ij} and χ''_{ij} are the real and imaginary parts of the high-frequency complex orientational susceptibility χ_{ij}^* and χ_{0ij} is the low-frequency susceptibility which is real. The τ 's; dimensionless parameters b 's involved with τ 's and linear coefficients β 's of $\chi'_{ij}-w_j$ curves are used to obtain dipole moments μ_1 and μ_2 of the flexible parts and the whole molecules. The theoretical weighted contributions c_1 and c_2 due to τ_1 and τ_2 towards dielectric dispersions from Fröhlich's equations are worked out to compare with experimental ones by graphical variations of χ'_{ij}/χ_{0ij} and χ''_{ij}/χ_{0ij} at $w_j \rightarrow 0$. The estimated τ 's from the ratio of the individual slopes of χ''_{ij} and χ'_{ij} with w_j 's at $w_j \rightarrow 0$ are compared with those of Murthy *et al* (1989 *Indian J. Phys.* B 63 491) and reported τ 's.

The symmetric and characteristic relaxation times τ_s and τ_{cs} by symmetric and asymmetric distribution parameters γ and δ are computed to suggest the symmetric relaxation behaviour of the molecules. The measured μ_1 and μ_2 from double relaxation phenomena and the reported μ 's signify the fact that a part of the molecule is rotating under a gigahertz electric field. The slight disagreement between the theoretical dipole moment μ_{theo} from available bond angles and bond moments of substituent polar groups attached to the parent molecules and measured μ_1 demands the inductive and mesomeric effects suffered by the substituent polar groups, in addition to structural and associational aspects of such molecules.

1. Introduction

The dielectric relaxation of a polar liquid molecule in a non-polar solvent under static and high-frequency (hf) electric fields provides one with valuable information on various types of molecular associations [1, 2] and the structural configuration of the polar molecule from relaxation parameters such as the relaxation time τ and dipole moment μ , measured by any standard method [3, 4]. μ_j 's determined by concentration variation of the real part of the hf dielectric susceptibility are concerned with the orientational polarization and are further used to shed more light on the structural and associational aspects of a polar molecule [5].

Srivastava and Chandra [6] measured the real ϵ'_{ij} and imaginary ϵ''_{ij} parts of the relative complex permittivity, ϵ_{ij}^* and the static and infinitely hf relative permittivities, ϵ_{0ij} and $\epsilon_{\infty ij}$, of isomers of anisidines and toluidines in C_6H_6 under 2.02, 3.86 and 22.06 GHz electric fields at 35 °C. The purpose of such a study was to observe the solute–solvent and solute–solute molecular associations, besides the possible existence of either double or single relaxation behaviour of anisidines and toluidines.

Nowadays, the usual practice is to study dielectric relaxation phenomena by dimensionless complex hf dielectric orientational susceptibility χ_{ij}^* [5] rather than the relative hf permittivity ϵ_{ij}^* or hf conductivity σ_{ij}^* . The ϵ_{ij}^* includes within

it all types of polarizations while σ_{ij}^* is concerned with the transport of bound charges. Hence it is better to work with χ_{ij} for its more direct link with orientational polarization. Moreover, the present system of study in the modern concept of internationally accepted symbols of dielectric terminology and parameters in SI units is interesting because of its rationalized, coherent and unified nature.

Under such a context we derived a linear equation (5) (see below) in terms of the real $\chi'_{ij} = (\epsilon'_{ij} - \epsilon_{\infty ij})$ and imaginary $\chi''_{ij} = \epsilon''_{ij}$ parts of the complex hf χ_{ij}^* and low-frequency dielectric susceptibility $\chi_{0ij} = (\epsilon_{0ij} - \epsilon_{\infty ij})$, which is real as presented in table 1 under a 9.945 GHz electric field, to obtain τ_1 and τ_2 of the flexible parts and the whole molecules in C_6H_6 at 35 °C.

The electric field frequency of $f = 9.945$ GHz was claimed to be the most effective dispersive region for such molecules [7]. When χ''_{ij} 's were plotted against frequency (f) they showed a peak in the neighbourhood of 9.945 GHz, at which point the dielectric orientation processes of polar molecules [8, 9] are invariably maximum. At this frequency χ'_{ij} , χ''_{ij} and χ_{0ij} were again adjusted by a careful graphical interpolation technique [7]. One could make a strong conclusion of double relaxation phenomena of a polar molecule in a non-polar solvent based on single-frequency measurement of the relaxation parameters, provided the accurate value of χ_{0ij} involved with ϵ_{0ij} and $\epsilon_{\infty ij}$ is available. The use of n_{Dij}^2 for $\epsilon_{\infty ij}$ [6] may often introduce additional error into the calculation. Nevertheless, the data are accurate up to 5% for χ''_{ij} and 2% for χ'_{ij} and χ_{0ij} . The liquid molecules at this f absorb electric energy much more strongly to exhibit reasonable τ_1 and τ_2 for all the chemical systems under identical environments. τ_1 and τ_2 are, however, measured from the intercept and slope of the derived straight-line equation (see equation (5) below) of $(\chi_{0ij} - \chi'_{ij})/\chi'_{ij}$ against χ''_{ij}/χ'_{ij} of figure 1 for different weight fractions w_j 's of polar solute at the single frequency $\omega (=2\pi f)$, signifying the material property of the systems. The correlation coefficients τ 's and minimum chisquare values to test the linearity of the curves of figure 1, along with the estimated τ_1 and τ_2 , are given in table 2. In absence of reliable τ , the ratio of the individual slopes of variation of χ''_{ij} and χ'_{ij} with w_j 's at $w_j \rightarrow 0$, as seen in figures 2 and 3, were conveniently used to evaluate τ_j to compare with those of Murthy *et al* [10] of figure 4 and Gopalakrishna's method [11].

The theoretical weighted contributions c_1 and c_2 due to the estimated τ_1 and τ_2 presented in table 3, towards dielectric dispersions, were calculated from Fröhlich's equations [12] in order to compare with the experimental contributions by the graphical extrapolation technique of figures 5 and 6 at $w_j \rightarrow 0$. The symmetric and asymmetric distribution parameters γ and δ were, however, worked out from the variation of χ'_{ij}/χ_{0ij} and χ''_{ij}/χ_{0ij} with w_j in the limit $w_j = 0$ to conclude the symmetric distribution behaviour obeyed by such molecules. The characteristic relaxation time τ_{cs} from δ and ϕ of figure 7 along with the symmetric relaxation time τ_s in terms of γ are found out to compare with τ_1 , τ_2 and τ_j in table 2.

The dipole moments μ_1 , μ_2 and μ_0 , in Coulomb metres (C m), in terms of b_1 , b_2 and b_0 involved with τ_1 , τ_2 and τ_0 , where τ_0 is the most probable relaxation time ($=\sqrt{\tau_1 \tau_2}$) and linear coefficient β 's of χ'_{ij} against w_j curves of figure 3

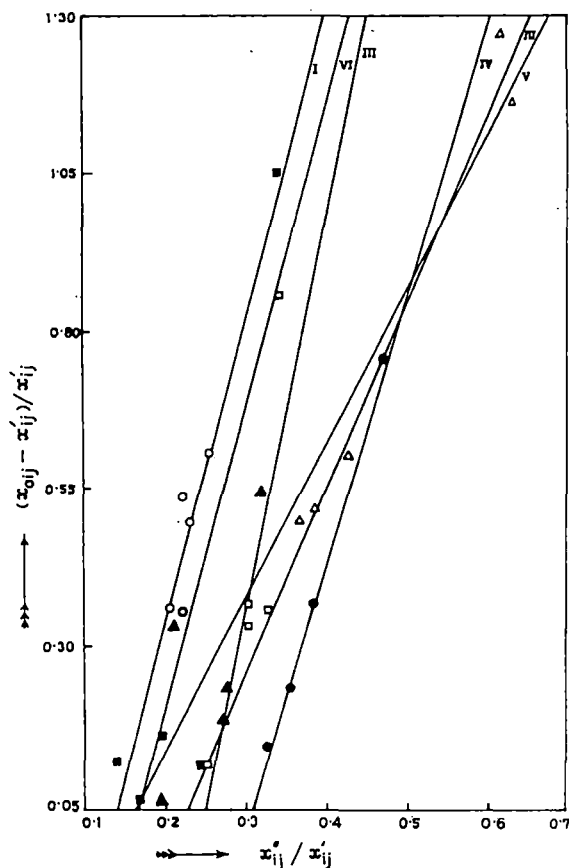


Figure 1. Linear variation of $(\chi_{0ij} - \chi'_{ij})/\chi'_{ij}$ against χ''_{ij}/χ'_{ij} of isomers of anisidines and toluidines in benzene at 35 °C under a 9.945 GHz electric field: (I) *o*-anisidine (—○—), (II) *m*-anisidine (—△—), (III) *p*-anisidine (—□—), (IV) *o*-toluidine (—●—), (V) *m*-toluidine (—▲—) and (VI) *p*-toluidine (—■—).

were determined in order to place them in table 4. The comparison, however, indicates that the flexible parts of the molecules rotate under X-band gigahertz electric fields. They are compared with μ_{theo} 's obtained from available bond angles and bond moments of the substituent polar groups attached to the parent molecules, as displayed in figure 8, and μ_j by freshly calculated Gopalakrishna's method of table 4. The slight disagreement between the measured μ 's and μ_{theo} 's invites the existence of inductive and mesomeric effects of substituent polar groups.

2. Theoretical formulations for τ_1 , τ_2 and τ_0

Bergmann *et al*'s equations [13] are concerned with molecular orientational polarization processes. We therefore introduce χ_{ij} 's to avoid clumsiness of algebra as $\epsilon_{\infty ij}$ includes a fast polarization process and frequently appears as a subtracted term in the equations. Thus, with the established symbols of parameters of dielectric terminology like $\chi'_{ij} = (\epsilon'_{ij} - \epsilon_{\infty ij})$, $\chi''_{ij} = \epsilon''_{ij}$ and $\chi_{0ij} = (\epsilon_{0ij} - \epsilon_{\infty ij})$ of table 1, Bergmann *et al*'s

Table 1. Concentration variations of the measured real ϵ'_{ij} and imaginary ϵ''_{ij} parts of the hf complex relative permittivity under a 9.945 GHz electric field, the static and hf relative permittivities ϵ_{0ij} and $\epsilon_{\infty ij}$ along with the real χ'_{ij} and imaginary χ''_{ij} parts of the complex dimensionless dielectric orientational susceptibility χ_{ij} and the low-frequency susceptibility χ_{0ij} which is real for isomers of anisidine and toluidine in benzene at 35 °C.

System with serial number and molecular weight (M_j)	Weight fraction, w_j , of solute	Measured dielectric relative permittivities				Dimensionless dielectric orientational susceptibilities		
		ϵ'_{ij}	ϵ''_{ij}	ϵ_{0ij}	$\epsilon_{\infty ij}$	χ'_{ij}	χ''_{ij}	χ_{0ij}
(i) <i>o</i> -anisidine $M_j = 0.123$ kg	0.0326	2.3104	0.0148	2.336	2.239	0.0714	0.0148	0.097
	0.0604	2.3520	0.0244	2.404	2.247	0.1050	0.0244	0.157
	0.0884	2.4064	0.0340	2.459	2.255	0.1514	0.0340	0.204
	0.1135	2.4416	0.0400	2.538	2.262	0.1796	0.0400	0.276
	0.1361	2.4672	0.0512	2.588	2.267	0.2002	0.0512	0.321
(ii) <i>m</i> -anisidine $M_j = 0.123$ kg	0.0160	2.2720	0.0234	2.315	2.235	0.0370	0.0234	0.080
	0.0336	2.3040	0.0390	2.384	2.241	0.0630	0.0390	0.143
	0.0579	2.3904	0.0618	2.477	2.246	0.1444	0.0618	0.231
	0.0823	2.4544	0.0744	2.553	2.253	0.2014	0.0744	0.300
	0.1109	2.5344	0.1056	2.675	2.261	0.2734	0.1056	0.414
(iii) <i>p</i> -anisidine $M_j = 0.123$ kg	0.0319	2.3104	0.0252	2.373	2.237	0.0734	0.0252	0.136
	0.0597	2.3904	0.0474	2.442	2.246	0.1444	0.0474	0.196
	0.0848	2.5088	0.0642	2.539	2.250	0.2588	0.0642	0.289
	0.1106	2.5376	0.0840	2.638	2.262	0.2756	0.0840	0.376
	0.1396	2.6272	0.1086	2.745	2.269	0.3582	0.1086	0.476
(iv) <i>o</i> -toluidine $M_j = 0.107$ kg	0.0137	2.2752	0.0162	2.301	2.241	0.0342	0.0162	0.060
	0.0459	2.3648	0.0408	2.392	2.250	0.1148	0.0408	0.142
	0.0622	2.4032	0.0570	2.457	2.255	0.1482	0.0570	0.202
	0.1048	2.5376	0.0900	2.577	2.264	0.2736	0.0900	0.313
	(v) <i>m</i> -toluidine $M_j = 0.107$ kg	0.0264	2.3136	0.0150	2.337	2.243	0.0706	0.0150
0.0538	2.3552	0.0342	2.413	2.248	0.1072	0.0342	0.165	
0.0781	2.4576	0.0402	2.470	2.252	0.2056	0.0402	0.218	
0.1015	2.4840	0.0618	2.526	2.258	0.2260	0.0618	0.268	
0.1225	2.5280	0.0732	2.591	2.262	0.2660	0.0732	0.329	
(vi) <i>p</i> -toluidine $M_j = 0.107$ kg	0.0213	2.3100	0.0102	2.319	2.237	0.0730	0.0102	0.082
	0.0428	2.3040	0.0204	2.367	2.244	0.0600	0.0204	0.123
	0.0616	2.3904	0.0276	2.413	2.249	0.1414	0.0276	0.164
	0.0916	2.4704	0.0384	2.483	2.254	0.2164	0.0384	0.229
	0.1048	2.4960	0.0582	2.523	2.260	0.2360	0.0582	0.263

equations become

$$\frac{\chi'_{ij}}{\chi_{0ij}} = c_1 \frac{1}{1 + \omega^2 \tau_1^2} + c_2 \frac{1}{1 + \omega^2 \tau_2^2} \quad (1)$$

and

$$\frac{\chi''_{ij}}{\chi_{0ij}} = c_1 \frac{\omega \tau_1}{1 + \omega^2 \tau_1^2} + c_2 \frac{\omega \tau_2}{1 + \omega^2 \tau_2^2} \quad (2)$$

assuming the molecules possess two separate broad dispersions for which the relative weight factors c_1 and c_2 are such that $c_1 + c_2 = 1$. χ'_{ij} and χ''_{ij} are the real and imaginary parts of the hf complex susceptibility χ_{ij} and χ_{0ij} is the static or low-frequency susceptibility which is real.

Let $\alpha_1 = \omega \tau_1$ and $\alpha_2 = \omega \tau_2$, equations (1) and (2) are solved to obtain

$$c_1 = \frac{(\chi'_{ij} \alpha_2 - \chi''_{ij})(1 + \alpha_1^2)}{\chi_{0ij}(\alpha_2 - \alpha_1)} \quad (3)$$

and

$$c_2 = \frac{(\chi''_{ij} - \chi'_{ij} \alpha_1)(1 + \alpha_2^2)}{\chi_{0ij}(\alpha_2 - \alpha_1)} \quad (4)$$

provided $\alpha_2 > \alpha_1$. Now adding equations (3) and (4), since $c_1 + c_2 = 1$, one obtains

$$\frac{\chi_{0ij} - \chi'_{ij}}{\chi'_{ij}} = \omega(\tau_1 + \tau_2) \frac{\chi''_{ij}}{\chi'_{ij}} - \omega^2 \tau_1 \tau_2. \quad (5)$$

Equation (5) gives a straight line between the variables $(\chi_{0ij} - \chi'_{ij})/\chi'_{ij}$ and χ''_{ij}/χ'_{ij} having intercept $-\omega^2 \tau_1 \tau_2$ and slope $\omega(\tau_1 + \tau_2)$. It was solved for different concentrations w_j 's of each of the polar molecules of table 1 for a given fixed value of the angular frequency $\omega (=2\pi f)$ of the applied electric field at 35 °C, where $f = 9.945$ GHz. The values of τ_1 and τ_2 from the intercept and slope of equation (5) are found as shown in table 2:

The theoretical values of c_1 and c_2 towards dielectric relaxations were obtained from equations (3) and (4) using values of χ'_{ij}/χ_{0ij} and χ''_{ij}/χ_{0ij} of Fröhlich's [12] following equations, (6) and (7), in terms of the estimated τ_1 and τ_2 of table 2 from the intercepts and slopes of equation (5):

$$\chi'_{ij}/\chi_{0ij} = 1 - \frac{1}{2A} \ln \left(\frac{1 + \omega^2 \tau_2^2}{1 + \omega^2 \tau_1^2} \right) \quad (6)$$

$$\chi''_{ij}/\chi_{0ij} = \frac{1}{A} [\tan^{-1}(\omega \tau_2) - \tan^{-1}(\omega \tau_1)]. \quad (7)$$

The theoretical c_1 and c_2 are given in table 3 in order to compare them with the experimental values obtained by graphically extrapolated values of χ'_{ij}/χ_{0ij} and χ''_{ij}/χ_{0ij} in the limit $w_j = 0$ in figures 5 and 6 and equations (3) and (4). The Fröhlich's parameter A , where $A = \ln(\tau_2/\tau_1)$ is given in table 3 for each compound.

Table 2. Slope and intercept of the linear equations of $(\chi_{0ij} - \chi'_{ij})/\chi'_{ij}$ against χ''_{ij}/χ'_{ij} , correlation coefficient (r), minimum chisquare values, relaxation times τ_1 and τ_2 of the flexible part as well as the whole molecules, measured τ from equations (9) and (10), reported τ (Gopalakrishna) and most probable relaxation time τ_0 , together with symmetric τ_s and characteristic τ_{cs} from symmetric and asymmetric distribution parameters γ and δ of some monosubstituted anilines at 35 °C under a 9.945 GHz (X-band microwave) electric field.

System with serial number and molecular weight (M_j)	Intercept and slope from (5) for $((\chi_{0ij} - \chi'_{ij})/\chi'_{ij})$ against χ''_{ij}/χ'_{ij}		Correlation coefficient (r)	Chisquare value ($\times 10^2$)	Estimated relaxation times τ_1 and τ_2 (ps)		Most probable relaxation time $\tau_0 = \sqrt{\tau_1 \tau_2}$	Measured τ (ps) ^a	Ratio of slopes of χ''_{ij} and χ'_{ij} with w_j of (10) $\frac{(d\chi''_{ij}/dw_j)_{w_j \rightarrow 0}}{(d\chi'_{ij}/dw_j)_{w_j \rightarrow 0}}$
	Intercept	Slope							
	(c)	(m)							
(i) <i>o</i> -anisidine $M_j = 0.123$ kg	0.6373	4.8390	0.7743	4.36	2.17	75.31	12.78	4.18	0.1560
(ii) <i>m</i> -anisidine $M_j = 0.123$ kg	0.6075	2.9047	0.9888	1.22	3.63	42.88	12.48	5.20	0.3033
(iii) <i>p</i> -anisidine $M_j = 0.123$ kg	1.4948	6.2149	0.8310	24.77	4.01	95.50	19.57	4.47	0.1824
(iv) <i>o</i> -toluidine $M_j = 0.107$ kg	1.2684	4.2603	0.9986	0.13	5.15	63.06	18.02	4.95	0.4025
(v) <i>m</i> -toluidine $M_j = 0.107$ kg	0.3501	2.4337	0.6864	30.10	2.46	36.51	9.48	4.18	0.1605
(vi) <i>p</i> -toluidine $M_j = 0.107$ kg	0.7348	4.7136	0.8687	-23.25	2.58	72.89	13.71	3.36	0.1755

System with serial number and molecular weight (M_j)	Relaxation times			
	τ (ps) ^b	τ (ps) ^c	τ (ps) ^d	τ (ps) ^e
(i) <i>o</i> -anisidine $M_j = 0.123$ kg	2.50	3.29	2.46	130.40
(ii) <i>m</i> -anisidine $M_j = 0.123$ kg	4.86	4.28	3.02	64.22
(iii) <i>p</i> -anisidine $M_j = 0.123$ kg	2.92	3.70	140.19	305.52
(iv) <i>o</i> -toluidine $M_j = 0.107$ kg	6.44	4.15	16.05	82.37
(v) <i>m</i> -toluidine $M_j = 0.107$ kg	2.57	4.01	5.85	458.51
(vi) <i>p</i> -toluidine $M_j = 0.107$ kg	2.81	3.34	1.38	12.07

^a Measured by the slope of χ''_{ij} against χ'_{ij} using the straight-line equation (9).

^b From the ratio of individual slopes.

^c By Gopalakrishna's method [11].

^d From the symmetric distribution parameter γ of (17).

^e From the asymmetric distribution parameter δ of (19).

3. Theoretical formulation for the dipole moment

The real ϵ'_{ij} and imaginary ϵ''_{ij} parts of the hf complex relative permittivity are written as

$$\epsilon'_{ij} = \epsilon_{\infty ij} + (1/\omega\tau)\epsilon''_{ij}$$

or

$$\epsilon'_{ij} - \epsilon_{\infty ij} = (1/\omega\tau)\epsilon''_{ij}$$

or

$$\chi'_{ij} = (1/\omega\tau)\chi''_{ij} \quad (8)$$

and

$$(d\chi''_{ij}/d\chi'_{ij}) = \omega\tau_j. \quad (9)$$

The variation of susceptibility χ''_{ij} with χ'_{ij} of equation (9) is caused by variation in concentrations, w_j 's, of the polar liquids under the fixed frequency of the electric field. As χ''_{ij} is, however, claimed to vary linearly with χ'_{ij} [10] of different concentrations and the frequency is fixed, the slope of χ''_{ij} with χ'_{ij} can conveniently be used to obtain τ_j from equation (9).

However, in case of monosubstituted anilines the variations of χ''_{ij} with χ'_{ij} , as seen in figure 4, are not strictly linear. The ratio of individual slopes from the variations of χ''_{ij} and χ'_{ij} with w_j 's in figures 2 and 3 is, however, thought to be a better representation of equation (9) to obtain τ_j where polar-polar interactions are supposed to be fully avoided.

Table 3. Fröhlich's parameter A , relative contributions c_1 and c_2 due to τ_1 and τ_2 theoretical values of χ_{ij}'/χ_{0ij} and χ_{ij}''/χ_{0ij} of Fröhlich's equations, (6) and (7), and those by the graphical method at $w_j \rightarrow 0$, symmetric γ and asymmetric δ distribution parameters of some monosubstituted anilines at 35 °C under a 9.945 GHz (X-band microwave) electric field.

System with serial number	Fröhlich's Parameter $A = \ln(\tau_2/\tau_1)$	Estimated values of χ_{ij}'/χ_{0ij} and χ_{ij}''/χ_{0ij} of Fröhlich's equations (6) and (7)		Weighted contributions c_1 and c_2 from (3) and (4)		Estimated values of χ_{ij}'/χ_{0ij} and χ_{ij}''/χ_{0ij} from figures 5 and 6 at $w_j \rightarrow 0$		Weighted contributions c_1 and c_2 from the graphical technique		Symmetric distribution parameter γ	Asymmetric distribution parameter δ
		c_1	c_2	c_1	c_2	c_1	c_2	c_1	c_2		
(i) <i>o</i> -anisidine	3.5469	0.5598	0.3458	0.5099	1.3664	0.7100	0.1470	0.7117	0.2570	0.5716	0.1360
(ii) <i>m</i> -anisidine	2.4692	0.5848	0.4011	0.4997	0.8952	0.3339	0.3094	0.2508	0.7791	0.2475	0.5671
(iii) <i>p</i> -anisidine	3.1703	0.4419	0.3656	0.4222	1.6317	0.2114	0.1523	0.2062	0.6360	0.4813	0.4111
(iv) <i>o</i> -toluidine	2.5051	0.4600	0.4035	0.4296	1.1665	0.4995	0.2638	0.5197	0.4708	0.3821	0.3524
(v) <i>m</i> -toluidine	2.6974	0.6661	0.3726	0.5517	0.7879	0.5894	0.1308	0.5839	0.1173	0.6650	0.1422
(vi) <i>p</i> -toluidine	3.3412	0.5432	0.3576	0.4818	1.3361	0.9550	0.1148	0.9889	-0.1933	0.1617	0.1853

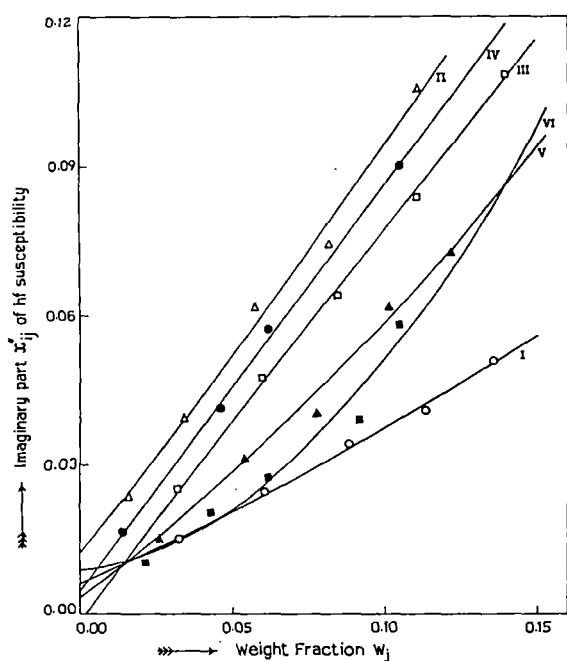


Figure 2. Variation of the imaginary part χ_{ij}'' of the hf susceptibility against the weight fraction w_j of solute in benzene at 35 °C under a 9.945 GHz electric field: (I) *o*-anisidine (—○—), (II) *m*-anisidine (—△—), (III) *p*-anisidine (—□—), (IV) *o*-toluidine (—●—), (V) *m*-toluidine (—▲—) and (VI) *p*-toluidine (—■—).

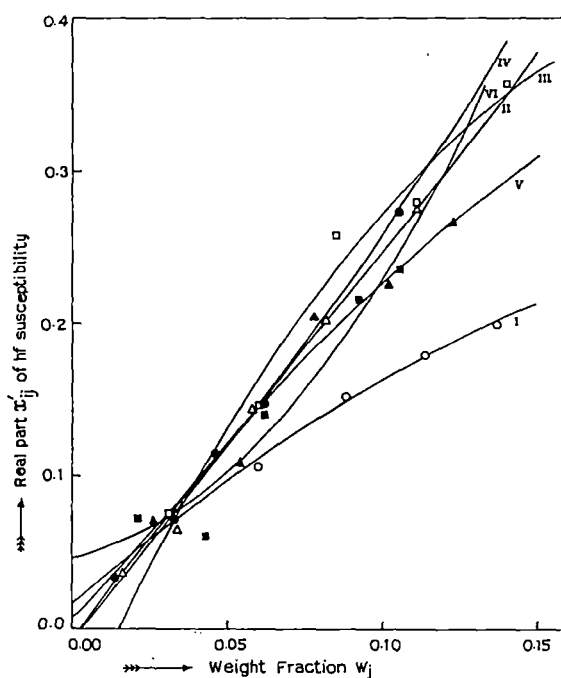


Figure 3. Variation of the real part χ_{ij}' of the hf susceptibility against the weight fraction w_j of solute in benzene at 35 °C under a 9.945 GHz electric field: (I) *o*-anisidine (—○—), (II) *m*-anisidine (—△—), (III) *p*-anisidine (—□—), (IV) *o*-toluidine (—●—), (V) *m*-toluidine (—▲—) and (VI) *p*-toluidine (—■—).

Thus

$$\left(\frac{d\chi_{ij}''}{dw_j}\right)_{w_j \rightarrow 0} \left[\left(\frac{d\chi_{ij}'}{dw_j}\right)_{w_j \rightarrow 0}\right]^{-1} = \omega\tau_j. \quad (10)$$

The imaginary part χ_{ij}'' of χ_{ij}^* is [14, 15]

$$\chi_{ij}'' = \frac{N\rho_{ij}\mu_j^2}{27\epsilon_0 M_j k_B T} \left(\frac{\omega\tau}{1 + \omega^2\tau^2}\right) (\epsilon_{ij} + 2)^2 w_j. \quad (11)$$

Equation (11), when differentiated with respect to w_j and at

$w_j \rightarrow 0$ yields

$$\left(\frac{d\chi_{ij}''}{dw_j}\right)_{w_j \rightarrow 0} = \frac{N\rho_i\mu_j^2}{27\epsilon_0 M_j k_B T} \left(\frac{\omega\tau}{1 + \omega^2\tau^2}\right) (\epsilon_i + 2)^2. \quad (12)$$

At $w_j \rightarrow 0$, the density of solution ρ_{ij} and $(\epsilon_{ij} + 2)^2$ tends to ρ_i and $(\epsilon_i + 2)^2$ where ρ_i and ϵ_i are the density and relative permittivity of solvent i , respectively.

In comparison to earlier works presented elsewhere [15, 16] the approximation that $\chi_{ij} \approx \chi_{ij}'$, as $\sigma_{ij} \approx \sigma_{ij}''$, is not necessary to obtain the μ_j 's from the τ_j 's where σ_{ij}'' is the

Table 4. Coefficients α , β and γ of the $\chi'_{ij}-w_j$ curve (figure 3) with correlation coefficients and percentage of errors, dimensionless parameter b , estimated μ_j 's where μ is from $\mu_1 = \mu_2(c_1/c_2)^{1/2}$ and theoretical μ from bond angles and bond moments together with reported μ (Gopalakrishna [11]) of some monosubstituted anilines in benzene at 35 °C under a 9.945 GHz (X-band microwave) electric field.

Systems with serial number and molecular weight (M_j)	Coefficients of the equation $\chi'_{ij} = \alpha + \beta w_j + \gamma w_j^2$			Correlation coefficient of the $\chi'_{ij}-w_j$ equation	Percentage error involved in the $\chi'_{ij}-w_j$ equations	Dimensionless parameters			Estimated dipole moments μ ($\times 10^{30}$ C m)		
	α	β	γ			b_0^a	b_1^b	b_2^c	μ_0	μ_1	μ_2
(i) <i>o</i> -anisidine $M_j = 0.123$ kg	0.0149	1.7546	-2.8056	0.9960	0.24	0.6108	0.9820	0.0432	6.17	4.87	23.21
(ii) <i>m</i> -anisidine $M_j = 0.123$ kg	-0.0094	2.5108	0.4641	0.9968	0.19	0.6221	0.9511	0.1224	7.31	5.91	16.49
(iii) <i>p</i> -anisidine $M_j = 0.123$ kg	-0.0634	4.4003	-10.2107	0.9962	0.23	0.4010	0.9410	0.0273	12.06	7.87	46.23
(iv) <i>o</i> -toluidine $M_j = 0.107$ kg	0.0063	2.0495	4.7368	0.9979	0.14	0.4412	0.9062	0.0606	7.32	5.11	19.75
(v) <i>m</i> -toluidine $M_j = 0.107$ kg	-0.0078	2.8140	-4.6071	0.9782	1.30	0.7404	0.9769	0.1613	6.62	5.76	14.19
(vi) <i>p</i> -toluidine $M_j = 0.107$ kg	0.0464	0.3863	14.5432	0.9593	2.41	0.5770	0.9747	0.0460	2.78	2.14	9.84

Systems with serial number and molecular weight (M_j)	Dipole moments		
	Estimated μ ($\times 10^{30}$ Cm) ^d	Theoretical μ ($\times 10^{30}$ Cm) ^e	μ ($\times 10^{30}$ Cm) ^f
(i) <i>o</i> -anisidine $M_j = 0.123$ kg	14.18	3.40	4.50
(ii) <i>m</i> -anisidine $M_j = 0.123$ kg	12.32	5.50	6.17
(iii) <i>p</i> -anisidine $M_j = 0.123$ kg	23.51	6.30	6.53
(iv) <i>o</i> -toluidine $M_j = 0.107$ kg	11.98	4.63	5.77
(v) <i>m</i> -toluidine $M_j = 0.107$ kg	11.87	3.43	5.17
(vi) <i>p</i> -toluidine $M_j = 0.107$ kg	5.91	5.13	5.30

$$^a b_0 = \frac{1}{1 + \omega^2 \tau_0^2}$$

$$^b b_1 = \frac{1}{1 + \omega^2 \tau_1^2}$$

$$^c b_2 = \frac{1}{1 + \omega^2 \tau_2^2}$$

$$^d \text{From } \mu_1 = \mu_2 \left(\frac{c_1}{c_2}\right)^{1/2}$$

^e From bond angles and bond moments.

^f From Gopalakrishna's method [11].

imaginary part of the complex hf conductivity and σ_{ij} is the total hf conductivity of the polar-non-polar liquid mixture.

From equations (8) and (12) one obtains

$$\omega \tau_j \left(\frac{d\chi'_{ij}}{dw_j} \right)_{w_j \rightarrow 0} = \frac{N \rho_i \mu_j^2}{27 \epsilon_0 M_j k_B T} \left(\frac{\omega \tau_j}{1 + \omega^2 \tau_j^2} \right) (\epsilon_i + 2)^2$$

or

$$\mu_j = \left[\frac{27 \epsilon_0 M_j k_B T \beta}{N \rho_i (\epsilon_i + 2)^2 b} \right]^{1/2} \quad (13)$$

where τ_j and μ_j are the relaxation time and the dipole moment of the j th solute and ϵ_0 is the permittivity of free space, $8.854 \times$

$10^{-12} \text{ F m}^{-1}$. Here N is the Avogadro number, 6.023×10^{23} ; ρ_i is the density of the solvent, 865 kg m^{-3} ; k_B is the Boltzmann constant, $1.38 \times 10^{-23} \text{ J mol}^{-1} \text{ K}^{-1}$; ϵ_i is the dielectric relative permittivity of the solvent, benzene, 2.253; M_j is the molecular weight of the solute in kilogrammes; β is the linear coefficient of the $\chi'_{ij} - w_j$ curve at $w_j \rightarrow 0$; and $b = 1/(1 + \omega^2 \tau_j^2)$ is a dimensionless parameter involved with the measured τ_j .

The μ_1 , μ_2 and μ_0 in terms of b_1 , b_2 and b_0 involved with τ_1 , τ_2 and τ_0 , respectively, were then computed with the knowledge of β of $\chi'_{ij}-w_j$ curves of figure 3. The μ 's thus obtained from equation (13) are given in table 4 in order to compare with those of Gopalakrishna [11] and μ_{theo} 's obtained

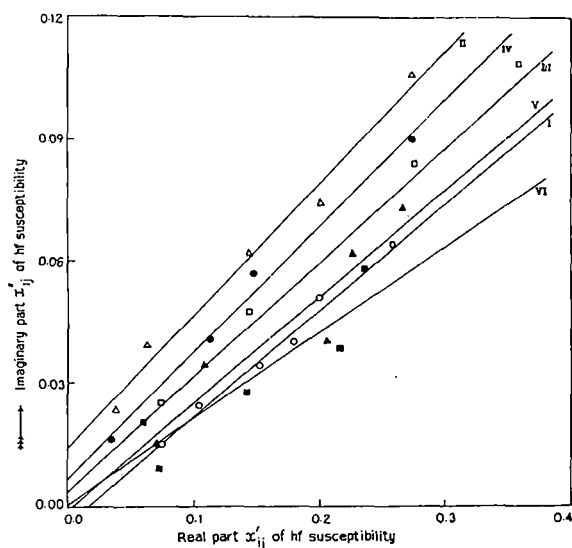


Figure 4. Linear plot of the imaginary part χ''_{ij} of the hf susceptibility against the real part χ'_{ij} of the isomers of the anisidine and toluidine in benzene at 35 °C under a 9.945 GHz electric field: (I) *o*-anisidine (—○—), (II) *m*-anisidine (—△—), (III) *p*-anisidine (—□—), (IV) *o*-toluidine (—●—), (V) *m*-toluidine (—▲—) and (VI) *p*-toluidine (—■—).

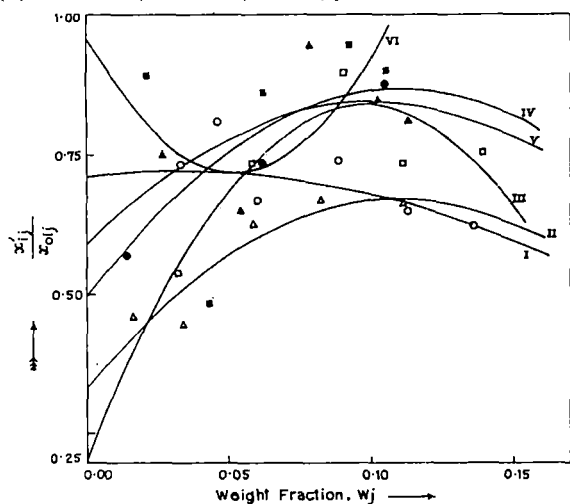


Figure 5. Plot of χ'_{ij}/χ_{0ij} against the weight fraction w_j of the solute of the isomers of the anisidine and toluidine in benzene at 35 °C under a 9.945 GHz electric field:

(I) *o*-anisidine (—○—), (II) *m*-anisidine (—△—), (III) *p*-anisidine (—□—), (IV) *o*-toluidine (—●—), (V) *m*-toluidine (—▲—) and (VI) *p*-toluidine (—■—).

from bond angles and bond moments of the substituent polar groups of the molecules of figure 8.

4. Symmetric and characteristic relaxation times τ_s and τ_{cs}

The symmetric and asymmetric distribution parameters γ and δ appear in the following equations:

$$\chi_{ij}^*/\chi_{0ij} = \frac{1}{1 + (j\omega\tau_s)^{1-\gamma}} \quad (14)$$

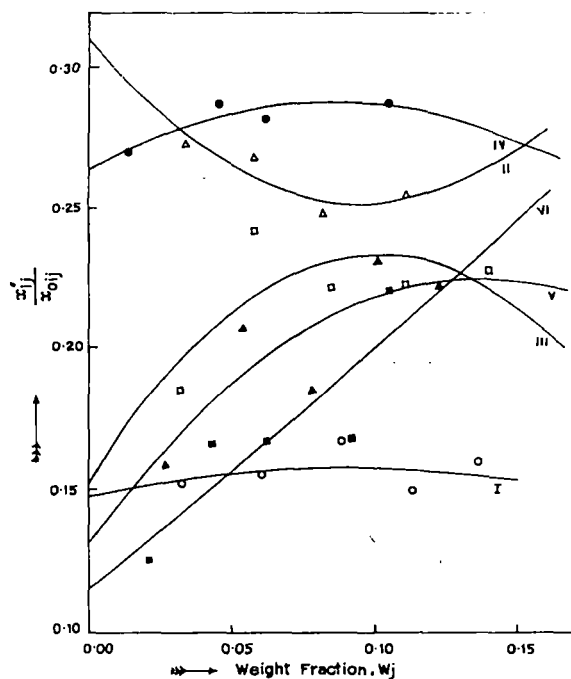


Figure 6. Plot of χ''_{ij}/χ_{0ij} against the weight fraction w_j of the solute of the isomers of the anisidine and toluidine in benzene at 35 °C under a 9.945 GHz electric field:

(I) *o*-anisidine (—○—), (II) *m*-anisidine (—△—), (III) *p*-anisidine (—□—), (IV) *o*-toluidine (—●—), (V) *m*-toluidine (—▲—) and (VI) *p*-toluidine (—■—).

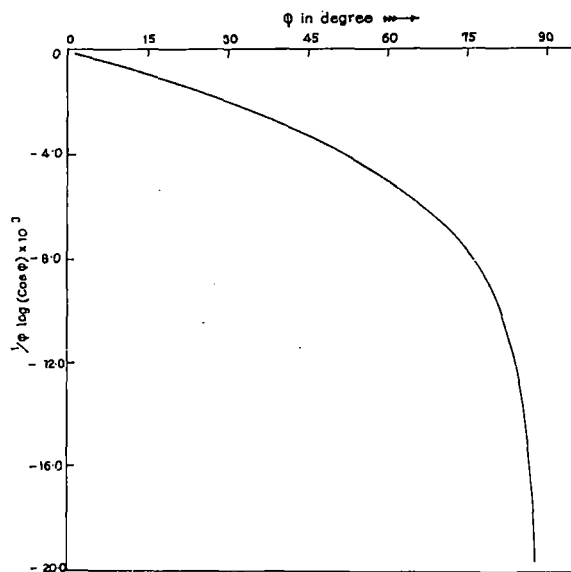


Figure 7. Variation of $(1/\phi) \log(\cos \phi) \times 10^3$ against ϕ in degrees.

$$\chi_{ij}^*/\chi_{0ij} = \frac{1}{(1 + j\omega\tau_{cs})^\delta} \quad (15)$$

Although the left-hand side of equations (14) and (15) are identical, the former is associated with the symmetric relaxation time τ_s and latter with the characteristic relaxation

time τ_{cs} . Separating the real and imaginary parts of equations (14) and (15) and rearranging them in terms of $(\chi'_{ij}/\chi_{0ij})_{w_j \rightarrow 0}$ and $(\chi''_{ij}/\chi_{0ij})_{w_j \rightarrow 0}$ obtained from figures 5 and 6 the γ and τ_s were found using

$$\gamma = \frac{2}{\pi} \tan^{-1} \left[\left(1 - \frac{\chi'_{ij}}{\chi_{0ij}} \right) \frac{\chi'_{ij}}{\chi''_{ij}} - \frac{\chi''_{ij}}{\chi_{0ij}} \right] \quad (16)$$

and

$$\tau_s = \frac{1}{\omega} \left[\frac{1}{(\chi'_{ij}/\chi''_{ij}) \cos(\gamma\pi/2) - \sin(\gamma\pi/2)} \right]^{1/(1-\gamma)} \quad (17)$$

Again δ and τ_{cs} can be obtained from equation (15)

$$\tan(\phi\delta) = \frac{\chi''_{ij}}{\chi'_{ij}} \quad (18)$$

and

$$\tan \phi = \omega \tau_{cs} \quad (19)$$

As ϕ cannot be evaluated directly, an arbitrary theoretical curve between $(1/\phi) \log(\cos \phi)$ against ϕ in degrees was drawn in figure 7, from which

$$\frac{1}{\phi} \log(\cos \phi) = \frac{\log[(\chi'_{ij}/\chi_{0ij}) / \cos(\phi\delta)]}{\phi\delta} \quad (20)$$

can be found. The known value of $(1/\phi) \log(\cos \phi)$ is used to obtain ϕ . With known ϕ and δ , τ_{cs} were found out from equations (18) and (19). τ_s and τ_{cs} so evaluated are given in table 2 in order to compare with values of τ by Murthy *et al* [10], Gopalakrishna [11] and τ_1 and τ_2 determined by double relaxation methods. The estimated values of γ and δ are however, given in table 3.

5. Results and discussion

The least-squares fitted linear equations of $(\chi_{0ij} - \chi'_{ij})/\chi'_{ij}$ against χ''_{ij}/χ'_{ij} for different weight fractions w_j 's of the monosubstituted anilines in benzene at 35°C under a 9.945 GHz electric field are shown graphically in figure 1, with the symbols denoting the experimental points. The experimental points are found to satisfy equation (5). χ'_{ij} and χ''_{ij} are the real and imaginary parts of the complex dielectric orientational susceptibility χ_{ij}^* and χ_{0ij} is the low-frequency dielectric susceptibility which is real. They are, however, derived from the measured relative permittivities [7] ϵ'_{ij} , ϵ''_{ij} , ϵ_{0ij} and $\epsilon_{\infty ij}$ of table 1. The linearity of all the curves of figure 1 are confirmed by correlation coefficients, r 's, lying in the range 0.6894–0.9986. The chisquare test of all the curves were again made to support their linearity. The slopes and intercepts of all the linear curves of figure 1 are placed in the second and third columns of table 2. The chisquare values are, however, large for *o*-anisidine, *p*-anisidine and *m*-toluidine probably because of the large errors introduced in the ϵ'_{ij} , ϵ''_{ij} , ϵ_{0ij} and $\epsilon_{\infty ij}$ measurements for the molecules. In order to find the existence of double relaxation phenomena, accurate measurements of ϵ_{0ij} and $\epsilon_{\infty ij}$ are necessary. The refractive index n_{Dij} measured by Abbe's refractometer yields $\epsilon_{\infty ij} = n_{Dij}^2$ [6], although a Cole–Cole [3, 4] plot often gives $\epsilon_{\infty ij}$ as 1–1.15 times n_{Dij}^2 .

The slope and intercept of each straight-line equation, (5), obtained from χ'_{ij} , χ''_{ij} and χ_{0ij} of different w_j 's of table 1 by least-squares fitting are used to determine τ_1 and τ_2 for each compound, as seen in the sixth and seventh columns of table 2. τ_2 's are found to increase gradually from the *meta* to the *ortho* and to the *para* forms for all the anisidines and toluidines, probably due to the presence of the C \rightarrow NH₂ group in them. The electric field of nearly 3 cm wavelength greatly influences the C \rightarrow NH₂ group. On the other hand, τ_1 increases from *ortho* to *para* for the anisidines, while the reverse is true for the toluidines. The increase in the τ_1 values indicates that the flexible parts of the molecules are more loosely bound to the parent molecules [17, 18], which signifies that the material property of the system is undergoing relaxation.

In the absence of a reliable τ_j under a hf electric field we tried to calculate τ_j 's from the slopes of the least-squares fitted straight-line equations of χ''_{ij} against χ'_{ij} as claimed by Murthy *et al* [10], and give them in the ninth column of table 2. The available experimental points were found to deviate from linearity as illustrated in figure 4. The individual plots of χ'_{ij} and χ''_{ij} against the w_j 's of the isomers of the anisidines and toluidines are not strictly linear as observed in figures 2 and 3. This at once prompted us to use the ratio of the individual slopes of variations of χ''_{ij} and χ'_{ij} with the w_j 's at $w_j \rightarrow 0$ of figures 2 and 3 to obtain τ_j 's. The τ_j 's thus obtained agree well with τ_1 from double relaxation and Gopalakrishna's [11] methods. This confirms the basic soundness of the latter method to determine τ_j where polar–polar interactions are fully avoided. Moreover, it shows that the hf dielectric susceptibility measurement yields a microscopic relaxation time whereas the double relaxation method gives both microscopic and macroscopic τ_1 and τ_2 , as observed elsewhere [19].

Larger τ_2 's signify the larger sizes of the rotating units of solute–solvent, i.e. monomer formation under a hf electric field. The existence of a distribution of τ 's between τ_2 and τ_1 helps us to test the symmetric and asymmetric distribution parameters γ and δ of such compounds. These are calculated from equations (16) and (18) with the values of χ'_{ij}/χ_{0ij} and χ''_{ij}/χ_{0ij} at $w_j \rightarrow 0$ of figures 5 and 6. The values of $(1/\phi) \log(\cos \phi)$ against ϕ in degrees as shown in figure 7 is essential to obtain δ . Knowing ϕ from the curve of figure 7, δ 's were obtained. γ and δ so obtained are seen in the 11th and 12th columns of table 3. The values of γ establishes the non-rigid behaviour of the molecules in benzene in a 9.945 GHz electric field. They obey symmetric relaxation phenomena as δ 's are found to be low.

The symmetric relaxation time τ_s from equation (17) agrees with the τ_1 's and τ 's due to Gopalakrishna's method [11] indicating symmetric relaxation behaviour for such molecules; but in case of *p*-anisidine the agreement is poor. It may probably be due to the experimental uncertainty or the presence of two flexible polar units in a line. The characteristic relaxation time τ_{cs} obtained from δ gives high values. They thus rule out the applicability of asymmetric relaxation behaviour for such polar molecules in benzene.

We find the relative contributions c_1 and c_2 towards dielectric dispersions for each polar compound, reported in tables and figures from equations (3) and (4) for fixed τ_1 and τ_2 of equation (5) and χ'_{ij}/χ_{0ij} and χ''_{ij}/χ_{0ij} of Fröhlich's equations, (6) and (7). The same could, however, be obtained

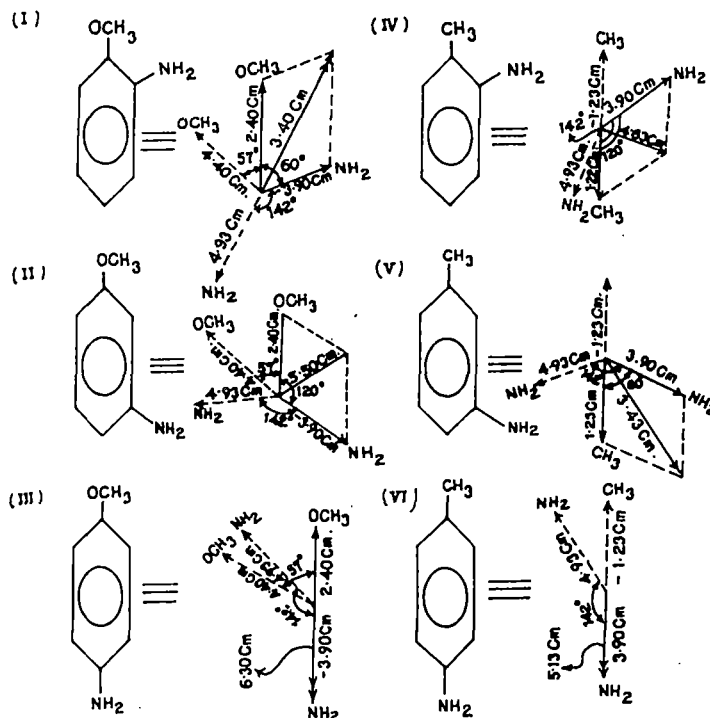


Figure 8. Conformational structures of the isomers of the anisidine and toluidine. (The bond moments ($\times 10^{30}$ C m) are given in the figures).

by a graphical technique. The c_1 and c_2 by both the methods are given in table 3. The Fröhlich's equations, (6) and (7), are related to Fröhlich's parameter, A , which predicts the temperature variation of the width of the distribution of τ . A is equal to $\ln(\tau_2/\tau_1)$. c_1 and c_2 obtained with χ'_{ij}/χ_{0ij} and χ''_{ij}/χ_{0ij} of Fröhlich's equations and the least-squares fitted graphically estimated values from figures 5 and 6 satisfy $c_1 + c_2 \approx 1$. The variation of χ'_{ij}/χ_{0ij} and χ''_{ij}/χ_{0ij} with w_j usually do not obey Bergmann *et al.*'s [13] equations, (1) and (2); as observed elsewhere [17, 18]. For *p*-toluidine c_2 becomes negative as seen in the tenth column of table 3. This arises due to the inertia of the whole molecule with respect to its flexible part under a nearly 10 GHz electric field [7, 19].

The dipole moments μ_1 and μ_2 of the flexible parts and whole molecules of all the compounds under investigation were obtained in terms of the dimensionless parameters b_1 and b_2 related to τ_1 and τ_2 and the linear coefficient β of the $\chi'_{ij}-w_j$ curve of figure 3. They are placed in the 11th and 12th columns of table 4 together with μ_0 in terms of b_0 related to τ_0 , where τ_0 is the most probable relaxation time ($=\sqrt{\tau_1\tau_2}$) for the distribution of τ 's between two fixed values. The correlation coefficients, τ 's, of the $\chi'_{ij}-w_j$ curves were also estimated and are entered in the fifth column of table 4, but only to show how far the χ'_{ij} 's are correlated with the w_j 's. The corresponding percentage of error in terms of τ are entered in the sixth column of table 4. The variation of the χ'_{ij} 's with the w_j 's gives a reliable slope of β to yield reliable μ_1 , μ_2 and μ_0 values. Almost all $\chi'_{ij}-w_j$ curves in figure 3 show a tendency to be closer in the region $0.00 \leq w_j \leq 0.03$, indicating an almost identical polarity of the solute molecules in addition to solute-solvent (monomer) and solute-solute (dimer) formations [9].

The solvent, benzene, is a cyclic compound with three double bonds and six p-electrons on six carbon atoms. Hence the $\pi-\pi$ interaction or resonance effect combined with an inductive effect, known as the mesomeric effect, is expected to play an important role in the measured hf μ_j . Special attention is therefore paid to obtain the conformational structures of the isomers of anisidine and toluidine from the available bond angles and bond moments of the substituent polar groups. The polar groups $C \rightarrow NH_2$ ($\angle 142^\circ$), $C \rightarrow OCH_3$ ($\angle 120^\circ$) and $C \rightarrow CH_3$ ($\angle 180^\circ$) having bond moments of 3.90×10^{-30} , 2.40×10^{-30} and 1.23×10^{-30} C m, respectively, are used to obtain the theoretical μ_{theo} of figure 8. In the case of the anisidines, the amino group, $-NH_2$, exhibits a mesomeric effect by pushing the electrons towards the C atom of the benzene ring, but the inductive effect is more prominent in the $-OCH_3$ group rather than mesomeric effect; so the latter pulls the electrons from the C atom of the ring. Hence the resultant μ_{theo} increases from the *para* to the *ortho* and to the *meta* forms, as seen in table 4. In the case of the methyl group, $-CH_3$, in toluidines the inductive effect is important as the sp^2 hybridized C atom of benzene is more electronegative than the C atom of the $-CH_3$ group, which is sp^3 hybridized. Thus the direction of the bond moment is towards the benzene ring. For the $-NH_2$ group the mesomeric and inductive effects act oppositely, but as the mesomeric effect is more pronounced so resultant bond moment is towards the C_6H_6 ring. In the *ortho*, *meta* and *para* toluidines, the angle between the $-CH_3$ and $-NH_2$ groups are 60° , 120° and 180° , respectively. Hence there is an increment in μ_{theo} from the *ortho* to the *meta* and to the *para* forms (table 4).

In the absence of reliable μ_j values of these compounds Gopalakrishna's method [11] was employed to obtain hf μ_j 's

(reported data). The close agreement between the reported μ_j (Gopalakrishna), μ_1 and μ_{rheo} as seen in table 4 establishes the basic soundness of the method prescribed for obtaining hf μ_j . It also confirms the fact that a part of the molecule is rotating under a nearly 3 cm wavelength electric field.

6. Conclusions

The theoretical considerations for the effective utilization of the established symbols of the dielectric susceptibilities, χ_{ij} 's, from the dielectric relative permittivities ϵ_{ij} 's appear to be sound to study the dielectric relaxation mechanism as χ_{ij} 's are directly concerned with orientational polarization. The significant equations in terms of the χ_{ij} 's help one to grasp new physical insight into polar-polar and polar-non-polar molecular interactions in solution. The single-frequency measurement of the relaxation parameters thus provides a unique method to obtain macroscopic and microscopic relaxation times and hence dipole moments of the whole and the flexible parts of the molecules. The estimation of τ from the linear equation (5) is a very simple, straightforward and significant one to obtain μ from equation (13) in terms of linear coefficient β of the familiar $\chi'_{ij}-w_j$ curve. The correlation coefficient r and the chisquare values signify the minimum error introduced into the desired parameters. The molecules under identical states show interesting phenomena of a double or, often, a single relaxation mechanism depending upon the solvent used. The probability of showing the double relaxation phenomena of monosubstituted anilines in benzene depends upon the electric field frequency of nearly 10 GHz. Various types of molecular associations, such as solute-solute and solute-solvent interactions, are thus inferred from the usual departure of graphically fitted plots of χ'_{ij}/χ_{0ij} and χ''_{ij}/χ_{0ij} with w_j following Bergmann's equations [13]. Non-rigid characteristics of the molecules are ascertained

by estimation of symmetric and asymmetric distribution parameters in benzene. The molecular associations are also supported by the conformational structures of the molecules in which the mesomeric, inductive and electromeric effects play prominent roles.

References

- [1] Sharma A and Sharma D R 1992 *J. Phys. Soc. Japan* **61** 1049
- [2] Sit S K, Ghosh N, Saha U and Acharyya S 1997 *Indian J. Phys. B* **71** 533
- [3] Cole K S and Cole R H 1941 *J. Chem. Phys.* **9** 341
- [4] Davidson D W and Cole R H 1951 *J. Chem. Phys.* **19** 1484
- [5] Jonscher A K 1980 *Physics of Dielectric Solids, Invited Papers* CHL Goodman
- [6] Srivasta S C and Chandra S 1975 *Indian J. Pure Appl. Phys.* **13** 101
- [7] Sit S K and Acharyya S 1996 *Indian J. Pure Appl. Phys.* **34** 255
- [8] Jonscher A K 1980 *Inst. Phys. Conf. (Canterbury)* ed C H L Goodman
- [9] Ghosh N, Karmakar A, Sit S K and Acharyya S 2000 *Indian J. Pure Appl. Phys.* **38** 574
- [10] Murthy M B R, Patil R L and Deshpande D K 1989 *Indian J. Phys. B* **63** 491
- [11] Gopalakrishna K V 1957 *Trans. Faraday Soc.* **53** 767
- [12] Fröhlich H 1949 *Theory of Dielectrics* (Oxford: Oxford University Press)
- [13] Bergmann K, Roberti D M and Smyth C P 1960 *J. Chem. Phys.* **64** 665
- [14] Smyth C P 1955 *Dielectric Behaviour and Structure* (New York: McGraw-Hill)
- [15] Dutta K, Sit S K and Acharyya S 2000 *Pramana: J. Phys.* at press
- [16] Ghosh N, Basak R C, Sit S K and Acharyya S 2000 *J. Mol. Liquids* **85** 375
- [17] Saha U, Sit S K, Basak R C and Acharyya S 1994 *J. Phys. D: Appl. Phys.* **27** 596
- [18] Sit S K, Basak R C, Saha U and Acharyya S 1994 *J. Phys. D: Appl. Phys.* **27** 2194
- [19] Sit S K, Ghosh N and Acharyya S 1997 *Indian J. Pure Appl. Phys.* **35** 329

Journal of MOLECULAR LIQUIDS

Editor-in-Chief:

Professor Josef Barthel

Institute of Physical and
Theoretical Chemistry
University of Regensburg
93040 Regensburg
Germany

Tel. No.: +49-941-943-4042

Fax No.: +49-941-943-4532

e-mail: Josef.Barthel@chemie.uni-regensburg.de

Dr. S. Acharyya
Dept. of physics
Raiganj College
Raiganj – 733134
Uttar Dinajpur, India
e-mail: gkdutta@rediffmail.com

Associate Editor

Professor Werner Kunz

Institute of Physical and
Theoretical Chemistry
University of Regensburg
93040 Regensburg
Germany

Tel. No.: +49-941-943-4041

Fax No.: +49-941-943-4531

e-mail: Werner.Kunz@chemie.uni-regensburg.de

27.11.01

Our Ref.: MS 01045

Dear Dr. Acharyya

Thank you for the revised version of your paper MS 01026:

Double Relaxation Phenomena of Monosubstituted Anilines in
Benzene under High Frequency Electric Field.
N. Gosh, S.K.Sit and S. Acharyya

I will continue the publishing procedure. If there is no serious argument by the referees, you will not receive further mail. Minor errors of spelling etc. will be corrected here. You will be contacted by the publishing company for the copy-right and the reprints.

Please, do not hesitate to contact me when you think that I could be of any help to you.

We highly appreciated receiving a manuscript from you and hope that you will submit more manuscripts to us in the future.

With kind regards.


Yours sincerely

Josef Barthel
Editor-in-Chief

Received on
7. 12. 01

Double relaxation phenomena of monosubstituted anilines in benzene under high frequency electric field.

N. Ghosh, S. K. Sit and S. Acharyya

Department of Physics, Raiganj College (University College) P.O. Raiganj, Dist. Uttar Dinajpur, Pin- 733134 (W.B.), India.

ABSTRACT

The intercept and slope of a derived linear equation : $(\chi_{oij} - \chi'_{ij}) / \chi'_{ij} = \omega (\tau_1 + \tau_2) \chi''_{ij} / \chi'_{ij} - \omega^2 \tau_1 \tau_2$ for different weight fractions w_j 's of monosubstituted anilines (j) in benzene(i) at 35°C under different electric field frequencies are used to yield the double relaxation times τ_1 and τ_2 of the flexible parts and the whole molecules. χ'_{ij} and χ''_{ij} are the real and imaginary parts of hf complex dielectric orientational susceptibility χ^*_{ij} and χ_{oij} is the low frequency dielectric susceptibility which is real. τ_j 's obtained from the ratio of the individual slopes of variations of χ''_{ij} and χ'_{ij} with w_j 's at $w_j \rightarrow 0$ are compared with Murthy et al (Indian J Phys **63 B** 1989 491) and Gopalakrishna (Trans Faraday. Soc. **53** 1957 767). The theoretical weighted contributions c_1 and c_2 for τ_1 and τ_2 from Fröhlich's equations are compared with the experimental ones from the graphically fitted curves of χ'_{ij} / χ_{oij} and χ''_{ij} / χ_{oij} with w_j 's in the limit $w_j = 0$. The values of $(\chi'_{ij} / \chi_{oij})_{w_j \rightarrow 0}$ and $(\chi''_{ij} / \chi_{oij})_{w_j \rightarrow 0}$ are again employed to get symmetric and asymmetric distribution parameters γ and δ , the latter one is from the curve of $1/\phi \log \text{Cos}\phi$ against ϕ^0 to yield the symmetric and characteristic relaxation times τ_s and τ_{cs} respectively only to show that symmetric relaxation behaviour obeyed by the molecules. The dipole moments μ_1 and μ_2 for the rotation of flexible parts and the whole molecules are measured from τ_1 and τ_2 and linear coefficient β 's of the variations of χ'_{ij} and hf conductivity σ_{ij} with w_j 's. The measured μ_1 and μ_2 are compared with the reported μ 's and μ_{theo} 's of available bond angles and bond moments of the substituent polar groups of the parent molecules. The slight disagreement of measured μ 's from μ_{theo} 's indicates the existence of inductive, mesomeric and electromeric effects suffered by the polar groups under hf electric field.

1. INTRODUCTION

In recent years, single or double relaxation phenomenon of polar liquid molecules in nonpolar solvents under high frequency (hf) electric field attracted the attention of a large number of workers [1, 2]. The study often provides the valuable information on the shape, size and structure, in addition to solute-solvent or solute-solute molecular associations in terms of the measured relaxation time τ and dipole moment μ by any conventional method [3, 4]. The stability and unstability [5] of the molecules towards dielectric relaxations, is, however, inferred from such study. τ_1 and τ_2 of the double relaxation method, τ_j from the ratio of slopes of the individual variations of χ''_{ij} and χ'_{ij} with weight fractions w_j 's in the limit $w_j = 0$ and μ_j 's from the linear coefficient β 's of either $\chi'_{ij} - w_j$ or hf conductivity $\sigma_{ij} - w_j$ curves shed more light on the structural aspects of such dielectropolar liquid molecules [6].

The real ϵ'_{ij} and imaginary ϵ''_{ij} parts of hf complex relative permittivity ϵ^*_{ij} together with the low frequency or static and optical relative permittivities ϵ_{oij} and $\epsilon_{\infty ij}$ of isomers of methoxy substituted anilines (anisidines) and methyl substituted anilines (toluidines) in benzene under 2.02, 3.86 and 22.06 GHz electric field for different weight fractions w_j 's were measured by Srivastava and Chandra [7] at 35°C. The analytical grade ortho, para toluidines and para-anisidines were supplied by M/S Riedel (Germany) and the others were of M/S BDH (London). The liquids were further purified by repeated fractional distillations and their physical constants like density ρ , viscosity η and refractive indices n_{Dij} were carefully checked in agreement with the literature values before use. The purpose of the study [7] was to detect the possible existence of solute-solvent (monomer) and solute-solute (dimer) molecular associations in the mixtures of various concentrations.

Nowadays, the usual trend is to study the dielectric relaxation processes in terms of hf complex dielectric orientational susceptibility χ^*_{ij} rather than hf complex conductivity σ^*_{ij} or hf relative permittivity ϵ^*_{ij} . ϵ^*_{ij} includes within it all types of polarisations while σ^*_{ij} is associated with transport of bound molecular charges. Hence it is more reasonable to work with χ_{ij} 's as they have direct link with the orientational polarisations [8]. Moreover, the present method of study in S.I unit is superior because of its unified, coherent and rationalised nature.

The dielectric susceptibilities like real $\chi'_{ij} = (\epsilon'_{ij} - \epsilon_{\infty ij})$ imaginary $\chi''_{ij} = \epsilon''_{ij}$ parts of complex susceptibility $\chi^*_{ij} = (\epsilon^*_{ij} - \epsilon_{\infty ij})$ and the low frequency susceptibility $\chi_{oij} = (\epsilon_{oij} - \epsilon_{\infty ij})$ which is real, were derived from the measured relative permittivities ϵ'_{ij} , ϵ''_{ij} , ϵ_{oij} and $\epsilon_{\infty ij}$ in each system for different w_j 's of the respective solute [7]. The experimental results of χ_{ij} 's for different w_j 's are thus collected together in Table 1 for use. One could make a strong conclusion of double relaxation phenomena of a polar molecule in a nonpolar solvent based on single frequency measurement of the relaxation parameters provided the accurate value of χ_{oij} involved with ϵ_{oij} and $\epsilon_{\infty ij}$ is available. The use of n^2_{Dij} for $\epsilon_{\infty ij}$ [7] may often introduce additional error in the calculation. Nevertheless, the data presented in Table 1 are accurate up to 5% for χ''_{ij} and 2% for χ'_{ij} and χ_{oij} respectively.

The polar liquids like monosubstituted anilines often possess two or more τ 's in GHz electric field for the rotation of their flexible polar groups to the parent molecules and the whole molecule itself [9]. Bergmann et al [10] devised a graphical method to obtain double relaxation times τ_1 and τ_2 and hence weighted contributions c_1 and c_2 towards dielectric dispersions for some complex polar liquid molecules. The method is based on plotting the measured values of ϵ' , ϵ'' , ϵ_0 , ϵ_{∞} at various frequencies ω on a semicircle in a complex plane. A point was then selected on the chord through two fixed points on the semicircle drawn in consistency with the experimental data. Bhattacharyya et al [11] subsequently modified the above procedure to get the same with experimental values measured at two different frequencies of GHz range.

Thus the object of the present paper is to detect the double relaxation times τ_1 and τ_2 due to rotations of the flexible parts and the whole molecules using χ_{ij} 's based on a single frequency measurement technique [7, 12-13]. The aniline derivatives are thought to absorb electric energy much more strongly at nearly 10 GHz electric field. The parameters measured at 2.02, 3.86 and

Table-1 : Real ϵ'_{ij} and imaginary ϵ''_{ij} parts of hf complex relative permittivity ϵ_{ij}^* static and optical frequency hf relative permittivities ϵ_{oij} and $\epsilon_{\infty ij}$ together with real χ'_{ij} and imaginary χ''_{ij} parts of hf complex dielectric orientational susceptibility χ_{ij}^* along with low frequency susceptibility χ_{oij} which is real for some monosubstituted anilines in benzene under different electric field frequencies at 35°C for various concentrations.

Systems with serial number & molecular weight M_j	Frequency (f) in GHz	Weight fraction w_j of solute	Measured dielectric relative permittivities				Dimensionless dielectric orientational susceptibilities		
			ϵ'_{ij}	ϵ''_{ij}	ϵ_{oij}	$\epsilon_{\infty ij}$	χ'_{ij}	χ''_{ij}	χ_{oij}
(I) o-anisidine in benzene $M_j = 0.123\text{kg}$	(a) 3.86	0.0326	2.32	0.011	2.336	2.239	0.081	0.011	0.097
		0.0604	2.37	0.021	2.404	2.247	0.123	0.021	0.157
		0.0884	2.44	0.029	2.459	2.255	0.185	0.029	0.204
		0.1135	2.49	0.033	2.538	2.262	0.228	0.033	0.276
		0.1361	2.53	0.041	2.588	2.267	0.263	0.041	0.321
	(b) 22.06	0.0326	2.31	0.015	2.336	2.239	0.071	0.015	0.097
		0.0604	2.36	0.026	2.404	2.247	0.113	0.026	0.157
		0.0884	2.40	0.041	2.459	2.255	0.145	0.041	0.204
		0.1135	2.42	0.053	2.538	2.262	0.158	0.053	0.276
		0.1361	2.56	0.065	2.588	2.267	0.293	0.065	0.321
(II) m-anisidine in benzene $M_j = 0.123\text{kg}$	(a) 3.86	0.0160	2.31	0.018	2.315	2.235	0.075	0.018	0.080
		0.0336	2.25	0.026	2.384	2.241	0.009	0.026	0.143
		0.0579	2.43	0.043	2.477	2.246	0.184	0.043	0.231
		0.0823	2.51	0.059	2.553	2.253	0.257	0.059	0.300
		0.1109	2.61	0.084	2.675	2.261	0.349	0.084	0.414
	(b) 22.06	0.0160	2.29	0.021	2.315	2.235	0.055	0.021	0.080
		0.0336	2.32	0.038	2.384	2.241	0.079	0.038	0.143
		0.0579	2.36	0.068	2.477	2.246	0.114	0.068	0.231
		0.0823	2.40	0.080	2.553	2.253	0.147	0.080	0.300
		0.1109	2.43	0.115	2.675	2.261	0.169	0.115	0.414
(III) o-toluidine in benzene $M_j = 0.107\text{kg}$	2.02	0.0137	2.30	0.005	2.301	2.241	0.059	0.005	0.060
		0.0459	2.38	0.013	2.392	2.250	0.130	0.013	0.142
		0.0622	2.42	0.015	2.457	2.255	0.165	0.015	0.202
		0.1048	2.55	0.022	2.577	2.264	0.286	0.022	0.313
(IV) m-toluidine in benzene $M_j = 0.107\text{kg}$	3.86	0.0264	2.31	0.007	2.337	2.243	0.067	0.007	0.094
		0.0538	2.37	0.016	2.413	2.248	0.122	0.016	0.165
		0.0781	2.44	0.024	2.470	2.252	0.188	0.024	0.218
		0.1015	2.39	0.036	2.526	2.258	0.132	0.036	0.268
		0.1225	2.54	0.045	2.591	2.262	0.278	0.045	0.329
(V) p-toluidine in benzene $M_j = 0.107\text{kg}$	(a) 3.86	0.0213	2.31	0.010	2.319	2.237	0.073	0.010	0.082
		0.0428	2.32	0.016	2.367	2.244	0.076	0.016	0.123
		0.0616	2.38	0.018	2.413	2.249	0.131	0.018	0.164
		0.0916	2.46	0.029	2.483	2.254	0.206	0.029	0.229
		0.1048	2.48	0.046	2.523	2.260	0.220	0.046	0.263
	(b) 22.06	0.0213	2.31	0.009	2.319	2.237	0.073	0.009	0.082
		0.0428	2.33	0.020	2.367	2.244	0.086	0.020	0.123
		0.0616	2.36	0.033	2.413	2.249	0.111	0.033	0.164
		0.0916	2.40	0.046	2.483	2.254	0.146	0.046	0.229
		0.1048	2.44	0.058	2.523	2.260	0.180	0.058	0.263

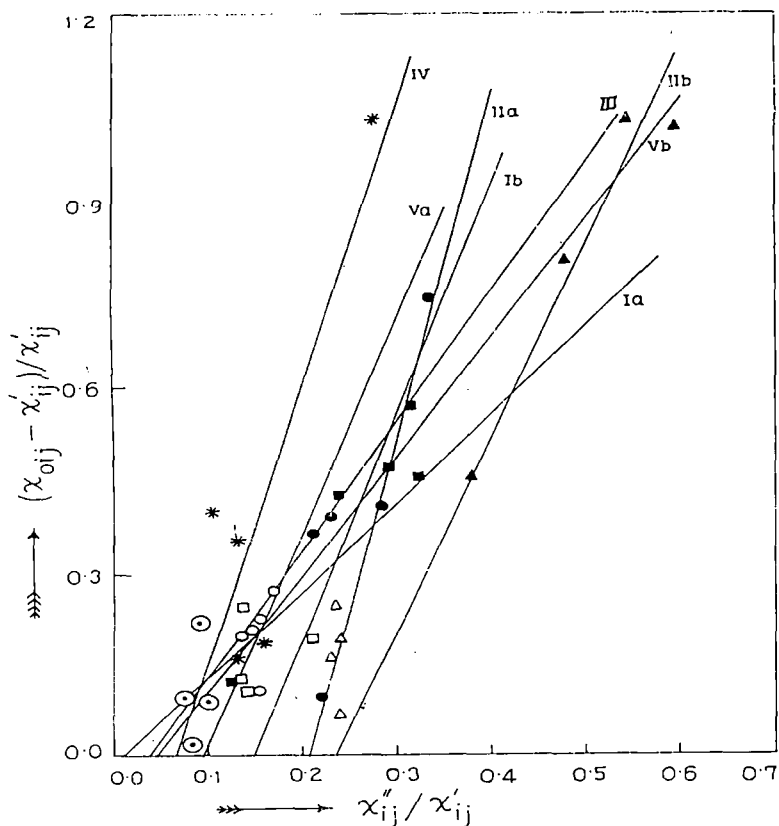


Figure 1 : Linear variation of $(\chi_{oij} - \chi'_{ij}) / \chi'_{ij}$ against χ''_{ij} / χ'_{ij} of monosubstituted anilines in benzene at 35°C under GHz electric field. (Ia) o-anisidine at 3.86 GHz (-O-), (Ib) o-anisidine at 22.06 GHz (-●-), (IIa) m-anisidine at 3.86 GHz (-Δ-), (IIb) m-anisidine at 22.06 GHz (-▲-), (III) o-toluidine at 2.02 GHz (-○-), (IV) m-toluidine at 3.86 GHz (-*-), (Va) p-toluidine at 3.86 GHz (-□-) and (Vb) p-toluidine at 22.06 GHz (-■-) respectively.

$$\chi'_{ij} / \chi_{oij} = c_1 / (1 + \omega^2 \tau_1^2) + c_2 / (1 + \omega^2 \tau_2^2) \quad (1)$$

$$\chi''_{ij} / \chi_{oij} = c_1 \omega \tau_1 / (1 + \omega^2 \tau_1^2) + c_2 \omega \tau_2 / (1 + \omega^2 \tau_2^2) \quad (2)$$

assuming two separate broad dispersions for which the sum of c_1 and c_2 is unity. Equations (1) and (2) are now solved to get

$$(\chi_{oij} - \chi'_{ij}) / \chi'_{ij} = \omega(\tau_1 + \tau_2) \chi''_{ij} / \chi'_{ij} - \omega^2 \tau_1 \tau_2 \quad (3)$$

When the variables $(\chi_{oij} - \chi'_{ij}) / \chi'_{ij}$ and χ''_{ij} / χ'_{ij} of equation (3) are plotted for different ω 's of a polar liquid at any given frequency ω of the applied electric field, a straight line results with intercept $-\omega^2 \tau_1 \tau_2$ and slope $\omega(\tau_1 + \tau_2)$, as shown in Figure 1. The intercept and slope of equation (3) are, however, obtained by linear regression analysis on the measured χ_{ij} 's of different ω 's of the monosubstituted anilines in C_6H_6 of Table 1 to get τ_1 and τ_2 as entered in the 7th and 8th columns of Table 2 extracted from the data of Table 1. The reliability of the data are checked through chisquares values. In absence of reliable τ_i , the ratio of individual slopes of variations of χ''_{ij} and χ'_{ij} with ω 's at $\omega \rightarrow 0$, as seen in Figures 2 and 3; were conveniently used to evaluate τ_i to compare with those of Murthy et al [14] of Figure 4 and Gopalakrishna [15].

22.06 GHz electric fields may yield considerable τ_1 and τ_2 . Moreover, the present systems in terms of new physical parameters like χ_{ij} 's seem to yield a better insight into the relaxation phenomena. One is further tempted to see how far the linear coefficients β 's of the variations of χ'_{ij} 's and σ_{ij} with ω_j affect μ 's. The aspect of molecular orientational polarisation, is, however, achieved by introducing χ_{ij} 's because $\epsilon_{\infty ij}$ which includes the fast polarisation, always appears as a subtracted term in Bergmann et al's equations [10]. Thus in order to exclude the fast polarisation process and to avoid the clumsiness of algebra the established symbols of dielectric terminologies and parameters like $\chi'_{ij} = (\epsilon'_{ij} - \epsilon_{\infty ij})$, $\chi''_{ij} = \epsilon''_{ij}$ and $\chi_{oij} = (\epsilon_{oij} - \epsilon_{\infty ij})$ of Table 1 are used in the Bergmann et. al's equations [10]:

Table 2: Intercept and slope of linear equation of $(\chi_{oij} - \chi'_{ij}) / \chi'_{ij}$ against χ''_{ij} / χ'_{ij} , correlation coefficient (r) and chisquare values, estimated relaxation times τ_1 and τ_2 due to rotation of flexible polar group and whole molecule, measured τ_j from Eq (16) and (17), reported τ (Gopalakrishna) symmetric and characteristic relaxation times τ_s and τ_{cs} of Eq. (11) and (13) of some monosubstituted anilines in benzene at 35°C under different GHz electric field frequencies.

Systems with serial number	Frequency (f) in GHz	Intercept and slope of Eq (3)		Correlation coefficient(r) and chisquares values of Eq(3)		Estimated relaxation times τ_1 & τ_2 in p.sec		Measured τ (ps) ^a	Ratio of slopes of $\chi''_{ij}-w_j$ & $\chi'_{ij}-w_j$ curves at $w_j \rightarrow 0$
(I) o-anisidine in benzene	(a) 3.86	0.0179	1.4360	0.3032	0.07	0.52	58.73	6.29	0.1891
	(b) 22.06	0.5406	3.6741	0.8277	0.23	1.11	25.41	1.59	0.1601
(II) m-anisidine in benzene	(a) 3.86	1.1404	5.5485	0.9999	0.15	8.82	220.07	7.61	0.2188
	(b) 22.06	0.7318	3.1447	0.9803	0.02	1.83	20.87	5.55	0.5413
(III) o-toluidine in benzene	2.02	0.0773	2.0910	0.2402	0.02	2.97	161.86	5.70	0.1536
(IV) m-toluidine in benzene	3.86	0.2938	4.5092	0.8469	0.51	2.73	183.29	6.53	0.3792
(V) p-toluidine in benzene	(a) 3.86	0.3149	3.4446	0.6480	0.30	3.88	183.22	7.64	0.2116
	(b) 22.06	0.0821	1.9151	0.9408	0.03	0.32	13.51	3.19	46.1743

Systems with serial number	Frequency (f) in GHz	Relaxation times			
		τ (ps) ^b	τ (ps) ^c	τ_s (ps)	τ_{cs} (ps) ^{cs}
(I) o-anisidine in benzene	(a) 3.86	7.80	5.25	0.92	471.52
	(b) 22.06	1.15	1.56	0.90	—
(II) m-anisidine in benzene	(a) 3.86	9.02	8.05	12.30	90.52
	(b) 22.06	3.91	4.41	2.33	14.80
(III) o-toluidine in benzene	2.02	12.11	4.97	17.06	—
(IV) m-toluidine in benzene	3.86	15.64	7.05	2.23	1181.32
(V) p-toluidine in benzene	(a) 3.86	8.73	7.65	8.15	—
	(b) 22.06	333.30	5.53	2.11	—

a. Measured by slope of χ''_{ij} against χ'_{ij} using Eq. (16)

b. From the ratio of individual slopes

c. By Gopalakrishna's method [15]

The theoretical weighted contributions c_1 and c_2 due to measured τ_1 and τ_2 from equation (3) were worked out from Fröhlich's equations [16] and are placed in Table 3 in order to compare them with the experimental ones from the intercepts of the least squares fitted curves of χ'_{ij}/χ_{oij} and χ''_{ij}/χ_{oij} against w_j 's from Figures 5 and 6 in the limit $w_j = 0$. The values of χ'_{ij}/χ_{oij} and χ''_{ij}/χ_{oij} at $w_j = 0$ together with arbitrary curve of $1/\varphi \log (\cos \varphi)$ against φ in degrees shown elsewhere [17] are further used to obtain symmetric and asymmetric distribution parameters γ and δ as seen in Table 3 to conclude the symmetric relaxation behaviour of such molecules. Symmetric relaxation time τ_s from γ and characteristic relaxation time τ_{cs} from δ and φ are further estimated in order to compare with τ_1 , τ_2 and τ_j of Table 2.

The dipole moments μ_1 and μ_2 by both hf susceptibility and conductivity measurement techniques are, however, worked out from linear coefficient β 's of $\chi'_{ij}-w_j$ and $\sigma_{ij}-w_j$ curves of Figures 3 and 7 in terms of b_1 , b_2 involved with the estimated τ_1 , τ_2 by double relaxation method. The μ_1 and μ_2 thus obtained are placed in Table 4 to see how far they are affected by the orientational polarisation and bound molecular charge in connection with χ_{ij} 's and σ_{ij} 's respectively. The estimated μ_1 and μ_2 by both the methods are finally compared with reported μ 's (Gopalakrishna) and μ_{theo} 's from bond angles and bond moments of polar groups of the molecules to support their conformations. The slight disagreement between measured μ_j 's and μ_{theo} 's invites the existence of inductive, mesomeric and electromeric effects suffered by polar groups, in addition to weak molecular associations between the polar molecules.

2. WEIGHTED CONTRIBUTIONS C_1 AND C_2 FOR τ_1 AND τ_2

By putting $\alpha_1 = \omega\tau_1$ and $\alpha_2 = \omega\tau_2$ the equations (1) and (2) are solved to get

$$c_1 = \frac{(\chi'_{ij}\alpha_2 - \chi''_{ij})(1 + \alpha_1^2)}{\chi_{oij}(\alpha_2 - \alpha_1)} \quad (4)$$

and

$$c_2 = \frac{(\chi''_{ij} - \chi'_{ij}\alpha_1)(1 + \alpha_2^2)}{\chi_{oij}(\alpha_2 - \alpha_1)} \quad (5)$$

provided $\alpha_2 > \alpha_1$. The theoretical values of c_1 and c_2 towards dielectric relaxations were, however, obtained from equations (4) and (5) with the help of Fröhlich's following theoretical equations [16]:

$$\chi'_{ij}/\chi_{oij} = 1 - \frac{1}{2A} \ln \left[\frac{1 + \omega^2 \tau_2^2}{1 + \omega^2 \tau_1^2} \right] \quad (6)$$

$$\chi''_{ij}/\chi_{oij} = 1/A [\tan^{-1}(\omega\tau_2) - \tan^{-1}(\omega\tau_1)] \quad (7)$$

in terms of the measured τ_1 and τ_2 as presented in Table 2 from equation (3) of double relaxation method.

The theoretical c_1 and c_2 as entered in Table 3 are compared with the experimental ones obtained from the intercepts of fitted parabolic curves of χ'_{ij}/χ_{oij} and χ''_{ij}/χ_{oij} against w_j of Figures 5 and 6 in the limit $w_j = 0$ and equations (3) and (4). The curves in Figure 5 and 6 drawn

by the regression analysis of polynomial fitting, are thought to yield the accurate values of χ'_{ij}/χ_{oij} and χ''_{ij}/χ_{oij} in the limit $w_j = 0$ in comparison to earlier graphical extrapolation technique based on personal judgement. The Fröhlich's parameter $A = \ln(\tau_2/\tau_1)$ are placed in Table 3 for each compound at different frequencies.

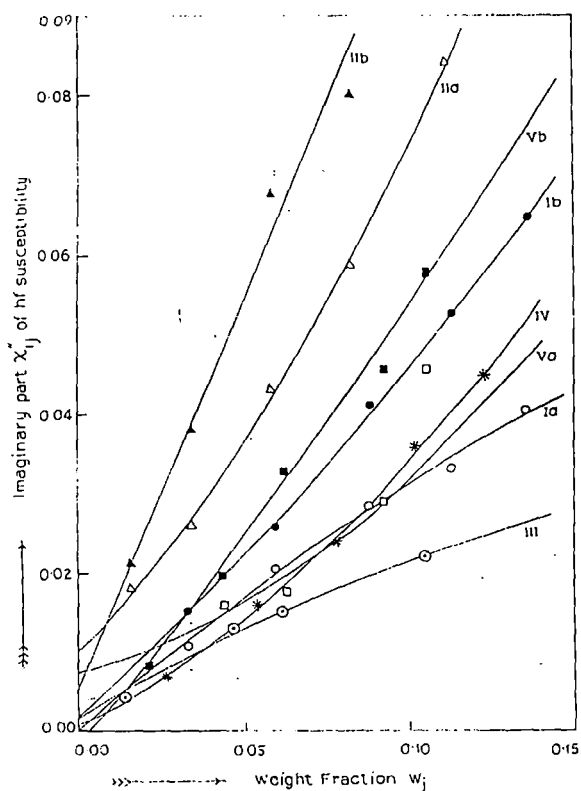


Figure 2 : Variation of imaginary part of hf susceptibility χ''_{ij} against weight fraction w_j of monosubstituted anilines in benzene at 35°C under GHz electric field.

(Ia) o-anisidine at 3.86 GHz (—○—), (Ib) o-anisidine at 22.06 GHz (—●—), (IIa) m-anisidine at 3.86 GHz (—△—), (IIb) m-anisidine at 22.06 GHz (—▲—), (III) o-toluidine at 2.02 GHz (—○—), (IV) m-toluidine at 3.86 GHz (—*—), (Va) p-toluidine at 3.86 GHz (—□—) and (Vb) p-toluidine at 22.06 GHz (—■—) respectively.

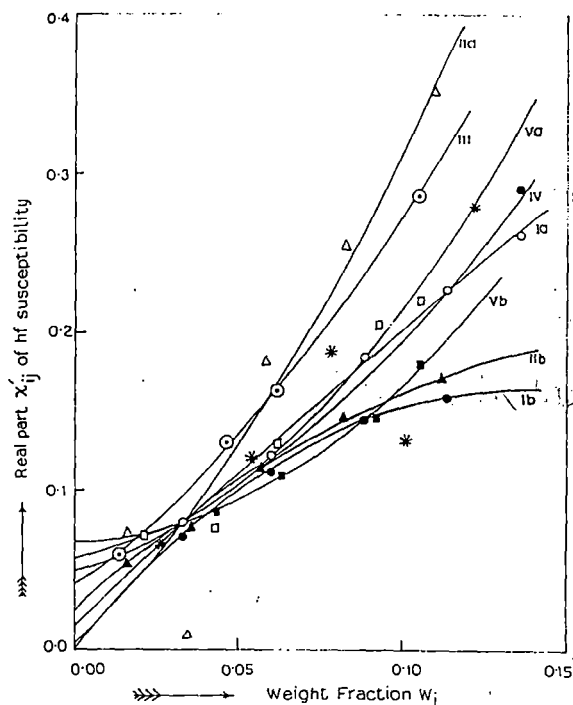


Figure 3 : Variation of real part of hf susceptibility χ'_{ij} against weight fraction w_j of monosubstituted anilines in benzene at 35°C under GHz electric field.

(Ia) o-anisidine at 3.86 GHz (—○—), (Ib) o-anisidine at 22.06 GHz (—●—), (IIa) m-anisidine at 3.86 GHz (—△—), (IIb) m-anisidine at 22.06 GHz (—▲—), (III) o-toluidine at 2.02 GHz (—○—), (IV) m-toluidine at 3.86 GHz (—*—), (Va) p-toluidine at 3.86 GHz (—□—) and (Vb) p-toluidine at 22.06 GHz (—■—) respectively.

3. SYMMETRIC AND CHARACTERISTIC RELAXATION TIMES τ_s AND τ_{cs}

The molecules under the present investigation appear to behave like non-rigid ones at 2.02, 3.86 and 22.06 GHz electric field having either symmetric or asymmetric distribution parameters γ and δ involved in the equations (8) and (9):

$$\frac{\chi_{ij}^{*}}{\chi_{oij}} = \frac{1}{1 + (j\omega\tau_s)^{1-\gamma}} \quad (8)$$

$$\frac{\chi_{ij}^{*}}{\chi_{oij}} = \frac{1}{(1 + j\omega\tau_{cs})^\delta} \quad (9)$$

Table 3 : Fröhlich's parameter A, χ'_{ij}/χ_{oij} and χ''_{ij}/χ_{oij} values estimated from Fröhlich's equations (6) and (7) with estimated τ_1 and τ_2 and those obtained from figures (5) and (6) at $\omega_j \rightarrow 0$, weighted contributions c_1 and c_2 from Fröhlich's method and those by graphical technique together with symmetric and asymmetric distribution parameters γ and δ of some monosubstituted anilines in benzene at 35°C under different electric field frequencies in GHz range.

Systems with serial number	Frequ.-ency (f) in GHz	Fröhlich parameter (A)	Estimated values of χ'_{ij}/χ_{oij} & χ''_{ij}/χ_{oij} of Fröhlich's equations (6) & (7)		Weighted contributions c_1 & c_2 from Eqs(4) & (5)		Estimated values of χ'_{ij}/χ_{oij} & χ''_{ij}/χ_{oij} from Figs.(5) & (6) at $\omega_j \rightarrow 0$	
(I) o-anisidine	(a) 3.86	4.7269	0.8829	0.2001	0.7491	0.4053	0.7613	0.0859
	(b) 22.06	3.1308	0.5893	0.3646	0.5200	1.0893	1.0006	0.1086
(II) m-anisidine	(a) 3.86	3.2169	0.4811	0.3650	0.4496	1.5081	0.7527	0.2389
	(b) 22.06	2.4340	0.5534	0.4063	0.4816	0.9439	0.7468	0.2508
(III) o-toluidine	2.02	3.9982	0.7936	0.2699	0.6755	0.6212	1.0700	0.0841
(IV) m-toluidine	3.86	4.2068	0.6401	0.3049	0.5826	1.2450	0.7858	0.0475
(V) p-toluidine	(a) 3.86	3.5730	0.6509	0.3320	0.5727	1.0167	0.9901	0.1639
	(b) 22.06	3.7429	0.7992	0.2766	0.6685	0.5943	1.1134	0.0399
Systems with serial number	Frequ.-ency (f) in GHz	Weighted contributions c_1 & c_2 from graphical technique		symmetric distribution parameter γ	Asymmetric distribution parameter δ			
(I) o-anisidine	(a) 3.86	0.7073	0.1637	0.7089	0.0757			
	(b) 22.06	1.0380	-0.1801	-0.0724	—			
(II) m-anisidine	(a) 3.86	0.7712	0.4485	0.3155	0.2688			
	(b) 22.06	0.7699	0.2181	0.2969	0.2901			
(III) o-toluidine	2.02	1.0498	0.1133	-0.4921	—			
(IV) m-toluidine	3.86	0.7903	-0.0213	0.8230	0.0393			
(V) p-toluidine	(a) 3.86	0.9769	0.2657	-0.0661	—			
	(b) 22.06	1.1208	-0.0233	-0.8078	—			

The former one (eq. 8) is associated with symmetric relaxation time τ_s and the latter one (eq. 9) with characteristic relaxation time τ_{cs} . Separating the real and imaginary parts of equations (8)

and (9) and rearranging them in terms of χ'_{ij}/χ_{oij} and χ''_{ij}/χ_{oij} at $w_j \rightarrow 0$ of Figures 5 and 6, γ and τ_s were obtained from :

$$\gamma = \frac{2}{\pi} \tan^{-1} \left[(1 - \chi'_{ij}/\chi_{oij}) \frac{\chi'_{ij}}{\chi''_{ij}} - \frac{\chi''_{ij}}{\chi_{oij}} \right] \quad (10)$$

and

$$\tau_s = \frac{1}{\omega} \left[\frac{1}{(\chi'_{ij}/\chi''_{ij}) \cos(\gamma\pi/2) - \sin(\gamma\pi/2)} \right]^{1/(1-\gamma)} \quad (11)$$

Similarly, δ and τ_{cs} can be had from equation (9) :

$$\tan(\phi\delta) = \frac{(\chi''_{ij}/\chi_{oij}) w_j \rightarrow 0}{(\chi'_{ij}/\chi_{oij}) w_j \rightarrow 0} \quad (12)$$

$$\text{and, } \tan \phi = \omega\tau_{cs} \quad (13)$$

As ϕ can not be evaluated directly; an arbitrary theoretical curve between $1/\phi \log \cos \phi$ against ϕ in degrees was drawn elsewhere [17] from which

$$\frac{1}{\phi} \log \cos \phi = \log \left[\frac{\chi'_{ij}/\chi_{oij}}{\cos \phi\delta} \right] / \phi\delta \quad (14)$$

can be known. The known values of $1/\phi \log \cos \phi$, is used to know ϕ from $1/\phi \log \cos \phi$ against ϕ curve. With known ϕ equations (12) and (13) were used to obtain δ and τ_{cs} respectively. τ_s and τ_{cs} so evaluated are in Table 2 to compare with τ_j 's by Murthy et al [14], freshly calculated Gopalakrishna [15] and τ_1 & τ_2 by double relaxation methods. Estimated γ and δ are shown in Table 3.

4. THEORETICAL FORMULATIONS TO OBTAIN HF DIPOLE MOMENT μ_j

(A) hf susceptibility method

The real ϵ'_{ij} and imaginary ϵ''_{ij} parts of hf complex relative permittivity ϵ^*_{ij} are related by:

$$\begin{aligned} \epsilon'_{ij} &= \epsilon_{\infty ij} + (1/\omega\tau) \epsilon''_{ij} \\ \epsilon'_{ij} - \epsilon_{\infty ij} &= (1/\omega\tau) \epsilon''_{ij} \\ \chi'_{ij} &= (1/\omega\tau) \epsilon''_{ij} \end{aligned} \quad (15)$$

$$\text{and, } (d\chi''_{ij} / d\chi'_{ij}) = \omega\tau \quad (16)$$

χ''_{ij} 's are expected to vary linearly with χ'_{ij} [14] as seen in Figure 4. The slope of linear equation of χ''_{ij} and χ'_{ij} was used to get τ_j from equation (16).

But the variations of χ''_{ij} with χ'_{ij} in Figure 4 are not strictly linear, the ratio of individual slopes of variations of χ''_{ij} and χ'_{ij} with w_j 's in Figures 2 and 3 is a better representation of

equation (16) to get τ_j where the polar - polar interactions are supposed to be almost eliminated. Thus

$$(d\chi''_{ij}/dw_j) w_j \rightarrow 0 / (d\chi'_{ij}/dw_j) w_j \rightarrow 0 = \omega\tau_j \quad (17)$$

The imaginary part χ''_{ij} of χ^*_{ij} is [18,19]

$$\chi''_{ij} = (N\rho_{ij}\mu_j^2 / 27\varepsilon_0 M_j K_B T) \cdot \omega\tau / (1 + \omega^2\tau^2) (\varepsilon_{ij} + 2)^2 w_j \quad (18)$$

which on differentiation with respect to w_j and at $w_j \rightarrow 0$ yields that

$$(d\chi''_{ij}/dw_j)w_j \rightarrow 0 = (N\rho_{ij}\mu_j^2 / 27\varepsilon_0 M_j K_B T) \cdot \omega\tau / (1 + \omega^2\tau^2) (\varepsilon_{ij} + 2)^2 \quad (19)$$

From equations (17) and (19) one obtains

$$\omega\tau (d\chi'_{ij}/dw_j) w_j \rightarrow 0 = (N\rho_{ij}\mu_j^2 / 27\varepsilon_0 M_j K_B T) \cdot \omega\tau / (1 + \omega^2\tau^2) (\varepsilon_{ij} + 2)^2$$

$$\text{or, } \mu_j = \left[\frac{27\varepsilon_0 M_j K_B T \beta}{N\rho_{ij} (\varepsilon_{ij} + 2)^2 b} \right]^{1/2} \quad (20)$$

Where ε_0 = the permittivity of free space = 8.854×10^{-12} F.m.⁻¹ and

β = linear coefficient of χ'_{ij} - w_j curves of Figure 3 at $w_j \rightarrow 0$.

(B) hf conductivity method

According to Murphy and Morgan [20] the real and imaginary parts of hf conductivity are related by :

$$\sigma''_{ij} = \sigma_{\infty ij} + (1/\omega\tau) \sigma'_{ij} \quad (21)$$

$\sigma'_{ij} = \omega\varepsilon_0 \varepsilon''_{ij}$ and $\sigma''_{ij} = \omega\varepsilon_0 \varepsilon'_{ij}$ are the real and imaginary parts of hf complex conductivity σ^*_{ij} . $\omega = 2\pi f$ and f is the frequency of applied electric field in GHz.

$$(d\sigma''_{ij}/dw_j) w_j \rightarrow 0 = (1/\omega\tau) (d\sigma'_{ij}/dw_j) w_j \rightarrow 0$$

Since in hf region $\sigma''_{ij} \cong \sigma_{ij}$ and σ_{ij} = the total hf conductivity = $\omega\varepsilon_0 (\varepsilon'_{ij}{}^2 + \varepsilon''_{ij}{}^2)^{1/2}$

$$\text{one has } (d\sigma'_{ij}/dw_j)w_j \rightarrow 0 = \omega\tau\beta \quad (22)$$

where β is the linear coefficient of σ_{ij} - w_j curve of Figure 7 in the limit $w_j = 0$.

Again, the real part σ'_{ij} of hf complex conductivity σ^*_{ij} is [18,22].

$$\sigma'_{ij} = \frac{N\mu_j^2 \rho_{ij}}{27M_j K_B T} \left[\frac{\omega^2\tau}{1 + \omega^2\tau^2} \right] (\varepsilon_{ij} + 2)^2 w_j \quad (23)$$

which on differentiation with respect to w_j and at $w_j \rightarrow 0$ yields

$$(d\sigma'_{ij}/dw_j)w_j \rightarrow 0 = \frac{N\mu_j^2 \rho_{ij}}{27M_j K_B T} \left[\frac{\omega^2\tau}{1 + \omega^2\tau^2} \right] (\varepsilon_{ij} + 2)^2 \quad (24)$$

From equations (22) and (24) one gets

$$\mu_j = \left[\frac{27M_j K_B T \beta}{N \rho_i (\epsilon_i + 2)^2 \omega b} \right]^{1/2} \quad (25)$$

Where β = linear coefficient of $\sigma_{ij} - w_j$ curve of Figure 7 at $w_j \rightarrow 0$. In both the equations (20) and (25) N = Avogadro's number = 6.023×10^{23} , ρ_i = density of solvent (C_6H_6) = 865 kg.m^{-3} , ϵ_i = relative permittivity of solvent (C_6H_6) = 2.253, M_j = molecular weight of solute in kg., K_B = Boltzmann constant = $1.38 \times 10^{-23} \text{ J. mole}^{-1} \text{ K}^{-1}$ and $b = 1 / (1 + \omega^2 \tau^2)$ = dimensionless parameter involved with measured τ .

Dipole moments μ_1 & μ_2 in terms of b_1, b_2 involved with τ_1 & τ_2 were computed from both the equations (20) and (25) as well with the linear coefficients β 's of both, $\chi'_{ij} - w_j$ and $\sigma_{ij} - w_j$ curves of Figures 3 and 7 respectively. All μ_j 's are placed in Table 4 together with μ_{theo} 's and reported μ_j 's (Gopalakrishna) for comparison.

Table 4 : Linear coefficient β 's, correlation coefficient (r) and % of error of $\chi'_{ij} - w_j$ and $\sigma_{ij} - w_j$ curves of figures 3 and 7, estimated dipole moments μ_1 & μ_2 for rotations of flexible polar groups and whole molecule by susceptibility and conductivity measurement techniques, dimensionless parameters b_1 and b_2 together with theoretical dipole moment μ_{theo} obtained from bond angles and bond moments, reported μ (Gopalakrishna) of some monosubstituted anilines in benzene at 35°C under different electric field frequencies.

Systems with serial number & molecular weight M_j	Frequ.-ency (f) in GHz	Liner coefficient of curves of figs 3 & 7	Correlation coefficient and % of error involved in curves of figs 3 & 7		Dimensionless parameters		Estimated $\mu \times 10^{30}$ in C.m from Eqs. (20) & (25)		$\mu_{theo} \times 10^{30}$ in C.m	$\mu \times 10^{30}$ in C.m from Gopalakrishna's method
					$b_1 = 1/(1+\omega^2\tau_1^2)$	$b_2 = 1/(1+\omega^2\tau_2^2)$	μ_1	μ_2		
(I) o-anisidine in C_6H_6 $M_j = 0.123 \text{ kg}$	(a) 3.86	1.9358 0.4890	0.9980 0.9984	0.12 0.10	0.9998	0.3304	5.07 5.50	8.81 9.56	3.40	5.23
	(b) 22.06	2.4031 17.3978	0.9102 0.9316	5.18 3.98	0.9769	0.0747	5.71 13.88	20.66 50.19		
(II) m-anisidine in C_6H_6 $M_j = 0.123 \text{ kg}$	(a) 3.86	1.8788 0.4623	0.9417 0.9508	3.41 2.89	0.9563	0.0339	5.10 5.46	27.10 29.01	5.50	5.13
	(b) 22.06	1.8214 2.5571	0.9934 0.9963	0.40 0.22	0.9396	0.1068	5.07 5.42	15.03 16.08		
(III) o-toluidine in C_6H_6 $M_j = 0.107 \text{ kg}$	2.02	1.4846	0.9966	0.23	0.9986	0.1917	4.14	9.45	4.63	5.37
		0.1981	0.9981	0.13			4.51	10.30		
(IV) m-toluidine in C_6H_6 $M_j = 0.107 \text{ kg}$	3.86	0.5720	0.8479	8.48	0.9956	0.0482	2.57	11.69	3.43	4.90
		0.1265	0.8732	7.16			2.61	11.87		
(V) p-toluidine in C_6H_6 $M_j = 0.107 \text{ kg}$	(a) 3.86	0.4791 0.1638	0.9755 0.9825	1.46 1.04	0.9912	0.0818	2.36 2.98	8.22 10.38	5.13	5.00
	(b) 22.06	0.0109 0.3762	0.9819 0.9864	1.08 0.81	0.9980	0.2221	0.35 1.88	0.75 3.99		

5. RESULTS AND DISCUSSION

The least squares fitted straight line equations in terms of χ'_{ij} , χ''_{ij} and χ_{oij} of Table 1 were worked out for each system as shown graphically in Figure 1 at different w_j of solute in benzene at 35°C under GHz electric field with the experimental points placed upon them. χ'_{ij} and χ''_{ij} are real and imaginary parts of hf complex dimensionless dielectric orientational susceptibility χ^*_{ij} and χ_{oij} is the static or low frequency real dielectric susceptibility. They are, however, derived from measured [7] relative permittivities ϵ'_{ij} , ϵ''_{ij} , ϵ_{oij} and $\epsilon_{\infty ij}$ of Table 1. The correlation coefficients (r) and chisquare values placed in the 5th and 6th columns of Table 2 are estimated to show how far the variables $(\chi_{oij} - \chi'_{ij}) / \chi'_{ij}$ and χ''_{ij} / χ'_{ij} of equation (3) are correlated. It is seen that r is low for *o*-anisidine at 3.86 GHz and *o*-toluidine at 2.02 GHz possibly for errors introduced in the measurement of ϵ'_{ij} , ϵ''_{ij} , ϵ_{oij} and $\epsilon_{\infty ij}$. This fact is also confirmed by remarkable deviations of experimental data from linear curves of

Figure 1. In order to locate the double relaxation phenomena accurate measurements of ϵ_{oij} and $\epsilon_{\infty ij}$ are essential. The refractive index n_{Dij} measured by Abbes refractometer often yields $\epsilon_{\infty ij} = n_{Dij}^2$ [7] although Cole - Cole [3] and Cole - Davidson [21] plots give $\epsilon_{\infty ij}$ as (1.0 - 1.15) times of n_{Dij}^2 . The intercepts and slopes of linear curves of Figure 1 are seen in the 3rd and 4th columns of Table 2, to get τ_1 and τ_2 due to rotation of flexible polar groups and end over end rotations of the whole molecules. τ_1 and τ_2 thus measured are presented in the 7th and 8th columns of Table 2. τ_2 's in Table 2 increases gradually from meta to ortho for anisidines at 22.06 GHz while the reverse is true at 3.86 GHz. But incase of toluidines τ_2 increases from para to ortho and to meta forms. This behaviour is, however, explained by the fact that C \rightarrow NH₂ group is significantly influenced by GHz electric field. On the other hand τ_1 increases from ortho to meta forms for anisidines while it increases from meta to ortho and to para forms for toluidines. This behaviour, however, indicates that flexible parts of the molecules are loosely bound to the parent molecules [12, 13].

In absence of reliable τ_j 's of monosubstituted anilines the slopes of the least squares fitted straight line curves of χ''_{ij} against χ'_{ij} of Figure 4 as claimed by Murthy et al [14] were used to

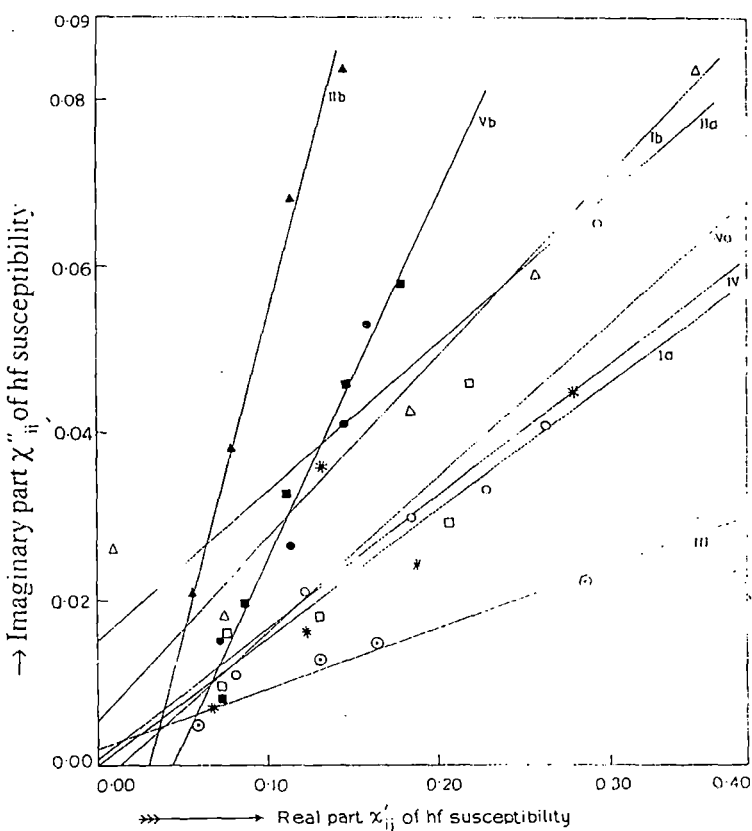


Figure 4 : Linear plot of imaginary part of hf susceptibility χ''_{ij} against real part χ'_{ij} of monosubstituted anilines in benzene at 35°C under GHz electric field.

(Ia) *o*-anisidine at 3.86 GHz (—○—), (Ib) *o*-anisidine at 22.06 GHz (—●—), (IIa) *m*-anisidine at 3.86 GHz (—△—), (IIb) *m*-anisidine at 22.06 GHz (—▲—), (III) *o*-toluidine at 2.02 GHz (—○—), (IV) *m*-toluidine at 3.86 GHz (—*—), (Va) *p*-toluidine at 3.86 GHz (—□—) and (Vb) *p*-toluidine at 22.06 GHz (—■—) respectively.

get τ_1 from equation (16). They are placed in the 9th column of Table 2. The experimental points of Table 1 are found to deviate from linearity of Figure 4 due to solute - solute molecular interactions. The individual variations of χ''_{ij} and χ'_{ij} with w_j are not strictly linear as seen in Figures 2 and 3. This fact at once prompted one to use the ratio of slopes of the individual variations of χ''_{ij} and χ'_{ij} with w_j 's entered in 10th column of Table 2 to evaluate τ_1 from equation (17) at $w_j \rightarrow 0$. τ_1 's thus obtained are in close agreement with τ_1 from double relaxation and Gopalakrishna's [15] method and are placed in the Table 2. τ_1 for p-toluidine at 22.06 GHz shows large value probably for error introduced in ϵ'_{ij} , ϵ''_{ij} , ϵ_{oij} and $\epsilon_{\infty ij}$ measurements. The basic soundness of the latter method in getting τ_1 is thus confirmed because polar-polar interactions are fully avoided [22]. Moreover, it shows that hf susceptibility measurement yields microscopic τ where as double relaxation method gives both microscopic and macroscopic τ_1 and τ_2 as observed else where [23].

Larger τ_2 arises for the bigger size of rotating unit ($\tau_j T / \eta \gamma$) due to solvent environment around solute molecules. The distribution of τ between two extreme τ_1 and τ_2 values yields the symmetric and asymmetric distribution parameters γ and δ . They are however, obtained from equations (10) and (12) with $(\chi'_{ij} / \chi_{oij}) w_j \rightarrow 0$ and $(\chi''_{ij} / \chi_{oij}) w_j \rightarrow 0$ of Figures 5 and 6. The value of $1/\phi \log \cos \phi$ against ϕ in degree as shown elsewhere [17] is essential to know δ . Knowing ϕ , δ 's were obtained. γ and δ are entered in Table 3.

The symmetric relaxation times τ_s from equation (11) in terms of γ of equation (10) are presented in Table 2. The close agreement of τ_s 's with τ_1 's and reported τ 's by freshly calculated from Gopalakrishna's method, indicates symmetric relaxation behaviour of such molecules in C_6H_6 . The agreement is however, poor incase of o-toluidine. The characteristic relaxation times τ_{cs} obtained from equation (13) for o-anisidine at 3.86 GHz, m-anisidine at 3.86 & 22.06 GHz and m-toluidine at 3.86 GHz as in Table 2 are found to be low due to high values of δ . For other

systems τ_{cs} and δ could not be found out as $1/\phi \log \cos \phi$ for them are positive. This fact rules out the applicability of asymmetric relaxation behaviour for such compounds.

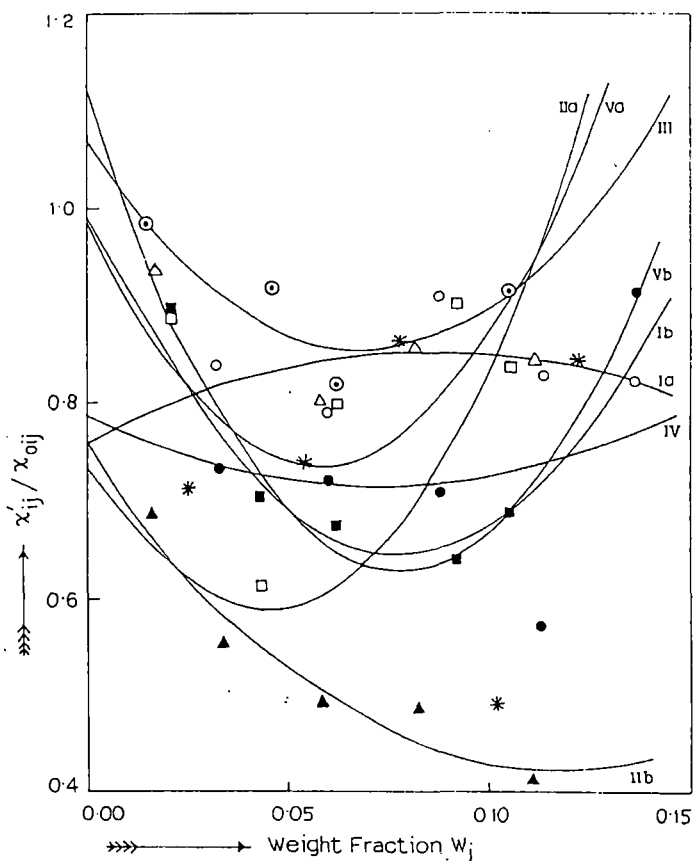


Figure 5 : Plot of χ'_{ij} / χ_{oij} against weight fraction w_j of monosubstituted anilines in benzene at 35°C under GHz electric field.

(Ia) o-anisidine at 3.86 GHz (○), (Ib) o-anisidine at 22.06 GHz (●), (IIa) m-anisidine at 3.86 GHz (△), (IIb) m-anisidine at 22.06 GHz (▲), (III) o-toluidine at 2.02 GHz (⊖), (IV) m-toluidine at 3.86 GHz (*), (Va) p-toluidine at 3.86 GHz (□) and (Vb) p-toluidine at 22.06 GHz (■) respectively.

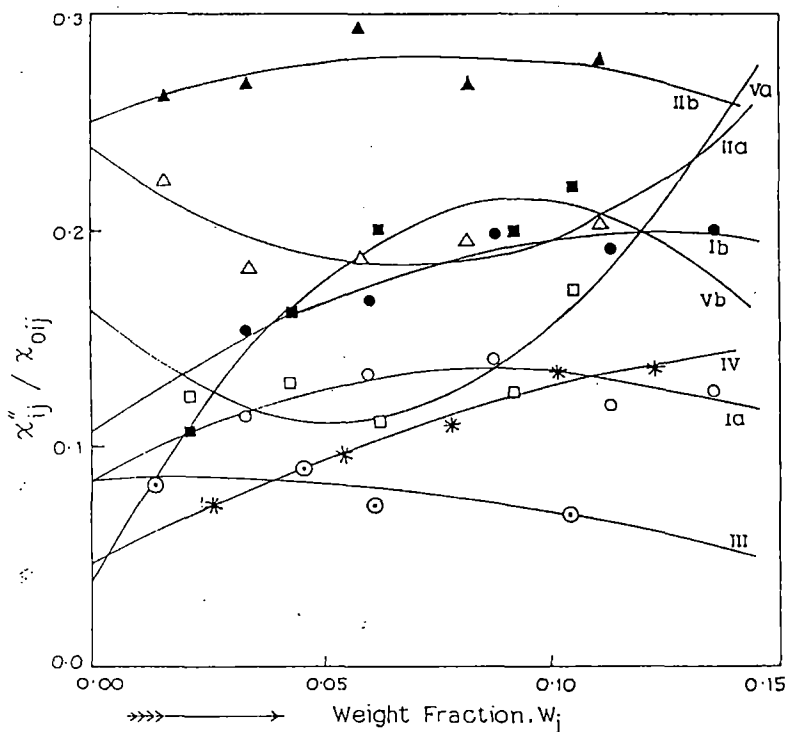


Figure 6 : Plot of χ''_{ij} / χ_{oij} against weight fraction w_j of monosubstituted anilines in benzene at 35°C under GHz electric field.

(Ia) o-anisidine at 3.86 GHz (—○—), (Ib) o-anisidine at 22.06 GHz (—●—), (IIa) m-anisidine at 3.86 GHz (—△—), (IIb) m-anisidine at 22.06 GHz (—▲—), (III) o-toluidine at 2.02 GHz (—○—), (IV) m-toluidine at 3.86 GHz (—*—), (Va) p-toluidine at 3.86 GHz (—□—) and (Vb) p-toluidine at 22.06 GHz (—■—) respectively.

hing the validity of equation (3). It is interesting to note that experimental c_2 's are negative in case of o-anisidine and p-toluidine at 22.06 GHz and m-toluidine for the inertia of the flexible parts [23]. In Figures 5 and 6 it is also seen that the experimental points often do not lie on the smooth fitted curves probably due to solute - solute or solute - solvent molecular associations.

The dipole moments μ_1 and μ_2 of the flexible parts and the whole molecules were estimated from the linear coefficients β 's in the 3rd column of Table 4 of both $\chi'_{ij} - w_j$ and $\sigma_{ij} - w_j$ curves of Figures 3 and 7 and dimensionless parameters b_1 and b_2 involved with measured τ_1 and τ_2 from equation (3). The μ_1 and μ_2 thus obtained from equations (20) and (25) are placed in the 8th and 9th columns of Table 4 for comparison. Correlation coefficients r 's and % of errors involved in the regression analysis in the 4th and 5th columns of Table 4 were made only to show how far χ'_{ij} 's and σ_{ij} 's are correlated with w_j 's. Both the χ'_{ij} 's and σ_{ij} 's with w_j in Figures 3 and 7 give reliable β to yield accurate μ_1 and μ_2 . It is seen in Figures 3 and 7 that almost all the curves show a tendency to be closer within the region $0.00 \leq w_j \leq 0.03$ indicating the same polarity of the molecules, in addition to solute - solvent (monomer) or solute - solute (dimer) molecular associations [6,22]. μ_1 and μ_2 in Table 4 from $\chi'_{ij} - w_j$ curves of Figure 3 are always smaller in magnitude than $\sigma_{ij} - w_j$ curves of Figure 7, as χ'_{ij} 's are associated with orientational polarisation while σ_{ij} is linked with bound molecular charges. Theoretical dipole moments μ_{theo} 's of monosubstituted anilines as estimated elsewhere [17] in terms of available bond angles and

The theoretical weighted contributions of c_1 and c_2 towards dielectric relaxations were obtained from equations (4) and (5) by the measured τ_1 and τ_2 of equation (3) and χ'_{ij} / χ_{oij} and χ''_{ij} / χ_{oij} of Fröhlich's equations (6) and (7). The 6th and 7th columns of Table 3 contain c_1 and c_2 . The experimental c_1 and c_2 values were also obtained from $(\chi'_{ij} / \chi_{oij}) w_j \rightarrow 0$ and $(\chi''_{ij} / \chi_{oij}) w_j \rightarrow 0$ of the concentration variations of χ'_{ij} / χ_{oij} and χ''_{ij} / χ_{oij} of Figures 5 and 6 by using equations (4) and (5). They are presented in Table 3 for comparison with the theoretical ones. Fröhlich's equations (6) and (7) are related to Fröhlich parameter A, where $A = \ln(\tau_2 / \tau_1)$. Both the theoretical and experimental c_1 and c_2 as seen in Table 3 showed that $|c_1 + c_2| \approx 1$ establis-

bond moments of polar groups $C \rightarrow NH_2$, $C \rightarrow OCH_3$, $C \rightarrow CH_3$ are entered in the 10th column of Table 4 to compare with experimental μ_j 's. The contribution of inductive, mesomeric and electromeric moments of the substituent polar groups of the molecules towards the hf μ_j 's are, however, explained by the factor $\mu_{(expt)}/\mu_{(theo)}$ of values 1.49, 1.68, 0.93, 0.92, 0.89, 0.75, 0.46 and 0.07 of Ia, Ib, IIa, IIb, III, IV, Va and Vb respectively. The amount of bound molecular charge is judged from the difference $\Delta\mu_j$ between μ_j 's of hf σ_{ij} and χ'_{ij} respectively to contribute to hf σ_{ij} [8].

In absence of reliable μ_j 's Gopalakrishna's method [15] were reemployed. The close agreement between reported μ_j 's, (Gopalakrishna) μ and $\mu_{(theo)}$'s confirms the basic soundness of the methods prescribed in getting hf μ_j , in addition to the fact that a part of the molecule is rotating under GHz electric field.

6. CONCLUSION

The methodology so far presented in SI units with internationally accepted symbols of dielectric terminologies and parameters appears to be more topical, simple, straightforward and significant contribution to predict relaxation parameters as χ_{ij} 's are directly linked with molecular orientational polarisation. The interesting equations to evaluate τ_j 's and μ_j 's in terms of χ_{ij} 's helps one to shed more light on the relaxation phenomena of complicated molecules. The simple straight line equation (3) provides with microscopic τ_1 and macroscopic τ_2 respectively. The method to evaluate τ_j from the ratio of slopes of individual variations of χ''_{ij} and χ'_{ij} with w_j is a better representation of the earlier one of Murthy et al as it eliminates polar - polar interactions in a given solution. The relative weight factors c_1 and c_2 towards dielectric dispersions by Fröhlich and graphical methods show $|c_1 + c_2| \approx 1$ confirming the applicability of the linear equation (3) to estimate τ_1 and τ_2 respectively for such dipolar liquids. The close agreement of τ_j , τ_1 and τ_2 confirms the nonrigid character of the molecules under hf electric field in C_6H_6 . μ_1 and μ_2 by hf susceptibility and conductivity methods establish the fact that different types of polarisations are associated with χ_{ij} 's and σ_{ij} 's. The theoretical reasons of evaluating τ_1 's and μ_1 's in agreement

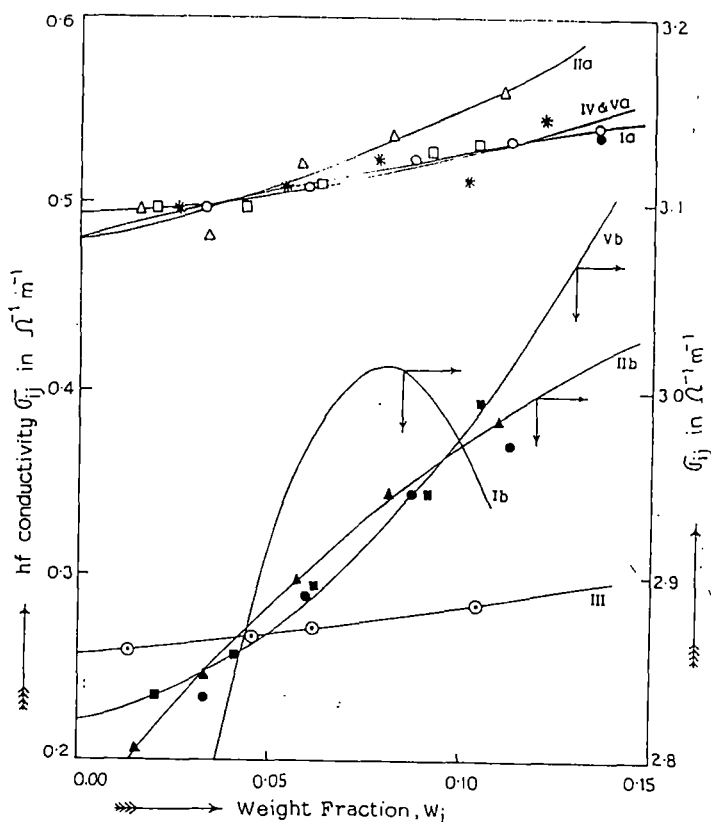


Figure 7 : Plot of σ_{ij} against weight fraction w_j of monosubstituted anilines in benzene at 35°C under GHz electric field.

(Ia) o-anisidine at 3.86 GHz (—○—), (Ib) o-anisidine at 22.06 GHz (—●—), (IIa) m-anisidine at 3.86 GHz (—△—), (IIb) m-anisidine at 22.06 GHz (—▲—), (III) o-toluidine at 2.02 GHz (—○—), (IV) m-toluidine at 3.86 GHz (—*—), (Va) p-toluidine at 3.86 GHz (—□—) and (Vb) p-toluidine at 22.06 GHz (—■—) respectively.

of τ_j 's and μ_j 's from freshly calculated Gopalakrishna's method is really sound. Various types of molecular associations are inferred from usual departure of graphically fitted plots of χ'_{ij} / χ_{oij} and χ''_{ij} / χ_{oij} with ω_j 's and conformational structure of the molecules in which the effects of inductive, mesomeric and electromeric moments of the polar groups of the molecule play the prominent role.

REFERENCES

- [1] A. Sharma, D.R Sharma and M.S Chauhan Indian J Pure & Appl Phys **31** (1993) 841.
- [2] K. Higasi, Y. Koga and M. Nakamura Bull Chem Soc. Japan **44** (1971) 988.
- [3] K.S. Cole and R.H. Cole J Chem Phys **9** (1941) 341.
- [4] E.A. Guggenheim Trans Faraday Soc **45** (1949) 714.
- [5] S.K. Sit, N.Ghosh, U.Saha and S. Acharyya Indian J Phys **71B** (1997) 533.
- [6] N.Ghosh, A. Karmakar, S.K. Sit and S. Acharyya Indian J Pure & Appl. Phys **38** (2000) 574.
- [7] S.C. Srivastava and S Chandra Indian J Pure & Appl. Phys **13** (1975) 101.
- [8] A. K. Jonscher Physics of Dielectric Solids, invited papers ed C H L Goodman Canterbury (1980).
- [9] A. Budo Phys Z **39** (1938) 706.
- [10] K. Bergmann, D.M. Roberti and C.P. Smyth J Phys Chem **64** (1960) 665.
- [11] J. Bhattacharyya, A. Hasan, S.B. Roy and G.S. Kastha J Phys Soc Japan **28** (1970) 204.
- [12] U. Saha, S.K. Sit, R.C. Basak and S. Acharyya J Phys D : Appl. Phys **27** (1994) 596.
- [13] S. K. Sit, R. C. Basak, U. Saha and S. Acharyya J Phys D : Appl. Phys **27** (1994) 2194.
- [14] M.B.R. Murthy, R.L. Patil and D.K. Deshpande Indian J Phys **63B** (1989) 491.
- [15] K. V. Gopalakrishna Trans Faraday Soc **53** (1957) 767.
- [16] H. Fröhlich "*Theory of Dielectrics*" (Oxford University Press: Oxford..1949).
- [17] N.Ghosh, S. K. Sit, A.K. Bothra and S. Acharyya J Phys D : Appl. Phys (UK) **34** (2001) 379.
- [18] C.P. Smyth "*Dielectric Behaviour and Structure*" (New York : Mc Graw Hill 1955)
- [19] K. Dutta, S.K. Sit and S. Acharyya, Pramana J Phys (2001) Accepted for Publication.
- [20] F. J. Murphy and S.O. Morgan Bell Syst Tech J **18** (1939) 502.
- [21] D.W. Davidson and R.H. Cole J Chem Phys **19** (1951) 1484.
- [22] N. Ghosh, R.C. Basak, S.K. Sit and S. Acharyya J. Mol. Liquids **85** (2000) 375.
- [23] S. K. Sit, N. Ghosh and S. Acharyya Indian J Pure & Appl. Phys **35** (1997) 329.